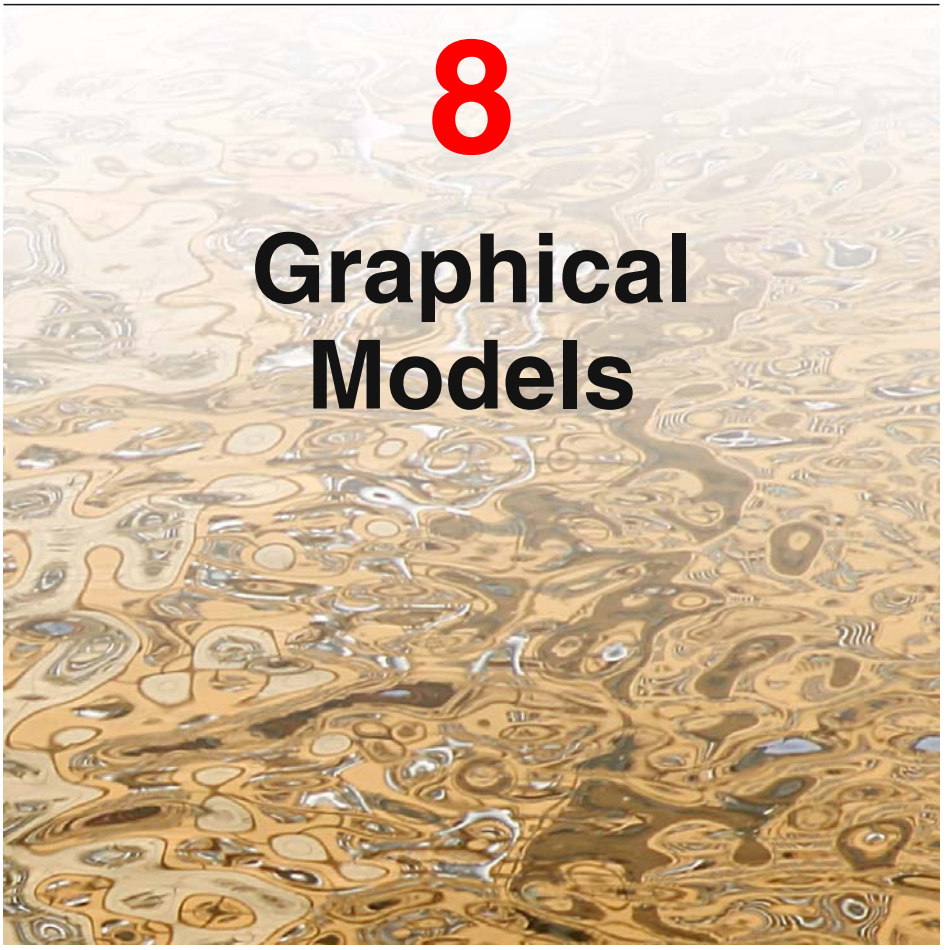

8 Graphical Models

Probabilities play a central role in modern pattern recognition. We have seen in Chapter 1 that probability theory can be expressed in terms of two simple equations corresponding to the sum rule and the product rule. All of the probabilistic inference and learning manipulations discussed in this book, no matter how complex, amount to repeated application of these two equations. We could therefore proceed to formulate and solve complicated probabilistic models purely by algebraic manipulation. However, we shall find it highly advantageous to augment the analysis using diagrammatic representations of probability distributions, called *probabilistic graphical models*. These offer several useful properties:

1. They provide a simple way to visualize the structure of a probabilistic model and can be used to design and motivate new models.

2. Insights into the properties of the model, including conditional independence properties, can be obtained by inspection of the graph.

3. Complex computations, required to perform inference and learning in sophisticated models, can be expressed in terms of graphical manipulations, in which underlying mathematical expressions are carried along implicitly.

A graph comprises *nodes* (also called *vertices*) connected by *links* (also known as *edges* or *arcs*). In a probabilistic graphical model, each node represents a random variable (or group of random variables), and the links express probabilistic relationships between these variables. The graph then captures the way in which the joint distribution over all of the random variables can be decomposed into a product of factors each depending only on a subset of the variables. We shall begin by discussing *Bayesian networks*, also known as *directed graphical models*, in which the links of the graphs have a particular directionality indicated by arrows. The other major class of graphical models are *Markov random fields*, also known as *undirected graphical models*, in which the links do not carry arrows and have no directional significance. Directed graphs are useful for expressing causal relationships between random variables, whereas undirected graphs are better suited to expressing soft constraints between random variables. For the purposes of solving inference problems, it is often convenient to convert both directed and undirected graphs into a different representation called a *factor graph*.

In this chapter, we shall focus on the key aspects of graphical models as needed for applications in pattern recognition and machine learning. More general treatments of graphical models can be found in the books by Whittaker (1990), Lauritzen (1996), Jensen (1996), Castillo *et al.* (1997), Jordan (1999), Cowell *et al.* (1999), and Jordan (2007).

8.1. Bayesian Networks

In order to motivate the use of directed graphs to describe probability distributions, consider first an arbitrary joint distribution $p(a, b, c)$ over three variables a, b, and c. Note that at this stage, we do not need to specify anything further about these variables, such as whether they are discrete or continuous. Indeed, one of the powerful aspects of graphical models is that a specific graph can make probabilistic statements for a broad class of distributions. By application of the product rule of probability (1.11), we can write the joint distribution in the form

$$p(a, b, c) = p(c|a, b)p(a, b). \tag{8.1}$$

A second application of the product rule, this time to the second term on the right-hand side of (8.1), gives

$$p(a, b, c) = p(c|a, b)p(b|a)p(a). \tag{8.2}$$

Note that this decomposition holds for any choice of the joint distribution. We now represent the right-hand side of (8.2) in terms of a simple graphical model as follows. First we introduce a node for each of the random variables a, b, and c and associate each node with the corresponding conditional distribution on the right-hand side of

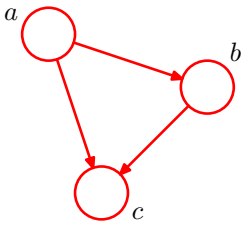

Figure 8.1 A directed graphical model representing the joint probability distribution over three variables a, b, and c, corresponding to the decomposition on the right-hand side of (8.2).

(8.2). Then, for each conditional distribution we add directed links (arrows) to the graph from the nodes corresponding to the variables on which the distribution is conditioned. Thus for the factor $p(c|a, b)$, there will be links from nodes a and b to node c, whereas for the factor $p(a)$ there will be no incoming links. The result is the graph shown in Figure 8.1. If there is a link going from a node a to a node b, then we say that node a is the *parent* of node b, and we say that node b is the *child* of node a. Note that we shall not make any formal distinction between a node and the variable to which it corresponds but will simply use the same symbol to refer to both.

An interesting point to note about (8.2) is that the left-hand side is symmetrical with respect to the three variables a, b, and c, whereas the right-hand side is not. Indeed, in making the decomposition in (8.2), we have implicitly chosen a particular ordering, namely a, b, c, and had we chosen a different ordering we would have obtained a different decomposition and hence a different graphical representation. We shall return to this point later.

For the moment let us extend the example of Figure 8.1 by considering the joint distribution over K variables given by $p(x_1, \ldots, x_K)$. By repeated application of the product rule of probability, this joint distribution can be written as a product of conditional distributions, one for each of the variables

$$p(x_1, \ldots, x_K) = p(x_K|x_1, \ldots, x_{K-1}) \ldots p(x_2|x_1)p(x_1). \tag{8.3}$$

For a given choice of K, we can again represent this as a directed graph having K nodes, one for each conditional distribution on the right-hand side of (8.3), with each node having incoming links from all lower numbered nodes. We say that this graph is *fully connected* because there is a link between every pair of nodes.

So far, we have worked with completely general joint distributions, so that the decompositions, and their representations as fully connected graphs, will be applicable to any choice of distribution. As we shall see shortly, it is the *absence* of links in the graph that conveys interesting information about the properties of the class of distributions that the graph represents. Consider the graph shown in Figure 8.2. This is not a fully connected graph because, for instance, there is no link from x_1 to x_2 or from x_3 to x_7.

We shall now go from this graph to the corresponding representation of the joint probability distribution written in terms of the product of a set of conditional distributions, one for each node in the graph. Each such conditional distribution will be conditioned only on the parents of the corresponding node in the graph. For instance, x_5 will be conditioned on x_1 and x_3. The joint distribution of all 7 variables

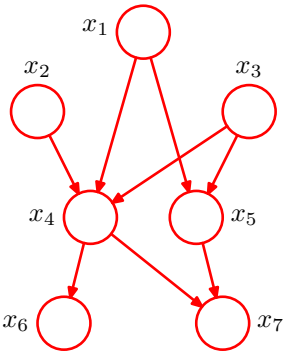

Figure 8.2 Example of a directed acyclic graph describing the joint distribution over variables $x_1, \ldots, x_7$. The corresponding decomposition of the joint distribution is given by (8.4).

is therefore given by

$$p(x_1)p(x_2)p(x_3)p(x_4|x_1, x_2, x_3)p(x_5|x_1, x_3)p(x_6|x_4)p(x_7|x_4, x_5). \tag{8.4}$$

The reader should take a moment to study carefully the correspondence between (8.4) and Figure 8.2.

We can now state in general terms the relationship between a given directed graph and the corresponding distribution over the variables. The joint distribution defined by a graph is given by the product, over all of the nodes of the graph, of a conditional distribution for each node conditioned on the variables corresponding to the parents of that node in the graph. Thus, for a graph with K nodes, the joint distribution is given by

$$p(\mathbf{x}) = \prod_{k=1}^{K} p(x_k|\mathrm{pa}_k) \tag{8.5}$$

where pa_k denotes the set of parents of x_k, and $\mathbf{x} = \{x_1, \ldots, x_K\}$. This key equation expresses the *factorization* properties of the joint distribution for a directed graphical model. Although we have considered each node to correspond to a single variable, we can equally well associate sets of variables and vector-valued variables with the nodes of a graph. It is easy to show that the representation on the right-hand side of (8.5) is always correctly normalized provided the individual conditional distributions are normalized.

Exercise 8.1

The directed graphs that we are considering are subject to an important restriction namely that there must be no *directed cycles*, in other words there are no closed paths within the graph such that we can move from node to node along links following the direction of the arrows and end up back at the starting node. Such graphs are also called *directed acyclic graphs*, or *DAGs*. This is equivalent to the statement that there exists an ordering of the nodes such that there are no links that go from any node to any lower numbered node.

Exercise 8.2

8.1.1 Example: Polynomial regression

As an illustration of the use of directed graphs to describe probability distributions, we consider the Bayesian polynomial regression model introduced in Sec-

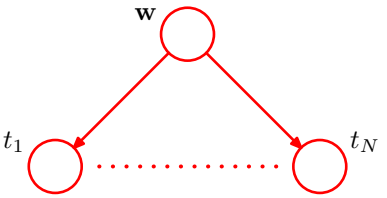

Figure 8.3 Directed graphical model representing the joint distribution (8.6) corresponding to the Bayesian polynomial regression model introduced in Section 1.2.6.

tion 1.2.6. The random variables in this model are the vector of polynomial coefficients $\mathbf{w}$ and the observed data $\mathbf{t} = (t_1, \ldots, t_N)^{\mathrm{T}}$. In addition, this model contains the input data $\mathbf{x} = (x_1, \ldots, x_N)^{\mathrm{T}}$, the noise variance σ^2, and the hyperparameter α representing the precision of the Gaussian prior over $\mathbf{w}$, all of which are parameters of the model rather than random variables. Focussing just on the random variables for the moment, we see that the joint distribution is given by the product of the prior $p(\mathbf{w})$ and N conditional distributions $p(t_n|\mathbf{w})$ for $n = 1, \ldots, N$ so that

$$p(\mathbf{t}, \mathbf{w}) = p(\mathbf{w}) \prod_{n=1}^{N} p(t_n|\mathbf{w}). \tag{8.6}$$

This joint distribution can be represented by a graphical model shown in Figure 8.3.

When we start to deal with more complex models later in the book, we shall find it inconvenient to have to write out multiple nodes of the form $t_1, \ldots, t_N$ explicitly as in Figure 8.3. We therefore introduce a graphical notation that allows such multiple nodes to be expressed more compactly, in which we draw a single representative node t_n and then surround this with a box, called a *plate*, labelled with N indicating that there are N nodes of this kind. Re-writing the graph of Figure 8.3 in this way, we obtain the graph shown in Figure 8.4.

We shall sometimes find it helpful to make the parameters of a model, as well as its stochastic variables, explicit. In this case, (8.6) becomes

$$p(\mathbf{t}, \mathbf{w}|\mathbf{x}, \alpha, \sigma^2) = p(\mathbf{w}|\alpha) \prod_{n=1}^{N} p(t_n|\mathbf{w}, x_n, \sigma^2).$$

Correspondingly, we can make $\mathbf{x}$ and α explicit in the graphical representation. To do this, we shall adopt the convention that random variables will be denoted by open circles, and deterministic parameters will be denoted by smaller solid circles. If we take the graph of Figure 8.4 and include the deterministic parameters, we obtain the graph shown in Figure 8.5.

When we apply a graphical model to a problem in machine learning or pattern recognition, we will typically set some of the random variables to specific observed

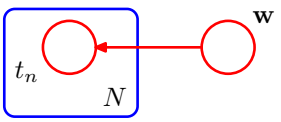

Figure 8.4 An alternative, more compact, representation of the graph shown in Figure 8.3 in which we have introduced a *plate* (the box labelled N) that represents N nodes of which only a single example t_n is shown explicitly.

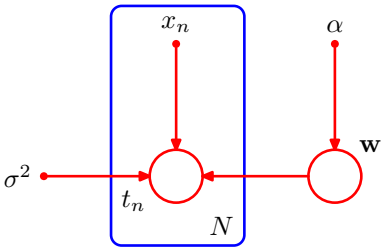

Figure 8.5 This shows the same model as in Figure 8.4 but with the deterministic parameters shown explicitly by the smaller solid nodes.

values, for example the variables $\{t_n\}$ from the training set in the case of polynomial curve fitting. In a graphical model, we will denote such *observed variables* by shading the corresponding nodes. Thus the graph corresponding to Figure 8.5 in which the variables $\{t_n\}$ are observed is shown in Figure 8.6. Note that the value of $\mathbf{w}$ is not observed, and so $\mathbf{w}$ is an example of a *latent* variable, also known as a *hidden* variable. Such variables play a crucial role in many probabilistic models and will form the focus of Chapters 9 and 12.

Having observed the values $\{t_n\}$ we can, if desired, evaluate the posterior distribution of the polynomial coefficients $\mathbf{w}$ as discussed in Section 1.2.5. For the moment, we note that this involves a straightforward application of Bayes' theorem

$$p(\mathbf{w}|\mathbf{T}) \propto p(\mathbf{w}) \prod_{n=1}^{N} p(t_n|\mathbf{w}) \tag{8.7}$$

where again we have omitted the deterministic parameters in order to keep the notation uncluttered.

In general, model parameters such as $\mathbf{w}$ are of little direct interest in themselves, because our ultimate goal is to make predictions for new input values. Suppose we are given a new input value $\widehat{x}$ and we wish to find the corresponding probability distribution for $\widehat{t}$ conditioned on the observed data. The graphical model that describes this problem is shown in Figure 8.7, and the corresponding joint distribution of all of the random variables in this model, conditioned on the deterministic parameters, is then given by

$$p(\widehat{t}, \mathbf{t}, \mathbf{w}|\widehat{x}, \mathbf{x}, \alpha, \sigma^2) = \left[\prod_{n=1}^{N} p(t_n|x_n, \mathbf{w}, \sigma^2)\right] p(\mathbf{w}|\alpha) p(\widehat{t}|\widehat{x}, \mathbf{w}, \sigma^2). \tag{8.8}$$

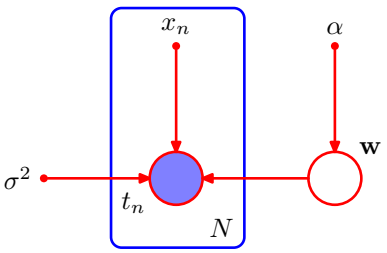

Figure 8.6 As in Figure 8.5 but with the nodes $\{t_n\}$ shaded to indicate that the corresponding random variables have been set to their observed (training set) values.

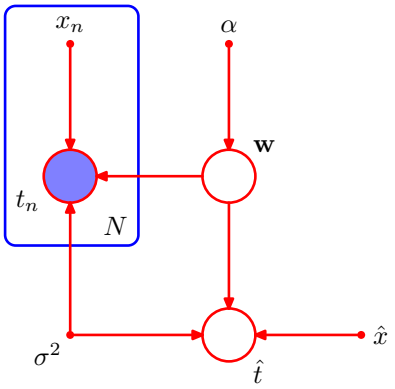

Figure 8.7 The polynomial regression model, corresponding to Figure 8.6, showing also a new input value $\widehat{x}$ together with the corresponding model prediction $\widehat{t}$.

The required predictive distribution for $\widehat{t}$ is then obtained, from the sum rule of probability, by integrating out the model parameters $\mathbf{w}$ so that

$$p(\widehat{t}|\widehat{x}, \mathbf{x}, \mathbf{t}, \alpha, \sigma^2) \propto \int p(\widehat{t}, \mathbf{t}, \mathbf{w}|\widehat{x}, \mathbf{x}, \alpha, \sigma^2)\, \mathrm{d}\mathbf{w}$$

where we are implicitly setting the random variables in $\mathbf{t}$ to the specific values observed in the data set. The details of this calculation were discussed in Chapter 3.

8.1.2 Generative models

There are many situations in which we wish to draw samples from a given probability distribution. Although we shall devote the whole of Chapter 11 to a detailed discussion of sampling methods, it is instructive to outline here one technique, called *ancestral sampling*, which is particularly relevant to graphical models. Consider a joint distribution $p(x_1, \ldots, x_K)$ over K variables that factorizes according to (8.5) corresponding to a directed acyclic graph. We shall suppose that the variables have been ordered such that there are no links from any node to any lower numbered node, in other words each node has a higher number than any of its parents. Our goal is to draw a sample $\widehat{x}_1, \ldots, \widehat{x}_K$ from the joint distribution.

To do this, we start with the lowest-numbered node and draw a sample from the distribution $p(x_1)$, which we call $\widehat{x}_1$. We then work through each of the nodes in order, so that for node n we draw a sample from the conditional distribution $p(x_n|\mathrm{pa}_n)$ in which the parent variables have been set to their sampled values. Note that at each stage, these parent values will always be available because they correspond to lower-numbered nodes that have already been sampled. Techniques for sampling from specific distributions will be discussed in detail in Chapter 11. Once we have sampled from the final variable x_K, we will have achieved our objective of obtaining a sample from the joint distribution. To obtain a sample from some marginal distribution corresponding to a subset of the variables, we simply take the sampled values for the required nodes and ignore the sampled values for the remaining nodes. For example, to draw a sample from the distribution $p(x_2, x_4)$, we simply sample from the full joint distribution and then retain the values $\widehat{x}_2, \widehat{x}_4$ and discard the remaining values $\{\widehat{x}_{j\neq 2,4}\}$.

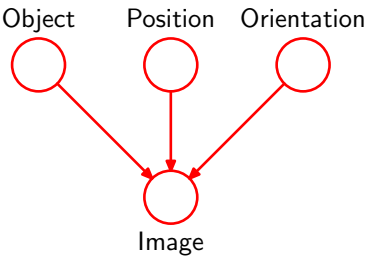

Figure 8.8 A graphical model representing the process by which images of objects are created, in which the identity of an object (a discrete variable) and the position and orientation of that object (continuous variables) have independent prior probabilities. The image (a vector of pixel intensities) has a probability distribution that is dependent on the identity of the object as well as on its position and orientation.

For practical applications of probabilistic models, it will typically be the higher-numbered variables corresponding to terminal nodes of the graph that represent the observations, with lower-numbered nodes corresponding to latent variables. The primary role of the latent variables is to allow a complicated distribution over the observed variables to be represented in terms of a model constructed from simpler (typically exponential family) conditional distributions.

We can interpret such models as expressing the processes by which the observed data arose. For instance, consider an object recognition task in which each observed data point corresponds to an image (comprising a vector of pixel intensities) of one of the objects. In this case, the latent variables might have an interpretation as the position and orientation of the object. Given a particular observed image, our goal is to find the posterior distribution over objects, in which we integrate over all possible positions and orientations. We can represent this problem using a graphical model of the form show in Figure 8.8.

The graphical model captures the *causal* process (Pearl, 1988) by which the observed data was generated. For this reason, such models are often called *generative* models. By contrast, the polynomial regression model described by Figure 8.5 is not generative because there is no probability distribution associated with the input variable x, and so it is not possible to generate synthetic data points from this model. We could make it generative by introducing a suitable prior distribution $p(x)$, at the expense of a more complex model.

The hidden variables in a probabilistic model need not, however, have any explicit physical interpretation but may be introduced simply to allow a more complex joint distribution to be constructed from simpler components. In either case, the technique of ancestral sampling applied to a generative model mimics the creation of the observed data and would therefore give rise to 'fantasy' data whose probability distribution (if the model were a perfect representation of reality) would be the same as that of the observed data. In practice, producing synthetic observations from a generative model can prove informative in understanding the form of the probability distribution represented by that model.

8.1.3 Discrete variables

Section 2.4

We have discussed the importance of probability distributions that are members of the exponential family, and we have seen that this family includes many well-known distributions as particular cases. Although such distributions are relatively simple, they form useful building blocks for constructing more complex probability

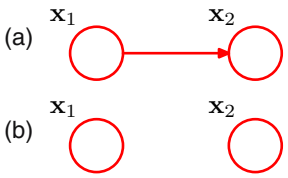

Figure 8.9 (a) This fully-connected graph describes a general distribution over two K-state discrete variables having a total of $K^2 - 1$ parameters. (b) By dropping the link between the nodes, the number of parameters is reduced to $2(K - 1)$.

distributions, and the framework of graphical models is very useful in expressing the way in which these building blocks are linked together.

Such models have particularly nice properties if we choose the relationship between each parent-child pair in a directed graph to be conjugate, and we shall explore several examples of this shortly. Two cases are particularly worthy of note, namely when the parent and child node each correspond to discrete variables and when they each correspond to Gaussian variables, because in these two cases the relationship can be extended hierarchically to construct arbitrarily complex directed acyclic graphs. We begin by examining the discrete case.

The probability distribution $p(\mathbf{x}|\boldsymbol{\mu})$ for a single discrete variable $\mathbf{x}$ having K possible states (using the 1-of-K representation) is given by

$$p(\mathbf{x}|\boldsymbol{\mu}) = \prod_{k=1}^{K} \mu_k^{x_k} \tag{8.9}$$

and is governed by the parameters $\boldsymbol{\mu} = (\mu_1, \ldots, \mu_K)^{\mathrm{T}}$. Due to the constraint $\sum_k \mu_k = 1$, only $K - 1$ values for μ_k need to be specified in order to define the distribution.

Now suppose that we have two discrete variables, $\mathbf{x}_1$ and $\mathbf{x}_2$, each of which has K states, and we wish to model their joint distribution. We denote the probability of observing both $x_{1k} = 1$ and $x_{2l} = 1$ by the parameter μ_{kl}, where x_{1k} denotes the k^{th} component of $\mathbf{x}_1$, and similarly for x_{2l}. The joint distribution can be written

$$p(\mathbf{x}_1, \mathbf{x}_2|\boldsymbol{\mu}) = \prod_{k=1}^{K} \prod_{l=1}^{K} \mu_{kl}^{x_{1k}x_{2l}}.$$

Because the parameters μ_{kl} are subject to the constraint $\sum_k \sum_l \mu_{kl} = 1$, this distribution is governed by $K^2 - 1$ parameters. It is easily seen that the total number of parameters that must be specified for an arbitrary joint distribution over M variables is $K^M - 1$ and therefore grows exponentially with the number M of variables.

Using the product rule, we can factor the joint distribution $p(\mathbf{x}_1, \mathbf{x}_2)$ in the form $p(\mathbf{x}_2|\mathbf{x}_1)p(\mathbf{x}_1)$, which corresponds to a two-node graph with a link going from the $\mathbf{x}_1$ node to the $\mathbf{x}_2$ node as shown in Figure 8.9(a). The marginal distribution $p(\mathbf{x}_1)$ is governed by $K - 1$ parameters, as before, Similarly, the conditional distribution $p(\mathbf{x}_2|\mathbf{x}_1)$ requires the specification of $K - 1$ parameters for each of the K possible values of $\mathbf{x}_1$. The total number of parameters that must be specified in the joint distribution is therefore $(K - 1) + K(K - 1) = K^2 - 1$ as before.

Now suppose that the variables $\mathbf{x}_1$ and $\mathbf{x}_2$ were independent, corresponding to the graphical model shown in Figure 8.9(b). Each variable is then described by

Figure 8.10 This chain of M discrete nodes, each having K states, requires the specification of $K-1+(M-1)K(K-1)$ parameters, which grows linearly with the length M of the chain. In contrast, a fully connected graph of M nodes would have K^M-1 parameters, which grows exponentially with M.

a separate multinomial distribution, and the total number of parameters would be $2(K-1)$. For a distribution over M independent discrete variables, each having K states, the total number of parameters would be $M(K-1)$, which therefore grows linearly with the number of variables. From a graphical perspective, we have reduced the number of parameters by dropping links in the graph, at the expense of having a restricted class of distributions.

More generally, if we have M discrete variables $\mathbf{x}_1,\ldots,\mathbf{x}_M$, we can model the joint distribution using a directed graph with one variable corresponding to each node. The conditional distribution at each node is given by a set of nonnegative parameters subject to the usual normalization constraint. If the graph is fully connected then we have a completely general distribution having K^M-1 parameters, whereas if there are no links in the graph the joint distribution factorizes into the product of the marginals, and the total number of parameters is $M(K-1)$. Graphs having intermediate levels of connectivity allow for more general distributions than the fully factorized one while requiring fewer parameters than the general joint distribution. As an illustration, consider the chain of nodes shown in Figure 8.10. The marginal distribution $p(\mathbf{x}_1)$ requires $K-1$ parameters, whereas each of the $M-1$ conditional distributions $p(\mathbf{x}_i|\mathbf{x}_{i-1})$, for $i=2,\ldots,M$, requires $K(K-1)$ parameters. This gives a total parameter count of $K-1+(M-1)K(K-1)$, which is quadratic in K and which grows linearly (rather than exponentially) with the length M of the chain.

An alternative way to reduce the number of independent parameters in a model is by *sharing* parameters (also known as *tying* of parameters). For instance, in the chain example of Figure 8.10, we can arrange that all of the conditional distributions $p(\mathbf{x}_i|\mathbf{x}_{i-1})$, for $i=2,\ldots,M$, are governed by the same set of $K(K-1)$ parameters. Together with the $K-1$ parameters governing the distribution of $\mathbf{x}_1$, this gives a total of K^2-1 parameters that must be specified in order to define the joint distribution.

We can turn a graph over discrete variables into a Bayesian model by introducing Dirichlet priors for the parameters. From a graphical point of view, each node then acquires an additional parent representing the Dirichlet distribution over the parameters associated with the corresponding discrete node. This is illustrated for the chain model in Figure 8.11. The corresponding model in which we tie the parameters governing the conditional distributions $p(\mathbf{x}_i|\mathbf{x}_{i-1})$, for $i=2,\ldots,M$, is shown in Figure 8.12.

Another way of controlling the exponential growth in the number of parameters in models of discrete variables is to use parameterized models for the conditional distributions instead of complete tables of conditional probability values. To illustrate this idea, consider the graph in Figure 8.13 in which all of the nodes represent binary variables. Each of the parent variables x_i is governed by a single parame-

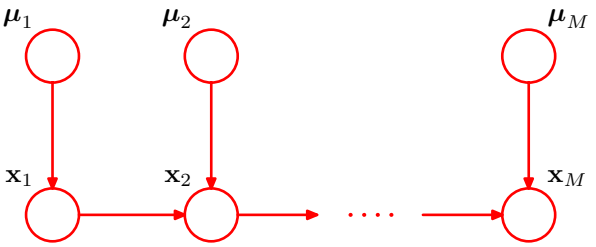

Figure 8.11 An extension of the model of Figure 8.10 to include Dirichlet priors over the parameters governing the discrete distributions.

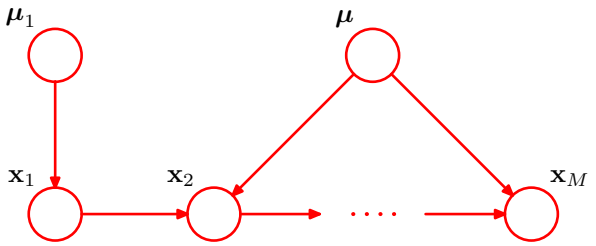

Figure 8.12 As in Figure 8.11 but with a single set of parameters $\boldsymbol{\mu}$ shared amongst all of the conditional distributions $p(\mathbf{x}_i|\mathbf{x}_{i-1})$.

ter μ_i representing the probability $p(x_i = 1)$, giving M parameters in total for the parent nodes. The conditional distribution $p(y|x_1, \ldots, x_M)$, however, would require 2^M parameters representing the probability $p(y = 1)$ for each of the 2^M possible settings of the parent variables. Thus in general the number of parameters required to specify this conditional distribution will grow exponentially with M. We can obtain a more parsimonious form for the conditional distribution by using a logistic sigmoid function acting on a linear combination of the parent variables, giving

Section 2.4

$$p(y = 1|x_1, \ldots, x_M) = \sigma\left(w_0 + \sum_{i=1}^{M} w_i x_i\right) = \sigma(\mathbf{w}^{\mathrm{T}}\mathbf{x}) \tag{8.10}$$

where $\sigma(a) = (1+\exp(-a))^{-1}$ is the logistic sigmoid, $\mathbf{x} = (x_0, x_1, \ldots, x_M)^{\mathrm{T}}$ is an $(M + 1)$-dimensional vector of parent states augmented with an additional variable x_0 whose value is clamped to 1, and $\mathbf{w} = (w_0, w_1, \ldots, w_M)^{\mathrm{T}}$ is a vector of $M + 1$ parameters. This is a more restricted form of conditional distribution than the general case but is now governed by a number of parameters that grows linearly with M. In this sense, it is analogous to the choice of a restrictive form of covariance matrix (for example, a diagonal matrix) in a multivariate Gaussian distribution. The motivation for the logistic sigmoid representation was discussed in Section 4.2.

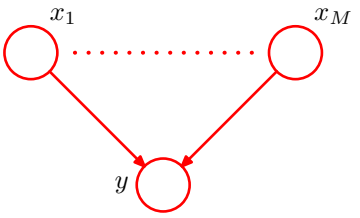

Figure 8.13 A graph comprising M parents $x_1, \ldots, x_M$ and a single child y, used to illustrate the idea of parameterized conditional distributions for discrete variables.

8.1.4 Linear-Gaussian models

In the previous section, we saw how to construct joint probability distributions over a set of discrete variables by expressing the variables as nodes in a directed acyclic graph. Here we show how a multivariate Gaussian can be expressed as a directed graph corresponding to a linear-Gaussian model over the component variables. This allows us to impose interesting structure on the distribution, with the general Gaussian and the diagonal covariance Gaussian representing opposite extremes. Several widely used techniques are examples of linear-Gaussian models, such as probabilistic principal component analysis, factor analysis, and linear dynamical systems (Roweis and Ghahramani, 1999). We shall make extensive use of the results of this section in later chapters when we consider some of these techniques in detail.

Consider an arbitrary directed acyclic graph over D variables in which node i represents a single continuous random variable x_i having a Gaussian distribution. The mean of this distribution is taken to be a linear combination of the states of its parent nodes pa_i of node i

$$p(x_i|\mathrm{pa}_i) = \mathcal{N}\left(x_i \,\middle|\, \sum_{j\in\mathrm{pa}_i} w_{ij}x_j + b_i, v_i\right) \tag{8.11}$$

where w_{ij} and b_i are parameters governing the mean, and v_i is the variance of the conditional distribution for x_i. The log of the joint distribution is then the log of the product of these conditionals over all nodes in the graph and hence takes the form

$$\ln p(\mathbf{x}) = \sum_{i=1}^{D} \ln p(x_i|\mathrm{pa}_i) \tag{8.12}$$

$$= -\sum_{i=1}^{D} \frac{1}{2v_i}\left(x_i - \sum_{j\in\mathrm{pa}_i} w_{ij}x_j - b_i\right)^2 + \text{const} \tag{8.13}$$

where $\mathbf{x} = (x_1, \ldots, x_D)^{\mathrm{T}}$ and 'const' denotes terms independent of $\mathbf{x}$. We see that this is a quadratic function of the components of $\mathbf{x}$, and hence the joint distribution $p(\mathbf{x})$ is a multivariate Gaussian.

We can determine the mean and covariance of the joint distribution recursively as follows. Each variable x_i has (conditional on the states of its parents) a Gaussian distribution of the form (8.11) and so

$$x_i = \sum_{j\in\mathrm{pa}_i} w_{ij}x_j + b_i + \sqrt{v_i}\epsilon_i \tag{8.14}$$

where ϵ_i is a zero mean, unit variance Gaussian random variable satisfying $\mathbb{E}[\epsilon_i] = 0$ and $\mathbb{E}[\epsilon_i\epsilon_j] = I_{ij}$, where I_{ij} is the i, j element of the identity matrix. Taking the expectation of (8.14), we have

$$\mathbb{E}[x_i] = \sum_{j\in\mathrm{pa}_i} w_{ij}\mathbb{E}[x_j] + b_i. \tag{8.15}$$

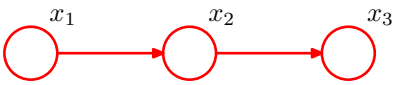

Figure 8.14 A directed graph over three Gaussian variables, with one missing link.

Thus we can find the components of $\mathbb{E}[\mathbf{x}] = (\mathbb{E}[x_1], \ldots, \mathbb{E}[x_D])^{\mathrm{T}}$ by starting at the lowest numbered node and working recursively through the graph (here we again assume that the nodes are numbered such that each node has a higher number than its parents). Similarly, we can use (8.14) and (8.15) to obtain the i, j element of the covariance matrix for $p(\mathbf{x})$ in the form of a recursion relation

$$\begin{aligned}
\mathrm{cov}[x_i, x_j] &= \mathbb{E}\left[(x_i - \mathbb{E}[x_i])(x_j - \mathbb{E}[x_j])\right] \\
&= \mathbb{E}\left[(x_i - \mathbb{E}[x_i])\left\{\sum_{k \in \mathrm{pa}_j} w_{jk}(x_k - \mathbb{E}[x_k]) + \sqrt{v_j}\epsilon_j\right\}\right] \\
&= \sum_{k \in \mathrm{pa}_j} w_{jk}\mathrm{cov}[x_i, x_k] + I_{ij}v_j \qquad (8.16)
\end{aligned}$$

and so the covariance can similarly be evaluated recursively starting from the lowest numbered node.

Let us consider two extreme cases. First of all, suppose that there are no links in the graph, which therefore comprises D isolated nodes. In this case, there are no parameters w_{ij} and so there are just D parameters b_i and D parameters v_i. From the recursion relations (8.15) and (8.16), we see that the mean of $p(\mathbf{x})$ is given by $(b_1, \ldots, b_D)^{\mathrm{T}}$ and the covariance matrix is diagonal of the form $\mathrm{diag}(v_1, \ldots, v_D)$. The joint distribution has a total of $2D$ parameters and represents a set of D independent univariate Gaussian distributions.

Now consider a fully connected graph in which each node has all lower numbered nodes as parents. The matrix w_{ij} then has $i - 1$ entries on the i^{th} row and hence is a lower triangular matrix (with no entries on the leading diagonal). Then the total number of parameters w_{ij} is obtained by taking the number D^2 of elements in a $D \times D$ matrix, subtracting D to account for the absence of elements on the leading diagonal, and then dividing by 2 because the matrix has elements only below the diagonal, giving a total of $D(D-1)/2$. The total number of independent parameters $\{w_{ij}\}$ and $\{v_i\}$ in the covariance matrix is therefore $D(D+1)/2$ corresponding to a general symmetric covariance matrix.

Section 2.3

Graphs having some intermediate level of complexity correspond to joint Gaussian distributions with partially constrained covariance matrices. Consider for example the graph shown in Figure 8.14, which has a link missing between variables x_1 and x_3. Using the recursion relations (8.15) and (8.16), we see that the mean and covariance of the joint distribution are given by

Exercise 8.7

$$\boldsymbol{\mu} = (b_1, b_2 + w_{21}b_1, b_3 + w_{32}b_2 + w_{32}w_{21}b_1)^{\mathrm{T}} \qquad (8.17)$$

$$\boldsymbol{\Sigma} = \begin{pmatrix} v_1 & w_{21}v_1 & w_{32}w_{21}v_1 \\ w_{21}v_1 & v_2 + w_{21}^2 v_1 & w_{32}(v_2 + w_{21}^2 v_1) \\ w_{32}w_{21}v_1 & w_{32}(v_2 + w_{21}^2 v_1) & v_3 + w_{32}^2(v_2 + w_{21}^2 v_1) \end{pmatrix}. \qquad (8.18)$$

We can readily extend the linear-Gaussian graphical model to the case in which the nodes of the graph represent multivariate Gaussian variables. In this case, we can write the conditional distribution for node i in the form

$$p(\mathbf{x}_i|\mathrm{pa}_i) = \mathcal{N}\left(\mathbf{x}_i \left| \sum_{j\in \mathrm{pa}_i} \mathbf{W}_{ij}\mathbf{x}_j + \mathbf{b}_i, \mathbf{\Sigma}_i\right.\right) \tag{8.19}$$

where now $\mathbf{W}_{ij}$ is a matrix (which is nonsquare if $\mathbf{x}_i$ and $\mathbf{x}_j$ have different dimensionalities). Again it is easy to verify that the joint distribution over all variables is Gaussian.

Section 2.3.6

Note that we have already encountered a specific example of the linear-Gaussian relationship when we saw that the conjugate prior for the mean $\boldsymbol{\mu}$ of a Gaussian variable $\mathbf{x}$ is itself a Gaussian distribution over $\boldsymbol{\mu}$. The joint distribution over $\mathbf{x}$ and $\boldsymbol{\mu}$ is therefore Gaussian. This corresponds to a simple two-node graph in which the node representing $\boldsymbol{\mu}$ is the parent of the node representing $\mathbf{x}$. The mean of the distribution over $\boldsymbol{\mu}$ is a parameter controlling a prior, and so it can be viewed as a hyperparameter. Because the value of this hyperparameter may itself be unknown, we can again treat it from a Bayesian perspective by introducing a prior over the hyperparameter, sometimes called a *hyperprior*, which is again given by a Gaussian distribution. This type of construction can be extended in principle to any level and is an illustration of a *hierarchical Bayesian model*, of which we shall encounter further examples in later chapters.

8.2. Conditional Independence

An important concept for probability distributions over multiple variables is that of *conditional independence* (Dawid, 1980). Consider three variables a, b, and c, and suppose that the conditional distribution of a, given b and c, is such that it does not depend on the value of b, so that

$$p(a|b,c) = p(a|c). \tag{8.20}$$

We say that a is conditionally independent of b given c. This can be expressed in a slightly different way if we consider the joint distribution of a and b conditioned on c, which we can write in the form

$$\begin{aligned} p(a,b|c) &= p(a|b,c)p(b|c) \\ &= p(a|c)p(b|c). \end{aligned} \tag{8.21}$$

where we have used the product rule of probability together with (8.20). Thus we see that, conditioned on c, the joint distribution of a and b factorizes into the product of the marginal distribution of a and the marginal distribution of b (again both conditioned on c). This says that the variables a and b are statistically independent, given c. Note that our definition of conditional independence will require that (8.20),

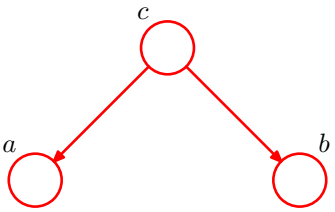

Figure 8.15 The first of three examples of graphs over three variables a, b, and c used to discuss conditional independence properties of directed graphical models.

or equivalently (8.21), must hold for every possible value of c, and not just for some values. We shall sometimes use a shorthand notation for conditional independence (Dawid, 1979) in which

$$a \perp\!\!\!\perp b \mid c \tag{8.22}$$

denotes that a is conditionally independent of b given c and is equivalent to (8.20).

Conditional independence properties play an important role in using probabilistic models for pattern recognition by simplifying both the structure of a model and the computations needed to perform inference and learning under that model. We shall see examples of this shortly.

If we are given an expression for the joint distribution over a set of variables in terms of a product of conditional distributions (i.e., the mathematical representation underlying a directed graph), then we could in principle test whether any potential conditional independence property holds by repeated application of the sum and product rules of probability. In practice, such an approach would be very time consuming. An important and elegant feature of graphical models is that conditional independence properties of the joint distribution can be read directly from the graph without having to perform any analytical manipulations. The general framework for achieving this is called *d-separation*, where the 'd' stands for 'directed' (Pearl, 1988). Here we shall motivate the concept of d-separation and give a general statement of the d-separation criterion. A formal proof can be found in Lauritzen (1996).

8.2.1 Three example graphs

We begin our discussion of the conditional independence properties of directed graphs by considering three simple examples each involving graphs having just three nodes. Together, these will motivate and illustrate the key concepts of d-separation. The first of the three examples is shown in Figure 8.15, and the joint distribution corresponding to this graph is easily written down using the general result (8.5) to give

$$p(a, b, c) = p(a|c)p(b|c)p(c). \tag{8.23}$$

If none of the variables are observed, then we can investigate whether a and b are independent by marginalizing both sides of (8.23) with respect to c to give

$$p(a, b) = \sum_c p(a|c)p(b|c)p(c). \tag{8.24}$$

In general, this does not factorize into the product $p(a)p(b)$, and so

$$a \not\perp\!\!\!\perp b \mid \emptyset \tag{8.25}$$

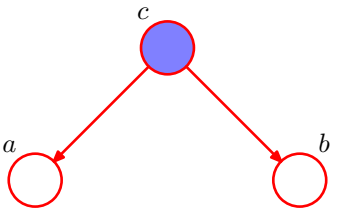

Figure 8.16 As in Figure 8.15 but where we have conditioned on the value of variable c.

where $\emptyset$ denotes the empty set, and the symbol $\not\perp\!\!\!\perp$ means that the conditional independence property does not hold in general. Of course, it may hold for a particular distribution by virtue of the specific numerical values associated with the various conditional probabilities, but it does not follow in general from the structure of the graph.

Now suppose we condition on the variable c, as represented by the graph of Figure 8.16. From (8.23), we can easily write down the conditional distribution of a and b, given c, in the form

$$\begin{aligned} p(a,b|c) &= \frac{p(a,b,c)}{p(c)} \\ &= p(a|c)p(b|c) \end{aligned}$$

and so we obtain the conditional independence property

$$a \perp\!\!\!\perp b \mid c.$$

We can provide a simple graphical interpretation of this result by considering the path from node a to node b via c. The node c is said to be *tail-to-tail* with respect to this path because the node is connected to the tails of the two arrows, and the presence of such a path connecting nodes a and b causes these nodes to be dependent. However, when we condition on node c, as in Figure 8.16, the conditioned node 'blocks' the path from a to b and causes a and b to become (conditionally) independent.

We can similarly consider the graph shown in Figure 8.17. The joint distribution corresponding to this graph is again obtained from our general formula (8.5) to give

$$p(a,b,c) = p(a)p(c|a)p(b|c). \tag{8.26}$$

First of all, suppose that none of the variables are observed. Again, we can test to see if a and b are independent by marginalizing over c to give

$$p(a,b) = p(a)\sum_c p(c|a)p(b|c) = p(a)p(b|a).$$

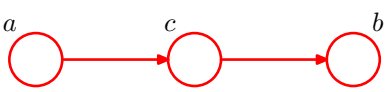

Figure 8.17 The second of our three examples of 3-node graphs used to motivate the conditional independence framework for directed graphical models.

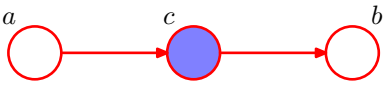

Figure 8.18 As in Figure 8.17 but now conditioning on node c.

which in general does not factorize into $p(a)p(b)$, and so

$$a \not\perp\!\!\!\perp b \mid \emptyset \tag{8.27}$$

as before.

Now suppose we condition on node c, as shown in Figure 8.18. Using Bayes' theorem, together with (8.26), we obtain

$$\begin{aligned} p(a,b|c) &= \frac{p(a,b,c)}{p(c)} \\ &= \frac{p(a)p(c|a)p(b|c)}{p(c)} \\ &= p(a|c)p(b|c) \end{aligned}$$

and so again we obtain the conditional independence property

$$a \perp\!\!\!\perp b \mid c.$$

As before, we can interpret these results graphically. The node c is said to be *head-to-tail* with respect to the path from node a to node b. Such a path connects nodes a and b and renders them dependent. If we now observe c, as in Figure 8.18, then this observation 'blocks' the path from a to b and so we obtain the conditional independence property $a \perp\!\!\!\perp b \mid c$.

Finally, we consider the third of our 3-node examples, shown by the graph in Figure 8.19. As we shall see, this has a more subtle behaviour than the two previous graphs.

The joint distribution can again be written down using our general result (8.5) to give

$$p(a,b,c) = p(a)p(b)p(c|a,b). \tag{8.28}$$

Consider first the case where none of the variables are observed. Marginalizing both sides of (8.28) over c we obtain

$$p(a,b) = p(a)p(b)$$

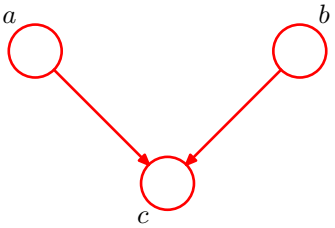

Figure 8.19 The last of our three examples of 3-node graphs used to explore conditional independence properties in graphical models. This graph has rather different properties from the two previous examples.

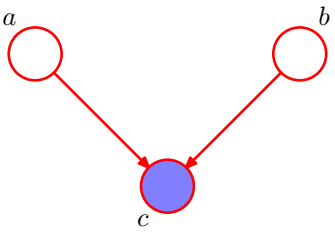

Figure 8.20 As in Figure 8.19 but conditioning on the value of node c. In this graph, the act of conditioning induces a dependence between a and b.

and so a and b are independent with no variables observed, in contrast to the two previous examples. We can write this result as

$$a \perp\!\!\!\perp b \mid \emptyset. \tag{8.29}$$

Now suppose we condition on c, as indicated in Figure 8.20. The conditional distribution of a and b is then given by

$$\begin{aligned} p(a, b|c) &= \frac{p(a, b, c)}{p(c)} \\ &= \frac{p(a)p(b)p(c|a, b)}{p(c)} \end{aligned}$$

which in general does not factorize into the product $p(a)p(b)$, and so

$$a \not\perp\!\!\!\perp b \mid c.$$

Thus our third example has the opposite behaviour from the first two. Graphically, we say that node c is *head-to-head* with respect to the path from a to b because it connects to the heads of the two arrows. When node c is unobserved, it 'blocks' the path, and the variables a and b are independent. However, conditioning on c 'unblocks' the path and renders a and b dependent.

There is one more subtlety associated with this third example that we need to consider. First we introduce some more terminology. We say that node y is a *descendant* of node x if there is a path from x to y in which each step of the path follows the directions of the arrows. Then it can be shown that a head-to-head path will become unblocked if either the node, *or any of its descendants*, is observed.

Exercise 8.10

In summary, a tail-to-tail node or a head-to-tail node leaves a path unblocked unless it is observed in which case it blocks the path. By contrast, a head-to-head node blocks a path if it is unobserved, but once the node, and/or at least one of its descendants, is observed the path becomes unblocked.

It is worth spending a moment to understand further the unusual behaviour of the graph of Figure 8.20. Consider a particular instance of such a graph corresponding to a problem with three binary random variables relating to the fuel system on a car, as shown in Figure 8.21. The variables are called B, representing the state of a battery that is either charged ($B = 1$) or flat ($B = 0$), F representing the state of the fuel tank that is either full of fuel ($F = 1$) or empty ($F = 0$), and G, which is the state of an electric fuel gauge and which indicates either full ($G = 1$) or empty

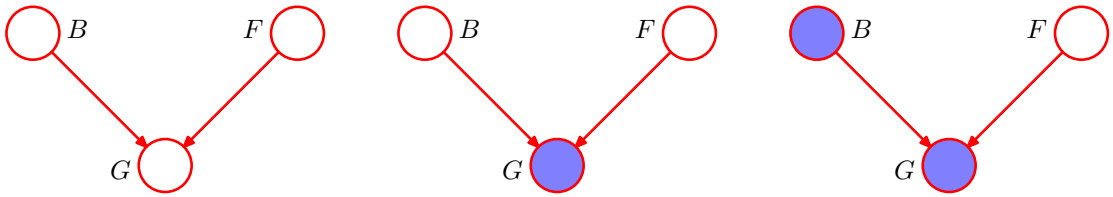

Figure 8.21 An example of a 3-node graph used to illustrate the phenomenon of 'explaining away'. The three nodes represent the state of the battery (B), the state of the fuel tank (F) and the reading on the electric fuel gauge (G). See the text for details.

($G = 0$). The battery is either charged or flat, and independently the fuel tank is either full or empty, with prior probabilities

$$\begin{aligned} p(B = 1) &= 0.9 \\ p(F = 1) &= 0.9. \end{aligned}$$

Given the state of the fuel tank and the battery, the fuel gauge reads full with probabilities given by

$$\begin{aligned} p(G = 1|B = 1, F = 1) &= 0.8 \\ p(G = 1|B = 1, F = 0) &= 0.2 \\ p(G = 1|B = 0, F = 1) &= 0.2 \\ p(G = 1|B = 0, F = 0) &= 0.1 \end{aligned}$$

so this is a rather unreliable fuel gauge! All remaining probabilities are determined by the requirement that probabilities sum to one, and so we have a complete specification of the probabilistic model.

Before we observe any data, the prior probability of the fuel tank being empty is $p(F = 0) = 0.1$. Now suppose that we observe the fuel gauge and discover that it reads empty, i.e., $G = 0$, corresponding to the middle graph in Figure 8.21. We can use Bayes' theorem to evaluate the posterior probability of the fuel tank being empty. First we evaluate the denominator for Bayes' theorem given by

$$p(G = 0) = \sum_{B \in \{0,1\}} \sum_{F \in \{0,1\}} p(G = 0|B, F)p(B)p(F) = 0.315 \tag{8.30}$$

and similarly we evaluate

$$p(G = 0|F = 0) = \sum_{B \in \{0,1\}} p(G = 0|B, F = 0)p(B) = 0.81 \tag{8.31}$$

and using these results we have

$$p(F = 0|G = 0) = \frac{p(G = 0|F = 0)p(F = 0)}{p(G = 0)} \simeq 0.257 \tag{8.32}$$

and so $p(F = 0|G = 0) > p(F = 0)$. Thus observing that the gauge reads empty makes it more likely that the tank is indeed empty, as we would intuitively expect. Next suppose that we also check the state of the battery and find that it is flat, i.e., $B = 0$. We have now observed the states of both the fuel gauge and the battery, as shown by the right-hand graph in Figure 8.21. The posterior probability that the fuel tank is empty given the observations of both the fuel gauge and the battery state is then given by

$$p(F = 0|G = 0, B = 0) = \frac{p(G = 0|B = 0, F = 0)p(F = 0)}{\sum_{F \in \{0,1\}} p(G = 0|B = 0, F)p(F)} \simeq 0.111 \quad (8.33)$$

where the prior probability $p(B = 0)$ has cancelled between numerator and denominator. Thus the probability that the tank is empty has *decreased* (from 0.257 to 0.111) as a result of the observation of the state of the battery. This accords with our intuition that finding out that the battery is flat *explains away* the observation that the fuel gauge reads empty. We see that the state of the fuel tank and that of the battery have indeed become dependent on each other as a result of observing the reading on the fuel gauge. In fact, this would also be the case if, instead of observing the fuel gauge directly, we observed the state of some descendant of G. Note that the probability $p(F = 0|G = 0, B = 0) \simeq 0.111$ is greater than the prior probability $p(F = 0) = 0.1$ because the observation that the fuel gauge reads zero still provides some evidence in favour of an empty fuel tank.

8.2.2 D-separation

We now give a general statement of the d-separation property (Pearl, 1988) for directed graphs. Consider a general directed graph in which A, B, and C are arbitrary nonintersecting sets of nodes (whose union may be smaller than the complete set of nodes in the graph). We wish to ascertain whether a particular conditional independence statement $A \perp\!\!\!\perp B \mid C$ is implied by a given directed acyclic graph. To do so, we consider all possible paths from any node in A to any node in B. Any such path is said to be *blocked* if it includes a node such that either

(a) the arrows on the path meet either head-to-tail or tail-to-tail at the node, and the node is in the set C, or

(b) the arrows meet head-to-head at the node, and neither the node, nor any of its descendants, is in the set C.

If all paths are blocked, then A is said to be d-separated from B by C, and the joint distribution over all of the variables in the graph will satisfy $A \perp\!\!\!\perp B \mid C$.

The concept of d-separation is illustrated in Figure 8.22. In graph (a), the path from a to b is not blocked by node f because it is a tail-to-tail node for this path and is not observed, nor is it blocked by node e because, although the latter is a head-to-head node, it has a descendant c because is in the conditioning set. Thus the conditional independence statement $a \perp\!\!\!\perp b \mid c$ does *not* follow from this graph. In graph (b), the path from a to b is blocked by node f because this is a tail-to-tail node that is observed, and so the conditional independence property $a \perp\!\!\!\perp b \mid f$ will

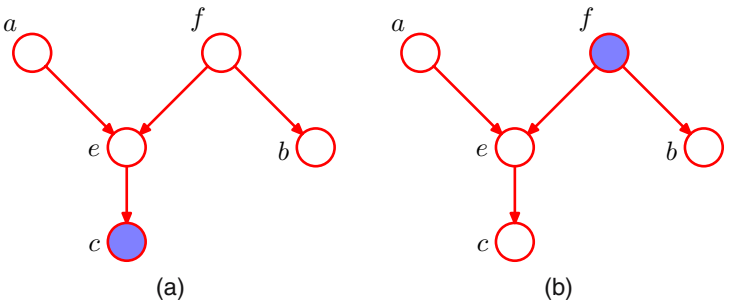

Figure 8.22 Illustration of the concept of d-separation. See the text for details.

be satisfied by any distribution that factorizes according to this graph. Note that this path is also blocked by node e because e is a head-to-head node and neither it nor its descendant are in the conditioning set.

For the purposes of d-separation, parameters such as α and σ^2 in Figure 8.5, indicated by small filled circles, behave in the same was as observed nodes. However, there are no marginal distributions associated with such nodes. Consequently parameter nodes never themselves have parents and so all paths through these nodes will always be tail-to-tail and hence blocked. Consequently they play no role in d-separation.

Another example of conditional independence and d-separation is provided by the concept of i.i.d. (independent identically distributed) data introduced in Section 1.2.4. Consider the problem of finding the posterior distribution for the mean of a univariate Gaussian distribution. This can be represented by the directed graph shown in Figure 8.23 in which the joint distribution is defined by a prior $p(\mu)$ together with a set of conditional distributions $p(x_n|\mu)$ for $n = 1, \ldots, N$. In practice, we observe $\mathcal{D} = \{x_1, \ldots, x_N\}$ and our goal is to infer μ. Suppose, for a moment, that we condition on μ and consider the joint distribution of the observations. Using d-separation, we note that there is a unique path from any x_i to any other $x_{j\neq i}$ and that this path is tail-to-tail with respect to the observed node μ. Every such path is blocked and so the observations $D = \{x_1, \ldots, x_N\}$ are independent given μ, so that

Section 2.3

$$p(\mathcal{D}|\mu) = \prod_{n=1}^{N} p(x_n|\mu). \tag{8.34}$$

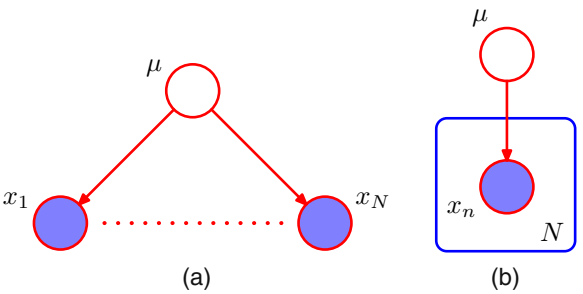

Figure 8.23 (a) Directed graph corresponding to the problem of inferring the mean μ of a univariate Gaussian distribution from observations $x_1, \ldots, x_N$. (b) The same graph drawn using the plate notation.

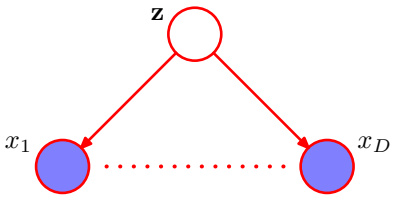

Figure 8.24 A graphical representation of the 'naive Bayes' model for classification. Conditioned on the class label $\mathbf{z}$, the components of the observed vector $\mathbf{x} = (x_1, \ldots, x_D)^{\mathrm{T}}$ are assumed to be independent.

However, if we integrate over μ, the observations are in general no longer independent

$$p(\mathcal{D}) = \int_0^\infty p(\mathcal{D}|\mu)p(\mu)\,\mathrm{d}\mu \neq \prod_{n=1}^{N} p(x_n). \tag{8.35}$$

Here μ is a latent variable, because its value is not observed.

Another example of a model representing i.i.d. data is the graph in Figure 8.7 corresponding to Bayesian polynomial regression. Here the stochastic nodes correspond to $\{t_n\}$, $\mathbf{w}$ and $\widehat{t}$. We see that the node for $\mathbf{w}$ is tail-to-tail with respect to the path from $\widehat{t}$ to any one of the nodes t_n and so we have the following conditional independence property

$$\widehat{t} \perp\!\!\!\perp t_n \mid \mathbf{w}. \tag{8.36}$$

Thus, conditioned on the polynomial coefficients $\mathbf{w}$, the predictive distribution for $\widehat{t}$ is independent of the training data $\{t_1, \ldots, t_N\}$. We can therefore first use the training data to determine the posterior distribution over the coefficients $\mathbf{w}$ and then we can discard the training data and use the posterior distribution for $\mathbf{w}$ to make predictions of $\widehat{t}$ for new input observations $\widehat{x}$.

Section 3.3

A related graphical structure arises in an approach to classification called the *naive Bayes* model, in which we use conditional independence assumptions to simplify the model structure. Suppose our observed variable consists of a D-dimensional vector $\mathbf{x} = (x_1, \ldots, x_D)^{\mathrm{T}}$, and we wish to assign observed values of $\mathbf{x}$ to one of K classes. Using the 1-of-K encoding scheme, we can represent these classes by a K-dimensional binary vector $\mathbf{z}$. We can then define a generative model by introducing a multinomial prior $p(\mathbf{z}|\boldsymbol{\mu})$ over the class labels, where the k^{th} component μ_k of $\boldsymbol{\mu}$ is the prior probability of class $\mathcal{C}_k$, together with a conditional distribution $p(\mathbf{x}|\mathbf{z})$ for the observed vector $\mathbf{x}$. The key assumption of the naive Bayes model is that, conditioned on the class $\mathbf{z}$, the distributions of the input variables $x_1, \ldots, x_D$ are independent. The graphical representation of this model is shown in Figure 8.24. We see that observation of $\mathbf{z}$ blocks the path between x_i and x_j for $j \neq i$ (because such paths are tail-to-tail at the node $\mathbf{z}$) and so x_i and x_j are conditionally independent given $\mathbf{z}$. If, however, we marginalize out $\mathbf{z}$ (so that $\mathbf{z}$ is unobserved) the tail-to-tail path from x_i to x_j is no longer blocked. This tells us that in general the marginal density $p(\mathbf{x})$ will not factorize with respect to the components of $\mathbf{x}$. We encountered a simple application of the naive Bayes model in the context of fusing data from different sources for medical diagnosis in Section 1.5.

If we are given a labelled training set, comprising inputs $\{\mathbf{x}_1, \ldots, \mathbf{x}_N\}$ together with their class labels, then we can fit the naive Bayes model to the training data

using maximum likelihood assuming that the data are drawn independently from the model. The solution is obtained by fitting the model for each class separately using the correspondingly labelled data. As an example, suppose that the probability density within each class is chosen to be Gaussian. In this case, the naive Bayes assumption then implies that the covariance matrix for each Gaussian is diagonal, and the contours of constant density within each class will be axis-aligned ellipsoids. The marginal density, however, is given by a superposition of diagonal Gaussians (with weighting coefficients given by the class priors) and so will no longer factorize with respect to its components.

The naive Bayes assumption is helpful when the dimensionality D of the input space is high, making density estimation in the full D-dimensional space more challenging. It is also useful if the input vector contains both discrete and continuous variables, since each can be represented separately using appropriate models (e.g., Bernoulli distributions for binary observations or Gaussians for real-valued variables). The conditional independence assumption of this model is clearly a strong one that may lead to rather poor representations of the class-conditional densities. Nevertheless, even if this assumption is not precisely satisfied, the model may still give good classification performance in practice because the decision boundaries can be insensitive to some of the details in the class-conditional densities, as illustrated in Figure 1.27.

We have seen that a particular directed graph represents a specific decomposition of a joint probability distribution into a product of conditional probabilities. The graph also expresses a set of conditional independence statements obtained through the d-separation criterion, and the d-separation theorem is really an expression of the equivalence of these two properties. In order to make this clear, it is helpful to think of a directed graph as a filter. Suppose we consider a particular joint probability distribution $p(\mathbf{x})$ over the variables $\mathbf{x}$ corresponding to the (nonobserved) nodes of the graph. The filter will allow this distribution to pass through if, and only if, it can be expressed in terms of the factorization (8.5) implied by the graph. If we present to the filter the set of all possible distributions $p(\mathbf{x})$ over the set of variables $\mathbf{x}$, then the subset of distributions that are passed by the filter will be denoted $\mathcal{DF}$, for *directed factorization*. This is illustrated in Figure 8.25. Alternatively, we can use the graph as a different kind of filter by first listing all of the conditional independence properties obtained by applying the d-separation criterion to the graph, and then allowing a distribution to pass only if it satisfies all of these properties. If we present all possible distributions $p(\mathbf{x})$ to this second kind of filter, then the d-separation theorem tells us that the set of distributions that will be allowed through is precisely the set $\mathcal{DF}$.

It should be emphasized that the conditional independence properties obtained from d-separation apply to any probabilistic model described by that particular directed graph. This will be true, for instance, whether the variables are discrete or continuous or a combination of these. Again, we see that a particular graph is describing a whole family of probability distributions.

At one extreme we have a fully connected graph that exhibits no conditional independence properties at all, and which can represent any possible joint probability distribution over the given variables. The set $\mathcal{DF}$ will contain all possible distribu-

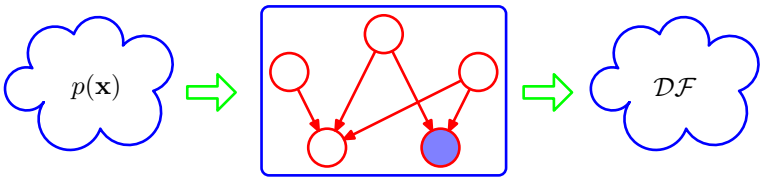

Figure 8.25 We can view a graphical model (in this case a directed graph) as a filter in which a probability distribution $p(\mathbf{x})$ is allowed through the filter if, and only if, it satisfies the directed factorization property (8.5). The set of all possible probability distributions $p(\mathbf{x})$ that pass through the filter is denoted $\mathcal{DF}$. We can alternatively use the graph to filter distributions according to whether they respect all of the conditional independencies implied by the d-separation properties of the graph. The d-separation theorem says that it is the same set of distributions $\mathcal{DF}$ that will be allowed through this second kind of filter.

tions $p(\mathbf{x})$. At the other extreme, we have the fully disconnected graph, i.e., one having no links at all. This corresponds to joint distributions which factorize into the product of the marginal distributions over the variables comprising the nodes of the graph.

Note that for any given graph, the set of distributions $\mathcal{DF}$ will include any distributions that have additional independence properties beyond those described by the graph. For instance, a fully factorized distribution will always be passed through the filter implied by any graph over the corresponding set of variables.

We end our discussion of conditional independence properties by exploring the concept of a *Markov blanket* or *Markov boundary*. Consider a joint distribution $p(\mathbf{x}_1, \ldots, \mathbf{x}_D)$ represented by a directed graph having D nodes, and consider the conditional distribution of a particular node with variables $\mathbf{x}_i$ conditioned on all of the remaining variables $\mathbf{x}_{j\neq i}$. Using the factorization property (8.5), we can express this conditional distribution in the form

$$\begin{aligned} p(\mathbf{x}_i|\mathbf{x}_{\{j\neq i\}}) &= \frac{p(\mathbf{x}_1, \ldots, \mathbf{x}_D)}{\displaystyle\int p(\mathbf{x}_1, \ldots, \mathbf{x}_D)\, \mathrm{d}\mathbf{x}_i} \\ &= \frac{\displaystyle\prod_k p(\mathbf{x}_k|\mathrm{pa}_k)}{\displaystyle\int \prod_k p(\mathbf{x}_k|\mathrm{pa}_k)\, \mathrm{d}\mathbf{x}_i} \end{aligned}$$

in which the integral is replaced by a summation in the case of discrete variables. We now observe that any factor $p(\mathbf{x}_k|\mathrm{pa}_k)$ that does not have any functional dependence on $\mathbf{x}_i$ can be taken outside the integral over $\mathbf{x}_i$, and will therefore cancel between numerator and denominator. The only factors that remain will be the conditional distribution $p(\mathbf{x}_i|\mathrm{pa}_i)$ for node $\mathbf{x}_i$ itself, together with the conditional distributions for any nodes $\mathbf{x}_k$ such that node $\mathbf{x}_i$ is in the conditioning set of $p(\mathbf{x}_k|\mathrm{pa}_k)$, in other words for which $\mathbf{x}_i$ is a parent of $\mathbf{x}_k$. The conditional $p(\mathbf{x}_i|\mathrm{pa}_i)$ will depend on the parents of node $\mathbf{x}_i$, whereas the conditionals $p(\mathbf{x}_k|\mathrm{pa}_k)$ will depend on the children

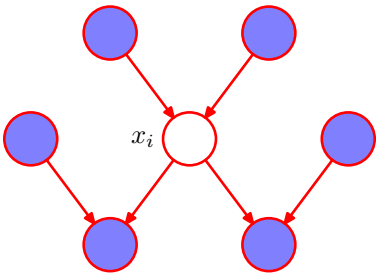

Figure 8.26 The Markov blanket of a node $\mathbf{x}_i$ comprises the set of parents, children and co-parents of the node. It has the property that the conditional distribution of $\mathbf{x}_i$, conditioned on all the remaining variables in the graph, is dependent only on the variables in the Markov blanket.

of $\mathbf{x}_i$ as well as on the *co-parents*, in other words variables corresponding to parents of node $\mathbf{x}_k$ other than node $\mathbf{x}_i$. The set of nodes comprising the parents, the children and the co-parents is called the Markov blanket and is illustrated in Figure 8.26. We can think of the Markov blanket of a node $\mathbf{x}_i$ as being the minimal set of nodes that isolates $\mathbf{x}_i$ from the rest of the graph. Note that it is not sufficient to include only the parents and children of node $\mathbf{x}_i$ because the phenomenon of explaining away means that observations of the child nodes will not block paths to the co-parents. We must therefore observe the co-parent nodes also.

8.3. Markov Random Fields

We have seen that directed graphical models specify a factorization of the joint distribution over a set of variables into a product of local conditional distributions. They also define a set of conditional independence properties that must be satisfied by any distribution that factorizes according to the graph. We turn now to the second major class of graphical models that are described by undirected graphs and that again specify both a factorization and a set of conditional independence relations.

A *Markov random field*, also known as a *Markov network* or an *undirected graphical model* (Kindermann and Snell, 1980), has a set of nodes each of which corresponds to a variable or group of variables, as well as a set of links each of which connects a pair of nodes. The links are undirected, that is they do not carry arrows. In the case of undirected graphs, it is convenient to begin with a discussion of conditional independence properties.

8.3.1 Conditional independence properties

Section 8.2

In the case of directed graphs, we saw that it was possible to test whether a particular conditional independence property holds by applying a graphical test called d-separation. This involved testing whether or not the paths connecting two sets of nodes were 'blocked'. The definition of blocked, however, was somewhat subtle due to the presence of paths having head-to-head nodes. We might ask whether it is possible to define an alternative graphical semantics for probability distributions such that conditional independence is determined by simple graph separation. This is indeed the case and corresponds to undirected graphical models. By removing the

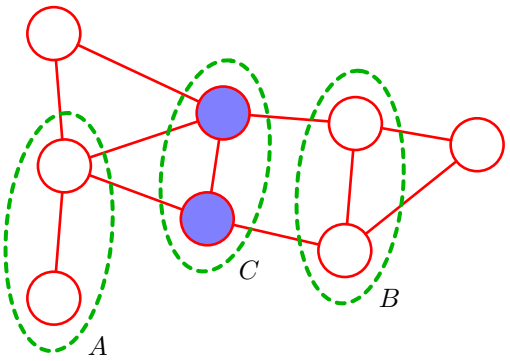

Figure 8.27 An example of an undirected graph in which every path from any node in set A to any node in set B passes through at least one node in set C. Consequently the conditional independence property $A \perp\!\!\!\perp B \mid C$ holds for any probability distribution described by this graph.

directionality from the links of the graph, the asymmetry between parent and child nodes is removed, and so the subtleties associated with head-to-head nodes no longer arise.

Suppose that in an undirected graph we identify three sets of nodes, denoted A, B, and C, and that we consider the conditional independence property

$$A \perp\!\!\!\perp B \mid C. \tag{8.37}$$

To test whether this property is satisfied by a probability distribution defined by a graph we consider all possible paths that connect nodes in set A to nodes in set B. If all such paths pass through one or more nodes in set C, then all such paths are 'blocked' and so the conditional independence property holds. However, if there is at least one such path that is not blocked, then the property does not necessarily hold, or more precisely there will exist at least some distributions corresponding to the graph that do not satisfy this conditional independence relation. This is illustrated with an example in Figure 8.27. Note that this is exactly the same as the d-separation criterion except that there is no 'explaining away' phenomenon. Testing for conditional independence in undirected graphs is therefore simpler than in directed graphs.

An alternative way to view the conditional independence test is to imagine removing all nodes in set C from the graph together with any links that connect to those nodes. We then ask if there exists a path that connects any node in A to any node in B. If there are no such paths, then the conditional independence property must hold.

The Markov blanket for an undirected graph takes a particularly simple form, because a node will be conditionally independent of all other nodes conditioned only on the neighbouring nodes, as illustrated in Figure 8.28.

8.3.2 Factorization properties

We now seek a factorization rule for undirected graphs that will correspond to the above conditional independence test. Again, this will involve expressing the joint distribution $p(\mathbf{x})$ as a product of functions defined over sets of variables that are local to the graph. We therefore need to decide what is the appropriate notion of locality in this case.

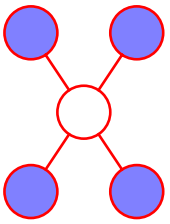

Figure 8.28 For an undirected graph, the Markov blanket of a node x_i consists of the set of neighbouring nodes. It has the property that the conditional distribution of x_i, conditioned on all the remaining variables in the graph, is dependent only on the variables in the Markov blanket.

If we consider two nodes x_i and x_j that are not connected by a link, then these variables must be conditionally independent given all other nodes in the graph. This follows from the fact that there is no direct path between the two nodes, and all other paths pass through nodes that are observed, and hence those paths are blocked. This conditional independence property can be expressed as

$$p(x_i, x_j|\mathbf{x}_{\setminus\{i,j\}}) = p(x_i|\mathbf{x}_{\setminus\{i,j\}})p(x_j|\mathbf{x}_{\setminus\{i,j\}}) \tag{8.38}$$

where $\mathbf{x}_{\setminus\{i,j\}}$ denotes the set $\mathbf{x}$ of all variables with x_i and x_j removed. The factorization of the joint distribution must therefore be such that x_i and x_j do not appear in the same factor in order for the conditional independence property to hold for all possible distributions belonging to the graph.

This leads us to consider a graphical concept called a *clique*, which is defined as a subset of the nodes in a graph such that there exists a link between all pairs of nodes in the subset. In other words, the set of nodes in a clique is fully connected. Furthermore, a *maximal clique* is a clique such that it is not possible to include any other nodes from the graph in the set without it ceasing to be a clique. These concepts are illustrated by the undirected graph over four variables shown in Figure 8.29. This graph has five cliques of two nodes given by $\{x_1, x_2\}$, $\{x_2, x_3\}$, $\{x_3, x_4\}$, $\{x_4, x_2\}$, and $\{x_1, x_3\}$, as well as two maximal cliques given by $\{x_1, x_2, x_3\}$ and $\{x_2, x_3, x_4\}$. The set $\{x_1, x_2, x_3, x_4\}$ is not a clique because of the missing link from x_1 to x_4.

We can therefore define the factors in the decomposition of the joint distribution to be functions of the variables in the cliques. In fact, we can consider functions of the maximal cliques, without loss of generality, because other cliques must be subsets of maximal cliques. Thus, if $\{x_1, x_2, x_3\}$ is a maximal clique and we define an arbitrary function over this clique, then including another factor defined over a subset of these variables would be redundant.

Let us denote a clique by C and the set of variables in that clique by $\mathbf{x}_C$. Then

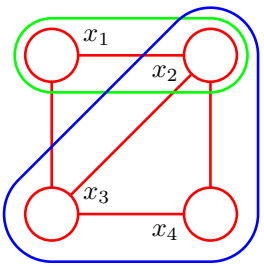

Figure 8.29 A four-node undirected graph showing a clique (outlined in green) and a maximal clique (outlined in blue).

the joint distribution is written as a product of *potential functions* $\psi_C(\mathbf{x}_C)$ over the maximal cliques of the graph

$$p(\mathbf{x}) = \frac{1}{Z} \prod_C \psi_C(\mathbf{x}_C). \tag{8.39}$$

Here the quantity Z, sometimes called the *partition function*, is a normalization constant and is given by

$$Z = \sum_{\mathbf{x}} \prod_C \psi_C(\mathbf{x}_C) \tag{8.40}$$

which ensures that the distribution $p(\mathbf{x})$ given by (8.39) is correctly normalized. By considering only potential functions which satisfy $\psi_C(\mathbf{x}_C) \geqslant 0$ we ensure that $p(\mathbf{x}) \geqslant 0$. In (8.40) we have assumed that $\mathbf{x}$ comprises discrete variables, but the framework is equally applicable to continuous variables, or a combination of the two, in which the summation is replaced by the appropriate combination of summation and integration.

Note that we do not restrict the choice of potential functions to those that have a specific probabilistic interpretation as marginal or conditional distributions. This is in contrast to directed graphs in which each factor represents the conditional distribution of the corresponding variable, conditioned on the state of its parents. However, in special cases, for instance where the undirected graph is constructed by starting with a directed graph, the potential functions may indeed have such an interpretation, as we shall see shortly.

One consequence of the generality of the potential functions $\psi_C(\mathbf{x}_C)$ is that their product will in general not be correctly normalized. We therefore have to introduce an explicit normalization factor given by (8.40). Recall that for directed graphs, the joint distribution was automatically normalized as a consequence of the normalization of each of the conditional distributions in the factorization.

The presence of this normalization constant is one of the major limitations of undirected graphs. If we have a model with M discrete nodes each having K states, then the evaluation of the normalization term involves summing over K^M states and so (in the worst case) is exponential in the size of the model. The partition function is needed for parameter learning because it will be a function of any parameters that govern the potential functions $\psi_C(\mathbf{x}_C)$. However, for evaluation of local conditional distributions, the partition function is not needed because a conditional is the ratio of two marginals, and the partition function cancels between numerator and denominator when evaluating this ratio. Similarly, for evaluating local marginal probabilities we can work with the unnormalized joint distribution and then normalize the marginals explicitly at the end. Provided the marginals only involves a small number of variables, the evaluation of their normalization coefficient will be feasible.

So far, we have discussed the notion of conditional independence based on simple graph separation and we have proposed a factorization of the joint distribution that is intended to correspond to this conditional independence structure. However, we have not made any formal connection between conditional independence and factorization for undirected graphs. To do so we need to restrict attention to potential functions $\psi_C(\mathbf{x}_C)$ that are strictly positive (i.e., never zero or negative for any

choice of $\mathbf{x}_C$). Given this restriction, we can make a precise relationship between factorization and conditional independence.

To do this we again return to the concept of a graphical model as a filter, corresponding to Figure 8.25. Consider the set of all possible distributions defined over a fixed set of variables corresponding to the nodes of a particular undirected graph. We can define $\mathcal{UI}$ to be the set of such distributions that are consistent with the set of conditional independence statements that can be read from the graph using graph separation. Similarly, we can define $\mathcal{UF}$ to be the set of such distributions that can be expressed as a factorization of the form (8.39) with respect to the maximal cliques of the graph. The *Hammersley-Clifford* theorem (Clifford, 1990) states that the sets $\mathcal{UI}$ and $\mathcal{UF}$ are identical.

Because we are restricted to potential functions which are strictly positive it is convenient to express them as exponentials, so that

$$\psi_C(\mathbf{x}_C) = \exp\{-E(\mathbf{x}_C)\} \tag{8.41}$$

where $E(\mathbf{x}_C)$ is called an *energy function*, and the exponential representation is called the *Boltzmann distribution*. The joint distribution is defined as the product of potentials, and so the total energy is obtained by adding the energies of each of the maximal cliques.

In contrast to the factors in the joint distribution for a directed graph, the potentials in an undirected graph do not have a specific probabilistic interpretation. Although this gives greater flexibility in choosing the potential functions, because there is no normalization constraint, it does raise the question of how to motivate a choice of potential function for a particular application. This can be done by viewing the potential function as expressing which configurations of the local variables are preferred to others. Global configurations that have a relatively high probability are those that find a good balance in satisfying the (possibly conflicting) influences of the clique potentials. We turn now to a specific example to illustrate the use of undirected graphs.

8.3.3 Illustration: Image de-noising

We can illustrate the application of undirected graphs using an example of noise removal from a binary image (Besag, 1974; Geman and Geman, 1984; Besag, 1986). Although a very simple example, this is typical of more sophisticated applications. Let the observed noisy image be described by an array of binary pixel values $y_i \in \{-1, +1\}$, where the index $i = 1, \ldots, D$ runs over all pixels. We shall suppose that the image is obtained by taking an unknown noise-free image, described by binary pixel values $x_i \in \{-1, +1\}$ and randomly flipping the sign of pixels with some small probability. An example binary image, together with a noise corrupted image obtained by flipping the sign of the pixels with probability 10%, is shown in Figure 8.30. Given the noisy image, our goal is to recover the original noise-free image.

Because the noise level is small, we know that there will be a strong correlation between x_i and y_i. We also know that neighbouring pixels x_i and x_j in an image are strongly correlated. This prior knowledge can be captured using the Markov

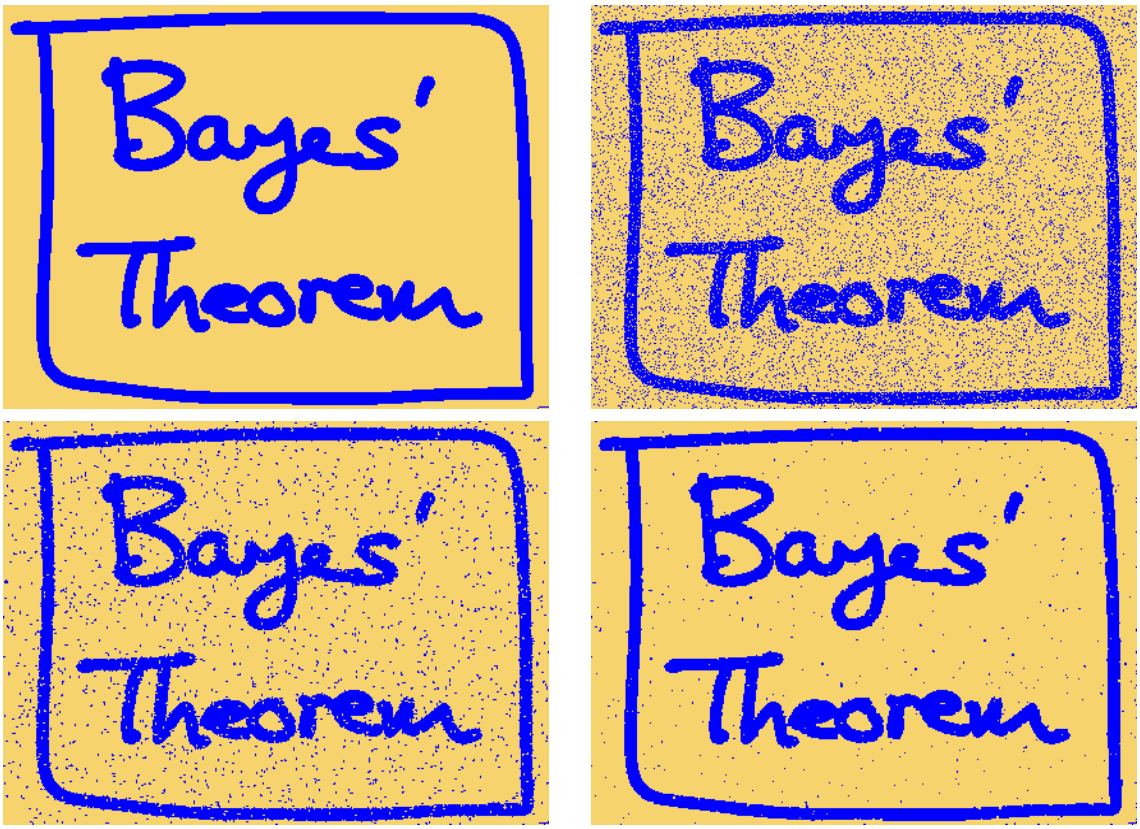

Figure 8.30 Illustration of image de-noising using a Markov random field. The top row shows the original binary image on the left and the corrupted image after randomly changing 10% of the pixels on the right. The bottom row shows the restored images obtained using iterated conditional models (ICM) on the left and using the graph-cut algorithm on the right. ICM produces an image where 96% of the pixels agree with the original image, whereas the corresponding number for graph-cut is 99%.

random field model whose undirected graph is shown in Figure 8.31. This graph has two types of cliques, each of which contains two variables. The cliques of the form $\{x_i, y_i\}$ have an associated energy function that expresses the correlation between these variables. We choose a very simple energy function for these cliques of the form $-\eta x_i y_i$ where η is a positive constant. This has the desired effect of giving a lower energy (thus encouraging a higher probability) when x_i and y_i have the same sign and a higher energy when they have the opposite sign.

The remaining cliques comprise pairs of variables $\{x_i, x_j\}$ where i and j are indices of neighbouring pixels. Again, we want the energy to be lower when the pixels have the same sign than when they have the opposite sign, and so we choose an energy given by $-\beta x_i x_j$ where β is a positive constant.

Because a potential function is an arbitrary, nonnegative function over a maximal clique, we can multiply it by any nonnegative functions of subsets of the clique, or

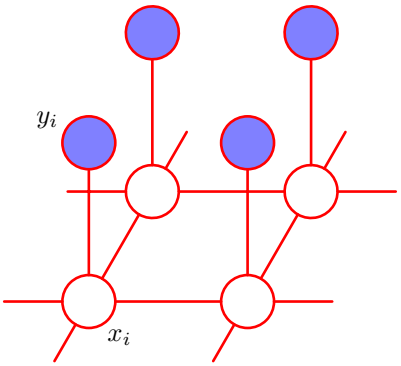

Figure 8.31 An undirected graphical model representing a Markov random field for image de-noising, in which x_i is a binary variable denoting the state of pixel i in the unknown noise-free image, and y_i denotes the corresponding value of pixel i in the observed noisy image.

equivalently we can add the corresponding energies. In this example, this allows us to add an extra term hx_i for each pixel i in the noise-free image. Such a term has the effect of biasing the model towards pixel values that have one particular sign in preference to the other.

The complete energy function for the model then takes the form

$$E(\mathbf{x}, \mathbf{y}) = h \sum_i x_i - \beta \sum_{\{i,j\}} x_i x_j - \eta \sum_i x_i y_i \tag{8.42}$$

which defines a joint distribution over $\mathbf{x}$ and $\mathbf{y}$ given by

$$p(\mathbf{x}, \mathbf{y}) = \frac{1}{Z} \exp\{-E(\mathbf{x}, \mathbf{y})\}. \tag{8.43}$$

We now fix the elements of $\mathbf{y}$ to the observed values given by the pixels of the noisy image, which implicitly defines a conditional distribution $p(\mathbf{x}|\mathbf{y})$ over noise-free images. This is an example of the *Ising model*, which has been widely studied in statistical physics. For the purposes of image restoration, we wish to find an image $\mathbf{x}$ having a high probability (ideally the maximum probability). To do this we shall use a simple iterative technique called *iterated conditional modes*, or *ICM* (Kittler and Föglein, 1984), which is simply an application of coordinate-wise gradient ascent. The idea is first to initialize the variables $\{x_i\}$, which we do by simply setting $x_i = y_i$ for all i. Then we take one node x_j at a time and we evaluate the total energy for the two possible states $x_j = +1$ and $x_j = -1$, keeping all other node variables fixed, and set x_j to whichever state has the lower energy. This will either leave the probability unchanged, if x_j is unchanged, or will increase it. Because only one variable is changed, this is a simple local computation that can be performed efficiently. We then repeat the update for another site, and so on, until some suitable stopping criterion is satisfied. The nodes may be updated in a systematic way, for instance by repeatedly raster scanning through the image, or by choosing nodes at random.

Exercise 8.13

If we have a sequence of updates in which every site is visited at least once, and in which no changes to the variables are made, then by definition the algorithm

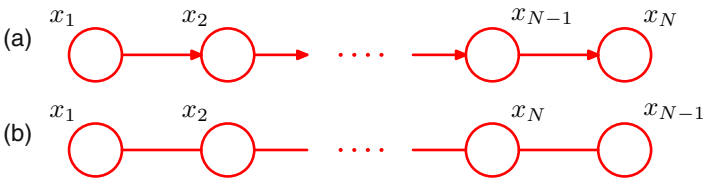

Figure 8.32 (a) Example of a directed graph. (b) The equivalent undirected graph.

will have converged to a local maximum of the probability. This need not, however, correspond to the global maximum.

For the purposes of this simple illustration, we have fixed the parameters to be $\beta = 1.0$, $\eta = 2.1$ and $h = 0$. Note that leaving $h = 0$ simply means that the prior probabilities of the two states of x_i are equal. Starting with the observed noisy image as the initial configuration, we run ICM until convergence, leading to the de-noised image shown in the lower left panel of Figure 8.30. Note that if we set $\beta = 0$, which effectively removes the links between neighbouring pixels, then the global most probable solution is given by $x_i = y_i$ for all i, corresponding to the observed noisy image.

Exercise 8.14

Section 8.4

Later we shall discuss a more effective algorithm for finding high probability solutions called the max-product algorithm, which typically leads to better solutions, although this is still not guaranteed to find the global maximum of the posterior distribution. However, for certain classes of model, including the one given by (8.42), there exist efficient algorithms based on *graph cuts* that are guaranteed to find the global maximum (Greig *et al.*, 1989; Boykov *et al.*, 2001; Kolmogorov and Zabih, 2004). The lower right panel of Figure 8.30 shows the result of applying a graph-cut algorithm to the de-noising problem.

8.3.4 Relation to directed graphs

We have introduced two graphical frameworks for representing probability distributions, corresponding to directed and undirected graphs, and it is instructive to discuss the relation between these. Consider first the problem of taking a model that is specified using a directed graph and trying to convert it to an undirected graph. In some cases this is straightforward, as in the simple example in Figure 8.32. Here the joint distribution for the directed graph is given as a product of conditionals in the form

$$p(\mathbf{x}) = p(x_1)p(x_2|x_1)p(x_3|x_2)\cdots p(x_N|x_{N-1}). \tag{8.44}$$

Now let us convert this to an undirected graph representation, as shown in Figure 8.32. In the undirected graph, the maximal cliques are simply the pairs of neighbouring nodes, and so from (8.39) we wish to write the joint distribution in the form

$$p(\mathbf{x}) = \frac{1}{Z}\psi_{1,2}(x_1, x_2)\psi_{2,3}(x_2, x_3)\cdots\psi_{N-1,N}(x_{N-1}, x_N). \tag{8.45}$$

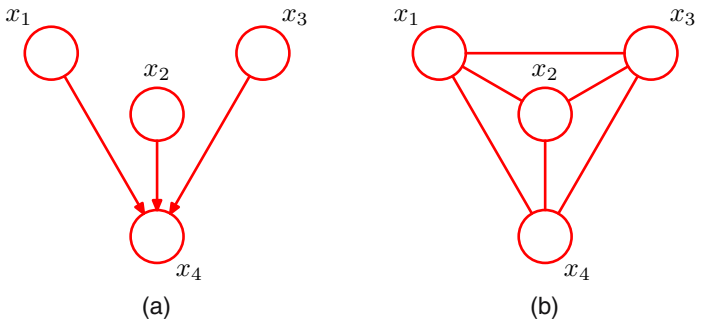

Figure 8.33 Example of a simple directed graph (a) and the corresponding moral graph (b).

This is easily done by identifying

$$\begin{aligned} \psi_{1,2}(x_1, x_2) &= p(x_1)p(x_2|x_1) \\ \psi_{2,3}(x_2, x_3) &= p(x_3|x_2) \\ &\vdots \\ \psi_{N-1,N}(x_{N-1}, x_N) &= p(x_N|x_{N-1}) \end{aligned}$$

where we have absorbed the marginal $p(x_1)$ for the first node into the first potential function. Note that in this case, the partition function $Z = 1$.

Let us consider how to generalize this construction, so that we can convert any distribution specified by a factorization over a directed graph into one specified by a factorization over an undirected graph. This can be achieved if the clique potentials of the undirected graph are given by the conditional distributions of the directed graph. In order for this to be valid, we must ensure that the set of variables that appears in each of the conditional distributions is a member of at least one clique of the undirected graph. For nodes on the directed graph having just one parent, this is achieved simply by replacing the directed link with an undirected link. However, for nodes in the directed graph having more than one parent, this is not sufficient. These are nodes that have 'head-to-head' paths encountered in our discussion of conditional independence. Consider a simple directed graph over 4 nodes shown in Figure 8.33. The joint distribution for the directed graph takes the form

$$p(\mathbf{x}) = p(x_1)p(x_2)p(x_3)p(x_4|x_1, x_2, x_3). \tag{8.46}$$

We see that the factor $p(x_4|x_1, x_2, x_3)$ involves the four variables x_1, x_2, x_3, and x_4, and so these must all belong to a single clique if this conditional distribution is to be absorbed into a clique potential. To ensure this, we add extra links between all pairs of parents of the node x_4. Anachronistically, this process of 'marrying the parents' has become known as *moralization*, and the resulting undirected graph, after dropping the arrows, is called the *moral graph*. It is important to observe that the moral graph in this example is fully connected and so exhibits no conditional independence properties, in contrast to the original directed graph.

Thus in general to convert a directed graph into an undirected graph, we first add additional undirected links between all pairs of parents for each node in the graph and

then drop the arrows on the original links to give the moral graph. Then we initialize all of the clique potentials of the moral graph to 1. We then take each conditional distribution factor in the original directed graph and multiply it into one of the clique potentials. There will always exist at least one maximal clique that contains all of the variables in the factor as a result of the moralization step. Note that in all cases the partition function is given by $Z = 1$.

The process of converting a directed graph into an undirected graph plays an important role in exact inference techniques such as the *junction tree algorithm*. Converting from an undirected to a directed representation is much less common and in general presents problems due to the normalization constraints.

Section 8.4

We saw that in going from a directed to an undirected representation we had to discard some conditional independence properties from the graph. Of course, we could always trivially convert any distribution over a directed graph into one over an undirected graph by simply using a fully connected undirected graph. This would, however, discard all conditional independence properties and so would be vacuous. The process of moralization adds the fewest extra links and so retains the maximum number of independence properties.

We have seen that the procedure for determining the conditional independence properties is different between directed and undirected graphs. It turns out that the two types of graph can express different conditional independence properties, and it is worth exploring this issue in more detail. To do so, we return to the view of a specific (directed or undirected) graph as a filter, so that the set of all possible distributions over the given variables could be reduced to a subset that respects the conditional independencies implied by the graph. A graph is said to be a *D map* (for 'dependency map') of a distribution if every conditional independence statement satisfied by the distribution is reflected in the graph. Thus a completely disconnected graph (no links) will be a trivial D map for any distribution.

Section 8.2

Alternatively, we can consider a specific distribution and ask which graphs have the appropriate conditional independence properties. If every conditional independence statement implied by a graph is satisfied by a specific distribution, then the graph is said to be an *I map* (for 'independence map') of that distribution. Clearly a fully connected graph will be a trivial I map for any distribution.

If it is the case that every conditional independence property of the distribution is reflected in the graph, and vice versa, then the graph is said to be a *perfect map* for

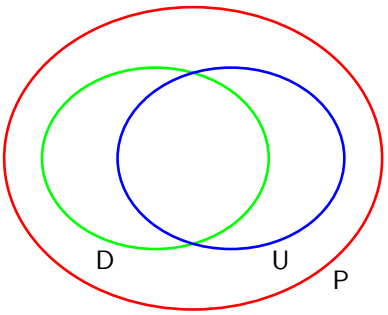

Figure 8.34 Venn diagram illustrating the set of all distributions P over a given set of variables, together with the set of distributions D that can be represented as a perfect map using a directed graph, and the set U that can be represented as a perfect map using an undirected graph.

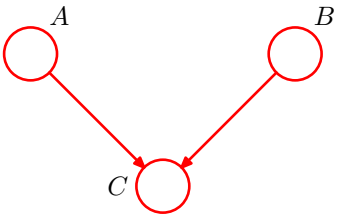

Figure 8.35 A directed graph whose conditional independence properties cannot be expressed using an undirected graph over the same three variables.

that distribution. A perfect map is therefore both an I map and a D map.

Consider the set of distributions such that for each distribution there exists a directed graph that is a perfect map. This set is distinct from the set of distributions such that for each distribution there exists an undirected graph that is a perfect map. In addition there are distributions for which neither directed nor undirected graphs offer a perfect map. This is illustrated as a Venn diagram in Figure 8.34.

Figure 8.35 shows an example of a directed graph that is a perfect map for a distribution satisfying the conditional independence properties $A \perp\!\!\!\perp B \mid \emptyset$ and $A \not\perp\!\!\!\perp B \mid C$. There is no corresponding undirected graph over the same three variables that is a perfect map.

Conversely, consider the undirected graph over four variables shown in Figure 8.36. This graph exhibits the properties $A \not\perp\!\!\!\perp B \mid \emptyset$, $C \perp\!\!\!\perp D \mid A \cup B$ and $A \perp\!\!\!\perp B \mid C \cup D$. There is no directed graph over four variables that implies the same set of conditional independence properties.

The graphical framework can be extended in a consistent way to graphs that include both directed and undirected links. These are called *chain graphs* (Lauritzen and Wermuth, 1989; Frydenberg, 1990), and contain the directed and undirected graphs considered so far as special cases. Although such graphs can represent a broader class of distributions than either directed or undirected alone, there remain distributions for which even a chain graph cannot provide a perfect map. Chain graphs are not discussed further in this book.

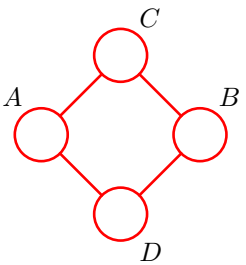

Figure 8.36 An undirected graph whose conditional independence properties cannot be expressed in terms of a directed graph over the same variables.

8.4. Inference in Graphical Models

We turn now to the problem of inference in graphical models, in which some of the nodes in a graph are clamped to observed values, and we wish to compute the posterior distributions of one or more subsets of other nodes. As we shall see, we can exploit the graphical structure both to find efficient algorithms for inference, and

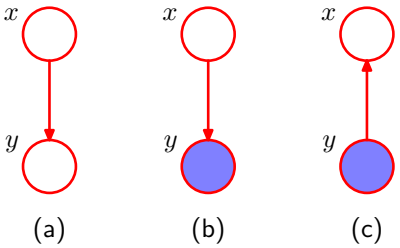

Figure 8.37 A graphical representation of Bayes' theorem. See the text for details.

to make the structure of those algorithms transparent. Specifically, we shall see that many algorithms can be expressed in terms of the propagation of local *messages* around the graph. In this section, we shall focus primarily on techniques for exact inference, and in Chapter 10 we shall consider a number of approximate inference algorithms.

To start with, let us consider the graphical interpretation of Bayes' theorem. Suppose we decompose the joint distribution $p(x, y)$ over two variables x and y into a product of factors in the form $p(x, y) = p(x)p(y|x)$. This can be represented by the directed graph shown in Figure 8.37(a). Now suppose we observe the value of y, as indicated by the shaded node in Figure 8.37(b). We can view the marginal distribution $p(x)$ as a prior over the latent variable x, and our goal is to infer the corresponding posterior distribution over x. Using the sum and product rules of probability we can evaluate

$$p(y) = \sum_{x'} p(y|x')p(x') \tag{8.47}$$

which can then be used in Bayes' theorem to calculate

$$p(x|y) = \frac{p(y|x)p(x)}{p(y)}. \tag{8.48}$$

Thus the joint distribution is now expressed in terms of $p(y)$ and $p(x|y)$. From a graphical perspective, the joint distribution $p(x, y)$ is now represented by the graph shown in Figure 8.37(c), in which the direction of the arrow is reversed. This is the simplest example of an inference problem for a graphical model.

8.4.1 Inference on a chain

Now consider a more complex problem involving the chain of nodes of the form shown in Figure 8.32. This example will lay the foundation for a discussion of exact inference in more general graphs later in this section.

Specifically, we shall consider the undirected graph in Figure 8.32(b). We have already seen that the directed chain can be transformed into an equivalent undirected chain. Because the directed graph does not have any nodes with more than one parent, this does not require the addition of any extra links, and the directed and undirected versions of this graph express exactly the same set of conditional independence statements.

The joint distribution for this graph takes the form

$$p(\mathbf{x}) = \frac{1}{Z}\psi_{1,2}(x_1, x_2)\psi_{2,3}(x_2, x_3)\cdots\psi_{N-1,N}(x_{N-1}, x_N). \tag{8.49}$$

We shall consider the specific case in which the N nodes represent discrete variables each having K states, in which case each potential function $\psi_{n-1,n}(x_{n-1}, x_n)$ comprises an $K \times K$ table, and so the joint distribution has $(N-1)K^2$ parameters.

Let us consider the inference problem of finding the marginal distribution $p(x_n)$ for a specific node x_n that is part way along the chain. Note that, for the moment, there are no observed nodes. By definition, the required marginal is obtained by summing the joint distribution over all variables except x_n, so that

$$p(x_n) = \sum_{x_1}\cdots\sum_{x_{n-1}}\sum_{x_{n+1}}\cdots\sum_{x_N} p(\mathbf{x}). \tag{8.50}$$

In a naive implementation, we would first evaluate the joint distribution and then perform the summations explicitly. The joint distribution can be represented as a set of numbers, one for each possible value for $\mathbf{x}$. Because there are N variables each with K states, there are K^N values for $\mathbf{x}$ and so evaluation and storage of the joint distribution, as well as marginalization to obtain $p(x_n)$, all involve storage and computation that scale exponentially with the length N of the chain.

We can, however, obtain a much more efficient algorithm by exploiting the conditional independence properties of the graphical model. If we substitute the factorized expression (8.49) for the joint distribution into (8.50), then we can rearrange the order of the summations and the multiplications to allow the required marginal to be evaluated much more efficiently. Consider for instance the summation over x_N. The potential $\psi_{N-1,N}(x_{N-1}, x_N)$ is the only one that depends on x_N, and so we can perform the summation

$$\sum_{x_N}\psi_{N-1,N}(x_{N-1}, x_N) \tag{8.51}$$

first to give a function of x_{N-1}. We can then use this to perform the summation over x_{N-1}, which will involve only this new function together with the potential $\psi_{N-2,N-1}(x_{N-2}, x_{N-1})$, because this is the only other place that x_{N-1} appears. Similarly, the summation over x_1 involves only the potential $\psi_{1,2}(x_1, x_2)$ and so can be performed separately to give a function of x_2, and so on. Because each summation effectively removes a variable from the distribution, this can be viewed as the removal of a node from the graph.

If we group the potentials and summations together in this way, we can express

the desired marginal in the form

$$p(x_n) = \frac{1}{Z} \underbrace{\left[\sum_{x_{n-1}} \psi_{n-1,n}(x_{n-1}, x_n) \cdots \left[\sum_{x_2} \psi_{2,3}(x_2, x_3) \left[\sum_{x_1} \psi_{1,2}(x_1, x_2)\right]\right] \cdots\right]}_{\mu_\alpha(x_n)} \underbrace{\left[\sum_{x_{n+1}} \psi_{n,n+1}(x_n, x_{n+1}) \cdots \left[\sum_{x_N} \psi_{N-1,N}(x_{N-1}, x_N)\right] \cdots\right]}_{\mu_\beta(x_n)}. \tag{8.52}$$

The reader is encouraged to study this re-ordering carefully as the underlying idea forms the basis for the later discussion of the general sum-product algorithm. Here the key concept that we are exploiting is that multiplication is distributive over addition, so that

$$ab + ac = a(b + c) \tag{8.53}$$

in which the left-hand side involves three arithmetic operations whereas the right-hand side reduces this to two operations.

Let us work out the computational cost of evaluating the required marginal using this re-ordered expression. We have to perform $N - 1$ summations each of which is over K states and each of which involves a function of two variables. For instance, the summation over x_1 involves only the function $\psi_{1,2}(x_1, x_2)$, which is a table of $K \times K$ numbers. We have to sum this table over x_1 for each value of x_2 and so this has $O(K^2)$ cost. The resulting vector of K numbers is multiplied by the matrix of numbers $\psi_{2,3}(x_2, x_3)$ and so is again $O(K^2)$. Because there are $N - 1$ summations and multiplications of this kind, the total cost of evaluating the marginal $p(x_n)$ is $O(NK^2)$. This is linear in the length of the chain, in contrast to the exponential cost of a naive approach. We have therefore been able to exploit the many conditional independence properties of this simple graph in order to obtain an efficient calculation. If the graph had been fully connected, there would have been no conditional independence properties, and we would have been forced to work directly with the full joint distribution.

We now give a powerful interpretation of this calculation in terms of the passing of local *messages* around on the graph. From (8.52) we see that the expression for the marginal $p(x_n)$ decomposes into the product of two factors times the normalization constant

$$p(x_n) = \frac{1}{Z}\mu_\alpha(x_n)\mu_\beta(x_n). \tag{8.54}$$

We shall interpret $\mu_\alpha(x_n)$ as a message passed forwards along the chain from node x_{n-1} to node x_n. Similarly, $\mu_\beta(x_n)$ can be viewed as a message passed backwards

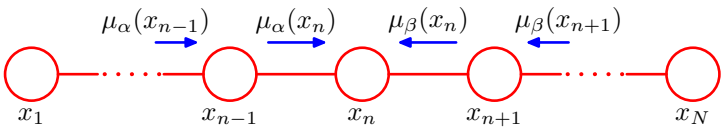

Figure 8.38 The marginal distribution $p(x_n)$ for a node x_n along the chain is obtained by multiplying the two messages $\mu_\alpha(x_n)$ and $\mu_\beta(x_n)$, and then normalizing. These messages can themselves be evaluated recursively by passing messages from both ends of the chain towards node x_n.

along the chain to node x_n from node x_{n+1}. Note that each of the messages comprises a set of K values, one for each choice of x_n, and so the product of two messages should be interpreted as the point-wise multiplication of the elements of the two messages to give another set of K values.

The message $\mu_\alpha(x_n)$ can be evaluated recursively because

$$\begin{aligned}\mu_\alpha(x_n) &= \sum_{x_{n-1}} \psi_{n-1,n}(x_{n-1}, x_n) \left[\sum_{x_{n-2}} \cdots \right] \\ &= \sum_{x_{n-1}} \psi_{n-1,n}(x_{n-1}, x_n)\mu_\alpha(x_{n-1}). \end{aligned} \tag{8.55}$$

We therefore first evaluate

$$\mu_\alpha(x_2) = \sum_{x_1} \psi_{1,2}(x_1, x_2) \tag{8.56}$$

and then apply (8.55) repeatedly until we reach the desired node. Note carefully the structure of the message passing equation. The outgoing message $\mu_\alpha(x_n)$ in (8.55) is obtained by multiplying the incoming message $\mu_\alpha(x_{n-1})$ by the local potential involving the node variable and the outgoing variable and then summing over the node variable.

Similarly, the message $\mu_\beta(x_n)$ can be evaluated recursively by starting with node x_N and using

$$\begin{aligned}\mu_\beta(x_n) &= \sum_{x_{n+1}} \psi_{n+1,n}(x_{n+1}, x_n) \left[\sum_{x_{n+2}} \cdots \right] \\ &= \sum_{x_{n+1}} \psi_{n+1,n}(x_{n+1}, x_n)\mu_\beta(x_{n+1}). \end{aligned} \tag{8.57}$$

This recursive message passing is illustrated in Figure 8.38. The normalization constant Z is easily evaluated by summing the right-hand side of (8.54) over all states of x_n, an operation that requires only $O(K)$ computation.

Graphs of the form shown in Figure 8.38 are called *Markov chains*, and the corresponding message passing equations represent an example of the *Chapman-Kolmogorov* equations for Markov processes (Papoulis, 1984).

Now suppose we wish to evaluate the marginals $p(x_n)$ for every node $n \in \{1, \ldots, N\}$ in the chain. Simply applying the above procedure separately for each node will have computational cost that is $O(N^2M^2)$. However, such an approach would be very wasteful of computation. For instance, to find $p(x_1)$ we need to propagate a message $\mu_\beta(\cdot)$ from node x_N back to node x_2. Similarly, to evaluate $p(x_2)$ we need to propagate a messages $\mu_\beta(\cdot)$ from node x_N back to node x_3. This will involve much duplicated computation because most of the messages will be identical in the two cases.

Suppose instead we first launch a message $\mu_\beta(x_{N-1})$ starting from node x_N and propagate corresponding messages all the way back to node x_1, and suppose we similarly launch a message $\mu_\alpha(x_2)$ starting from node x_1 and propagate the corresponding messages all the way forward to node x_N. Provided we store all of the intermediate messages along the way, then any node can evaluate its marginal simply by applying (8.54). The computational cost is only twice that for finding the marginal of a single node, rather than N times as much. Observe that a message has passed once in each direction across each link in the graph. Note also that the normalization constant Z need be evaluated only once, using any convenient node.

If some of the nodes in the graph are observed, then the corresponding variables are simply clamped to their observed values and there is no summation. To see this, note that the effect of clamping a variable x_n to an observed value $\widehat{x}_n$ can be expressed by multiplying the joint distribution by (one or more copies of) an additional function $I(x_n, \widehat{x}_n)$, which takes the value 1 when $x_n = \widehat{x}_n$ and the value 0 otherwise. One such function can then be absorbed into each of the potentials that contain x_n. Summations over x_n then contain only one term in which $x_n = \widehat{x}_n$.

Now suppose we wish to calculate the joint distribution $p(x_{n-1}, x_n)$ for two neighbouring nodes on the chain. This is similar to the evaluation of the marginal for a single node, except that there are now two variables that are not summed out. *Exercise 8.15* A few moments thought will show that the required joint distribution can be written in the form

$$p(x_{n-1}, x_n) = \frac{1}{Z}\mu_\alpha(x_{n-1})\psi_{n-1,n}(x_{n-1}, x_n)\mu_\beta(x_n). \tag{8.58}$$

Thus we can obtain the joint distributions over all of the sets of variables in each of the potentials directly once we have completed the message passing required to obtain the marginals.

This is a useful result because in practice we may wish to use parametric forms for the clique potentials, or equivalently for the conditional distributions if we started from a directed graph. In order to learn the parameters of these potentials in situations where not all of the variables are observed, we can employ the *EM algorithm*, *Chapter 9* and it turns out that the local joint distributions of the cliques, conditioned on any observed data, is precisely what is needed in the E step. We shall consider some examples of this in detail in Chapter 13.

8.4.2 Trees

We have seen that exact inference on a graph comprising a chain of nodes can be performed efficiently in time that is linear in the number of nodes, using an algorithm

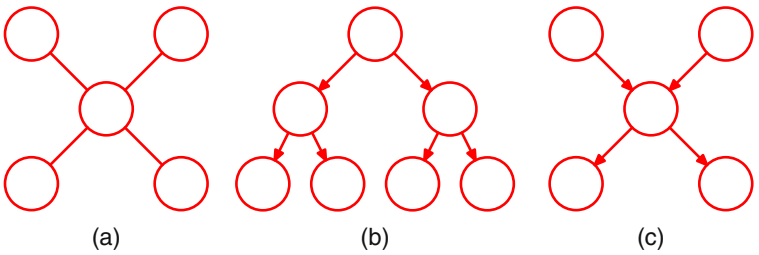

Figure 8.39 Examples of tree-structured graphs, showing (a) an undirected tree, (b) a directed tree, and (c) a directed polytree.

that can be interpreted in terms of messages passed along the chain. More generally, inference can be performed efficiently using local message passing on a broader class of graphs called *trees*. In particular, we shall shortly generalize the message passing formalism derived above for chains to give the *sum-product* algorithm, which provides an efficient framework for exact inference in tree-structured graphs.

In the case of an undirected graph, a tree is defined as a graph in which there is one, and only one, path between any pair of nodes. Such graphs therefore do not have loops. In the case of directed graphs, a tree is defined such that there is a single node, called the *root*, which has no parents, and all other nodes have one parent. If we convert a directed tree into an undirected graph, we see that the moralization step will not add any links as all nodes have at most one parent, and as a consequence the corresponding moralized graph will be an undirected tree. Examples of undirected and directed trees are shown in Figure 8.39(a) and 8.39(b). Note that a distribution represented as a directed tree can easily be converted into one represented by an undirected tree, and vice versa.

Exercise 8.18

If there are nodes in a directed graph that have more than one parent, but there is still only one path (ignoring the direction of the arrows) between any two nodes, then the graph is a called a *polytree*, as illustrated in Figure 8.39(c). Such a graph will have more than one node with the property of having no parents, and furthermore, the corresponding moralized undirected graph will have loops.

8.4.3 Factor graphs

The sum-product algorithm that we derive in the next section is applicable to undirected and directed trees and to polytrees. It can be cast in a particularly simple and general form if we first introduce a new graphical construction called a *factor graph* (Frey, 1998; Kschischnang *et al.*, 2001).

Both directed and undirected graphs allow a global function of several variables to be expressed as a product of factors over subsets of those variables. Factor graphs make this decomposition explicit by introducing additional nodes for the factors themselves in addition to the nodes representing the variables. They also allow us to be more explicit about the details of the factorization, as we shall see.

Let us write the joint distribution over a set of variables in the form of a product of factors

$$p(\mathbf{x}) = \prod_s f_s(\mathbf{x}_s) \tag{8.59}$$

where $\mathbf{x}_s$ denotes a subset of the variables. For convenience, we shall denote the

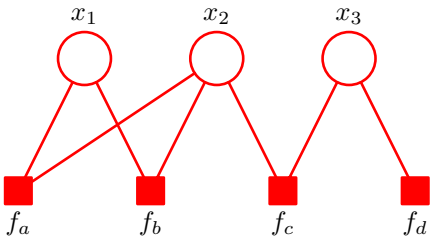

Figure 8.40 Example of a factor graph, which corresponds to the factorization (8.60).

individual variables by x_i, however, as in earlier discussions, these can comprise groups of variables (such as vectors or matrices). Each factor f_s is a function of a corresponding set of variables $\mathbf{x}_s$.

Directed graphs, whose factorization is defined by (8.5), represent special cases of (8.59) in which the factors $f_s(\mathbf{x}_s)$ are local conditional distributions. Similarly, undirected graphs, given by (8.39), are a special case in which the factors are potential functions over the maximal cliques (the normalizing coefficient $1/Z$ can be viewed as a factor defined over the empty set of variables).

In a factor graph, there is a node (depicted as usual by a circle) for every variable in the distribution, as was the case for directed and undirected graphs. There are also additional nodes (depicted by small squares) for each factor $f_s(\mathbf{x}_s)$ in the joint distribution. Finally, there are undirected links connecting each factor node to all of the variables nodes on which that factor depends. Consider, for example, a distribution that is expressed in terms of the factorization

$$p(\mathbf{x}) = f_a(x_1, x_2) f_b(x_1, x_2) f_c(x_2, x_3) f_d(x_3). \tag{8.60}$$

This can be expressed by the factor graph shown in Figure 8.40. Note that there are two factors $f_a(x_1, x_2)$ and $f_b(x_1, x_2)$ that are defined over the same set of variables. In an undirected graph, the product of two such factors would simply be lumped together into the same clique potential. Similarly, $f_c(x_2, x_3)$ and $f_d(x_3)$ could be combined into a single potential over x_2 and x_3. The factor graph, however, keeps such factors explicit and so is able to convey more detailed information about the underlying factorization.

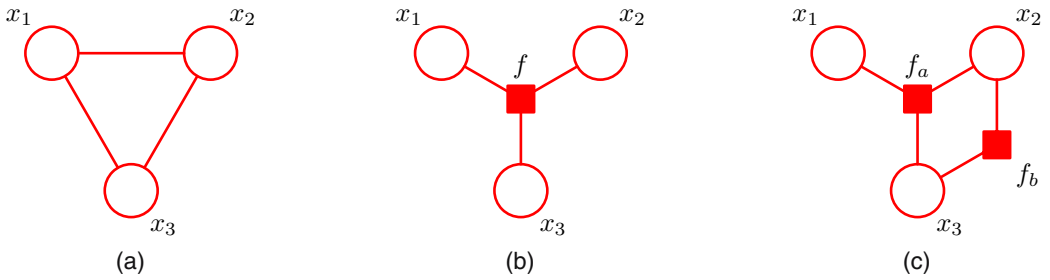

Figure 8.41 (a) An undirected graph with a single clique potential $\psi(x_1, x_2, x_3)$. (b) A factor graph with factor $f(x_1, x_2, x_3) = \psi(x_1, x_2, x_3)$ representing the same distribution as the undirected graph. (c) A different factor graph representing the same distribution, whose factors satisfy $f_a(x_1, x_2, x_3) f_b(x_1, x_2) = \psi(x_1, x_2, x_3)$.

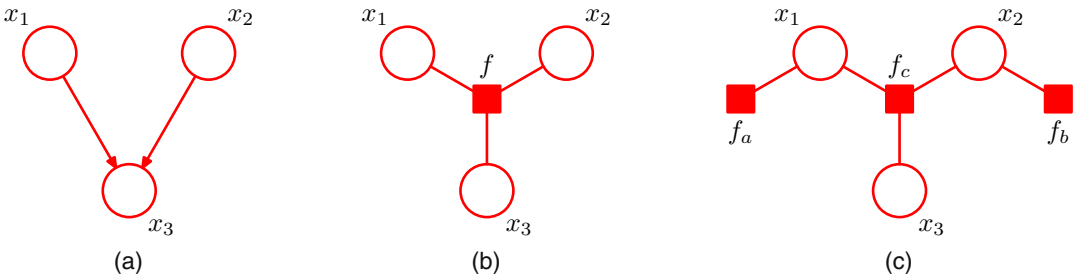

Figure 8.42 (a) A directed graph with the factorization $p(x_1)p(x_2)p(x_3|x_1, x_2)$. (b) A factor graph representing the same distribution as the directed graph, whose factor satisfies $f(x_1, x_2, x_3) = p(x_1)p(x_2)p(x_3|x_1, x_2)$. (c) A different factor graph representing the same distribution with factors $f_a(x_1) = p(x_1)$, $f_b(x_2) = p(x_2)$ and $f_c(x_1, x_2, x_3) = p(x_3|x_1, x_2)$.

Factor graphs are said to be *bipartite* because they consist of two distinct kinds of nodes, and all links go between nodes of opposite type. In general, factor graphs can therefore always be drawn as two rows of nodes (variable nodes at the top and factor nodes at the bottom) with links between the rows, as shown in the example in Figure 8.40. In some situations, however, other ways of laying out the graph may be more intuitive, for example when the factor graph is derived from a directed or undirected graph, as we shall see.

If we are given a distribution that is expressed in terms of an undirected graph, then we can readily convert it to a factor graph. To do this, we create variable nodes corresponding to the nodes in the original undirected graph, and then create additional factor nodes corresponding to the maximal cliques $\mathbf{x}_s$. The factors $f_s(\mathbf{x}_s)$ are then set equal to the clique potentials. Note that there may be several different factor graphs that correspond to the same undirected graph. These concepts are illustrated in Figure 8.41.

Similarly, to convert a directed graph to a factor graph, we simply create variable nodes in the factor graph corresponding to the nodes of the directed graph, and then create factor nodes corresponding to the conditional distributions, and then finally add the appropriate links. Again, there can be multiple factor graphs all of which correspond to the same directed graph. The conversion of a directed graph to a factor graph is illustrated in Figure 8.42.

We have already noted the importance of tree-structured graphs for performing efficient inference. If we take a directed or undirected tree and convert it into a factor graph, then the result will again be a tree (in other words, the factor graph will have no loops, and there will be one and only one path connecting any two nodes). In the case of a directed polytree, conversion to an undirected graph results in loops due to the moralization step, whereas conversion to a factor graph again results in a tree, as illustrated in Figure 8.43. In fact, local cycles in a directed graph due to links connecting parents of a node can be removed on conversion to a factor graph by defining the appropriate factor function, as shown in Figure 8.44.

We have seen that multiple different factor graphs can represent the same directed or undirected graph. This allows factor graphs to be more specific about the

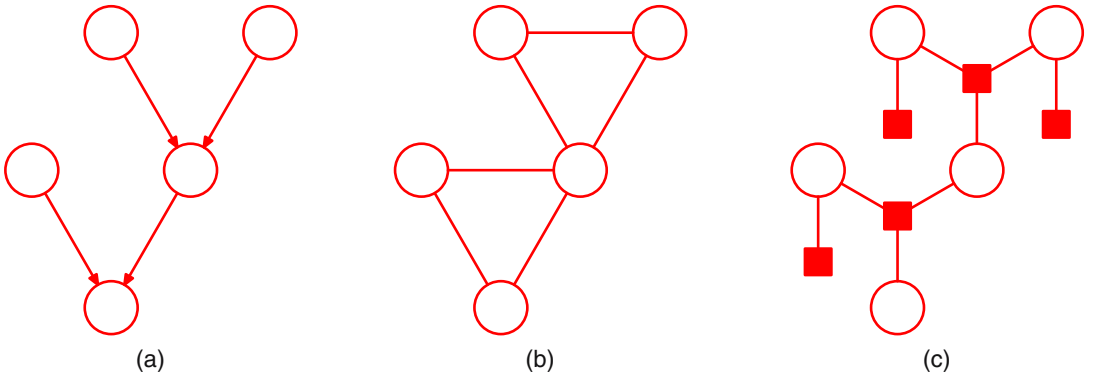

Figure 8.43 (a) A directed polytree. (b) The result of converting the polytree into an undirected graph showing the creation of loops. (c) The result of converting the polytree into a factor graph, which retains the tree structure.

precise form of the factorization. Figure 8.45 shows an example of a fully connected undirected graph along with two different factor graphs. In (b), the joint distribution is given by a general form $p(\mathbf{x}) = f(x_1, x_2, x_3)$, whereas in (c), it is given by the more specific factorization $p(\mathbf{x}) = f_a(x_1, x_2)f_b(x_1, x_3)f_c(x_2, x_3)$. It should be emphasized that the factorization in (c) does not correspond to any conditional independence properties.

8.4.4 The sum-product algorithm

We shall now make use of the factor graph framework to derive a powerful class of efficient, exact inference algorithms that are applicable to tree-structured graphs. Here we shall focus on the problem of evaluating local marginals over nodes or subsets of nodes, which will lead us to the *sum-product* algorithm. Later we shall modify the technique to allow the most probable state to be found, giving rise to the *max-sum* algorithm.

Also we shall suppose that all of the variables in the model are discrete, and so marginalization corresponds to performing sums. The framework, however, is equally applicable to linear-Gaussian models in which case marginalization involves integration, and we shall consider an example of this in detail when we discuss linear dynamical systems.

Section 13.3

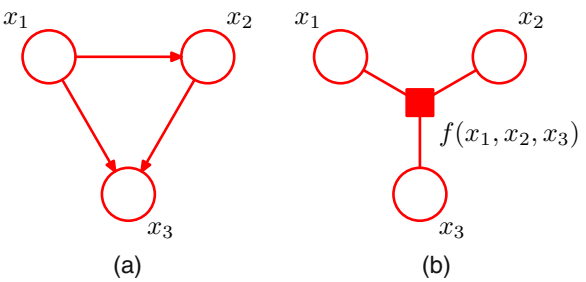

Figure 8.44 (a) A fragment of a directed graph having a local cycle. (b) Conversion to a fragment of a factor graph having a tree structure, in which $f(x_1, x_2, x_3) = p(x_1)p(x_2|x_1)p(x_3|x_1, x_2)$.

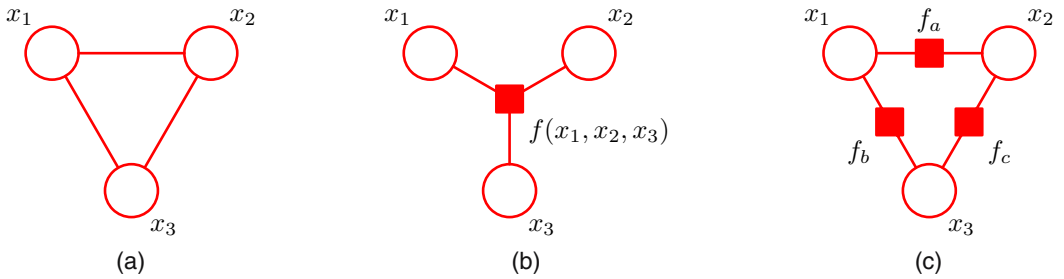

Figure 8.45 (a) A fully connected undirected graph. (b) and (c) Two factor graphs each of which corresponds to the undirected graph in (a).

There is an algorithm for exact inference on directed graphs without loops known as *belief propagation* (Pearl, 1988; Lauritzen and Spiegelhalter, 1988), and is equivalent to a special case of the sum-product algorithm. Here we shall consider only the sum-product algorithm because it is simpler to derive and to apply, as well as being more general.

We shall assume that the original graph is an undirected tree or a directed tree or polytree, so that the corresponding factor graph has a tree structure. We first convert the original graph into a factor graph so that we can deal with both directed and undirected models using the same framework. Our goal is to exploit the structure of the graph to achieve two things: (i) to obtain an efficient, exact inference algorithm for finding marginals; (ii) in situations where several marginals are required to allow computations to be shared efficiently.

We begin by considering the problem of finding the marginal $p(x)$ for particular variable node x. For the moment, we shall suppose that all of the variables are hidden. Later we shall see how to modify the algorithm to incorporate evidence corresponding to observed variables. By definition, the marginal is obtained by summing the joint distribution over all variables except x so that

$$p(x) = \sum_{\mathbf{x} \setminus x} p(\mathbf{x}) \tag{8.61}$$

where $\mathbf{x} \setminus x$ denotes the set of variables in $\mathbf{x}$ with variable x omitted. The idea is to substitute for $p(\mathbf{x})$ using the factor graph expression (8.59) and then interchange summations and products in order to obtain an efficient algorithm. Consider the fragment of graph shown in Figure 8.46 in which we see that the tree structure of the graph allows us to partition the factors in the joint distribution into groups, with one group associated with each of the factor nodes that is a neighbour of the variable node x. We see that the joint distribution can be written as a product of the form

$$p(\mathbf{x}) = \prod_{s \in \mathrm{ne}(x)} F_s(x, X_s) \tag{8.62}$$

$\mathrm{ne}(x)$ denotes the set of factor nodes that are neighbours of x, and X_s denotes the set of all variables in the subtree connected to the variable node x via the factor node

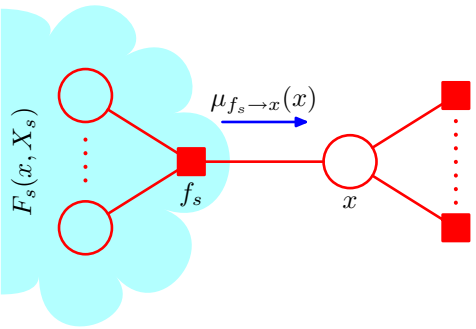

Figure 8.46 A fragment of a factor graph illustrating the evaluation of the marginal $p(x)$.

f_s, and $F_s(x, X_s)$ represents the product of all the factors in the group associated with factor f_s.

Substituting (8.62) into (8.61) and interchanging the sums and products, we obtain

$$\begin{aligned} p(x) &= \prod_{s \in \mathrm{ne}(x)} \left[\sum_{X_s} F_s(x, X_s) \right] \\ &= \prod_{s \in \mathrm{ne}(x)} \mu_{f_s \to x}(x). \end{aligned} \tag{8.63}$$

Here we have introduced a set of functions $\mu_{f_s \to x}(x)$, defined by

$$\mu_{f_s \to x}(x) \equiv \sum_{X_s} F_s(x, X_s) \tag{8.64}$$

which can be viewed as *messages* from the factor nodes f_s to the variable node x. We see that the required marginal $p(x)$ is given by the product of all the incoming messages arriving at node x.

In order to evaluate these messages, we again turn to Figure 8.46 and note that each factor $F_s(x, X_s)$ is described by a factor (sub-)graph and so can itself be factorized. In particular, we can write

$$F_s(x, X_s) = f_s(x, x_1, \ldots, x_M) G_1(x_1, X_{s1}) \ldots G_M(x_M, X_{sM}) \tag{8.65}$$

where, for convenience, we have denoted the variables associated with factor f_x, in addition to x, by $x_1, \ldots, x_M$. This factorization is illustrated in Figure 8.47. Note that the set of variables $\{x, x_1, \ldots, x_M\}$ is the set of variables on which the factor f_s depends, and so it can also be denoted $\mathbf{x}_s$, using the notation of (8.59).

Substituting (8.65) into (8.64) we obtain

$$\begin{aligned} \mu_{f_s \to x}(x) &= \sum_{x_1} \ldots \sum_{x_M} f_s(x, x_1, \ldots, x_M) \prod_{m \in \mathrm{ne}(f_s) \setminus x} \left[\sum_{X_{xm}} G_m(x_m, X_{sm}) \right] \\ &= \sum_{x_1} \ldots \sum_{x_M} f_s(x, x_1, \ldots, x_M) \prod_{m \in \mathrm{ne}(f_s) \setminus x} \mu_{x_m \to f_s}(x_m) \end{aligned} \tag{8.66}$$

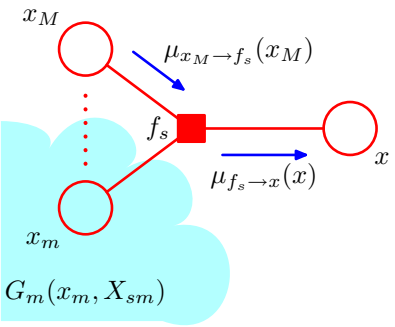

Figure 8.47 Illustration of the factorization of the subgraph associated with factor node f_s.

where $\mathrm{ne}(f_s)$ denotes the set of variable nodes that are neighbours of the factor node f_s, and $\mathrm{ne}(f_s) \setminus x$ denotes the same set but with node x removed. Here we have defined the following messages from variable nodes to factor nodes

$$\mu_{x_m \to f_s}(x_m) \equiv \sum_{X_{sm}} G_m(x_m, X_{sm}). \tag{8.67}$$

We have therefore introduced two distinct kinds of message, those that go from factor nodes to variable nodes denoted $\mu_{f \to x}(x)$, and those that go from variable nodes to factor nodes denoted $\mu_{x \to f}(x)$. In each case, we see that messages passed along a link are always a function of the variable associated with the variable node that link connects to.

The result (8.66) says that to evaluate the message sent by a factor node to a variable node along the link connecting them, take the product of the incoming messages along all other links coming into the factor node, multiply by the factor associated with that node, and then marginalize over all of the variables associated with the incoming messages. This is illustrated in Figure 8.47. It is important to note that a factor node can send a message to a variable node once it has received incoming messages from all other neighbouring variable nodes.

Finally, we derive an expression for evaluating the messages from variable nodes to factor nodes, again by making use of the (sub-)graph factorization. From Figure 8.48, we see that term $G_m(x_m, X_{sm})$ associated with node x_m is given by a product of terms $F_l(x_m, X_{ml})$ each associated with one of the factor nodes f_l that is linked to node x_m (excluding node f_s), so that

$$G_m(x_m, X_{sm}) = \prod_{l \in \mathrm{ne}(x_m) \setminus f_s} F_l(x_m, X_{ml}) \tag{8.68}$$

where the product is taken over all neighbours of node x_m except for node f_s. Note that each of the factors $F_l(x_m, X_{ml})$ represents a subtree of the original graph of precisely the same kind as introduced in (8.62). Substituting (8.68) into (8.67), we

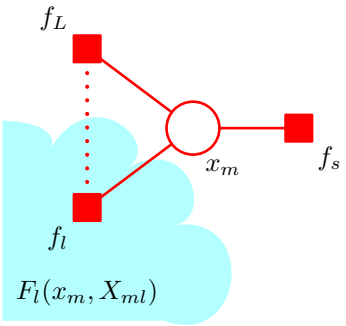

Figure 8.48 Illustration of the evaluation of the message sent by a variable node to an adjacent factor node.

then obtain

$$\begin{aligned}\mu_{x_m \to f_s}(x_m) &= \prod_{l \in \mathrm{ne}(x_m) \setminus f_s} \left[\sum_{X_{ml}} F_l(x_m, X_{ml}) \right] \\ &= \prod_{l \in \mathrm{ne}(x_m) \setminus f_s} \mu_{f_l \to x_m}(x_m) \end{aligned} \tag{8.69}$$

where we have used the definition (8.64) of the messages passed from factor nodes to variable nodes. Thus to evaluate the message sent by a variable node to an adjacent factor node along the connecting link, we simply take the product of the incoming messages along all of the other links. Note that any variable node that has only two neighbours performs no computation but simply passes messages through unchanged. Also, we note that a variable node can send a message to a factor node once it has received incoming messages from all other neighbouring factor nodes.

Recall that our goal is to calculate the marginal for variable node x, and that this marginal is given by the product of incoming messages along all of the links arriving at that node. Each of these messages can be computed recursively in terms of other messages. In order to start this recursion, we can view the node x as the root of the tree and begin at the leaf nodes. From the definition (8.69), we see that if a leaf node is a variable node, then the message that it sends along its one and only link is given by

$$\mu_{x \to f}(x) = 1 \tag{8.70}$$

as illustrated in Figure 8.49(a). Similarly, if the leaf node is a factor node, we see from (8.66) that the message sent should take the form

$$\mu_{f \to x}(x) = f(x) \tag{8.71}$$

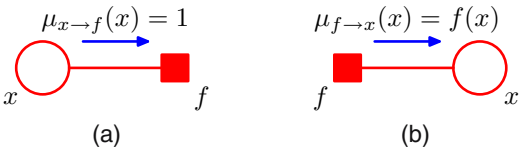

Figure 8.49 The sum-product algorithm begins with messages sent by the leaf nodes, which depend on whether the leaf node is (a) a variable node, or (b) a factor node.

as illustrated in Figure 8.49(b).

At this point, it is worth pausing to summarize the particular version of the sum-product algorithm obtained so far for evaluating the marginal $p(x)$. We start by viewing the variable node x as the root of the factor graph and initiating messages at the leaves of the graph using (8.70) and (8.71). The message passing steps (8.66) and (8.69) are then applied recursively until messages have been propagated along every link, and the root node has received messages from all of its neighbours. Each node can send a message towards the root once it has received messages from all of its other neighbours. Once the root node has received messages from all of its neighbours, the required marginal can be evaluated using (8.63). We shall illustrate this process shortly.

To see that each node will always receive enough messages to be able to send out a message, we can use a simple inductive argument as follows. Clearly, for a graph comprising a variable root node connected directly to several factor leaf nodes, the algorithm trivially involves sending messages of the form (8.71) directly from the leaves to the root. Now imagine building up a general graph by adding nodes one at a time, and suppose that for some particular graph we have a valid algorithm. When one more (variable or factor) node is added, it can be connected only by a single link because the overall graph must remain a tree, and so the new node will be a leaf node. It therefore sends a message to the node to which it is linked, which in turn will therefore receive all the messages it requires in order to send its own message towards the root, and so again we have a valid algorithm, thereby completing the proof.

Now suppose we wish to find the marginals for every variable node in the graph. This could be done by simply running the above algorithm afresh for each such node. However, this would be very wasteful as many of the required computations would be repeated. We can obtain a much more efficient procedure by 'overlaying' these multiple message passing algorithms to obtain the general sum-product algorithm as follows. Arbitrarily pick any (variable or factor) node and designate it as the root. Propagate messages from the leaves to the root as before. At this point, the root node will have received messages from all of its neighbours. It can therefore send out messages to all of its neighbours. These in turn will then have received messages from all of their neighbours and so can send out messages along the links going away from the root, and so on. In this way, messages are passed outwards from the root all the way to the leaves. By now, a message will have passed in both directions across every link in the graph, and every node will have received a message from all of its neighbours. Again a simple inductive argument can be used to verify the validity of this message passing protocol. Because every variable node will have received messages from all of its neighbours, we can readily calculate the marginal distribution for every variable in the graph. The number of messages that have to be computed is given by twice the number of links in the graph and so involves only twice the computation involved in finding a single marginal. By comparison, if we had run the sum-product algorithm separately for each node, the amount of computation would grow quadratically with the size of the graph. Note that this algorithm is in fact independent of which node was designated as the root,

Exercise 8.20

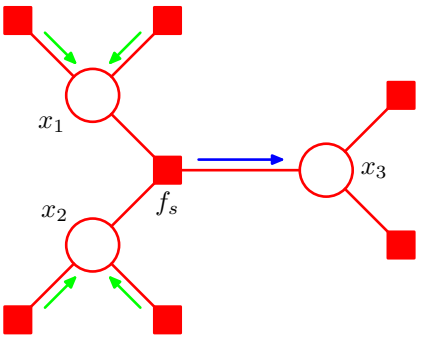

Figure 8.50 The sum-product algorithm can be viewed purely in terms of messages sent out by factor nodes to other factor nodes. In this example, the outgoing message shown by the blue arrow is obtained by taking the product of all the incoming messages shown by green arrows, multiplying by the factor f_s, and marginalizing over the variables x_1 and x_2.

and indeed the notion of one node having a special status was introduced only as a convenient way to explain the message passing protocol.

Next suppose we wish to find the marginal distributions $p(\mathbf{x}_s)$ associated with the sets of variables belonging to each of the factors. By a similar argument to that used above, it is easy to see that the marginal associated with a factor is given by the product of messages arriving at the factor node and the local factor at that node

Exercise 8.21

$$p(\mathbf{x}_s) = f_s(\mathbf{x}_s) \prod_{i \in \mathrm{ne}(f_s)} \mu_{x_i \to f_s}(x_i) \tag{8.72}$$

in complete analogy with the marginals at the variable nodes. If the factors are parameterized functions and we wish to learn the values of the parameters using the EM algorithm, then these marginals are precisely the quantities we will need to calculate in the E step, as we shall see in detail when we discuss the hidden Markov model in Chapter 13.

The message sent by a variable node to a factor node, as we have seen, is simply the product of the incoming messages on other links. We can if we wish view the sum-product algorithm in a slightly different form by eliminating messages from variable nodes to factor nodes and simply considering messages that are sent out by factor nodes. This is most easily seen by considering the example in Figure 8.50.

So far, we have rather neglected the issue of normalization. If the factor graph was derived from a directed graph, then the joint distribution is already correctly normalized, and so the marginals obtained by the sum-product algorithm will similarly be normalized correctly. However, if we started from an undirected graph, then in general there will be an unknown normalization coefficient $1/Z$. As with the simple chain example of Figure 8.38, this is easily handled by working with an unnormalized version $\widetilde{p}(\mathbf{x})$ of the joint distribution, where $p(\mathbf{x}) = \widetilde{p}(\mathbf{x})/Z$. We first run the sum-product algorithm to find the corresponding unnormalized marginals $\widetilde{p}(x_i)$. The coefficient $1/Z$ is then easily obtained by normalizing any one of these marginals, and this is computationally efficient because the normalization is done over a single variable rather than over the entire set of variables as would be required to normalize $\widetilde{p}(\mathbf{x})$ directly.

At this point, it may be helpful to consider a simple example to illustrate the operation of the sum-product algorithm. Figure 8.51 shows a simple 4-node factor

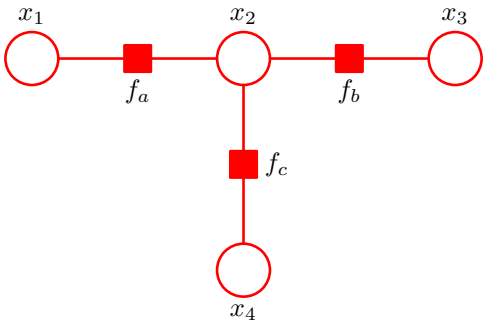

Figure 8.51 A simple factor graph used to illustrate the sum-product algorithm.

graph whose unnormalized joint distribution is given by

$$\widetilde{p}(\mathbf{x}) = f_a(x_1, x_2) f_b(x_2, x_3) f_c(x_2, x_4). \tag{8.73}$$

In order to apply the sum-product algorithm to this graph, let us designate node x_3 as the root, in which case there are two leaf nodes x_1 and x_4. Starting with the leaf nodes, we then have the following sequence of six messages

$$\mu_{x_1 \to f_a}(x_1) = 1 \tag{8.74}$$

$$\mu_{f_a \to x_2}(x_2) = \sum_{x_1} f_a(x_1, x_2) \tag{8.75}$$

$$\mu_{x_4 \to f_c}(x_4) = 1 \tag{8.76}$$

$$\mu_{f_c \to x_2}(x_2) = \sum_{x_4} f_c(x_2, x_4) \tag{8.77}$$

$$\mu_{x_2 \to f_b}(x_2) = \mu_{f_a \to x_2}(x_2) \mu_{f_c \to x_2}(x_2) \tag{8.78}$$

$$\mu_{f_b \to x_3}(x_3) = \sum_{x_2} f_b(x_2, x_3) \mu_{x_2 \to f_b}. \tag{8.79}$$

The direction of flow of these messages is illustrated in Figure 8.52. Once this message propagation is complete, we can then propagate messages from the root node out to the leaf nodes, and these are given by

$$\mu_{x_3 \to f_b}(x_3) = 1 \tag{8.80}$$

$$\mu_{f_b \to x_2}(x_2) = \sum_{x_3} f_b(x_2, x_3) \tag{8.81}$$

$$\mu_{x_2 \to f_a}(x_2) = \mu_{f_b \to x_2}(x_2) \mu_{f_c \to x_2}(x_2) \tag{8.82}$$

$$\mu_{f_a \to x_1}(x_1) = \sum_{x_2} f_a(x_1, x_2) \mu_{x_2 \to f_a}(x_2) \tag{8.83}$$

$$\mu_{x_2 \to f_c}(x_2) = \mu_{f_a \to x_2}(x_2) \mu_{f_b \to x_2}(x_2) \tag{8.84}$$

$$\mu_{f_c \to x_4}(x_4) = \sum_{x_2} f_c(x_2, x_4) \mu_{x_2 \to f_c}(x_2). \tag{8.85}$$

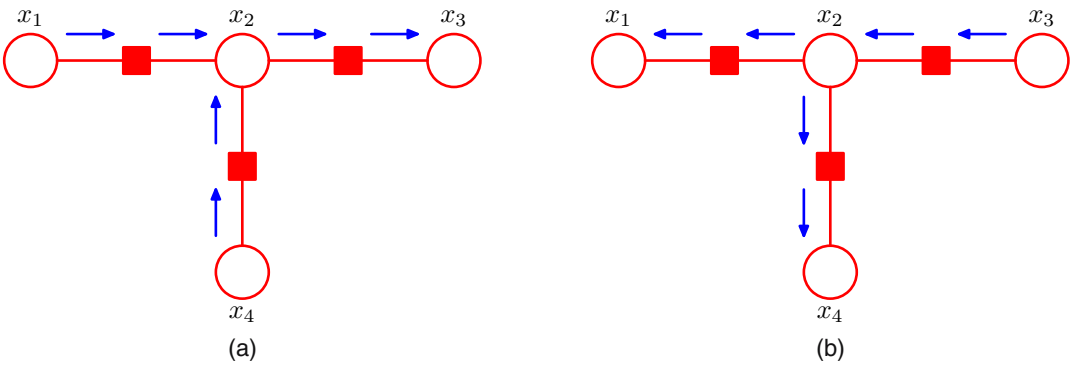

Figure 8.52 Flow of messages for the sum-product algorithm applied to the example graph in Figure 8.51. (a) From the leaf nodes x_1 and x_4 towards the root node x_3. (b) From the root node towards the leaf nodes.

One message has now passed in each direction across each link, and we can now evaluate the marginals. As a simple check, let us verify that the marginal $p(x_2)$ is given by the correct expression. Using (8.63) and substituting for the messages using the above results, we have

$$\begin{aligned}
\widetilde{p}(x_2) &= \mu_{f_a \to x_2}(x_2)\mu_{f_b \to x_2}(x_2)\mu_{f_c \to x_2}(x_2) \\
&= \left[\sum_{x_1} f_a(x_1, x_2)\right]\left[\sum_{x_3} f_b(x_2, x_3)\right]\left[\sum_{x_4} f_c(x_2, x_4)\right] \\
&= \sum_{x_1}\sum_{x_2}\sum_{x_4} f_a(x_1, x_2) f_b(x_2, x_3) f_c(x_2, x_4) \\
&= \sum_{x_1}\sum_{x_3}\sum_{x_4} \widetilde{p}(\mathbf{x}) \qquad (8.86)
\end{aligned}$$

as required.

So far, we have assumed that all of the variables in the graph are hidden. In most practical applications, a subset of the variables will be observed, and we wish to calculate posterior distributions conditioned on these observations. Observed nodes are easily handled within the sum-product algorithm as follows. Suppose we partition $\mathbf{x}$ into hidden variables $\mathbf{h}$ and observed variables $\mathbf{v}$, and that the observed value of $\mathbf{v}$ is denoted $\widehat{\mathbf{v}}$. Then we simply multiply the joint distribution $p(\mathbf{x})$ by $\prod_i I(v_i, \widehat{v}_i)$, where $I(v, \widehat{v}) = 1$ if $v = \widehat{v}$ and $I(v, \widehat{v}) = 0$ otherwise. This product corresponds to $p(\mathbf{h}, \mathbf{v} = \widehat{\mathbf{v}})$ and hence is an unnormalized version of $p(\mathbf{h}|\mathbf{v} = \widehat{\mathbf{v}})$. By running the sum-product algorithm, we can efficiently calculate the posterior marginals $p(h_i|\mathbf{v} = \widehat{\mathbf{v}})$ up to a normalization coefficient whose value can be found efficiently using a local computation. Any summations over variables in $\mathbf{v}$ then collapse into a single term.

We have assumed throughout this section that we are dealing with discrete variables. However, there is nothing specific to discrete variables either in the graphical framework or in the probabilistic construction of the sum-product algorithm. For

Table 8.1 Example of a joint distribution over two binary variables for which the maximum of the joint distribution occurs for different variable values compared to the maxima of the two marginals.

	$x = 0$	$x = 1$
$y = 0$	0.3	0.4
$y = 1$	0.3	0.0

continuous variables the summations are simply replaced by integrations. We shall give an example of the sum-product algorithm applied to a graph of linear-Gaussian variables when we consider linear dynamical systems.

Section 13.3

8.4.5 The max-sum algorithm

The sum-product algorithm allows us to take a joint distribution $p(\mathbf{x})$ expressed as a factor graph and efficiently find marginals over the component variables. Two other common tasks are to find a setting of the variables that has the largest probability and to find the value of that probability. These can be addressed through a closely related algorithm called *max-sum*, which can be viewed as an application of *dynamic programming* in the context of graphical models (Cormen *et al.*, 2001).

A simple approach to finding latent variable values having high probability would be to run the sum-product algorithm to obtain the marginals $p(x_i)$ for every variable, and then, for each marginal in turn, to find the value $x_i^\star$ that maximizes that marginal. However, this would give the set of values that are *individually* the most probable. In practice, we typically wish to find the set of values that *jointly* have the largest probability, in other words the vector $\mathbf{x}^{\max}$ that maximizes the joint distribution, so that

$$\mathbf{x}^{\max} = \arg\max_{\mathbf{x}} p(\mathbf{x}) \tag{8.87}$$

for which the corresponding value of the joint probability will be given by

$$p(\mathbf{x}^{\max}) = \max_{\mathbf{x}} p(\mathbf{x}). \tag{8.88}$$

In general, $\mathbf{x}^{\max}$ is not the same as the set of $x_i^\star$ values, as we can easily show using a simple example. Consider the joint distribution $p(x, y)$ over two binary variables $x, y \in \{0, 1\}$ given in Table 8.1. The joint distribution is maximized by setting $x = 1$ and $y = 0$, corresponding the value 0.4. However, the marginal for $p(x)$, obtained by summing over both values of y, is given by $p(x = 0) = 0.6$ and $p(x = 1) = 0.4$, and similarly the marginal for y is given by $p(y = 0) = 0.7$ and $p(y = 1) = 0.3$, and so the marginals are maximized by $x = 0$ and $y = 0$, which corresponds to a value of 0.3 for the joint distribution. In fact, it is not difficult to construct examples for which the set of individually most probable values has probability zero under the joint distribution.

Exercise 8.27

We therefore seek an efficient algorithm for finding the value of $\mathbf{x}$ that maximizes the joint distribution $p(\mathbf{x})$ and that will allow us to obtain the value of the joint distribution at its maximum. To address the second of these problems, we shall simply write out the max operator in terms of its components

$$\max_{\mathbf{x}} p(\mathbf{x}) = \max_{x_1} \ldots \max_{x_M} p(\mathbf{x}) \tag{8.89}$$

where M is the total number of variables, and then substitute for $p(\mathbf{x})$ using its expansion in terms of a product of factors. In deriving the sum-product algorithm, we made use of the distributive law (8.53) for multiplication. Here we make use of the analogous law for the max operator

$$\max(ab, ac) = a \max(b, c) \tag{8.90}$$

which holds if $a \geqslant 0$ (as will always be the case for the factors in a graphical model). This allows us to exchange products with maximizations.

Consider first the simple example of a chain of nodes described by (8.49). The evaluation of the probability maximum can be written as

$$\begin{aligned} \max_{\mathbf{x}} p(\mathbf{x}) &= \frac{1}{Z} \max_{x_1} \cdots \max_{x_N} [\psi_{1,2}(x_1, x_2) \cdots \psi_{N-1,N}(x_{N-1}, x_N)] \\ &= \frac{1}{Z} \max_{x_1} \left[\psi_{1,2}(x_1, x_2) \left[\cdots \max_{x_N} \psi_{N-1,N}(x_{N-1}, x_N) \right] \right]. \end{aligned}$$

As with the calculation of marginals, we see that exchanging the max and product operators results in a much more efficient computation, and one that is easily interpreted in terms of messages passed from node x_N backwards along the chain to node x_1.

We can readily generalize this result to arbitrary tree-structured factor graphs by substituting the expression (8.59) for the factor graph expansion into (8.89) and again exchanging maximizations with products. The structure of this calculation is identical to that of the sum-product algorithm, and so we can simply translate those results into the present context. In particular, suppose that we designate a particular variable node as the 'root' of the graph. Then we start a set of messages propagating inwards from the leaves of the tree towards the root, with each node sending its message towards the root once it has received all incoming messages from its other neighbours. The final maximization is performed over the product of all messages arriving at the root node, and gives the maximum value for $p(\mathbf{x})$. This could be called the *max-product* algorithm and is identical to the sum-product algorithm except that summations are replaced by maximizations. Note that at this stage, messages have been sent from leaves to the root, but not in the other direction.

In practice, products of many small probabilities can lead to numerical underflow problems, and so it is convenient to work with the logarithm of the joint distribution. The logarithm is a monotonic function, so that if $a > b$ then $\ln a > \ln b$, and hence the max operator and the logarithm function can be interchanged, so that

$$\ln \left(\max_{\mathbf{x}} p(\mathbf{x}) \right) = \max_{\mathbf{x}} \ln p(\mathbf{x}). \tag{8.91}$$

The distributive property is preserved because

$$\max(a + b, a + c) = a + \max(b, c). \tag{8.92}$$

Thus taking the logarithm simply has the effect of replacing the products in the max-product algorithm with sums, and so we obtain the *max-sum* algorithm. From

the results (8.66) and (8.69) derived earlier for the sum-product algorithm, we can readily write down the max-sum algorithm in terms of message passing simply by replacing 'sum' with 'max' and replacing products with sums of logarithms to give

$$\mu_{f\to x}(x) = \max_{x_1,\ldots,x_M}\left[\ln f(x,x_1,\ldots,x_M) + \sum_{m\in \mathrm{ne}(f_s)\setminus x} \mu_{x_m\to f}(x_m)\right] \tag{8.93}$$

$$\mu_{x\to f}(x) = \sum_{l\in \mathrm{ne}(x)\setminus f} \mu_{f_l\to x}(x). \tag{8.94}$$

The initial messages sent by the leaf nodes are obtained by analogy with (8.70) and (8.71) and are given by

$$\mu_{x\to f}(x) = 0 \tag{8.95}$$

$$\mu_{f\to x}(x) = \ln f(x) \tag{8.96}$$

while at the root node the maximum probability can then be computed, by analogy with (8.63), using

$$p^{\max} = \max_x \left[\sum_{s\in \mathrm{ne}(x)} \mu_{f_s\to x}(x)\right]. \tag{8.97}$$

So far, we have seen how to find the maximum of the joint distribution by propagating messages from the leaves to an arbitrarily chosen root node. The result will be the same irrespective of which node is chosen as the root. Now we turn to the second problem of finding the configuration of the variables for which the joint distribution attains this maximum value. So far, we have sent messages from the leaves to the root. The process of evaluating (8.97) will also give the value $x^{\max}$ for the most probable value of the root node variable, defined by

$$x^{\max} = \arg\max_x \left[\sum_{s\in \mathrm{ne}(x)} \mu_{f_s\to x}(x)\right]. \tag{8.98}$$

At this point, we might be tempted simply to continue with the message passing algorithm and send messages from the root back out to the leaves, using (8.93) and (8.94), then apply (8.98) to all of the remaining variable nodes. However, because we are now maximizing rather than summing, it is possible that there may be multiple configurations of $\mathbf{x}$ all of which give rise to the maximum value for $p(\mathbf{x})$. In such cases, this strategy can fail because it is possible for the individual variable values obtained by maximizing the product of messages at each node to belong to different maximizing configurations, giving an overall configuration that no longer corresponds to a maximum.

The problem can be resolved by adopting a rather different kind of message passing from the root node to the leaves. To see how this works, let us return once again to the simple chain example of N variables $x_1,\ldots,x_N$ each having K states,

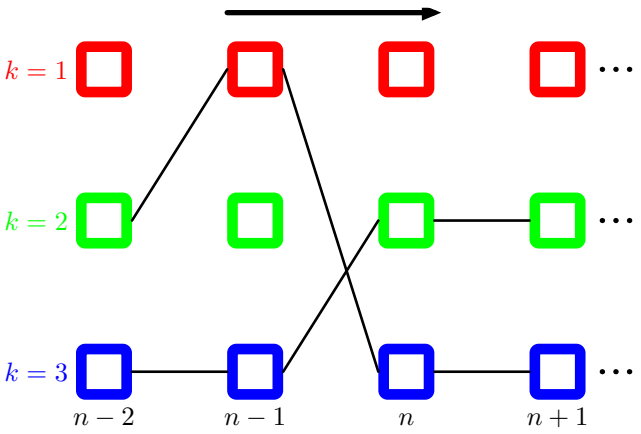

Figure 8.53 A lattice, or trellis, diagram showing explicitly the K possible states (one per row of the diagram) for each of the variables x_n in the chain model. In this illustration $K = 3$. The arrow shows the direction of message passing in the max-product algorithm. For every state k of each variable x_n (corresponding to column n of the diagram) the function $\phi(x_n)$ defines a unique state at the previous variable, indicated by the black lines. The two paths through the lattice correspond to configurations that give the global maximum of the joint probability distribution, and either of these can be found by tracing back along the black lines in the opposite direction to the arrow.

corresponding to the graph shown in Figure 8.38. Suppose we take node x_N to be the root node. Then in the first phase, we propagate messages from the leaf node x_1 to the root node using

$$\begin{aligned}\mu_{x_n \to f_{n,n+1}}(x_n) &= \mu_{f_{n-1,n} \to x_n}(x_n) \\ \mu_{f_{n-1,n} \to x_n}(x_n) &= \max_{x_{n-1}} \left[\ln f_{n-1,n}(x_{n-1}, x_n) + \mu_{x_{n-1} \to fn-1,n}(x_n)\right]\end{aligned}$$

which follow from applying (8.94) and (8.93) to this particular graph. The initial message sent from the leaf node is simply

$$\mu_{x_1 \to f_{1,2}}(x_1) = 0. \tag{8.99}$$

The most probable value for x_N is then given by

$$x_N^{\max} = \arg\max_{x_N} \left[\mu_{f_{N-1,N} \to x_N}(x_N)\right]. \tag{8.100}$$

Now we need to determine the states of the previous variables that correspond to the same maximizing configuration. This can be done by keeping track of which values of the variables gave rise to the maximum state of each variable, in other words by storing quantities given by

$$\phi(x_n) = \arg\max_{x_{n-1}} \left[\ln f_{n-1,n}(x_{n-1}, x_n) + \mu_{x_{n-1} \to fn-1,n}(x_n)\right]. \tag{8.101}$$

To understand better what is happening, it is helpful to represent the chain of variables in terms of a *lattice* or *trellis* diagram as shown in Figure 8.53. Note that this is not a probabilistic graphical model because the nodes represent individual states of variables, while each variable corresponds to a column of such states in the diagram. For each state of a given variable, there is a unique state of the previous variable that maximizes the probability (ties are broken either systematically or at random), corresponding to the function $\phi(x_n)$ given by (8.101), and this is indicated

by the lines connecting the nodes. Once we know the most probable value of the final node x_N, we can then simply follow the link back to find the most probable state of node x_{N-1} and so on back to the initial node x_1. This corresponds to propagating a message back down the chain using

$$x_{n-1}^{\max} = \phi(x_n^{\max}) \tag{8.102}$$

and is known as *back-tracking*. Note that there could be several values of x_{n-1} all of which give the maximum value in (8.101). Provided we chose one of these values when we do the back-tracking, we are assured of a globally consistent maximizing configuration.

In Figure 8.53, we have indicated two paths, each of which we shall suppose corresponds to a global maximum of the joint probability distribution. If $k = 2$ and $k = 3$ each represent possible values of $x_N^{\max}$, then starting from either state and tracing back along the black lines, which corresponds to iterating (8.102), we obtain a valid global maximum configuration. Note that if we had run a forward pass of max-sum message passing followed by a backward pass and then applied (8.98) at each node separately, we could end up selecting some states from one path and some from the other path, giving an overall configuration that is not a global maximizer. We see that it is necessary instead to keep track of the maximizing states during the forward pass using the functions $\phi(x_n)$ and then use back-tracking to find a consistent solution.

The extension to a general tree-structured factor graph should now be clear. If a message is sent from a factor node f to a variable node x, a maximization is performed over all other variable nodes $x_1, \ldots, x_M$ that are neighbours of that factor node, using (8.93). When we perform this maximization, we keep a record of which values of the variables $x_1, \ldots, x_M$ gave rise to the maximum. Then in the back-tracking step, having found $x^{\max}$, we can then use these stored values to assign consistent maximizing states $x_1^{\max}, \ldots, x_M^{\max}$. The max-sum algorithm, with back-tracking, gives an exact maximizing configuration for the variables provided the factor graph is a tree. An important application of this technique is for finding the most probable sequence of hidden states in a hidden Markov model, in which case it is known as the *Viterbi* algorithm.

Section 13.2

As with the sum-product algorithm, the inclusion of evidence in the form of observed variables is straightforward. The observed variables are clamped to their observed values, and the maximization is performed over the remaining hidden variables. This can be shown formally by including identity functions for the observed variables into the factor functions, as we did for the sum-product algorithm.

It is interesting to compare max-sum with the iterated conditional modes (ICM) algorithm described on page 389. Each step in ICM is computationally simpler because the 'messages' that are passed from one node to the next comprise a single value consisting of the new state of the node for which the conditional distribution is maximized. The max-sum algorithm is more complex because the messages are functions of node variables x and hence comprise a set of K values for each possible state of x. Unlike max-sum, however, ICM is not guaranteed to find a global maximum even for tree-structured graphs.

8.4.6 Exact inference in general graphs

The sum-product and max-sum algorithms provide efficient and exact solutions to inference problems in tree-structured graphs. For many practical applications, however, we have to deal with graphs having loops.

The message passing framework can be generalized to arbitrary graph topologies, giving an exact inference procedure known as the *junction tree algorithm* (Lauritzen and Spiegelhalter, 1988; Jordan, 2007). Here we give a brief outline of the key steps involved. This is not intended to convey a detailed understanding of the algorithm, but rather to give a flavour of the various stages involved. If the starting point is a directed graph, it is first converted to an undirected graph by moralization, whereas if starting from an undirected graph this step is not required. Next the graph is *triangulated*, which involves finding chord-less cycles containing four or more nodes and adding extra links to eliminate such chord-less cycles. For instance, in the graph in Figure 8.36, the cycle A–C–B–D–A is chord-less a link could be added between A and B or alternatively between C and D. Note that the joint distribution for the resulting triangulated graph is still defined by a product of the same potential functions, but these are now considered to be functions over expanded sets of variables. Next the triangulated graph is used to construct a new tree-structured undirected graph called a *join tree*, whose nodes correspond to the maximal cliques of the triangulated graph, and whose links connect pairs of cliques that have variables in common. The selection of which pairs of cliques to connect in this way is important and is done so as to give a *maximal spanning tree* defined as follows. Of all possible trees that link up the cliques, the one that is chosen is one for which the *weight* of the tree is largest, where the weight for a link is the number of nodes shared by the two cliques it connects, and the weight for the tree is the sum of the weights for the links. If the tree is condensed, so that any clique that is a subset of another clique is absorbed into the larger clique, this gives a *junction tree*. As a consequence of the triangulation step, the resulting tree satisfies the *running intersection property*, which means that if a variable is contained in two cliques, then it must also be contained in every clique on the path that connects them. This ensures that inference about variables will be consistent across the graph. Finally, a two-stage message passing algorithm, essentially equivalent to the sum-product algorithm, can now be applied to this junction tree in order to find marginals and conditionals. Although the junction tree algorithm sounds complicated, at its heart is the simple idea that we have used already of exploiting the factorization properties of the distribution to allow sums and products to be interchanged so that partial summations can be performed, thereby avoiding having to work directly with the joint distribution. The role of the junction tree is to provide a precise and efficient way to organize these computations. It is worth emphasizing that this is achieved using purely graphical operations!

The junction tree is exact for arbitrary graphs and is efficient in the sense that for a given graph there does not in general exist a computationally cheaper approach. Unfortunately, the algorithm must work with the joint distributions within each node (each of which corresponds to a clique of the triangulated graph) and so the computational cost of the algorithm is determined by the number of variables in the largest

clique and will grow exponentially with this number in the case of discrete variables. An important concept is the *treewidth* of a graph (Bodlaender, 1993), which is defined in terms of the number of variables in the largest clique. In fact, it is defined to be as one less than the size of the largest clique, to ensure that a tree has a treewidth of 1. Because there in general there can be multiple different junction trees that can be constructed from a given starting graph, the treewidth is defined by the junction tree for which the largest clique has the fewest variables. If the treewidth of the original graph is high, the junction tree algorithm becomes impractical.

8.4.7 Loopy belief propagation

For many problems of practical interest, it will not be feasible to use exact inference, and so we need to exploit effective approximation methods. An important class of such approximations, that can broadly be called *variational* methods, will be discussed in detail in Chapter 10. Complementing these deterministic approaches is a wide range of *sampling* methods, also called *Monte Carlo* methods, that are based on stochastic numerical sampling from distributions and that will be discussed at length in Chapter 11.

Here we consider one simple approach to approximate inference in graphs with loops, which builds directly on the previous discussion of exact inference in trees. The idea is simply to apply the sum-product algorithm even though there is no guarantee that it will yield good results. This approach is known as *loopy belief propagation* (Frey and MacKay, 1998) and is possible because the message passing rules (8.66) and (8.69) for the sum-product algorithm are purely local. However, because the graph now has cycles, information can flow many times around the graph. For some models, the algorithm will converge, whereas for others it will not.

In order to apply this approach, we need to define a *message passing schedule*. Let us assume that one message is passed at a time on any given link and in any given direction. Each message sent from a node replaces any previous message sent in the same direction across the same link and will itself be a function only of the most recent messages received by that node at previous steps of the algorithm.

We have seen that a message can only be sent across a link from a node when all other messages have been received by that node across its other links. Because there are loops in the graph, this raises the problem of how to initiate the message passing algorithm. To resolve this, we suppose that an initial message given by the unit function has been passed across every link in each direction. Every node is then in a position to send a message.

There are now many possible ways to organize the message passing schedule. For example, the *flooding schedule* simultaneously passes a message across every link in both directions at each time step, whereas schedules that pass one message at a time are called *serial schedules*.

Following Kschischnang *et al.* (2001), we will say that a (variable or factor) node a has a message *pending* on its link to a node b if node a has received any message on any of its other links since the last time it send a message to b. Thus, when a node receives a message on one of its links, this creates pending messages on all of its other links. Only pending messages need to be transmitted because

other messages would simply duplicate the previous message on the same link. For graphs that have a tree structure, any schedule that sends only pending messages will eventually terminate once a message has passed in each direction across every link. At this point, there are no pending messages, and the product of the received messages at every variable give the exact marginal. In graphs having loops, however, the algorithm may never terminate because there might always be pending messages, although in practice it is generally found to converge within a reasonable time for most applications. Once the algorithm has converged, or once it has been stopped if convergence is not observed, the (approximate) local marginals can be computed using the product of the most recently received incoming messages to each variable node or factor node on every link.

Exercise 8.29

In some applications, the loopy belief propagation algorithm can give poor results, whereas in other applications it has proven to be very effective. In particular, state-of-the-art algorithms for decoding certain kinds of error-correcting codes are equivalent to loopy belief propagation (Gallager, 1963; Berrou *et al.*, 1993; McEliece *et al.*, 1998; MacKay and Neal, 1999; Frey, 1998).

8.4.8 Learning the graph structure

In our discussion of inference in graphical models, we have assumed that the structure of the graph is known and fixed. However, there is also interest in going beyond the inference problem and learning the graph structure itself from data (Friedman and Koller, 2003). This requires that we define a space of possible structures as well as a measure that can be used to score each structure.

From a Bayesian viewpoint, we would ideally like to compute a posterior distribution over graph structures and to make predictions by averaging with respect to this distribution. If we have a prior $p(m)$ over graphs indexed by m, then the posterior distribution is given by

$$p(m|\mathcal{D}) \propto p(m)p(\mathcal{D}|m) \tag{8.103}$$

where $\mathcal{D}$ is the observed data set. The model evidence $p(\mathcal{D}|m)$ then provides the score for each model. However, evaluation of the evidence involves marginalization over the latent variables and presents a challenging computational problem for many models.

Exploring the space of structures can also be problematic. Because the number of different graph structures grows exponentially with the number of nodes, it is often necessary to resort to heuristics to find good candidates.

Exercises

8.1 ($\star$) **www** By marginalizing out the variables in order, show that the representation (8.5) for the joint distribution of a directed graph is correctly normalized, provided each of the conditional distributions is normalized.

8.2 ($\star$) **www** Show that the property of there being no directed cycles in a directed graph follows from the statement that there exists an ordered numbering of the nodes such that for each node there are no links going to a lower-numbered node.

Table 8.2 The joint distribution over three binary variables.

a	b	c	$p(a, b, c)$
0	0	0	0.192
0	0	1	0.144
0	1	0	0.048
0	1	1	0.216
1	0	0	0.192
1	0	1	0.064
1	1	0	0.048
1	1	1	0.096

8.3 ($\star\star$) Consider three binary variables $a, b, c \in \{0, 1\}$ having the joint distribution given in Table 8.2. Show by direct evaluation that this distribution has the property that a and b are marginally dependent, so that $p(a, b) \neq p(a)p(b)$, but that they become independent when conditioned on c, so that $p(a, b|c) = p(a|c)p(b|c)$ for both $c = 0$ and $c = 1$.

8.4 ($\star\star$) Evaluate the distributions $p(a)$, $p(b|c)$, and $p(c|a)$ corresponding to the joint distribution given in Table 8.2. Hence show by direct evaluation that $p(a, b, c) = p(a)p(c|a)p(b|c)$. Draw the corresponding directed graph.

8.5 ($\star$) **www** Draw a directed probabilistic graphical model corresponding to the relevance vector machine described by (7.79) and (7.80).

8.6 ($\star$) For the model shown in Figure 8.13, we have seen that the number of parameters required to specify the conditional distribution $p(y|x_1, \ldots, x_M)$, where $x_i \in \{0, 1\}$, could be reduced from 2^M to $M + 1$ by making use of the logistic sigmoid representation (8.10). An alternative representation (Pearl, 1988) is given by

$$p(y = 1|x_1, \ldots, x_M) = 1 - (1 - \mu_0) \prod_{i=1}^{M} (1 - \mu_i)^{x_i} \tag{8.104}$$

where the parameters μ_i represent the probabilities $p(x_i = 1)$, and μ_0 is an additional parameters satisfying $0 \leqslant \mu_0 \leqslant 1$. The conditional distribution (8.104) is known as the *noisy-OR*. Show that this can be interpreted as a 'soft' (probabilistic) form of the logical OR function (i.e., the function that gives $y = 1$ whenever at least one of the $x_i = 1$). Discuss the interpretation of μ_0.

8.7 ($\star\star$) Using the recursion relations (8.15) and (8.16), show that the mean and covariance of the joint distribution for the graph shown in Figure 8.14 are given by (8.17) and (8.18), respectively.

8.8 ($\star$) **www** Show that $a \perp\!\!\!\perp b, c \mid d$ implies $a \perp\!\!\!\perp b \mid d$.

8.9 ($\star$) **www** Using the d-separation criterion, show that the conditional distribution for a node $\mathbf{x}$ in a directed graph, conditioned on all of the nodes in the Markov blanket, is independent of the remaining variables in the graph.

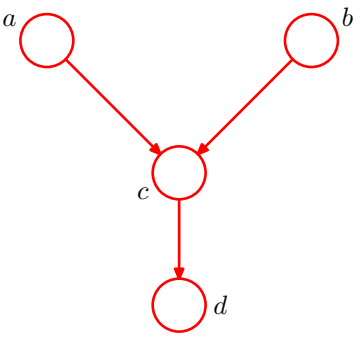

Figure 8.54 Example of a graphical model used to explore the conditional independence properties of the head-to-head path a–c–b when a descendant of c, namely the node d, is observed.

8.10 ($\star$) Consider the directed graph shown in Figure 8.54 in which none of the variables is observed. Show that $a \perp\!\!\!\perp b \mid \emptyset$. Suppose we now observe the variable d. Show that in general $a \not\perp\!\!\!\perp b \mid d$.

8.11 ($\star\star$) Consider the example of the car fuel system shown in Figure 8.21, and suppose that instead of observing the state of the fuel gauge G directly, the gauge is seen by the driver D who reports to us the reading on the gauge. This report is either that the gauge shows full $D = 1$ or that it shows empty $D = 0$. Our driver is a bit unreliable, as expressed through the following probabilities

$$p(D = 1|G = 1) = 0.9 \tag{8.105}$$
$$p(D = 0|G = 0) = 0.9. \tag{8.106}$$

Suppose that the driver tells us that the fuel gauge shows empty, in other words that we observe $D = 0$. Evaluate the probability that the tank is empty given only this observation. Similarly, evaluate the corresponding probability given also the observation that the battery is flat, and note that this second probability is lower. Discuss the intuition behind this result, and relate the result to Figure 8.54.

8.12 ($\star$) **www** Show that there are $2^{M(M-1)/2}$ distinct undirected graphs over a set of M distinct random variables. Draw the 8 possibilities for the case of $M = 3$.

8.13 ($\star$) Consider the use of iterated conditional modes (ICM) to minimize the energy function given by (8.42). Write down an expression for the difference in the values of the energy associated with the two states of a particular variable x_j, with all other variables held fixed, and show that it depends only on quantities that are local to x_j in the graph.

8.14 ($\star$) Consider a particular case of the energy function given by (8.42) in which the coefficients $\beta = h = 0$. Show that the most probable configuration of the latent variables is given by $x_i = y_i$ for all i.

8.15 ($\star\star$) **www** Show that the joint distribution $p(x_{n-1}, x_n)$ for two neighbouring nodes in the graph shown in Figure 8.38 is given by an expression of the form (8.58).

8.16 (⋆⋆) Consider the inference problem of evaluating $p(\mathbf{x}_n|\mathbf{x}_N)$ for the graph shown in Figure 8.38, for all nodes $n \in \{1, \ldots, N-1\}$. Show that the message passing algorithm discussed in Section 8.4.1 can be used to solve this efficiently, and discuss which messages are modified and in what way.

8.17 (⋆⋆) Consider a graph of the form shown in Figure 8.38 having $N = 5$ nodes, in which nodes x_3 and x_5 are observed. Use d-separation to show that $x_2 \perp\!\!\!\perp x_5 \mid x_3$. Show that if the message passing algorithm of Section 8.4.1 is applied to the evaluation of $p(x_2|x_3, x_5)$, the result will be independent of the value of x_5.

8.18 (⋆⋆) **www** Show that a distribution represented by a directed tree can trivially be written as an equivalent distribution over the corresponding undirected tree. Also show that a distribution expressed as an undirected tree can, by suitable normalization of the clique potentials, be written as a directed tree. Calculate the number of distinct directed trees that can be constructed from a given undirected tree.

8.19 (⋆⋆) Apply the sum-product algorithm derived in Section 8.4.4 to the chain-of-nodes model discussed in Section 8.4.1 and show that the results (8.54), (8.55), and (8.57) are recovered as a special case.

8.20 (⋆) **www** Consider the message passing protocol for the sum-product algorithm on a tree-structured factor graph in which messages are first propagated from the leaves to an arbitrarily chosen root node and then from the root node out to the leaves. Use proof by induction to show that the messages can be passed in such an order that at every step, each node that must send a message has received all of the incoming messages necessary to construct its outgoing messages.

8.21 (⋆⋆) **www** Show that the marginal distributions $p(\mathbf{x}_s)$ over the sets of variables $\mathbf{x}_s$ associated with each of the factors $f_x(\mathbf{x}_s)$ in a factor graph can be found by first running the sum-product message passing algorithm and then evaluating the required marginals using (8.72).

8.22 (⋆) Consider a tree-structured factor graph, in which a given subset of the variable nodes form a connected subgraph (i.e., any variable node of the subset is connected to at least one of the other variable nodes via a single factor node). Show how the sum-product algorithm can be used to compute the marginal distribution over that subset.

8.23 (⋆⋆) **www** In Section 8.4.4, we showed that the marginal distribution $p(x_i)$ for a variable node x_i in a factor graph is given by the product of the messages arriving at this node from neighbouring factor nodes in the form (8.63). Show that the marginal $p(x_i)$ can also be written as the product of the incoming message along any one of the links with the outgoing message along the same link.

8.24 (⋆⋆) Show that the marginal distribution for the variables $\mathbf{x}_s$ in a factor $f_s(\mathbf{x}_s)$ in a tree-structured factor graph, after running the sum-product message passing algorithm, can be written as the product of the message arriving at the factor node along all its links, times the local factor $f(\mathbf{x}_s)$, in the form (8.72).

8.25 ($\star\star$) In (8.86), we verified that the sum-product algorithm run on the graph in Figure 8.51 with node x_3 designated as the root node gives the correct marginal for x_2. Show that the correct marginals are obtained also for x_1 and x_3. Similarly, show that the use of the result (8.72) after running the sum-product algorithm on this graph gives the correct joint distribution for x_1, x_2.

8.26 ($\star$) Consider a tree-structured factor graph over discrete variables, and suppose we wish to evaluate the joint distribution $p(x_a, x_b)$ associated with two variables x_a and x_b that do not belong to a common factor. Define a procedure for using the sum-product algorithm to evaluate this joint distribution in which one of the variables is successively clamped to each of its allowed values.

8.27 ($\star\star$) Consider two discrete variables x and y each having three possible states, for example $x, y \in \{0, 1, 2\}$. Construct a joint distribution $p(x, y)$ over these variables having the property that the value $\widehat{x}$ that maximizes the marginal $p(x)$, along with the value $\widehat{y}$ that maximizes the marginal $p(y)$, together have probability zero under the joint distribution, so that $p(\widehat{x}, \widehat{y}) = 0$.

8.28 ($\star\star$) **WWW** The concept of a *pending* message in the sum-product algorithm for a factor graph was defined in Section 8.4.7. Show that if the graph has one or more cycles, there will always be at least one pending message irrespective of how long the algorithm runs.

8.29 ($\star\star$) **WWW** Show that if the sum-product algorithm is run on a factor graph with a tree structure (no loops), then after a finite number of messages have been sent, there will be no pending messages.

9 Mixture Models and EM

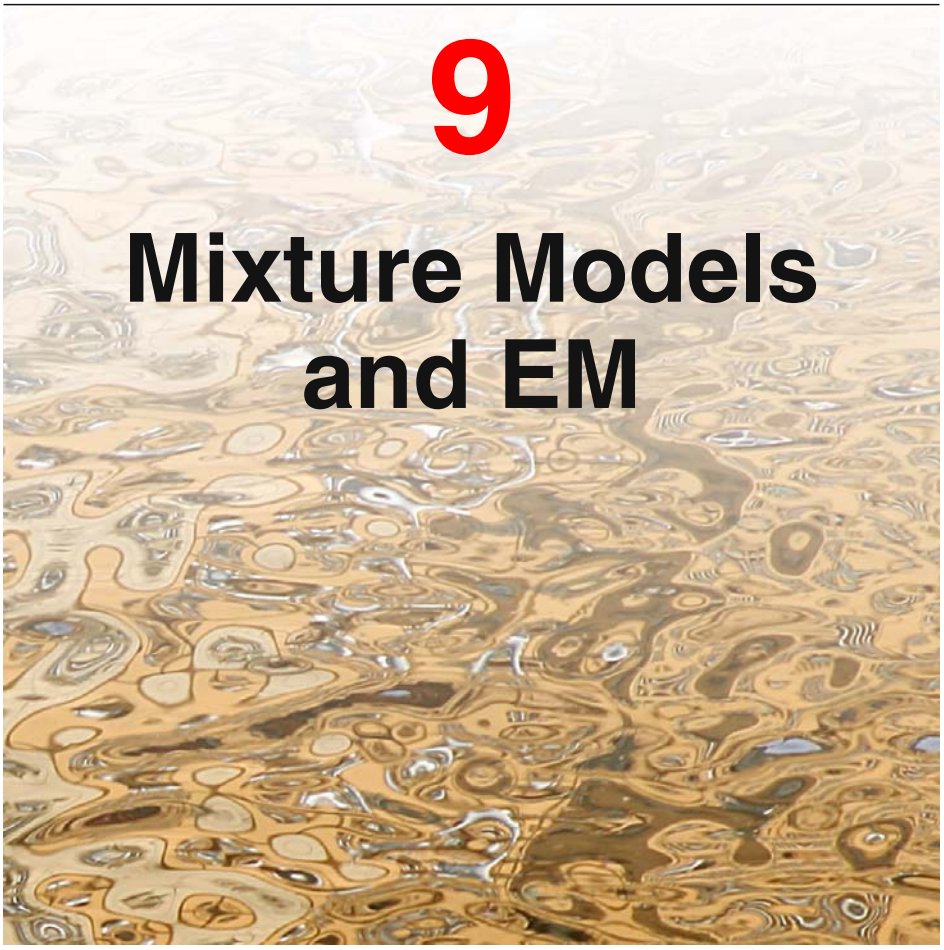

If we define a joint distribution over observed and latent variables, the corresponding distribution of the observed variables alone is obtained by marginalization. This allows relatively complex marginal distributions over observed variables to be expressed in terms of more tractable joint distributions over the expanded space of observed and latent variables. The introduction of latent variables thereby allows complicated distributions to be formed from simpler components. In this chapter, we shall see that mixture distributions, such as the Gaussian mixture discussed in Section 2.3.9, can be interpreted in terms of discrete latent variables. Continuous latent variables will form the subject of Chapter 12.

As well as providing a framework for building more complex probability distributions, mixture models can also be used to cluster data. We therefore begin our discussion of mixture distributions by considering the problem of finding clusters in a set of data points, which we approach first using a nonprobabilistic technique called the K-means algorithm (Lloyd, 1982). Then we introduce the latent variable

Section 9.1

view of mixture distributions in which the discrete latent variables can be interpreted as defining assignments of data points to specific components of the mixture. A general technique for finding maximum likelihood estimators in latent variable models is the expectation-maximization (EM) algorithm. We first of all use the Gaussian mixture distribution to motivate the EM algorithm in a fairly informal way, and then we give a more careful treatment based on the latent variable viewpoint. We shall see that the K-means algorithm corresponds to a particular nonprobabilistic limit of EM applied to mixtures of Gaussians. Finally, we discuss EM in some generality.

Section 9.2

Section 9.3

Section 9.4

Gaussian mixture models are widely used in data mining, pattern recognition, machine learning, and statistical analysis. In many applications, their parameters are determined by maximum likelihood, typically using the EM algorithm. However, as we shall see there are some significant limitations to the maximum likelihood approach, and in Chapter 10 we shall show that an elegant Bayesian treatment can be given using the framework of variational inference. This requires little additional computation compared with EM, and it resolves the principal difficulties of maximum likelihood while also allowing the number of components in the mixture to be inferred automatically from the data.

9.1. K-means Clustering

We begin by considering the problem of identifying groups, or clusters, of data points in a multidimensional space. Suppose we have a data set $\{\mathbf{x}_1, \ldots, \mathbf{x}_N\}$ consisting of N observations of a random D-dimensional Euclidean variable $\mathbf{x}$. Our goal is to partition the data set into some number K of clusters, where we shall suppose for the moment that the value of K is given. Intuitively, we might think of a cluster as comprising a group of data points whose inter-point distances are small compared with the distances to points outside of the cluster. We can formalize this notion by first introducing a set of D-dimensional vectors $\boldsymbol{\mu}_k$, where $k = 1, \ldots, K$, in which $\boldsymbol{\mu}_k$ is a prototype associated with the k^{th} cluster. As we shall see shortly, we can think of the $\boldsymbol{\mu}_k$ as representing the centres of the clusters. Our goal is then to find an assignment of data points to clusters, as well as a set of vectors $\{\boldsymbol{\mu}_k\}$, such that the sum of the squares of the distances of each data point to its closest vector $\boldsymbol{\mu}_k$, is a minimum.

It is convenient at this point to define some notation to describe the assignment of data points to clusters. For each data point $\mathbf{x}_n$, we introduce a corresponding set of binary indicator variables $r_{nk} \in \{0, 1\}$, where $k = 1, \ldots, K$ describing which of the K clusters the data point $\mathbf{x}_n$ is assigned to, so that if data point $\mathbf{x}_n$ is assigned to cluster k then $r_{nk} = 1$, and $r_{nj} = 0$ for $j \neq k$. This is known as the 1-of-K coding scheme. We can then define an objective function, sometimes called a *distortion measure*, given by

$$J = \sum_{n=1}^{N} \sum_{k=1}^{K} r_{nk} \|\mathbf{x}_n - \boldsymbol{\mu}_k\|^2 \tag{9.1}$$

which represents the sum of the squares of the distances of each data point to its

assigned vector $\boldsymbol{\mu}_k$. Our goal is to find values for the $\{r_{nk}\}$ and the $\{\boldsymbol{\mu}_k\}$ so as to minimize J. We can do this through an iterative procedure in which each iteration involves two successive steps corresponding to successive optimizations with respect to the r_{nk} and the $\boldsymbol{\mu}_k$. First we choose some initial values for the $\boldsymbol{\mu}_k$. Then in the first phase we minimize J with respect to the r_{nk}, keeping the $\boldsymbol{\mu}_k$ fixed. In the second phase we minimize J with respect to the $\boldsymbol{\mu}_k$, keeping r_{nk} fixed. This two-stage optimization is then repeated until convergence. We shall see that these two stages of updating r_{nk} and updating $\boldsymbol{\mu}_k$ correspond respectively to the E (expectation) and M (maximization) steps of the EM algorithm, and to emphasize this we shall use the terms E step and M step in the context of the K-means algorithm.

Section 9.4

Consider first the determination of the r_{nk}. Because J in (9.1) is a linear function of r_{nk}, this optimization can be performed easily to give a closed form solution. The terms involving different n are independent and so we can optimize for each n separately by choosing r_{nk} to be 1 for whichever value of k gives the minimum value of $\|\mathbf{x}_n - \boldsymbol{\mu}_k\|^2$. In other words, we simply assign the n^{th} data point to the closest cluster centre. More formally, this can be expressed as

$$r_{nk} = \begin{cases} 1 & \text{if } k = \arg\min_j \|\mathbf{x}_n - \boldsymbol{\mu}_j\|^2 \\ 0 & \text{otherwise.} \end{cases} \tag{9.2}$$

Now consider the optimization of the $\boldsymbol{\mu}_k$ with the r_{nk} held fixed. The objective function J is a quadratic function of $\boldsymbol{\mu}_k$, and it can be minimized by setting its derivative with respect to $\boldsymbol{\mu}_k$ to zero giving

$$2\sum_{n=1}^{N} r_{nk}(\mathbf{x}_n - \boldsymbol{\mu}_k) = 0 \tag{9.3}$$

which we can easily solve for $\boldsymbol{\mu}_k$ to give

$$\boldsymbol{\mu}_k = \frac{\sum_n r_{nk}\mathbf{x}_n}{\sum_n r_{nk}}. \tag{9.4}$$

The denominator in this expression is equal to the number of points assigned to cluster k, and so this result has a simple interpretation, namely set $\boldsymbol{\mu}_k$ equal to the mean of all of the data points $\mathbf{x}_n$ assigned to cluster k. For this reason, the procedure is known as the K-*means* algorithm.

The two phases of re-assigning data points to clusters and re-computing the cluster means are repeated in turn until there is no further change in the assignments (or until some maximum number of iterations is exceeded). Because each phase reduces the value of the objective function J, convergence of the algorithm is assured. However, it may converge to a local rather than global minimum of J. The convergence properties of the K-means algorithm were studied by MacQueen (1967).

Exercise 9.1

Appendix A

The K-means algorithm is illustrated using the Old Faithful data set in Figure 9.1. For the purposes of this example, we have made a linear re-scaling of the data, known as *standardizing*, such that each of the variables has zero mean and unit standard deviation. For this example, we have chosen $K = 2$, and so in this

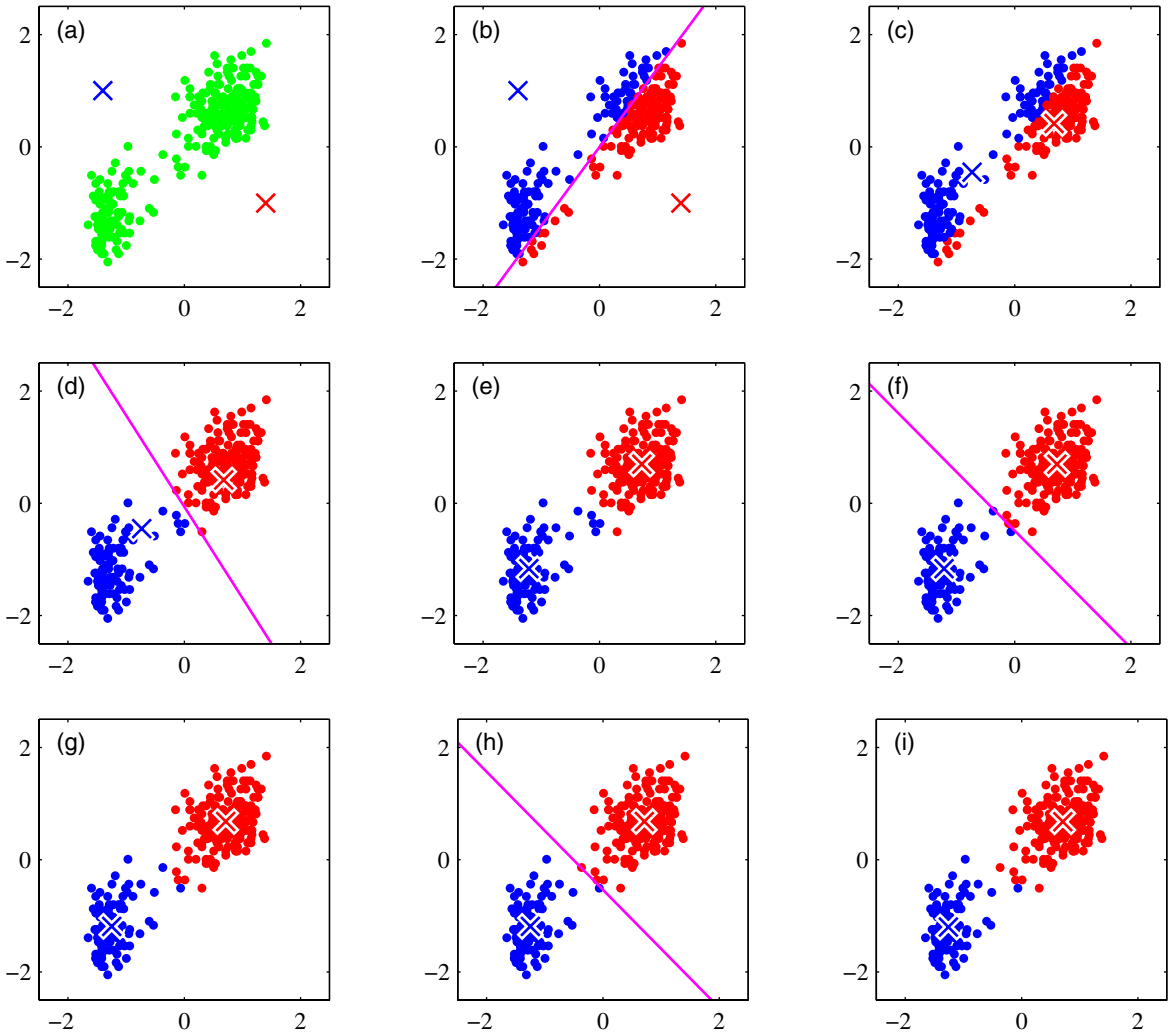

Figure 9.1 Illustration of the K-means algorithm using the re-scaled Old Faithful data set. (a) Green points denote the data set in a two-dimensional Euclidean space. The initial choices for centres $\boldsymbol{\mu}_1$ and $\boldsymbol{\mu}_2$ are shown by the red and blue crosses, respectively. (b) In the initial E step, each data point is assigned either to the red cluster or to the blue cluster, according to which cluster centre is nearer. This is equivalent to classifying the points according to which side of the perpendicular bisector of the two cluster centres, shown by the magenta line, they lie on. (c) In the subsequent M step, each cluster centre is re-computed to be the mean of the points assigned to the corresponding cluster. (d)–(i) show successive E and M steps through to final convergence of the algorithm.

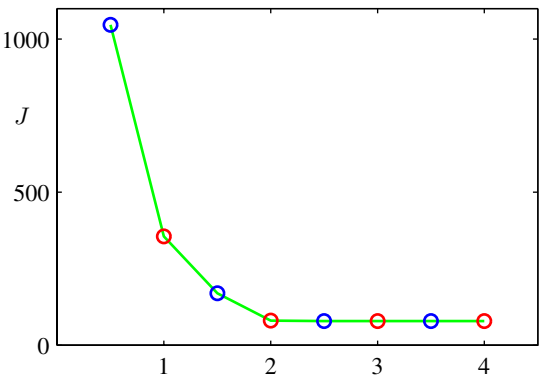

Figure 9.2 Plot of the cost function J given by (9.1) after each E step (blue points) and M step (red points) of the K-means algorithm for the example shown in Figure 9.1. The algorithm has converged after the third M step, and the final EM cycle produces no changes in either the assignments or the prototype vectors.

case, the assignment of each data point to the nearest cluster centre is equivalent to a classification of the data points according to which side they lie of the perpendicular bisector of the two cluster centres. A plot of the cost function J given by (9.1) for the Old Faithful example is shown in Figure 9.2.

Note that we have deliberately chosen poor initial values for the cluster centres so that the algorithm takes several steps before convergence. In practice, a better initialization procedure would be to choose the cluster centres $\boldsymbol{\mu}_k$ to be equal to a random subset of K data points. It is also worth noting that the K-means algorithm itself is often used to initialize the parameters in a Gaussian mixture model before applying the EM algorithm.

Section 9.2.2

A direct implementation of the K-means algorithm as discussed here can be relatively slow, because in each E step it is necessary to compute the Euclidean distance between every prototype vector and every data point. Various schemes have been proposed for speeding up the K-means algorithm, some of which are based on precomputing a data structure such as a tree such that nearby points are in the same subtree (Ramasubramanian and Paliwal, 1990; Moore, 2000). Other approaches make use of the triangle inequality for distances, thereby avoiding unnecessary distance calculations (Hodgson, 1998; Elkan, 2003).

So far, we have considered a batch version of K-means in which the whole data set is used together to update the prototype vectors. We can also derive an on-line stochastic algorithm (MacQueen, 1967) by applying the Robbins-Monro procedure to the problem of finding the roots of the regression function given by the derivatives of J in (9.1) with respect to $\boldsymbol{\mu}_k$. This leads to a sequential update in which, for each data point $\mathbf{x}_n$ in turn, we update the nearest prototype $\boldsymbol{\mu}_k$ using

Section 2.3.5

Exercise 9.2

$$\boldsymbol{\mu}_k^{\text{new}} = \boldsymbol{\mu}_k^{\text{old}} + \eta_n(\mathbf{x}_n - \boldsymbol{\mu}_k^{\text{old}}) \tag{9.5}$$

where η_n is the learning rate parameter, which is typically made to decrease monotonically as more data points are considered.

The K-means algorithm is based on the use of squared Euclidean distance as the measure of dissimilarity between a data point and a prototype vector. Not only does this limit the type of data variables that can be considered (it would be inappropriate for cases where some or all of the variables represent categorical labels for instance),

Section 2.3.7

but it can also make the determination of the cluster means nonrobust to outliers. We can generalize the K-means algorithm by introducing a more general dissimilarity measure $\mathcal{V}(\mathbf{x}, \mathbf{x}')$ between two vectors $\mathbf{x}$ and $\mathbf{x}'$ and then minimizing the following distortion measure

$$\widetilde{J} = \sum_{n=1}^{N} \sum_{k=1}^{K} r_{nk} \mathcal{V}(\mathbf{x}_n, \boldsymbol{\mu}_k) \tag{9.6}$$

which gives the *K-medoids* algorithm. The E step again involves, for given cluster prototypes $\boldsymbol{\mu}_k$, assigning each data point to the cluster for which the dissimilarity to the corresponding prototype is smallest. The computational cost of this is $O(KN)$, as is the case for the standard K-means algorithm. For a general choice of dissimilarity measure, the M step is potentially more complex than for K-means, and so it is common to restrict each cluster prototype to be equal to one of the data vectors assigned to that cluster, as this allows the algorithm to be implemented for any choice of dissimilarity measure $\mathcal{V}(\cdot, \cdot)$ so long as it can be readily evaluated. Thus the M step involves, for each cluster k, a discrete search over the N_k points assigned to that cluster, which requires $O(N_k^2)$ evaluations of $\mathcal{V}(\cdot, \cdot)$.

One notable feature of the K-means algorithm is that at each iteration, every data point is assigned uniquely to one, and only one, of the clusters. Whereas some data points will be much closer to a particular centre $\boldsymbol{\mu}_k$ than to any other centre, there may be other data points that lie roughly midway between cluster centres. In the latter case, it is not clear that the hard assignment to the nearest cluster is the most appropriate. We shall see in the next section that by adopting a probabilistic approach, we obtain 'soft' assignments of data points to clusters in a way that reflects the level of uncertainty over the most appropriate assignment. This probabilistic formulation brings with it numerous benefits.

9.1.1 Image segmentation and compression

As an illustration of the application of the K-means algorithm, we consider the related problems of image segmentation and image compression. The goal of segmentation is to partition an image into regions each of which has a reasonably homogeneous visual appearance or which corresponds to objects or parts of objects (Forsyth and Ponce, 2003). Each pixel in an image is a point in a 3-dimensional space comprising the intensities of the red, blue, and green channels, and our segmentation algorithm simply treats each pixel in the image as a separate data point. Note that strictly this space is not Euclidean because the channel intensities are bounded by the interval $[0, 1]$. Nevertheless, we can apply the K-means algorithm without difficulty. We illustrate the result of running K-means to convergence, for any particular value of K, by re-drawing the image replacing each pixel vector with the $\{R, G, B\}$ intensity triplet given by the centre $\boldsymbol{\mu}_k$ to which that pixel has been assigned. Results for various values of K are shown in Figure 9.3. We see that for a given value of K, the algorithm is representing the image using a palette of only K colours. It should be emphasized that this use of K-means is not a particularly sophisticated approach to image segmentation, not least because it takes no account of the spatial proximity of different pixels. The image segmentation problem is in general extremely difficult

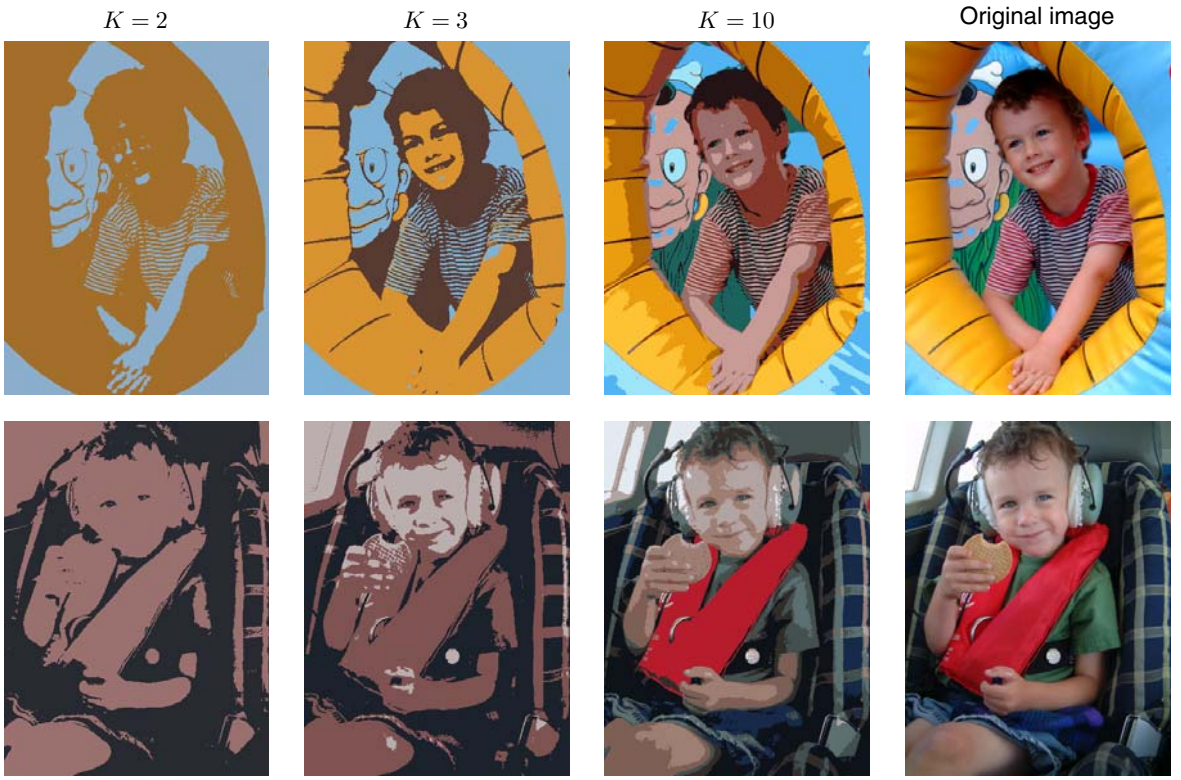

Figure 9.3 Two examples of the application of the K-means clustering algorithm to image segmentation showing the initial images together with their K-means segmentations obtained using various values of K. This also illustrates of the use of vector quantization for data compression, in which smaller values of K give higher compression at the expense of poorer image quality.

and remains the subject of active research and is introduced here simply to illustrate the behaviour of the K-means algorithm.

We can also use the result of a clustering algorithm to perform data compression. It is important to distinguish between *lossless data compression*, in which the goal is to be able to reconstruct the original data exactly from the compressed representation, and *lossy data compression*, in which we accept some errors in the reconstruction in return for higher levels of compression than can be achieved in the lossless case. We can apply the K-means algorithm to the problem of lossy data compression as follows. For each of the N data points, we store only the identity k of the cluster to which it is assigned. We also store the values of the K cluster centres $\boldsymbol{\mu}_k$, which typically requires significantly less data, provided we choose $K \ll N$. Each data point is then approximated by its nearest centre $\boldsymbol{\mu}_k$. New data points can similarly be compressed by first finding the nearest $\boldsymbol{\mu}_k$ and then storing the label k instead of the original data vector. This framework is often called *vector quantization*, and the vectors $\boldsymbol{\mu}_k$ are called *code-book vectors*.

The image segmentation problem discussed above also provides an illustration of the use of clustering for data compression. Suppose the original image has N pixels comprising $\{R, G, B\}$ values each of which is stored with 8 bits of precision. Then to transmit the whole image directly would cost $24N$ bits. Now suppose we first run K-means on the image data, and then instead of transmitting the original pixel intensity vectors we transmit the identity of the nearest vector $\boldsymbol{\mu}_k$. Because there are K such vectors, this requires $\log_2 K$ bits per pixel. We must also transmit the K code book vectors $\boldsymbol{\mu}_k$, which requires $24K$ bits, and so the total number of bits required to transmit the image is $24K + N \log_2 K$ (rounding up to the nearest integer). The original image shown in Figure 9.3 has $240 \times 180 = 43,200$ pixels and so requires $24 \times 43,200 = 1,036,800$ bits to transmit directly. By comparison, the compressed images require $43,248$ bits ($K = 2$), $86,472$ bits ($K = 3$), and $173,040$ bits ($K = 10$), respectively, to transmit. These represent compression ratios compared to the original image of 4.2%, 8.3%, and 16.7%, respectively. We see that there is a trade-off between degree of compression and image quality. Note that our aim in this example is to illustrate the K-means algorithm. If we had been aiming to produce a good image compressor, then it would be more fruitful to consider small blocks of adjacent pixels, for instance 5×5, and thereby exploit the correlations that exist in natural images between nearby pixels.

9.2. Mixtures of Gaussians

In Section 2.3.9 we motivated the Gaussian mixture model as a simple linear superposition of Gaussian components, aimed at providing a richer class of density models than the single Gaussian. We now turn to a formulation of Gaussian mixtures in terms of discrete *latent* variables. This will provide us with a deeper insight into this important distribution, and will also serve to motivate the expectation-maximization algorithm.

Recall from (2.188) that the Gaussian mixture distribution can be written as a linear superposition of Gaussians in the form

$$p(\mathbf{x}) = \sum_{k=1}^{K} \pi_k \mathcal{N}(\mathbf{x}|\boldsymbol{\mu}_k, \boldsymbol{\Sigma}_k). \tag{9.7}$$

Let us introduce a K-dimensional binary random variable $\mathbf{z}$ having a 1-of-K representation in which a particular element z_k is equal to 1 and all other elements are equal to 0. The values of z_k therefore satisfy $z_k \in \{0, 1\}$ and $\sum_k z_k = 1$, and we see that there are K possible states for the vector $\mathbf{z}$ according to which element is nonzero. We shall define the joint distribution $p(\mathbf{x}, \mathbf{z})$ in terms of a marginal distribution $p(\mathbf{z})$ and a conditional distribution $p(\mathbf{x}|\mathbf{z})$, corresponding to the graphical model in Figure 9.4. The marginal distribution over $\mathbf{z}$ is specified in terms of the mixing coefficients π_k, such that

$$p(z_k = 1) = \pi_k$$

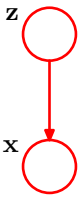

Figure 9.4 Graphical representation of a mixture model, in which the joint distribution is expressed in the form $p(\mathbf{x}, \mathbf{z}) = p(\mathbf{z})p(\mathbf{x}|\mathbf{z})$.

where the parameters $\{\pi_k\}$ must satisfy

$$0 \leqslant \pi_k \leqslant 1 \tag{9.8}$$

together with

$$\sum_{k=1}^{K} \pi_k = 1 \tag{9.9}$$

in order to be valid probabilities. Because $\mathbf{z}$ uses a 1-of-K representation, we can also write this distribution in the form

$$p(\mathbf{z}) = \prod_{k=1}^{K} \pi_k^{z_k}. \tag{9.10}$$

Similarly, the conditional distribution of $\mathbf{x}$ given a particular value for $\mathbf{z}$ is a Gaussian

$$p(\mathbf{x}|z_k = 1) = \mathcal{N}(\mathbf{x}|\boldsymbol{\mu}_k, \boldsymbol{\Sigma}_k)$$

which can also be written in the form

$$p(\mathbf{x}|\mathbf{z}) = \prod_{k=1}^{K} \mathcal{N}(\mathbf{x}|\boldsymbol{\mu}_k, \boldsymbol{\Sigma}_k)^{z_k}. \tag{9.11}$$

Exercise 9.3

The joint distribution is given by $p(\mathbf{z})p(\mathbf{x}|\mathbf{z})$, and the marginal distribution of $\mathbf{x}$ is then obtained by summing the joint distribution over all possible states of $\mathbf{z}$ to give

$$p(\mathbf{x}) = \sum_{\mathbf{z}} p(\mathbf{z})p(\mathbf{x}|\mathbf{z}) = \sum_{k=1}^{K} \pi_k \mathcal{N}(\mathbf{x}|\boldsymbol{\mu}_k, \boldsymbol{\Sigma}_k) \tag{9.12}$$

where we have made use of (9.10) and (9.11). Thus the marginal distribution of $\mathbf{x}$ is a Gaussian mixture of the form (9.7). If we have several observations $\mathbf{x}_1, \ldots, \mathbf{x}_N$, then, because we have represented the marginal distribution in the form $p(\mathbf{x}) = \sum_{\mathbf{z}} p(\mathbf{x}, \mathbf{z})$, it follows that for every observed data point $\mathbf{x}_n$ there is a corresponding latent variable $\mathbf{z}_n$.

We have therefore found an equivalent formulation of the Gaussian mixture involving an explicit latent variable. It might seem that we have not gained much by doing so. However, we are now able to work with the joint distribution $p(\mathbf{x}, \mathbf{z})$

instead of the marginal distribution $p(\mathbf{x})$, and this will lead to significant simplifications, most notably through the introduction of the expectation-maximization (EM) algorithm.

Another quantity that will play an important role is the conditional probability of $\mathbf{z}$ given $\mathbf{x}$. We shall use $\gamma(z_k)$ to denote $p(z_k = 1|\mathbf{x})$, whose value can be found using Bayes' theorem

$$\begin{aligned}\gamma(z_k) \equiv p(z_k = 1|\mathbf{x}) &= \frac{p(z_k = 1)p(\mathbf{x}|z_k = 1)}{\sum_{j=1}^{K} p(z_j = 1)p(\mathbf{x}|z_j = 1)} \\ &= \frac{\pi_k \mathcal{N}(\mathbf{x}|\boldsymbol{\mu}_k, \boldsymbol{\Sigma}_k)}{\sum_{j=1}^{K} \pi_j \mathcal{N}(\mathbf{x}|\boldsymbol{\mu}_j, \boldsymbol{\Sigma}_j)}. \end{aligned} \tag{9.13}$$

We shall view π_k as the prior probability of $z_k = 1$, and the quantity $\gamma(z_k)$ as the corresponding posterior probability once we have observed $\mathbf{x}$. As we shall see later, $\gamma(z_k)$ can also be viewed as the *responsibility* that component k takes for 'explaining' the observation $\mathbf{x}$.

Section 8.1.2

We can use the technique of ancestral sampling to generate random samples distributed according to the Gaussian mixture model. To do this, we first generate a value for $\mathbf{z}$, which we denote $\widehat{\mathbf{z}}$, from the marginal distribution $p(\mathbf{z})$ and then generate a value for $\mathbf{x}$ from the conditional distribution $p(\mathbf{x}|\widehat{\mathbf{z}})$. Techniques for sampling from standard distributions are discussed in Chapter 11. We can depict samples from the joint distribution $p(\mathbf{x}, \mathbf{z})$ by plotting points at the corresponding values of $\mathbf{x}$ and then colouring them according to the value of $\mathbf{z}$, in other words according to which Gaussian component was responsible for generating them, as shown in Figure 9.5(a). Similarly samples from the marginal distribution $p(\mathbf{x})$ are obtained by taking the samples from the joint distribution and ignoring the values of $\mathbf{z}$. These are illustrated in Figure 9.5(b) by plotting the $\mathbf{x}$ values without any coloured labels.

We can also use this synthetic data set to illustrate the 'responsibilities' by evaluating, for every data point, the posterior probability for each component in the mixture distribution from which this data set was generated. In particular, we can represent the value of the responsibilities $\gamma(z_{nk})$ associated with data point $\mathbf{x}_n$ by plotting the corresponding point using proportions of red, blue, and green ink given by $\gamma(z_{nk})$ for $k = 1, 2, 3$, respectively, as shown in Figure 9.5(c). So, for instance, a data point for which $\gamma(z_{n1}) = 1$ will be coloured red, whereas one for which $\gamma(z_{n2}) = \gamma(z_{n3}) = 0.5$ will be coloured with equal proportions of blue and green ink and so will appear cyan. This should be compared with Figure 9.5(a) in which the data points were labelled using the true identity of the component from which they were generated.

9.2.1 Maximum likelihood

Suppose we have a data set of observations $\{\mathbf{x}_1, \ldots, \mathbf{x}_N\}$, and we wish to model this data using a mixture of Gaussians. We can represent this data set as an $N \times D$

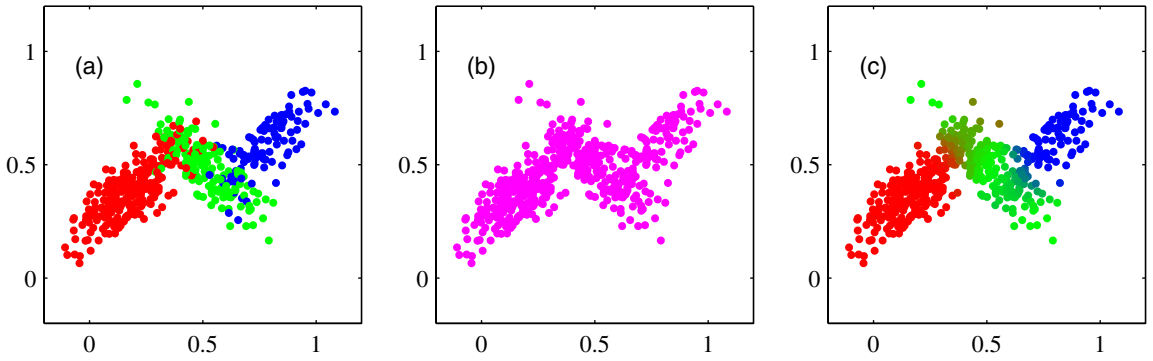

Figure 9.5 Example of 500 points drawn from the mixture of 3 Gaussians shown in Figure 2.23. (a) Samples from the joint distribution $p(\mathbf{z})p(\mathbf{x}|\mathbf{z})$ in which the three states of $\mathbf{z}$, corresponding to the three components of the mixture, are depicted in red, green, and blue, and (b) the corresponding samples from the marginal distribution $p(\mathbf{x})$, which is obtained by simply ignoring the values of $\mathbf{z}$ and just plotting the $\mathbf{x}$ values. The data set in (a) is said to be *complete*, whereas that in (b) is *incomplete*. (c) The same samples in which the colours represent the value of the responsibilities $\gamma(z_{nk})$ associated with data point $\mathbf{x}_n$, obtained by plotting the corresponding point using proportions of red, blue, and green ink given by $\gamma(z_{nk})$ for $k = 1, 2, 3$, respectively

matrix $\mathbf{X}$ in which the n^{th} row is given by $\mathbf{x}_n^{\mathrm{T}}$. Similarly, the corresponding latent variables will be denoted by an $N \times K$ matrix $\mathbf{Z}$ with rows $\mathbf{z}_n^{\mathrm{T}}$. If we assume that the data points are drawn independently from the distribution, then we can express the Gaussian mixture model for this i.i.d. data set using the graphical representation shown in Figure 9.6. From (9.7) the log of the likelihood function is given by

$$\ln p(\mathbf{X}|\boldsymbol{\pi}, \boldsymbol{\mu}, \boldsymbol{\Sigma}) = \sum_{n=1}^{N} \ln \left\{ \sum_{k=1}^{K} \pi_k \mathcal{N}(\mathbf{x}_n|\boldsymbol{\mu}_k, \boldsymbol{\Sigma}_k) \right\}. \tag{9.14}$$

Before discussing how to maximize this function, it is worth emphasizing that there is a significant problem associated with the maximum likelihood framework applied to Gaussian mixture models, due to the presence of singularities. For simplicity, consider a Gaussian mixture whose components have covariance matrices given by $\boldsymbol{\Sigma}_k = \sigma_k^2 \mathbf{I}$, where $\mathbf{I}$ is the unit matrix, although the conclusions will hold for general covariance matrices. Suppose that one of the components of the mixture model, let us say the j^{th} component, has its mean $\boldsymbol{\mu}_j$ exactly equal to one of the data

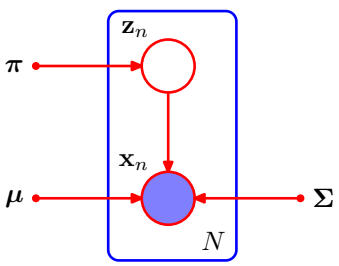

Figure 9.6 Graphical representation of a Gaussian mixture model for a set of N i.i.d. data points $\{\mathbf{x}_n\}$, with corresponding latent points $\{\mathbf{z}_n\}$, where $n = 1, \ldots, N$.

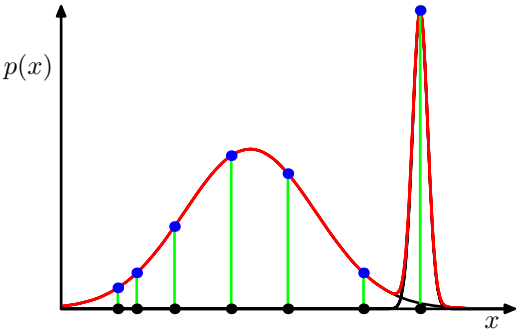

Figure 9.7 Illustration of how singularities in the likelihood function arise with mixtures of Gaussians. This should be compared with the case of a single Gaussian shown in Figure 1.14 for which no singularities arise.

points so that $\boldsymbol{\mu}_j = \mathbf{x}_n$ for some value of n. This data point will then contribute a term in the likelihood function of the form

$$\mathcal{N}(\mathbf{x}_n|\mathbf{x}_n, \sigma_j^2\mathbf{I}) = \frac{1}{(2\pi)^{1/2}}\frac{1}{\sigma_j}. \tag{9.15}$$

If we consider the limit $\sigma_j \to 0$, then we see that this term goes to infinity and so the log likelihood function will also go to infinity. Thus the maximization of the log likelihood function is not a well posed problem because such singularities will always be present and will occur whenever one of the Gaussian components 'collapses' onto a specific data point. Recall that this problem did not arise in the case of a single Gaussian distribution. To understand the difference, note that if a single Gaussian collapses onto a data point it will contribute multiplicative factors to the likelihood function arising from the other data points and these factors will go to zero exponentially fast, giving an overall likelihood that goes to zero rather than infinity. However, once we have (at least) two components in the mixture, one of the components can have a finite variance and therefore assign finite probability to all of the data points while the other component can shrink onto one specific data point and thereby contribute an ever increasing additive value to the log likelihood. This is illustrated in Figure 9.7. These singularities provide another example of the severe over-fitting that can occur in a maximum likelihood approach. We shall see that this difficulty does not occur if we adopt a Bayesian approach. For the moment, however, we simply note that in applying maximum likelihood to Gaussian mixture models we must take steps to avoid finding such pathological solutions and instead seek local maxima of the likelihood function that are well behaved. We can hope to avoid the singularities by using suitable heuristics, for instance by detecting when a Gaussian component is collapsing and resetting its mean to a randomly chosen value while also resetting its covariance to some large value, and then continuing with the optimization.

Section 10.1

A further issue in finding maximum likelihood solutions arises from the fact that for any given maximum likelihood solution, a K-component mixture will have a total of $K!$ equivalent solutions corresponding to the $K!$ ways of assigning K sets of parameters to K components. In other words, for any given (nondegenerate) point in the space of parameter values there will be a further $K! - 1$ additional points all of which give rise to exactly the same distribution. This problem is known as

identifiability (Casella and Berger, 2002) and is an important issue when we wish to interpret the parameter values discovered by a model. Identifiability will also arise when we discuss models having continuous latent variables in Chapter 12. However, for the purposes of finding a good density model, it is irrelevant because any of the equivalent solutions is as good as any other.

Maximizing the log likelihood function (9.14) for a Gaussian mixture model turns out to be a more complex problem than for the case of a single Gaussian. The difficulty arises from the presence of the summation over k that appears inside the logarithm in (9.14), so that the logarithm function no longer acts directly on the Gaussian. If we set the derivatives of the log likelihood to zero, we will no longer obtain a closed form solution, as we shall see shortly.

One approach is to apply gradient-based optimization techniques (Fletcher, 1987; Nocedal and Wright, 1999; Bishop and Nabney, 2008). Although gradient-based techniques are feasible, and indeed will play an important role when we discuss mixture density networks in Chapter 5, we now consider an alternative approach known as the EM algorithm which has broad applicability and which will lay the foundations for a discussion of variational inference techniques in Chapter 10.

9.2.2 EM for Gaussian mixtures

An elegant and powerful method for finding maximum likelihood solutions for models with latent variables is called the *expectation-maximization* algorithm, or *EM* algorithm (Dempster *et al.*, 1977; McLachlan and Krishnan, 1997). Later we shall give a general treatment of EM, and we shall also show how EM can be generalized to obtain the variational inference framework. Initially, we shall motivate the EM algorithm by giving a relatively informal treatment in the context of the Gaussian mixture model. We emphasize, however, that EM has broad applicability, and indeed it will be encountered in the context of a variety of different models in this book.

Section 10.1

Let us begin by writing down the conditions that must be satisfied at a maximum of the likelihood function. Setting the derivatives of $\ln p(\mathbf{X}|\boldsymbol{\pi}, \boldsymbol{\mu}, \boldsymbol{\Sigma})$ in (9.14) with respect to the means $\boldsymbol{\mu}_k$ of the Gaussian components to zero, we obtain

$$0 = -\sum_{n=1}^{N} \underbrace{\frac{\pi_k \mathcal{N}(\mathbf{x}_n|\boldsymbol{\mu}_k, \boldsymbol{\Sigma}_k)}{\sum_j \pi_j \mathcal{N}(\mathbf{x}_n|\boldsymbol{\mu}_j, \boldsymbol{\Sigma}_j)}}_{\gamma(z_{nk})} \boldsymbol{\Sigma}_k(\mathbf{x}_n - \boldsymbol{\mu}_k) \tag{9.16}$$

where we have made use of the form (2.43) for the Gaussian distribution. Note that the posterior probabilities, or responsibilities, given by (9.13) appear naturally on the right-hand side. Multiplying by $\boldsymbol{\Sigma}_k^{-1}$ (which we assume to be nonsingular) and rearranging we obtain

$$\boldsymbol{\mu}_k = \frac{1}{N_k} \sum_{n=1}^{N} \gamma(z_{nk}) \mathbf{x}_n \tag{9.17}$$

where we have defined

$$N_k = \sum_{n=1}^{N} \gamma(z_{nk}). \tag{9.18}$$

We can interpret N_k as the effective number of points assigned to cluster k. Note carefully the form of this solution. We see that the mean $\boldsymbol{\mu}_k$ for the k^{th} Gaussian component is obtained by taking a weighted mean of all of the points in the data set, in which the weighting factor for data point $\mathbf{x}_n$ is given by the posterior probability $\gamma(z_{nk})$ that component k was responsible for generating $\mathbf{x}_n$.

If we set the derivative of $\ln p(\mathbf{X}|\boldsymbol{\pi}, \boldsymbol{\mu}, \boldsymbol{\Sigma})$ with respect to $\boldsymbol{\Sigma}_k$ to zero, and follow a similar line of reasoning, making use of the result for the maximum likelihood solution for the covariance matrix of a single Gaussian, we obtain

Section 2.3.4

$$\boldsymbol{\Sigma}_k = \frac{1}{N_k} \sum_{n=1}^{N} \gamma(z_{nk})(\mathbf{x}_n - \boldsymbol{\mu}_k)(\mathbf{x}_n - \boldsymbol{\mu}_k)^{\mathrm{T}} \tag{9.19}$$

which has the same form as the corresponding result for a single Gaussian fitted to the data set, but again with each data point weighted by the corresponding posterior probability and with the denominator given by the effective number of points associated with the corresponding component.

Finally, we maximize $\ln p(\mathbf{X}|\boldsymbol{\pi}, \boldsymbol{\mu}, \boldsymbol{\Sigma})$ with respect to the mixing coefficients π_k. Here we must take account of the constraint (9.9), which requires the mixing coefficients to sum to one. This can be achieved using a Lagrange multiplier and maximizing the following quantity

Appendix E

$$\ln p(\mathbf{X}|\boldsymbol{\pi}, \boldsymbol{\mu}, \boldsymbol{\Sigma}) + \lambda \left(\sum_{k=1}^{K} \pi_k - 1 \right) \tag{9.20}$$

which gives

$$0 = \sum_{n=1}^{N} \frac{\mathcal{N}(\mathbf{x}_n|\boldsymbol{\mu}_k, \boldsymbol{\Sigma}_k)}{\sum_j \pi_j \mathcal{N}(\mathbf{x}_n|\boldsymbol{\mu}_j, \boldsymbol{\Sigma}_j)} + \lambda \tag{9.21}$$

where again we see the appearance of the responsibilities. If we now multiply both sides by π_k and sum over k making use of the constraint (9.9), we find $\lambda = -N$. Using this to eliminate λ and rearranging we obtain

$$\pi_k = \frac{N_k}{N} \tag{9.22}$$

so that the mixing coefficient for the k^{th} component is given by the average responsibility which that component takes for explaining the data points.

It is worth emphasizing that the results (9.17), (9.19), and (9.22) do not constitute a closed-form solution for the parameters of the mixture model because the responsibilities $\gamma(z_{nk})$ depend on those parameters in a complex way through (9.13). However, these results do suggest a simple iterative scheme for finding a solution to the maximum likelihood problem, which as we shall see turns out to be an instance of the EM algorithm for the particular case of the Gaussian mixture model. We first choose some initial values for the means, covariances, and mixing coefficients. Then we alternate between the following two updates that we shall call the E step

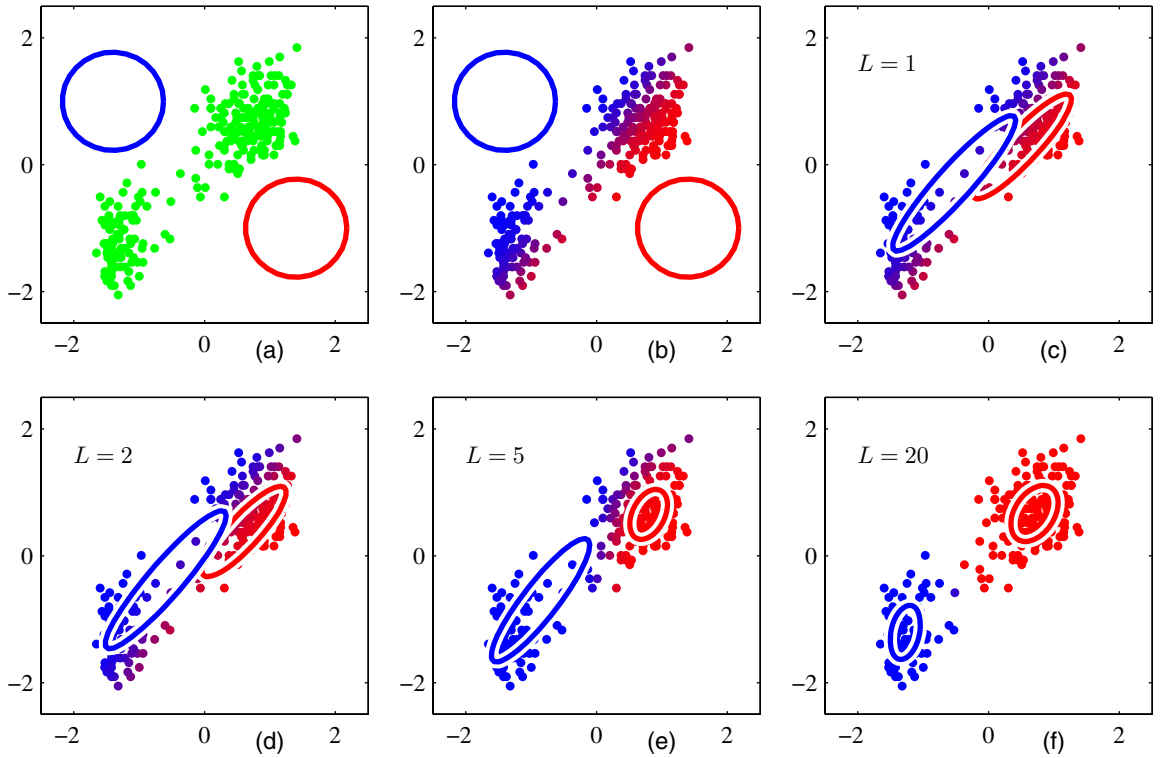

Figure 9.8 Illustration of the EM algorithm using the Old Faithful set as used for the illustration of the K-means algorithm in Figure 9.1. See the text for details.

and the M step, for reasons that will become apparent shortly. In the *expectation* step, or E step, we use the current values for the parameters to evaluate the posterior probabilities, or responsibilities, given by (9.13). We then use these probabilities in the *maximization* step, or M step, to re-estimate the means, covariances, and mixing coefficients using the results (9.17), (9.19), and (9.22). Note that in so doing we first evaluate the new means using (9.17) and then use these new values to find the covariances using (9.19), in keeping with the corresponding result for a single Gaussian distribution. We shall show that each update to the parameters resulting from an E step followed by an M step is guaranteed to increase the log likelihood function. In practice, the algorithm is deemed to have converged when the change in the log likelihood function, or alternatively in the parameters, falls below some threshold. We illustrate the EM algorithm for a mixture of two Gaussians applied to the rescaled Old Faithful data set in Figure 9.8. Here a mixture of two Gaussians is used, with centres initialized using the same values as for the K-means algorithm in Figure 9.1, and with precision matrices initialized to be proportional to the unit matrix. Plot (a) shows the data points in green, together with the initial configuration of the mixture model in which the one standard-deviation contours for the two

Section 9.4

Gaussian components are shown as blue and red circles. Plot (b) shows the result of the initial E step, in which each data point is depicted using a proportion of blue ink equal to the posterior probability of having been generated from the blue component, and a corresponding proportion of red ink given by the posterior probability of having been generated by the red component. Thus, points that have a significant probability for belonging to either cluster appear purple. The situation after the first M step is shown in plot (c), in which the mean of the blue Gaussian has moved to the mean of the data set, weighted by the probabilities of each data point belonging to the blue cluster, in other words it has moved to the centre of mass of the blue ink. Similarly, the covariance of the blue Gaussian is set equal to the covariance of the blue ink. Analogous results hold for the red component. Plots (d), (e), and (f) show the results after 2, 5, and 20 complete cycles of EM, respectively. In plot (f) the algorithm is close to convergence.

Note that the EM algorithm takes many more iterations to reach (approximate) convergence compared with the K-means algorithm, and that each cycle requires significantly more computation. It is therefore common to run the K-means algorithm in order to find a suitable initialization for a Gaussian mixture model that is subsequently adapted using EM. The covariance matrices can conveniently be initialized to the sample covariances of the clusters found by the K-means algorithm, and the mixing coefficients can be set to the fractions of data points assigned to the respective clusters. As with gradient-based approaches for maximizing the log likelihood, techniques must be employed to avoid singularities of the likelihood function in which a Gaussian component collapses onto a particular data point. It should be emphasized that there will generally be multiple local maxima of the log likelihood function, and that EM is not guaranteed to find the largest of these maxima. Because the EM algorithm for Gaussian mixtures plays such an important role, we summarize it below.

EM for Gaussian Mixtures

Given a Gaussian mixture model, the goal is to maximize the likelihood function with respect to the parameters (comprising the means and covariances of the components and the mixing coefficients).

1. Initialize the means $\boldsymbol{\mu}_k$, covariances $\boldsymbol{\Sigma}_k$ and mixing coefficients π_k, and evaluate the initial value of the log likelihood.
2. **E step**. Evaluate the responsibilities using the current parameter values

$$\gamma(z_{nk}) = \frac{\pi_k \mathcal{N}(\mathbf{x}_n|\boldsymbol{\mu}_k, \boldsymbol{\Sigma}_k)}{\sum_{j=1}^{K} \pi_j \mathcal{N}(\mathbf{x}_n|\boldsymbol{\mu}_j, \boldsymbol{\Sigma}_j)}. \tag{9.23}$$

3. **M step**. Re-estimate the parameters using the current responsibilities

$$\boldsymbol{\mu}_k^{\text{new}} = \frac{1}{N_k}\sum_{n=1}^{N}\gamma(z_{nk})\mathbf{x}_n \tag{9.24}$$

$$\boldsymbol{\Sigma}_k^{\text{new}} = \frac{1}{N_k}\sum_{n=1}^{N}\gamma(z_{nk})\left(\mathbf{x}_n-\boldsymbol{\mu}_k^{\text{new}}\right)\left(\mathbf{x}_n-\boldsymbol{\mu}_k^{\text{new}}\right)^{\mathrm{T}} \tag{9.25}$$

$$\pi_k^{\text{new}} = \frac{N_k}{N} \tag{9.26}$$

where

$$N_k = \sum_{n=1}^{N}\gamma(z_{nk}). \tag{9.27}$$

4. Evaluate the log likelihood

$$\ln p(\mathbf{X}|\boldsymbol{\mu},\boldsymbol{\Sigma},\boldsymbol{\pi}) = \sum_{n=1}^{N}\ln\left\{\sum_{k=1}^{K}\pi_k\mathcal{N}(\mathbf{x}_n|\boldsymbol{\mu}_k,\boldsymbol{\Sigma}_k)\right\} \tag{9.28}$$

and check for convergence of either the parameters or the log likelihood. If the convergence criterion is not satisfied return to step 2.

9.3. An Alternative View of EM

In this section, we present a complementary view of the EM algorithm that recognizes the key role played by latent variables. We discuss this approach first of all in an abstract setting, and then for illustration we consider once again the case of Gaussian mixtures.

The goal of the EM algorithm is to find maximum likelihood solutions for models having latent variables. We denote the set of all observed data by $\mathbf{X}$, in which the n^{th} row represents $\mathbf{x}_n^{\mathrm{T}}$, and similarly we denote the set of all latent variables by $\mathbf{Z}$, with a corresponding row $\mathbf{z}_n^{\mathrm{T}}$. The set of all model parameters is denoted by $\boldsymbol{\theta}$, and so the log likelihood function is given by

$$\ln p(\mathbf{X}|\boldsymbol{\theta}) = \ln\left\{\sum_{\mathbf{Z}}p(\mathbf{X},\mathbf{Z}|\boldsymbol{\theta})\right\}. \tag{9.29}$$

Note that our discussion will apply equally well to continuous latent variables simply by replacing the sum over $\mathbf{Z}$ with an integral.

A key observation is that the summation over the latent variables appears inside the logarithm. Even if the joint distribution $p(\mathbf{X},\mathbf{Z}|\boldsymbol{\theta})$ belongs to the exponential

family, the marginal distribution $p(\mathbf{X}|\boldsymbol{\theta})$ typically does not as a result of this summation. The presence of the sum prevents the logarithm from acting directly on the joint distribution, resulting in complicated expressions for the maximum likelihood solution.

Now suppose that, for each observation in $\mathbf{X}$, we were told the corresponding value of the latent variable $\mathbf{Z}$. We shall call $\{\mathbf{X}, \mathbf{Z}\}$ the *complete* data set, and we shall refer to the actual observed data $\mathbf{X}$ as *incomplete*, as illustrated in Figure 9.5. The likelihood function for the complete data set simply takes the form $\ln p(\mathbf{X}, \mathbf{Z}|\boldsymbol{\theta})$, and we shall suppose that maximization of this complete-data log likelihood function is straightforward.

In practice, however, we are not given the complete data set $\{\mathbf{X}, \mathbf{Z}\}$, but only the incomplete data $\mathbf{X}$. Our state of knowledge of the values of the latent variables in $\mathbf{Z}$ is given only by the posterior distribution $p(\mathbf{Z}|\mathbf{X}, \boldsymbol{\theta})$. Because we cannot use the complete-data log likelihood, we consider instead its expected value under the posterior distribution of the latent variable, which corresponds (as we shall see) to the E step of the EM algorithm. In the subsequent M step, we maximize this expectation. If the current estimate for the parameters is denoted $\boldsymbol{\theta}^{\text{old}}$, then a pair of successive E and M steps gives rise to a revised estimate $\boldsymbol{\theta}^{\text{new}}$. The algorithm is initialized by choosing some starting value for the parameters $\boldsymbol{\theta}_0$. The use of the expectation may seem somewhat arbitrary. However, we shall see the motivation for this choice when we give a deeper treatment of EM in Section 9.4.

In the E step, we use the current parameter values $\boldsymbol{\theta}^{\text{old}}$ to find the posterior distribution of the latent variables given by $p(\mathbf{Z}|\mathbf{X}, \boldsymbol{\theta}^{\text{old}})$. We then use this posterior distribution to find the expectation of the complete-data log likelihood evaluated for some general parameter value $\boldsymbol{\theta}$. This expectation, denoted $\mathcal{Q}(\boldsymbol{\theta}, \boldsymbol{\theta}^{\text{old}})$, is given by

$$\mathcal{Q}(\boldsymbol{\theta}, \boldsymbol{\theta}^{\text{old}}) = \sum_{\mathbf{Z}} p(\mathbf{Z}|\mathbf{X}, \boldsymbol{\theta}^{\text{old}}) \ln p(\mathbf{X}, \mathbf{Z}|\boldsymbol{\theta}). \tag{9.30}$$

In the M step, we determine the revised parameter estimate $\boldsymbol{\theta}^{\text{new}}$ by maximizing this function

$$\boldsymbol{\theta}^{\text{new}} = \arg\max_{\boldsymbol{\theta}} \mathcal{Q}(\boldsymbol{\theta}, \boldsymbol{\theta}^{\text{old}}). \tag{9.31}$$

Note that in the definition of $\mathcal{Q}(\boldsymbol{\theta}, \boldsymbol{\theta}^{\text{old}})$, the logarithm acts directly on the joint distribution $p(\mathbf{X}, \mathbf{Z}|\boldsymbol{\theta})$, and so the corresponding M-step maximization will, by supposition, be tractable.

The general EM algorithm is summarized below. It has the property, as we shall show later, that each cycle of EM will increase the incomplete-data log likelihood (unless it is already at a local maximum).

Section 9.4

The General EM Algorithm

Given a joint distribution $p(\mathbf{X}, \mathbf{Z}|\boldsymbol{\theta})$ over observed variables $\mathbf{X}$ and latent variables $\mathbf{Z}$, governed by parameters $\boldsymbol{\theta}$, the goal is to maximize the likelihood function $p(\mathbf{X}|\boldsymbol{\theta})$ with respect to $\boldsymbol{\theta}$.

1. Choose an initial setting for the parameters $\boldsymbol{\theta}^{\text{old}}$.

2. **E step** Evaluate $p(\mathbf{Z}|\mathbf{X}, \boldsymbol{\theta}^{\text{old}})$.

3. **M step** Evaluate $\boldsymbol{\theta}^{\text{new}}$ given by

$$\boldsymbol{\theta}^{\text{new}} = \arg\max_{\boldsymbol{\theta}} \mathcal{Q}(\boldsymbol{\theta}, \boldsymbol{\theta}^{\text{old}}) \tag{9.32}$$

where

$$\mathcal{Q}(\boldsymbol{\theta}, \boldsymbol{\theta}^{\text{old}}) = \sum_{\mathbf{Z}} p(\mathbf{Z}|\mathbf{X}, \boldsymbol{\theta}^{\text{old}}) \ln p(\mathbf{X}, \mathbf{Z}|\boldsymbol{\theta}). \tag{9.33}$$

4. Check for convergence of either the log likelihood or the parameter values. If the convergence criterion is not satisfied, then let

$$\boldsymbol{\theta}^{\text{old}} \leftarrow \boldsymbol{\theta}^{\text{new}} \tag{9.34}$$

and return to step 2.

Exercise 9.4

The EM algorithm can also be used to find MAP (maximum posterior) solutions for models in which a prior $p(\boldsymbol{\theta})$ is defined over the parameters. In this case the E step remains the same as in the maximum likelihood case, whereas in the M step the quantity to be maximized is given by $\mathcal{Q}(\boldsymbol{\theta}, \boldsymbol{\theta}^{\text{old}}) + \ln p(\boldsymbol{\theta})$. Suitable choices for the prior will remove the singularities of the kind illustrated in Figure 9.7.

Here we have considered the use of the EM algorithm to maximize a likelihood function when there are discrete latent variables. However, it can also be applied when the unobserved variables correspond to missing values in the data set. The distribution of the observed values is obtained by taking the joint distribution of all the variables and then marginalizing over the missing ones. EM can then be used to maximize the corresponding likelihood function. We shall show an example of the application of this technique in the context of principal component analysis in Figure 12.11. This will be a valid procedure if the data values are *missing at random*, meaning that the mechanism causing values to be missing does not depend on the unobserved values. In many situations this will not be the case, for instance if a sensor fails to return a value whenever the quantity it is measuring exceeds some threshold.

9.3.1 Gaussian mixtures revisited

We now consider the application of this latent variable view of EM to the specific case of a Gaussian mixture model. Recall that our goal is to maximize the log likelihood function (9.14), which is computed using the observed data set $\mathbf{X}$, and we saw that this was more difficult than for the case of a single Gaussian distribution due to the presence of the summation over k that occurs inside the logarithm. Suppose then that in addition to the observed data set $\mathbf{X}$, we were also given the values of the corresponding discrete variables $\mathbf{Z}$. Recall that Figure 9.5(a) shows a 'complete' data set (i.e., one that includes labels showing which component generated each data point) while Figure 9.5(b) shows the corresponding 'incomplete' data set. The graphical model for the complete data is shown in Figure 9.9.

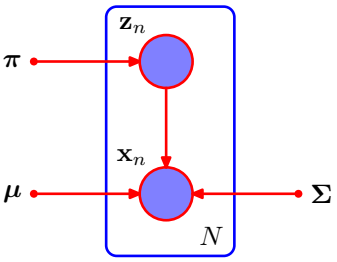

Figure 9.9 This shows the same graph as in Figure 9.6 except that we now suppose that the discrete variables $\mathbf{z}_n$ are observed, as well as the data variables $\mathbf{x}_n$.

Now consider the problem of maximizing the likelihood for the complete data set $\{\mathbf{X}, \mathbf{Z}\}$. From (9.10) and (9.11), this likelihood function takes the form

$$p(\mathbf{X}, \mathbf{Z}|\boldsymbol{\mu}, \boldsymbol{\Sigma}, \boldsymbol{\pi}) = \prod_{n=1}^{N} \prod_{k=1}^{K} \pi_k^{z_{nk}} \mathcal{N}(\mathbf{x}_n|\boldsymbol{\mu}_k, \boldsymbol{\Sigma}_k)^{z_{nk}} \tag{9.35}$$

where z_{nk} denotes the k^{th} component of $\mathbf{z}_n$. Taking the logarithm, we obtain

$$\ln p(\mathbf{X}, \mathbf{Z}|\boldsymbol{\mu}, \boldsymbol{\Sigma}, \boldsymbol{\pi}) = \sum_{n=1}^{N} \sum_{k=1}^{K} z_{nk} \left\{ \ln \pi_k + \ln \mathcal{N}(\mathbf{x}_n|\boldsymbol{\mu}_k, \boldsymbol{\Sigma}_k) \right\}. \tag{9.36}$$

Comparison with the log likelihood function (9.14) for the incomplete data shows that the summation over k and the logarithm have been interchanged. The logarithm now acts directly on the Gaussian distribution, which itself is a member of the exponential family. Not surprisingly, this leads to a much simpler solution to the maximum likelihood problem, as we now show. Consider first the maximization with respect to the means and covariances. Because $\mathbf{z}_n$ is a K-dimensional vector with all elements equal to 0 except for a single element having the value 1, the complete-data log likelihood function is simply a sum of K independent contributions, one for each mixture component. Thus the maximization with respect to a mean or a covariance is exactly as for a single Gaussian, except that it involves only the subset of data points that are 'assigned' to that component. For the maximization with respect to the mixing coefficients, we note that these are coupled for different values of k by virtue of the summation constraint (9.9). Again, this can be enforced using a Lagrange multiplier as before, and leads to the result

$$\pi_k = \frac{1}{N} \sum_{n=1}^{N} z_{nk} \tag{9.37}$$

so that the mixing coefficients are equal to the fractions of data points assigned to the corresponding components.

Thus we see that the complete-data log likelihood function can be maximized trivially in closed form. In practice, however, we do not have values for the latent variables so, as discussed earlier, we consider the expectation, with respect to the posterior distribution of the latent variables, of the complete-data log likelihood.

Using (9.10) and (9.11) together with Bayes' theorem, we see that this posterior distribution takes the form

$$p(\mathbf{Z}|\mathbf{X},\boldsymbol{\mu},\boldsymbol{\Sigma},\boldsymbol{\pi}) \propto \prod_{n=1}^{N}\prod_{k=1}^{K}\left[\pi_k \mathcal{N}(\mathbf{x}_n|\boldsymbol{\mu}_k,\boldsymbol{\Sigma}_k)\right]^{z_{nk}}. \tag{9.38}$$

and hence factorizes over n so that under the posterior distribution the $\{\mathbf{z}_n\}$ are independent. This is easily verified by inspection of the directed graph in Figure 9.6 and making use of the d-separation criterion. The expected value of the indicator variable z_{nk} under this posterior distribution is then given by

Exercise 9.5
Section 8.2

$$\begin{aligned}\mathbb{E}[z_{nk}] &= \frac{\sum_{z_{nk}} z_{nk}\left[\pi_k \mathcal{N}(\mathbf{x}_n|\boldsymbol{\mu}_k,\boldsymbol{\Sigma}_k)\right]^{z_{nk}}}{\sum_{z_{nj}}\left[\pi_j \mathcal{N}(\mathbf{x}_n|\boldsymbol{\mu}_j,\boldsymbol{\Sigma}_j)\right]^{z_{nj}}} \\ &= \frac{\pi_k \mathcal{N}(\mathbf{x}_n|\boldsymbol{\mu}_k,\boldsymbol{\Sigma}_k)}{\sum_{j=1}^{K}\pi_j \mathcal{N}(\mathbf{x}_n|\boldsymbol{\mu}_j,\boldsymbol{\Sigma}_j)} = \gamma(z_{nk})\end{aligned} \tag{9.39}$$

which is just the responsibility of component k for data point $\mathbf{x}_n$. The expected value of the complete-data log likelihood function is therefore given by

$$\mathbb{E}_{\mathbf{Z}}[\ln p(\mathbf{X},\mathbf{Z}|\boldsymbol{\mu},\boldsymbol{\Sigma},\boldsymbol{\pi})] = \sum_{n=1}^{N}\sum_{k=1}^{K}\gamma(z_{nk})\left\{\ln \pi_k + \ln \mathcal{N}(\mathbf{x}_n|\boldsymbol{\mu}_k,\boldsymbol{\Sigma}_k)\right\}. \tag{9.40}$$

We can now proceed as follows. First we choose some initial values for the parameters $\boldsymbol{\mu}^{\text{old}}$, $\boldsymbol{\Sigma}^{\text{old}}$ and $\boldsymbol{\pi}^{\text{old}}$, and use these to evaluate the responsibilities (the E step). We then keep the responsibilities fixed and maximize (9.40) with respect to $\boldsymbol{\mu}_k$, $\boldsymbol{\Sigma}_k$ and π_k (the M step). This leads to closed form solutions for $\boldsymbol{\mu}^{\text{new}}$, $\boldsymbol{\Sigma}^{\text{new}}$ and $\boldsymbol{\pi}^{\text{new}}$ given by (9.17), (9.19), and (9.22) as before. This is precisely the EM algorithm for Gaussian mixtures as derived earlier. We shall gain more insight into the role of the expected complete-data log likelihood function when we give a proof of convergence of the EM algorithm in Section 9.4.

Exercise 9.8

9.3.2 Relation to K-means

Comparison of the K-means algorithm with the EM algorithm for Gaussian mixtures shows that there is a close similarity. Whereas the K-means algorithm performs a *hard* assignment of data points to clusters, in which each data point is associated uniquely with one cluster, the EM algorithm makes a *soft* assignment based on the posterior probabilities. In fact, we can derive the K-means algorithm as a particular limit of EM for Gaussian mixtures as follows.

Consider a Gaussian mixture model in which the covariance matrices of the mixture components are given by $\epsilon\mathbf{I}$, where ϵ is a variance parameter that is shared

by all of the components, and $\mathbf{I}$ is the identity matrix, so that

$$p(\mathbf{x}|\boldsymbol{\mu}_k, \boldsymbol{\Sigma}_k) = \frac{1}{(2\pi\epsilon)^{1/2}} \exp\left\{-\frac{1}{2\epsilon}\|\mathbf{x} - \boldsymbol{\mu}_k\|^2\right\}. \tag{9.41}$$

We now consider the EM algorithm for a mixture of K Gaussians of this form in which we treat ϵ as a fixed constant, instead of a parameter to be re-estimated. From (9.13) the posterior probabilities, or responsibilities, for a particular data point $\mathbf{x}_n$, are given by

$$\gamma(z_{nk}) = \frac{\pi_k \exp\{-\|\mathbf{x}_n - \boldsymbol{\mu}_k\|^2/2\epsilon\}}{\sum_j \pi_j \exp\{-\|\mathbf{x}_n - \boldsymbol{\mu}_j\|^2/2\epsilon\}}. \tag{9.42}$$

If we consider the limit $\epsilon \to 0$, we see that in the denominator the term for which $\|\mathbf{x}_n - \boldsymbol{\mu}_j\|^2$ is smallest will go to zero most slowly, and hence the responsibilities $\gamma(z_{nk})$ for the data point $\mathbf{x}_n$ all go to zero except for term j, for which the responsibility $\gamma(z_{nj})$ will go to unity. Note that this holds independently of the values of the π_k so long as none of the π_k is zero. Thus, in this limit, we obtain a hard assignment of data points to clusters, just as in the K-means algorithm, so that $\gamma(z_{nk}) \to r_{nk}$ where r_{nk} is defined by (9.2). Each data point is thereby assigned to the cluster having the closest mean.

The EM re-estimation equation for the $\boldsymbol{\mu}_k$, given by (9.17), then reduces to the K-means result (9.4). Note that the re-estimation formula for the mixing coefficients (9.22) simply re-sets the value of π_k to be equal to the fraction of data points assigned to cluster k, although these parameters no longer play an active role in the algorithm.

Finally, in the limit $\epsilon \to 0$ the expected complete-data log likelihood, given by (9.40), becomes

Exercise 9.11

$$\mathbb{E}_{\mathbf{Z}}[\ln p(\mathbf{X}, \mathbf{Z}|\boldsymbol{\mu}, \boldsymbol{\Sigma}, \boldsymbol{\pi})] \to -\frac{1}{2}\sum_{n=1}^{N}\sum_{k=1}^{K} r_{nk}\|\mathbf{x}_n - \boldsymbol{\mu}_k\|^2 + \text{const.} \tag{9.43}$$

Thus we see that in this limit, maximizing the expected complete-data log likelihood is equivalent to minimizing the distortion measure J for the K-means algorithm given by (9.1).

Note that the K-means algorithm does not estimate the covariances of the clusters but only the cluster means. A hard-assignment version of the Gaussian mixture model with general covariance matrices, known as the *elliptical K-means* algorithm, has been considered by Sung and Poggio (1994).

9.3.3 Mixtures of Bernoulli distributions

So far in this chapter, we have focussed on distributions over continuous variables described by mixtures of Gaussians. As a further example of mixture modelling, and to illustrate the EM algorithm in a different context, we now discuss mixtures of discrete binary variables described by Bernoulli distributions. This model is also known as *latent class analysis* (Lazarsfeld and Henry, 1968; McLachlan and Peel, 2000). As well as being of practical importance in its own right, our discussion of Bernoulli mixtures will also lay the foundation for a consideration of hidden Markov models over discrete variables.

Section 13.2

Consider a set of D binary variables x_i, where $i = 1, \ldots, D$, each of which is governed by a Bernoulli distribution with parameter μ_i, so that

$$p(\mathbf{x}|\boldsymbol{\mu}) = \prod_{i=1}^{D} \mu_i^{x_i}(1-\mu_i)^{(1-x_i)} \tag{9.44}$$

where $\mathbf{x} = (x_1, \ldots, x_D)^{\mathrm{T}}$ and $\boldsymbol{\mu} = (\mu_1, \ldots, \mu_D)^{\mathrm{T}}$. We see that the individual variables x_i are independent, given $\boldsymbol{\mu}$. The mean and covariance of this distribution are easily seen to be

$$\mathbb{E}[\mathbf{x}] = \boldsymbol{\mu} \tag{9.45}$$

$$\mathrm{cov}[\mathbf{x}] = \mathrm{diag}\{\mu_i(1-\mu_i)\}. \tag{9.46}$$

Now let us consider a finite mixture of these distributions given by

$$p(\mathbf{x}|\boldsymbol{\mu}, \boldsymbol{\pi}) = \sum_{k=1}^{K} \pi_k p(\mathbf{x}|\boldsymbol{\mu}_k) \tag{9.47}$$

where $\boldsymbol{\mu} = \{\boldsymbol{\mu}_1, \ldots, \boldsymbol{\mu}_K\}$, $\boldsymbol{\pi} = \{\pi_1, \ldots, \pi_K\}$, and

$$p(\mathbf{x}|\boldsymbol{\mu}_k) = \prod_{i=1}^{D} \mu_{ki}^{x_i}(1-\mu_{ki})^{(1-x_i)}. \tag{9.48}$$

Exercise 9.12

The mean and covariance of this mixture distribution are given by

$$\mathbb{E}[\mathbf{x}] = \sum_{k=1}^{K} \pi_k \boldsymbol{\mu}_k \tag{9.49}$$

$$\mathrm{cov}[\mathbf{x}] = \sum_{k=1}^{K} \pi_k \left\{\boldsymbol{\Sigma}_k + \boldsymbol{\mu}_k \boldsymbol{\mu}_k^{\mathrm{T}}\right\} - \mathbb{E}[\mathbf{x}]\mathbb{E}[\mathbf{x}]^{\mathrm{T}} \tag{9.50}$$

where $\boldsymbol{\Sigma}_k = \mathrm{diag}\{\mu_{ki}(1-\mu_{ki})\}$. Because the covariance matrix $\mathrm{cov}[\mathbf{x}]$ is no longer diagonal, the mixture distribution can capture correlations between the variables, unlike a single Bernoulli distribution.

If we are given a data set $\mathbf{X} = \{\mathbf{x}_1, \ldots, \mathbf{x}_N\}$ then the log likelihood function for this model is given by

$$\ln p(\mathbf{X}|\boldsymbol{\mu}, \boldsymbol{\pi}) = \sum_{n=1}^{N} \ln \left\{ \sum_{k=1}^{K} \pi_k p(\mathbf{x}_n|\boldsymbol{\mu}_k) \right\}. \tag{9.51}$$

Again we see the appearance of the summation inside the logarithm, so that the maximum likelihood solution no longer has closed form.

We now derive the EM algorithm for maximizing the likelihood function for the mixture of Bernoulli distributions. To do this, we first introduce an explicit latent

variable $\mathbf{z}$ associated with each instance of $\mathbf{x}$. As in the case of the Gaussian mixture, $\mathbf{z} = (z_1, \ldots, z_K)^{\mathrm{T}}$ is a binary K-dimensional variable having a single component equal to 1, with all other components equal to 0. We can then write the conditional distribution of $\mathbf{x}$, given the latent variable, as

$$p(\mathbf{x}|\mathbf{z}, \boldsymbol{\mu}) = \prod_{k=1}^{K} p(\mathbf{x}|\boldsymbol{\mu}_k)^{z_k} \tag{9.52}$$

while the prior distribution for the latent variables is the same as for the mixture of Gaussians model, so that

$$p(\mathbf{z}|\boldsymbol{\pi}) = \prod_{k=1}^{K} \pi_k^{z_k}. \tag{9.53}$$

If we form the product of $p(\mathbf{x}|\mathbf{z}, \boldsymbol{\mu})$ and $p(\mathbf{z}|\boldsymbol{\pi})$ and then marginalize over $\mathbf{z}$, then we recover (9.47).

Exercise 9.14

In order to derive the EM algorithm, we first write down the complete-data log likelihood function, which is given by

$$\ln p(\mathbf{X}, \mathbf{Z}|\boldsymbol{\mu}, \boldsymbol{\pi}) = \sum_{n=1}^{N} \sum_{k=1}^{K} z_{nk} \left\{ \ln \pi_k + \sum_{i=1}^{D} [x_{ni} \ln \mu_{ki} + (1 - x_{ni}) \ln(1 - \mu_{ki})] \right\} \tag{9.54}$$

where $\mathbf{X} = \{\mathbf{x}_n\}$ and $\mathbf{Z} = \{\mathbf{z}_n\}$. Next we take the expectation of the complete-data log likelihood with respect to the posterior distribution of the latent variables to give

$$\mathbb{E}_{\mathbf{Z}}[\ln p(\mathbf{X}, \mathbf{Z}|\boldsymbol{\mu}, \boldsymbol{\pi})] = \sum_{n=1}^{N} \sum_{k=1}^{K} \gamma(z_{nk}) \left\{ \ln \pi_k + \sum_{i=1}^{D} [x_{ni} \ln \mu_{ki} + (1 - x_{ni}) \ln(1 - \mu_{ki})] \right\} \tag{9.55}$$

where $\gamma(z_{nk}) = \mathbb{E}[z_{nk}]$ is the posterior probability, or responsibility, of component k given data point $\mathbf{x}_n$. In the E step, these responsibilities are evaluated using Bayes' theorem, which takes the form

$$\begin{aligned} \gamma(z_{nk}) = \mathbb{E}[z_{nk}] &= \frac{\sum_{z_{nk}} z_{nk} \left[\pi_k p(\mathbf{x}_n|\boldsymbol{\mu}_k)\right]^{z_{nk}}}{\sum_{z_{nj}} \left[\pi_j p(\mathbf{x}_n|\boldsymbol{\mu}_j)\right]^{z_{nj}}} \\ &= \frac{\pi_k p(\mathbf{x}_n|\boldsymbol{\mu}_k)}{\sum_{j=1}^{K} \pi_j p(\mathbf{x}_n|\boldsymbol{\mu}_j)}. \end{aligned} \tag{9.56}$$

If we consider the sum over n in (9.55), we see that the responsibilities enter only through two terms, which can be written as

$$N_k = \sum_{n=1}^{N} \gamma(z_{nk}) \tag{9.57}$$

$$\overline{\mathbf{x}}_k = \frac{1}{N_k} \sum_{n=1}^{N} \gamma(z_{nk}) \mathbf{x}_n \tag{9.58}$$

where N_k is the effective number of data points associated with component k. In the M step, we maximize the expected complete-data log likelihood with respect to the parameters $\boldsymbol{\mu}_k$ and $\boldsymbol{\pi}$. If we set the derivative of (9.55) with respect to $\boldsymbol{\mu}_k$ equal to zero and rearrange the terms, we obtain

Exercise 9.15

$$\boldsymbol{\mu}_k = \overline{\mathbf{x}}_k. \tag{9.59}$$

We see that this sets the mean of component k equal to a weighted mean of the data, with weighting coefficients given by the responsibilities that component k takes for data points. For the maximization with respect to π_k, we need to introduce a Lagrange multiplier to enforce the constraint $\sum_k \pi_k = 1$. Following analogous steps to those used for the mixture of Gaussians, we then obtain

Exercise 9.16

$$\pi_k = \frac{N_k}{N} \tag{9.60}$$

which represents the intuitively reasonable result that the mixing coefficient for component k is given by the effective fraction of points in the data set explained by that component.

Note that in contrast to the mixture of Gaussians, there are no singularities in which the likelihood function goes to infinity. This can be seen by noting that the likelihood function is bounded above because $0 \leqslant p(\mathbf{x}_n|\boldsymbol{\mu}_k) \leqslant 1$. There exist singularities at which the likelihood function goes to zero, but these will not be found by EM provided it is not initialized to a pathological starting point, because the EM algorithm always increases the value of the likelihood function, until a local maximum is found. We illustrate the Bernoulli mixture model in Figure 9.10 by using it to model handwritten digits. Here the digit images have been turned into binary vectors by setting all elements whose values exceed 0.5 to 1 and setting the remaining elements to 0. We now fit a data set of $N = 600$ such digits, comprising the digits '2', '3', and '4', with a mixture of $K = 3$ Bernoulli distributions by running 10 iterations of the EM algorithm. The mixing coefficients were initialized to $\pi_k = 1/K$, and the parameters μ_{kj} were set to random values chosen uniformly in the range $(0.25, 0.75)$ and then normalized to satisfy the constraint that $\sum_j \mu_{kj} = 1$. We see that a mixture of 3 Bernoulli distributions is able to find the three clusters in the data set corresponding to the different digits.

Exercise 9.17

Section 9.4

The conjugate prior for the parameters of a Bernoulli distribution is given by the beta distribution, and we have seen that a beta prior is equivalent to introducing

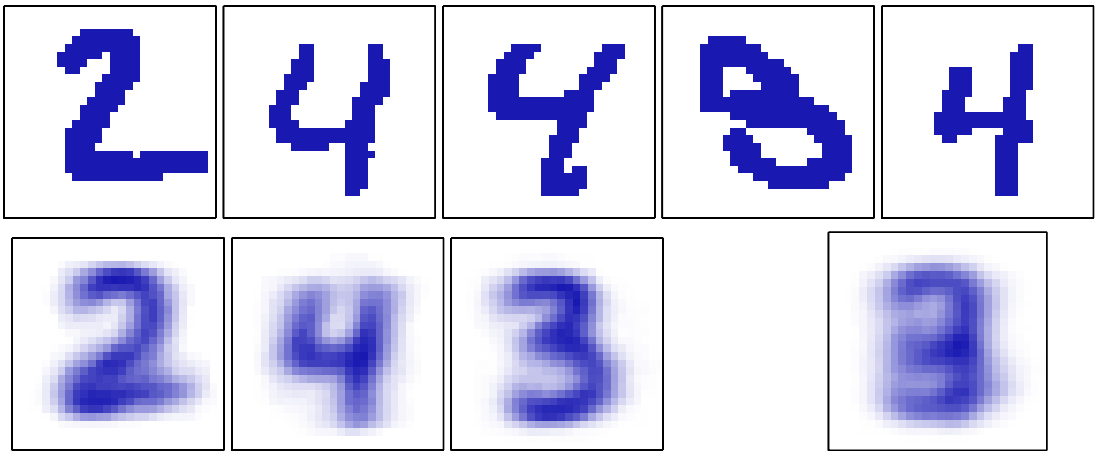

Figure 9.10 Illustration of the Bernoulli mixture model in which the top row shows examples from the digits data set after converting the pixel values from grey scale to binary using a threshold of 0.5. On the bottom row the first three images show the parameters μ_{ki} for each of the three components in the mixture model. As a comparison, we also fit the same data set using a single multivariate Bernoulli distribution, again using maximum likelihood. This amounts to simply averaging the counts in each pixel and is shown by the right-most image on the bottom row.

Section 2.1.1 additional effective observations of $\mathbf{x}$. We can similarly introduce priors into the Bernoulli mixture model, and use EM to maximize the posterior probability distributions.

Exercise 9.18

It is straightforward to extend the analysis of Bernoulli mixtures to the case of multinomial binary variables having $M > 2$ states by making use of the discrete distribution (2.26). Again, we can introduce Dirichlet priors over the model parameters if desired.

Exercise 9.19

9.3.4 EM for Bayesian linear regression

As a third example of the application of EM, we return to the evidence approximation for Bayesian linear regression. In Section 3.5.2, we obtained the re-estimation equations for the hyperparameters α and β by evaluation of the evidence and then setting the derivatives of the resulting expression to zero. We now turn to an alternative approach for finding α and β based on the EM algorithm. Recall that our goal is to maximize the evidence function $p(\mathbf{t}|\alpha, \beta)$ given by (3.77) with respect to α and β. Because the parameter vector $\mathbf{w}$ is marginalized out, we can regard it as a latent variable, and hence we can optimize this marginal likelihood function using EM. In the E step, we compute the posterior distribution of $\mathbf{w}$ given the current setting of the parameters α and β and then use this to find the expected complete-data log likelihood. In the M step, we maximize this quantity with respect to α and β. We have already derived the posterior distribution of $\mathbf{w}$ because this is given by (3.49). The complete-data log likelihood function is then given by

$$\ln p(\mathbf{t}, \mathbf{w}|\alpha, \beta) = \ln p(\mathbf{t}|\mathbf{w}, \beta) + \ln p(\mathbf{w}|\alpha) \tag{9.61}$$

where the likelihood $p(\mathbf{t}|\mathbf{w}, \beta)$ and the prior $p(\mathbf{w}|\alpha)$ are given by (3.10) and (3.52), respectively, and $y(\mathbf{x}, \mathbf{w})$ is given by (3.3). Taking the expectation with respect to the posterior distribution of $\mathbf{w}$ then gives

$$\begin{aligned}\mathbb{E}\left[\ln p(\mathbf{t}, \mathbf{w}|\alpha, \beta)\right] &= \frac{M}{2}\ln\left(\frac{\alpha}{2\pi}\right) - \frac{\alpha}{2}\mathbb{E}\left[\mathbf{w}^{\mathrm{T}}\mathbf{w}\right] + \frac{N}{2}\ln\left(\frac{\beta}{2\pi}\right) \\ &\quad -\frac{\beta}{2}\sum_{n=1}^{N}\mathbb{E}\left[(t_n - \mathbf{w}^{\mathrm{T}}\boldsymbol{\phi}_n)^2\right]. \end{aligned} \tag{9.62}$$

Setting the derivatives with respect to α to zero, we obtain the M step re-estimation equation

Exercise 9.20

$$\alpha = \frac{M}{\mathbb{E}\left[\mathbf{w}^{\mathrm{T}}\mathbf{w}\right]} = \frac{M}{\mathbf{m}_N^{\mathrm{T}}\mathbf{m}_N + \mathrm{Tr}(\mathbf{S}_N)}. \tag{9.63}$$

Exercise 9.21

An analogous result holds for β.

Note that this re-estimation equation takes a slightly different form from the corresponding result (3.92) derived by direct evaluation of the evidence function. However, they each involve computation and inversion (or eigen decomposition) of an $M \times M$ matrix and hence will have comparable computational cost per iteration.

These two approaches to determining α should of course converge to the same result (assuming they find the same local maximum of the evidence function). This can be verified by first noting that the quantity γ is defined by

$$\gamma = M - \alpha\sum_{i=1}^{M}\frac{1}{\lambda_i + \alpha} = M - \alpha\mathrm{Tr}(\mathbf{S}_N). \tag{9.64}$$

At a stationary point of the evidence function, the re-estimation equation (3.92) will be self-consistently satisfied, and hence we can substitute for γ to give

$$\alpha\mathbf{m}_N^{\mathrm{T}}\mathbf{m}_N = \gamma = M - \alpha\mathrm{Tr}(\mathbf{S}_N) \tag{9.65}$$

and solving for α we obtain (9.63), which is precisely the EM re-estimation equation.

As a final example, we consider a closely related model, namely the relevance vector machine for regression discussed in Section 7.2.1. There we used direct maximization of the marginal likelihood to derive re-estimation equations for the hyperparameters α and β. Here we consider an alternative approach in which we view the weight vector $\mathbf{w}$ as a latent variable and apply the EM algorithm. The E step involves finding the posterior distribution over the weights, and this is given by (7.81). In the M step we maximize the expected complete-data log likelihood, which is defined by

$$\mathbb{E}_{\mathbf{w}}\left[\ln p(\mathbf{t}|\mathbf{X}, \mathbf{w}, \beta)p(\mathbf{w}|\boldsymbol{\alpha})\right] \tag{9.66}$$

where the expectation is taken with respect to the posterior distribution computed using the 'old' parameter values. To compute the new parameter values we maximize with respect to $\boldsymbol{\alpha}$ and β to give

Exercise 9.22

$$\alpha_i^{\text{new}} = \frac{1}{m_i^2 + \Sigma_{ii}} \tag{9.67}$$

$$(\beta^{\text{new}})^{-1} = \frac{\|\mathbf{t} - \mathbf{\Phi}\mathbf{m}_N\|^2 + \beta^{-1}\sum_i \gamma_i}{N} \tag{9.68}$$

These re-estimation equations are formally equivalent to those obtained by direct maxmization.

Exercise 9.23

9.4. The EM Algorithm in General

The *expectation maximization* algorithm, or EM algorithm, is a general technique for finding maximum likelihood solutions for probabilistic models having latent variables (Dempster *et al.*, 1977; McLachlan and Krishnan, 1997). Here we give a very general treatment of the EM algorithm and in the process provide a proof that the EM algorithm derived heuristically in Sections 9.2 and 9.3 for Gaussian mixtures does indeed maximize the likelihood function (Csiszàr and Tusnàdy, 1984; Hathaway, 1986; Neal and Hinton, 1999). Our discussion will also form the basis for the derivation of the variational inference framework.

Section 10.1

Consider a probabilistic model in which we collectively denote all of the observed variables by $\mathbf{X}$ and all of the hidden variables by $\mathbf{Z}$. The joint distribution $p(\mathbf{X}, \mathbf{Z}|\boldsymbol{\theta})$ is governed by a set of parameters denoted $\boldsymbol{\theta}$. Our goal is to maximize the likelihood function that is given by

$$p(\mathbf{X}|\boldsymbol{\theta}) = \sum_{\mathbf{Z}} p(\mathbf{X}, \mathbf{Z}|\boldsymbol{\theta}). \tag{9.69}$$

Here we are assuming $\mathbf{Z}$ is discrete, although the discussion is identical if $\mathbf{Z}$ comprises continuous variables or a combination of discrete and continuous variables, with summation replaced by integration as appropriate.

We shall suppose that direct optimization of $p(\mathbf{X}|\boldsymbol{\theta})$ is difficult, but that optimization of the complete-data likelihood function $p(\mathbf{X}, \mathbf{Z}|\boldsymbol{\theta})$ is significantly easier. Next we introduce a distribution $q(\mathbf{Z})$ defined over the latent variables, and we observe that, for any choice of $q(\mathbf{Z})$, the following decomposition holds

$$\ln p(\mathbf{X}|\boldsymbol{\theta}) = \mathcal{L}(q, \boldsymbol{\theta}) + \mathrm{KL}(q\|p) \tag{9.70}$$

where we have defined

$$\mathcal{L}(q, \boldsymbol{\theta}) = \sum_{\mathbf{Z}} q(\mathbf{Z}) \ln \left\{ \frac{p(\mathbf{X}, \mathbf{Z}|\boldsymbol{\theta})}{q(\mathbf{Z})} \right\} \tag{9.71}$$

$$\mathrm{KL}(q\|p) = -\sum_{\mathbf{Z}} q(\mathbf{Z}) \ln \left\{ \frac{p(\mathbf{Z}|\mathbf{X}, \boldsymbol{\theta})}{q(\mathbf{Z})} \right\}. \tag{9.72}$$

Note that $\mathcal{L}(q, \boldsymbol{\theta})$ is a functional (see Appendix D for a discussion of functionals) of the distribution $q(\mathbf{Z})$, and a function of the parameters $\boldsymbol{\theta}$. It is worth studying

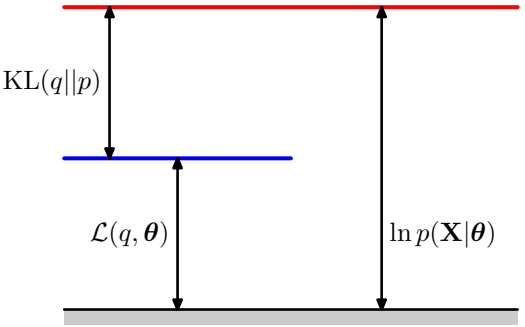

Figure 9.11 Illustration of the decomposition given by (9.70), which holds for any choice of distribution $q(\mathbf{Z})$. Because the Kullback-Leibler divergence satisfies $\mathrm{KL}(q\|p) \geqslant 0$, we see that the quantity $\mathcal{L}(q, \boldsymbol{\theta})$ is a lower bound on the log likelihood function $\ln p(\mathbf{X}|\boldsymbol{\theta})$.

carefully the forms of the expressions (9.71) and (9.72), and in particular noting that they differ in sign and also that $\mathcal{L}(q, \boldsymbol{\theta})$ contains the joint distribution of $\mathbf{X}$ and $\mathbf{Z}$ while $\mathrm{KL}(q\|p)$ contains the conditional distribution of $\mathbf{Z}$ given $\mathbf{X}$. To verify the

Exercise 9.24

decomposition (9.70), we first make use of the product rule of probability to give

$$\ln p(\mathbf{X}, \mathbf{Z}|\boldsymbol{\theta}) = \ln p(\mathbf{Z}|\mathbf{X}, \boldsymbol{\theta}) + \ln p(\mathbf{X}|\boldsymbol{\theta}) \tag{9.73}$$

which we then substitute into the expression for $\mathcal{L}(q, \boldsymbol{\theta})$. This gives rise to two terms, one of which cancels $\mathrm{KL}(q\|p)$ while the other gives the required log likelihood $\ln p(\mathbf{X}|\boldsymbol{\theta})$ after noting that $q(\mathbf{Z})$ is a normalized distribution that sums to 1.

From (9.72), we see that $\mathrm{KL}(q\|p)$ is the Kullback-Leibler divergence between $q(\mathbf{Z})$ and the posterior distribution $p(\mathbf{Z}|\mathbf{X}, \boldsymbol{\theta})$. Recall that the Kullback-Leibler di-

Section 1.6.1

vergence satisfies $\mathrm{KL}(q\|p) \geqslant 0$, with equality if, and only if, $q(\mathbf{Z}) = p(\mathbf{Z}|\mathbf{X}, \boldsymbol{\theta})$. It therefore follows from (9.70) that $\mathcal{L}(q, \boldsymbol{\theta}) \leqslant \ln p(\mathbf{X}|\boldsymbol{\theta})$, in other words that $\mathcal{L}(q, \boldsymbol{\theta})$ is a lower bound on $\ln p(\mathbf{X}|\boldsymbol{\theta})$. The decomposition (9.70) is illustrated in Figure 9.11.

The EM algorithm is a two-stage iterative optimization technique for finding maximum likelihood solutions. We can use the decomposition (9.70) to define the EM algorithm and to demonstrate that it does indeed maximize the log likelihood. Suppose that the current value of the parameter vector is $\boldsymbol{\theta}^{\mathrm{old}}$. In the E step, the lower bound $\mathcal{L}(q, \boldsymbol{\theta}^{\mathrm{old}})$ is maximized with respect to $q(\mathbf{Z})$ while holding $\boldsymbol{\theta}^{\mathrm{old}}$ fixed. The solution to this maximization problem is easily seen by noting that the value of $\ln p(\mathbf{X}|\boldsymbol{\theta}^{\mathrm{old}})$ does not depend on $q(\mathbf{Z})$ and so the largest value of $\mathcal{L}(q, \boldsymbol{\theta}^{\mathrm{old}})$ will occur when the Kullback-Leibler divergence vanishes, in other words when $q(\mathbf{Z})$ is equal to the posterior distribution $p(\mathbf{Z}|\mathbf{X}, \boldsymbol{\theta}^{\mathrm{old}})$. In this case, the lower bound will equal the log likelihood, as illustrated in Figure 9.12.

In the subsequent M step, the distribution $q(\mathbf{Z})$ is held fixed and the lower bound $\mathcal{L}(q, \boldsymbol{\theta})$ is maximized with respect to $\boldsymbol{\theta}$ to give some new value $\boldsymbol{\theta}^{\mathrm{new}}$. This will cause the lower bound $\mathcal{L}$ to increase (unless it is already at a maximum), which will necessarily cause the corresponding log likelihood function to increase. Because the distribution q is determined using the old parameter values rather than the new values and is held fixed during the M step, it will not equal the new posterior distribution $p(\mathbf{Z}|\mathbf{X}, \boldsymbol{\theta}^{\mathrm{new}})$, and hence there will be a nonzero KL divergence. The increase in the log likelihood function is therefore greater than the increase in the lower bound, as

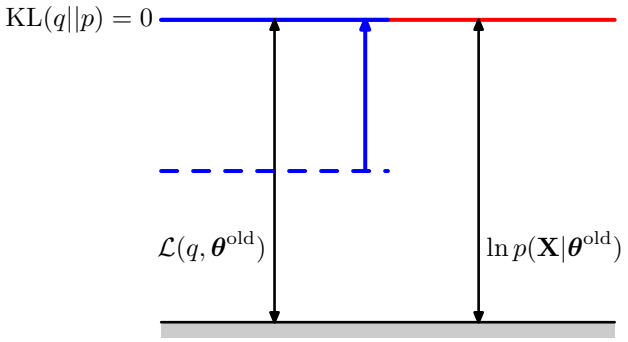

Figure 9.12 Illustration of the E step of the EM algorithm. The q distribution is set equal to the posterior distribution for the current parameter values $\boldsymbol{\theta}^{\text{old}}$, causing the lower bound to move up to the same value as the log likelihood function, with the KL divergence vanishing.

shown in Figure 9.13. If we substitute $q(\mathbf{Z}) = p(\mathbf{Z}|\mathbf{X}, \boldsymbol{\theta}^{\text{old}})$ into (9.71), we see that, after the E step, the lower bound takes the form

$$\begin{aligned} \mathcal{L}(q, \boldsymbol{\theta}) &= \sum_{\mathbf{Z}} p(\mathbf{Z}|\mathbf{X}, \boldsymbol{\theta}^{\text{old}}) \ln p(\mathbf{X}, \mathbf{Z}|\boldsymbol{\theta}) - \sum_{\mathbf{Z}} p(\mathbf{Z}|\mathbf{X}, \boldsymbol{\theta}^{\text{old}}) \ln p(\mathbf{Z}|\mathbf{X}, \boldsymbol{\theta}^{\text{old}}) \\ &= \mathcal{Q}(\boldsymbol{\theta}, \boldsymbol{\theta}^{\text{old}}) + \text{const} \end{aligned} \tag{9.74}$$

where the constant is simply the negative entropy of the q distribution and is therefore independent of $\boldsymbol{\theta}$. Thus in the M step, the quantity that is being maximized is the expectation of the complete-data log likelihood, as we saw earlier in the case of mixtures of Gaussians. Note that the variable $\boldsymbol{\theta}$ over which we are optimizing appears only inside the logarithm. If the joint distribution $p(\mathbf{Z}, \mathbf{X}|\boldsymbol{\theta})$ comprises a member of the exponential family, or a product of such members, then we see that the logarithm will cancel the exponential and lead to an M step that will be typically much simpler than the maximization of the corresponding incomplete-data log likelihood function $p(\mathbf{X}|\boldsymbol{\theta})$.

The operation of the EM algorithm can also be viewed in the space of parameters, as illustrated schematically in Figure 9.14. Here the red curve depicts the (in-

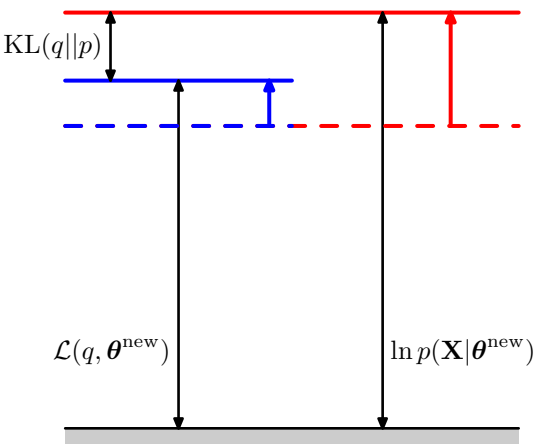

Figure 9.13 Illustration of the M step of the EM algorithm. The distribution $q(\mathbf{Z})$ is held fixed and the lower bound $\mathcal{L}(q, \boldsymbol{\theta})$ is maximized with respect to the parameter vector $\boldsymbol{\theta}$ to give a revised value $\boldsymbol{\theta}^{\text{new}}$. Because the KL divergence is nonnegative, this causes the log likelihood $\ln p(\mathbf{X}|\boldsymbol{\theta})$ to increase by at least as much as the lower bound does.

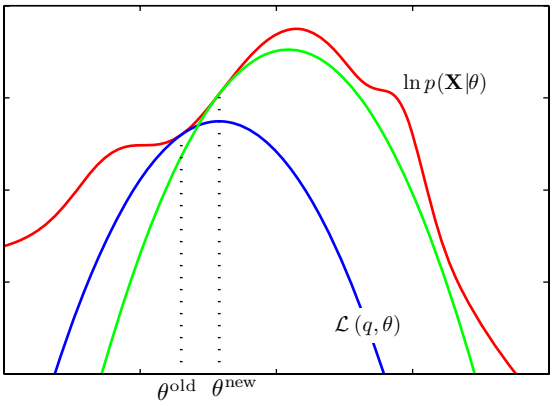

Figure 9.14 The EM algorithm involves alternately computing a lower bound on the log likelihood for the current parameter values and then maximizing this bound to obtain the new parameter values. See the text for a full discussion.

complete data) log likelihood function whose value we wish to maximize. We start with some initial parameter value $\boldsymbol{\theta}^{\text{old}}$, and in the first E step we evaluate the posterior distribution over latent variables, which gives rise to a lower bound $\mathcal{L}(\boldsymbol{\theta}, \boldsymbol{\theta}^{(\text{old})})$ whose value equals the log likelihood at $\boldsymbol{\theta}^{(\text{old})}$, as shown by the blue curve. Note that the bound makes a tangential contact with the log likelihood at $\boldsymbol{\theta}^{(\text{old})}$, so that both curves have the same gradient. This bound is a convex function having a unique maximum (for mixture components from the exponential family). In the M step, the bound is maximized giving the value $\boldsymbol{\theta}^{(\text{new})}$, which gives a larger value of log likelihood than $\boldsymbol{\theta}^{(\text{old})}$. The subsequent E step then constructs a bound that is tangential at $\boldsymbol{\theta}^{(\text{new})}$ as shown by the green curve.

Exercise 9.25

For the particular case of an independent, identically distributed data set, $\mathbf{X}$ will comprise N data points $\{\mathbf{x}_n\}$ while $\mathbf{Z}$ will comprise N corresponding latent variables $\{\mathbf{z}_n\}$, where $n = 1, \ldots, N$. From the independence assumption, we have $p(\mathbf{X}, \mathbf{Z}) = \prod_n p(\mathbf{x}_n, \mathbf{z}_n)$ and, by marginalizing over the $\{\mathbf{z}_n\}$ we have $p(\mathbf{X}) = \prod_n p(\mathbf{x}_n)$. Using the sum and product rules, we see that the posterior probability that is evaluated in the E step takes the form

$$p(\mathbf{Z}|\mathbf{X}, \boldsymbol{\theta}) = \frac{p(\mathbf{X}, \mathbf{Z}|\boldsymbol{\theta})}{\sum_{\mathbf{Z}} p(\mathbf{X}, \mathbf{Z}|\boldsymbol{\theta})} = \frac{\prod_{n=1}^{N} p(\mathbf{x}_n, \mathbf{z}_n|\boldsymbol{\theta})}{\sum_{\mathbf{Z}} \prod_{n=1}^{N} p(\mathbf{x}_n, \mathbf{z}_n|\boldsymbol{\theta})} = \prod_{n=1}^{N} p(\mathbf{z}_n|\mathbf{x}_n, \boldsymbol{\theta}) \tag{9.75}$$

and so the posterior distribution also factorizes with respect to n. In the case of the Gaussian mixture model this simply says that the responsibility that each of the mixture components takes for a particular data point $\mathbf{x}_n$ depends only on the value of $\mathbf{x}_n$ and on the parameters $\boldsymbol{\theta}$ of the mixture components, not on the values of the other data points.

We have seen that both the E and the M steps of the EM algorithm are increasing the value of a well-defined bound on the log likelihood function and that the

complete EM cycle will change the model parameters in such a way as to cause the log likelihood to increase (unless it is already at a maximum, in which case the parameters remain unchanged).

We can also use the EM algorithm to maximize the posterior distribution $p(\boldsymbol{\theta}|\mathbf{X})$ for models in which we have introduced a prior $p(\boldsymbol{\theta})$ over the parameters. To see this, we note that as a function of $\boldsymbol{\theta}$, we have $p(\boldsymbol{\theta}|\mathbf{X}) = p(\boldsymbol{\theta}, \mathbf{X})/p(\mathbf{X})$ and so

$$\ln p(\boldsymbol{\theta}|\mathbf{X}) = \ln p(\boldsymbol{\theta}, \mathbf{X}) - \ln p(\mathbf{X}). \tag{9.76}$$

Making use of the decomposition (9.70), we have

$$\begin{aligned} \ln p(\boldsymbol{\theta}|\mathbf{X}) &= \mathcal{L}(q, \boldsymbol{\theta}) + \mathrm{KL}(q\|p) + \ln p(\boldsymbol{\theta}) - \ln p(\mathbf{X}) \\ &\geqslant \mathcal{L}(q, \boldsymbol{\theta}) + \ln p(\boldsymbol{\theta}) - \ln p(\mathbf{X}). \end{aligned} \tag{9.77}$$

where $\ln p(\mathbf{X})$ is a constant. We can again optimize the right-hand side alternately with respect to q and $\boldsymbol{\theta}$. The optimization with respect to q gives rise to the same E-step equations as for the standard EM algorithm, because q only appears in $\mathcal{L}(q, \boldsymbol{\theta})$. The M-step equations are modified through the introduction of the prior term $\ln p(\boldsymbol{\theta})$, which typically requires only a small modification to the standard maximum likelihood M-step equations.

The EM algorithm breaks down the potentially difficult problem of maximizing the likelihood function into two stages, the E step and the M step, each of which will often prove simpler to implement. Nevertheless, for complex models it may be the case that either the E step or the M step, or indeed both, remain intractable. This leads to two possible extensions of the EM algorithm, as follows.

The *generalized EM*, or *GEM*, algorithm addresses the problem of an intractable M step. Instead of aiming to maximize $\mathcal{L}(q, \boldsymbol{\theta})$ with respect to $\boldsymbol{\theta}$, it seeks instead to change the parameters in such a way as to increase its value. Again, because $\mathcal{L}(q, \boldsymbol{\theta})$ is a lower bound on the log likelihood function, each complete EM cycle of the GEM algorithm is guaranteed to increase the value of the log likelihood (unless the parameters already correspond to a local maximum). One way to exploit the GEM approach would be to use one of the nonlinear optimization strategies, such as the conjugate gradients algorithm, during the M step. Another form of GEM algorithm, known as the *expectation conditional maximization*, or ECM, algorithm, involves making several constrained optimizations within each M step (Meng and Rubin, 1993). For instance, the parameters might be partitioned into groups, and the M step is broken down into multiple steps each of which involves optimizing one of the subset with the remainder held fixed.

We can similarly generalize the E step of the EM algorithm by performing a partial, rather than complete, optimization of $\mathcal{L}(q, \boldsymbol{\theta})$ with respect to $q(\mathbf{Z})$ (Neal and Hinton, 1999). As we have seen, for any given value of $\boldsymbol{\theta}$ there is a unique maximum of $\mathcal{L}(q, \boldsymbol{\theta})$ with respect to $q(\mathbf{Z})$ that corresponds to the posterior distribution $q_{\boldsymbol{\theta}}(\mathbf{Z}) = p(\mathbf{Z}|\mathbf{X}, \boldsymbol{\theta})$ and that for this choice of $q(\mathbf{Z})$ the bound $\mathcal{L}(q, \boldsymbol{\theta})$ is equal to the log likelihood function $\ln p(\mathbf{X}|\boldsymbol{\theta})$. It follows that any algorithm that converges to the global maximum of $\mathcal{L}(q, \boldsymbol{\theta})$ will find a value of $\boldsymbol{\theta}$ that is also a global maximum of the log likelihood $\ln p(\mathbf{X}|\boldsymbol{\theta})$. Provided $p(\mathbf{X}, \mathbf{Z}|\boldsymbol{\theta})$ is a continuous function of $\boldsymbol{\theta}$

then, by continuity, any local maximum of $\mathcal{L}(q, \boldsymbol{\theta})$ will also be a local maximum of $\ln p(\mathbf{X}|\boldsymbol{\theta})$.

Consider the case of N independent data points $\mathbf{x}_1, \ldots, \mathbf{x}_N$ with corresponding latent variables $\mathbf{z}_1, \ldots, \mathbf{z}_N$. The joint distribution $p(\mathbf{X}, \mathbf{Z}|\boldsymbol{\theta})$ factorizes over the data points, and this structure can be exploited in an incremental form of EM in which at each EM cycle only one data point is processed at a time. In the E step, instead of recomputing the responsibilities for all of the data points, we just re-evaluate the responsibilities for one data point. It might appear that the subsequent M step would require computation involving the responsibilities for all of the data points. However, if the mixture components are members of the exponential family, then the responsibilities enter only through simple sufficient statistics, and these can be updated efficiently. Consider, for instance, the case of a Gaussian mixture, and suppose we perform an update for data point m in which the corresponding old and new values of the responsibilities are denoted $\gamma^{\text{old}}(z_{mk})$ and $\gamma^{\text{new}}(z_{mk})$. In the M step, the required sufficient statistics can be updated incrementally. For instance, for the means the sufficient statistics are defined by (9.17) and (9.18) from which we obtain

Exercise 9.26

$$\boldsymbol{\mu}_k^{\text{new}} = \boldsymbol{\mu}_k^{\text{old}} + \left(\frac{\gamma^{\text{new}}(z_{mk}) - \gamma^{\text{old}}(z_{mk})}{N_k^{\text{new}}} \right) \left(\mathbf{x}_m - \boldsymbol{\mu}_k^{\text{old}} \right) \tag{9.78}$$

together with

$$N_k^{\text{new}} = N_k^{\text{old}} + \gamma^{\text{new}}(z_{mk}) - \gamma^{\text{old}}(z_{mk}). \tag{9.79}$$

The corresponding results for the covariances and the mixing coefficients are analogous.

Thus both the E step and the M step take fixed time that is independent of the total number of data points. Because the parameters are revised after each data point, rather than waiting until after the whole data set is processed, this incremental version can converge faster than the batch version. Each E or M step in this incremental algorithm is increasing the value of $\mathcal{L}(q, \boldsymbol{\theta})$ and, as we have shown above, if the algorithm converges to a local (or global) maximum of $\mathcal{L}(q, \boldsymbol{\theta})$, this will correspond to a local (or global) maximum of the log likelihood function $\ln p(\mathbf{X}|\boldsymbol{\theta})$.

Exercises

9.1 (⋆) **www** Consider the K-means algorithm discussed in Section 9.1. Show that as a consequence of there being a finite number of possible assignments for the set of discrete indicator variables r_{nk}, and that for each such assignment there is a unique optimum for the $\{\boldsymbol{\mu}_k\}$, the K-means algorithm must converge after a finite number of iterations.

9.2 (⋆) Apply the Robbins-Monro sequential estimation procedure described in Section 2.3.5 to the problem of finding the roots of the regression function given by the derivatives of J in (9.1) with respect to $\boldsymbol{\mu}_k$. Show that this leads to a stochastic K-means algorithm in which, for each data point $\mathbf{x}_n$, the nearest prototype $\boldsymbol{\mu}_k$ is updated using (9.5).

9.3 (⋆) **www** Consider a Gaussian mixture model in which the marginal distribution $p(\mathbf{z})$ for the latent variable is given by (9.10), and the conditional distribution $p(\mathbf{x}|\mathbf{z})$ for the observed variable is given by (9.11). Show that the marginal distribution $p(\mathbf{x})$, obtained by summing $p(\mathbf{z})p(\mathbf{x}|\mathbf{z})$ over all possible values of $\mathbf{z}$, is a Gaussian mixture of the form (9.7).

9.4 (⋆) Suppose we wish to use the EM algorithm to maximize the posterior distribution over parameters $p(\boldsymbol{\theta}|\mathbf{X})$ for a model containing latent variables, where $\mathbf{X}$ is the observed data set. Show that the E step remains the same as in the maximum likelihood case, whereas in the M step the quantity to be maximized is given by $\mathcal{Q}(\boldsymbol{\theta}, \boldsymbol{\theta}^{\text{old}}) + \ln p(\boldsymbol{\theta})$ where $\mathcal{Q}(\boldsymbol{\theta}, \boldsymbol{\theta}^{\text{old}})$ is defined by (9.30).

9.5 (⋆) Consider the directed graph for a Gaussian mixture model shown in Figure 9.6. By making use of the d-separation criterion discussed in Section 8.2, show that the posterior distribution of the latent variables factorizes with respect to the different data points so that

$$p(\mathbf{Z}|\mathbf{X}, \boldsymbol{\mu}, \boldsymbol{\Sigma}, \boldsymbol{\pi}) = \prod_{n=1}^{N} p(\mathbf{z}_n|\mathbf{x}_n, \boldsymbol{\mu}, \boldsymbol{\Sigma}, \boldsymbol{\pi}). \tag{9.80}$$

9.6 (⋆⋆) Consider a special case of a Gaussian mixture model in which the covariance matrices $\boldsymbol{\Sigma}_k$ of the components are all constrained to have a common value $\boldsymbol{\Sigma}$. Derive the EM equations for maximizing the likelihood function under such a model.

9.7 (⋆) **www** Verify that maximization of the complete-data log likelihood (9.36) for a Gaussian mixture model leads to the result that the means and covariances of each component are fitted independently to the corresponding group of data points, and the mixing coefficients are given by the fractions of points in each group.

9.8 (⋆) **www** Show that if we maximize (9.40) with respect to $\boldsymbol{\mu}_k$ while keeping the responsibilities $\gamma(z_{nk})$ fixed, we obtain the closed form solution given by (9.17).

9.9 (⋆) Show that if we maximize (9.40) with respect to $\boldsymbol{\Sigma}_k$ and π_k while keeping the responsibilities $\gamma(z_{nk})$ fixed, we obtain the closed form solutions given by (9.19) and (9.22).

9.10 (⋆⋆) Consider a density model given by a mixture distribution

$$p(\mathbf{x}) = \sum_{k=1}^{K} \pi_k p(\mathbf{x}|k) \tag{9.81}$$

and suppose that we partition the vector $\mathbf{x}$ into two parts so that $\mathbf{x} = (\mathbf{x}_a, \mathbf{x}_b)$. Show that the conditional density $p(\mathbf{x}_b|\mathbf{x}_a)$ is itself a mixture distribution and find expressions for the mixing coefficients and for the component densities.

9.11 ($\star$) In Section 9.3.2, we obtained a relationship between K means and EM for Gaussian mixtures by considering a mixture model in which all components have covariance $\epsilon\mathbf{I}$. Show that in the limit $\epsilon \to 0$, maximizing the expected complete-data log likelihood for this model, given by (9.40), is equivalent to minimizing the distortion measure J for the K-means algorithm given by (9.1).

9.12 ($\star$) **www** Consider a mixture distribution of the form

$$p(\mathbf{x}) = \sum_{k=1}^{K} \pi_k p(\mathbf{x}|k) \tag{9.82}$$

where the elements of $\mathbf{x}$ could be discrete or continuous or a combination of these. Denote the mean and covariance of $p(\mathbf{x}|k)$ by $\boldsymbol{\mu}_k$ and $\boldsymbol{\Sigma}_k$, respectively. Show that the mean and covariance of the mixture distribution are given by (9.49) and (9.50).

9.13 ($\star\star$) Using the re-estimation equations for the EM algorithm, show that a mixture of Bernoulli distributions, with its parameters set to values corresponding to a maximum of the likelihood function, has the property that

$$\mathbb{E}[\mathbf{x}] = \frac{1}{N}\sum_{n=1}^{N} \mathbf{x}_n \equiv \overline{\mathbf{x}}. \tag{9.83}$$

Hence show that if the parameters of this model are initialized such that all components have the same mean $\boldsymbol{\mu}_k = \widehat{\boldsymbol{\mu}}$ for $k = 1, \ldots, K$, then the EM algorithm will converge after one iteration, for any choice of the initial mixing coefficients, and that this solution has the property $\boldsymbol{\mu}_k = \overline{\mathbf{x}}$. Note that this represents a degenerate case of the mixture model in which all of the components are identical, and in practice we try to avoid such solutions by using an appropriate initialization.

9.14 ($\star$) Consider the joint distribution of latent and observed variables for the Bernoulli distribution obtained by forming the product of $p(\mathbf{x}|\mathbf{z}, \boldsymbol{\mu})$ given by (9.52) and $p(\mathbf{z}|\boldsymbol{\pi})$ given by (9.53). Show that if we marginalize this joint distribution with respect to $\mathbf{z}$, then we obtain (9.47).

9.15 ($\star$) **www** Show that if we maximize the expected complete-data log likelihood function (9.55) for a mixture of Bernoulli distributions with respect to $\boldsymbol{\mu}_k$, we obtain the M step equation (9.59).

9.16 ($\star$) Show that if we maximize the expected complete-data log likelihood function (9.55) for a mixture of Bernoulli distributions with respect to the mixing coefficients π_k, using a Lagrange multiplier to enforce the summation constraint, we obtain the M step equation (9.60).

9.17 ($\star$) **www** Show that as a consequence of the constraint $0 \leqslant p(\mathbf{x}_n|\boldsymbol{\mu}_k) \leqslant 1$ for the discrete variable $\mathbf{x}_n$, the incomplete-data log likelihood function for a mixture of Bernoulli distributions is bounded above, and hence that there are no singularities for which the likelihood goes to infinity.

9.18 ($\star\star$) Consider a Bernoulli mixture model as discussed in Section 9.3.3, together with a prior distribution $p(\boldsymbol{\mu}_k|a_k, b_k)$ over each of the parameter vectors $\boldsymbol{\mu}_k$ given by the beta distribution (2.13), and a Dirichlet prior $p(\boldsymbol{\pi}|\boldsymbol{\alpha})$ given by (2.38). Derive the EM algorithm for maximizing the posterior probability $p(\boldsymbol{\mu}, \boldsymbol{\pi}|\mathbf{X})$.

9.19 ($\star\star$) Consider a D-dimensional variable $\mathbf{x}$ each of whose components i is itself a multinomial variable of degree M so that $\mathbf{x}$ is a binary vector with components x_{ij} where $i = 1, \ldots, D$ and $j = 1, \ldots, M$, subject to the constraint that $\sum_j x_{ij} = 1$ for all i. Suppose that the distribution of these variables is described by a mixture of the discrete multinomial distributions considered in Section 2.2 so that

$$p(\mathbf{x}) = \sum_{k=1}^{K} \pi_k p(\mathbf{x}|\boldsymbol{\mu}_k) \tag{9.84}$$

where

$$p(\mathbf{x}|\boldsymbol{\mu}_k) = \prod_{i=1}^{D} \prod_{j=1}^{M} \mu_{kij}^{x_{ij}}. \tag{9.85}$$

The parameters μ_{kij} represent the probabilities $p(x_{ij} = 1|\boldsymbol{\mu}_k)$ and must satisfy $0 \leqslant \mu_{kij} \leqslant 1$ together with the constraint $\sum_j \mu_{kij} = 1$ for all values of k and i. Given an observed data set $\{\mathbf{x}_n\}$, where $n = 1, \ldots, N$, derive the E and M step equations of the EM algorithm for optimizing the mixing coefficients π_k and the component parameters μ_{kij} of this distribution by maximum likelihood.

9.20 ($\star$) **www** Show that maximization of the expected complete-data log likelihood function (9.62) for the Bayesian linear regression model leads to the M step re-estimation result (9.63) for α.

9.21 ($\star\star$) Using the evidence framework of Section 3.5, derive the M-step re-estimation equations for the parameter β in the Bayesian linear regression model, analogous to the result (9.63) for α.

9.22 ($\star\star$) By maximization of the expected complete-data log likelihood defined by (9.66), derive the M step equations (9.67) and (9.68) for re-estimating the hyperparameters of the relevance vector machine for regression.

9.23 ($\star\star$) **www** In Section 7.2.1 we used direct maximization of the marginal likelihood to derive the re-estimation equations (7.87) and (7.88) for finding values of the hyperparameters $\boldsymbol{\alpha}$ and β for the regression RVM. Similarly, in Section 9.3.4 we used the EM algorithm to maximize the same marginal likelihood, giving the re-estimation equations (9.67) and (9.68). Show that these two sets of re-estimation equations are formally equivalent.

9.24 ($\star$) Verify the relation (9.70) in which $\mathcal{L}(q, \boldsymbol{\theta})$ and $\mathrm{KL}(q\|p)$ are defined by (9.71) and (9.72), respectively.

9.25 ($\star$) **www** Show that the lower bound $\mathcal{L}(q, \boldsymbol{\theta})$ given by (9.71), with $q(\mathbf{Z}) = p(\mathbf{Z}|\mathbf{X}, \boldsymbol{\theta}^{(\text{old})})$, has the same gradient with respect to $\boldsymbol{\theta}$ as the log likelihood function $\ln p(\mathbf{X}|\boldsymbol{\theta})$ at the point $\boldsymbol{\theta} = \boldsymbol{\theta}^{(\text{old})}$.

9.26 ($\star$) **www** Consider the incremental form of the EM algorithm for a mixture of Gaussians, in which the responsibilities are recomputed only for a specific data point $\mathbf{x}_m$. Starting from the M-step formulae (9.17) and (9.18), derive the results (9.78) and (9.79) for updating the component means.

9.27 ($\star\star$) Derive M-step formulae for updating the covariance matrices and mixing coefficients in a Gaussian mixture model when the responsibilities are updated incrementally, analogous to the result (9.78) for updating the means.

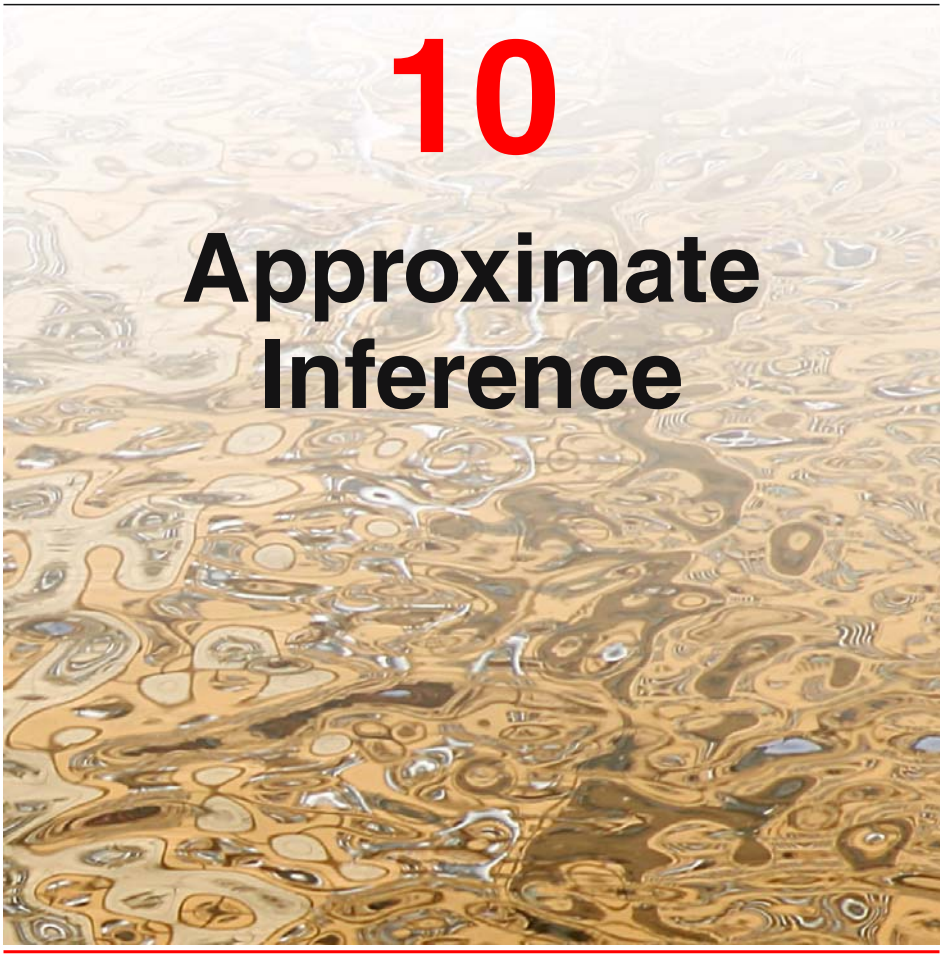

10 Approximate Inference

A central task in the application of probabilistic models is the evaluation of the posterior distribution $p(\mathbf{Z}|\mathbf{X})$ of the latent variables $\mathbf{Z}$ given the observed (visible) data variables $\mathbf{X}$, and the evaluation of expectations computed with respect to this distribution. The model might also contain some deterministic parameters, which we will leave implicit for the moment, or it may be a fully Bayesian model in which any unknown parameters are given prior distributions and are absorbed into the set of latent variables denoted by the vector $\mathbf{Z}$. For instance, in the EM algorithm we need to evaluate the expectation of the complete-data log likelihood with respect to the posterior distribution of the latent variables. For many models of practical interest, it will be infeasible to evaluate the posterior distribution or indeed to compute expectations with respect to this distribution. This could be because the dimensionality of the latent space is too high to work with directly or because the posterior distribution has a highly complex form for which expectations are not analytically tractable. In the case of continuous variables, the required integrations may not have closed-form

analytical solutions, while the dimensionality of the space and the complexity of the integrand may prohibit numerical integration. For discrete variables, the marginalizations involve summing over all possible configurations of the hidden variables, and though this is always possible in principle, we often find in practice that there may be exponentially many hidden states so that exact calculation is prohibitively expensive.

In such situations, we need to resort to approximation schemes, and these fall broadly into two classes, according to whether they rely on stochastic or deterministic approximations. Stochastic techniques such as Markov chain Monte Carlo, described in Chapter 11, have enabled the widespread use of Bayesian methods across many domains. They generally have the property that given infinite computational resource, they can generate exact results, and the approximation arises from the use of a finite amount of processor time. In practice, sampling methods can be computationally demanding, often limiting their use to small-scale problems. Also, it can be difficult to know whether a sampling scheme is generating independent samples from the required distribution.

In this chapter, we introduce a range of deterministic approximation schemes, some of which scale well to large applications. These are based on analytical approximations to the posterior distribution, for example by assuming that it factorizes in a particular way or that it has a specific parametric form such as a Gaussian. As such, they can never generate exact results, and so their strengths and weaknesses are complementary to those of sampling methods.

In Section 4.4, we discussed the Laplace approximation, which is based on a local Gaussian approximation to a mode (i.e., a maximum) of the distribution. Here we turn to a family of approximation techniques called *variational inference* or *variational Bayes*, which use more global criteria and which have been widely applied. We conclude with a brief introduction to an alternative variational framework known as *expectation propagation*.

10.1. Variational Inference

Variational methods have their origins in the 18^{th} century with the work of Euler, Lagrange, and others on the *calculus of variations*. Standard calculus is concerned with finding derivatives of functions. We can think of a function as a mapping that takes the value of a variable as the input and returns the value of the function as the output. The derivative of the function then describes how the output value varies as we make infinitesimal changes to the input value. Similarly, we can define a *functional* as a mapping that takes a function as the input and that returns the value of the functional as the output. An example would be the entropy $\mathrm{H}[p]$, which takes a probability distribution $p(x)$ as the input and returns the quantity

$$\mathrm{H}[p] = \int p(x) \ln p(x) \, \mathrm{d}x \tag{10.1}$$

as the output. We can the introduce the concept of a *functional derivative*, which expresses how the value of the functional changes in response to infinitesimal changes to the input function (Feynman *et al.*, 1964). The rules for the calculus of variations mirror those of standard calculus and are discussed in Appendix D. Many problems can be expressed in terms of an optimization problem in which the quantity being optimized is a functional. The solution is obtained by exploring all possible input functions to find the one that maximizes, or minimizes, the functional. Variational methods have broad applicability and include such areas as finite element methods (Kapur, 1989) and maximum entropy (Schwarz, 1988).

Although there is nothing intrinsically approximate about variational methods, they do naturally lend themselves to finding approximate solutions. This is done by restricting the range of functions over which the optimization is performed, for instance by considering only quadratic functions or by considering functions composed of a linear combination of fixed basis functions in which only the coefficients of the linear combination can vary. In the case of applications to probabilistic inference, the restriction may for example take the form of factorization assumptions (Jordan *et al.*, 1999; Jaakkola, 2001).

Now let us consider in more detail how the concept of variational optimization can be applied to the inference problem. Suppose we have a fully Bayesian model in which all parameters are given prior distributions. The model may also have latent variables as well as parameters, and we shall denote the set of all latent variables and parameters by $\mathbf{Z}$. Similarly, we denote the set of all observed variables by $\mathbf{X}$. For example, we might have a set of N independent, identically distributed data, for which $\mathbf{X} = \{\mathbf{x}_1, \ldots, \mathbf{x}_N\}$ and $\mathbf{Z} = \{\mathbf{z}_1, \ldots, \mathbf{z}_N\}$. Our probabilistic model specifies the joint distribution $p(\mathbf{X}, \mathbf{Z})$, and our goal is to find an approximation for the posterior distribution $p(\mathbf{Z}|\mathbf{X})$ as well as for the model evidence $p(\mathbf{X})$. As in our discussion of EM, we can decompose the log marginal probability using

$$\ln p(\mathbf{X}) = \mathcal{L}(q) + \mathrm{KL}(q\|p) \tag{10.2}$$

where we have defined

$$\mathcal{L}(q) = \int q(\mathbf{Z}) \ln \left\{ \frac{p(\mathbf{X}, \mathbf{Z})}{q(\mathbf{Z})} \right\} \mathrm{d}\mathbf{Z} \tag{10.3}$$

$$\mathrm{KL}(q\|p) = -\int q(\mathbf{Z}) \ln \left\{ \frac{p(\mathbf{Z}|\mathbf{X})}{q(\mathbf{Z})} \right\} \mathrm{d}\mathbf{Z}. \tag{10.4}$$

This differs from our discussion of EM only in that the parameter vector $\boldsymbol{\theta}$ no longer appears, because the parameters are now stochastic variables and are absorbed into $\mathbf{Z}$. Since in this chapter we will mainly be interested in continuous variables we have used integrations rather than summations in formulating this decomposition. However, the analysis goes through unchanged if some or all of the variables are discrete simply by replacing the integrations with summations as required. As before, we can maximize the lower bound $\mathcal{L}(q)$ by optimization with respect to the distribution $q(\mathbf{Z})$, which is equivalent to minimizing the KL divergence. If we allow any possible choice for $q(\mathbf{Z})$, then the maximum of the lower bound occurs when the KL divergence vanishes, which occurs when $q(\mathbf{Z})$ equals the posterior distribution $p(\mathbf{Z}|\mathbf{X})$.

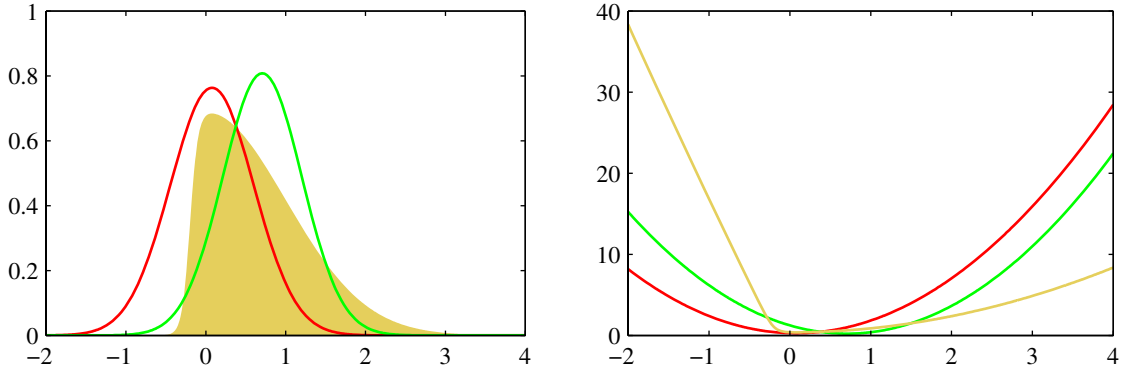

Figure 10.1 Illustration of the variational approximation for the example considered earlier in Figure 4.14. The left-hand plot shows the original distribution (yellow) along with the Laplace (red) and variational (green) approximations, and the right-hand plot shows the negative logarithms of the corresponding curves.

However, we shall suppose the model is such that working with the true posterior distribution is intractable.

We therefore consider instead a restricted family of distributions $q(\mathbf{Z})$ and then seek the member of this family for which the KL divergence is minimized. Our goal is to restrict the family sufficiently that they comprise only tractable distributions, while at the same time allowing the family to be sufficiently rich and flexible that it can provide a good approximation to the true posterior distribution. It is important to emphasize that the restriction is imposed purely to achieve tractability, and that subject to this requirement we should use as rich a family of approximating distributions as possible. In particular, there is no 'over-fitting' associated with highly flexible distributions. Using more flexible approximations simply allows us to approach the true posterior distribution more closely.

One way to restrict the family of approximating distributions is to use a parametric distribution $q(\mathbf{Z}|\boldsymbol{\omega})$ governed by a set of parameters $\boldsymbol{\omega}$. The lower bound $\mathcal{L}(q)$ then becomes a function of $\boldsymbol{\omega}$, and we can exploit standard nonlinear optimization techniques to determine the optimal values for the parameters. An example of this approach, in which the variational distribution is a Gaussian and we have optimized with respect to its mean and variance, is shown in Figure 10.1.

10.1.1 Factorized distributions

Here we consider an alternative way in which to restrict the family of distributions $q(\mathbf{Z})$. Suppose we partition the elements of $\mathbf{Z}$ into disjoint groups that we denote by $\mathbf{Z}_i$ where $i = 1, \ldots, M$. We then assume that the q distribution factorizes with respect to these groups, so that

$$q(\mathbf{Z}) = \prod_{i=1}^{M} q_i(\mathbf{Z}_i). \tag{10.5}$$

It should be emphasized that we are making no further assumptions about the distribution. In particular, we place no restriction on the functional forms of the individual factors $q_i(\mathbf{Z}_i)$. This factorized form of variational inference corresponds to an approximation framework developed in physics called *mean field theory* (Parisi, 1988).

Amongst all distributions $q(\mathbf{Z})$ having the form (10.5), we now seek that distribution for which the lower bound $\mathcal{L}(q)$ is largest. We therefore wish to make a free form (variational) optimization of $\mathcal{L}(q)$ with respect to all of the distributions $q_i(\mathbf{Z}_i)$, which we do by optimizing with respect to each of the factors in turn. To achieve this, we first substitute (10.5) into (10.3) and then dissect out the dependence on one of the factors $q_j(\mathbf{Z}_j)$. Denoting $q_j(\mathbf{Z}_j)$ by simply q_j to keep the notation uncluttered, we then obtain

$$\begin{aligned}\mathcal{L}(q) &= \int \prod_i q_i \left\{ \ln p(\mathbf{X}, \mathbf{Z}) - \sum_i \ln q_i \right\} \mathrm{d}\mathbf{Z} \\ &= \int q_j \left\{ \int \ln p(\mathbf{X}, \mathbf{Z}) \prod_{i \neq j} q_i \, \mathrm{d}\mathbf{Z}_i \right\} \mathrm{d}\mathbf{Z}_j - \int q_j \ln q_j \, \mathrm{d}\mathbf{Z}_j + \text{const} \\ &= \int q_j \ln \widetilde{p}(\mathbf{X}, \mathbf{Z}_j) \, \mathrm{d}\mathbf{Z}_j - \int q_j \ln q_j \, \mathrm{d}\mathbf{Z}_j + \text{const} \end{aligned} \tag{10.6}$$

where we have defined a new distribution $\widetilde{p}(\mathbf{X}, \mathbf{Z}_j)$ by the relation

$$\ln \widetilde{p}(\mathbf{X}, \mathbf{Z}_j) = \mathbb{E}_{i \neq j}[\ln p(\mathbf{X}, \mathbf{Z})] + \text{const}. \tag{10.7}$$

Here the notation $\mathbb{E}_{i \neq j}[\cdots]$ denotes an expectation with respect to the q distributions over all variables $\mathbf{z}_i$ for $i \neq j$, so that

$$\mathbb{E}_{i \neq j}[\ln p(\mathbf{X}, \mathbf{Z})] = \int \ln p(\mathbf{X}, \mathbf{Z}) \prod_{i \neq j} q_i \, \mathrm{d}\mathbf{Z}_i. \tag{10.8}$$

Now suppose we keep the $\{q_{i \neq j}\}$ fixed and maximize $\mathcal{L}(q)$ in (10.6) with respect to all possible forms for the distribution $q_j(\mathbf{Z}_j)$. This is easily done by recognizing that (10.6) is a negative Kullback-Leibler divergence between $q_j(\mathbf{Z}_j)$ and $\widetilde{p}(\mathbf{X}, \mathbf{Z}_j)$. Thus maximizing (10.6) is equivalent to minimizing the Kullback-Leibler

Leonhard Euler
1707–1783

Euler was a Swiss mathematician and physicist who worked in St. Petersburg and Berlin and who is widely considered to be one of the greatest mathematicians of all time. He is certainly the most prolific, and his collected works fill 75 volumes. Amongst his many contributions, he formulated the modern theory of the function, he developed (together with Lagrange) the calculus of variations, and he discovered the formula $e^{i\pi} = -1$, which relates four of the most important numbers in mathematics. During the last 17 years of his life, he was almost totally blind, and yet he produced nearly half of his results during this period.

divergence, and the minimum occurs when $q_j(\mathbf{Z}_j) = \widetilde{p}(\mathbf{X}, \mathbf{Z}_j)$. Thus we obtain a general expression for the optimal solution $q_j^\star(\mathbf{Z}_j)$ given by

$$\ln q_j^\star(\mathbf{Z}_j) = \mathbb{E}_{i \neq j}[\ln p(\mathbf{X}, \mathbf{Z})] + \text{const.} \tag{10.9}$$

It is worth taking a few moments to study the form of this solution as it provides the basis for applications of variational methods. It says that the log of the optimal solution for factor q_j is obtained simply by considering the log of the joint distribution over all hidden and visible variables and then taking the expectation with respect to all of the other factors $\{q_i\}$ for $i \neq j$.

The additive constant in (10.9) is set by normalizing the distribution $q_j^\star(\mathbf{Z}_j)$. Thus if we take the exponential of both sides and normalize, we have

$$q_j^\star(\mathbf{Z}_j) = \frac{\exp\left(\mathbb{E}_{i \neq j}[\ln p(\mathbf{X}, \mathbf{Z})]\right)}{\displaystyle\int \exp\left(\mathbb{E}_{i \neq j}[\ln p(\mathbf{X}, \mathbf{Z})]\right) \, \mathrm{d}\mathbf{Z}_j}.$$

In practice, we shall find it more convenient to work with the form (10.9) and then reinstate the normalization constant (where required) by inspection. This will become clear from subsequent examples.

The set of equations given by (10.9) for $j = 1, \ldots, M$ represent a set of consistency conditions for the maximum of the lower bound subject to the factorization constraint. However, they do not represent an explicit solution because the expression on the right-hand side of (10.9) for the optimum $q_j^\star(\mathbf{Z}_j)$ depends on expectations computed with respect to the other factors $q_i(\mathbf{Z}_i)$ for $i \neq j$. We will therefore seek a consistent solution by first initializing all of the factors $q_i(\mathbf{Z}_i)$ appropriately and then cycling through the factors and replacing each in turn with a revised estimate given by the right-hand side of (10.9) evaluated using the current estimates for all of the other factors. Convergence is guaranteed because bound is convex with respect to each of the factors $q_i(\mathbf{Z}_i)$ (Boyd and Vandenberghe, 2004).

10.1.2 Properties of factorized approximations

Our approach to variational inference is based on a factorized approximation to the true posterior distribution. Let us consider for a moment the problem of approximating a general distribution by a factorized distribution. To begin with, we discuss the problem of approximating a Gaussian distribution using a factorized Gaussian, which will provide useful insight into the types of inaccuracy introduced in using factorized approximations. Consider a Gaussian distribution $p(\mathbf{z}) = \mathcal{N}(\mathbf{z}|\boldsymbol{\mu}, \boldsymbol{\Lambda}^{-1})$ over two correlated variables $\mathbf{z} = (z_1, z_2)$ in which the mean and precision have elements

$$\boldsymbol{\mu} = \begin{pmatrix} \mu_1 \\ \mu_2 \end{pmatrix}, \qquad \boldsymbol{\Lambda} = \begin{pmatrix} \Lambda_{11} & \Lambda_{12} \\ \Lambda_{21} & \Lambda_{22} \end{pmatrix} \tag{10.10}$$

and $\Lambda_{21} = \Lambda_{12}$ due to the symmetry of the precision matrix. Now suppose we wish to approximate this distribution using a factorized Gaussian of the form $q(\mathbf{z}) = q_1(z_1)q_2(z_2)$. We first apply the general result (10.9) to find an expression for the

optimal factor $q_1^\star(z_1)$. In doing so it is useful to note that on the right-hand side we only need to retain those terms that have some functional dependence on z_1 because all other terms can be absorbed into the normalization constant. Thus we have

$$\begin{aligned}\ln q_1^\star(z_1) &= \mathbb{E}_{z_2}[\ln p(\mathbf{z})] + \text{const} \\ &= \mathbb{E}_{z_2}\left[-\frac{1}{2}(z_1-\mu_1)^2\Lambda_{11} - (z_1-\mu_1)\Lambda_{12}(z_2-\mu_2)\right] + \text{const} \\ &= -\frac{1}{2}z_1^2\Lambda_{11} + z_1\mu_1\Lambda_{11} - z_1\Lambda_{12}\left(\mathbb{E}[z_2]-\mu_2\right) + \text{const}. \end{aligned} \tag{10.11}$$

Next we observe that the right-hand side of this expression is a quadratic function of z_1, and so we can identify $q^\star(z_1)$ as a Gaussian distribution. It is worth emphasizing that we did not assume that $q(z_i)$ is Gaussian, but rather we derived this result by variational optimization of the KL divergence over all possible distributions $q(z_i)$. Note also that we do not need to consider the additive constant in (10.9) explicitly because it represents the normalization constant that can be found at the end by inspection if required. Using the technique of completing the square, we can identify the mean and precision of this Gaussian, giving

Section 2.3.1

$$q^\star(z_1) = \mathcal{N}(z_1|m_1, \Lambda_{11}^{-1}) \tag{10.12}$$

where

$$m_1 = \mu_1 - \Lambda_{11}^{-1}\Lambda_{12}\left(\mathbb{E}[z_2]-\mu_2\right). \tag{10.13}$$

By symmetry, $q_2^\star(z_2)$ is also Gaussian and can be written as

$$q_2^\star(z_2) = \mathcal{N}(z_2|m_2, \Lambda_{22}^{-1}) \tag{10.14}$$

in which

$$m_2 = \mu_2 - \Lambda_{22}^{-1}\Lambda_{21}\left(\mathbb{E}[z_1]-\mu_1\right). \tag{10.15}$$

Note that these solutions are coupled, so that $q^\star(z_1)$ depends on expectations computed with respect to $q^\star(z_2)$ and vice versa. In general, we address this by treating the variational solutions as re-estimation equations and cycling through the variables in turn updating them until some convergence criterion is satisfied. We shall see an example of this shortly. Here, however, we note that the problem is sufficiently simple that a closed form solution can be found. In particular, because $\mathbb{E}[z_1] = m_1$ and $\mathbb{E}[z_2] = m_2$, we see that the two equations are satisfied if we take $\mathbb{E}[z_1] = \mu_1$ and $\mathbb{E}[z_2] = \mu_2$, and it is easily shown that this is the only solution provided the distribution is nonsingular. This result is illustrated in Figure 10.2(a). We see that the mean is correctly captured but that the variance of $q(\mathbf{z})$ is controlled by the direction of smallest variance of $p(\mathbf{z})$, and that the variance along the orthogonal direction is significantly under-estimated. It is a general result that a factorized variational approximation tends to give approximations to the posterior distribution that are too compact.

Exercise 10.2

By way of comparison, suppose instead that we had been minimizing the reverse Kullback-Leibler divergence $\mathrm{KL}(p\|q)$. As we shall see, this form of KL divergence

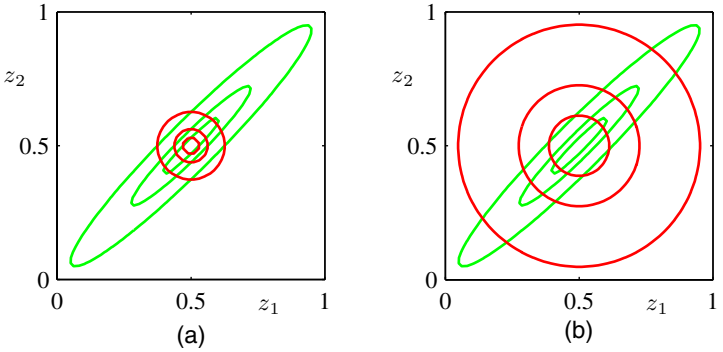

Figure 10.2 Comparison of the two alternative forms for the Kullback-Leibler divergence. The green contours corresponding to 1, 2, and 3 standard deviations for a correlated Gaussian distribution $p(\mathbf{z})$ over two variables z_1 and z_2, and the red contours represent the corresponding levels for an approximating distribution $q(\mathbf{z})$ over the same variables given by the product of two independent univariate Gaussian distributions whose parameters are obtained by minimization of (a) the Kullback-Leibler divergence $\mathrm{KL}(q\|p)$, and (b) the reverse Kullback-Leibler divergence $\mathrm{KL}(p\|q)$.

Section 10.7

is used in an alternative approximate inference framework called *expectation propagation*. We therefore consider the general problem of minimizing $\mathrm{KL}(p\|q)$ when $q(\mathbf{Z})$ is a factorized approximation of the form (10.5). The KL divergence can then be written in the form

$$\mathrm{KL}(p\|q) = -\int p(\mathbf{Z}) \left[\sum_{i=1}^{M} \ln q_i(\mathbf{Z}_i) \right] \mathrm{d}\mathbf{Z} + \text{const} \tag{10.16}$$

Exercise 10.3

where the constant term is simply the entropy of $p(\mathbf{Z})$ and so does not depend on $q(\mathbf{Z})$. We can now optimize with respect to each of the factors $q_j(\mathbf{Z}_j)$, which is easily done using a Lagrange multiplier to give

$$q_j^\star(\mathbf{Z}_j) = \int p(\mathbf{Z}) \prod_{i \neq j} \mathrm{d}\mathbf{Z}_i = p(\mathbf{Z}_j). \tag{10.17}$$

In this case, we find that the optimal solution for $q_j(\mathbf{Z}_j)$ is just given by the corresponding marginal distribution of $p(\mathbf{Z})$. Note that this is a closed-form solution and so does not require iteration.

To apply this result to the illustrative example of a Gaussian distribution $p(\mathbf{z})$ over a vector $\mathbf{z}$ we can use (2.98), which gives the result shown in Figure 10.2(b). We see that once again the mean of the approximation is correct, but that it places significant probability mass in regions of variable space that have very low probability.

The difference between these two results can be understood by noting that there is a large positive contribution to the Kullback-Leibler divergence

$$\mathrm{KL}(q\|p) = -\int q(\mathbf{Z}) \ln \left\{ \frac{p(\mathbf{Z})}{q(\mathbf{Z})} \right\} \mathrm{d}\mathbf{Z} \tag{10.18}$$

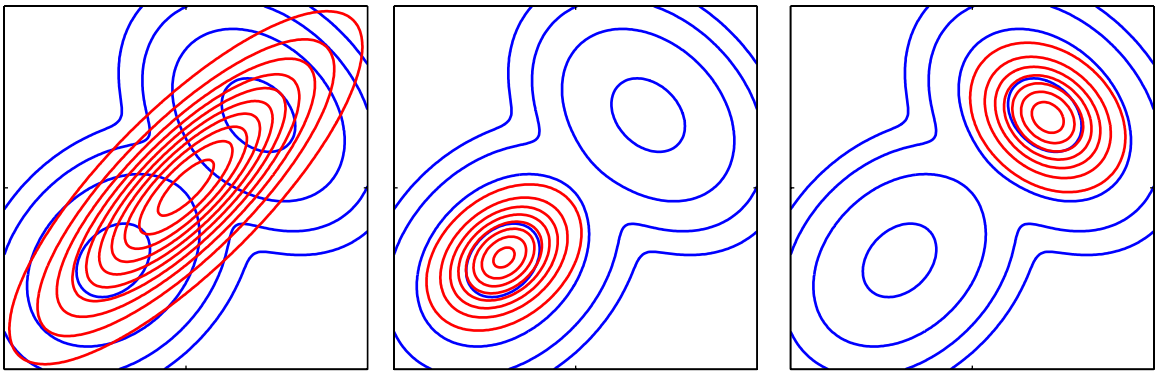

Figure 10.3 Another comparison of the two alternative forms for the Kullback-Leibler divergence. (a) The blue contours show a bimodal distribution $p(\mathbf{Z})$ given by a mixture of two Gaussians, and the red contours correspond to the single Gaussian distribution $q(\mathbf{Z})$ that best approximates $p(\mathbf{Z})$ in the sense of minimizing the Kullback-Leibler divergence $\mathrm{KL}(p\|q)$. (b) As in (a) but now the red contours correspond to a Gaussian distribution $q(\mathbf{Z})$ found by numerical minimization of the Kullback-Leibler divergence $\mathrm{KL}(q\|p)$. (c) As in (b) but showing a different local minimum of the Kullback-Leibler divergence.

from regions of $\mathbf{Z}$ space in which $p(\mathbf{Z})$ is near zero unless $q(\mathbf{Z})$ is also close to zero. Thus minimizing this form of KL divergence leads to distributions $q(\mathbf{Z})$ that avoid regions in which $p(\mathbf{Z})$ is small. Conversely, the Kullback-Leibler divergence $\mathrm{KL}(p\|q)$ is minimized by distributions $q(\mathbf{Z})$ that are nonzero in regions where $p(\mathbf{Z})$ is nonzero.

We can gain further insight into the different behaviour of the two KL divergences if we consider approximating a multimodal distribution by a unimodal one, as illustrated in Figure 10.3. In practical applications, the true posterior distribution will often be multimodal, with most of the posterior mass concentrated in some number of relatively small regions of parameter space. These multiple modes may arise through nonidentifiability in the latent space or through complex nonlinear dependence on the parameters. Both types of multimodality were encountered in Chapter 9 in the context of Gaussian mixtures, where they manifested themselves as multiple maxima in the likelihood function, and a variational treatment based on the minimization of $\mathrm{KL}(q\|p)$ will tend to find one of these modes. By contrast, if we were to minimize $\mathrm{KL}(p\|q)$, the resulting approximations would average across all of the modes and, in the context of the mixture model, would lead to poor predictive distributions (because the average of two good parameter values is typically itself not a good parameter value). It is possible to make use of $\mathrm{KL}(p\|q)$ to define a useful inference procedure, but this requires a rather different approach to the one discussed here, and will be considered in detail when we discuss expectation propagation.

Section 10.7

The two forms of Kullback-Leibler divergence are members of the *alpha family*

of divergences (Ali and Silvey, 1966; Amari, 1985; Minka, 2005) defined by

$$\mathrm{D}_\alpha(p\|q) = \frac{4}{1-\alpha^2}\left(1 - \int p(x)^{(1+\alpha)/2} q(x)^{(1-\alpha)/2}\,\mathrm{d}x\right) \tag{10.19}$$

where $-\infty < \alpha < \infty$ is a continuous parameter. The Kullback-Leibler divergence $\mathrm{KL}(p\|q)$ corresponds to the limit $\alpha \to 1$, whereas $\mathrm{KL}(q\|p)$ corresponds to the limit $\alpha \to -1$. For all values of α we have $\mathrm{D}_\alpha(p\|q) \geqslant 0$, with equality if, and only if, $p(x) = q(x)$. Suppose $p(x)$ is a fixed distribution, and we minimize $\mathrm{D}_\alpha(p\|q)$ with respect to some set of distributions $q(x)$. Then for $\alpha \leqslant -1$ the divergence is *zero forcing*, so that any values of x for which $p(x) = 0$ will have $q(x) = 0$, and typically $q(x)$ will under-estimate the support of $p(x)$ and will tend to seek the mode with the largest mass. Conversely for $\alpha \geqslant 1$ the divergence is *zero-avoiding*, so that values of x for which $p(x) > 0$ will have $q(x) > 0$, and typically $q(x)$ will stretch to cover all of $p(x)$, and will over-estimate the support of $p(x)$. When $\alpha = 0$ we obtain a symmetric divergence that is linearly related to the *Hellinger distance* given by

Exercise 10.6

$$\mathrm{D}_\mathrm{H}(p\|q) = \int \left(p(x)^{1/2} - q(x)^{1/2}\right)\,\mathrm{d}x. \tag{10.20}$$

The square root of the Hellinger distance is a valid distance metric.

10.1.3 Example: The univariate Gaussian

We now illustrate the factorized variational approximation using a Gaussian distribution over a single variable x (MacKay, 2003). Our goal is to infer the posterior distribution for the mean μ and precision τ, given a data set $\mathcal{D} = \{x_1, \ldots, x_N\}$ of observed values of x which are assumed to be drawn independently from the Gaussian. The likelihood function is given by

$$p(\mathcal{D}|\mu,\tau) = \left(\frac{\tau}{2\pi}\right)^{N/2} \exp\left\{-\frac{\tau}{2}\sum_{n=1}^{N}(x_n-\mu)^2\right\}. \tag{10.21}$$

We now introduce conjugate prior distributions for μ and τ given by

$$p(\mu|\tau) = \mathcal{N}\left(\mu|\mu_0, (\lambda_0\tau)^{-1}\right) \tag{10.22}$$

$$p(\tau) = \mathrm{Gam}(\tau|a_0, b_0) \tag{10.23}$$

where $\mathrm{Gam}(\tau|a_0, b_0)$ is the gamma distribution defined by (2.146). Together these distributions constitute a Gaussian-Gamma conjugate prior distribution.

Section 2.3.6

For this simple problem the posterior distribution can be found exactly, and again takes the form of a Gaussian-gamma distribution. However, for tutorial purposes we will consider a factorized variational approximation to the posterior distribution given by

Exercise 2.44

$$q(\mu,\tau) = q_\mu(\mu)q_\tau(\tau). \tag{10.24}$$

Note that the true posterior distribution does not factorize in this way. The optimum factors $q_\mu(\mu)$ and $q_\tau(\tau)$ can be obtained from the general result (10.9) as follows. For $q_\mu(\mu)$ we have

$$\begin{aligned}\ln q_\mu^\star(\mu) &= \mathbb{E}_\tau\left[\ln p(\mathcal{D}|\mu,\tau)+\ln p(\mu|\tau)\right]+\text{const} \\ &= -\frac{\mathbb{E}[\tau]}{2}\left\{\lambda_0(\mu-\mu_0)^2+\sum_{n=1}^{N}(x_n-\mu)^2\right\}+\text{const}. \quad (10.25)\end{aligned}$$

Completing the square over μ we see that $q_\mu(\mu)$ is a Gaussian $\mathcal{N}\left(\mu|\mu_N,\lambda_N^{-1}\right)$ with mean and precision given by

Exercise 10.7

$$\mu_N = \frac{\lambda_0\mu_0+N\overline{x}}{\lambda_0+N} \quad (10.26)$$

$$\lambda_N = (\lambda_0+N)\mathbb{E}[\tau]. \quad (10.27)$$

Note that for $N\to\infty$ this gives the maximum likelihood result in which $\mu_N=\overline{x}$ and the precision is infinite.

Similarly, the optimal solution for the factor $q_\tau(\tau)$ is given by

$$\begin{aligned}\ln q_\tau^\star(\tau) &= \mathbb{E}_\mu\left[\ln p(\mathcal{D}|\mu,\tau)+\ln p(\mu|\tau)\right]+\ln p(\tau)+\text{const} \\ &= (a_0-1)\ln\tau-b_0\tau+\frac{N}{2}\ln\tau \\ &\quad -\frac{\tau}{2}\mathbb{E}_\mu\left[\sum_{n=1}^{N}(x_n-\mu)^2+\lambda_0(\mu-\mu_0)^2\right]+\text{const} \quad (10.28)\end{aligned}$$

and hence $q_\tau(\tau)$ is a gamma distribution $\text{Gam}(\tau|a_N,b_N)$ with parameters

$$a_N = a_0+\frac{N}{2} \quad (10.29)$$

$$b_N = b_0+\frac{1}{2}\mathbb{E}_\mu\left[\sum_{n=1}^{N}(x_n-\mu)^2+\lambda_0(\mu-\mu_0)^2\right]. \quad (10.30)$$

Exercise 10.8

Again this exhibits the expected behaviour when $N\to\infty$.

It should be emphasized that we did not assume these specific functional forms for the optimal distributions $q_\mu(\mu)$ and $q_\tau(\tau)$. They arose naturally from the structure of the likelihood function and the corresponding conjugate priors.

Section 10.4.1

Thus we have expressions for the optimal distributions $q_\mu(\mu)$ and $q_\tau(\tau)$ each of which depends on moments evaluated with respect to the other distribution. One approach to finding a solution is therefore to make an initial guess for, say, the moment $\mathbb{E}[\tau]$ and use this to re-compute the distribution $q_\mu(\mu)$. Given this revised distribution we can then extract the required moments $\mathbb{E}[\mu]$ and $\mathbb{E}[\mu^2]$, and use these to recompute the distribution $q_\tau(\tau)$, and so on. Since the space of hidden variables for this example is only two dimensional, we can illustrate the variational approximation to the posterior distribution by plotting contours of both the true posterior and the factorized approximation, as illustrated in Figure 10.4.

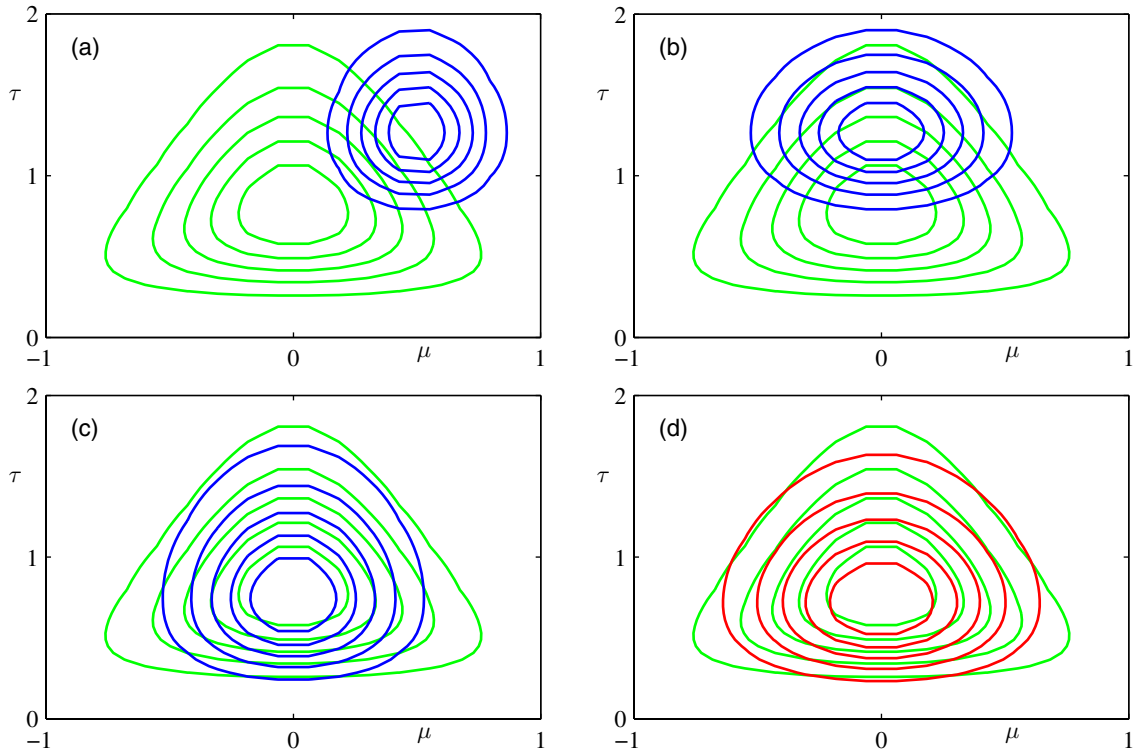

Figure 10.4 Illustration of variational inference for the mean μ and precision τ of a univariate Gaussian distribution. Contours of the true posterior distribution $p(\mu, \tau|D)$ are shown in green. (a) Contours of the initial factorized approximation $q_\mu(\mu)q_\tau(\tau)$ are shown in blue. (b) After re-estimating the factor $q_\mu(\mu)$. (c) After re-estimating the factor $q_\tau(\tau)$. (d) Contours of the optimal factorized approximation, to which the iterative scheme converges, are shown in red.

In general, we will need to use an iterative approach such as this in order to solve for the optimal factorized posterior distribution. For the very simple example we are considering here, however, we can find an explicit solution by solving the simultaneous equations for the optimal factors $q_\mu(\mu)$ and $q_\tau(\tau)$. Before doing this, we can simplify these expressions by considering broad, noninformative priors in which $\mu_0 = a_0 = b_0 = \lambda_0 = 0$. Although these parameter settings correspond to improper priors, we see that the posterior distribution is still well defined. Using the standard result $\mathbb{E}[\tau] = a_N/b_N$ for the mean of a gamma distribution, together with (10.29) and (10.30), we have

Appendix B

$$\frac{1}{\mathbb{E}[\tau]} = \mathbb{E}\left[\frac{1}{N}\sum_{n=1}^{N}(x_n - \mu)^2\right] = \overline{x^2} - 2\overline{x}\mathbb{E}[\mu] + \mathbb{E}[\mu^2]. \tag{10.31}$$

Then, using (10.26) and (10.27), we obtain the first and second order moments of

$q_\mu(\mu)$ in the form

$$\mathbb{E}[\mu] = \overline{x}, \qquad \mathbb{E}[\mu^2] = \overline{x}^2 + \frac{1}{N\mathbb{E}[\tau]}. \tag{10.32}$$

Exercise 10.9 We can now substitute these moments into (10.31) and then solve for $\mathbb{E}[\tau]$ to give

$$\begin{aligned} \frac{1}{\mathbb{E}[\tau]} &= \frac{1}{N-1}(\overline{x^2} - \overline{x}^2) \\ &= \frac{1}{N-1}\sum_{n=1}^{N}(x_n - \overline{x})^2. \end{aligned} \tag{10.33}$$

We recognize the right-hand side as the familiar unbiased estimator for the variance of a univariate Gaussian distribution, and so we see that the use of a Bayesian approach has avoided the bias of the maximum likelihood solution.

Section 1.2.4

10.1.4 Model comparison

As well as performing inference over the hidden variables $\mathbf{Z}$, we may also wish to compare a set of candidate models, labelled by the index m, and having prior probabilities $p(m)$. Our goal is then to approximate the posterior probabilities $p(m|\mathbf{X})$, where $\mathbf{X}$ is the observed data. This is a slightly more complex situation than that considered so far because different models may have different structure and indeed different dimensionality for the hidden variables $\mathbf{Z}$. We cannot therefore simply consider a factorized approximation $q(\mathbf{Z})q(m)$, but must instead recognize that the posterior over $\mathbf{Z}$ must be conditioned on m, and so we must consider $q(\mathbf{Z}, m) = q(\mathbf{Z}|m)q(m)$. We can readily verify the following decomposition based on this variational distribution

Exercise 10.10

$$\ln p(\mathbf{X}) = \mathcal{L}_m - \sum_m \sum_{\mathbf{Z}} q(\mathbf{Z}|m)q(m) \ln \left\{ \frac{p(\mathbf{Z}, m|\mathbf{X})}{q(\mathbf{Z}|m)q(m)} \right\} \tag{10.34}$$

where the $\mathcal{L}_m$ is a lower bound on $\ln p(\mathbf{X})$ and is given by

$$\mathcal{L}_m = \sum_m \sum_{\mathbf{Z}} q(\mathbf{Z}|m)q(m) \ln \left\{ \frac{p(\mathbf{Z}, \mathbf{X}, m)}{q(\mathbf{Z}|m)q(m)} \right\}. \tag{10.35}$$

Here we are assuming discrete $\mathbf{Z}$, but the same analysis applies to continuous latent variables provided the summations are replaced with integrations. We can maximize $\mathcal{L}_m$ with respect to the distribution $q(m)$ using a Lagrange multiplier, with the result

Exercise 10.11

$$q(m) \propto p(m) \exp\{\mathcal{L}_m\}. \tag{10.36}$$

However, if we maximize $\mathcal{L}_m$ with respect to the $q(\mathbf{Z}|m)$, we find that the solutions for different m are coupled, as we expect because they are conditioned on m. We proceed instead by first optimizing each of the $q(\mathbf{Z}|m)$ individually by optimization

of (10.35), and then subsequently determining the $q(m)$ using (10.36). After normalization the resulting values for $q(m)$ can be used for model selection or model averaging in the usual way.

10.2. Illustration: Variational Mixture of Gaussians

We now return to our discussion of the Gaussian mixture model and apply the variational inference machinery developed in the previous section. This will provide a good illustration of the application of variational methods and will also demonstrate how a Bayesian treatment elegantly resolves many of the difficulties associated with the maximum likelihood approach (Attias, 1999b). The reader is encouraged to work through this example in detail as it provides many insights into the practical application of variational methods. Many Bayesian models, corresponding to much more sophisticated distributions, can be solved by straightforward extensions and generalizations of this analysis.

Our starting point is the likelihood function for the Gaussian mixture model, illustrated by the graphical model in Figure 9.6. For each observation $\mathbf{x}_n$ we have a corresponding latent variable $\mathbf{z}_n$ comprising a 1-of-K binary vector with elements z_{nk} for $k = 1, \ldots, K$. As before we denote the observed data set by $\mathbf{X} = \{\mathbf{x}_1, \ldots, \mathbf{x}_N\}$, and similarly we denote the latent variables by $\mathbf{Z} = \{\mathbf{z}_1, \ldots, \mathbf{z}_N\}$. From (9.10) we can write down the conditional distribution of $\mathbf{Z}$, given the mixing coefficients $\boldsymbol{\pi}$, in the form

$$p(\mathbf{Z}|\boldsymbol{\pi}) = \prod_{n=1}^{N}\prod_{k=1}^{K} \pi_k^{z_{nk}}. \tag{10.37}$$

Similarly, from (9.11), we can write down the conditional distribution of the observed data vectors, given the latent variables and the component parameters

$$p(\mathbf{X}|\mathbf{Z}, \boldsymbol{\mu}, \boldsymbol{\Lambda}) = \prod_{n=1}^{N}\prod_{k=1}^{K} \mathcal{N}\left(\mathbf{x}_n|\boldsymbol{\mu}_k, \boldsymbol{\Lambda}_k^{-1}\right)^{z_{nk}} \tag{10.38}$$

where $\boldsymbol{\mu} = \{\boldsymbol{\mu}_k\}$ and $\boldsymbol{\Lambda} = \{\boldsymbol{\Lambda}_k\}$. Note that we are working in terms of precision matrices rather than covariance matrices as this somewhat simplifies the mathematics.

Next we introduce priors over the parameters $\boldsymbol{\mu}$, $\boldsymbol{\Lambda}$ and $\boldsymbol{\pi}$. The analysis is considerably simplified if we use conjugate prior distributions. We therefore choose a Dirichlet distribution over the mixing coefficients $\boldsymbol{\pi}$

Section 10.4.1

$$p(\boldsymbol{\pi}) = \mathrm{Dir}(\boldsymbol{\pi}|\boldsymbol{\alpha}_0) = C(\boldsymbol{\alpha}_0)\prod_{k=1}^{K} \pi_k^{\alpha_0 - 1} \tag{10.39}$$

where by symmetry we have chosen the same parameter α_0 for each of the components, and $C(\boldsymbol{\alpha}_0)$ is the normalization constant for the Dirichlet distribution defined

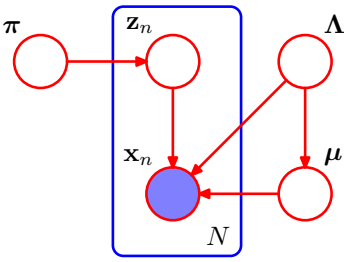

Figure 10.5 Directed acyclic graph representing the Bayesian mixture of Gaussians model, in which the box (plate) denotes a set of N i.i.d. observations. Here $\boldsymbol{\mu}$ denotes $\{\boldsymbol{\mu}_k\}$ and $\boldsymbol{\Lambda}$ denotes $\{\boldsymbol{\Lambda}_k\}$.

Section 2.2.1

by (B.23). As we have seen, the parameter α_0 can be interpreted as the effective prior number of observations associated with each component of the mixture. If the value of α_0 is small, then the posterior distribution will be influenced primarily by the data rather than by the prior.

Similarly, we introduce an independent Gaussian-Wishart prior governing the mean and precision of each Gaussian component, given by

$$\begin{aligned} p(\boldsymbol{\mu}, \boldsymbol{\Lambda}) &= p(\boldsymbol{\mu}|\boldsymbol{\Lambda})p(\boldsymbol{\Lambda}) \\ &= \prod_{k=1}^{K} \mathcal{N}\left(\boldsymbol{\mu}_k|\mathbf{m}_0, (\beta_0\boldsymbol{\Lambda}_k)^{-1}\right) \mathcal{W}(\boldsymbol{\Lambda}_k|\mathbf{W}_0, \nu_0) \end{aligned} \tag{10.40}$$

because this represents the conjugate prior distribution when both the mean and precision are unknown. Typically we would choose $\mathbf{m}_0 = \mathbf{0}$ by symmetry.

Section 2.3.6

The resulting model can be represented as a directed graph as shown in Figure 10.5. Note that there is a link from $\boldsymbol{\Lambda}$ to $\boldsymbol{\mu}$ since the variance of the distribution over $\boldsymbol{\mu}$ in (10.40) is a function of $\boldsymbol{\Lambda}$.

This example provides a nice illustration of the distinction between latent variables and parameters. Variables such as $\mathbf{z}_n$ that appear inside the plate are regarded as latent variables because the number of such variables grows with the size of the data set. By contrast, variables such as $\boldsymbol{\mu}$ that are outside the plate are fixed in number independently of the size of the data set, and so are regarded as parameters. From the perspective of graphical models, however, there is really no fundamental difference between them.

10.2.1 Variational distribution

In order to formulate a variational treatment of this model, we next write down the joint distribution of all of the random variables, which is given by

$$p(\mathbf{X}, \mathbf{Z}, \boldsymbol{\pi}, \boldsymbol{\mu}, \boldsymbol{\Lambda}) = p(\mathbf{X}|\mathbf{Z}, \boldsymbol{\mu}, \boldsymbol{\Lambda})p(\mathbf{Z}|\boldsymbol{\pi})p(\boldsymbol{\pi})p(\boldsymbol{\mu}|\boldsymbol{\Lambda})p(\boldsymbol{\Lambda}) \tag{10.41}$$

in which the various factors are defined above. The reader should take a moment to verify that this decomposition does indeed correspond to the probabilistic graphical model shown in Figure 10.5. Note that only the variables $\mathbf{X} = \{\mathbf{x}_1, \ldots, \mathbf{x}_N\}$ are observed.

We now consider a variational distribution which factorizes between the latent variables and the parameters so that

$$q(\mathbf{Z}, \boldsymbol{\pi}, \boldsymbol{\mu}, \boldsymbol{\Lambda}) = q(\mathbf{Z})q(\boldsymbol{\pi}, \boldsymbol{\mu}, \boldsymbol{\Lambda}). \tag{10.42}$$

It is remarkable that this is the *only* assumption that we need to make in order to obtain a tractable practical solution to our Bayesian mixture model. In particular, the functional form of the factors $q(\mathbf{Z})$ and $q(\boldsymbol{\pi}, \boldsymbol{\mu}, \boldsymbol{\Lambda})$ will be determined automatically by optimization of the variational distribution. Note that we are omitting the subscripts on the q distributions, much as we do with the p distributions in (10.41), and are relying on the arguments to distinguish the different distributions.

The corresponding sequential update equations for these factors can be easily derived by making use of the general result (10.9). Let us consider the derivation of the update equation for the factor $q(\mathbf{Z})$. The log of the optimized factor is given by

$$\ln q^\star(\mathbf{Z}) = \mathbb{E}_{\boldsymbol{\pi},\boldsymbol{\mu},\boldsymbol{\Lambda}}[\ln p(\mathbf{X}, \mathbf{Z}, \boldsymbol{\pi}, \boldsymbol{\mu}, \boldsymbol{\Lambda})] + \text{const}. \tag{10.43}$$

We now make use of the decomposition (10.41). Note that we are only interested in the functional dependence of the right-hand side on the variable $\mathbf{Z}$. Thus any terms that do not depend on $\mathbf{Z}$ can be absorbed into the additive normalization constant, giving

$$\ln q^\star(\mathbf{Z}) = \mathbb{E}_{\boldsymbol{\pi}}[\ln p(\mathbf{Z}|\boldsymbol{\pi})] + \mathbb{E}_{\boldsymbol{\mu},\boldsymbol{\Lambda}}[\ln p(\mathbf{X}|\mathbf{Z}, \boldsymbol{\mu}, \boldsymbol{\Lambda})] + \text{const}. \tag{10.44}$$

Substituting for the two conditional distributions on the right-hand side, and again absorbing any terms that are independent of $\mathbf{Z}$ into the additive constant, we have

$$\ln q^\star(\mathbf{Z}) = \sum_{n=1}^{N}\sum_{k=1}^{K} z_{nk} \ln \rho_{nk} + \text{const} \tag{10.45}$$

where we have defined

$$\begin{aligned} \ln \rho_{nk} &= \mathbb{E}[\ln \pi_k] + \frac{1}{2}\mathbb{E}\left[\ln |\boldsymbol{\Lambda}_k|\right] - \frac{D}{2}\ln(2\pi) \\ &\quad -\frac{1}{2}\mathbb{E}_{\boldsymbol{\mu}_k,\boldsymbol{\Lambda}_k}\left[(\mathbf{x}_n - \boldsymbol{\mu}_k)^{\mathrm{T}}\boldsymbol{\Lambda}_k(\mathbf{x}_n - \boldsymbol{\mu}_k)\right] \end{aligned} \tag{10.46}$$

where D is the dimensionality of the data variable $\mathbf{x}$. Taking the exponential of both sides of (10.45) we obtain

$$q^\star(\mathbf{Z}) \propto \prod_{n=1}^{N}\prod_{k=1}^{K} \rho_{nk}^{z_{nk}}. \tag{10.47}$$

Requiring that this distribution be normalized, and noting that for each value of n the quantities z_{nk} are binary and sum to 1 over all values of k, we obtain

Exercise 10.12

$$q^\star(\mathbf{Z}) = \prod_{n=1}^{N}\prod_{k=1}^{K} r_{nk}^{z_{nk}} \tag{10.48}$$

where

$$r_{nk} = \frac{\rho_{nk}}{\sum_{j=1}^{K} \rho_{nj}}. \tag{10.49}$$

We see that the optimal solution for the factor $q(\mathbf{Z})$ takes the same functional form as the prior $p(\mathbf{Z}|\boldsymbol{\pi})$. Note that because ρ_{nk} is given by the exponential of a real quantity, the quantities r_{nk} will be nonnegative and will sum to one, as required.

For the discrete distribution $q^\star(\mathbf{Z})$ we have the standard result

$$\mathbb{E}[z_{nk}] = r_{nk} \tag{10.50}$$

from which we see that the quantities r_{nk} are playing the role of responsibilities. Note that the optimal solution for $q^\star(\mathbf{Z})$ depends on moments evaluated with respect to the distributions of other variables, and so again the variational update equations are coupled and must be solved iteratively.

At this point, we shall find it convenient to define three statistics of the observed data set evaluated with respect to the responsibilities, given by

$$N_k = \sum_{n=1}^{N} r_{nk} \tag{10.51}$$

$$\overline{\mathbf{x}}_k = \frac{1}{N_k} \sum_{n=1}^{N} r_{nk} \mathbf{x}_n \tag{10.52}$$

$$\mathbf{S}_k = \frac{1}{N_k} \sum_{n=1}^{N} r_{nk} (\mathbf{x}_n - \overline{\mathbf{x}}_k)(\mathbf{x}_n - \overline{\mathbf{x}}_k)^{\mathrm{T}}. \tag{10.53}$$

Note that these are analogous to quantities evaluated in the maximum likelihood EM algorithm for the Gaussian mixture model.

Now let us consider the factor $q(\boldsymbol{\pi}, \boldsymbol{\mu}, \boldsymbol{\Lambda})$ in the variational posterior distribution. Again using the general result (10.9) we have

$$\ln q^\star(\boldsymbol{\pi}, \boldsymbol{\mu}, \boldsymbol{\Lambda}) = \ln p(\boldsymbol{\pi}) + \sum_{k=1}^{K} \ln p(\boldsymbol{\mu}_k, \boldsymbol{\Lambda}_k) + \mathbb{E}_{\mathbf{Z}} \left[\ln p(\mathbf{Z}|\boldsymbol{\pi}) \right]$$
$$+ \sum_{k=1}^{K} \sum_{n=1}^{N} \mathbb{E}[z_{nk}] \ln \mathcal{N}\left(\mathbf{x}_n | \boldsymbol{\mu}_k, \boldsymbol{\Lambda}_k^{-1} \right) + \text{const}. \tag{10.54}$$

We observe that the right-hand side of this expression decomposes into a sum of terms involving only $\boldsymbol{\pi}$ together with terms only involving $\boldsymbol{\mu}$ and $\boldsymbol{\Lambda}$, which implies that the variational posterior $q(\boldsymbol{\pi}, \boldsymbol{\mu}, \boldsymbol{\Lambda})$ factorizes to give $q(\boldsymbol{\pi})q(\boldsymbol{\mu}, \boldsymbol{\Lambda})$. Furthermore, the terms involving $\boldsymbol{\mu}$ and $\boldsymbol{\Lambda}$ themselves comprise a sum over k of terms involving $\boldsymbol{\mu}_k$ and $\boldsymbol{\Lambda}_k$ leading to the further factorization

$$q(\boldsymbol{\pi}, \boldsymbol{\mu}, \boldsymbol{\Lambda}) = q(\boldsymbol{\pi}) \prod_{k=1}^{K} q(\boldsymbol{\mu}_k, \boldsymbol{\Lambda}_k). \tag{10.55}$$

Identifying the terms on the right-hand side of (10.54) that depend on $\boldsymbol{\pi}$, we have

$$\ln q^\star(\boldsymbol{\pi}) = (\alpha_0 - 1)\sum_{k=1}^{K} \ln \pi_k + \sum_{k=1}^{K}\sum_{n=1}^{N} r_{nk} \ln \pi_k + \text{const} \tag{10.56}$$

where we have used (10.50). Taking the exponential of both sides, we recognize $q^\star(\boldsymbol{\pi})$ as a Dirichlet distribution

$$q^\star(\boldsymbol{\pi}) = \text{Dir}(\boldsymbol{\pi}|\boldsymbol{\alpha}) \tag{10.57}$$

where $\boldsymbol{\alpha}$ has components α_k given by

$$\alpha_k = \alpha_0 + N_k. \tag{10.58}$$

Finally, the variational posterior distribution $q^\star(\boldsymbol{\mu}_k, \boldsymbol{\Lambda}_k)$ does not factorize into the product of the marginals, but we can always use the product rule to write it in the form $q^\star(\boldsymbol{\mu}_k, \boldsymbol{\Lambda}_k) = q^\star(\boldsymbol{\mu}_k|\boldsymbol{\Lambda}_k)q^\star(\boldsymbol{\Lambda}_k)$. The two factors can be found by inspecting (10.54) and reading off those terms that involve $\boldsymbol{\mu}_k$ and $\boldsymbol{\Lambda}_k$. The result, as expected, is a Gaussian-Wishart distribution and is given by

Exercise 10.13

$$q^\star(\boldsymbol{\mu}_k, \boldsymbol{\Lambda}_k) = \mathcal{N}\left(\boldsymbol{\mu}_k|\mathbf{m}_k, (\beta_k\boldsymbol{\Lambda}_k)^{-1}\right)\, \mathcal{W}(\boldsymbol{\Lambda}_k|\mathbf{W}_k, \nu_k) \tag{10.59}$$

where we have defined

$$\begin{aligned}
\beta_k &= \beta_0 + N_k && (10.60)\\
\mathbf{m}_k &= \frac{1}{\beta_k}(\beta_0\mathbf{m}_0 + N_k\overline{\mathbf{x}}_k) && (10.61)\\
\mathbf{W}_k^{-1} &= \mathbf{W}_0^{-1} + N_k\mathbf{S}_k + \frac{\beta_0 N_k}{\beta_0 + N_k}(\overline{\mathbf{x}}_k - \mathbf{m}_0)(\overline{\mathbf{x}}_k - \mathbf{m}_0)^{\mathrm{T}} && (10.62)\\
\nu_k &= \nu_0 + N_k. && (10.63)
\end{aligned}$$

These update equations are analogous to the M-step equations of the EM algorithm for the maximum likelihood solution of the mixture of Gaussians. We see that the computations that must be performed in order to update the variational posterior distribution over the model parameters involve evaluation of the same sums over the data set, as arose in the maximum likelihood treatment.

In order to perform this variational M step, we need the expectations $\mathbb{E}[z_{nk}] = r_{nk}$ representing the responsibilities. These are obtained by normalizing the ρ_{nk} that are given by (10.46). We see that this expression involves expectations with respect to the variational distributions of the parameters, and these are easily evaluated to give

Exercise 10.14

$$\begin{aligned}
&\mathbb{E}_{\boldsymbol{\mu}_k,\boldsymbol{\Lambda}_k}\left[(\mathbf{x}_n - \boldsymbol{\mu}_k)^{\mathrm{T}}\boldsymbol{\Lambda}_k(\mathbf{x}_n - \boldsymbol{\mu}_k)\right]\\
&\qquad = D\beta_k^{-1} + \nu_k(\mathbf{x}_n - \mathbf{m}_k)^{\mathrm{T}}\mathbf{W}_k(\mathbf{x}_n - \mathbf{m}_k) && (10.64)\\
\ln\widetilde{\Lambda}_k \equiv \mathbb{E}\left[\ln|\boldsymbol{\Lambda}_k|\right] &= \sum_{i=1}^{D}\psi\left(\frac{\nu_k + 1 - i}{2}\right) + D\ln 2 + \ln|\mathbf{W}_k| && (10.65)\\
\ln\widetilde{\pi}_k \equiv \mathbb{E}\left[\ln\pi_k\right] &= \psi(\alpha_k) - \psi(\widehat{\alpha}) && (10.66)
\end{aligned}$$

where we have introduced definitions of $\widetilde{\Lambda}_k$ and $\widetilde{\pi}_k$, and $\psi(\cdot)$ is the digamma function defined by (B.25), with $\widehat{\alpha} = \sum_k \alpha_k$. The results (10.65) and (10.66) follow from the standard properties of the Wishart and Dirichlet distributions.

Appendix B

If we substitute (10.64), (10.65), and (10.66) into (10.46) and make use of (10.49), we obtain the following result for the responsibilities

$$r_{nk} \propto \widetilde{\pi}_k \widetilde{\Lambda}_k^{1/2} \exp\left\{-\frac{D}{2\beta_k} - \frac{\nu_k}{2}(\mathbf{x}_n - \mathbf{m}_k)^{\mathrm{T}} \mathbf{W}_k (\mathbf{x}_n - \mathbf{m}_k)\right\}. \tag{10.67}$$

Notice the similarity to the corresponding result for the responsibilities in maximum likelihood EM, which from (9.13) can be written in the form

$$r_{nk} \propto \pi_k |\boldsymbol{\Lambda}_k|^{1/2} \exp\left\{-\frac{1}{2}(\mathbf{x}_n - \boldsymbol{\mu}_k)^{\mathrm{T}} \boldsymbol{\Lambda}_k (\mathbf{x}_n - \boldsymbol{\mu}_k)\right\} \tag{10.68}$$

where we have used the precision in place of the covariance to highlight the similarity to (10.67).

Thus the optimization of the variational posterior distribution involves cycling between two stages analogous to the E and M steps of the maximum likelihood EM algorithm. In the variational equivalent of the E step, we use the current distributions over the model parameters to evaluate the moments in (10.64), (10.65), and (10.66) and hence evaluate $\mathbb{E}[z_{nk}] = r_{nk}$. Then in the subsequent variational equivalent of the M step, we keep these responsibilities fixed and use them to re-compute the variational distribution over the parameters using (10.57) and (10.59). In each case, we see that the variational posterior distribution has the same functional form as the corresponding factor in the joint distribution (10.41). This is a general result and is a consequence of the choice of conjugate distributions.

Section 10.4.1

Figure 10.6 shows the results of applying this approach to the rescaled Old Faithful data set for a Gaussian mixture model having $K = 6$ components. We see that after convergence, there are only two components for which the expected values of the mixing coefficients are numerically distinguishable from their prior values. This effect can be understood qualitatively in terms of the automatic trade-off in a Bayesian model between fitting the data and the complexity of the model, in which the complexity penalty arises from components whose parameters are pushed away from their prior values. Components that take essentially no responsibility for explaining the data points have $r_{nk} \simeq 0$ and hence $N_k \simeq 0$. From (10.58), we see that $\alpha_k \simeq \alpha_0$ and from (10.60)–(10.63) we see that the other parameters revert to their prior values. In principle such components are fitted slightly to the data points, but for broad priors this effect is too small to be seen numerically. For the variational Gaussian mixture model the expected values of the mixing coefficients in the posterior distribution are given by

Section 3.4

Exercise 10.15

$$\mathbb{E}[\pi_k] = \frac{\alpha_k + N_k}{K\alpha_0 + N}. \tag{10.69}$$

Consider a component for which $N_k \simeq 0$ and $\alpha_k \simeq \alpha_0$. If the prior is broad so that $\alpha_0 \to 0$, then $\mathbb{E}[\pi_k] \to 0$ and the component plays no role in the model, whereas if

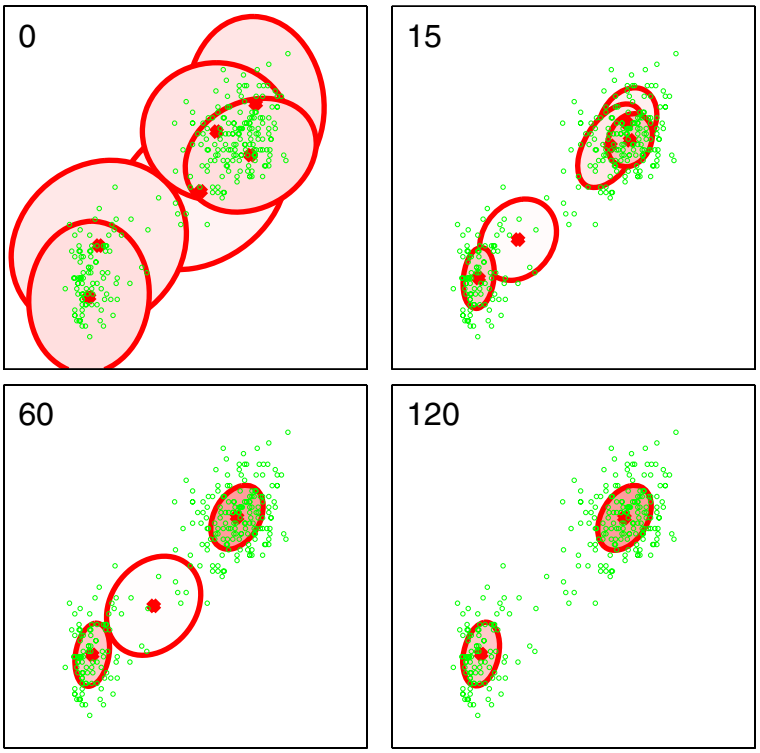

Figure 10.6 Variational Bayesian mixture of $K = 6$ Gaussians applied to the Old Faithful data set, in which the ellipses denote the one standard-deviation density contours for each of the components, and the density of red ink inside each ellipse corresponds to the mean value of the mixing coefficient for each component. The number in the top left of each diagram shows the number of iterations of variational inference. Components whose expected mixing coefficient are numerically indistinguishable from zero are not plotted.

the prior tightly constrains the mixing coefficients so that $\alpha_0 \to \infty$, then $\mathbb{E}[\pi_k] \to 1/K$.

In Figure 10.6, the prior over the mixing coefficients is a Dirichlet of the form (10.39). Recall from Figure 2.5 that for $\alpha_0 < 1$ the prior favours solutions in which some of the mixing coefficients are zero. Figure 10.6 was obtained using $\alpha_0 = 10^{-3}$, and resulted in two components having nonzero mixing coefficients. If instead we choose $\alpha_0 = 1$ we obtain three components with nonzero mixing coefficients, and for $\alpha = 10$ all six components have nonzero mixing coefficients.

As we have seen there is a close similarity between the variational solution for the Bayesian mixture of Gaussians and the EM algorithm for maximum likelihood. In fact if we consider the limit $N \to \infty$ then the Bayesian treatment converges to the maximum likelihood EM algorithm. For anything other than very small data sets, the dominant computational cost of the variational algorithm for Gaussian mixtures arises from the evaluation of the responsibilities, together with the evaluation and inversion of the weighted data covariance matrices. These computations mirror precisely those that arise in the maximum likelihood EM algorithm, and so there is little computational overhead in using this Bayesian approach as compared to the traditional maximum likelihood one. There are, however, some substantial advantages. First of all, the singularities that arise in maximum likelihood when a Gaussian component 'collapses' onto a specific data point are absent in the Bayesian treatment.

Indeed, these singularities are removed if we simply introduce a prior and then use a MAP estimate instead of maximum likelihood. Furthermore, there is no over-fitting if we choose a large number K of components in the mixture, as we saw in Figure 10.6. Finally, the variational treatment opens up the possibility of determining the optimal number of components in the mixture without resorting to techniques such as cross validation.

Section 10.2.4

10.2.2 Variational lower bound

We can also straightforwardly evaluate the lower bound (10.3) for this model. In practice, it is useful to be able to monitor the bound during the re-estimation in order to test for convergence. It can also provide a valuable check on both the mathematical expressions for the solutions and their software implementation, because at each step of the iterative re-estimation procedure the value of this bound should not decrease. We can take this a stage further to provide a deeper test of the correctness of both the mathematical derivation of the update equations and of their software implementation by using finite differences to check that each update does indeed give a (constrained) maximum of the bound (Svensén and Bishop, 2004).

For the variational mixture of Gaussians, the lower bound (10.3) is given by

$$\begin{aligned}\mathcal{L} &= \sum_{\mathbf{Z}} \iiint q(\mathbf{Z}, \boldsymbol{\pi}, \boldsymbol{\mu}, \boldsymbol{\Lambda}) \ln \left\{ \frac{p(\mathbf{X}, \mathbf{Z}, \boldsymbol{\pi}, \boldsymbol{\mu}, \boldsymbol{\Lambda})}{q(\mathbf{Z}, \boldsymbol{\pi}, \boldsymbol{\mu}, \boldsymbol{\Lambda})} \right\} \mathrm{d}\boldsymbol{\pi}\, \mathrm{d}\boldsymbol{\mu}\, \mathrm{d}\boldsymbol{\Lambda} \\ &= \mathbb{E}[\ln p(\mathbf{X}, \mathbf{Z}, \boldsymbol{\pi}, \boldsymbol{\mu}, \boldsymbol{\Lambda})] - \mathbb{E}[\ln q(\mathbf{Z}, \boldsymbol{\pi}, \boldsymbol{\mu}, \boldsymbol{\Lambda})] \\ &= \mathbb{E}[\ln p(\mathbf{X}|\mathbf{Z}, \boldsymbol{\mu}, \boldsymbol{\Lambda})] + \mathbb{E}[\ln p(\mathbf{Z}|\boldsymbol{\pi})] + \mathbb{E}[\ln p(\boldsymbol{\pi})] + \mathbb{E}[\ln p(\boldsymbol{\mu}, \boldsymbol{\Lambda})] \\ &\quad - \mathbb{E}[\ln q(\mathbf{Z})] - \mathbb{E}[\ln q(\boldsymbol{\pi})] - \mathbb{E}[\ln q(\boldsymbol{\mu}, \boldsymbol{\Lambda})] \end{aligned} \tag{10.70}$$

where, to keep the notation uncluttered, we have omitted the $\star$ superscript on the q distributions, along with the subscripts on the expectation operators because each expectation is taken with respect to all of the random variables in its argument. The various terms in the bound are easily evaluated to give the following results

Exercise 10.16

$$\begin{aligned}\mathbb{E}[\ln p(\mathbf{X}|\mathbf{Z}, \boldsymbol{\mu}, \boldsymbol{\Lambda})] = \frac{1}{2} \sum_{k=1}^{K} N_k \Big\{ &\ln \widetilde{\Lambda}_k - D\beta_k^{-1} - \nu_k \mathrm{Tr}(\mathbf{S}_k \mathbf{W}_k) \\ &- \nu_k (\overline{\mathbf{x}}_k - \mathbf{m}_k)^{\mathrm{T}} \mathbf{W}_k (\overline{\mathbf{x}}_k - \mathbf{m}_k) - D \ln(2\pi) \Big\} \end{aligned} \tag{10.71}$$

$$\mathbb{E}[\ln p(\mathbf{Z}|\boldsymbol{\pi})] = \sum_{n=1}^{N} \sum_{k=1}^{K} r_{nk} \ln \widetilde{\pi}_k \tag{10.72}$$

$$\mathbb{E}[\ln p(\boldsymbol{\pi})] = \ln C(\boldsymbol{\alpha}_0) + (\alpha_0 - 1) \sum_{k=1}^{K} \ln \widetilde{\pi}_k \tag{10.73}$$

$$\mathbb{E}[\ln p(\boldsymbol{\mu}, \boldsymbol{\Lambda})] = \frac{1}{2}\sum_{k=1}^{K}\left\{D\ln(\beta_0/2\pi) + \ln\widetilde{\Lambda}_k - \frac{D\beta_0}{\beta_k}\right.$$
$$\left. -\beta_0\nu_k(\mathbf{m}_k - \mathbf{m}_0)^{\mathrm{T}}\mathbf{W}_k(\mathbf{m}_k - \mathbf{m}_0)\right\} + K\ln B(\mathbf{W}_0, \nu_0)$$
$$+\frac{(\nu_0 - D - 1)}{2}\sum_{k=1}^{K}\ln\widetilde{\Lambda}_k - \frac{1}{2}\sum_{k=1}^{K}\nu_k\mathrm{Tr}(\mathbf{W}_0^{-1}\mathbf{W}_k) \tag{10.74}$$

$$\mathbb{E}[\ln q(\mathbf{Z})] = \sum_{n=1}^{N}\sum_{k=1}^{K} r_{nk}\ln r_{nk} \tag{10.75}$$

$$\mathbb{E}[\ln q(\boldsymbol{\pi})] = \sum_{k=1}^{K}(\alpha_k - 1)\ln\widetilde{\pi}_k + \ln C(\boldsymbol{\alpha}) \tag{10.76}$$

$$\mathbb{E}[\ln q(\boldsymbol{\mu}, \boldsymbol{\Lambda})] = \sum_{k=1}^{K}\left\{\frac{1}{2}\ln\widetilde{\Lambda}_k + \frac{D}{2}\ln\left(\frac{\beta_k}{2\pi}\right) - \frac{D}{2} - \mathrm{H}\left[q(\boldsymbol{\Lambda}_k)\right]\right\} \tag{10.77}$$

where D is the dimensionality of $\mathbf{x}$, $\mathrm{H}[q(\boldsymbol{\Lambda}_k)]$ is the entropy of the Wishart distribution given by (B.82), and the coefficients $C(\boldsymbol{\alpha})$ and $B(\mathbf{W}, \nu)$ are defined by (B.23) and (B.79), respectively. Note that the terms involving expectations of the logs of the q distributions simply represent the negative entropies of those distributions. Some simplifications and combination of terms can be performed when these expressions are summed to give the lower bound. However, we have kept the expressions separate for ease of understanding.

Finally, it is worth noting that the lower bound provides an alternative approach for deriving the variational re-estimation equations obtained in Section 10.2.1. To do this we use the fact that, since the model has conjugate priors, the functional form of the factors in the variational posterior distribution is known, namely discrete for $\mathbf{Z}$, Dirichlet for π, and Gaussian-Wishart for $(\boldsymbol{\mu}_k, \boldsymbol{\Lambda}_k)$. By taking general parametric forms for these distributions we can derive the form of the lower bound as a function of the parameters of the distributions. Maximizing the bound with respect to these parameters then gives the required re-estimation equations.

Exercise 10.18

10.2.3 Predictive density

In applications of the Bayesian mixture of Gaussians model we will often be interested in the predictive density for a new value $\widehat{\mathbf{x}}$ of the observed variable. Associated with this observation will be a corresponding latent variable $\widehat{\mathbf{z}}$, and the predictive density is then given by

$$p(\widehat{\mathbf{x}}|\mathbf{X}) = \sum_{\widehat{\mathbf{z}}}\iiint p(\widehat{\mathbf{x}}|\widehat{\mathbf{z}}, \boldsymbol{\mu}, \boldsymbol{\Lambda})p(\widehat{\mathbf{z}}|\boldsymbol{\pi})p(\boldsymbol{\pi}, \boldsymbol{\mu}, \boldsymbol{\Lambda}|\mathbf{X})\,\mathrm{d}\boldsymbol{\pi}\,\mathrm{d}\boldsymbol{\mu}\,\mathrm{d}\boldsymbol{\Lambda} \tag{10.78}$$

where $p(\boldsymbol{\pi}, \boldsymbol{\mu}, \boldsymbol{\Lambda}|\mathbf{X})$ is the (unknown) true posterior distribution of the parameters. Using (10.37) and (10.38) we can first perform the summation over $\widehat{\mathbf{z}}$ to give

$$p(\widehat{\mathbf{x}}|\mathbf{X}) = \sum_{k=1}^{K} \iiint \pi_k \mathcal{N}\left(\widehat{\mathbf{x}}|\boldsymbol{\mu}_k, \boldsymbol{\Lambda}_k^{-1}\right) p(\boldsymbol{\pi}, \boldsymbol{\mu}, \boldsymbol{\Lambda}|\mathbf{X}) \, \mathrm{d}\boldsymbol{\pi} \, \mathrm{d}\boldsymbol{\mu} \, \mathrm{d}\boldsymbol{\Lambda}. \tag{10.79}$$

Because the remaining integrations are intractable, we approximate the predictive density by replacing the true posterior distribution $p(\boldsymbol{\pi}, \boldsymbol{\mu}, \boldsymbol{\Lambda}|\mathbf{X})$ with its variational approximation $q(\boldsymbol{\pi})q(\boldsymbol{\mu}, \boldsymbol{\Lambda})$ to give

$$p(\widehat{\mathbf{x}}|\mathbf{X}) = \sum_{k=1}^{K} \iiint \pi_k \mathcal{N}\left(\widehat{\mathbf{x}}|\boldsymbol{\mu}_k, \boldsymbol{\Lambda}_k^{-1}\right) q(\boldsymbol{\pi}) q(\boldsymbol{\mu}_k, \boldsymbol{\Lambda}_k) \, \mathrm{d}\boldsymbol{\pi} \, \mathrm{d}\boldsymbol{\mu}_k \, \mathrm{d}\boldsymbol{\Lambda}_k \tag{10.80}$$

where we have made use of the factorization (10.55) and in each term we have implicitly integrated out all variables $\{\boldsymbol{\mu}_j, \boldsymbol{\Lambda}_j\}$ for $j \neq k$ The remaining integrations can now be evaluated analytically giving a mixture of Student's t-distributions

Exercise 10.19

$$p(\widehat{\mathbf{x}}|\mathbf{X}) = \frac{1}{\widehat{\alpha}} \sum_{k=1}^{K} \alpha_k \mathrm{St}(\widehat{\mathbf{x}}|\mathbf{m}_k, \mathbf{L}_k, \nu_k + 1 - D) \tag{10.81}$$

in which the k^{th} component has mean $\mathbf{m}_k$, and the precision is given by

$$\mathbf{L}_k = \frac{(\nu_k + 1 - D)\beta_k}{(1 + \beta_k)} \mathbf{W}_k \tag{10.82}$$

in which ν_k is given by (10.63). When the size N of the data set is large the predictive distribution (10.81) reduces to a mixture of Gaussians.

Exercise 10.20

10.2.4 Determining the number of components

Section 10.1.4

We have seen that the variational lower bound can be used to determine a posterior distribution over the number K of components in the mixture model. There is, however, one subtlety that needs to be addressed. For any given setting of the parameters in a Gaussian mixture model (except for specific degenerate settings), there will exist other parameter settings for which the density over the observed variables will be identical. These parameter values differ only through a re-labelling of the components. For instance, consider a mixture of two Gaussians and a single observed variable x, in which the parameters have the values $\pi_1 = a$, $\pi_2 = b$, $\mu_1 = c$, $\mu_2 = d$, $\sigma_1 = e$, $\sigma_2 = f$. Then the parameter values $\pi_1 = b$, $\pi_2 = a$, $\mu_1 = d$, $\mu_2 = c$, $\sigma_1 = f$, $\sigma_2 = e$, in which the two components have been exchanged, will by symmetry give rise to the same value of $p(x)$. If we have a mixture model comprising K components, then each parameter setting will be a member of a family of $K!$ equivalent settings.

Exercise 10.21

In the context of maximum likelihood, this redundancy is irrelevant because the parameter optimization algorithm (for example EM) will, depending on the initialization of the parameters, find one specific solution, and the other equivalent solutions play no role. In a Bayesian setting, however, we marginalize over all possible

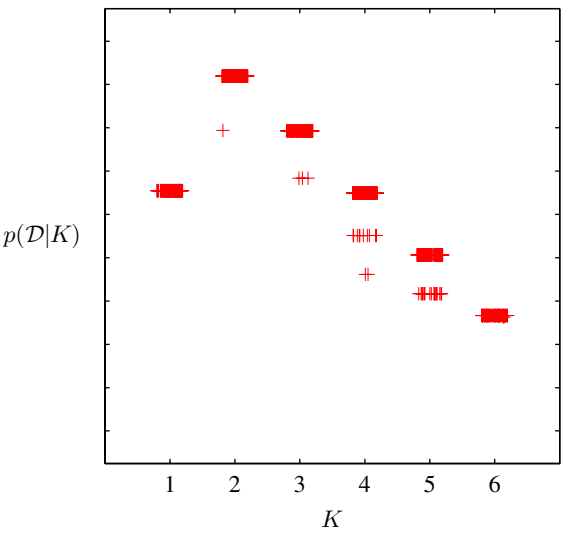

Figure 10.7 Plot of the variational lower bound $\mathcal{L}$ versus the number K of components in the Gaussian mixture model, for the Old Faithful data, showing a distinct peak at $K = 2$ components. For each value of K, the model is trained from 100 different random starts, and the results shown as '+' symbols plotted with small random horizontal perturbations so that they can be distinguished. Note that some solutions find suboptimal local maxima, but that this happens infrequently.

parameter values. We have seen in Figure 10.2 that if the true posterior distribution is multimodal, variational inference based on the minimization of $\mathrm{KL}(q\|p)$ will tend to approximate the distribution in the neighbourhood of one of the modes and ignore the others. Again, because equivalent modes have equivalent predictive densities, this is of no concern provided we are considering a model having a specific number K of components. If, however, we wish to compare different values of K, then we need to take account of this multimodality. A simple approximate solution is to add a term $\ln K!$ onto the lower bound when used for model comparison and averaging.

Exercise 10.22

Figure 10.7 shows a plot of the lower bound, including the multimodality factor, versus the number K of components for the Old Faithful data set. It is worth emphasizing once again that maximum likelihood would lead to values of the likelihood function that increase monotonically with K (assuming the singular solutions have been avoided, and discounting the effects of local maxima) and so cannot be used to determine an appropriate model complexity. By contrast, Bayesian inference automatically makes the trade-off between model complexity and fitting the data.

Section 3.4

This approach to the determination of K requires that a range of models having different K values be trained and compared. An alternative approach to determining a suitable value for K is to treat the mixing coefficients $\boldsymbol{\pi}$ as parameters and make point estimates of their values by maximizing the lower bound (Corduneanu and Bishop, 2001) with respect to $\boldsymbol{\pi}$ instead of maintaining a probability distribution over them as in the fully Bayesian approach. This leads to the re-estimation equation

Exercise 10.23

$$\pi_k = \frac{1}{N}\sum_{n=1}^{N} r_{nk} \tag{10.83}$$

and this maximization is interleaved with the variational updates for the q distribution over the remaining parameters. Components that provide insufficient contribution

to explaining the data will have their mixing coefficients driven to zero during the optimization, and so they are effectively removed from the model through *automatic relevance determination*. This allows us to make a single training run in which we start with a relatively large initial value of K, and allow surplus components to be pruned out of the model. The origins of the sparsity when optimizing with respect to hyperparameters is discussed in detail in the context of the relevance vector machine.

Section 7.2.2

10.2.5 Induced factorizations

In deriving these variational update equations for the Gaussian mixture model, we assumed a particular factorization of the variational posterior distribution given by (10.42). However, the optimal solutions for the various factors exhibit additional factorizations. In particular, the solution for $q^\star(\boldsymbol{\mu}, \boldsymbol{\Lambda})$ is given by the product of an independent distribution $q^\star(\boldsymbol{\mu}_k, \boldsymbol{\Lambda}_k)$ over each of the components k of the mixture, whereas the variational posterior distribution $q^\star(\mathbf{Z})$ over the latent variables, given by (10.48), factorizes into an independent distribution $q^\star(\mathbf{z}_n)$ for each observation n (note that it does not further factorize with respect to k because, for each value of n, the z_{nk} are constrained to sum to one over k). These additional factorizations are a consequence of the interaction between the assumed factorization and the conditional independence properties of the true distribution, as characterized by the directed graph in Figure 10.5.

We shall refer to these additional factorizations as *induced factorizations* because they arise from an interaction between the factorization assumed in the variational posterior distribution and the conditional independence properties of the true joint distribution. In a numerical implementation of the variational approach it is important to take account of such additional factorizations. For instance, it would be very inefficient to maintain a full precision matrix for the Gaussian distribution over a set of variables if the optimal form for that distribution always had a diagonal precision matrix (corresponding to a factorization with respect to the individual variables described by that Gaussian).

Such induced factorizations can easily be detected using a simple graphical test based on d-separation as follows. We partition the latent variables into three disjoint groups $\mathbf{A}, \mathbf{B}, \mathbf{C}$ and then let us suppose that we are assuming a factorization between $\mathbf{C}$ and the remaining latent variables, so that

$$q(\mathbf{A}, \mathbf{B}, \mathbf{C}) = q(\mathbf{A}, \mathbf{B})q(\mathbf{C}). \tag{10.84}$$

Using the general result (10.9), together with the product rule for probabilities, we see that the optimal solution for $q(\mathbf{A}, \mathbf{B})$ is given by

$$\begin{aligned} \ln q^\star(\mathbf{A}, \mathbf{B}) &= \mathbb{E}_{\mathbf{C}}[\ln p(\mathbf{X}, \mathbf{A}, \mathbf{B}, \mathbf{C})] + \text{const} \\ &= \mathbb{E}_{\mathbf{C}}[\ln p(\mathbf{A}, \mathbf{B}|\mathbf{X}, \mathbf{C})] + \text{const}. \end{aligned} \tag{10.85}$$

We now ask whether this resulting solution will factorize between $\mathbf{A}$ and $\mathbf{B}$, in other words whether $q^\star(\mathbf{A}, \mathbf{B}) = q^\star(\mathbf{A})q^\star(\mathbf{B})$. This will happen if, and only if, $\ln p(\mathbf{A}, \mathbf{B}|\mathbf{X}, \mathbf{C}) = \ln p(\mathbf{A}|\mathbf{X}, \mathbf{C}) + \ln p(\mathbf{B}|\mathbf{X}, \mathbf{C})$, that is, if the conditional independence relation

$$\mathbf{A} \perp\!\!\!\perp \mathbf{B} \mid \mathbf{X}, \mathbf{C} \tag{10.86}$$

is satisfied. We can test to see if this relation does hold, for any choice of $\mathbf{A}$ and $\mathbf{B}$ by making use of the d-separation criterion.

To illustrate this, consider again the Bayesian mixture of Gaussians represented by the directed graph in Figure 10.5, in which we are assuming a variational factorization given by (10.42). We can see immediately that the variational posterior distribution over the parameters must factorize between $\boldsymbol{\pi}$ and the remaining parameters $\boldsymbol{\mu}$ and $\boldsymbol{\Lambda}$ because all paths connecting $\boldsymbol{\pi}$ to either $\boldsymbol{\mu}$ or $\boldsymbol{\Lambda}$ must pass through one of the nodes $\mathbf{z}_n$ all of which are in the conditioning set for our conditional independence test and all of which are head-to-tail with respect to such paths.

10.3. Variational Linear Regression

As a second illustration of variational inference, we return to the Bayesian linear regression model of Section 3.3. In the evidence framework, we approximated the integration over α and β by making point estimates obtained by maximizing the log marginal likelihood. A fully Bayesian approach would integrate over the hyperparameters as well as over the parameters. Although exact integration is intractable, we can use variational methods to find a tractable approximation. In order to simplify the discussion, we shall suppose that the noise precision parameter β is known, and is fixed to its true value, although the framework is easily extended to include the distribution over β. For the linear regression model, the variational treatment will turn out to be equivalent to the evidence framework. Nevertheless, it provides a good exercise in the use of variational methods and will also lay the foundation for variational treatment of Bayesian logistic regression in Section 10.6.

Exercise 10.26

Recall that the likelihood function for $\mathbf{w}$, and the prior over $\mathbf{w}$, are given by

$$p(\mathbf{t}|\mathbf{w}) = \prod_{n=1}^{N} \mathcal{N}(t_n|\mathbf{w}^{\mathrm{T}}\boldsymbol{\phi}_n, \beta^{-1}) \tag{10.87}$$

$$p(\mathbf{w}|\alpha) = \mathcal{N}(\mathbf{w}|\mathbf{0}, \alpha^{-1}\mathbf{I}) \tag{10.88}$$

where $\boldsymbol{\phi}_n = \boldsymbol{\phi}(\mathbf{x}_n)$. We now introduce a prior distribution over α. From our discussion in Section 2.3.6, we know that the conjugate prior for the precision of a Gaussian is given by a gamma distribution, and so we choose

$$p(\alpha) = \mathrm{Gam}(\alpha|a_0, b_0) \tag{10.89}$$

where $\mathrm{Gam}(\cdot|\cdot,\cdot)$ is defined by (B.26). Thus the joint distribution of all the variables is given by

$$p(\mathbf{t}, \mathbf{w}, \alpha) = p(\mathbf{t}|\mathbf{w})p(\mathbf{w}|\alpha)p(\alpha). \tag{10.90}$$

This can be represented as a directed graphical model as shown in Figure 10.8.

10.3.1 Variational distribution

Our first goal is to find an approximation to the posterior distribution $p(\mathbf{w}, \alpha|\mathbf{t})$. To do this, we employ the variational framework of Section 10.1, with a variational

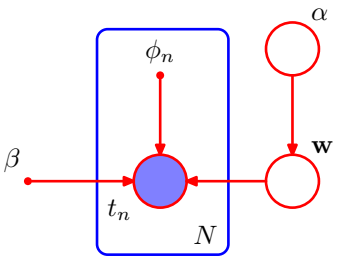

Figure 10.8 Probabilistic graphical model representing the joint distribution (10.90) for the Bayesian linear regression model.

posterior distribution given by the factorized expression

$$q(\mathbf{w}, \alpha) = q(\mathbf{w})q(\alpha). \tag{10.91}$$

We can find re-estimation equations for the factors in this distribution by making use of the general result (10.9). Recall that for each factor, we take the log of the joint distribution over all variables and then average with respect to those variables not in that factor. Consider first the distribution over α. Keeping only terms that have a functional dependence on α, we have

$$\begin{aligned} \ln q^\star(\alpha) &= \ln p(\alpha) + \mathbb{E}_{\mathbf{w}}\left[\ln p(\mathbf{w}|\alpha)\right] + \text{const} \\ &= (a_0 - 1)\ln\alpha - b_0\alpha + \frac{M}{2}\ln\alpha - \frac{\alpha}{2}\mathbb{E}[\mathbf{w}^{\mathrm{T}}\mathbf{w}] + \text{const}. \end{aligned} \tag{10.92}$$

We recognize this as the log of a gamma distribution, and so identifying the coefficients of α and $\ln\alpha$ we obtain

$$q^\star(\alpha) = \mathrm{Gam}(\alpha|a_N, b_N) \tag{10.93}$$

where

$$a_N = a_0 + \frac{M}{2} \tag{10.94}$$

$$b_N = b_0 + \frac{1}{2}\mathbb{E}[\mathbf{w}^{\mathrm{T}}\mathbf{w}]. \tag{10.95}$$

Similarly, we can find the variational re-estimation equation for the posterior distribution over $\mathbf{w}$. Again, using the general result (10.9), and keeping only those terms that have a functional dependence on $\mathbf{w}$, we have

$$\ln q^\star(\mathbf{w}) = \ln p(\mathbf{t}|\mathbf{w}) + \mathbb{E}_\alpha\left[\ln p(\mathbf{w}|\alpha)\right] + \text{const} \tag{10.96}$$

$$= -\frac{\beta}{2}\sum_{n=1}^{N}\{\mathbf{w}^{\mathrm{T}}\boldsymbol{\phi}_n - t_n\}^2 - \frac{1}{2}\mathbb{E}[\alpha]\mathbf{w}^{\mathrm{T}}\mathbf{w} + \text{const} \tag{10.97}$$

$$= -\frac{1}{2}\mathbf{w}^{\mathrm{T}}\left(\mathbb{E}[\alpha]\mathbf{I} + \beta\boldsymbol{\Phi}^{\mathrm{T}}\boldsymbol{\Phi}\right)\mathbf{w} + \beta\mathbf{w}^{\mathrm{T}}\boldsymbol{\Phi}^{\mathrm{T}}\mathbf{t} + \text{const}. \tag{10.98}$$

Because this is a quadratic form, the distribution $q^\star(\mathbf{w})$ is Gaussian, and so we can complete the square in the usual way to identify the mean and covariance, giving

$$q^\star(\mathbf{w}) = \mathcal{N}(\mathbf{w}|\mathbf{m}_N, \mathbf{S}_N) \tag{10.99}$$

where

$$\mathbf{m}_N = \beta \mathbf{S}_N \boldsymbol{\Phi}^{\mathrm{T}} \mathbf{t} \tag{10.100}$$

$$\mathbf{S}_N = \left(\mathbb{E}[\alpha] \mathbf{I} + \beta \boldsymbol{\Phi}^{\mathrm{T}} \boldsymbol{\Phi} \right)^{-1}. \tag{10.101}$$

Note the close similarity to the posterior distribution (3.52) obtained when α was treated as a fixed parameter. The difference is that here α is replaced by its expectation $\mathbb{E}[\alpha]$ under the variational distribution. Indeed, we have chosen to use the same notation for the covariance matrix $\mathbf{S}_N$ in both cases.

Using the standard results (B.27), (B.38), and (B.39), we can obtain the required moments as follows

$$\mathbb{E}[\alpha] = a_N / b_N \tag{10.102}$$

$$\mathbb{E}[\mathbf{w}\mathbf{w}^{\mathrm{T}}] = \mathbf{m}_N \mathbf{m}_N^{\mathrm{T}} + \mathbf{S}_N. \tag{10.103}$$

The evaluation of the variational posterior distribution begins by initializing the parameters of one of the distributions $q(\mathbf{w})$ or $q(\alpha)$, and then alternately re-estimates these factors in turn until a suitable convergence criterion is satisfied (usually specified in terms of the lower bound to be discussed shortly).

It is instructive to relate the variational solution to that found using the evidence framework in Section 3.5. To do this consider the case $a_0 = b_0 = 0$, corresponding to the limit of an infinitely broad prior over α. The mean of the variational posterior distribution $q(\alpha)$ is then given by

$$\mathbb{E}[\alpha] = \frac{a_N}{b_N} = \frac{M/2}{\mathbb{E}[\mathbf{w}^{\mathrm{T}}\mathbf{w}]/2} = \frac{M}{\mathbf{m}_N^{\mathrm{T}}\mathbf{m}_N + \mathrm{Tr}(\mathbf{S}_N)}. \tag{10.104}$$

Comparison with (9.63) shows that in the case of this particularly simple model, the variational approach gives precisely the same expression as that obtained by maximizing the evidence function using EM except that the point estimate for α is replaced by its expected value. Because the distribution $q(\mathbf{w})$ depends on $q(\alpha)$ only through the expectation $\mathbb{E}[\alpha]$, we see that the two approaches will give identical results for the case of an infinitely broad prior.

10.3.2 Predictive distribution

The predictive distribution over t, given a new input $\mathbf{x}$, is easily evaluated for this model using the Gaussian variational posterior for the parameters

$$\begin{aligned} p(t|\mathbf{x}, \mathbf{t}) &= \int p(t|\mathbf{x}, \mathbf{w}) p(\mathbf{w}|\mathbf{t}) \, \mathrm{d}\mathbf{w} \\ &\simeq \int p(t|\mathbf{x}, \mathbf{w}) q(\mathbf{w}) \, \mathrm{d}\mathbf{w} \\ &= \int \mathcal{N}(t|\mathbf{w}^{\mathrm{T}}\boldsymbol{\phi}(\mathbf{x}), \beta^{-1}) \mathcal{N}(\mathbf{w}|\mathbf{m}_N, \mathbf{S}_N) \, \mathrm{d}\mathbf{w} \\ &= \mathcal{N}(t|\mathbf{m}_N^{\mathrm{T}}\boldsymbol{\phi}(\mathbf{x}), \sigma^2(\mathbf{x})) \end{aligned} \tag{10.105}$$

where we have evaluated the integral by making use of the result (2.115) for the linear-Gaussian model. Here the input-dependent variance is given by

$$\sigma^2(\mathbf{x}) = \frac{1}{\beta} + \boldsymbol{\phi}(\mathbf{x})^{\mathrm{T}}\mathbf{S}_N\boldsymbol{\phi}(\mathbf{x}). \tag{10.106}$$

Note that this takes the same form as the result (3.59) obtained with fixed α except that now the expected value $\mathbb{E}[\alpha]$ appears in the definition of $\mathbf{S}_N$.

10.3.3 Lower bound

Another quantity of importance is the lower bound $\mathcal{L}$ defined by

$$\begin{aligned}\mathcal{L}(q) &= \mathbb{E}[\ln p(\mathbf{w},\alpha,\mathbf{t})] - \mathbb{E}[\ln q(\mathbf{w},\alpha)] \\ &= \mathbb{E}_{\mathbf{w}}[\ln p(\mathbf{t}|\mathbf{w})] + \mathbb{E}_{\mathbf{w},\alpha}[\ln p(\mathbf{w}|\alpha)] + \mathbb{E}_{\alpha}[\ln p(\alpha)] \\ &\quad -\mathbb{E}_{\alpha}[\ln q(\mathbf{w})]_{\mathbf{w}} - \mathbb{E}[\ln q(\alpha)].\end{aligned} \tag{10.107}$$

Exercise 10.27

Evaluation of the various terms is straightforward, making use of results obtained in previous chapters, and gives

$$\begin{aligned}\mathbb{E}[\ln p(\mathbf{t}|\mathbf{w})]_{\mathbf{w}} &= \frac{N}{2}\ln\left(\frac{\beta}{2\pi}\right) - \frac{\beta}{2}\mathbf{t}^{\mathrm{T}}\mathbf{t} + \beta\mathbf{m}_N^{\mathrm{T}}\boldsymbol{\Phi}^{\mathrm{T}}\mathbf{t} \\ &\quad -\frac{\beta}{2}\mathrm{Tr}\left[\boldsymbol{\Phi}^{\mathrm{T}}\boldsymbol{\Phi}(\mathbf{m}_N\mathbf{m}_N^{\mathrm{T}} + \mathbf{S}_N)\right] \qquad (10.108) \\ \mathbb{E}[\ln p(\mathbf{w}|\alpha)]_{\mathbf{w},\alpha} &= -\frac{M}{2}\ln(2\pi) + \frac{M}{2}(\psi(a_N) - \ln b_N) \\ &\quad -\frac{a_N}{2b_N}\left[\mathbf{m}_N^{\mathrm{T}}\mathbf{m}_N + \mathrm{Tr}(\mathbf{S}_N)\right] \qquad (10.109) \\ \mathbb{E}[\ln p(\alpha)]_{\alpha} &= a_0\ln b_0 + (a_0 - 1)\left[\psi(a_N) - \ln b_N\right] \\ &\quad -b_0\frac{a_N}{b_N} - \ln\Gamma(a_N) \qquad (10.110) \\ -\mathbb{E}[\ln q(\mathbf{w})]_{\mathbf{w}} &= \frac{1}{2}\ln|\mathbf{S}_N| + \frac{M}{2}\left[1 + \ln(2\pi)\right] \qquad (10.111) \\ -\mathbb{E}[\ln q(\alpha)]_{\alpha} &= \ln\Gamma(a_N) - (a_N - 1)\psi(a_N) - \ln b_N + a_N. \qquad (10.112)\end{aligned}$$

Figure 10.9 shows a plot of the lower bound $\mathcal{L}(q)$ versus the degree of a polynomial model for a synthetic data set generated from a degree three polynomial. Here the prior parameters have been set to $a_0 = b_0 = 0$, corresponding to the noninformative prior $p(\alpha) \propto 1/\alpha$, which is uniform over $\ln\alpha$ as discussed in Section 2.3.6. As we saw in Section 10.1, the quantity $\mathcal{L}$ represents lower bound on the log marginal likelihood $p(\mathbf{t}|M)$ for the model. If we assign equal prior probabilities $p(M)$ to the different values of M, then we can interpret $\mathcal{L}$ as an approximation to the posterior model probability $p(M|\mathbf{t})$. Thus the variational framework assigns the highest probability to the model with $M = 3$. This should be contrasted with the maximum likelihood result, which assigns ever smaller residual error to models of increasing complexity until the residual error is driven to zero, causing maximum likelihood to favour severely over-fitted models.

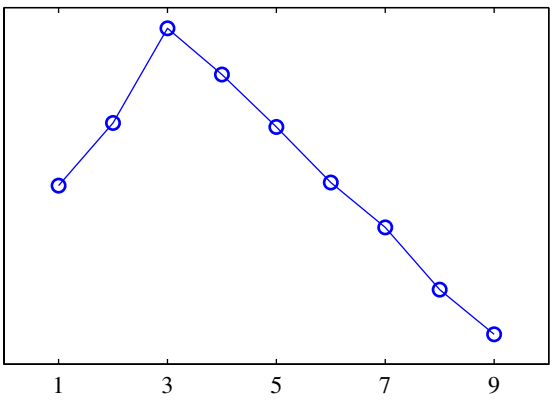

Figure 10.9 Plot of the lower bound $\mathcal{L}$ versus the order M of the polynomial, for a polynomial model, in which a set of 10 data points is generated from a polynomial with $M = 3$ sampled over the interval $(-5, 5)$ with additive Gaussian noise of variance 0.09. The value of the bound gives the log probability of the model, and we see that the value of the bound peaks at $M = 3$, corresponding to the true model from which the data set was generated.

10.4. Exponential Family Distributions

In Chapter 2, we discussed the important role played by the exponential family of distributions and their conjugate priors. For many of the models discussed in this book, the complete-data likelihood is drawn from the exponential family. However, in general this will not be the case for the marginal likelihood function for the observed data. For example, in a mixture of Gaussians, the joint distribution of observations $\mathbf{x}_n$ and corresponding hidden variables $\mathbf{z}_n$ is a member of the exponential family, whereas the marginal distribution of $\mathbf{x}_n$ is a mixture of Gaussians and hence is not.

Up to now we have grouped the variables in the model into observed variables and hidden variables. We now make a further distinction between latent variables, denoted $\mathbf{Z}$, and parameters, denoted $\boldsymbol{\theta}$, where parameters are *intensive* (fixed in number independent of the size of the data set), whereas latent variables are *extensive* (scale in number with the size of the data set). For example, in a Gaussian mixture model, the indicator variables z_{kn} (which specify which component k is responsible for generating data point $\mathbf{x}_n$) represent the latent variables, whereas the means $\boldsymbol{\mu}_k$, precisions $\boldsymbol{\Lambda}_k$ and mixing proportions π_k represent the parameters.

Consider the case of independent identically distributed data. We denote the data values by $\mathbf{X} = \{\mathbf{x}_n\}$, where $n = 1, \ldots N$, with corresponding latent variables $\mathbf{Z} = \{\mathbf{z}_n\}$. Now suppose that the joint distribution of observed and latent variables is a member of the exponential family, parameterized by natural parameters $\boldsymbol{\eta}$ so that

$$p(\mathbf{X}, \mathbf{Z}|\boldsymbol{\eta}) = \prod_{n=1}^{N} h(\mathbf{x}_n, \mathbf{z}_n) g(\boldsymbol{\eta}) \exp\left\{\boldsymbol{\eta}^{\mathrm{T}} \mathbf{u}(\mathbf{x}_n, \mathbf{z}_n)\right\}. \tag{10.113}$$

We shall also use a conjugate prior for $\boldsymbol{\eta}$, which can be written as

$$p(\boldsymbol{\eta}|\nu_0, \mathbf{v}_0) = f(\nu_0, \boldsymbol{\chi}_0) g(\boldsymbol{\eta})^{\nu_0} \exp\left\{\nu_o \boldsymbol{\eta}^{\mathrm{T}} \boldsymbol{\chi}_0\right\}. \tag{10.114}$$

Recall that the conjugate prior distribution can be interpreted as a prior number ν_0 of observations all having the value $\boldsymbol{\chi}_0$ for the $\mathbf{u}$ vector. Now consider a variational

distribution that factorizes between the latent variables and the parameters, so that $q(\mathbf{Z}, \boldsymbol{\eta}) = q(\mathbf{Z})q(\boldsymbol{\eta})$. Using the general result (10.9), we can solve for the two factors as follows

$$\begin{aligned} \ln q^\star(\mathbf{Z}) &= \mathbb{E}_{\boldsymbol{\eta}}[\ln p(\mathbf{X}, \mathbf{Z}|\boldsymbol{\eta})] + \text{const} \\ &= \sum_{n=1}^{N} \left\{ \ln h(\mathbf{x}_n, \mathbf{z}_n) + \mathbb{E}[\boldsymbol{\eta}^{\mathrm{T}}]\mathbf{u}(\mathbf{x}_n, \mathbf{z}_n) \right\} + \text{const}. \end{aligned} \tag{10.115}$$

Thus we see that this decomposes into a sum of independent terms, one for each value of n, and hence the solution for $q^\star(\mathbf{Z})$ will factorize over n so that $q^\star(\mathbf{Z}) = \prod_n q^\star(\mathbf{z}_n)$. This is an example of an induced factorization. Taking the exponential of both sides, we have

Section 10.2.5

$$q^\star(\mathbf{z}_n) = h(\mathbf{x}_n, \mathbf{z}_n) g\left(\mathbb{E}[\boldsymbol{\eta}]\right) \exp\left\{ \mathbb{E}[\boldsymbol{\eta}^{\mathrm{T}}]\mathbf{u}(\mathbf{x}_n, \mathbf{z}_n) \right\} \tag{10.116}$$

where the normalization coefficient has been re-instated by comparison with the standard form for the exponential family.

Similarly, for the variational distribution over the parameters, we have

$$\ln q^\star(\boldsymbol{\eta}) = \ln p(\boldsymbol{\eta}|\nu_0, \boldsymbol{\chi}_0) + \mathbb{E}_{\mathbf{Z}}[\ln p(\mathbf{X}, \mathbf{Z}|\boldsymbol{\eta})] + \text{const} \tag{10.117}$$

$$= \nu_0 \ln g(\boldsymbol{\eta}) + \boldsymbol{\eta}^{\mathrm{T}}\boldsymbol{\chi}_0 + \sum_{n=1}^{N} \left\{ \ln g(\boldsymbol{\eta}) + \boldsymbol{\eta}^{\mathrm{T}} \mathbb{E}_{\mathbf{z}_n}[\mathbf{u}(\mathbf{x}_n, \mathbf{z}_n)] \right\} + \text{const}. \tag{10.118}$$

Again, taking the exponential of both sides, and re-instating the normalization coefficient by inspection, we have

$$q^\star(\boldsymbol{\eta}) = f(\nu_N, \boldsymbol{\chi}_N) g(\boldsymbol{\eta})^{\nu_N} \exp\left\{ \boldsymbol{\eta}^{\mathrm{T}}\boldsymbol{\chi}_N \right\} \tag{10.119}$$

where we have defined

$$\nu_N = \nu_0 + N \tag{10.120}$$

$$\boldsymbol{\chi}_N = \boldsymbol{\chi}_0 + \sum_{n=1}^{N} \mathbb{E}_{\mathbf{z}_n}[\mathbf{u}(\mathbf{x}_n, \mathbf{z}_n)]. \tag{10.121}$$

Note that the solutions for $q^\star(\mathbf{z}_n)$ and $q^\star(\boldsymbol{\eta})$ are coupled, and so we solve them iteratively in a two-stage procedure. In the variational E step, we evaluate the expected sufficient statistics $\mathbb{E}[\mathbf{u}(\mathbf{x}_n, \mathbf{z}_n)]$ using the current posterior distribution $q(\mathbf{z}_n)$ over the latent variables and use this to compute a revised posterior distribution $q(\boldsymbol{\eta})$ over the parameters. Then in the subsequent variational M step, we use this revised parameter posterior distribution to find the expected natural parameters $\mathbb{E}[\boldsymbol{\eta}^{\mathrm{T}}]$, which gives rise to a revised variational distribution over the latent variables.

10.4.1 Variational message passing

We have illustrated the application of variational methods by considering a specific model, the Bayesian mixture of Gaussians, in some detail. This model can be

described by the directed graph shown in Figure 10.5. Here we consider more generally the use of variational methods for models described by directed graphs and derive a number of widely applicable results.

The joint distribution corresponding to a directed graph can be written using the decomposition

$$p(\mathbf{x}) = \prod_i p(\mathbf{x}_i|\mathrm{pa}_i) \tag{10.122}$$

where $\mathbf{x}_i$ denotes the variable(s) associated with node i, and pa_i denotes the parent set corresponding to node i. Note that $\mathbf{x}_i$ may be a latent variable or it may belong to the set of observed variables. Now consider a variational approximation in which the distribution $q(\mathbf{x})$ is assumed to factorize with respect to the $\mathbf{x}_i$ so that

$$q(\mathbf{x}) = \prod_i q_i(\mathbf{x}_i). \tag{10.123}$$

Note that for observed nodes, there is no factor $q(\mathbf{x}_i)$ in the variational distribution. We now substitute (10.122) into our general result (10.9) to give

$$\ln q_j^\star(\mathbf{x}_j) = \mathbb{E}_{i\neq j}\left[\sum_i \ln p(\mathbf{x}_i|\mathrm{pa}_i)\right] + \text{const.} \tag{10.124}$$

Any terms on the right-hand side that do not depend on $\mathbf{x}_j$ can be absorbed into the additive constant. In fact, the only terms that do depend on $\mathbf{x}_j$ are the conditional distribution for $\mathbf{x}_j$ given by $p(\mathbf{x}_j|\mathrm{pa}_j)$ together with any other conditional distributions that have $\mathbf{x}_j$ in the conditioning set. By definition, these conditional distributions correspond to the children of node j, and they therefore also depend on the *co-parents* of the child nodes, i.e., the other parents of the child nodes besides node $\mathbf{x}_j$ itself. We see that the set of all nodes on which $q^\star(\mathbf{x}_j)$ depends corresponds to the Markov blanket of node $\mathbf{x}_j$, as illustrated in Figure 8.26. Thus the update of the factors in the variational posterior distribution represents a local calculation on the graph. This makes possible the construction of general purpose software for variational inference in which the form of the model does not need to be specified in advance (Bishop *et al.*, 2003).

If we now specialize to the case of a model in which all of the conditional distributions have a conjugate-exponential structure, then the variational update procedure can be cast in terms of a local message passing algorithm (Winn and Bishop, 2005). In particular, the distribution associated with a particular node can be updated once that node has received messages from all of its parents and all of its children. This in turn requires that the children have already received messages from their co-parents. The evaluation of the lower bound can also be simplified because many of the required quantities are already evaluated as part of the message passing scheme. This distributed message passing formulation has good scaling properties and is well suited to large networks.

10.5. Local Variational Methods

The variational framework discussed in Sections 10.1 and 10.2 can be considered a 'global' method in the sense that it directly seeks an approximation to the full posterior distribution over all random variables. An alternative 'local' approach involves finding bounds on functions over individual variables or groups of variables within a model. For instance, we might seek a bound on a conditional distribution $p(y|x)$, which is itself just one factor in a much larger probabilistic model specified by a directed graph. The purpose of introducing the bound of course is to simplify the resulting distribution. This local approximation can be applied to multiple variables in turn until a tractable approximation is obtained, and in Section 10.6.1 we shall give a practical example of this approach in the context of logistic regression. Here we focus on developing the bounds themselves.

We have already seen in our discussion of the Kullback-Leibler divergence that the convexity of the logarithm function played a key role in developing the lower bound in the global variational approach. We have defined a (strictly) convex function as one for which every chord lies above the function. Convexity also plays a central role in the local variational framework. Note that our discussion will apply equally to concave functions with 'min' and 'max' interchanged and with lower bounds replaced by upper bounds.

Section 1.6.1

Let us begin by considering a simple example, namely the function $f(x) = \exp(-x)$, which is a convex function of x, and which is shown in the left-hand plot of Figure 10.10. Our goal is to approximate $f(x)$ by a simpler function, in particular a linear function of x. From Figure 10.10, we see that this linear function will be a lower bound on $f(x)$ if it corresponds to a tangent. We can obtain the tangent line $y(x)$ at a specific value of x, say $x = \xi$, by making a first order Taylor expansion

$$y(x) = f(\xi) + f'(\xi)(x - \xi) \tag{10.125}$$

so that $y(x) \leqslant f(x)$ with equality when $x = \xi$. For our example function $f(x) =$

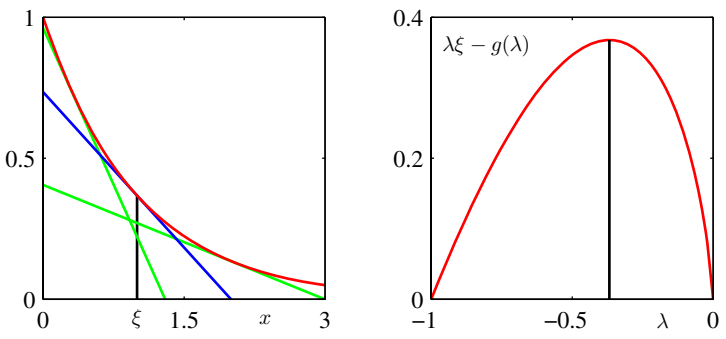

Figure 10.10 In the left-hand figure the red curve shows the function $\exp(-x)$, and the blue line shows the tangent at $x = \xi$ defined by (10.125) with $\xi = 1$. This line has slope $\lambda = f'(\xi) = -\exp(-\xi)$. Note that any other tangent line, for example the ones shown in green, will have a smaller value of y at $x = \xi$. The right-hand figure shows the corresponding plot of the function $\lambda\xi - g(\lambda)$, where $g(\lambda)$ is given by (10.131), versus λ for $\xi = 1$, in which the maximum corresponds to $\lambda = -\exp(-\xi) = -1/e$.

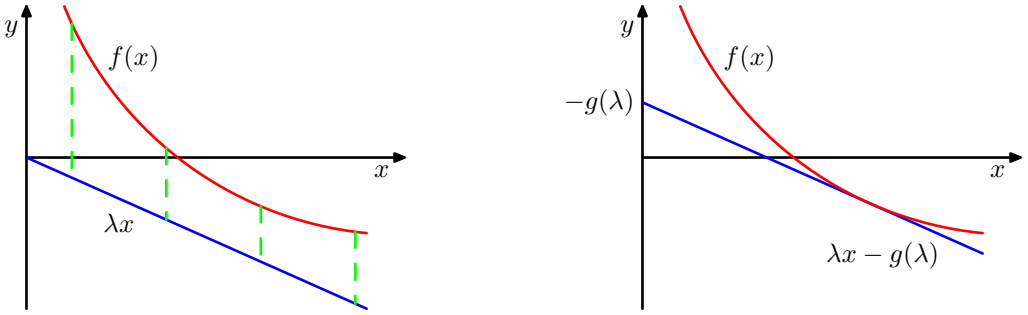

Figure 10.11 In the left-hand plot the red curve shows a convex function $f(x)$, and the blue line represents the linear function λx, which is a lower bound on $f(x)$ because $f(x) > \lambda x$ for all x. For the given value of slope λ the contact point of the tangent line having the same slope is found by minimizing with respect to x the discrepancy (shown by the green dashed lines) given by $f(x) - \lambda x$. This defines the dual function $g(\lambda)$, which corresponds to the (negative of the) intercept of the tangent line having slope λ.

$\exp(-x)$, we therefore obtain the tangent line in the form

$$y(x) = \exp(-\xi) - \exp(-\xi)(x - \xi) \tag{10.126}$$

which is a linear function parameterized by ξ. For consistency with subsequent discussion, let us define $\lambda = -\exp(-\xi)$ so that

$$y(x, \lambda) = \lambda x - \lambda + \lambda \ln(-\lambda). \tag{10.127}$$

Different values of λ correspond to different tangent lines, and because all such lines are lower bounds on the function, we have $f(x) \geqslant y(x, \lambda)$. Thus we can write the function in the form

$$f(x) = \max_{\lambda} \{\lambda x - \lambda + \lambda \ln(-\lambda)\}. \tag{10.128}$$

We have succeeded in approximating the convex function $f(x)$ by a simpler, linear function $y(x, \lambda)$. The price we have paid is that we have introduced a variational parameter λ, and to obtain the tightest bound we must optimize with respect to λ.

We can formulate this approach more generally using the framework of *convex duality* (Rockafellar, 1972; Jordan *et al.*, 1999). Consider the illustration of a convex function $f(x)$ shown in the left-hand plot in Figure 10.11. In this example, the function λx is a lower bound on $f(x)$ but it is not the best lower bound that can be achieved by a linear function having slope λ, because the tightest bound is given by the tangent line. Let us write the equation of the tangent line, having slope λ as $\lambda x - g(\lambda)$ where the (negative) intercept $g(\lambda)$ clearly depends on the slope λ of the tangent. To determine the intercept, we note that the line must be moved vertically by an amount equal to the smallest vertical distance between the line and the function, as shown in Figure 10.11. Thus

$$\begin{aligned} g(\lambda) &= -\min_{x} \{f(x) - \lambda x\} \\ &= \max_{x} \{\lambda x - f(x)\}. \end{aligned} \tag{10.129}$$

Now, instead of fixing λ and varying x, we can consider a particular x and then adjust λ until the tangent plane is tangent at that particular x. Because the y value of the tangent line at a particular x is maximized when that value coincides with its contact point, we have

$$f(x) = \max_{\lambda} \{\lambda x - g(\lambda)\}. \tag{10.130}$$

We see that the functions $f(x)$ and $g(\lambda)$ play a dual role, and are related through (10.129) and (10.130).

Let us apply these duality relations to our simple example $f(x) = \exp(-x)$. From (10.129) we see that the maximizing value of x is given by $\xi = -\ln(-\lambda)$, and back-substituting we obtain the conjugate function $g(\lambda)$ in the form

$$g(\lambda) = \lambda - \lambda \ln(-\lambda) \tag{10.131}$$

as obtained previously. The function $\lambda\xi - g(\lambda)$ is shown, for $\xi = 1$ in the right-hand plot in Figure 10.10. As a check, we can substitute (10.131) into (10.130), which gives the maximizing value of $\lambda = -\exp(-x)$, and back-substituting then recovers the original function $f(x) = \exp(-x)$.

For concave functions, we can follow a similar argument to obtain upper bounds, in which 'max' is replaced with 'min', so that

$$f(x) = \min_{\lambda} \{\lambda x - g(\lambda)\} \tag{10.132}$$

$$g(\lambda) = \min_{x} \{\lambda x - f(x)\}. \tag{10.133}$$

If the function of interest is not convex (or concave), then we cannot directly apply the method above to obtain a bound. However, we can first seek invertible transformations either of the function or of its argument which change it into a convex form. We then calculate the conjugate function and then transform back to the original variables.

An important example, which arises frequently in pattern recognition, is the logistic sigmoid function defined by

$$\sigma(x) = \frac{1}{1 + e^{-x}}. \tag{10.134}$$

As it stands this function is neither convex nor concave. However, if we take the logarithm we obtain a function which is concave, as is easily verified by finding the second derivative. From (10.133) the corresponding conjugate function then takes the form

Exercise 10.30

$$g(\lambda) = \min_{x} \{\lambda x - f(x)\} = -\lambda \ln \lambda - (1 - \lambda) \ln(1 - \lambda) \tag{10.135}$$

which we recognize as the binary entropy function for a variable whose probability of having the value 1 is λ. Using (10.132), we then obtain an upper bound on the log sigmoid

Appendix B

$$\ln \sigma(x) \leqslant \lambda x - g(\lambda) \tag{10.136}$$

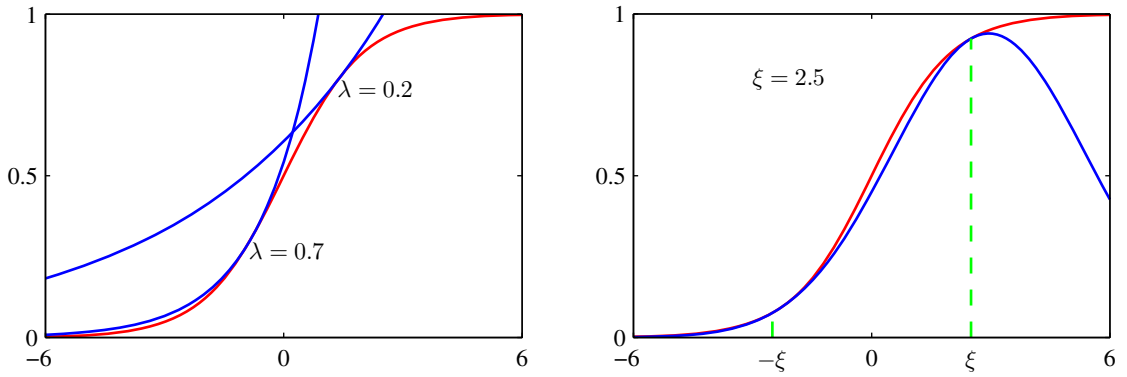

Figure 10.12 The left-hand plot shows the logistic sigmoid function $\sigma(x)$ defined by (10.134) in red, together with two examples of the exponential upper bound (10.137) shown in blue. The right-hand plot shows the logistic sigmoid again in red together with the Gaussian lower bound (10.144) shown in blue. Here the parameter $\xi = 2.5$, and the bound is exact at $x = \xi$ and $x = -\xi$, denoted by the dashed green lines.

and taking the exponential, we obtain an upper bound on the logistic sigmoid itself of the form

$$\sigma(x) \leqslant \exp(\lambda x - g(\lambda)) \tag{10.137}$$

which is plotted for two values of λ on the left-hand plot in Figure 10.12.

We can also obtain a lower bound on the sigmoid having the functional form of a Gaussian. To do this, we follow Jaakkola and Jordan (2000) and make transformations both of the input variable and of the function itself. First we take the log of the logistic function and then decompose it so that

$$\begin{aligned} \ln \sigma(x) &= -\ln(1 + e^{-x}) = -\ln\left\{e^{-x/2}(e^{x/2} + e^{-x/2})\right\} \\ &= x/2 - \ln(e^{x/2} + e^{-x/2}). \end{aligned} \tag{10.138}$$

Exercise 10.31

We now note that the function $f(x) = -\ln(e^{x/2} + e^{-x/2})$ is a convex function of the variable x^2, as can again be verified by finding the second derivative. This leads to a lower bound on $f(x)$, which is a linear function of x^2 whose conjugate function is given by

$$g(\lambda) = \max_{x^2} \left\{\lambda x^2 - f\left(\sqrt{x^2}\right)\right\}. \tag{10.139}$$

The stationarity condition leads to

$$0 = \lambda - \frac{dx}{dx^2}\frac{d}{dx} f(x) = \lambda + \frac{1}{4x}\tanh\left(\frac{x}{2}\right). \tag{10.140}$$

If we denote this value of x, corresponding to the contact point of the tangent line for this particular value of λ, by ξ, then we have

$$\lambda(\xi) = -\frac{1}{4\xi}\tanh\left(\frac{\xi}{2}\right) = -\frac{1}{2\xi}\left[\sigma(\xi) - \frac{1}{2}\right]. \tag{10.141}$$

Instead of thinking of λ as the variational parameter, we can let ξ play this role as this leads to simpler expressions for the conjugate function, which is then given by

$$g(\lambda) = \lambda(\xi)\xi^2 - f(\xi) = \lambda(\xi)\xi^2 + \ln(e^{\xi/2} + e^{-\xi/2}). \tag{10.142}$$

Hence the bound on $f(x)$ can be written as

$$f(x) \geqslant \lambda x^2 - g(\lambda) = \lambda x^2 - \lambda\xi^2 - \ln(e^{\xi/2} + e^{-\xi/2}). \tag{10.143}$$

The bound on the sigmoid then becomes

$$\sigma(x) \geqslant \sigma(\xi) \exp\left\{(x-\xi)/2 - \lambda(\xi)(x^2 - \xi^2)\right\} \tag{10.144}$$

where $\lambda(\xi)$ is defined by (10.141). This bound is illustrated in the right-hand plot of Figure 10.12. We see that the bound has the form of the exponential of a quadratic function of x, which will prove useful when we seek Gaussian representations of posterior distributions defined through logistic sigmoid functions.

Section 4.5

The logistic sigmoid arises frequently in probabilistic models over binary variables because it is the function that transforms a log odds ratio into a posterior probability. The corresponding transformation for a multiclass distribution is given by the softmax function. Unfortunately, the lower bound derived here for the logistic sigmoid does not directly extend to the softmax. Gibbs (1997) proposes a method for constructing a Gaussian distribution that is conjectured to be a bound (although no rigorous proof is given), which may be used to apply local variational methods to multiclass problems.

Section 4.3

We shall see an example of the use of local variational bounds in Sections 10.6.1. For the moment, however, it is instructive to consider in general terms how these bounds can be used. Suppose we wish to evaluate an integral of the form

$$I = \int \sigma(a)p(a)\,\mathrm{d}a \tag{10.145}$$

where $\sigma(a)$ is the logistic sigmoid, and $p(a)$ is a Gaussian probability density. Such integrals arise in Bayesian models when, for instance, we wish to evaluate the predictive distribution, in which case $p(a)$ represents a posterior parameter distribution. Because the integral is intractable, we employ the variational bound (10.144), which we write in the form $\sigma(a) \geqslant f(a, \xi)$ where ξ is a variational parameter. The integral now becomes the product of two exponential-quadratic functions and so can be integrated analytically to give a bound on I

$$I \geqslant \int f(a,\xi)p(a)\,\mathrm{d}a = F(\xi). \tag{10.146}$$

We now have the freedom to choose the variational parameter ξ, which we do by finding the value $\xi^\star$ that maximizes the function $F(\xi)$. The resulting value $F(\xi^\star)$ represents the tightest bound within this family of bounds and can be used as an approximation to I. This optimized bound, however, will in general not be exact.

Although the bound $\sigma(a) \geqslant f(a, \xi)$ on the logistic sigmoid can be optimized exactly, the required choice for ξ depends on the value of a, so that the bound is exact for one value of a only. Because the quantity $F(\xi)$ is obtained by integrating over all values of a, the value of $\xi^\star$ represents a compromise, weighted by the distribution $p(a)$.

10.6. Variational Logistic Regression

We now illustrate the use of local variational methods by returning to the Bayesian logistic regression model studied in Section 4.5. There we focussed on the use of the Laplace approximation, while here we consider a variational treatment based on the approach of Jaakkola and Jordan (2000). Like the Laplace method, this also leads to a Gaussian approximation to the posterior distribution. However, the greater flexibility of the variational approximation leads to improved accuracy compared to the Laplace method. Furthermore (unlike the Laplace method), the variational approach is optimizing a well defined objective function given by a rigourous bound on the model evidence. Logistic regression has also been treated by Dybowski and Roberts (2005) from a Bayesian perspective using Monte Carlo sampling techniques.

10.6.1 Variational posterior distribution

Here we shall make use of a variational approximation based on the local bounds introduced in Section 10.5. This allows the likelihood function for logistic regression, which is governed by the logistic sigmoid, to be approximated by the exponential of a quadratic form. It is therefore again convenient to choose a conjugate Gaussian prior of the form (4.140). For the moment, we shall treat the hyperparameters $\mathbf{m}_0$ and $\mathbf{S}_0$ as fixed constants. In Section 10.6.3, we shall demonstrate how the variational formalism can be extended to the case where there are unknown hyperparameters whose values are to be inferred from the data.

In the variational framework, we seek to maximize a lower bound on the marginal likelihood. For the Bayesian logistic regression model, the marginal likelihood takes the form

$$p(\mathbf{t}) = \int p(\mathbf{t}|\mathbf{w})p(\mathbf{w})\,\mathrm{d}\mathbf{w} = \int \left[\prod_{n=1}^{N} p(t_n|\mathbf{w})\right] p(\mathbf{w})\,\mathrm{d}\mathbf{w}. \tag{10.147}$$

We first note that the conditional distribution for t can be written as

$$\begin{aligned} p(t|\mathbf{w}) &= \sigma(a)^t \left\{1-\sigma(a)\right\}^{1-t} \\ &= \left(\frac{1}{1+e^{-a}}\right)^t \left(1-\frac{1}{1+e^{-a}}\right)^{1-t} \\ &= e^{at}\frac{e^{-a}}{1+e^{-a}} = e^{at}\sigma(-a) \end{aligned} \tag{10.148}$$

where $a = \mathbf{w}^{\mathrm{T}}\boldsymbol{\phi}$. In order to obtain a lower bound on $p(\mathbf{t})$, we make use of the variational lower bound on the logistic sigmoid function given by (10.144), which

we reproduce here for convenience

$$\sigma(z) \geqslant \sigma(\xi) \exp\left\{(z-\xi)/2 - \lambda(\xi)(z^2-\xi^2)\right\} \tag{10.149}$$

where

$$\lambda(\xi) = \frac{1}{2\xi}\left[\sigma(\xi) - \frac{1}{2}\right]. \tag{10.150}$$

We can therefore write

$$p(t|\mathbf{w}) = e^{at}\sigma(-a) \geqslant e^{at}\sigma(\xi)\exp\left\{-(a+\xi)/2 - \lambda(\xi)(a^2-\xi^2)\right\}. \tag{10.151}$$

Note that because this bound is applied to each of the terms in the likelihood function separately, there is a variational parameter ξ_n corresponding to each training set observation $(\boldsymbol{\phi}_n, t_n)$. Using $a = \mathbf{w}^{\mathrm{T}}\boldsymbol{\phi}$, and multiplying by the prior distribution, we obtain the following bound on the joint distribution of $\mathbf{t}$ and $\mathbf{w}$

$$p(\mathbf{t}, \mathbf{w}) = p(\mathbf{t}|\mathbf{w})p(\mathbf{w}) \geqslant h(\mathbf{w}, \boldsymbol{\xi})p(\mathbf{w}) \tag{10.152}$$

where $\boldsymbol{\xi}$ denotes the set $\{\xi_n\}$ of variational parameters, and

$$\begin{aligned} h(\mathbf{w}, \boldsymbol{\xi}) \quad = \quad & \prod_{n=1}^{N} \sigma(\xi_n) \exp\left\{\mathbf{w}^{\mathrm{T}}\boldsymbol{\phi}_n t_n - (\mathbf{w}^{\mathrm{T}}\boldsymbol{\phi}_n + \xi_n)/2 \right. \\ & \left. - \lambda(\xi_n)([\mathbf{w}^{\mathrm{T}}\boldsymbol{\phi}_n]^2 - \xi_n^2)\right\}. \end{aligned} \tag{10.153}$$

Evaluation of the exact posterior distribution would require normalization of the left-hand side of this inequality. Because this is intractable, we work instead with the right-hand side. Note that the function on the right-hand side cannot be interpreted as a probability density because it is not normalized. Once it is normalized to give a variational posterior distribution $q(\mathbf{w})$, however, it no longer represents a bound.

Because the logarithm function is monotonically increasing, the inequality $A \geqslant B$ implies $\ln A \geqslant \ln B$. This gives a lower bound on the log of the joint distribution of $\mathbf{t}$ and $\mathbf{w}$ of the form

$$\begin{aligned} \ln\{p(\mathbf{t}|\mathbf{w})p(\mathbf{w})\} \geqslant \ln p(\mathbf{w}) + \sum_{n=1}^{N} & \left\{\ln\sigma(\xi_n) + \mathbf{w}^{\mathrm{T}}\boldsymbol{\phi}_n t_n \right. \\ & \left. - (\mathbf{w}^{\mathrm{T}}\boldsymbol{\phi}_n + \xi_n)/2 - \lambda(\xi_n)([\mathbf{w}^{\mathrm{T}}\boldsymbol{\phi}_n]^2 - \xi_n^2)\right\}. \end{aligned} \tag{10.154}$$

Substituting for the prior $p(\mathbf{w})$, the right-hand side of this inequality becomes, as a function of $\mathbf{w}$

$$\begin{aligned} & -\frac{1}{2}(\mathbf{w}-\mathbf{m}_0)^{\mathrm{T}}\mathbf{S}_0^{-1}(\mathbf{w}-\mathbf{m}_0) \\ & + \sum_{n=1}^{N}\left\{\mathbf{w}^{\mathrm{T}}\boldsymbol{\phi}_n(t_n - 1/2) - \lambda(\xi_n)\mathbf{w}^{\mathrm{T}}(\boldsymbol{\phi}_n\boldsymbol{\phi}_n^{\mathrm{T}})\mathbf{w}\right\} + \text{const}. \end{aligned} \tag{10.155}$$

This is a quadratic function of $\mathbf{w}$, and so we can obtain the corresponding variational approximation to the posterior distribution by identifying the linear and quadratic terms in $\mathbf{w}$, giving a Gaussian variational posterior of the form

$$q(\mathbf{w}) = \mathcal{N}(\mathbf{w}|\mathbf{m}_N, \mathbf{S}_N) \tag{10.156}$$

where

$$\mathbf{m}_N = \mathbf{S}_N\left(\mathbf{S}_0^{-1}\mathbf{m}_0 + \sum_{n=1}^{N}(t_n - 1/2)\boldsymbol{\phi}_n\right) \tag{10.157}$$

$$\mathbf{S}_N^{-1} = \mathbf{S}_0^{-1} + 2\sum_{n=1}^{N}\lambda(\xi_n)\boldsymbol{\phi}_n\boldsymbol{\phi}_n^{\mathrm{T}}. \tag{10.158}$$

As with the Laplace framework, we have again obtained a Gaussian approximation to the posterior distribution. However, the additional flexibility provided by the variational parameters $\{\xi_n\}$ leads to improved accuracy in the approximation (Jaakkola and Jordan, 2000).

Here we have considered a batch learning context in which all of the training data is available at once. However, Bayesian methods are intrinsically well suited to sequential learning in which the data points are processed one at a time and then discarded. The formulation of this variational approach for the sequential case is straightforward. *Exercise 10.32*

Note that the bound given by (10.149) applies only to the two-class problem and so this approach does not directly generalize to classification problems with $K > 2$ classes. An alternative bound for the multiclass case has been explored by Gibbs (1997).

10.6.2 Optimizing the variational parameters

We now have a normalized Gaussian approximation to the posterior distribution, which we shall use shortly to evaluate the predictive distribution for new data points. First, however, we need to determine the variational parameters $\{\xi_n\}$ by maximizing the lower bound on the marginal likelihood.

To do this, we substitute the inequality (10.152) back into the marginal likelihood to give

$$\ln p(\mathbf{t}) = \ln \int p(\mathbf{t}|\mathbf{w})p(\mathbf{w})\,\mathrm{d}\mathbf{w} \geqslant \ln \int h(\mathbf{w}, \boldsymbol{\xi})p(\mathbf{w})\,\mathrm{d}\mathbf{w} = \mathcal{L}(\boldsymbol{\xi}). \tag{10.159}$$

As with the optimization of the hyperparameter α in the linear regression model of Section 3.5, there are two approaches to determining the ξ_n. In the first approach, we recognize that the function $\mathcal{L}(\boldsymbol{\xi})$ is defined by an integration over $\mathbf{w}$ and so we can view $\mathbf{w}$ as a latent variable and invoke the EM algorithm. In the second approach, we integrate over $\mathbf{w}$ analytically and then perform a direct maximization over $\boldsymbol{\xi}$. Let us begin by considering the EM approach.

The EM algorithm starts by choosing some initial values for the parameters $\{\xi_n\}$, which we denote collectively by $\boldsymbol{\xi}^{\mathrm{old}}$. In the E step of the EM algorithm,

we then use these parameter values to find the posterior distribution over $\mathbf{w}$, which is given by (10.156). In the M step, we then maximize the expected complete-data log likelihood which is given by

$$Q(\boldsymbol{\xi}, \boldsymbol{\xi}^{\text{old}}) = \mathbb{E}\left[\ln h(\mathbf{w}, \boldsymbol{\xi}) p(\mathbf{w})\right] \tag{10.160}$$

where the expectation is taken with respect to the posterior distribution $q(\mathbf{w})$ evaluated using $\boldsymbol{\xi}^{\text{old}}$. Noting that $p(\mathbf{w})$ does not depend on $\boldsymbol{\xi}$, and substituting for $h(\mathbf{w}, \boldsymbol{\xi})$ we obtain

$$Q(\boldsymbol{\xi}, \boldsymbol{\xi}^{\text{old}}) = \sum_{n=1}^{N} \left\{\ln \sigma(\xi_n) - \xi_n/2 - \lambda(\xi_n)(\boldsymbol{\phi}_n^{\mathrm{T}} \mathbb{E}[\mathbf{w}\mathbf{w}^{\mathrm{T}}] \boldsymbol{\phi}_n - \xi_n^2)\right\} + \text{const} \tag{10.161}$$

where 'const' denotes terms that are independent of $\boldsymbol{\xi}$. We now set the derivative with respect to ξ_n equal to zero. A few lines of algebra, making use of the definitions of $\sigma(\xi)$ and $\lambda(\xi)$, then gives

$$0 = \lambda'(\xi_n)(\boldsymbol{\phi}_n^{\mathrm{T}} \mathbb{E}[\mathbf{w}\mathbf{w}^{\mathrm{T}}] \boldsymbol{\phi}_n - \xi_n^2). \tag{10.162}$$

We now note that $\lambda'(\xi)$ is a monotonic function of ξ for $\xi \geqslant 0$, and that we can restrict attention to nonnegative values of ξ without loss of generality due to the symmetry of the bound around $\xi = 0$. Thus $\lambda'(\xi) \neq 0$, and hence we obtain the following re-estimation equations

Exercise 10.33

$$(\xi_n^{\text{new}})^2 = \boldsymbol{\phi}_n^{\mathrm{T}} \mathbb{E}[\mathbf{w}\mathbf{w}^{\mathrm{T}}] \boldsymbol{\phi}_n = \boldsymbol{\phi}_n^{\mathrm{T}} \left(\mathbf{S}_N + \mathbf{m}_N \mathbf{m}_N^{\mathrm{T}}\right) \boldsymbol{\phi}_n \tag{10.163}$$

where we have used (10.156).

Let us summarize the EM algorithm for finding the variational posterior distribution. We first initialize the variational parameters $\boldsymbol{\xi}^{\text{old}}$. In the E step, we evaluate the posterior distribution over $\mathbf{w}$ given by (10.156), in which the mean and covariance are defined by (10.157) and (10.158). In the M step, we then use this variational posterior to compute a new value for $\boldsymbol{\xi}$ given by (10.163). The E and M steps are repeated until a suitable convergence criterion is satisfied, which in practice typically requires only a few iterations.

An alternative approach to obtaining re-estimation equations for $\boldsymbol{\xi}$ is to note that in the integral over $\mathbf{w}$ in the definition (10.159) of the lower bound $\mathcal{L}(\boldsymbol{\xi})$, the integrand has a Gaussian-like form and so the integral can be evaluated analytically. Having evaluated the integral, we can then differentiate with respect to ξ_n. It turns out that this gives rise to exactly the same re-estimation equations as does the EM approach given by (10.163).

Exercise 10.34

As we have emphasized already, in the application of variational methods it is useful to be able to evaluate the lower bound $\mathcal{L}(\boldsymbol{\xi})$ given by (10.159). The integration over $\mathbf{w}$ can be performed analytically by noting that $p(\mathbf{w})$ is Gaussian and $h(\mathbf{w}, \boldsymbol{\xi})$ is the exponential of a quadratic function of $\mathbf{w}$. Thus, by completing the square and making use of the standard result for the normalization coefficient of a Gaussian distribution, we can obtain a closed form solution which takes the form

Exercise 10.35

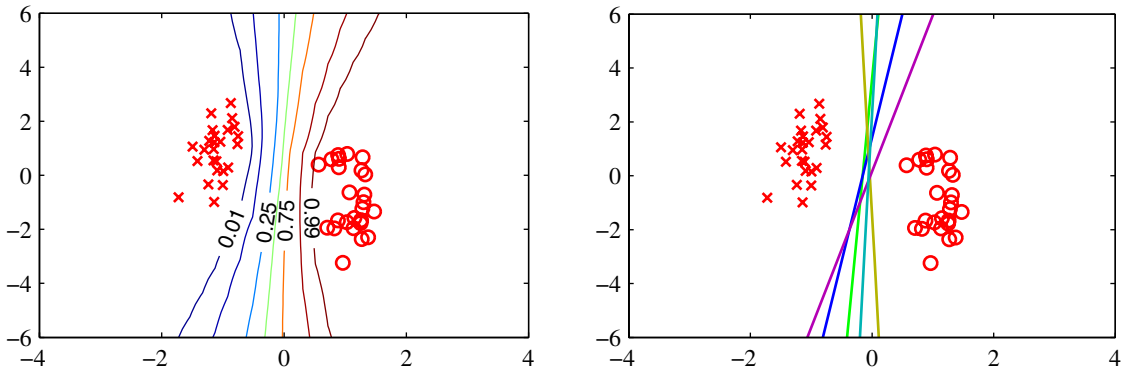

Figure 10.13 Illustration of the Bayesian approach to logistic regression for a simple linearly separable data set. The plot on the left shows the predictive distribution obtained using variational inference. We see that the decision boundary lies roughly mid way between the clusters of data points, and that the contours of the predictive distribution splay out away from the data reflecting the greater uncertainty in the classification of such regions. The plot on the right shows the decision boundaries corresponding to five samples of the parameter vector $\mathbf{w}$ drawn from the posterior distribution $p(\mathbf{w}|\mathbf{t})$.

$$\begin{aligned}\mathcal{L}(\boldsymbol{\xi}) &= \frac{1}{2}\ln\frac{|\mathbf{S}_N|}{|\mathbf{S}_0|} - \frac{1}{2}\mathbf{m}_N^{\mathrm{T}}\mathbf{S}_N^{-1}\mathbf{m}_N + \frac{1}{2}\mathbf{m}_0^{\mathrm{T}}\mathbf{S}_0^{-1}\mathbf{m}_0 \\ &\quad + \sum_{n=1}^{N}\left\{\ln\sigma(\xi_n) - \frac{1}{2}\xi_n - \lambda(\xi_n)\xi_n^2\right\}. \end{aligned} \tag{10.164}$$

This variational framework can also be applied to situations in which the data is arriving sequentially (Jaakkola and Jordan, 2000). In this case we maintain a Gaussian posterior distribution over $\mathbf{w}$, which is initialized using the prior $p(\mathbf{w})$. As each data point arrives, the posterior is updated by making use of the bound (10.151) and then normalized to give an updated posterior distribution.

The predictive distribution is obtained by marginalizing over the posterior distribution, and takes the same form as for the Laplace approximation discussed in Section 4.5.2. Figure 10.13 shows the variational predictive distributions for a synthetic data set. This example provides interesting insights into the concept of 'large margin', which was discussed in Section 7.1 and which has qualitatively similar behaviour to the Bayesian solution.

10.6.3 Inference of hyperparameters

So far, we have treated the hyperparameter α in the prior distribution as a known constant. We now extend the Bayesian logistic regression model to allow the value of this parameter to be inferred from the data set. This can be achieved by combining the global and local variational approximations into a single framework, so as to maintain a lower bound on the marginal likelihood at each stage. Such a combined approach was adopted by Bishop and Svensén (2003) in the context of a Bayesian treatment of the hierarchical mixture of experts model.

Specifically, we consider once again a simple isotropic Gaussian prior distribution of the form

$$p(\mathbf{w}|\alpha) = \mathcal{N}(\mathbf{w}|\mathbf{0}, \alpha^{-1}\mathbf{I}). \tag{10.165}$$

Our analysis is readily extended to more general Gaussian priors, for instance if we wish to associate a different hyperparameter with different subsets of the parameters w_j. As usual, we consider a conjugate hyperprior over α given by a gamma distribution

$$p(\alpha) = \mathrm{Gam}(\alpha|a_0, b_0) \tag{10.166}$$

governed by the constants a_0 and b_0.

The marginal likelihood for this model now takes the form

$$p(\mathbf{t}) = \iint p(\mathbf{w}, \alpha, \mathbf{t})\, \mathrm{d}\mathbf{w}\, \mathrm{d}\alpha \tag{10.167}$$

where the joint distribution is given by

$$p(\mathbf{w}, \alpha, \mathbf{t}) = p(\mathbf{t}|\mathbf{w})p(\mathbf{w}|\alpha)p(\alpha). \tag{10.168}$$

We are now faced with an analytically intractable integration over $\mathbf{w}$ and α, which we shall tackle by using both the local and global variational approaches in the same model

To begin with, we introduce a variational distribution $q(\mathbf{w}, \alpha)$, and then apply the decomposition (10.2), which in this instance takes the form

$$\ln p(\mathbf{t}) = \mathcal{L}(q) + \mathrm{KL}(q\|p) \tag{10.169}$$

where the lower bound $\mathcal{L}(q)$ and the Kullback-Leibler divergence $\mathrm{KL}(q\|p)$ are defined by

$$\mathcal{L}(q) = \iint q(\mathbf{w}, \alpha) \ln \left\{ \frac{p(\mathbf{w}, \alpha, \mathbf{t})}{q(\mathbf{w}, \alpha)} \right\} \mathrm{d}\mathbf{w}\, \mathrm{d}\alpha \tag{10.170}$$

$$\mathrm{KL}(q\|p) = -\iint q(\mathbf{w}, \alpha) \ln \left\{ \frac{p(\mathbf{w}, \alpha|\mathbf{t}))}{q(\mathbf{w}, \alpha)} \right\} \mathrm{d}\mathbf{w}\, \mathrm{d}\alpha. \tag{10.171}$$

At this point, the lower bound $\mathcal{L}(q)$ is still intractable due to the form of the likelihood factor $p(\mathbf{t}|\mathbf{w})$. We therefore apply the local variational bound to each of the logistic sigmoid factors as before. This allows us to use the inequality (10.152) and place a lower bound on $\mathcal{L}(q)$, which will therefore also be a lower bound on the log marginal likelihood

$$\begin{aligned} \ln p(\mathbf{t}) &\geqslant \mathcal{L}(q) \geqslant \widetilde{\mathcal{L}}(q, \boldsymbol{\xi}) \\ &= \iint q(\mathbf{w}, \alpha) \ln \left\{ \frac{h(\mathbf{w}, \boldsymbol{\xi})p(\mathbf{w}|\alpha)p(\alpha)}{q(\mathbf{w}, \alpha)} \right\} \mathrm{d}\mathbf{w}\, \mathrm{d}\alpha. \end{aligned} \tag{10.172}$$

Next we assume that the variational distribution factorizes between parameters and hyperparameters so that

$$q(\mathbf{w}, \alpha) = q(\mathbf{w})q(\alpha). \tag{10.173}$$

With this factorization we can appeal to the general result (10.9) to find expressions for the optimal factors. Consider first the distribution $q(\mathbf{w})$. Discarding terms that are independent of $\mathbf{w}$, we have

$$\begin{aligned}\ln q(\mathbf{w}) &= \mathbb{E}_\alpha \left[\ln \{h(\mathbf{w}, \boldsymbol{\xi}) p(\mathbf{w}|\alpha) p(\alpha)\}\right] + \text{const} \\ &= \ln h(\mathbf{w}, \boldsymbol{\xi}) + \mathbb{E}_\alpha \left[\ln p(\mathbf{w}|\alpha)\right] + \text{const}.\end{aligned}$$

We now substitute for $\ln h(\mathbf{w}, \boldsymbol{\xi})$ using (10.153), and for $\ln p(\mathbf{w}|\alpha)$ using (10.165), giving

$$\ln q(\mathbf{w}) = -\frac{\mathbb{E}[\alpha]}{2}\mathbf{w}^{\mathrm{T}}\mathbf{w} + \sum_{n=1}^{N}\left\{(t_n - 1/2)\mathbf{w}^{\mathrm{T}}\boldsymbol{\phi}_n - \lambda(\xi_n)\mathbf{w}^{\mathrm{T}}\boldsymbol{\phi}_n\boldsymbol{\phi}_n^{\mathrm{T}}\mathbf{w}\right\} + \text{const}.$$

We see that this is a quadratic function of $\mathbf{w}$ and so the solution for $q(\mathbf{w})$ will be Gaussian. Completing the square in the usual way, we obtain

$$q(\mathbf{w}) = \mathcal{N}(\mathbf{w}|\boldsymbol{\mu}_N, \boldsymbol{\Sigma}_N) \tag{10.174}$$

where we have defined

$$\boldsymbol{\Sigma}_N^{-1}\boldsymbol{\mu}_N = \sum_{n=1}^{N}(t_n - 1/2)\boldsymbol{\phi}_n \tag{10.175}$$

$$\boldsymbol{\Sigma}_N^{-1} = \mathbb{E}[\alpha]\mathbf{I} + 2\sum_{n=1}^{N}\lambda(\xi_n)\boldsymbol{\phi}_n\boldsymbol{\phi}_n^{\mathrm{T}}. \tag{10.176}$$

Similarly, the optimal solution for the factor $q(\alpha)$ is obtained from

$$\ln q(\alpha) = \mathbb{E}_{\mathbf{w}}\left[\ln p(\mathbf{w}|\alpha)\right] + \ln p(\alpha) + \text{const}.$$

Substituting for $\ln p(\mathbf{w}|\alpha)$ using (10.165), and for $\ln p(\alpha)$ using (10.166), we obtain

$$\ln q(\alpha) = \frac{M}{2}\ln\alpha - \frac{\alpha}{2}\mathbb{E}\left[\mathbf{w}^{\mathrm{T}}\mathbf{w}\right] + (a_0 - 1)\ln\alpha - b_0\alpha + \text{const}.$$

We recognize this as the log of a gamma distribution, and so we obtain

$$q(\alpha) = \mathrm{Gam}(\alpha|a_N, b_N) = \frac{1}{\Gamma(a_0)}a_0^{b_0}\alpha^{a_0-1}e^{-b_0\alpha} \tag{10.177}$$

where

$$a_N = a_0 + \frac{M}{2} \tag{10.178}$$

$$b_N = b_0 + \frac{1}{2}\mathbb{E}_{\mathbf{w}}\left[\mathbf{w}^{\mathrm{T}}\mathbf{w}\right]. \tag{10.179}$$

We also need to optimize the variational parameters ξ_n, and this is also done by maximizing the lower bound $\widetilde{\mathcal{L}}(q, \boldsymbol{\xi})$. Omitting terms that are independent of $\boldsymbol{\xi}$, and integrating over α, we have

$$\widetilde{\mathcal{L}}(q, \boldsymbol{\xi}) = \int q(\mathbf{w}) \ln h(\mathbf{w}, \boldsymbol{\xi}) \, \mathrm{d}\mathbf{w} + \text{const}. \tag{10.180}$$

Note that this has precisely the same form as (10.159), and so we can again appeal to our earlier result (10.163), which can be obtained by direct optimization of the marginal likelihood function, leading to re-estimation equations of the form

$$(\xi_n^{\text{new}})^2 = \boldsymbol{\phi}_n^{\mathrm{T}} \left(\boldsymbol{\Sigma}_N + \boldsymbol{\mu}_N \boldsymbol{\mu}_N^{\mathrm{T}} \right) \boldsymbol{\phi}_n. \tag{10.181}$$

We have obtained re-estimation equations for the three quantities $q(\mathbf{w})$, $q(\alpha)$, and $\boldsymbol{\xi}$, and so after making suitable initializations, we can cycle through these quantities, updating each in turn. The required moments are given by

Appendix B

$$\mathbb{E}\left[\alpha\right] = \frac{a_N}{b_N} \tag{10.182}$$

$$\mathbb{E}\left[\mathbf{w}^{\mathrm{T}}\mathbf{w}\right] = \boldsymbol{\Sigma}_N + \boldsymbol{\mu}_N^{\mathrm{T}} \boldsymbol{\mu}_N. \tag{10.183}$$

10.7. Expectation Propagation

We conclude this chapter by discussing an alternative form of deterministic approximate inference, known as *expectation propagation* or *EP* (Minka, 2001a; Minka, 2001b). As with the variational Bayes methods discussed so far, this too is based on the minimization of a Kullback-Leibler divergence but now of the reverse form, which gives the approximation rather different properties.

Consider for a moment the problem of minimizing $\mathrm{KL}(p\|q)$ with respect to $q(\mathbf{z})$ when $p(\mathbf{z})$ is a fixed distribution and $q(\mathbf{z})$ is a member of the exponential family and so, from (2.194), can be written in the form

$$q(\mathbf{z}) = h(\mathbf{z}) g(\boldsymbol{\eta}) \exp\left\{ \boldsymbol{\eta}^{\mathrm{T}} \mathbf{u}(\mathbf{z}) \right\}. \tag{10.184}$$

As a function of $\boldsymbol{\eta}$, the Kullback-Leibler divergence then becomes

$$\mathrm{KL}(p\|q) = -\ln g(\boldsymbol{\eta}) - \boldsymbol{\eta}^{\mathrm{T}} \mathbb{E}_{p(\mathbf{z})}[\mathbf{u}(\mathbf{z})] + \text{const} \tag{10.185}$$

where the constant terms are independent of the natural parameters $\boldsymbol{\eta}$. We can minimize $\mathrm{KL}(p\|q)$ within this family of distributions by setting the gradient with respect to $\boldsymbol{\eta}$ to zero, giving

$$-\nabla \ln g(\boldsymbol{\eta}) = \mathbb{E}_{p(\mathbf{z})}[\mathbf{u}(\mathbf{z})]. \tag{10.186}$$

However, we have already seen in (2.226) that the negative gradient of $\ln g(\boldsymbol{\eta})$ is given by the expectation of $\mathbf{u}(\mathbf{z})$ under the distribution $q(\mathbf{z})$. Equating these two results, we obtain

$$\mathbb{E}_{q(\mathbf{z})}[\mathbf{u}(\mathbf{z})] = \mathbb{E}_{p(\mathbf{z})}[\mathbf{u}(\mathbf{z})]. \tag{10.187}$$

We see that the optimum solution simply corresponds to matching the expected sufficient statistics. So, for instance, if $q(\mathbf{z})$ is a Gaussian $\mathcal{N}(\mathbf{z}|\boldsymbol{\mu}, \boldsymbol{\Sigma})$ then we minimize the Kullback-Leibler divergence by setting the mean $\boldsymbol{\mu}$ of $q(\mathbf{z})$ equal to the mean of the distribution $p(\mathbf{z})$ and the covariance $\boldsymbol{\Sigma}$ equal to the covariance of $p(\mathbf{z})$. This is sometimes called *moment matching*. An example of this was seen in Figure 10.3(a).

Now let us exploit this result to obtain a practical algorithm for approximate inference. For many probabilistic models, the joint distribution of data $\mathcal{D}$ and hidden variables (including parameters) $\boldsymbol{\theta}$ comprises a product of factors in the form

$$p(\mathcal{D}, \boldsymbol{\theta}) = \prod_i f_i(\boldsymbol{\theta}). \tag{10.188}$$

This would arise, for example, in a model for independent, identically distributed data in which there is one factor $f_n(\boldsymbol{\theta}) = p(\mathbf{x}_n|\boldsymbol{\theta})$ for each data point $\mathbf{x}_n$, along with a factor $f_0(\boldsymbol{\theta}) = p(\boldsymbol{\theta})$ corresponding to the prior. More generally, it would also apply to any model defined by a directed probabilistic graph in which each factor is a conditional distribution corresponding to one of the nodes, or an undirected graph in which each factor is a clique potential. We are interested in evaluating the posterior distribution $p(\boldsymbol{\theta}|\mathcal{D})$ for the purpose of making predictions, as well as the model evidence $p(\mathcal{D})$ for the purpose of model comparison. From (10.188) the posterior is given by

$$p(\boldsymbol{\theta}|\mathcal{D}) = \frac{1}{p(\mathcal{D})} \prod_i f_i(\boldsymbol{\theta}) \tag{10.189}$$

and the model evidence is given by

$$p(\mathcal{D}) = \int \prod_i f_i(\boldsymbol{\theta}) \, \mathrm{d}\boldsymbol{\theta}. \tag{10.190}$$

Here we are considering continuous variables, but the following discussion applies equally to discrete variables with integrals replaced by summations. We shall suppose that the marginalization over $\boldsymbol{\theta}$, along with the marginalizations with respect to the posterior distribution required to make predictions, are intractable so that some form of approximation is required.

Expectation propagation is based on an approximation to the posterior distribution which is also given by a product of factors

$$q(\boldsymbol{\theta}) = \frac{1}{Z} \prod_i \widetilde{f}_i(\boldsymbol{\theta}) \tag{10.191}$$

in which each factor $\widetilde{f}_i(\boldsymbol{\theta})$ in the approximation corresponds to one of the factors $f_i(\boldsymbol{\theta})$ in the true posterior (10.189), and the factor $1/Z$ is the normalizing constant needed to ensure that the left-hand side of (10.191) integrates to unity. In order to obtain a practical algorithm, we need to constrain the factors $\widetilde{f}_i(\boldsymbol{\theta})$ in some way, and in particular we shall assume that they come from the exponential family. The product of the factors will therefore also be from the exponential family and so can

be described by a finite set of sufficient statistics. For example, if each of the $\widetilde{f}_i(\boldsymbol{\theta})$ is a Gaussian, then the overall approximation $q(\boldsymbol{\theta})$ will also be Gaussian.

Ideally we would like to determine the $\widetilde{f}_i(\boldsymbol{\theta})$ by minimizing the Kullback-Leibler divergence between the true posterior and the approximation given by

$$\mathrm{KL}\left(p\|q\right) = \mathrm{KL}\left(\frac{1}{p(\mathcal{D})}\prod_i f_i(\boldsymbol{\theta})\middle\|\frac{1}{Z}\prod_i \widetilde{f}_i(\boldsymbol{\theta})\right). \tag{10.192}$$

Note that this is the reverse form of KL divergence compared with that used in variational inference. In general, this minimization will be intractable because the KL divergence involves averaging with respect to the true distribution. As a rough approximation, we could instead minimize the KL divergences between the corresponding pairs $f_i(\boldsymbol{\theta})$ and $\widetilde{f}_i(\boldsymbol{\theta})$ of factors. This represents a much simpler problem to solve, and has the advantage that the algorithm is noniterative. However, because each factor is individually approximated, the product of the factors could well give a poor approximation.

Expectation propagation makes a much better approximation by optimizing each factor in turn in the context of all of the remaining factors. It starts by initializing the factors $\widetilde{f}_i(\boldsymbol{\theta})$, and then cycles through the factors refining them one at a time. This is similar in spirit to the update of factors in the variational Bayes framework considered earlier. Suppose we wish to refine factor $\widetilde{f}_j(\boldsymbol{\theta})$. We first remove this factor from the product to give $\prod_{i\neq j}\widetilde{f}_i(\boldsymbol{\theta})$. Conceptually, we will now determine a revised form of the factor $\widetilde{f}_j(\boldsymbol{\theta})$ by ensuring that the product

$$q^{\mathrm{new}}(\boldsymbol{\theta}) \propto \widetilde{f}_j(\boldsymbol{\theta})\prod_{i\neq j}\widetilde{f}_i(\boldsymbol{\theta}) \tag{10.193}$$

is as close as possible to

$$f_j(\boldsymbol{\theta})\prod_{i\neq j}\widetilde{f}_i(\boldsymbol{\theta}) \tag{10.194}$$

in which we keep fixed all of the factors $\widetilde{f}_i(\boldsymbol{\theta})$ for $i \neq j$. This ensures that the approximation is most accurate in the regions of high posterior probability as defined by the remaining factors. We shall see an example of this effect when we apply EP to the 'clutter problem'. To achieve this, we first remove the factor $\widetilde{f}_j(\boldsymbol{\theta})$ from the current approximation to the posterior by defining the unnormalized distribution

Section 10.7.1

$$q^{\backslash j}(\boldsymbol{\theta}) = \frac{q(\boldsymbol{\theta})}{\widetilde{f}_j(\boldsymbol{\theta})}. \tag{10.195}$$

Note that we could instead find $q^{\backslash j}(\boldsymbol{\theta})$ from the product of factors $i \neq j$, although in practice division is usually easier. This is now combined with the factor $f_j(\boldsymbol{\theta})$ to give a distribution

$$\frac{1}{Z_j}f_j(\boldsymbol{\theta})q^{\backslash j}(\boldsymbol{\theta}) \tag{10.196}$$

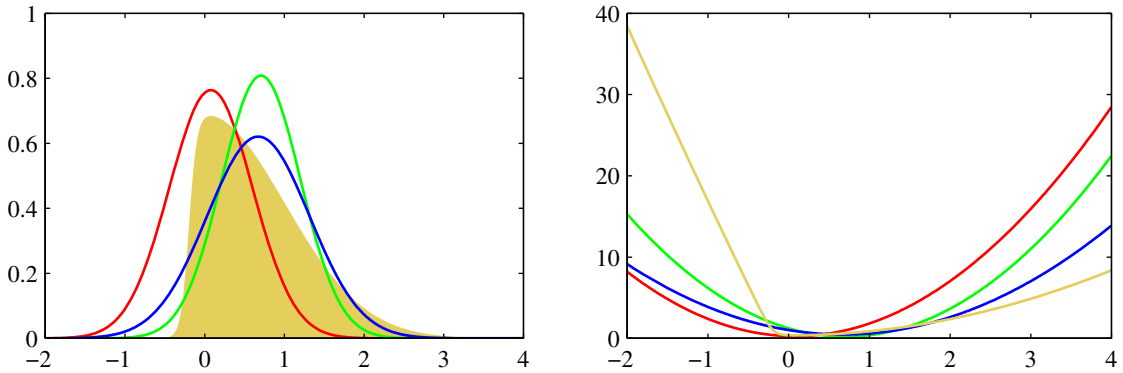

Figure 10.14 Illustration of the expectation propagation approximation using a Gaussian distribution for the example considered earlier in Figures 4.14 and 10.1. The left-hand plot shows the original distribution (yellow) along with the Laplace (red), global variational (green), and EP (blue) approximations, and the right-hand plot shows the corresponding negative logarithms of the distributions. Note that the EP distribution is broader than that variational inference, as a consequence of the different form of KL divergence.

where Z_j is the normalization constant given by

$$Z_j = \int f_j(\boldsymbol{\theta}) q^{\backslash j}(\boldsymbol{\theta}) \, \mathrm{d}\boldsymbol{\theta}. \tag{10.197}$$

We now determine a revised factor $\widetilde{f}_j(\boldsymbol{\theta})$ by minimizing the Kullback-Leibler divergence

$$\mathrm{KL}\left(\frac{f_j(\boldsymbol{\theta}) q^{\backslash j}(\boldsymbol{\theta})}{Z_j} \middle\| q^{\mathrm{new}}(\boldsymbol{\theta}) \right). \tag{10.198}$$

This is easily solved because the approximating distribution $q^{\mathrm{new}}(\boldsymbol{\theta})$ is from the exponential family, and so we can appeal to the result (10.187), which tells us that the parameters of $q^{\mathrm{new}}(\boldsymbol{\theta})$ are obtained by matching its expected sufficient statistics to the corresponding moments of (10.196). We shall assume that this is a tractable operation. For example, if we choose $q(\boldsymbol{\theta})$ to be a Gaussian distribution $\mathcal{N}(\boldsymbol{\theta}|\boldsymbol{\mu}, \boldsymbol{\Sigma})$, then $\boldsymbol{\mu}$ is set equal to the mean of the (unnormalized) distribution $f_j(\boldsymbol{\theta}) q^{\backslash j}(\boldsymbol{\theta})$, and $\boldsymbol{\Sigma}$ is set to its covariance. More generally, it is straightforward to obtain the required expectations for any member of the exponential family, provided it can be normalized, because the expected statistics can be related to the derivatives of the normalization coefficient, as given by (2.226). The EP approximation is illustrated in Figure 10.14.

From (10.193), we see that the revised factor $\widetilde{f}_j(\boldsymbol{\theta})$ can be found by taking $q^{\mathrm{new}}(\boldsymbol{\theta})$ and dividing out the remaining factors so that

$$\widetilde{f}_j(\boldsymbol{\theta}) = K \frac{q^{\mathrm{new}}(\boldsymbol{\theta})}{q^{\backslash j}(\boldsymbol{\theta})} \tag{10.199}$$

where we have used (10.195). The coefficient K is determined by multiplying both

sides of (10.199) by $q^{\backslash i}(\boldsymbol{\theta})$ and integrating to give

$$K = \int \widetilde{f}_j(\boldsymbol{\theta}) q^{\backslash j}(\boldsymbol{\theta}) \, \mathrm{d}\boldsymbol{\theta} \tag{10.200}$$

where we have used the fact that $q^{\text{new}}(\boldsymbol{\theta})$ is normalized. The value of K can therefore be found by matching zeroth-order moments

$$\int \widetilde{f}_j(\boldsymbol{\theta}) q^{\backslash j}(\boldsymbol{\theta}) \, \mathrm{d}\boldsymbol{\theta} = \int f_j(\boldsymbol{\theta}) q^{\backslash j}(\boldsymbol{\theta}) \, \mathrm{d}\boldsymbol{\theta}. \tag{10.201}$$

Combining this with (10.197), we then see that $K = Z_j$ and so can be found by evaluating the integral in (10.197).

In practice, several passes are made through the set of factors, revising each factor in turn. The posterior distribution $p(\boldsymbol{\theta}|\mathcal{D})$ is then approximated using (10.191), and the model evidence $p(\mathcal{D})$ can be approximated by using (10.190) with the factors $f_i(\boldsymbol{\theta})$ replaced by their approximations $\widetilde{f}_i(\boldsymbol{\theta})$.

Expectation Propagation

We are given a joint distribution over observed data $\mathcal{D}$ and stochastic variables $\boldsymbol{\theta}$ in the form of a product of factors

$$p(\mathcal{D}, \boldsymbol{\theta}) = \prod_i f_i(\boldsymbol{\theta}) \tag{10.202}$$

and we wish to approximate the posterior distribution $p(\boldsymbol{\theta}|\mathcal{D})$ by a distribution of the form

$$q(\boldsymbol{\theta}) = \frac{1}{Z} \prod_i \widetilde{f}_i(\boldsymbol{\theta}). \tag{10.203}$$

We also wish to approximate the model evidence $p(\mathcal{D})$.

1. Initialize all of the approximating factors $\widetilde{f}_i(\boldsymbol{\theta})$.
2. Initialize the posterior approximation by setting

$$q(\boldsymbol{\theta}) \propto \prod_i \widetilde{f}_i(\boldsymbol{\theta}). \tag{10.204}$$

3. Until convergence:
   (a) Choose a factor $\widetilde{f}_j(\boldsymbol{\theta})$ to refine.
   (b) Remove $\widetilde{f}_j(\boldsymbol{\theta})$ from the posterior by division

$$q^{\backslash j}(\boldsymbol{\theta}) = \frac{q(\boldsymbol{\theta})}{\widetilde{f}_j(\boldsymbol{\theta})}. \tag{10.205}$$

(c) Evaluate the new posterior by setting the sufficient statistics (moments) of $q^{\text{new}}(\boldsymbol{\theta})$ equal to those of $q^{\backslash j}(\boldsymbol{\theta})f_j(\boldsymbol{\theta})$, including evaluation of the normalization constant

$$Z_j = \int q^{\backslash j}(\boldsymbol{\theta})f_j(\boldsymbol{\theta})\,\mathrm{d}\boldsymbol{\theta}. \tag{10.206}$$

(d) Evaluate and store the new factor

$$\widetilde{f}_j(\boldsymbol{\theta}) = Z_j \frac{q^{\text{new}}(\boldsymbol{\theta})}{q^{\backslash j}(\boldsymbol{\theta})}. \tag{10.207}$$

4. Evaluate the approximation to the model evidence

$$p(\mathcal{D}) \simeq \int \prod_i \widetilde{f}_i(\boldsymbol{\theta})\,\mathrm{d}\boldsymbol{\theta}. \tag{10.208}$$

A special case of EP, known as *assumed density filtering* (ADF) or *moment matching* (Maybeck, 1982; Lauritzen, 1992; Boyen and Koller, 1998; Opper and Winther, 1999), is obtained by initializing all of the approximating factors except the first to unity and then making one pass through the factors updating each of them once. Assumed density filtering can be appropriate for on-line learning in which data points are arriving in a sequence and we need to learn from each data point and then discard it before considering the next point. However, in a batch setting we have the opportunity to re-use the data points many times in order to achieve improved accuracy, and it is this idea that is exploited in expectation propagation. Furthermore, if we apply ADF to batch data, the results will have an undesirable dependence on the (arbitrary) order in which the data points are considered, which again EP can overcome.

One disadvantage of expectation propagation is that there is no guarantee that the iterations will converge. However, for approximations $q(\boldsymbol{\theta})$ in the exponential family, if the iterations do converge, the resulting solution will be a stationary point of a particular energy function (Minka, 2001a), although each iteration of EP does not necessarily decrease the value of this energy function. This is in contrast to variational Bayes, which iteratively maximizes a lower bound on the log marginal likelihood, in which each iteration is guaranteed not to decrease the bound. It is possible to optimize the EP cost function directly, in which case it is guaranteed to converge, although the resulting algorithms can be slower and more complex to implement.

Another difference between variational Bayes and EP arises from the form of KL divergence that is minimized by the two algorithms, because the former minimizes $\mathrm{KL}(q\|p)$ whereas the latter minimizes $\mathrm{KL}(p\|q)$. As we saw in Figure 10.3, for distributions $p(\boldsymbol{\theta})$ which are multimodal, minimizing $\mathrm{KL}(p\|q)$ can lead to poor approximations. In particular, if EP is applied to mixtures the results are not sensible because the approximation tries to capture all of the modes of the posterior distribution. Conversely, in logistic-type models, EP often out-performs both local variational methods and the Laplace approximation (Kuss and Rasmussen, 2006).

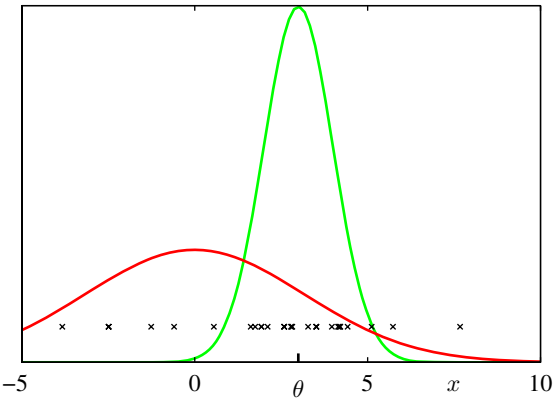

Figure 10.15 Illustration of the clutter problem for a data space dimensionality of $D = 1$. Training data points, denoted by the crosses, are drawn from a mixture of two Gaussians with components shown in red and green. The goal is to infer the mean of the green Gaussian from the observed data.

10.7.1 Example: The clutter problem

Following Minka (2001b), we illustrate the EP algorithm using a simple example in which the goal is to infer the mean $\boldsymbol{\theta}$ of a multivariate Gaussian distribution over a variable $\mathbf{x}$ given a set of observations drawn from that distribution. To make the problem more interesting, the observations are embedded in background clutter, which itself is also Gaussian distributed, as illustrated in Figure 10.15. The distribution of observed values $\mathbf{x}$ is therefore a mixture of Gaussians, which we take to be of the form

$$p(\mathbf{x}|\boldsymbol{\theta}) = (1-w)\mathcal{N}(\mathbf{x}|\boldsymbol{\theta}, \mathbf{I}) + w\mathcal{N}(\mathbf{x}|\mathbf{0}, a\mathbf{I}) \tag{10.209}$$

where w is the proportion of background clutter and is assumed to be known. The prior over $\boldsymbol{\theta}$ is taken to be Gaussian

$$p(\boldsymbol{\theta}) = \mathcal{N}(\boldsymbol{\theta}|\mathbf{0}, b\mathbf{I}) \tag{10.210}$$

and Minka (2001a) chooses the parameter values $a = 10$, $b = 100$ and $w = 0.5$. The joint distribution of N observations $\mathcal{D} = \{\mathbf{x}_1, \ldots, \mathbf{x}_N\}$ and $\boldsymbol{\theta}$ is given by

$$p(\mathcal{D}, \boldsymbol{\theta}) = p(\boldsymbol{\theta}) \prod_{n=1}^{N} p(\mathbf{x}_n|\boldsymbol{\theta}) \tag{10.211}$$

and so the posterior distribution comprises a mixture of 2^N Gaussians. Thus the computational cost of solving this problem exactly would grow exponentially with the size of the data set, and so an exact solution is intractable for moderately large N.

To apply EP to the clutter problem, we first identify the factors $f_0(\boldsymbol{\theta}) = p(\boldsymbol{\theta})$ and $f_n(\boldsymbol{\theta}) = p(\mathbf{x}_n|\boldsymbol{\theta})$. Next we select an approximating distribution from the exponential family, and for this example it is convenient to choose a spherical Gaussian

$$q(\boldsymbol{\theta}) = \mathcal{N}(\boldsymbol{\theta}|\mathbf{m}, v\mathbf{I}). \tag{10.212}$$

The factor approximations will therefore take the form of exponential-quadratic functions of the form

$$\widetilde{f}_n(\boldsymbol{\theta}) = s_n \mathcal{N}(\boldsymbol{\theta}|\mathbf{m}_n, v_n\mathbf{I}) \tag{10.213}$$

where $n = 1, \ldots, N$, and we set $\widetilde{f}_0(\boldsymbol{\theta})$ equal to the prior $p(\boldsymbol{\theta})$. Note that the use of $\mathcal{N}(\boldsymbol{\theta}|\cdot,\cdot)$ does not imply that the right-hand side is a well-defined Gaussian density (in fact, as we shall see, the variance parameter v_n can be negative) but is simply a convenient shorthand notation. The approximations $\widetilde{f}_n(\boldsymbol{\theta})$, for $n = 1, \ldots, N$, can be initialized to unity, corresponding to $s_n = (2\pi v_n)^{D/2}$, $v_n \to \infty$ and $\mathbf{m}_n = \mathbf{0}$, where D is the dimensionality of $\mathbf{x}$ and hence of $\boldsymbol{\theta}$. The initial $q(\boldsymbol{\theta})$, defined by (10.191), is therefore equal to the prior.

We then iteratively refine the factors by taking one factor $f_n(\boldsymbol{\theta})$ at a time and applying (10.205), (10.206), and (10.207). Note that we do not need to revise the term $f_0(\boldsymbol{\theta})$ because an EP update will leave this term unchanged. Here we state the results and leave the reader to fill in the details.

Exercise 10.37

First we remove the current estimate $\widetilde{f}_n(\boldsymbol{\theta})$ from $q(\boldsymbol{\theta})$ by division using (10.205) to give $q^{\backslash n}(\boldsymbol{\theta})$, which has mean and inverse variance given by

Exercise 10.38

$$\mathbf{m}^{\backslash n} = \mathbf{m} + v^{\backslash n} v_n^{-1}(\mathbf{m} - \mathbf{m}_n) \tag{10.214}$$

$$(v^{\backslash n})^{-1} = v^{-1} - v_n^{-1}. \tag{10.215}$$

Next we evaluate the normalization constant Z_n using (10.206) to give

$$Z_n = (1-w)\mathcal{N}(\mathbf{x}_n|\mathbf{m}^{\backslash n}, (v^{\backslash n} + 1)\mathbf{I}) + w\mathcal{N}(\mathbf{x}_n|\mathbf{0}, a\mathbf{I}). \tag{10.216}$$

Similarly, we compute the mean and variance of $q^{\text{new}}(\boldsymbol{\theta})$ by finding the mean and variance of $q^{\backslash n}(\boldsymbol{\theta}) f_n(\boldsymbol{\theta})$ to give

Exercise 10.39

$$\mathbf{m} = \mathbf{m}^{\backslash n} + \rho_n \frac{v^{\backslash n}}{v^{\backslash n} + 1}(\mathbf{x}_n - \mathbf{m}^{\backslash n}) \tag{10.217}$$

$$v = v^{\backslash n} - \rho_n \frac{(v^{\backslash n})^2}{v^{\backslash n} + 1} + \rho_n(1-\rho_n)\frac{(v^{\backslash n})^2 \|\mathbf{x}_n - \mathbf{m}^{\backslash n}\|^2}{D(v^{\backslash n} + 1)^2} \tag{10.218}$$

where the quantity

$$\rho_n = 1 - \frac{w}{Z_n}\mathcal{N}(\mathbf{x}_n|\mathbf{0}, a\mathbf{I}) \tag{10.219}$$

has a simple interpretation as the probability of the point $\mathbf{x}_n$ not being clutter. Then we use (10.207) to compute the refined factor $\widetilde{f}_n(\boldsymbol{\theta})$ whose parameters are given by

$$v_n^{-1} = (v^{\text{new}})^{-1} - (v^{\backslash n})^{-1} \tag{10.220}$$

$$\mathbf{m}_n = \mathbf{m}^{\backslash n} + (v_n + v^{\backslash n})(v^{\backslash n})^{-1}(\mathbf{m}^{\text{new}} - \mathbf{m}^{\backslash n}) \tag{10.221}$$

$$s_n = \frac{Z_n}{(2\pi v_n)^{D/2}\mathcal{N}(\mathbf{m}_n|\mathbf{m}^{\backslash n}, (v_n + v^{\backslash n})\mathbf{I})}. \tag{10.222}$$

This refinement process is repeated until a suitable termination criterion is satisfied, for instance that the maximum change in parameter values resulting from a complete

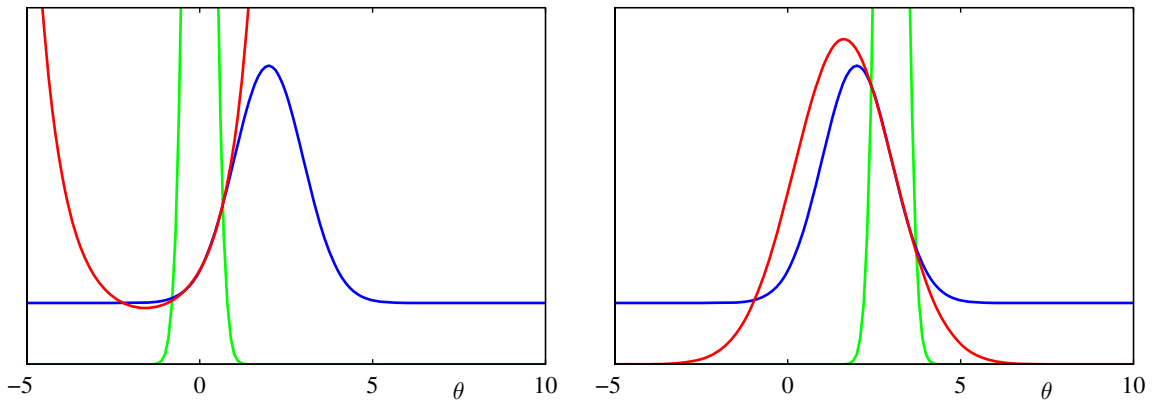

Figure 10.16 Examples of the approximation of specific factors for a one-dimensional version of the clutter problem, showing $f_n(\theta)$ in blue, $\widetilde{f}_n(\theta)$ in red, and $q^{\backslash n}(\theta)$ in green. Notice that the current form for $q^{\backslash n}(\theta)$ controls the range of θ over which $\widetilde{f}_n(\theta)$ will be a good approximation to $f_n(\theta)$.

pass through all factors is less than some threshold. Finally, we use (10.208) to evaluate the approximation to the model evidence, given by

$$p(\mathcal{D}) \simeq (2\pi v^{\text{new}})^{D/2} \exp(B/2) \prod_{n=1}^{N} \left\{ s_n (2\pi v_n)^{-D/2} \right\} \tag{10.223}$$

where

$$B = \frac{(\mathbf{m}^{\text{new}})^{\mathrm{T}} \mathbf{m}^{\text{new}}}{v} - \sum_{n=1}^{N} \frac{\mathbf{m}_n^{\mathrm{T}} \mathbf{m}_n}{v_n}. \tag{10.224}$$

Examples factor approximations for the clutter problem with a one-dimensional parameter space θ are shown in Figure 10.16. Note that the factor approximations can have infinite or even negative values for the 'variance' parameter v_n. This simply corresponds to approximations that curve upwards instead of downwards and are not necessarily problematic provided the overall approximate posterior $q(\boldsymbol{\theta})$ has positive variance. Figure 10.17 compares the performance of EP with variational Bayes (mean field theory) and the Laplace approximation on the clutter problem.

10.7.2 Expectation propagation on graphs

So far in our general discussion of EP, we have allowed the factors $f_i(\boldsymbol{\theta})$ in the distribution $p(\boldsymbol{\theta})$ to be functions of all of the components of $\boldsymbol{\theta}$, and similarly for the approximating factors $\widetilde{f}(\boldsymbol{\theta})$ in the approximating distribution $q(\boldsymbol{\theta})$. We now consider situations in which the factors depend only on subsets of the variables. Such restrictions can be conveniently expressed using the framework of probabilistic graphical models, as discussed in Chapter 8. Here we use a factor graph representation because this encompasses both directed and undirected graphs.

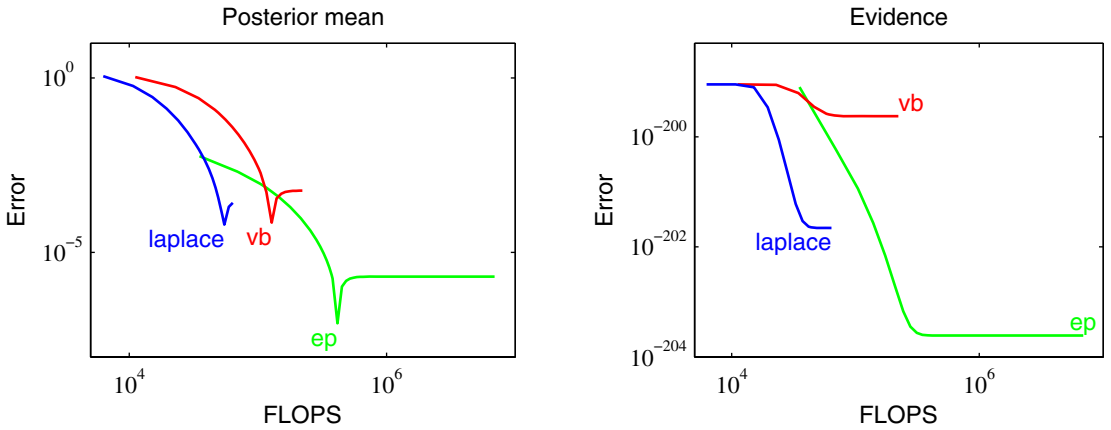

Figure 10.17 Comparison of expectation propagation, variational inference, and the Laplace approximation on the clutter problem. The left-hand plot shows the error in the predicted posterior mean versus the number of floating point operations, and the right-hand plot shows the corresponding results for the model evidence.

We shall focus on the case in which the approximating distribution is fully factorized, and we shall show that in this case expectation propagation reduces to loopy belief propagation (Minka, 2001a). To start with, we show this in the context of a simple example, and then we shall explore the general case.

First of all, recall from (10.17) that if we minimize the Kullback-Leibler divergence $\mathrm{KL}(p\|q)$ with respect to a factorized distribution q, then the optimal solution for each factor is simply the corresponding marginal of p.

Section 8.4.4

Now consider the factor graph shown on the left in Figure 10.18, which was introduced earlier in the context of the sum-product algorithm. The joint distribution is given by

$$p(\mathbf{x}) = f_a(x_1, x_2) f_b(x_2, x_3) f_c(x_2, x_4). \tag{10.225}$$

We seek an approximation $q(\mathbf{x})$ that has the same factorization, so that

$$q(\mathbf{x}) \propto \widetilde{f}_a(x_1, x_2)\widetilde{f}_b(x_2, x_3)\widetilde{f}_c(x_2, x_4). \tag{10.226}$$

Note that normalization constants have been omitted, and these can be re-instated at the end by local normalization, as is generally done in belief propagation. Now suppose we restrict attention to approximations in which the factors themselves factorize with respect to the individual variables so that

$$q(\mathbf{x}) \propto \widetilde{f}_{a1}(x_1)\widetilde{f}_{a2}(x_2)\widetilde{f}_{b2}(x_2)\widetilde{f}_{b3}(x_3)\widetilde{f}_{c2}(x_2)\widetilde{f}_{c4}(x_4) \tag{10.227}$$

which corresponds to the factor graph shown on the right in Figure 10.18. Because the individual factors are factorized, the overall distribution $q(\mathbf{x})$ is itself fully factorized.

Now we apply the EP algorithm using the fully factorized approximation. Suppose that we have initialized all of the factors and that we choose to refine factor

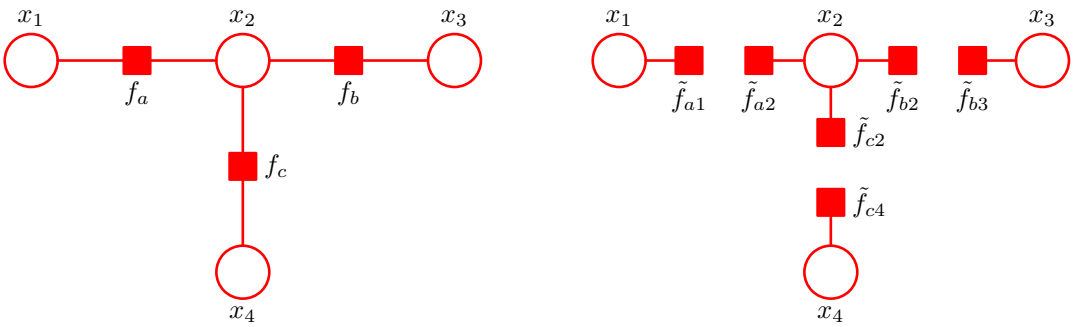

Figure 10.18 On the left is a simple factor graph from Figure 8.51 and reproduced here for convenience. On the right is the corresponding factorized approximation.

$\widetilde{f}_b(x_2, x_3) = \widetilde{f}_{b2}(x_2)\widetilde{f}_{b3}(x_3)$. We first remove this factor from the approximating distribution to give

$$q^{\backslash b}(\mathbf{x}) = \widetilde{f}_{a1}(x_1)\widetilde{f}_{a2}(x_2)\widetilde{f}_{c2}(x_2)\widetilde{f}_{c4}(x_4) \tag{10.228}$$

and we then multiply this by the exact factor $f_b(x_2, x_3)$ to give

$$\widehat{p}(\mathbf{x}) = q^{\backslash b}(\mathbf{x})f_b(x_2, x_3) = \widetilde{f}_{a1}(x_1)\widetilde{f}_{a2}(x_2)\widetilde{f}_{c2}(x_2)\widetilde{f}_{c4}(x_4)f_b(x_2, x_3). \tag{10.229}$$

We now find $q^{\text{new}}(\mathbf{x})$ by minimizing the Kullback-Leibler divergence $\text{KL}(\widehat{p}\|q^{\text{new}})$. The result, as noted above, is that $q^{\text{new}}(\mathbf{z})$ comprises the product of factors, one for each variable x_i, in which each factor is given by the corresponding marginal of $\widehat{p}(\mathbf{x})$. These four marginals are given by

$$\widehat{p}(x_1) \propto \widetilde{f}_{a1}(x_1) \tag{10.230}$$

$$\widehat{p}(x_2) \propto \widetilde{f}_{a2}(x_2)\widetilde{f}_{c2}(x_2)\sum_{x_3} f_b(x_2, x_3) \tag{10.231}$$

$$\widehat{p}(x_3) \propto \sum_{x_2}\left\{f_b(x_2, x_3)\widetilde{f}_{a2}(x_2)\widetilde{f}_{c2}(x_2)\right\} \tag{10.232}$$

$$\widehat{p}(x_4) \propto \widetilde{f}_{c4}(x_4) \tag{10.233}$$

and $q^{\text{new}}(\mathbf{x})$ is obtained by multiplying these marginals together. We see that the only factors in $q(\mathbf{x})$ that change when we update $\widetilde{f}_b(x_2, x_3)$ are those that involve the variables in f_b namely x_2 and x_3. To obtain the refined factor $\widetilde{f}_b(x_2, x_3) = \widetilde{f}_{b2}(x_2)\widetilde{f}_{b3}(x_3)$ we simply divide $q^{\text{new}}(\mathbf{x})$ by $q^{\backslash b}(\mathbf{x})$, which gives

$$\widetilde{f}_{b2}(x_2) \propto \sum_{x_3} f_b(x_2, x_3) \tag{10.234}$$

$$\widetilde{f}_{b3}(x_3) \propto \sum_{x_2}\left\{f_b(x_2, x_3)\widetilde{f}_{a2}(x_2)\widetilde{f}_{c2}(x_2)\right\}. \tag{10.235}$$

Section 8.4.4

These are precisely the messages obtained using belief propagation in which messages from variable nodes to factor nodes have been folded into the messages from factor nodes to variable nodes. In particular, $\widetilde{f}_{b2}(x_2)$ corresponds to the message $\mu_{f_b \to x_2}(x_2)$ sent by factor node f_b to variable node x_2 and is given by (8.81). Similarly, if we substitute (8.78) into (8.79), we obtain (10.235) in which $\widetilde{f}_{a2}(x_2)$ corresponds to $\mu_{f_a \to x_2}(x_2)$ and $\widetilde{f}_{c2}(x_2)$ corresponds to $\mu_{f_c \to x_2}(x_2)$, giving the message $\widetilde{f}_{b3}(x_3)$ which corresponds to $\mu_{f_b \to x_3}(x_3)$.

This result differs slightly from standard belief propagation in that messages are passed in both directions at the same time. We can easily modify the EP procedure to give the standard form of the sum-product algorithm by updating just one of the factors at a time, for instance if we refine only $\widetilde{f}_{b3}(x_3)$, then $\widetilde{f}_{b2}(x_2)$ is unchanged by definition, while the refined version of $\widetilde{f}_{b3}(x_3)$ is again given by (10.235). If we are refining only one term at a time, then we can choose the order in which the refinements are done as we wish. In particular, for a tree-structured graph we can follow a two-pass update scheme, corresponding to the standard belief propagation schedule, which will result in exact inference of the variable and factor marginals. The initialization of the approximation factors in this case is unimportant.

Now let us consider a general factor graph corresponding to the distribution

$$p(\boldsymbol{\theta}) = \prod_i f_i(\boldsymbol{\theta}_i) \tag{10.236}$$

where $\boldsymbol{\theta}_i$ represents the subset of variables associated with factor f_i. We approximate this using a fully factorized distribution of the form

$$q(\boldsymbol{\theta}) \propto \prod_i \prod_k \widetilde{f}_{ik}(\theta_k) \tag{10.237}$$

where θ_k corresponds to an individual variable node. Suppose that we wish to refine the particular term $\widetilde{f}_{jl}(\theta_l)$ keeping all other terms fixed. We first remove the term $\widetilde{f}_j(\boldsymbol{\theta}_j)$ from $q(\boldsymbol{\theta})$ to give

$$q^{\backslash j}(\boldsymbol{\theta}) \propto \prod_{i \neq j} \prod_k \widetilde{f}_{ik}(\theta_k) \tag{10.238}$$

and then multiply by the exact factor $f_j(\boldsymbol{\theta}_j)$. To determine the refined term $\widetilde{f}_{jl}(\theta_l)$, we need only consider the functional dependence on θ_l, and so we simply find the corresponding marginal of

$$q^{\backslash j}(\boldsymbol{\theta}) f_j(\boldsymbol{\theta}_j). \tag{10.239}$$

Up to a multiplicative constant, this involves taking the marginal of $f_j(\boldsymbol{\theta}_j)$ multiplied by any terms from $q^{\backslash j}(\boldsymbol{\theta})$ that are functions of any of the variables in $\boldsymbol{\theta}_j$. Terms that correspond to other factors $\widetilde{f}_i(\boldsymbol{\theta}_i)$ for $i \neq j$ will cancel between numerator and denominator when we subsequently divide by $q^{\backslash j}(\boldsymbol{\theta})$. We therefore obtain

$$\widetilde{f}_{jl}(\theta_l) \propto \sum_{\theta_{m \neq l} \in \boldsymbol{\theta}_j} f_j(\boldsymbol{\theta}_j) \prod_k \prod_{m \neq l} \widetilde{f}_{km}(\theta_m). \tag{10.240}$$

We recognize this as the sum-product rule in the form in which messages from variable nodes to factor nodes have been eliminated, as illustrated by the example shown in Figure 8.50. The quantity $\widetilde{f}_{jm}(\theta_m)$ corresponds to the message $\mu_{f_j \to \theta_m}(\theta_m)$, which factor node j sends to variable node m, and the product over k in (10.240) is over all factors that depend on the variables θ_m that have variables (other than variable θ_l) in common with factor $f_j(\boldsymbol{\theta}_j)$. In other words, to compute the outgoing message from a factor node, we take the product of all the incoming messages from other factor nodes, multiply by the local factor, and then marginalize.

Thus, the sum-product algorithm arises as a special case of expectation propagation if we use an approximating distribution that is fully factorized. This suggests that more flexible approximating distributions, corresponding to partially disconnected graphs, could be used to achieve higher accuracy. Another generalization is to group factors $f_i(\boldsymbol{\theta}_i)$ together into sets and to refine all the factors in a set together at each iteration. Both of these approaches can lead to improvements in accuracy (Minka, 2001b). In general, the problem of choosing the best combination of grouping and disconnection is an open research issue.

We have seen that variational message passing and expectation propagation optimize two different forms of the Kullback-Leibler divergence. Minka (2005) has shown that a broad range of message passing algorithms can be derived from a common framework involving minimization of members of the alpha family of divergences, given by (10.19). These include variational message passing, loopy belief propagation, and expectation propagation, as well as a range of other algorithms, which we do not have space to discuss here, such as *tree-reweighted message passing* (Wainwright *et al.*, 2005), *fractional belief propagation* (Wiegerinck and Heskes, 2003), and *power EP* (Minka, 2004).

Exercises

10.1 (⋆) **www** Verify that the log marginal distribution of the observed data $\ln p(\mathbf{X})$ can be decomposed into two terms in the form (10.2) where $\mathcal{L}(q)$ is given by (10.3) and $\mathrm{KL}(q\|p)$ is given by (10.4).

10.2 (⋆) Use the properties $\mathbb{E}[z_1] = m_1$ and $\mathbb{E}[z_2] = m_2$ to solve the simultaneous equations (10.13) and (10.15), and hence show that, provided the original distribution $p(\mathbf{z})$ is nonsingular, the unique solution for the means of the factors in the approximation distribution is given by $\mathbb{E}[z_1] = \mu_1$ and $\mathbb{E}[z_2] = \mu_2$.

10.3 (⋆⋆) **www** Consider a factorized variational distribution $q(\mathbf{Z})$ of the form (10.5). By using the technique of Lagrange multipliers, verify that minimization of the Kullback-Leibler divergence $\mathrm{KL}(p\|q)$ with respect to one of the factors $q_i(\mathbf{Z}_i)$, keeping all other factors fixed, leads to the solution (10.17).

10.4 (⋆⋆) Suppose that $p(\mathbf{x})$ is some fixed distribution and that we wish to approximate it using a Gaussian distribution $q(\mathbf{x}) = \mathcal{N}(\mathbf{x}|\boldsymbol{\mu}, \boldsymbol{\Sigma})$. By writing down the form of the KL divergence $\mathrm{KL}(p\|q)$ for a Gaussian $q(\mathbf{x})$ and then differentiating, show that

minimization of $\mathrm{KL}(p\|q)$ with respect to $\boldsymbol{\mu}$ and $\boldsymbol{\Sigma}$ leads to the result that $\boldsymbol{\mu}$ is given by the expectation of $\mathbf{x}$ under $p(\mathbf{x})$ and that $\boldsymbol{\Sigma}$ is given by the covariance.

10.5 ($\star\star$) **www** Consider a model in which the set of all hidden stochastic variables, denoted collectively by $\mathbf{Z}$, comprises some latent variables $\mathbf{z}$ together with some model parameters $\boldsymbol{\theta}$. Suppose we use a variational distribution that factorizes between latent variables and parameters so that $q(\mathbf{z}, \boldsymbol{\theta}) = q_{\mathbf{z}}(\mathbf{z})q_{\boldsymbol{\theta}}(\boldsymbol{\theta})$, in which the distribution $q_{\boldsymbol{\theta}}(\boldsymbol{\theta})$ is approximated by a point estimate of the form $q_{\boldsymbol{\theta}}(\boldsymbol{\theta}) = \delta(\boldsymbol{\theta} - \boldsymbol{\theta}_0)$ where $\boldsymbol{\theta}_0$ is a vector of free parameters. Show that variational optimization of this factorized distribution is equivalent to an EM algorithm, in which the E step optimizes $q_{\mathbf{z}}(\mathbf{z})$, and the M step maximizes the expected complete-data log posterior distribution of $\boldsymbol{\theta}$ with respect to $\boldsymbol{\theta}_0$.

10.6 ($\star\star$) The alpha family of divergences is defined by (10.19). Show that the Kullback-Leibler divergence $\mathrm{KL}(p\|q)$ corresponds to $\alpha \to 1$. This can be done by writing $p^\epsilon = \exp(\epsilon \ln p) = 1 + \epsilon \ln p + O(\epsilon^2)$ and then taking $\epsilon \to 0$. Similarly show that $\mathrm{KL}(q\|p)$ corresponds to $\alpha \to -1$.

10.7 ($\star\star$) Consider the problem of inferring the mean and precision of a univariate Gaussian using a factorized variational approximation, as considered in Section 10.1.3. Show that the factor $q_\mu(\mu)$ is a Gaussian of the form $\mathcal{N}(\mu|\mu_N, \lambda_N^{-1})$ with mean and precision given by (10.26) and (10.27), respectively. Similarly show that the factor $q_\tau(\tau)$ is a gamma distribution of the form $\mathrm{Gam}(\tau|a_N, b_N)$ with parameters given by (10.29) and (10.30).

10.8 ($\star$) Consider the variational posterior distribution for the precision of a univariate Gaussian whose parameters are given by (10.29) and (10.30). By using the standard results for the mean and variance of the gamma distribution given by (B.27) and (B.28), show that if we let $N \to \infty$, this variational posterior distribution has a mean given by the inverse of the maximum likelihood estimator for the variance of the data, and a variance that goes to zero.

10.9 ($\star\star$) By making use of the standard result $\mathbb{E}[\tau] = a_N/b_N$ for the mean of a gamma distribution, together with (10.26), (10.27), (10.29), and (10.30), derive the result (10.33) for the reciprocal of the expected precision in the factorized variational treatment of a univariate Gaussian.

10.10 ($\star$) **www** Derive the decomposition given by (10.34) that is used to find approximate posterior distributions over models using variational inference.

10.11 ($\star\star$) **www** By using a Lagrange multiplier to enforce the normalization constraint on the distribution $q(m)$, show that the maximum of the lower bound (10.35) is given by (10.36).

10.12 ($\star\star$) Starting from the joint distribution (10.41), and applying the general result (10.9), show that the optimal variational distribution $q^\star(\mathbf{Z})$ over the latent variables for the Bayesian mixture of Gaussians is given by (10.48) by verifying the steps given in the text.

10.13 (⋆⋆) **www** Starting from (10.54), derive the result (10.59) for the optimum variational posterior distribution over $\boldsymbol{\mu}_k$ and $\boldsymbol{\Lambda}_k$ in the Bayesian mixture of Gaussians, and hence verify the expressions for the parameters of this distribution given by (10.60)–(10.63).

10.14 (⋆⋆) Using the distribution (10.59), verify the result (10.64).

10.15 (⋆) Using the result (B.17), show that the expected value of the mixing coefficients in the variational mixture of Gaussians is given by (10.69).

10.16 (⋆⋆) **www** Verify the results (10.71) and (10.72) for the first two terms in the lower bound for the variational Gaussian mixture model given by (10.70).

10.17 (⋆⋆⋆) Verify the results (10.73)–(10.77) for the remaining terms in the lower bound for the variational Gaussian mixture model given by (10.70).

10.18 (⋆⋆⋆) In this exercise, we shall derive the variational re-estimation equations for the Gaussian mixture model by direct differentiation of the lower bound. To do this we assume that the variational distribution has the factorization defined by (10.42) and (10.55) with factors given by (10.48), (10.57), and (10.59). Substitute these into (10.70) and hence obtain the lower bound as a function of the parameters of the variational distribution. Then, by maximizing the bound with respect to these parameters, derive the re-estimation equations for the factors in the variational distribution, and show that these are the same as those obtained in Section 10.2.1.

10.19 (⋆⋆) Derive the result (10.81) for the predictive distribution in the variational treatment of the Bayesian mixture of Gaussians model.

10.20 (⋆⋆) **www** This exercise explores the variational Bayes solution for the mixture of Gaussians model when the size N of the data set is large and shows that it reduces (as we would expect) to the maximum likelihood solution based on EM derived in Chapter 9. Note that results from Appendix B may be used to help answer this exercise. First show that the posterior distribution $q^\star(\boldsymbol{\Lambda}_k)$ of the precisions becomes sharply peaked around the maximum likelihood solution. Do the same for the posterior distribution of the means $q^\star(\boldsymbol{\mu}_k|\boldsymbol{\Lambda}_k)$. Next consider the posterior distribution $q^\star(\boldsymbol{\pi})$ for the mixing coefficients and show that this too becomes sharply peaked around the maximum likelihood solution. Similarly, show that the responsibilities become equal to the corresponding maximum likelihood values for large N, by making use of the following asymptotic result for the digamma function for large x

$$\psi(x) = \ln x + O\left(1/x\right). \tag{10.241}$$

Finally, by making use of (10.80), show that for large N, the predictive distribution becomes a mixture of Gaussians.

10.21 (⋆) Show that the number of equivalent parameter settings due to interchange symmetries in a mixture model with K components is $K!$.

10.22 ($\star\star$) We have seen that each mode of the posterior distribution in a Gaussian mixture model is a member of a family of $K!$ equivalent modes. Suppose that the result of running the variational inference algorithm is an approximate posterior distribution q that is localized in the neighbourhood of one of the modes. We can then approximate the full posterior distribution as a mixture of $K!$ such q distributions, once centred on each mode and having equal mixing coefficients. Show that if we assume negligible overlap between the components of the q mixture, the resulting lower bound differs from that for a single component q distribution through the addition of an extra term $\ln K!$.

10.23 ($\star\star$) **www** Consider a variational Gaussian mixture model in which there is no prior distribution over mixing coefficients $\{\pi_k\}$. Instead, the mixing coefficients are treated as parameters, whose values are to be found by maximizing the variational lower bound on the log marginal likelihood. Show that maximizing this lower bound with respect to the mixing coefficients, using a Lagrange multiplier to enforce the constraint that the mixing coefficients sum to one, leads to the re-estimation result (10.83). Note that there is no need to consider all of the terms in the lower bound but only the dependence of the bound on the $\{\pi_k\}$.

10.24 ($\star\star$) **www** We have seen in Section 10.2 that the singularities arising in the maximum likelihood treatment of Gaussian mixture models do not arise in a Bayesian treatment. Discuss whether such singularities would arise if the Bayesian model were solved using maximum posterior (MAP) estimation.

10.25 ($\star\star$) The variational treatment of the Bayesian mixture of Gaussians, discussed in Section 10.2, made use of a factorized approximation (10.5) to the posterior distribution. As we saw in Figure 10.2, the factorized assumption causes the variance of the posterior distribution to be under-estimated for certain directions in parameter space. Discuss qualitatively the effect this will have on the variational approximation to the model evidence, and how this effect will vary with the number of components in the mixture. Hence explain whether the variational Gaussian mixture will tend to under-estimate or over-estimate the optimal number of components.

10.26 ($\star\star\star$) Extend the variational treatment of Bayesian linear regression to include a gamma hyperprior $\mathrm{Gam}(\beta|c_0, d_0)$ over β and solve variationally, by assuming a factorized variational distribution of the form $q(\mathbf{w})q(\alpha)q(\beta)$. Derive the variational update equations for the three factors in the variational distribution and also obtain an expression for the lower bound and for the predictive distribution.

10.27 ($\star\star$) By making use of the formulae given in Appendix B show that the variational lower bound for the linear basis function regression model, defined by (10.107), can be written in the form (10.107) with the various terms defined by (10.108)–(10.112).

10.28 ($\star\star\star$) Rewrite the model for the Bayesian mixture of Gaussians, introduced in Section 10.2, as a conjugate model from the exponential family, as discussed in Section 10.4. Hence use the general results (10.115) and (10.119) to derive the specific results (10.48), (10.57), and (10.59).

10.29 (⋆) **www** Show that the function $f(x) = \ln(x)$ is concave for $0 < x < \infty$ by computing its second derivative. Determine the form of the dual function $g(\lambda)$ defined by (10.133), and verify that minimization of $\lambda x - g(\lambda)$ with respect to λ according to (10.132) indeed recovers the function $\ln(x)$.

10.30 (⋆) By evaluating the second derivative, show that the log logistic function $f(x) = -\ln(1 + e^{-x})$ is concave. Derive the variational upper bound (10.137) directly by making a second order Taylor expansion of the log logistic function around a point $x = \xi$.

10.31 (⋆⋆) By finding the second derivative with respect to x, show that the function $f(x) = -\ln(e^{x/2} + e^{-x/2})$ is a concave function of x. Now consider the second derivatives with respect to the variable x^2 and hence show that it is a convex function of x^2. Plot graphs of $f(x)$ against x and against x^2. Derive the lower bound (10.144) on the logistic sigmoid function directly by making a first order Taylor series expansion of the function $f(x)$ in the variable x^2 centred on the value ξ^2.

10.32 (⋆⋆) **www** Consider the variational treatment of logistic regression with sequential learning in which data points are arriving one at a time and each must be processed and discarded before the next data point arrives. Show that a Gaussian approximation to the posterior distribution can be maintained through the use of the lower bound (10.151), in which the distribution is initialized using the prior, and as each data point is absorbed its corresponding variational parameter ξ_n is optimized.

10.33 (⋆) By differentiating the quantity $Q(\boldsymbol{\xi}, \boldsymbol{\xi}^{\text{old}})$ defined by (10.161) with respect to the variational parameter ξ_n show that the update equation for ξ_n for the Bayesian logistic regression model is given by (10.163).

10.34 (⋆⋆) In this exercise we derive re-estimation equations for the variational parameters $\boldsymbol{\xi}$ in the Bayesian logistic regression model of Section 4.5 by direct maximization of the lower bound given by (10.164). To do this set the derivative of $\mathcal{L}(\boldsymbol{\xi})$ with respect to ξ_n equal to zero, making use of the result (3.117) for the derivative of the log of a determinant, together with the expressions (10.157) and (10.158) which define the mean and covariance of the variational posterior distribution $q(\mathbf{w})$.

10.35 (⋆⋆) Derive the result (10.164) for the lower bound $\mathcal{L}(\boldsymbol{\xi})$ in the variational logistic regression model. This is most easily done by substituting the expressions for the Gaussian prior $q(\mathbf{w}) = \mathcal{N}(\mathbf{w}|\mathbf{m}_0, \mathbf{S}_0)$, together with the lower bound $h(\mathbf{w}, \boldsymbol{\xi})$ on the likelihood function, into the integral (10.159) which defines $\mathcal{L}(\boldsymbol{\xi})$. Next gather together the terms which depend on $\mathbf{w}$ in the exponential and complete the square to give a Gaussian integral, which can then be evaluated by invoking the standard result for the normalization coefficient of a multivariate Gaussian. Finally take the logarithm to obtain (10.164).

10.36 (⋆⋆) Consider the ADF approximation scheme discussed in Section 10.7, and show that inclusion of the factor $f_j(\boldsymbol{\theta})$ leads to an update of the model evidence of the form

$$p_j(\mathcal{D}) \simeq p_{j-1}(\mathcal{D}) Z_j \tag{10.242}$$

where Z_j is the normalization constant defined by (10.197). By applying this result recursively, and initializing with $p_0(\mathcal{D}) = 1$, derive the result

$$p(\mathcal{D}) \simeq \prod_j Z_j. \tag{10.243}$$

10.37 ($\star$) **www** Consider the expectation propagation algorithm from Section 10.7, and suppose that one of the factors $f_0(\boldsymbol{\theta})$ in the definition (10.188) has the same exponential family functional form as the approximating distribution $q(\boldsymbol{\theta})$. Show that if the factor $\widetilde{f}_0(\boldsymbol{\theta})$ is initialized to be $f_0(\boldsymbol{\theta})$, then an EP update to refine $\widetilde{f}_0(\boldsymbol{\theta})$ leaves $\widetilde{f}_0(\boldsymbol{\theta})$ unchanged. This situation typically arises when one of the factors is the prior $p(\boldsymbol{\theta})$, and so we see that the prior factor can be incorporated once exactly and does not need to be refined.

10.38 ($\star\star\star$) In this exercise and the next, we shall verify the results (10.214)–(10.224) for the expectation propagation algorithm applied to the clutter problem. Begin by using the division formula (10.205) to derive the expressions (10.214) and (10.215) by completing the square inside the exponential to identify the mean and variance. Also, show that the normalization constant Z_n, defined by (10.206), is given for the clutter problem by (10.216). This can be done by making use of the general result (2.115).

10.39 ($\star\star\star$) Show that the mean and variance of $q^{\text{new}}(\boldsymbol{\theta})$ for EP applied to the clutter problem are given by (10.217) and (10.218). To do this, first prove the following results for the expectations of $\boldsymbol{\theta}$ and $\boldsymbol{\theta}\boldsymbol{\theta}^{\mathrm{T}}$ under $q^{\text{new}}(\boldsymbol{\theta})$

$$\mathbb{E}[\boldsymbol{\theta}] = \mathbf{m}^{\backslash n} + v^{\backslash n}\nabla_{\mathbf{m}^{\backslash n}} \ln Z_n \tag{10.244}$$

$$\mathbb{E}[\boldsymbol{\theta}^{\mathrm{T}}\boldsymbol{\theta}] = 2(v^{\backslash n})^2\nabla_{v^{\backslash n}} \ln Z_n + 2\mathbb{E}[\boldsymbol{\theta}]^{\mathrm{T}}\mathbf{m}^{\backslash n} - \|\mathbf{m}^{\backslash n}\|^2 \tag{10.245}$$

and then make use of the result (10.216) for Z_n. Next, prove the results (10.220)–(10.222) by using (10.207) and completing the square in the exponential. Finally, use (10.208) to derive the result (10.223).

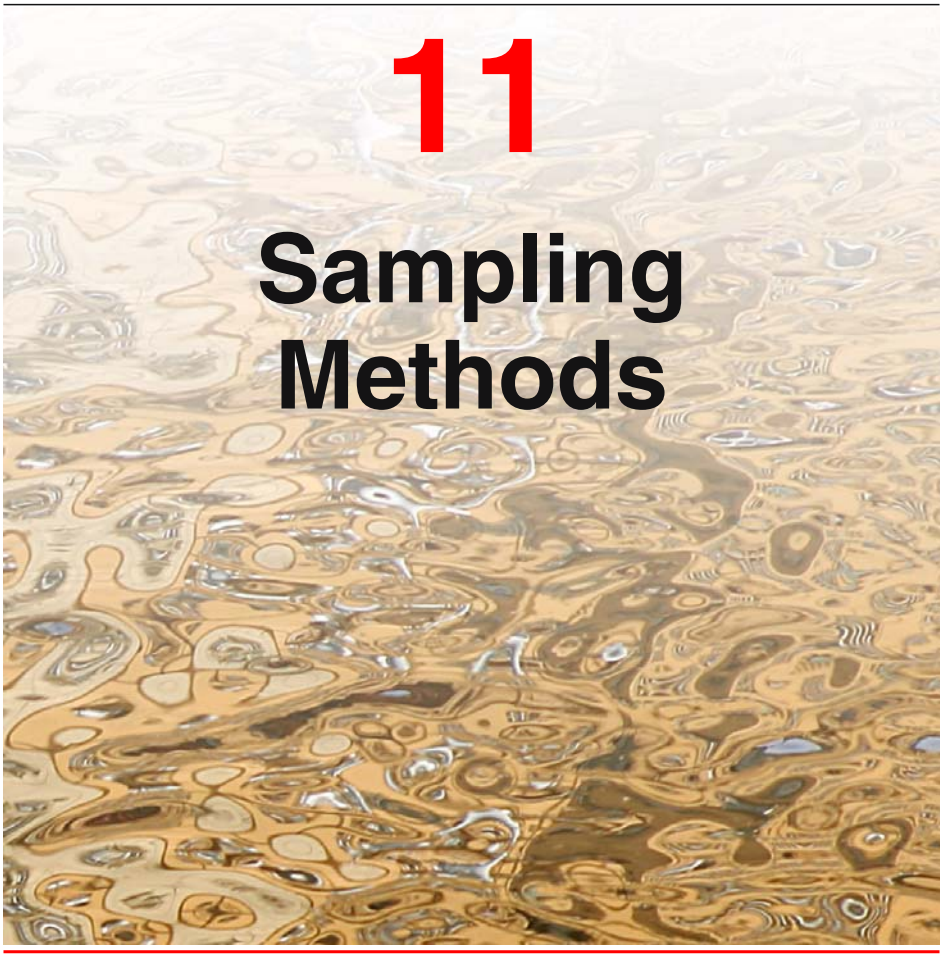

11 Sampling Methods

For most probabilistic models of practical interest, exact inference is intractable, and so we have to resort to some form of approximation. In Chapter 10, we discussed inference algorithms based on deterministic approximations, which include methods such as variational Bayes and expectation propagation. Here we consider approximate inference methods based on numerical sampling, also known as *Monte Carlo* techniques.

Although for some applications the posterior distribution over unobserved variables will be of direct interest in itself, for most situations the posterior distribution is required primarily for the purpose of evaluating expectations, for example in order to make predictions. The fundamental problem that we therefore wish to address in this chapter involves finding the expectation of some function $f(\mathbf{z})$ with respect to a probability distribution $p(\mathbf{z})$. Here, the components of $\mathbf{z}$ might comprise discrete or continuous variables or some combination of the two. Thus in the case of continuous

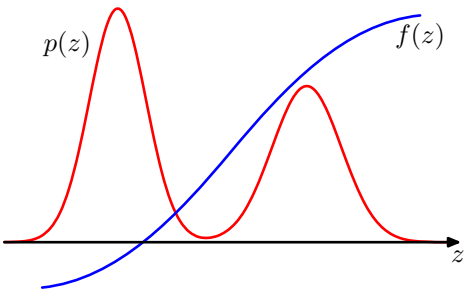

Figure 11.1 Schematic illustration of a function $f(z)$ whose expectation is to be evaluated with respect to a distribution $p(z)$.

variables, we wish to evaluate the expectation

$$\mathbb{E}[f] = \int f(\mathbf{z})p(\mathbf{z})\,\mathrm{d}\mathbf{z} \tag{11.1}$$

where the integral is replaced by summation in the case of discrete variables. This is illustrated schematically for a single continuous variable in Figure 11.1. We shall suppose that such expectations are too complex to be evaluated exactly using analytical techniques.

The general idea behind sampling methods is to obtain a set of samples $\mathbf{z}^{(l)}$ (where $l = 1, \ldots, L$) drawn independently from the distribution $p(\mathbf{z})$. This allows the expectation (11.1) to be approximated by a finite sum

$$\widehat{f} = \frac{1}{L}\sum_{l=1}^{L} f(\mathbf{z}^{(l)}). \tag{11.2}$$

As long as the samples $\mathbf{z}^{(l)}$ are drawn from the distribution $p(\mathbf{z})$, then $\mathbb{E}[\widehat{f}] = \mathbb{E}[f]$ and so the estimator $\widehat{f}$ has the correct mean. The variance of the estimator is given by

Exercise 11.1

$$\mathrm{var}[\widehat{f}] = \frac{1}{L}\mathbb{E}\left[(f - \mathbb{E}[f])^2\right] \tag{11.3}$$

is the variance of the function $f(\mathbf{z})$ under the distribution $p(\mathbf{z})$. It is worth emphasizing that the accuracy of the estimator therefore does not depend on the dimensionality of $\mathbf{z}$, and that, in principle, high accuracy may be achievable with a relatively small number of samples $\mathbf{z}^{(l)}$. In practice, ten or twenty independent samples may suffice to estimate an expectation to sufficient accuracy.

The problem, however, is that the samples $\{\mathbf{z}^{(l)}\}$ might not be independent, and so the effective sample size might be much smaller than the apparent sample size. Also, referring back to Figure 11.1, we note that if $f(\mathbf{z})$ is small in regions where $p(\mathbf{z})$ is large, and vice versa, then the expectation may be dominated by regions of small probability, implying that relatively large sample sizes will be required to achieve sufficient accuracy.

For many models, the joint distribution $p(\mathbf{z})$ is conveniently specified in terms of a graphical model. In the case of a directed graph with no observed variables, it is

straightforward to sample from the joint distribution (assuming that it is possible to sample from the conditional distributions at each node) using the following *ancestral sampling* approach, discussed briefly in Section 8.1.2. The joint distribution is specified by

$$p(\mathbf{z}) = \prod_{i=1}^{M} p(\mathbf{z}_i|\mathrm{pa}_i) \tag{11.4}$$

where $\mathbf{z}_i$ are the set of variables associated with node i, and pa_i denotes the set of variables associated with the parents of node i. To obtain a sample from the joint distribution, we make one pass through the set of variables in the order $\mathbf{z}_1, \ldots, \mathbf{z}_M$ sampling from the conditional distributions $p(\mathbf{z}_i|\mathrm{pa}_i)$. This is always possible because at each step all of the parent values will have been instantiated. After one pass through the graph, we will have obtained a sample from the joint distribution.

Now consider the case of a directed graph in which some of the nodes are instantiated with observed values. We can in principle extend the above procedure, at least in the case of nodes representing discrete variables, to give the following *logic sampling* approach (Henrion, 1988), which can be seen as a special case of *importance sampling* discussed in Section 11.1.4. At each step, when a sampled value is obtained for a variable $\mathbf{z}_i$ whose value is observed, the sampled value is compared to the observed value, and if they agree then the sample value is retained and the algorithm proceeds to the next variable in turn. However, if the sampled value and the observed value disagree, then the whole sample so far is discarded and the algorithm starts again with the first node in the graph. This algorithm samples correctly from the posterior distribution because it corresponds simply to drawing samples from the joint distribution of hidden variables and data variables and then discarding those samples that disagree with the observed data (with the slight saving of not continuing with the sampling from the joint distribution as soon as one contradictory value is observed). However, the overall probability of accepting a sample from the posterior decreases rapidly as the number of observed variables increases and as the number of states that those variables can take increases, and so this approach is rarely used in practice.

In the case of probability distributions defined by an undirected graph, there is no one-pass sampling strategy that will sample even from the prior distribution with no observed variables. Instead, computationally more expensive techniques must be employed, such as Gibbs sampling, which is discussed in Section 11.3.

As well as sampling from conditional distributions, we may also require samples from a marginal distribution. If we already have a strategy for sampling from a joint distribution $p(\mathbf{u}, \mathbf{v})$, then it is straightforward to obtain samples from the marginal distribution $p(\mathbf{u})$ simply by ignoring the values for $\mathbf{v}$ in each sample.

There are numerous texts dealing with Monte Carlo methods. Those of particular interest from the statistical inference perspective include Chen *et al.* (2001), Gamerman (1997), Gilks *et al.* (1996), Liu (2001), Neal (1996), and Robert and Casella (1999). Also there are review articles by Besag *et al.* (1995), Brooks (1998), Diaconis and Saloff-Coste (1998), Jerrum and Sinclair (1996), Neal (1993), Tierney (1994), and Andrieu *et al.* (2003) that provide additional information on sampling

methods for statistical inference.

Diagnostic tests for convergence of Markov chain Monte Carlo algorithms are summarized in Robert and Casella (1999), and some practical guidance on the use of sampling methods in the context of machine learning is given in Bishop and Nabney (2008).

11.1. Basic Sampling Algorithms

In this section, we consider some simple strategies for generating random samples from a given distribution. Because the samples will be generated by a computer algorithm they will in fact be *pseudo-random* numbers, that is, they will be deterministically calculated, but must nevertheless pass appropriate tests for randomness. Generating such numbers raises several subtleties (Press *et al.*, 1992) that lie outside the scope of this book. Here we shall assume that an algorithm has been provided that generates pseudo-random numbers distributed uniformly over $(0, 1)$, and indeed most software environments have such a facility built in.

11.1.1 Standard distributions

We first consider how to generate random numbers from simple nonuniform distributions, assuming that we already have available a source of uniformly distributed random numbers. Suppose that z is uniformly distributed over the interval $(0, 1)$, and that we transform the values of z using some function $f(\cdot)$ so that $y = f(z)$. The distribution of y will be governed by

$$p(y) = p(z)\left|\frac{dz}{dy}\right| \tag{11.5}$$

where, in this case, $p(z) = 1$. Our goal is to choose the function $f(z)$ such that the resulting values of y have some specific desired distribution $p(y)$. Integrating (11.5) we obtain

$$z = h(y) \equiv \int_{-\infty}^{y} p(\widehat{y})\,\mathrm{d}\widehat{y} \tag{11.6}$$

Exercise 11.2

which is the indefinite integral of $p(y)$. Thus, $y = h^{-1}(z)$, and so we have to transform the uniformly distributed random numbers using a function which is the inverse of the indefinite integral of the desired distribution. This is illustrated in Figure 11.2.

Consider for example the *exponential distribution*

$$p(y) = \lambda \exp(-\lambda y) \tag{11.7}$$

where $0 \leqslant y < \infty$. In this case the lower limit of the integral in (11.6) is 0, and so $h(y) = 1 - \exp(-\lambda y)$. Thus, if we transform our uniformly distributed variable z using $y = -\lambda^{-1}\ln(1 - z)$, then y will have an exponential distribution.

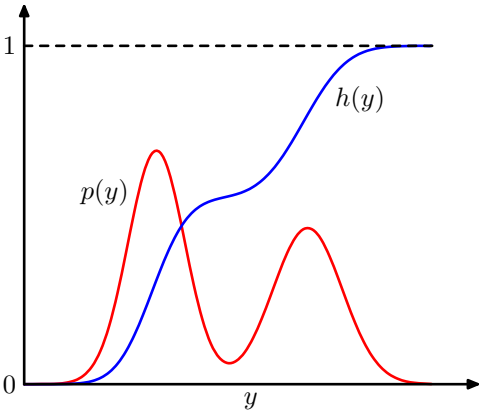

Figure 11.2 Geometrical interpretation of the transformation method for generating nonuniformly distributed random numbers. $h(y)$ is the indefinite integral of the desired distribution $p(y)$. If a uniformly distributed random variable z is transformed using $y = h^{-1}(z)$, then y will be distributed according to $p(y)$.

Another example of a distribution to which the transformation method can be applied is given by the Cauchy distribution

$$p(y) = \frac{1}{\pi}\frac{1}{1+y^2}. \tag{11.8}$$

Exercise 11.3 In this case, the inverse of the indefinite integral can be expressed in terms of the 'tan' function.

The generalization to multiple variables is straightforward and involves the Jacobian of the change of variables, so that

$$p(y_1, \ldots, y_M) = p(z_1, \ldots, z_M)\left|\frac{\partial(z_1, \ldots, z_M)}{\partial(y_1, \ldots, y_M)}\right|. \tag{11.9}$$

As a final example of the transformation method we consider the Box-Muller method for generating samples from a Gaussian distribution. First, suppose we generate pairs of uniformly distributed random numbers $z_1, z_2 \in (-1, 1)$, which we can do by transforming a variable distributed uniformly over $(0, 1)$ using $z \to 2z - 1$. Next we discard each pair unless it satisfies $z_1^2 + z_2^2 \leqslant 1$. This leads to a uniform distribution of points inside the unit circle with $p(z_1, z_2) = 1/\pi$, as illustrated in Figure 11.3. Then, for each pair z_1, z_2 we evaluate the quantities

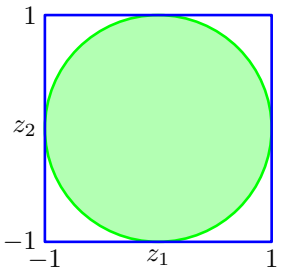

Figure 11.3 The Box-Muller method for generating Gaussian distributed random numbers starts by generating samples from a uniform distribution inside the unit circle.

$$y_1 = z_1 \left(\frac{-2 \ln z_1}{r^2} \right)^{1/2} \tag{11.10}$$

$$y_2 = z_2 \left(\frac{-2 \ln z_2}{r^2} \right)^{1/2} \tag{11.11}$$

Exercise 11.4

where $r^2 = z_1^2 + z_2^2$. Then the joint distribution of y_1 and y_2 is given by

$$\begin{aligned} p(y_1, y_2) &= p(z_1, z_2) \left| \frac{\partial(z_1, z_2)}{\partial(y_1, y_2)} \right| \\ &= \left[\frac{1}{\sqrt{2\pi}} \exp(-y_1^2/2) \right] \left[\frac{1}{\sqrt{2\pi}} \exp(-y_2^2/2) \right] \end{aligned} \tag{11.12}$$

and so y_1 and y_2 are independent and each has a Gaussian distribution with zero mean and unit variance.

If y has a Gaussian distribution with zero mean and unit variance, then $\sigma y + \mu$ will have a Gaussian distribution with mean μ and variance σ^2. To generate vector-valued variables having a multivariate Gaussian distribution with mean $\boldsymbol{\mu}$ and covariance $\boldsymbol{\Sigma}$, we can make use of the *Cholesky decomposition*, which takes the form $\boldsymbol{\Sigma} = \mathbf{L}\mathbf{L}^{\mathrm{T}}$ (Press *et al.*, 1992). Then, if $\mathbf{z}$ is a vector valued random variable whose components are independent and Gaussian distributed with zero mean and unit variance, then $\mathbf{y} = \boldsymbol{\mu} + \mathbf{L}\mathbf{z}$ will have mean $\boldsymbol{\mu}$ and covariance $\boldsymbol{\Sigma}$.

Exercise 11.5

Obviously, the transformation technique depends for its success on the ability to calculate and then invert the indefinite integral of the required distribution. Such operations will only be feasible for a limited number of simple distributions, and so we must turn to alternative approaches in search of a more general strategy. Here we consider two techniques called *rejection sampling* and *importance sampling*. Although mainly limited to univariate distributions and thus not directly applicable to complex problems in many dimensions, they do form important components in more general strategies.

11.1.2 Rejection sampling

The rejection sampling framework allows us to sample from relatively complex distributions, subject to certain constraints. We begin by considering univariate distributions and discuss the extension to multiple dimensions subsequently.

Suppose we wish to sample from a distribution $p(\mathbf{z})$ that is not one of the simple, standard distributions considered so far, and that sampling directly from $p(\mathbf{z})$ is difficult. Furthermore suppose, as is often the case, that we are easily able to evaluate $p(\mathbf{z})$ for any given value of $\mathbf{z}$, up to some normalizing constant Z, so that

$$p(z) = \frac{1}{Z_p} \widetilde{p}(z) \tag{11.13}$$

where $\widetilde{p}(z)$ can readily be evaluated, but Z_p is unknown.

In order to apply rejection sampling, we need some simpler distribution $q(z)$, sometimes called a *proposal distribution*, from which we can readily draw samples.

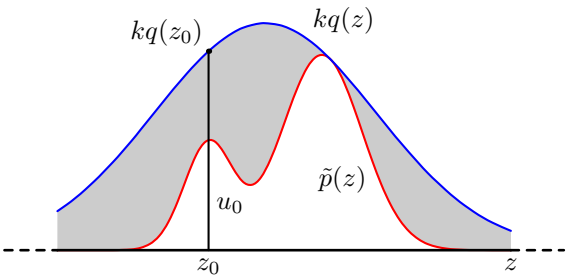

Figure 11.4 In the rejection sampling method, samples are drawn from a simple distribution $q(z)$ and rejected if they fall in the grey area between the unnormalized distribution $\widetilde{p}(z)$ and the scaled distribution $kq(z)$. The resulting samples are distributed according to $p(z)$, which is the normalized version of $\widetilde{p}(z)$.

We next introduce a constant k whose value is chosen such that $kq(z) \geqslant \widetilde{p}(z)$ for all values of z. The function $kq(z)$ is called the comparison function and is illustrated for a univariate distribution in Figure 11.4. Each step of the rejection sampler involves generating two random numbers. First, we generate a number z_0 from the distribution $q(z)$. Next, we generate a number u_0 from the uniform distribution over $[0, kq(z_0)]$. This pair of random numbers has uniform distribution under the curve of the function $kq(z)$. Finally, if $u_0 > \widetilde{p}(z_0)$ then the sample is rejected, otherwise u_0 is retained. Thus the pair is rejected if it lies in the grey shaded region in Figure 11.4. The remaining pairs then have uniform distribution under the curve of $\widetilde{p}(z)$, and hence the corresponding z values are distributed according to $p(z)$, as desired.

Exercise 11.6

The original values of z are generated from the distribution $q(z)$, and these samples are then accepted with probability $\widetilde{p}(z)/kq(z)$, and so the probability that a sample will be accepted is given by

$$\begin{aligned} p(\text{accept}) &= \int \{\widetilde{p}(z)/kq(z)\}\, q(z)\, \mathrm{d}z \\ &= \frac{1}{k} \int \widetilde{p}(z)\, \mathrm{d}z. \end{aligned} \tag{11.14}$$

Thus the fraction of points that are rejected by this method depends on the ratio of the area under the unnormalized distribution $\widetilde{p}(z)$ to the area under the curve $kq(z)$. We therefore see that the constant k should be as small as possible subject to the limitation that $kq(z)$ must be nowhere less than $\widetilde{p}(z)$.

As an illustration of the use of rejection sampling, consider the task of sampling from the gamma distribution

$$\mathrm{Gam}(z|a, b) = \frac{b^a z^{a-1} \exp(-bz)}{\Gamma(a)} \tag{11.15}$$

which, for $a > 1$, has a bell-shaped form, as shown in Figure 11.5. A suitable proposal distribution is therefore the Cauchy (11.8) because this too is bell-shaped and because we can use the transformation method, discussed earlier, to sample from it. We need to generalize the Cauchy slightly to ensure that it nowhere has a smaller value than the gamma distribution. This can be achieved by transforming a uniform random variable y using $z = b \tan y + c$, which gives random numbers distributed according to.

Exercise 11.7

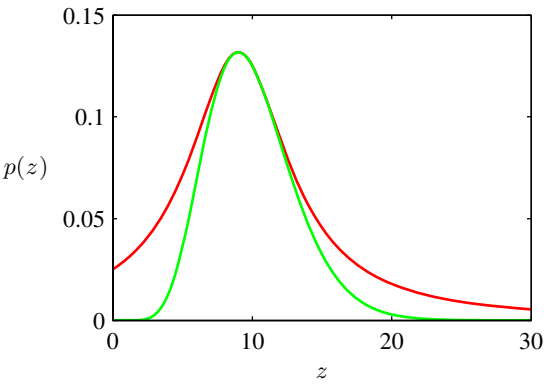

Figure 11.5 Plot showing the gamma distribution given by (11.15) as the green curve, with a scaled Cauchy proposal distribution shown by the red curve. Samples from the gamma distribution can be obtained by sampling from the Cauchy and then applying the rejection sampling criterion.

$$q(z) = \frac{k}{1 + (z - c)^2/b^2}. \tag{11.16}$$

The minimum reject rate is obtained by setting $c = a - 1$, $b^2 = 2a - 1$ and choosing the constant k to be as small as possible while still satisfying the requirement $kq(z) \geqslant \widetilde{p}(z)$. The resulting comparison function is also illustrated in Figure 11.5.

11.1.3 Adaptive rejection sampling

In many instances where we might wish to apply rejection sampling, it proves difficult to determine a suitable analytic form for the envelope distribution $q(z)$. An alternative approach is to construct the envelope function on the fly based on measured values of the distribution $p(z)$ (Gilks and Wild, 1992). Construction of an envelope function is particularly straightforward for cases in which $p(z)$ is log concave, in other words when $\ln p(z)$ has derivatives that are nonincreasing functions of z. The construction of a suitable envelope function is illustrated graphically in Figure 11.6.

The function $\ln p(z)$ and its gradient are evaluated at some initial set of grid points, and the intersections of the resulting tangent lines are used to construct the envelope function. Next a sample value is drawn from the envelope distribution. This is straightforward because the log of the envelope distribution is a succession

Exercise 11.9

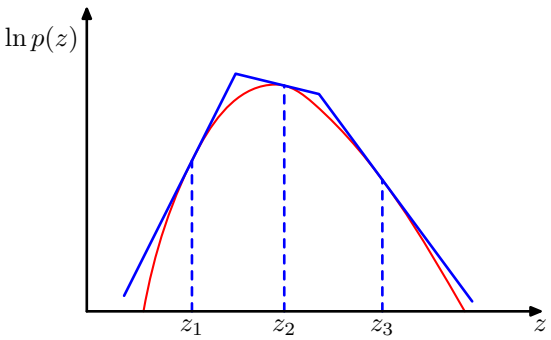

Figure 11.6 In the case of distributions that are log concave, an envelope function for use in rejection sampling can be constructed using the tangent lines computed at a set of grid points. If a sample point is rejected, it is added to the set of grid points and used to refine the envelope distribution.

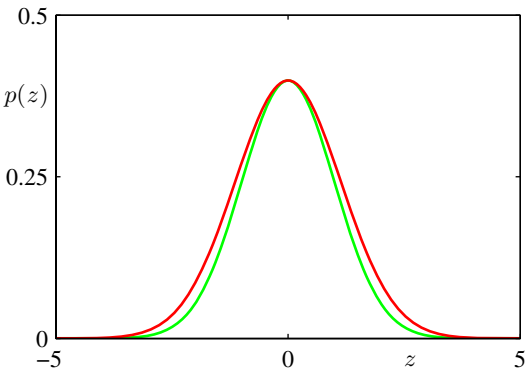

Figure 11.7 Illustrative example of rejection sampling involving sampling from a Gaussian distribution $p(z)$ shown by the green curve, by using rejection sampling from a proposal distribution $q(z)$ that is also Gaussian and whose scaled version $kq(z)$ is shown by the red curve.

of linear functions, and hence the envelope distribution itself comprises a piecewise exponential distribution of the form

$$q(z) = k_i \lambda_i \exp\{-\lambda_i(z - z_{i-1})\} \qquad z_{i-1} < z \leqslant z_i. \tag{11.17}$$

Once a sample has been drawn, the usual rejection criterion can be applied. If the sample is accepted, then it will be a draw from the desired distribution. If, however, the sample is rejected, then it is incorporated into the set of grid points, a new tangent line is computed, and the envelope function is thereby refined. As the number of grid points increases, so the envelope function becomes a better approximation of the desired distribution $p(z)$ and the probability of rejection decreases.

A variant of the algorithm exists that avoids the evaluation of derivatives (Gilks, 1992). The adaptive rejection sampling framework can also be extended to distributions that are not log concave, simply by following each rejection sampling step with a Metropolis-Hastings step (to be discussed in Section 11.2.2), giving rise to *adaptive rejection Metropolis* sampling (Gilks *et al.*, 1995).

Clearly for rejection sampling to be of practical value, we require that the comparison function be close to the required distribution so that the rate of rejection is kept to a minimum. Now let us examine what happens when we try to use rejection sampling in spaces of high dimensionality. Consider, for the sake of illustration, a somewhat artificial problem in which we wish to sample from a zero-mean multivariate Gaussian distribution with covariance $\sigma_p^2\mathbf{I}$, where $\mathbf{I}$ is the unit matrix, by rejection sampling from a proposal distribution that is itself a zero-mean Gaussian distribution having covariance $\sigma_q^2\mathbf{I}$. Obviously, we must have $\sigma_q^2 \geqslant \sigma_p^2$ in order that there exists a k such that $kq(z) \geqslant p(z)$. In D-dimensions the optimum value of k is given by $k = (\sigma_q/\sigma_p)^D$, as illustrated for $D = 1$ in Figure 11.7. The acceptance rate will be the ratio of volumes under $p(z)$ and $kq(z)$, which, because both distributions are normalized, is just $1/k$. Thus the acceptance rate diminishes exponentially with dimensionality. Even if σ_q exceeds σ_p by just one percent, for $D = 1,000$ the acceptance ratio will be approximately $1/20,000$. In this illustrative example the comparison function is close to the required distribution. For more practical examples, where the desired distribution may be multimodal and sharply peaked, it will be extremely difficult to find a good proposal distribution and comparison function.

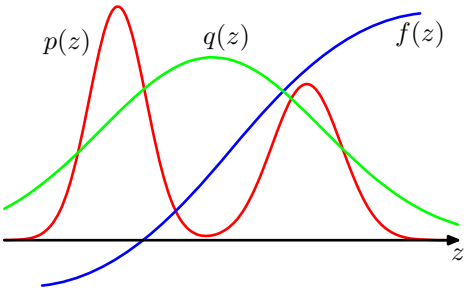

Figure 11.8 Importance sampling addresses the problem of evaluating the expectation of a function $f(z)$ with respect to a distribution $p(z)$ from which it is difficult to draw samples directly. Instead, samples $\{z^{(l)}\}$ are drawn from a simpler distribution $q(z)$, and the corresponding terms in the summation are weighted by the ratios $p(z^{(l)})/q(z^{(l)})$.

Furthermore, the exponential decrease of acceptance rate with dimensionality is a generic feature of rejection sampling. Although rejection can be a useful technique in one or two dimensions it is unsuited to problems of high dimensionality. It can, however, play a role as a subroutine in more sophisticated algorithms for sampling in high dimensional spaces.

11.1.4 Importance sampling

One of the principal reasons for wishing to sample from complicated probability distributions is to be able to evaluate expectations of the form (11.1). The technique of *importance sampling* provides a framework for approximating expectations directly but does not itself provide a mechanism for drawing samples from distribution $p(\mathbf{z})$.

The finite sum approximation to the expectation, given by (11.2), depends on being able to draw samples from the distribution $p(\mathbf{z})$. Suppose, however, that it is impractical to sample directly from $p(\mathbf{z})$ but that we can evaluate $p(\mathbf{z})$ easily for any given value of $\mathbf{z}$. One simplistic strategy for evaluating expectations would be to discretize $\mathbf{z}$-space into a uniform grid and to evaluate the integrand as a sum of the form

$$\mathbb{E}[f] \simeq \sum_{l=1}^{L} p(\mathbf{z}^{(l)}) f(\mathbf{z}^{(l)}). \tag{11.18}$$

An obvious problem with this approach is that the number of terms in the summation grows exponentially with the dimensionality of $\mathbf{z}$. Furthermore, as we have already noted, the kinds of probability distributions of interest will often have much of their mass confined to relatively small regions of $\mathbf{z}$ space and so uniform sampling will be very inefficient because in high-dimensional problems, only a very small proportion of the samples will make a significant contribution to the sum. We would really like to choose the sample points to fall in regions where $p(\mathbf{z})$ is large, or ideally where the product $p(\mathbf{z})f(\mathbf{z})$ is large.

As in the case of rejection sampling, importance sampling is based on the use of a proposal distribution $q(\mathbf{z})$ from which it is easy to draw samples, as illustrated in Figure 11.8. We can then express the expectation in the form of a finite sum over

samples $\{\mathbf{z}^{(l)}\}$ drawn from $q(\mathbf{z})$

$$\begin{aligned}\mathbb{E}[f] &= \int f(\mathbf{z})p(\mathbf{z})\,\mathrm{d}\mathbf{z} \\ &= \int f(\mathbf{z})\frac{p(\mathbf{z})}{q(\mathbf{z})}q(\mathbf{z})\,\mathrm{d}\mathbf{z} \\ &\simeq \frac{1}{L}\sum_{l=1}^{L}\frac{p(\mathbf{z}^{(l)})}{q(\mathbf{z}^{(l)})}f(\mathbf{z}^{(l)}).\end{aligned} \tag{11.19}$$

The quantities $r_l = p(\mathbf{z}^{(l)})/q(\mathbf{z}^{(l)})$ are known as *importance weights*, and they correct the bias introduced by sampling from the wrong distribution. Note that, unlike rejection sampling, all of the samples generated are retained.

It will often be the case that the distribution $p(\mathbf{z})$ can only be evaluated up to a normalization constant, so that $p(\mathbf{z}) = \widetilde{p}(\mathbf{z})/Z_p$ where $\widetilde{p}(\mathbf{z})$ can be evaluated easily, whereas Z_p is unknown. Similarly, we may wish to use an importance sampling distribution $q(\mathbf{z}) = \widetilde{q}(\mathbf{z})/Z_q$, which has the same property. We then have

$$\begin{aligned}\mathbb{E}[f] &= \int f(\mathbf{z})p(\mathbf{z})\,\mathrm{d}\mathbf{z} \\ &= \frac{Z_q}{Z_p}\int f(\mathbf{z})\frac{\widetilde{p}(\mathbf{z})}{\widetilde{q}(\mathbf{z})}q(\mathbf{z})\,\mathrm{d}\mathbf{z} \\ &\simeq \frac{Z_q}{Z_p}\frac{1}{L}\sum_{l=1}^{L}\widetilde{r}_l f(\mathbf{z}^{(l)}).\end{aligned} \tag{11.20}$$

where $\widetilde{r}_l = \widetilde{p}(\mathbf{z}^{(l)})/\widetilde{q}(\mathbf{z}^{(l)})$. We can use the same sample set to evaluate the ratio Z_p/Z_q with the result

$$\begin{aligned}\frac{Z_p}{Z_q} &= \frac{1}{Z_q}\int \widetilde{p}(\mathbf{z})\,\mathrm{d}\mathbf{z} = \int \frac{\widetilde{p}(\mathbf{z})}{\widetilde{q}(\mathbf{z})}q(\mathbf{z})\,\mathrm{d}\mathbf{z} \\ &\simeq \frac{1}{L}\sum_{l=1}^{L}\widetilde{r}_l\end{aligned} \tag{11.21}$$

and hence

$$\mathbb{E}[f] \simeq \sum_{l=1}^{L} w_l f(\mathbf{z}^{(l)}) \tag{11.22}$$

where we have defined

$$w_l = \frac{\widetilde{r}_l}{\sum_m \widetilde{r}_m} = \frac{\widetilde{p}(\mathbf{z}^{(l)})/q(\mathbf{z}^{(l)})}{\sum_m \widetilde{p}(\mathbf{z}^{(m)})/q(\mathbf{z}^{(m)})}. \tag{11.23}$$

As with rejection sampling, the success of the importance sampling approach depends crucially on how well the sampling distribution $q(\mathbf{z})$ matches the desired

distribution $p(\mathbf{z})$. If, as is often the case, $p(\mathbf{z})f(\mathbf{z})$ is strongly varying and has a significant proportion of its mass concentrated over relatively small regions of $\mathbf{z}$ space, then the set of importance weights $\{r_l\}$ may be dominated by a few weights having large values, with the remaining weights being relatively insignificant. Thus the effective sample size can be much smaller than the apparent sample size L. The problem is even more severe if none of the samples falls in the regions where $p(\mathbf{z})f(\mathbf{z})$ is large. In that case, the apparent variances of r_l and $r_l f(\mathbf{z}^{(l)})$ may be small even though the estimate of the expectation may be severely wrong. Hence a major drawback of the importance sampling method is the potential to produce results that are arbitrarily in error and with no diagnostic indication. This also highlights a key requirement for the sampling distribution $q(\mathbf{z})$, namely that it should not be small or zero in regions where $p(\mathbf{z})$ may be significant.

For distributions defined in terms of a graphical model, we can apply the importance sampling technique in various ways. For discrete variables, a simple approach is called *uniform sampling*. The joint distribution for a directed graph is defined by (11.4). Each sample from the joint distribution is obtained by first setting those variables $\mathbf{z}_i$ that are in the evidence set equal to their observed values. Each of the remaining variables is then sampled independently from a uniform distribution over the space of possible instantiations. To determine the corresponding weight associated with a sample $\mathbf{z}^{(l)}$, we note that the sampling distribution $\widetilde{q}(\mathbf{z})$ is uniform over the possible choices for $\mathbf{z}$, and that $\widetilde{p}(\mathbf{z}|\mathbf{x}) = \widetilde{p}(\mathbf{z})$, where $\mathbf{x}$ denotes the subset of variables that are observed, and the equality follows from the fact that every sample $\mathbf{z}$ that is generated is necessarily consistent with the evidence. Thus the weights r_l are simply proportional to $p(\mathbf{z})$. Note that the variables can be sampled in any order. This approach can yield poor results if the posterior distribution is far from uniform, as is often the case in practice.

An improvement on this approach is called *likelihood weighted sampling* (Fung and Chang, 1990; Shachter and Peot, 1990) and is based on ancestral sampling of the variables. For each variable in turn, if that variable is in the evidence set, then it is just set to its instantiated value. If it is not in the evidence set, then it is sampled from the conditional distribution $p(\mathbf{z}_i|\mathrm{pa}_i)$ in which the conditioning variables are set to their currently sampled values. The weighting associated with the resulting sample $\mathbf{z}$ is then given by

$$r(\mathbf{z}) = \prod_{\mathbf{z}_i \notin \mathbf{e}} \frac{p(\mathbf{z}_i|\mathrm{pa}_i)}{p(\mathbf{z}_i|\mathrm{pa}_i)} \prod_{\mathbf{z}_i \in \mathbf{e}} \frac{p(\mathbf{z}_i|\mathrm{pa}_i)}{1} = \prod_{\mathbf{z}_i \in \mathbf{e}} p(\mathbf{z}_i|\mathrm{pa}_i). \tag{11.24}$$

This method can be further extended using *self-importance sampling* (Shachter and Peot, 1990) in which the importance sampling distribution is continually updated to reflect the current estimated posterior distribution.

11.1.5 Sampling-importance-resampling

The rejection sampling method discussed in Section 11.1.2 depends in part for its success on the determination of a suitable value for the constant k. For many pairs of distributions $p(\mathbf{z})$ and $q(\mathbf{z})$, it will be impractical to determine a suitable

value for k in that any value that is sufficiently large to guarantee a bound on the desired distribution will lead to impractically small acceptance rates.

As in the case of rejection sampling, the *sampling-importance-resampling* (SIR) approach also makes use of a sampling distribution $q(\mathbf{z})$ but avoids having to determine the constant k. There are two stages to the scheme. In the first stage, L samples $\mathbf{z}^{(1)}, \ldots, \mathbf{z}^{(L)}$ are drawn from $q(\mathbf{z})$. Then in the second stage, weights $w_1, \ldots, w_L$ are constructed using (11.23). Finally, a second set of L samples is drawn from the discrete distribution $(\mathbf{z}^{(1)}, \ldots, \mathbf{z}^{(L)})$ with probabilities given by the weights $(w_1, \ldots, w_L)$.

The resulting L samples are only approximately distributed according to $p(\mathbf{z})$, but the distribution becomes correct in the limit $L \to \infty$. To see this, consider the univariate case, and note that the cumulative distribution of the resampled values is given by

$$\begin{aligned} p(z \leqslant a) &= \sum_{l: z^{(l)} \leqslant a} w_l \\ &= \frac{\sum_l I(z^{(l)} \leqslant a) \widetilde{p}(z^{(l)})/q(z^{(l)})}{\sum_l \widetilde{p}(z^{(l)})/q(z^{(l)})} \end{aligned} \tag{11.25}$$

where $I(.)$ is the indicator function (which equals 1 if its argument is true and 0 otherwise). Taking the limit $L \to \infty$, and assuming suitable regularity of the distributions, we can replace the sums by integrals weighted according to the original sampling distribution $q(z)$

$$\begin{aligned} p(z \leqslant a) &= \frac{\displaystyle\int I(z \leqslant a) \{\widetilde{p}(z)/q(z)\} q(z) \, \mathrm{d}z}{\displaystyle\int \{\widetilde{p}(z)/q(z)\} q(z) \, \mathrm{d}z} \\ &= \frac{\displaystyle\int I(z \leqslant a) \widetilde{p}(z) \, \mathrm{d}z}{\displaystyle\int \widetilde{p}(z) \, \mathrm{d}z} \\ &= \int I(z \leqslant a) p(z) \, \mathrm{d}z \end{aligned} \tag{11.26}$$

which is the cumulative distribution function of $p(z)$. Again, we see that the normalization of $p(z)$ is not required.

For a finite value of L, and a given initial sample set, the resampled values will only approximately be drawn from the desired distribution. As with rejection sampling, the approximation improves as the sampling distribution $q(\mathbf{z})$ gets closer to the desired distribution $p(\mathbf{z})$. When $q(\mathbf{z}) = p(\mathbf{z})$, the initial samples $(\mathbf{z}^{(1)}, \ldots, \mathbf{z}^{(L)})$ have the desired distribution, and the weights $w_n = 1/L$ so that the resampled values also have the desired distribution.

If moments with respect to the distribution $p(\mathbf{z})$ are required, then they can be

evaluated directly using the original samples together with the weights, because

$$\begin{aligned}\mathbb{E}[f(\mathbf{z})] &= \int f(\mathbf{z})p(\mathbf{z})\,\mathrm{d}\mathbf{z} \\ &= \frac{\int f(\mathbf{z})[\widetilde{p}(\mathbf{z})/q(\mathbf{z})]q(\mathbf{z})\,\mathrm{d}\mathbf{z}}{\int [\widetilde{p}(\mathbf{z})/q(\mathbf{z})]q(\mathbf{z})\,\mathrm{d}\mathbf{z}} \\ &\simeq \sum_{l=1}^{L} w_l f(\mathbf{z}_l). \end{aligned} \tag{11.27}$$

11.1.6 Sampling and the EM algorithm

In addition to providing a mechanism for direct implementation of the Bayesian framework, Monte Carlo methods can also play a role in the frequentist paradigm, for example to find maximum likelihood solutions. In particular, sampling methods can be used to approximate the E step of the EM algorithm for models in which the E step cannot be performed analytically. Consider a model with hidden variables $\mathbf{Z}$, visible (observed) variables $\mathbf{X}$, and parameters $\boldsymbol{\theta}$. The function that is optimized with respect to $\boldsymbol{\theta}$ in the M step is the expected complete-data log likelihood, given by

$$Q(\boldsymbol{\theta}, \boldsymbol{\theta}^{\mathrm{old}}) = \int p(\mathbf{Z}|\mathbf{X}, \boldsymbol{\theta}^{\mathrm{old}}) \ln p(\mathbf{Z}, \mathbf{X}|\boldsymbol{\theta})\,\mathrm{d}\mathbf{Z}. \tag{11.28}$$

We can use sampling methods to approximate this integral by a finite sum over samples $\{\mathbf{Z}^{(l)}\}$, which are drawn from the current estimate for the posterior distribution $p(\mathbf{Z}|\mathbf{X}, \boldsymbol{\theta}^{\mathrm{old}})$, so that

$$Q(\boldsymbol{\theta}, \boldsymbol{\theta}^{\mathrm{old}}) \simeq \frac{1}{L} \sum_{l=1}^{L} \ln p(\mathbf{Z}^{(l)}, \mathbf{X}|\boldsymbol{\theta}). \tag{11.29}$$

The Q function is then optimized in the usual way in the M step. This procedure is called the *Monte Carlo EM algorithm*.

It is straightforward to extend this to the problem of finding the mode of the posterior distribution over $\boldsymbol{\theta}$ (the MAP estimate) when a prior distribution $p(\boldsymbol{\theta})$ has been defined, simply by adding $\ln p(\boldsymbol{\theta})$ to the function $Q(\boldsymbol{\theta}, \boldsymbol{\theta}^{\mathrm{old}})$ before performing the M step.

A particular instance of the Monte Carlo EM algorithm, called *stochastic EM*, arises if we consider a finite mixture model, and draw just one sample at each E step. Here the latent variable $\mathbf{Z}$ characterizes which of the K components of the mixture is responsible for generating each data point. In the E step, a sample of $\mathbf{Z}$ is taken from the posterior distribution $p(\mathbf{Z}|\mathbf{X}, \boldsymbol{\theta}^{\mathrm{old}})$ where $\mathbf{X}$ is the data set. This effectively makes a hard assignment of each data point to one of the components in the mixture. In the M step, this sampled approximation to the posterior distribution is used to update the model parameters in the usual way.

Now suppose we move from a maximum likelihood approach to a full Bayesian treatment in which we wish to sample from the posterior distribution over the parameter vector $\boldsymbol{\theta}$. In principle, we would like to draw samples from the joint posterior $p(\boldsymbol{\theta}, \mathbf{Z}|\mathbf{X})$, but we shall suppose that this is computationally difficult. Suppose further that it is relatively straightforward to sample from the complete-data parameter posterior $p(\boldsymbol{\theta}|\mathbf{Z}, \mathbf{X})$. This inspires the *data augmentation* algorithm, which alternates between two steps known as the I-step (imputation step, analogous to an E step) and the P-step (posterior step, analogous to an M step).

IP Algorithm

I-step. We wish to sample from $p(\mathbf{Z}|\mathbf{X})$ but we cannot do this directly. We therefore note the relation

$$p(\mathbf{Z}|\mathbf{X}) = \int p(\mathbf{Z}|\boldsymbol{\theta}, \mathbf{X}) p(\boldsymbol{\theta}|\mathbf{X}) \, \mathrm{d}\boldsymbol{\theta} \tag{11.30}$$

and hence for $l = 1, \ldots, L$ we first draw a sample $\boldsymbol{\theta}^{(l)}$ from the current estimate for $p(\boldsymbol{\theta}|\mathbf{X})$, and then use this to draw a sample $\mathbf{Z}^{(l)}$ from $p(\mathbf{Z}|\boldsymbol{\theta}^{(l)}, \mathbf{X})$.

P-step. Given the relation

$$p(\boldsymbol{\theta}|\mathbf{X}) = \int p(\boldsymbol{\theta}|\mathbf{Z}, \mathbf{X}) p(\mathbf{Z}|\mathbf{X}) \, \mathrm{d}\mathbf{Z} \tag{11.31}$$

we use the samples $\{\mathbf{Z}^{(l)}\}$ obtained from the I-step to compute a revised estimate of the posterior distribution over $\boldsymbol{\theta}$ given by

$$p(\boldsymbol{\theta}|\mathbf{X}) \simeq \frac{1}{L} \sum_{l=1}^{L} p(\boldsymbol{\theta}|\mathbf{Z}^{(l)}, \mathbf{X}). \tag{11.32}$$

By assumption, it will be feasible to sample from this approximation in the I-step.

Note that we are making a (somewhat artificial) distinction between parameters $\boldsymbol{\theta}$ and hidden variables $\mathbf{Z}$. From now on, we blur this distinction and focus simply on the problem of drawing samples from a given posterior distribution.

11.2. Markov Chain Monte Carlo

In the previous section, we discussed the rejection sampling and importance sampling strategies for evaluating expectations of functions, and we saw that they suffer from severe limitations particularly in spaces of high dimensionality. We therefore turn in this section to a very general and powerful framework called Markov chain Monte Carlo (MCMC), which allows sampling from a large class of distributions,

and which scales well with the dimensionality of the sample space. Markov chain Monte Carlo methods have their origins in physics (Metropolis and Ulam, 1949), and it was only towards the end of the 1980s that they started to have a significant impact in the field of statistics.

As with rejection and importance sampling, we again sample from a proposal distribution. This time, however, we maintain a record of the current state $\mathbf{z}^{(\tau)}$, and the proposal distribution $q(\mathbf{z}|\mathbf{z}^{(\tau)})$ depends on this current state, and so the sequence of samples $\mathbf{z}^{(1)}, \mathbf{z}^{(2)}, \ldots$ forms a Markov chain. Again, if we write $p(\mathbf{z}) = \widetilde{p}(\mathbf{z})/Z_p$, we will assume that $\widetilde{p}(\mathbf{z})$ can readily be evaluated for any given value of $\mathbf{z}$, although the value of Z_p may be unknown. The proposal distribution itself is chosen to be sufficiently simple that it is straightforward to draw samples from it directly. At each cycle of the algorithm, we generate a candidate sample $\mathbf{z}^\star$ from the proposal distribution and then accept the sample according to an appropriate criterion.

Section 11.2.1

In the basic *Metropolis* algorithm (Metropolis *et al.*, 1953), we assume that the proposal distribution is symmetric, that is $q(\mathbf{z}_A|\mathbf{z}_B) = q(\mathbf{z}_B|\mathbf{z}_A)$ for all values of $\mathbf{z}_A$ and $\mathbf{z}_B$. The candidate sample is then accepted with probability

$$A(\mathbf{z}^\star, \mathbf{z}^{(\tau)}) = \min\left(1, \frac{\widetilde{p}(\mathbf{z}^\star)}{\widetilde{p}(\mathbf{z}^{(\tau)})}\right). \tag{11.33}$$

This can be achieved by choosing a random number u with uniform distribution over the unit interval $(0, 1)$ and then accepting the sample if $A(\mathbf{z}^\star, \mathbf{z}^{(\tau)}) > u$. Note that if the step from $\mathbf{z}^{(\tau)}$ to $\mathbf{z}^\star$ causes an increase in the value of $p(\mathbf{z})$, then the candidate point is certain to be kept.

If the candidate sample is accepted, then $\mathbf{z}^{(\tau+1)} = \mathbf{z}^\star$, otherwise the candidate point $\mathbf{z}^\star$ is discarded, $\mathbf{z}^{(\tau+1)}$ is set to $\mathbf{z}^{(\tau)}$ and another candidate sample is drawn from the distribution $q(\mathbf{z}|\mathbf{z}^{(\tau+1)})$. This is in contrast to rejection sampling, where rejected samples are simply discarded. In the Metropolis algorithm when a candidate point is rejected, the previous sample is included instead in the final list of samples, leading to multiple copies of samples. Of course, in a practical implementation, only a single copy of each retained sample would be kept, along with an integer weighting factor recording how many times that state appears. As we shall see, as long as $q(\mathbf{z}_A|\mathbf{z}_B)$ is positive for any values of $\mathbf{z}_A$ and $\mathbf{z}_B$ (this is a sufficient but not necessary condition), the distribution of $\mathbf{z}^{(\tau)}$ tends to $p(\mathbf{z})$ as $\tau \to \infty$. It should be emphasized, however, that the sequence $\mathbf{z}^{(1)}, \mathbf{z}^{(2)}, \ldots$ is not a set of independent samples from $p(\mathbf{z})$ because successive samples are highly correlated. If we wish to obtain independent samples, then we can discard most of the sequence and just retain every M^{th} sample. For M sufficiently large, the retained samples will for all practical purposes be independent. Figure 11.9 shows a simple illustrative example of sampling from a two-dimensional Gaussian distribution using the Metropolis algorithm in which the proposal distribution is an isotropic Gaussian.

Further insight into the nature of Markov chain Monte Carlo algorithms can be gleaned by looking at the properties of a specific example, namely a simple random

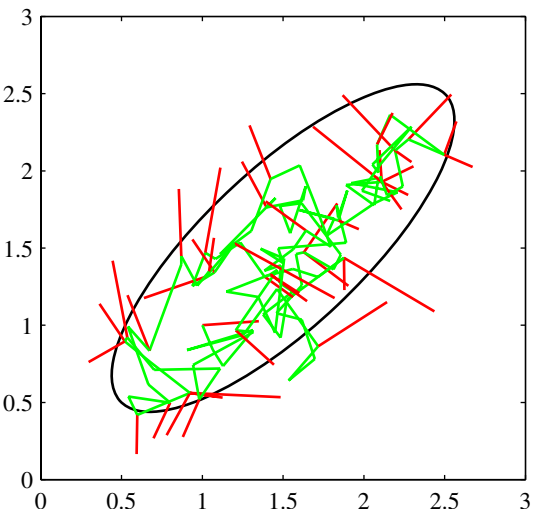

Figure 11.9 A simple illustration using Metropolis algorithm to sample from a Gaussian distribution whose one standard-deviation contour is shown by the ellipse. The proposal distribution is an isotropic Gaussian distribution whose standard deviation is 0.2. Steps that are accepted are shown as green lines, and rejected steps are shown in red. A total of 150 candidate samples are generated, of which 43 are rejected.

walk. Consider a state space z consisting of the integers, with probabilities

$$p(z^{(\tau+1)} = z^{(\tau)}) = 0.5 \tag{11.34}$$

$$p(z^{(\tau+1)} = z^{(\tau)} + 1) = 0.25 \tag{11.35}$$

$$p(z^{(\tau+1)} = z^{(\tau)} - 1) = 0.25 \tag{11.36}$$

where $z^{(\tau)}$ denotes the state at step τ. If the initial state is $z^{(1)} = 0$, then by symmetry the expected state at time τ will also be zero $\mathbb{E}[z^{(\tau)}] = 0$, and similarly it is easily seen that $\mathbb{E}[(z^{(\tau)})^2] = \tau/2$. Thus after τ steps, the random walk has only travelled a distance that on average is proportional to the square root of τ. This square root dependence is typical of random walk behaviour and shows that random walks are very inefficient in exploring the state space. As we shall see, a central goal in designing Markov chain Monte Carlo methods is to avoid random walk behaviour.

Exercise 11.10

11.2.1 Markov chains

Before discussing Markov chain Monte Carlo methods in more detail, it is useful to study some general properties of Markov chains in more detail. In particular, we ask under what circumstances will a Markov chain converge to the desired distribution. A first-order Markov chain is defined to be a series of random variables $\mathbf{z}^{(1)}, \ldots, \mathbf{z}^{(M)}$ such that the following conditional independence property holds for $m \in \{1, \ldots, M-1\}$

$$p(\mathbf{z}^{(m+1)}|\mathbf{z}^{(1)}, \ldots, \mathbf{z}^{(m)}) = p(\mathbf{z}^{(m+1)}|\mathbf{z}^{(m)}). \tag{11.37}$$

This of course can be represented as a directed graph in the form of a chain, an example of which is shown in Figure 8.38. We can then specify the Markov chain by giving the probability distribution for the initial variable $p(\mathbf{z}^{(0)})$ together with the

conditional probabilities for subsequent variables in the form of *transition probabilities* $T_m(\mathbf{z}^{(m)}, \mathbf{z}^{(m+1)}) \equiv p(\mathbf{z}^{(m+1)}|\mathbf{z}^{(m)})$. A Markov chain is called *homogeneous* if the transition probabilities are the same for all m.

The marginal probability for a particular variable can be expressed in terms of the marginal probability for the previous variable in the chain in the form

$$p(\mathbf{z}^{(m+1)}) = \sum_{\mathbf{z}^{(m)}} p(\mathbf{z}^{(m+1)}|\mathbf{z}^{(m)})p(\mathbf{z}^{(m)}). \tag{11.38}$$

A distribution is said to be invariant, or stationary, with respect to a Markov chain if each step in the chain leaves that distribution invariant. Thus, for a homogeneous Markov chain with transition probabilities $T(\mathbf{z}', \mathbf{z})$, the distribution $p^\star(\mathbf{z})$ is invariant if

$$p^\star(\mathbf{z}) = \sum_{\mathbf{z}'} T(\mathbf{z}', \mathbf{z})p^\star(\mathbf{z}'). \tag{11.39}$$

Note that a given Markov chain may have more than one invariant distribution. For instance, if the transition probabilities are given by the identity transformation, then any distribution will be invariant.

A sufficient (but not necessary) condition for ensuring that the required distribution $p(\mathbf{z})$ is invariant is to choose the transition probabilities to satisfy the property of *detailed balance*, defined by

$$p^\star(\mathbf{z})T(\mathbf{z}, \mathbf{z}') = p^\star(\mathbf{z}')T(\mathbf{z}', \mathbf{z}) \tag{11.40}$$

for the particular distribution $p^\star(\mathbf{z})$. It is easily seen that a transition probability that satisfies detailed balance with respect to a particular distribution will leave that distribution invariant, because

$$\sum_{\mathbf{z}'} p^\star(\mathbf{z}')T(\mathbf{z}', \mathbf{z}) = \sum_{\mathbf{z}'} p^\star(\mathbf{z})T(\mathbf{z}, \mathbf{z}') = p^\star(\mathbf{z}) \sum_{\mathbf{z}'} p(\mathbf{z}'|\mathbf{z}) = p^\star(\mathbf{z}). \tag{11.41}$$

A Markov chain that respects detailed balance is said to be *reversible*.

Our goal is to use Markov chains to sample from a given distribution. We can achieve this if we set up a Markov chain such that the desired distribution is invariant. However, we must also require that for $m \to \infty$, the distribution $p(\mathbf{z}^{(m)})$ converges to the required invariant distribution $p^\star(\mathbf{z})$, irrespective of the choice of initial distribution $p(\mathbf{z}^{(0)})$. This property is called *ergodicity*, and the invariant distribution is then called the *equilibrium* distribution. Clearly, an ergodic Markov chain can have only one equilibrium distribution. It can be shown that a homogeneous Markov chain will be ergodic, subject only to weak restrictions on the invariant distribution and the transition probabilities (Neal, 1993).

In practice we often construct the transition probabilities from a set of 'base' transitions $B_1, \ldots, B_K$. This can be achieved through a mixture distribution of the form

$$T(\mathbf{z}', \mathbf{z}) = \sum_{k=1}^{K} \alpha_k B_k(\mathbf{z}', \mathbf{z}) \tag{11.42}$$

for some set of mixing coefficients $\alpha_1, \ldots, \alpha_K$ satisfying $\alpha_k \geqslant 0$ and $\sum_k \alpha_k = 1$. Alternatively, the base transitions may be combined through successive application, so that

$$T(\mathbf{z}', \mathbf{z}) = \sum_{\mathbf{z}_1} \ldots \sum_{\mathbf{z}_{n-1}} B_1(\mathbf{z}', \mathbf{z}_1) \ldots B_{K-1}(\mathbf{z}_{K-2}, \mathbf{z}_{K-1}) B_K(\mathbf{z}_{K-1}, \mathbf{z}). \quad (11.43)$$

If a distribution is invariant with respect to each of the base transitions, then obviously it will also be invariant with respect to either of the $T(\mathbf{z}', \mathbf{z})$ given by (11.42) or (11.43). For the case of the mixture (11.42), if each of the base transitions satisfies detailed balance, then the mixture transition T will also satisfy detailed balance. This does not hold for the transition probability constructed using (11.43), although by symmetrizing the order of application of the base transitions, in the form $B_1, B_2, \ldots, B_K, B_K, \ldots, B_2, B_1$, detailed balance can be restored. A common example of the use of composite transition probabilities is where each base transition changes only a subset of the variables.

11.2.2 The Metropolis-Hastings algorithm

Earlier we introduced the basic Metropolis algorithm, without actually demonstrating that it samples from the required distribution. Before giving a proof, we first discuss a generalization, known as the *Metropolis-Hastings* algorithm (Hastings, 1970), to the case where the proposal distribution is no longer a symmetric function of its arguments. In particular at step τ of the algorithm, in which the current state is $\mathbf{z}^{(\tau)}$, we draw a sample $\mathbf{z}^\star$ from the distribution $q_k(\mathbf{z}|\mathbf{z}^{(\tau)})$ and then accept it with probability $A_k(\mathbf{z}^\star, \mathbf{z}_\tau)$ where

$$A_k(\mathbf{z}^\star, \mathbf{z}^{(\tau)}) = \min\left(1, \frac{\widetilde{p}(\mathbf{z}^\star) q_k(\mathbf{z}^{(\tau)}|\mathbf{z}^\star)}{\widetilde{p}(\mathbf{z}^{(\tau)}) q_k(\mathbf{z}^\star|\mathbf{z}^{(\tau)})}\right). \quad (11.44)$$

Here k labels the members of the set of possible transitions being considered. Again, the evaluation of the acceptance criterion does not require knowledge of the normalizing constant Z_p in the probability distribution $p(\mathbf{z}) = \widetilde{p}(\mathbf{z})/Z_p$. For a symmetric proposal distribution the Metropolis-Hastings criterion (11.44) reduces to the standard Metropolis criterion given by (11.33).

We can show that $p(\mathbf{z})$ is an invariant distribution of the Markov chain defined by the Metropolis-Hastings algorithm by showing that detailed balance, defined by (11.40), is satisfied. Using (11.44) we have

$$\begin{aligned} p(\mathbf{z}) q_k(\mathbf{z}|\mathbf{z}') A_k(\mathbf{z}', \mathbf{z}) &= \min\left(p(\mathbf{z}) q_k(\mathbf{z}|\mathbf{z}'), p(\mathbf{z}') q_k(\mathbf{z}'|\mathbf{z})\right) \\ &= \min\left(p(\mathbf{z}') q_k(\mathbf{z}'|\mathbf{z}), p(\mathbf{z}) q_k(\mathbf{z}|\mathbf{z}')\right) \\ &= p(\mathbf{z}') q_k(\mathbf{z}'|\mathbf{z}) A_k(\mathbf{z}, \mathbf{z}') \end{aligned} \quad (11.45)$$

as required.

The specific choice of proposal distribution can have a marked effect on the performance of the algorithm. For continuous state spaces, a common choice is a Gaussian centred on the current state, leading to an important trade-off in determining the variance parameter of this distribution. If the variance is small, then the

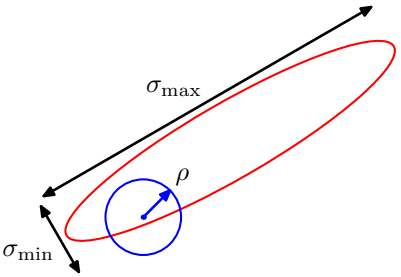

Figure 11.10 Schematic illustration of the use of an isotropic Gaussian proposal distribution (blue circle) to sample from a correlated multivariate Gaussian distribution (red ellipse) having very different standard deviations in different directions, using the Metropolis-Hastings algorithm. In order to keep the rejection rate low, the scale ρ of the proposal distribution should be on the order of the smallest standard deviation $\sigma_{\min}$, which leads to random walk behaviour in which the number of steps separating states that are approximately independent is of order $(\sigma_{\max}/\sigma_{\min})^2$ where $\sigma_{\max}$ is the largest standard deviation.

proportion of accepted transitions will be high, but progress through the state space takes the form of a slow random walk leading to long correlation times. However, if the variance parameter is large, then the rejection rate will be high because, in the kind of complex problems we are considering, many of the proposed steps will be to states for which the probability $p(\mathbf{z})$ is low. Consider a multivariate distribution $p(\mathbf{z})$ having strong correlations between the components of $\mathbf{z}$, as illustrated in Figure 11.10. The scale ρ of the proposal distribution should be as large as possible without incurring high rejection rates. This suggests that ρ should be of the same order as the smallest length scale $\sigma_{\min}$. The system then explores the distribution along the more extended direction by means of a random walk, and so the number of steps to arrive at a state that is more or less independent of the original state is of order $(\sigma_{\max}/\sigma_{\min})^2$. In fact in two dimensions, the increase in rejection rate as ρ increases is offset by the larger steps sizes of those transitions that are accepted, and more generally for a multivariate Gaussian the number of steps required to obtain independent samples scales like $(\sigma_{\max}/\sigma_2)^2$ where σ_2 is the second-smallest standard deviation (Neal, 1993). These details aside, it remains the case that if the length scales over which the distributions vary are very different in different directions, then the Metropolis Hastings algorithm can have very slow convergence.

11.3. Gibbs Sampling

Gibbs sampling (Geman and Geman, 1984) is a simple and widely applicable Markov chain Monte Carlo algorithm and can be seen as a special case of the Metropolis-Hastings algorithm.

Consider the distribution $p(\mathbf{z}) = p(z_1, \ldots, z_M)$ from which we wish to sample, and suppose that we have chosen some initial state for the Markov chain. Each step of the Gibbs sampling procedure involves replacing the value of one of the variables by a value drawn from the distribution of that variable conditioned on the values of the remaining variables. Thus we replace z_i by a value drawn from the distribution $p(z_i|\mathbf{z}_{\setminus i})$, where z_i denotes the i^{th} component of $\mathbf{z}$, and $\mathbf{z}_{\setminus i}$ denotes $z_1, \ldots, z_M$ but with z_i omitted. This procedure is repeated either by cycling through the variables

in some particular order or by choosing the variable to be updated at each step at random from some distribution.

For example, suppose we have a distribution $p(z_1, z_2, z_3)$ over three variables, and at step τ of the algorithm we have selected values $z_1^{(\tau)}$, $z_2^{(\tau)}$ and $z_3^{(\tau)}$. We first replace $z_1^{(\tau)}$ by a new value $z_1^{(\tau+1)}$ obtained by sampling from the conditional distribution

$$p(z_1|z_2^{(\tau)}, z_3^{(\tau)}). \tag{11.46}$$

Next we replace $z_2^{(\tau)}$ by a value $z_2^{(\tau+1)}$ obtained by sampling from the conditional distribution

$$p(z_2|z_1^{(\tau+1)}, z_3^{(\tau)}) \tag{11.47}$$

so that the new value for z_1 is used straight away in subsequent sampling steps. Then we update z_3 with a sample $z_3^{(\tau+1)}$ drawn from

$$p(z_3|z_1^{(\tau+1)}, z_2^{(\tau+1)}) \tag{11.48}$$

and so on, cycling through the three variables in turn.

Gibbs Sampling

1. Initialize $\{z_i : i = 1, \ldots, M\}$
2. For $\tau = 1, \ldots, T$:
   - Sample $z_1^{(\tau+1)} \sim p(z_1|z_2^{(\tau)}, z_3^{(\tau)}, \ldots, z_M^{(\tau)})$.
   - Sample $z_2^{(\tau+1)} \sim p(z_2|z_1^{(\tau+1)}, z_3^{(\tau)}, \ldots, z_M^{(\tau)})$.
   - $\vdots$
   - Sample $z_j^{(\tau+1)} \sim p(z_j|z_1^{(\tau+1)}, \ldots, z_{j-1}^{(\tau+1)}, z_{j+1}^{(\tau)}, \ldots, z_M^{(\tau)})$.
   - $\vdots$
   - Sample $z_M^{(\tau+1)} \sim p(z_M|z_1^{(\tau+1)}, z_2^{(\tau+1)}, \ldots, z_{M-1}^{(\tau+1)})$.

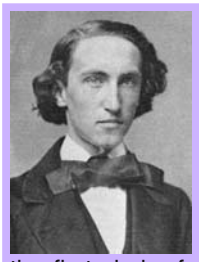

Josiah Willard Gibbs
1839–1903

Gibbs spent almost his entire life living in a house built by his father in New Haven, Connecticut. In 1863, Gibbs was granted the first PhD in engineering in the United States, and in 1871 he was appointed to the first chair of mathematical physics in the United States at Yale, a post for which he received no salary because at the time he had no publications. He developed the field of vector analysis and made contributions to crystallography and planetary orbits. His most famous work, entitled *On the Equilibrium of Heterogeneous Substances*, laid the foundations for the science of physical chemistry.

To show that this procedure samples from the required distribution, we first of all note that the distribution $p(\mathbf{z})$ is an invariant of each of the Gibbs sampling steps individually and hence of the whole Markov chain. This follows from the fact that when we sample from $p(z_i|\{\mathbf{z}_{\setminus i})$, the marginal distribution $p(\mathbf{z}_{\setminus i})$ is clearly invariant because the value of $\mathbf{z}_{\setminus i}$ is unchanged. Also, each step by definition samples from the correct conditional distribution $p(z_i|\mathbf{z}_{\setminus i})$. Because these conditional and marginal distributions together specify the joint distribution, we see that the joint distribution is itself invariant.

The second requirement to be satisfied in order that the Gibbs sampling procedure samples from the correct distribution is that it be ergodic. A sufficient condition for ergodicity is that none of the conditional distributions be anywhere zero. If this is the case, then any point in z space can be reached from any other point in a finite number of steps involving one update of each of the component variables. If this requirement is not satisfied, so that some of the conditional distributions have zeros, then ergodicity, if it applies, must be proven explicitly.

The distribution of initial states must also be specified in order to complete the algorithm, although samples drawn after many iterations will effectively become independent of this distribution. Of course, successive samples from the Markov chain will be highly correlated, and so to obtain samples that are nearly independent it will be necessary to subsample the sequence.

We can obtain the Gibbs sampling procedure as a particular instance of the Metropolis-Hastings algorithm as follows. Consider a Metropolis-Hastings sampling step involving the variable z_k in which the remaining variables $\mathbf{z}_{\setminus k}$ remain fixed, and for which the transition probability from $\mathbf{z}$ to $\mathbf{z}^\star$ is given by $q_k(\mathbf{z}^\star|\mathbf{z}) = p(z_k^\star|\mathbf{z}_{\setminus k})$. We note that $\mathbf{z}_{\setminus k}^\star = \mathbf{z}_{\setminus k}$ because these components are unchanged by the sampling step. Also, $p(\mathbf{z}) = p(z_k|\mathbf{z}_{\setminus k})p(\mathbf{z}_{\setminus k})$. Thus the factor that determines the acceptance probability in the Metropolis-Hastings (11.44) is given by

$$A(\mathbf{z}^\star, \mathbf{z}) = \frac{p(\mathbf{z}^\star)q_k(\mathbf{z}|\mathbf{z}^\star)}{p(\mathbf{z})q_k(\mathbf{z}^\star|\mathbf{z})} = \frac{p(z_k^\star|\mathbf{z}_{\setminus k}^\star)p(\mathbf{z}_{\setminus k}^\star)p(z_k|\mathbf{z}_{\setminus k}^\star)}{p(z_k|\mathbf{z}_{\setminus k})p(\mathbf{z}_{\setminus k})p(z_k^\star|\mathbf{z}_{\setminus k})} = 1 \tag{11.49}$$

where we have used $\mathbf{z}_{\setminus k}^\star = \mathbf{z}_{\setminus k}$. Thus the Metropolis-Hastings steps are always accepted.

As with the Metropolis algorithm, we can gain some insight into the behaviour of Gibbs sampling by investigating its application to a Gaussian distribution. Consider a correlated Gaussian in two variables, as illustrated in Figure 11.11, having conditional distributions of width l and marginal distributions of width L. The typical step size is governed by the conditional distributions and will be of order l. Because the state evolves according to a random walk, the number of steps needed to obtain independent samples from the distribution will be of order $(L/l)^2$. Of course if the Gaussian distribution were uncorrelated, then the Gibbs sampling procedure would be optimally efficient. For this simple problem, we could rotate the coordinate system in order to decorrelate the variables. However, in practical applications it will generally be infeasible to find such transformations.

One approach to reducing random walk behaviour in Gibbs sampling is called *over-relaxation* (Adler, 1981). In its original form, this applies to problems for which

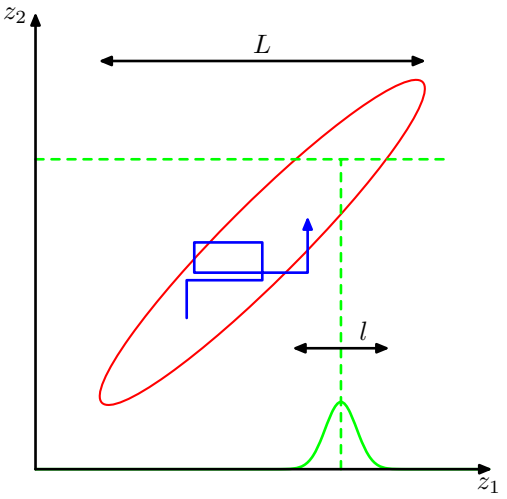

Figure 11.11 Illustration of Gibbs sampling by alternate updates of two variables whose distribution is a correlated Gaussian. The step size is governed by the standard deviation of the conditional distribution (green curve), and is $O(l)$, leading to slow progress in the direction of elongation of the joint distribution (red ellipse). The number of steps needed to obtain an independent sample from the distribution is $O((L/l)^2)$.

the conditional distributions are Gaussian, which represents a more general class of distributions than the multivariate Gaussian because, for example, the non-Gaussian distribution $p(z, y) \propto \exp(-z^2y^2)$ has Gaussian conditional distributions. At each step of the Gibbs sampling algorithm, the conditional distribution for a particular component z_i has some mean μ_i and some variance σ_i^2. In the over-relaxation framework, the value of z_i is replaced with

$$z_i' = \mu_i + \alpha(z_i - \mu_i) + \sigma_i(1 - \alpha_i^2)^{1/2}\nu \tag{11.50}$$

where ν is a Gaussian random variable with zero mean and unit variance, and α is a parameter such that $-1 < \alpha < 1$. For $\alpha = 0$, the method is equivalent to standard Gibbs sampling, and for $\alpha < 0$ the step is biased to the opposite side of the mean. This step leaves the desired distribution invariant because if z_i has mean μ_i and variance σ_i^2, then so too does z_i'. The effect of over-relaxation is to encourage directed motion through state space when the variables are highly correlated. The framework of *ordered over-relaxation* (Neal, 1999) generalizes this approach to non-Gaussian distributions.

The practical applicability of Gibbs sampling depends on the ease with which samples can be drawn from the conditional distributions $p(z_k|\mathbf{z}_{\setminus k})$. In the case of probability distributions specified using graphical models, the conditional distributions for individual nodes depend only on the variables in the corresponding Markov blankets, as illustrated in Figure 11.12. For directed graphs, a wide choice of conditional distributions for the individual nodes conditioned on their parents will lead to conditional distributions for Gibbs sampling that are log concave. The adaptive rejection sampling methods discussed in Section 11.1.3 therefore provide a framework for Monte Carlo sampling from directed graphs with broad applicability.

If the graph is constructed using distributions from the exponential family, and if the parent-child relationships preserve conjugacy, then the full conditional distributions arising in Gibbs sampling will have the same functional form as the orig-

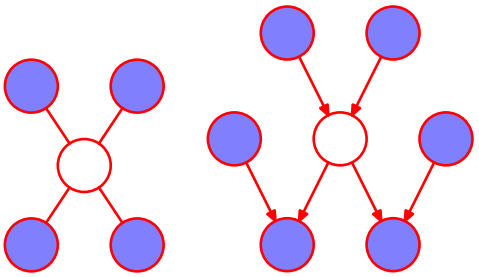

Figure 11.12 The Gibbs sampling method requires samples to be drawn from the conditional distribution of a variable conditioned on the remaining variables. For graphical models, this conditional distribution is a function only of the states of the nodes in the Markov blanket. For an undirected graph this comprises the set of neighbours, as shown on the left, while for a directed graph the Markov blanket comprises the parents, the children, and the co-parents, as shown on the right.

inal conditional distributions (conditioned on the parents) defining each node, and so standard sampling techniques can be employed. In general, the full conditional distributions will be of a complex form that does not permit the use of standard sampling algorithms. However, if these conditionals are log concave, then sampling can be done efficiently using adaptive rejection sampling (assuming the corresponding variable is a scalar).

If, at each stage of the Gibbs sampling algorithm, instead of drawing a sample from the corresponding conditional distribution, we make a point estimate of the variable given by the maximum of the conditional distribution, then we obtain the iterated conditional modes (ICM) algorithm discussed in Section 8.3.3. Thus ICM can be seen as a greedy approximation to Gibbs sampling.

Because the basic Gibbs sampling technique considers one variable at a time, there are strong dependencies between successive samples. At the opposite extreme, if we could draw samples directly from the joint distribution (an operation that we are supposing is intractable), then successive samples would be independent. We can hope to improve on the simple Gibbs sampler by adopting an intermediate strategy in which we sample successively from groups of variables rather than individual variables. This is achieved in the *blocking Gibbs* sampling algorithm by choosing blocks of variables, not necessarily disjoint, and then sampling jointly from the variables in each block in turn, conditioned on the remaining variables (Jensen *et al.*, 1995).

11.4. Slice Sampling

We have seen that one of the difficulties with the Metropolis algorithm is the sensitivity to step size. If this is too small, the result is slow decorrelation due to random walk behaviour, whereas if it is too large the result is inefficiency due to a high rejection rate. The technique of *slice sampling* (Neal, 2003) provides an adaptive step size that is automatically adjusted to match the characteristics of the distribution. Again it requires that we are able to evaluate the unnormalized distribution $\widetilde{p}(\mathbf{z})$.

Consider first the univariate case. Slice sampling involves augmenting z with an additional variable u and then drawing samples from the joint (z, u) space. We shall see another example of this approach when we discuss hybrid Monte Carlo in Section 11.5. The goal is to sample uniformly from the area under the distribution

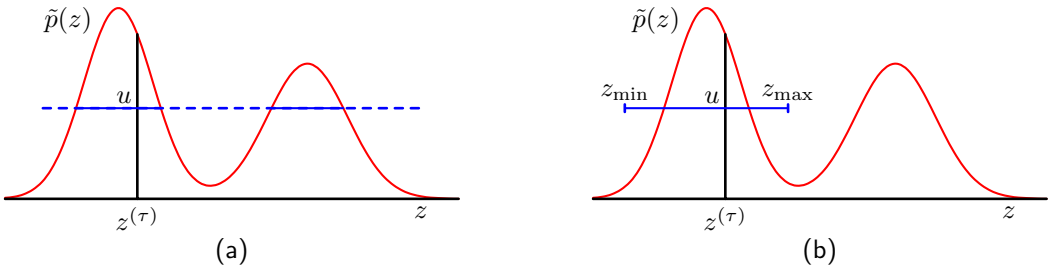

Figure 11.13 Illustration of slice sampling. (a) For a given value $z^{(\tau)}$, a value of u is chosen uniformly in the region $0 \leqslant u \leqslant \widetilde{p}(z^{(\tau)})$, which then defines a 'slice' through the distribution, shown by the solid horizontal lines. (b) Because it is infeasible to sample directly from a slice, a new sample of z is drawn from a region $z_{\min} \leqslant z \leqslant z_{\max}$, which contains the previous value $z^{(\tau)}$.

given by

$$\widehat{p}(z,u) = \begin{cases} 1/Z_p & \text{if } 0 \leqslant u \leqslant \widetilde{p}(z) \\ 0 & \text{otherwise} \end{cases} \tag{11.51}$$

where $Z_p = \int \widetilde{p}(z)\,\mathrm{d}z$. The marginal distribution over z is given by

$$\int \widehat{p}(z,u)\,\mathrm{d}u = \int_0^{\widetilde{p}(z)} \frac{1}{Z_p}\,\mathrm{d}u = \frac{\widetilde{p}(z)}{Z_p} = p(z) \tag{11.52}$$

and so we can sample from $p(z)$ by sampling from $\widehat{p}(z,u)$ and then ignoring the u values. This can be achieved by alternately sampling z and u. Given the value of z we evaluate $\widetilde{p}(z)$ and then sample u uniformly in the range $0 \leqslant u \leqslant \widetilde{p}(z)$, which is straightforward. Then we fix u and sample z uniformly from the 'slice' through the distribution defined by $\{z : \widetilde{p}(z) > u\}$. This is illustrated in Figure 11.13(a).

In practice, it can be difficult to sample directly from a slice through the distribution and so instead we define a sampling scheme that leaves the uniform distribution under $\widehat{p}(z,u)$ invariant, which can be achieved by ensuring that detailed balance is satisfied. Suppose the current value of z is denoted $z^{(\tau)}$ and that we have obtained a corresponding sample u. The next value of z is obtained by considering a region $z_{\min} \leqslant z \leqslant z_{\max}$ that contains $z^{(\tau)}$. It is in the choice of this region that the adaptation to the characteristic length scales of the distribution takes place. We want the region to encompass as much of the slice as possible so as to allow large moves in z space while having as little as possible of this region lying outside the slice, because this makes the sampling less efficient.

One approach to the choice of region involves starting with a region containing $z^{(\tau)}$ having some width w and then testing each of the end points to see if they lie within the slice. If either end point does not, then the region is extended in that direction by increments of value w until the end point lies outside the region. A candidate value z' is then chosen uniformly from this region, and if it lies within the slice, then it forms $z^{(\tau+1)}$. If it lies outside the slice, then the region is shrunk such that z' forms an end point and such that the region still contains $z^{(\tau)}$. Then another

candidate point is drawn uniformly from this reduced region and so on, until a value of z is found that lies within the slice.

Slice sampling can be applied to multivariate distributions by repeatedly sampling each variable in turn, in the manner of Gibbs sampling. This requires that we are able to compute, for each component z_i, a function that is proportional to $p(z_i|\mathbf{z}_{\setminus i})$.

11.5. The Hybrid Monte Carlo Algorithm

As we have already noted, one of the major limitations of the Metropolis algorithm is that it can exhibit random walk behaviour whereby the distance traversed through the state space grows only as the square root of the number of steps. The problem cannot be resolved simply by taking bigger steps as this leads to a high rejection rate.

In this section, we introduce a more sophisticated class of transitions based on an analogy with physical systems and that has the property of being able to make large changes to the system state while keeping the rejection probability small. It is applicable to distributions over continuous variables for which we can readily evaluate the gradient of the log probability with respect to the state variables. We will discuss the dynamical systems framework in Section 11.5.1, and then in Section 11.5.2 we explain how this may be combined with the Metropolis algorithm to yield the powerful hybrid Monte Carlo algorithm. A background in physics is not required as this section is self-contained and the key results are all derived from first principles.

11.5.1 Dynamical systems

The dynamical approach to stochastic sampling has its origins in algorithms for simulating the behaviour of physical systems evolving under Hamiltonian dynamics. In a Markov chain Monte Carlo simulation, the goal is to sample from a given probability distribution $p(\mathbf{z})$. The framework of *Hamiltonian dynamics* is exploited by casting the probabilistic simulation in the form of a Hamiltonian system. In order to remain in keeping with the literature in this area, we make use of the relevant dynamical systems terminology where appropriate, which will be defined as we go along.

The dynamics that we consider corresponds to the evolution of the state variable $\mathbf{z} = \{z_i\}$ under continuous time, which we denote by τ. Classical dynamics is described by Newton's second law of motion in which the acceleration of an object is proportional to the applied force, corresponding to a second-order differential equation over time. We can decompose a second-order equation into two coupled first-order equations by introducing intermediate *momentum* variables $\mathbf{r}$, corresponding to the rate of change of the state variables $\mathbf{z}$, having components

$$r_i = \frac{\mathrm{d}z_i}{\mathrm{d}\tau} \tag{11.53}$$

where the z_i can be regarded as *position* variables in this dynamics perspective. Thus

for each position variable there is a corresponding momentum variable, and the joint space of position and momentum variables is called *phase space*.

Without loss of generality, we can write the probability distribution $p(\mathbf{z})$ in the form

$$p(\mathbf{z}) = \frac{1}{Z_p} \exp\left(-E(\mathbf{z})\right) \tag{11.54}$$

where $E(\mathbf{z})$ is interpreted as the *potential energy* of the system when in state $\mathbf{z}$. The system acceleration is the rate of change of momentum and is given by the applied *force*, which itself is the negative gradient of the potential energy

$$\frac{\mathrm{d}r_i}{\mathrm{d}\tau} = -\frac{\partial E(\mathbf{z})}{\partial z_i}. \tag{11.55}$$

It is convenient to reformulate this dynamical system using the Hamiltonian framework. To do this, we first define the *kinetic energy* by

$$K(\mathbf{r}) = \frac{1}{2}\|\mathbf{r}\|^2 = \frac{1}{2}\sum_i r_i^2. \tag{11.56}$$

The total energy of the system is then the sum of its potential and kinetic energies

$$H(\mathbf{z}, \mathbf{r}) = E(\mathbf{z}) + K(\mathbf{r}) \tag{11.57}$$

where H is the *Hamiltonian* function. Using (11.53), (11.55), (11.56), and (11.57), we can now express the dynamics of the system in terms of the Hamiltonian equations given by

Exercise 11.15

$$\frac{\mathrm{d}z_i}{\mathrm{d}\tau} = \frac{\partial H}{\partial r_i} \tag{11.58}$$

$$\frac{\mathrm{d}r_i}{\mathrm{d}\tau} = -\frac{\partial H}{\partial z_i}. \tag{11.59}$$

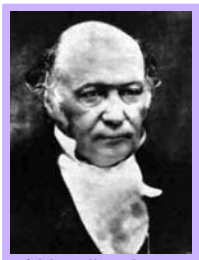

William Hamilton
1805–1865

William Rowan Hamilton was an Irish mathematician and physicist, and child prodigy, who was appointed Professor of Astronomy at Trinity College, Dublin, in 1827, before he had even graduated. One of Hamilton's most important contributions was a new formulation of dynamics, which played a significant role in the later development of quantum mechanics.

His other great achievement was the development of *quaternions*, which generalize the concept of complex numbers by introducing three distinct square roots of minus one, which satisfy $i^2 = j^2 = k^2 = ijk = -1$. It is said that these equations occurred to him while walking along the Royal Canal in Dublin with his wife, on 16 October 1843, and he promptly carved the equations into the side of Broome bridge. Although there is no longer any evidence of the carving, there is now a stone plaque on the bridge commemorating the discovery and displaying the quaternion equations.

During the evolution of this dynamical system, the value of the Hamiltonian H is constant, as is easily seen by differentiation

$$\begin{aligned}\frac{\mathrm{d}H}{\mathrm{d}\tau} &= \sum_i \left\{ \frac{\partial H}{\partial z_i}\frac{\mathrm{d}z_i}{\mathrm{d}\tau} + \frac{\partial H}{\partial r_i}\frac{\mathrm{d}r_i}{\mathrm{d}\tau} \right\} \\ &= \sum_i \left\{ \frac{\partial H}{\partial z_i}\frac{\partial H}{\partial r_i} - \frac{\partial H}{\partial r_i}\frac{\partial H}{\partial z_i} \right\} = 0. \end{aligned} \tag{11.60}$$

A second important property of Hamiltonian dynamical systems, known as *Liouville's Theorem*, is that they preserve volume in phase space. In other words, if we consider a region within the space of variables $(\mathbf{z}, \mathbf{r})$, then as this region evolves under the equations of Hamiltonian dynamics, its shape may change but its volume will not. This can be seen by noting that the flow field (rate of change of location in phase space) is given by

$$\mathbf{V} = \left(\frac{\mathrm{d}\mathbf{z}}{\mathrm{d}\tau}, \frac{\mathrm{d}\mathbf{r}}{\mathrm{d}\tau} \right) \tag{11.61}$$

and that the divergence of this field vanishes

$$\begin{aligned}\mathrm{div}\ \mathbf{V} &= \sum_i \left\{ \frac{\partial}{\partial z_i}\frac{\mathrm{d}z_i}{\mathrm{d}\tau} + \frac{\partial}{\partial r_i}\frac{\mathrm{d}r_i}{\mathrm{d}\tau} \right\} \\ &= \sum_i \left\{ -\frac{\partial}{\partial z_i}\frac{\partial H}{\partial r_i} + \frac{\partial}{\partial r_i}\frac{\partial H}{\partial z_i} \right\} = 0. \end{aligned} \tag{11.62}$$

Now consider the joint distribution over phase space whose total energy is the Hamiltonian, i.e., the distribution given by

$$p(\mathbf{z}, \mathbf{r}) = \frac{1}{Z_H} \exp(-H(\mathbf{z}, \mathbf{r})). \tag{11.63}$$

Using the two results of conservation of volume and conservation of H, it follows that the Hamiltonian dynamics will leave $p(\mathbf{z}, \mathbf{r})$ invariant. This can be seen by considering a small region of phase space over which H is approximately constant. If we follow the evolution of the Hamiltonian equations for a finite time, then the volume of this region will remain unchanged as will the value of H in this region, and hence the probability density, which is a function only of H, will also be unchanged.

Although H is invariant, the values of $\mathbf{z}$ and $\mathbf{r}$ will vary, and so by integrating the Hamiltonian dynamics over a finite time duration it becomes possible to make large changes to $\mathbf{z}$ in a systematic way that avoids random walk behaviour.

Evolution under the Hamiltonian dynamics will not, however, sample ergodically from $p(\mathbf{z}, \mathbf{r})$ because the value of H is constant. In order to arrive at an ergodic sampling scheme, we can introduce additional moves in phase space that change the value of H while also leaving the distribution $p(\mathbf{z}, \mathbf{r})$ invariant. The simplest way to achieve this is to replace the value of $\mathbf{r}$ with one drawn from its distribution conditioned on $\mathbf{z}$. This can be regarded as a Gibbs sampling step, and hence from

Section 11.3 we see that this also leaves the desired distribution invariant. Noting that $\mathbf{z}$ and $\mathbf{r}$ are independent in the distribution $p(\mathbf{z}, \mathbf{r})$, we see that the conditional distribution $p(\mathbf{r}|\mathbf{z})$ is a Gaussian from which it is straightforward to sample.

Exercise 11.16

In a practical application of this approach, we have to address the problem of performing a numerical integration of the Hamiltonian equations. This will necessarily introduce numerical errors and so we should devise a scheme that minimizes the impact of such errors. In fact, it turns out that integration schemes can be devised for which Liouville's theorem still holds exactly. This property will be important in the hybrid Monte Carlo algorithm, which is discussed in Section 11.5.2. One scheme for achieving this is called the *leapfrog* discretization and involves alternately updating discrete-time approximations $\widehat{\mathbf{z}}$ and $\widehat{\mathbf{r}}$ to the position and momentum variables using

$$\widehat{r}_i(\tau + \epsilon/2) = \widehat{r}_i(\tau) - \frac{\epsilon}{2}\frac{\partial E}{\partial z_i}(\widehat{\mathbf{z}}(\tau)) \tag{11.64}$$

$$\widehat{z}_i(\tau + \epsilon) = \widehat{z}_i(\tau) + \epsilon \widehat{r}_i(\tau + \epsilon/2) \tag{11.65}$$

$$\widehat{r}_i(\tau + \epsilon) = \widehat{r}_i(\tau + \epsilon/2) - \frac{\epsilon}{2}\frac{\partial E}{\partial z_i}(\widehat{\mathbf{z}}(\tau + \epsilon)). \tag{11.66}$$

We see that this takes the form of a half-step update of the momentum variables with step size $\epsilon/2$, followed by a full-step update of the position variables with step size ϵ, followed by a second half-step update of the momentum variables. If several leapfrog steps are applied in succession, it can be seen that half-step updates to the momentum variables can be combined into full-step updates with step size ϵ. The successive updates to position and momentum variables then leapfrog over each other. In order to advance the dynamics by a time interval τ, we need to take τ/ϵ steps. The error involved in the discretized approximation to the continuous time dynamics will go to zero, assuming a smooth function $E(\mathbf{z})$, in the limit $\epsilon \to 0$. However, for a nonzero ϵ as used in practice, some residual error will remain. We shall see in Section 11.5.2 how the effects of such errors can be eliminated in the hybrid Monte Carlo algorithm.

In summary then, the Hamiltonian dynamical approach involves alternating between a series of leapfrog updates and a resampling of the momentum variables from their marginal distribution.

Note that the Hamiltonian dynamics method, unlike the basic Metropolis algorithm, is able to make use of information about the gradient of the log probability distribution as well as about the distribution itself. An analogous situation is familiar from the domain of function optimization. In most cases where gradient information is available, it is highly advantageous to make use of it. Informally, this follows from the fact that in a space of dimension D, the additional computational cost of evaluating a gradient compared with evaluating the function itself will typically be a fixed factor independent of D, whereas the D-dimensional gradient vector conveys D pieces of information compared with the one piece of information given by the function itself.

11.5.2 Hybrid Monte Carlo

As we discussed in the previous section, for a nonzero step size ϵ, the discretization of the leapfrog algorithm will introduce errors into the integration of the Hamiltonian dynamical equations. *Hybrid Monte Carlo* (Duane *et al.*, 1987; Neal, 1996) combines Hamiltonian dynamics with the Metropolis algorithm and thereby removes any bias associated with the discretization.

Specifically, the algorithm uses a Markov chain consisting of alternate stochastic updates of the momentum variable $\mathbf{r}$ and Hamiltonian dynamical updates using the leapfrog algorithm. After each application of the leapfrog algorithm, the resulting candidate state is accepted or rejected according to the Metropolis criterion based on the value of the Hamiltonian H. Thus if $(\mathbf{z}, \mathbf{r})$ is the initial state and $(\mathbf{z}^\star, \mathbf{r}^\star)$ is the state after the leapfrog integration, then this candidate state is accepted with probability

$$\min\left(1, \exp\{H(\mathbf{z}, \mathbf{r}) - H(\mathbf{z}^\star, \mathbf{r}^\star)\}\right). \tag{11.67}$$

If the leapfrog integration were to simulate the Hamiltonian dynamics perfectly, then every such candidate step would automatically be accepted because the value of H would be unchanged. Due to numerical errors, the value of H may sometimes decrease, and we would like the Metropolis criterion to remove any bias due to this effect and ensure that the resulting samples are indeed drawn from the required distribution. In order for this to be the case, we need to ensure that the update equations corresponding to the leapfrog integration satisfy detailed balance (11.40). This is easily achieved by modifying the leapfrog scheme as follows.

Before the start of each leapfrog integration sequence, we choose at random, with equal probability, whether to integrate forwards in time (using step size ϵ) or backwards in time (using step size $-\epsilon$). We first note that the leapfrog integration scheme (11.64), (11.65), and (11.66) is time-reversible, so that integration for L steps using step size $-\epsilon$ will exactly undo the effect of integration for L steps using step size ϵ. Next we show that the leapfrog integration preserves phase-space volume exactly. This follows from the fact that each step in the leapfrog scheme updates either a z_i variable or an r_i variable by an amount that is a function only of the other variable. As shown in Figure 11.14, this has the effect of shearing a region of phase space while not altering its volume.

Finally, we use these results to show that detailed balance holds. Consider a small region $\mathcal{R}$ of phase space that, under a sequence of L leapfrog iterations of step size ϵ, maps to a region $\mathcal{R}'$. Using conservation of volume under the leapfrog iteration, we see that if $\mathcal{R}$ has volume δV then so too will $\mathcal{R}'$. If we choose an initial point from the distribution (11.63) and then update it using L leapfrog interactions, the probability of the transition going from $\mathcal{R}$ to $\mathcal{R}'$ is given by

$$\frac{1}{Z_H}\exp(-H(\mathcal{R}))\delta V \frac{1}{2}\min\left\{1, \exp(-H(\mathcal{R}) + H(\mathcal{R}'))\right\}. \tag{11.68}$$

where the factor of $1/2$ arises from the probability of choosing to integrate with a positive step size rather than a negative one. Similarly, the probability of starting in

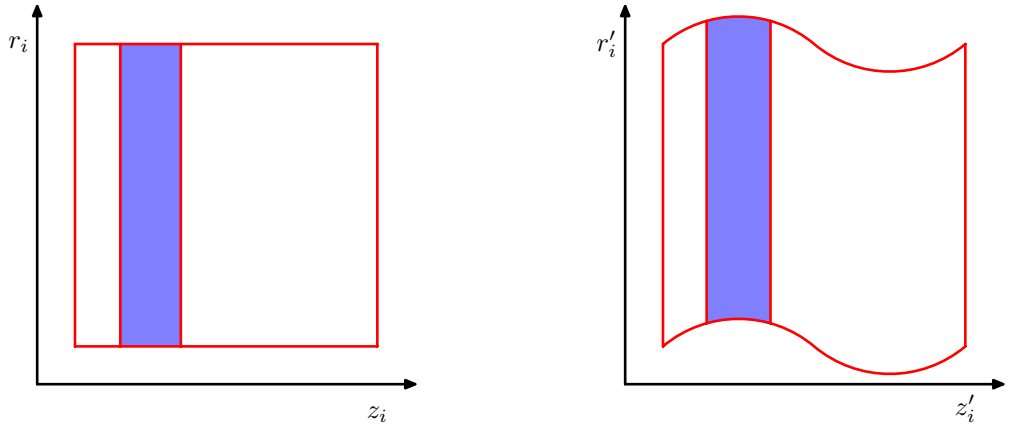

Figure 11.14 Each step of the leapfrog algorithm (11.64)–(11.66) modifies either a position variable z_i or a momentum variable r_i. Because the change to one variable is a function only of the other, any region in phase space will be sheared without change of volume.

region $\mathcal{R}'$ and integrating backwards in time to end up in region $\mathcal{R}$ is given by

$$\frac{1}{Z_H}\exp(-H(\mathcal{R}'))\delta V\frac{1}{2}\min\left\{1,\exp(-H(\mathcal{R}')+H(\mathcal{R}))\right\}. \tag{11.69}$$

Exercise 11.17 It is easily seen that the two probabilities (11.68) and (11.69) are equal, and hence detailed balance holds. Note that this proof ignores any overlap between the regions $\mathcal{R}$ and $\mathcal{R}'$ but is easily generalized to allow for such overlap.

It is not difficult to construct examples for which the leapfrog algorithm returns to its starting position after a finite number of iterations. In such cases, the random replacement of the momentum values before each leapfrog integration will not be sufficient to ensure ergodicity because the position variables will never be updated. Such phenomena are easily avoided by choosing the magnitude of the step size at random from some small interval, before each leapfrog integration.

We can gain some insight into the behaviour of the hybrid Monte Carlo algorithm by considering its application to a multivariate Gaussian. For convenience, consider a Gaussian distribution $p(\mathbf{z})$ with independent components, for which the Hamiltonian is given by

$$H(\mathbf{z},\mathbf{r})=\frac{1}{2}\sum_i\frac{1}{\sigma_i^2}z_i^2+\frac{1}{2}\sum_i r_i^2. \tag{11.70}$$

Our conclusions will be equally valid for a Gaussian distribution having correlated components because the hybrid Monte Carlo algorithm exhibits rotational isotropy. During the leapfrog integration, each pair of phase-space variables z_i, r_i evolves independently. However, the acceptance or rejection of the candidate point is based on the value of H, which depends on the values of all of the variables. Thus, a significant integration error in any one of the variables could lead to a high probability of rejection. In order that the discrete leapfrog integration be a reasonably

good approximation to the true continuous-time dynamics, it is necessary for the leapfrog integration scale ϵ to be smaller than the shortest length-scale over which the potential is varying significantly. This is governed by the smallest value of σ_i, which we denote by $\sigma_{\min}$. Recall that the goal of the leapfrog integration in hybrid Monte Carlo is to move a substantial distance through phase space to a new state that is relatively independent of the initial state and still achieve a high probability of acceptance. In order to achieve this, the leapfrog integration must be continued for a number of iterations of order $\sigma_{\max}/\sigma_{\min}$.

By contrast, consider the behaviour of a simple Metropolis algorithm with an isotropic Gaussian proposal distribution of variance s^2, considered earlier. In order to avoid high rejection rates, the value of s must be of order $\sigma_{\min}$. The exploration of state space then proceeds by a random walk and takes of order $(\sigma_{\max}/\sigma_{\min})^2$ steps to arrive at a roughly independent state.

11.6. Estimating the Partition Function

As we have seen, most of the sampling algorithms considered in this chapter require only the functional form of the probability distribution up to a multiplicative constant. Thus if we write

$$p_E(\mathbf{z}) = \frac{1}{Z_E}\exp(-E(\mathbf{z})) \tag{11.71}$$

then the value of the normalization constant Z_E, also known as the partition function, is not needed in order to draw samples from $p(\mathbf{z})$. However, knowledge of the value of Z_E can be useful for Bayesian model comparison since it represents the model evidence (i.e., the probability of the observed data given the model), and so it is of interest to consider how its value might be obtained. We assume that direct evaluation by summing, or integrating, the function $\exp(-E(\mathbf{z}))$ over the state space of $\mathbf{z}$ is intractable.

For model comparison, it is actually the ratio of the partition functions for two models that is required. Multiplication of this ratio by the ratio of prior probabilities gives the ratio of posterior probabilities, which can then be used for model selection or model averaging.

One way to estimate a ratio of partition functions is to use importance sampling from a distribution with energy function $G(\mathbf{z})$

$$\begin{aligned}
\frac{Z_E}{Z_G} &= \frac{\sum_{\mathbf{z}}\exp(-E(\mathbf{z}))}{\sum_{\mathbf{z}}\exp(-G(\mathbf{z}))} \\
&= \frac{\sum_{\mathbf{z}}\exp(-E(\mathbf{z})+G(\mathbf{z}))\exp(-G(\mathbf{z}))}{\sum_{\mathbf{z}}\exp(-G(\mathbf{z}))} \\
&= \mathbb{E}_{G(\mathbf{z})}[\exp(-E+G)] \\
&\simeq \sum_{l}\exp(-E(\mathbf{z}^{(l)})+G(\mathbf{z}^{(l)}))
\end{aligned} \tag{11.72}$$

where $\{\mathbf{z}^{(l)}\}$ are samples drawn from the distribution defined by $p_G(\mathbf{z})$. If the distribution p_G is one for which the partition function can be evaluated analytically, for example a Gaussian, then the absolute value of Z_E can be obtained.

This approach will only yield accurate results if the importance sampling distribution p_G is closely matched to the distribution p_E, so that the ratio p_E/p_G does not have wide variations. In practice, suitable analytically specified importance sampling distributions cannot readily be found for the kinds of complex models considered in this book.

An alternative approach is therefore to use the samples obtained from a Markov chain to define the importance-sampling distribution. If the transition probability for the Markov chain is given by $T(\mathbf{z}, \mathbf{z}')$, and the sample set is given by $\mathbf{z}^{(1)}, \ldots, \mathbf{z}^{(L)}$, then the sampling distribution can be written as

$$\frac{1}{Z_G} \exp\left(-G(\mathbf{z})\right) = \sum_{l=1}^{L} T(\mathbf{z}^{(l)}, \mathbf{z}) \tag{11.73}$$

which can be used directly in (11.72).

Methods for estimating the ratio of two partition functions require for their success that the two corresponding distributions be reasonably closely matched. This is especially problematic if we wish to find the absolute value of the partition function for a complex distribution because it is only for relatively simple distributions that the partition function can be evaluated directly, and so attempting to estimate the ratio of partition functions directly is unlikely to be successful. This problem can be tackled using a technique known as *chaining* (Neal, 1993; Barber and Bishop, 1997), which involves introducing a succession of intermediate distributions $p_2, \ldots, p_{M-1}$ that interpolate between a simple distribution $p_1(\mathbf{z})$ for which we can evaluate the normalization coefficient Z_1 and the desired complex distribution $p_M(\mathbf{z})$. We then have

$$\frac{Z_M}{Z_1} = \frac{Z_2}{Z_1}\frac{Z_3}{Z_2} \cdots \frac{Z_M}{Z_{M-1}} \tag{11.74}$$

in which the intermediate ratios can be determined using Monte Carlo methods as discussed above. One way to construct such a sequence of intermediate systems is to use an energy function containing a continuous parameter $0 \leqslant \alpha \leqslant 1$ that interpolates between the two distributions

$$E_\alpha(\mathbf{z}) = (1-\alpha)E_1(\mathbf{z}) + \alpha E_M(\mathbf{z}). \tag{11.75}$$

If the intermediate ratios in (11.74) are to be found using Monte Carlo, it may be more efficient to use a single Markov chain run than to restart the Markov chain for each ratio. In this case, the Markov chain is run initially for the system p_1 and then after some suitable number of steps moves on to the next distribution in the sequence. Note, however, that the system must remain close to the equilibrium distribution at each stage.

Exercises

11.1 ($\star$) **www** Show that the finite sample estimator $\widehat{f}$ defined by (11.2) has mean equal to $\mathbb{E}[f]$ and variance given by (11.3).

11.2 ($\star$) Suppose that z is a random variable with uniform distribution over $(0, 1)$ and that we transform z using $y = h^{-1}(z)$ where $h(y)$ is given by (11.6). Show that y has the distribution $p(y)$.

11.3 ($\star$) Given a random variable z that is uniformly distributed over $(0, 1)$, find a transformation $y = f(z)$ such that y has a Cauchy distribution given by (11.8).

11.4 ($\star\star$) Suppose that z_1 and z_2 are uniformly distributed over the unit circle, as shown in Figure 11.3, and that we make the change of variables given by (11.10) and (11.11). Show that (y_1, y_2) will be distributed according to (11.12).

11.5 ($\star$) **www** Let $\mathbf{z}$ be a D-dimensional random variable having a Gaussian distribution with zero mean and unit covariance matrix, and suppose that the positive definite symmetric matrix $\mathbf{\Sigma}$ has the Cholesky decomposition $\mathbf{\Sigma} = \mathbf{L}\mathbf{L}^{\mathrm{T}}$ where $\mathbf{L}$ is a lower-triangular matrix (i.e., one with zeros above the leading diagonal). Show that the variable $\mathbf{y} = \boldsymbol{\mu} + \mathbf{L}\mathbf{z}$ has a Gaussian distribution with mean $\boldsymbol{\mu}$ and covariance $\mathbf{\Sigma}$. This provides a technique for generating samples from a general multivariate Gaussian using samples from a univariate Gaussian having zero mean and unit variance.

11.6 ($\star\star$) **www** In this exercise, we show more carefully that rejection sampling does indeed draw samples from the desired distribution $p(\mathbf{z})$. Suppose the proposal distribution is $q(\mathbf{z})$ and show that the probability of a sample value $\mathbf{z}$ being accepted is given by $\widetilde{p}(\mathbf{z})/kq(\mathbf{z})$ where $\widetilde{p}$ is any unnormalized distribution that is proportional to $p(\mathbf{z})$, and the constant k is set to the smallest value that ensures $kq(\mathbf{z}) \geqslant \widetilde{p}(\mathbf{z})$ for all values of $\mathbf{z}$. Note that the probability of drawing a value $\mathbf{z}$ is given by the probability of drawing that value from $q(\mathbf{z})$ times the probability of accepting that value given that it has been drawn. Make use of this, along with the sum and product rules of probability, to write down the normalized form for the distribution over $\mathbf{z}$, and show that it equals $p(\mathbf{z})$.

11.7 ($\star$) Suppose that z has a uniform distribution over the interval $[0, 1]$. Show that the variable $y = b \tan z + c$ has a Cauchy distribution given by (11.16).

11.8 ($\star\star$) Determine expressions for the coefficients k_i in the envelope distribution (11.17) for adaptive rejection sampling using the requirements of continuity and normalization.

11.9 ($\star\star$) By making use of the technique discussed in Section 11.1.1 for sampling from a single exponential distribution, devise an algorithm for sampling from the piecewise exponential distribution defined by (11.17).

11.10 ($\star$) Show that the simple random walk over the integers defined by (11.34), (11.35), and (11.36) has the property that $\mathbb{E}[(z^{(\tau)})^2] = \mathbb{E}[(z^{(\tau-1)})^2] + 1/2$ and hence by induction that $\mathbb{E}[(z^{(\tau)})^2] = \tau/2$.

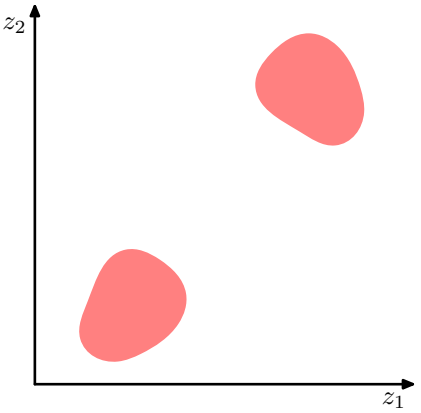

Figure 11.15 A probability distribution over two variables z_1 and z_2 that is uniform over the shaded regions and that is zero everywhere else.

11.11 ($\star\star$) **www** Show that the Gibbs sampling algorithm, discussed in Section 11.3, satisfies detailed balance as defined by (11.40).

11.12 ($\star$) Consider the distribution shown in Figure 11.15. Discuss whether the standard Gibbs sampling procedure for this distribution is ergodic, and therefore whether it would sample correctly from this distribution

11.13 ($\star\star$) Consider the simple 3-node graph shown in Figure 11.16 in which the observed node x is given by a Gaussian distribution $\mathcal{N}(x|\mu, \tau^{-1})$ with mean μ and precision τ. Suppose that the marginal distributions over the mean and precision are given by $\mathcal{N}(\mu|\mu_0, s_0)$ and $\mathrm{Gam}(\tau|a, b)$, where $\mathrm{Gam}(\cdot|\cdot, \cdot)$ denotes a gamma distribution. Write down expressions for the conditional distributions $p(\mu|x, \tau)$ and $p(\tau|x, \mu)$ that would be required in order to apply Gibbs sampling to the posterior distribution $p(\mu, \tau|x)$.

11.14 ($\star$) Verify that the over-relaxation update (11.50), in which z_i has mean μ_i and variance σ_i, and where ν has zero mean and unit variance, gives a value z_i' with mean μ_i and variance σ_i^2.

11.15 ($\star$) **www** Using (11.56) and (11.57), show that the Hamiltonian equation (11.58) is equivalent to (11.53). Similarly, using (11.57) show that (11.59) is equivalent to (11.55).

11.16 ($\star$) By making use of (11.56), (11.57), and (11.63), show that the conditional distribution $p(\mathbf{r}|\mathbf{z})$ is a Gaussian.

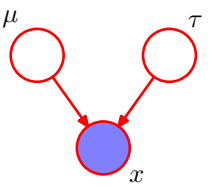

Figure 11.16 A graph involving an observed Gaussian variable x with prior distributions over its mean μ and precision τ.

11.17 ($\star$) **www** Verify that the two probabilities (11.68) and (11.69) are equal, and hence that detailed balance holds for the hybrid Monte Carlo algorithm.

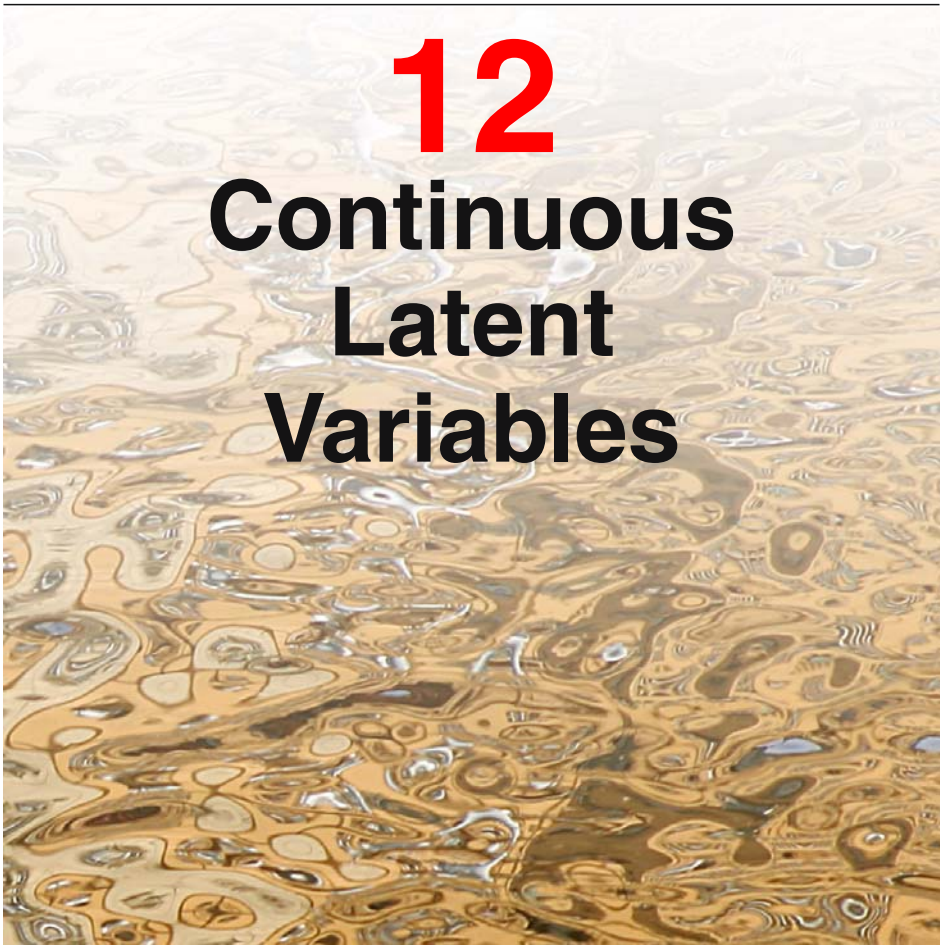

12 Continuous Latent Variables

In Chapter 9, we discussed probabilistic models having discrete latent variables, such as the mixture of Gaussians. We now explore models in which some, or all, of the latent variables are continuous. An important motivation for such models is that many data sets have the property that the data points all lie close to a manifold of much lower dimensionality than that of the original data space. To see why this might arise, consider an artificial data set constructed by taking one of the off-line digits, represented by a 64×64 pixel grey-level image, and embedding it in a larger image of size 100×100 by padding with pixels having the value zero (corresponding to white pixels) in which the location and orientation of the digit is varied at random, as illustrated in Figure 12.1. Each of the resulting images is represented by a point in the $100 \times 100 = 10,000$-dimensional data space. However, across a data set of such images, there are only three *degrees of freedom* of variability, corresponding to the vertical and horizontal translations and the rotations. The data points will therefore live on a subspace of the data space whose *intrinsic dimensionality* is three. Note

Appendix A

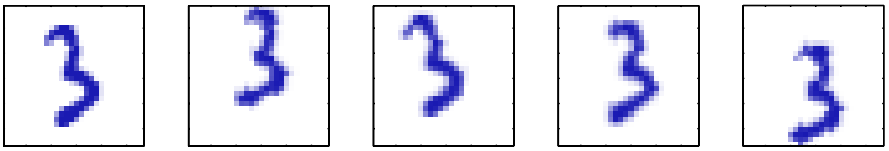

Figure 12.1 A synthetic data set obtained by taking one of the off-line digit images and creating multiple copies in each of which the digit has undergone a random displacement and rotation within some larger image field. The resulting images each have $100 \times 100 = 10,000$ pixels.

that the manifold will be nonlinear because, for instance, if we translate the digit past a particular pixel, that pixel value will go from zero (white) to one (black) and back to zero again, which is clearly a nonlinear function of the digit position. In this example, the translation and rotation parameters are latent variables because we observe only the image vectors and are not told which values of the translation or rotation variables were used to create them.

For real digit image data, there will be a further degree of freedom arising from scaling. Moreover there will be multiple additional degrees of freedom associated with more complex deformations due to the variability in an individual's writing as well as the differences in writing styles between individuals. Nevertheless, the number of such degrees of freedom will be small compared to the dimensionality of the data set.

Appendix A Another example is provided by the oil flow data set, in which (for a given geometrical configuration of the gas, water, and oil phases) there are only two degrees of freedom of variability corresponding to the fraction of oil in the pipe and the fraction of water (the fraction of gas then being determined). Although the data space comprises 12 measurements, a data set of points will lie close to a two-dimensional manifold embedded within this space. In this case, the manifold comprises several distinct segments corresponding to different flow regimes, each such segment being a (noisy) continuous two-dimensional manifold. If our goal is data compression, or density modelling, then there can be benefits in exploiting this manifold structure.

In practice, the data points will not be confined precisely to a smooth low-dimensional manifold, and we can interpret the departures of data points from the manifold as 'noise'. This leads naturally to a generative view of such models in which we first select a point within the manifold according to some latent variable distribution and then generate an observed data point by adding noise, drawn from some conditional distribution of the data variables given the latent variables.

The simplest continuous latent variable model assumes Gaussian distributions for both the latent and observed variables and makes use of a linear-Gaussian dependence of the observed variables on the state of the latent variables. This leads to a probabilistic formulation of the well-known technique of principal component analysis (PCA), as well as to a related model called factor analysis.

Section 8.1.4

Section 12.1 In this chapter w will begin with a standard, nonprobabilistic treatment of PCA, and then we show how PCA arises naturally as the maximum likelihood solution to

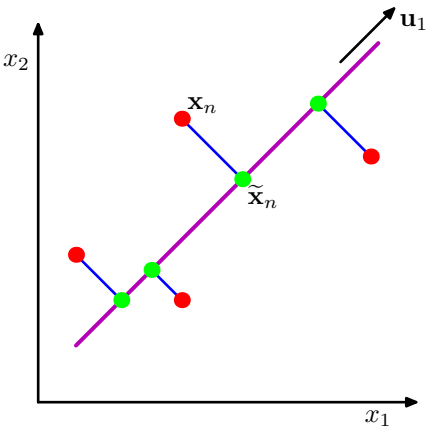

Figure 12.2 Principal component analysis seeks a space of lower dimensionality, known as the principal subspace and denoted by the magenta line, such that the orthogonal projection of the data points (red dots) onto this subspace maximizes the variance of the projected points (green dots). An alternative definition of PCA is based on minimizing the sum-of-squares of the projection errors, indicated by the blue lines.

Section 12.2 a particular form of linear-Gaussian latent variable model. This probabilistic reformulation brings many advantages, such as the use of EM for parameter estimation, principled extensions to mixtures of PCA models, and Bayesian formulations that allow the number of principal components to be determined automatically from the data. Finally, we discuss briefly several generalizations of the latent variable concept that go beyond the linear-Gaussian assumption including non-Gaussian latent variables, which leads to the framework of *independent component analysis*, as well as

Section 12.4 models having a nonlinear relationship between latent and observed variables.

12.1. Principal Component Analysis

Principal component analysis, or PCA, is a technique that is widely used for applications such as dimensionality reduction, lossy data compression, feature extraction, and data visualization (Jolliffe, 2002). It is also known as the *Karhunen-Loève* transform.

There are two commonly used definitions of PCA that give rise to the same algorithm. PCA can be defined as the orthogonal projection of the data onto a lower dimensional linear space, known as the *principal subspace*, such that the variance of the projected data is maximized (Hotelling, 1933). Equivalently, it can be defined as the linear projection that minimizes the average projection cost, defined as the mean squared distance between the data points and their projections (Pearson, 1901). The process of orthogonal projection is illustrated in Figure 12.2. We consider each of these definitions in turn.

12.1.1 Maximum variance formulation

Consider a data set of observations $\{\mathbf{x}_n\}$ where $n = 1, \ldots, N$, and $\mathbf{x}_n$ is a Euclidean variable with dimensionality D. Our goal is to project the data onto a space having dimensionality $M < D$ while maximizing the variance of the projected data. For the moment, we shall assume that the value of M is given. Later in this

chapter, we shall consider techniques to determine an appropriate value of M from the data.

To begin with, consider the projection onto a one-dimensional space ($M = 1$). We can define the direction of this space using a D-dimensional vector $\mathbf{u}_1$, which for convenience (and without loss of generality) we shall choose to be a unit vector so that $\mathbf{u}_1^{\mathrm{T}}\mathbf{u}_1 = 1$ (note that we are only interested in the direction defined by $\mathbf{u}_1$, not in the magnitude of $\mathbf{u}_1$ itself). Each data point $\mathbf{x}_n$ is then projected onto a scalar value $\mathbf{u}_1^{\mathrm{T}}\mathbf{x}_n$. The mean of the projected data is $\mathbf{u}_1^{\mathrm{T}}\overline{\mathbf{x}}$ where $\overline{\mathbf{x}}$ is the sample set mean given by

$$\overline{\mathbf{x}} = \frac{1}{N}\sum_{n=1}^{N}\mathbf{x}_n \tag{12.1}$$

and the variance of the projected data is given by

$$\frac{1}{N}\sum_{n=1}^{N}\left\{\mathbf{u}_1^{\mathrm{T}}\mathbf{x}_n - \mathbf{u}_1^{\mathrm{T}}\overline{\mathbf{x}}\right\}^2 = \mathbf{u}_1^{\mathrm{T}}\mathbf{S}\mathbf{u}_1 \tag{12.2}$$

where $\mathbf{S}$ is the data covariance matrix defined by

$$\mathbf{S} = \frac{1}{N}\sum_{n=1}^{N}(\mathbf{x}_n - \overline{\mathbf{x}})(\mathbf{x}_n - \overline{\mathbf{x}})^{\mathrm{T}}. \tag{12.3}$$

We now maximize the projected variance $\mathbf{u}_1^{\mathrm{T}}\mathbf{S}\mathbf{u}_1$ with respect to $\mathbf{u}_1$. Clearly, this has to be a constrained maximization to prevent $\|\mathbf{u}_1\| \to \infty$. The appropriate constraint comes from the normalization condition $\mathbf{u}_1^{\mathrm{T}}\mathbf{u}_1 = 1$. To enforce this constraint, we introduce a Lagrange multiplier that we shall denote by λ_1, and then make an unconstrained maximization of

Appendix E

$$\mathbf{u}_1^{\mathrm{T}}\mathbf{S}\mathbf{u}_1 + \lambda_1\left(1 - \mathbf{u}_1^{\mathrm{T}}\mathbf{u}_1\right). \tag{12.4}$$

By setting the derivative with respect to $\mathbf{u}_1$ equal to zero, we see that this quantity will have a stationary point when

$$\mathbf{S}\mathbf{u}_1 = \lambda_1\mathbf{u}_1 \tag{12.5}$$

which says that $\mathbf{u}_1$ must be an eigenvector of $\mathbf{S}$. If we left-multiply by $\mathbf{u}_1^{\mathrm{T}}$ and make use of $\mathbf{u}_1^{\mathrm{T}}\mathbf{u}_1 = 1$, we see that the variance is given by

$$\mathbf{u}_1^{\mathrm{T}}\mathbf{S}\mathbf{u}_1 = \lambda_1 \tag{12.6}$$

and so the variance will be a maximum when we set $\mathbf{u}_1$ equal to the eigenvector having the largest eigenvalue λ_1. This eigenvector is known as the first principal component.

We can define additional principal components in an incremental fashion by choosing each new direction to be that which maximizes the projected variance

amongst all possible directions orthogonal to those already considered. If we consider the general case of an M-dimensional projection space, the optimal linear projection for which the variance of the projected data is maximized is now defined by the M eigenvectors $\mathbf{u}_1, \ldots, \mathbf{u}_M$ of the data covariance matrix $\mathbf{S}$ corresponding to the M largest eigenvalues $\lambda_1, \ldots, \lambda_M$. This is easily shown using proof by induction.

Exercise 12.1

To summarize, principal component analysis involves evaluating the mean $\overline{\mathbf{x}}$ and the covariance matrix $\mathbf{S}$ of the data set and then finding the M eigenvectors of $\mathbf{S}$ corresponding to the M largest eigenvalues. Algorithms for finding eigenvectors and eigenvalues, as well as additional theorems related to eigenvector decomposition, can be found in Golub and Van Loan (1996). Note that the computational cost of computing the full eigenvector decomposition for a matrix of size $D \times D$ is $O(D^3)$. If we plan to project our data onto the first M principal components, then we only need to find the first M eigenvalues and eigenvectors. This can be done with more efficient techniques, such as the *power method* (Golub and Van Loan, 1996), that scale like $O(MD^2)$, or alternatively we can make use of the EM algorithm.

Section 12.2.2

12.1.2 Minimum-error formulation

We now discuss an alternative formulation of PCA based on projection error minimization. To do this, we introduce a complete orthonormal set of D-dimensional basis vectors $\{\mathbf{u}_i\}$ where $i = 1, \ldots, D$ that satisfy

Appendix C

$$\mathbf{u}_i^{\mathrm{T}} \mathbf{u}_j = \delta_{ij}. \tag{12.7}$$

Because this basis is complete, each data point can be represented exactly by a linear combination of the basis vectors

$$\mathbf{x}_n = \sum_{i=1}^{D} \alpha_{ni} \mathbf{u}_i \tag{12.8}$$

where the coefficients α_{ni} will be different for different data points. This simply corresponds to a rotation of the coordinate system to a new system defined by the $\{\mathbf{u}_i\}$, and the original D components $\{x_{n1}, \ldots, x_{nD}\}$ are replaced by an equivalent set $\{\alpha_{n1}, \ldots, \alpha_{nD}\}$. Taking the inner product with $\mathbf{u}_j$, and making use of the orthonormality property, we obtain $\alpha_{nj} = \mathbf{x}_n^{\mathrm{T}} \mathbf{u}_j$, and so without loss of generality we can write

$$\mathbf{x}_n = \sum_{i=1}^{D} \left(\mathbf{x}_n^{\mathrm{T}} \mathbf{u}_i \right) \mathbf{u}_i. \tag{12.9}$$

Our goal, however, is to approximate this data point using a representation involving a restricted number $M < D$ of variables corresponding to a projection onto a lower-dimensional subspace. The M-dimensional linear subspace can be represented, without loss of generality, by the first M of the basis vectors, and so we approximate each data point $\mathbf{x}_n$ by

$$\widetilde{\mathbf{x}}_n = \sum_{i=1}^{M} z_{ni} \mathbf{u}_i + \sum_{i=M+1}^{D} b_i \mathbf{u}_i \tag{12.10}$$

where the $\{z_{ni}\}$ depend on the particular data point, whereas the $\{b_i\}$ are constants that are the same for all data points. We are free to choose the $\{\mathbf{u}_i\}$, the $\{z_{ni}\}$, and the $\{b_i\}$ so as to minimize the distortion introduced by the reduction in dimensionality. As our distortion measure, we shall use the squared distance between the original data point $\mathbf{x}_n$ and its approximation $\widetilde{\mathbf{x}}_n$, averaged over the data set, so that our goal is to minimize

$$J = \frac{1}{N}\sum_{n=1}^{N} \|\mathbf{x}_n - \widetilde{\mathbf{x}}_n\|^2. \tag{12.11}$$

Consider first of all the minimization with respect to the quantities $\{z_{ni}\}$. Substituting for $\widetilde{\mathbf{x}}_n$, setting the derivative with respect to z_{nj} to zero, and making use of the orthonormality conditions, we obtain

$$z_{nj} = \mathbf{x}_n^{\mathrm{T}}\mathbf{u}_j \tag{12.12}$$

where $j = 1, \ldots, M$. Similarly, setting the derivative of J with respect to b_i to zero, and again making use of the orthonormality relations, gives

$$b_j = \overline{\mathbf{x}}^{\mathrm{T}}\mathbf{u}_j \tag{12.13}$$

where $j = M+1, \ldots, D$. If we substitute for z_{ni} and b_i, and make use of the general expansion (12.9), we obtain

$$\mathbf{x}_n - \widetilde{\mathbf{x}}_n = \sum_{i=M+1}^{D} \left\{(\mathbf{x}_n - \overline{\mathbf{x}})^{\mathrm{T}}\mathbf{u}_i\right\}\mathbf{u}_i \tag{12.14}$$

from which we see that the displacement vector from $\mathbf{x}_n$ to $\widetilde{\mathbf{x}}_n$ lies in the space orthogonal to the principal subspace, because it is a linear combination of $\{\mathbf{u}_i\}$ for $i = M+1, \ldots, D$, as illustrated in Figure 12.2. This is to be expected because the projected points $\widetilde{\mathbf{x}}_n$ must lie within the principal subspace, but we can move them freely within that subspace, and so the minimum error is given by the orthogonal projection.

We therefore obtain an expression for the distortion measure J as a function purely of the $\{\mathbf{u}_i\}$ in the form

$$J = \frac{1}{N}\sum_{n=1}^{N}\sum_{i=M+1}^{D}\left(\mathbf{x}_n^{\mathrm{T}}\mathbf{u}_i - \overline{\mathbf{x}}^{\mathrm{T}}\mathbf{u}_i\right)^2 = \sum_{i=M+1}^{D}\mathbf{u}_i^{\mathrm{T}}\mathbf{S}\mathbf{u}_i. \tag{12.15}$$

There remains the task of minimizing J with respect to the $\{\mathbf{u}_i\}$, which must be a constrained minimization otherwise we will obtain the vacuous result $\mathbf{u}_i = 0$. The constraints arise from the orthonormality conditions and, as we shall see, the solution will be expressed in terms of the eigenvector expansion of the covariance matrix. Before considering a formal solution, let us try to obtain some intuition about the result by considering the case of a two-dimensional data space $D = 2$ and a one-dimensional principal subspace $M = 1$. We have to choose a direction $\mathbf{u}_2$ so as to

minimize $J = \mathbf{u}_2^{\mathrm{T}}\mathbf{S}\mathbf{u}_2$, subject to the normalization constraint $\mathbf{u}_2^{\mathrm{T}}\mathbf{u}_2 = 1$. Using a Lagrange multiplier λ_2 to enforce the constraint, we consider the minimization of

$$\widetilde{J} = \mathbf{u}_2^{\mathrm{T}}\mathbf{S}\mathbf{u}_2 + \lambda_2\left(1 - \mathbf{u}_2^{\mathrm{T}}\mathbf{u}_2\right). \tag{12.16}$$

Setting the derivative with respect to $\mathbf{u}_2$ to zero, we obtain $\mathbf{S}\mathbf{u}_2 = \lambda_2\mathbf{u}_2$ so that $\mathbf{u}_2$ is an eigenvector of $\mathbf{S}$ with eigenvalue λ_2. Thus any eigenvector will define a stationary point of the distortion measure. To find the value of J at the minimum, we back-substitute the solution for $\mathbf{u}_2$ into the distortion measure to give $J = \lambda_2$. We therefore obtain the minimum value of J by choosing $\mathbf{u}_2$ to be the eigenvector corresponding to the smaller of the two eigenvalues. Thus we should choose the principal subspace to be aligned with the eigenvector having the *larger* eigenvalue. This result accords with our intuition that, in order to minimize the average squared projection distance, we should choose the principal component subspace to pass through the mean of the data points and to be aligned with the directions of maximum variance. For the case when the eigenvalues are equal, any choice of principal direction will give rise to the same value of J.

Exercise 12.2

The general solution to the minimization of J for arbitrary D and arbitrary $M < D$ is obtained by choosing the $\{\mathbf{u}_i\}$ to be eigenvectors of the covariance matrix given by

$$\mathbf{S}\mathbf{u}_i = \lambda_i\mathbf{u}_i \tag{12.17}$$

where $i = 1, \ldots, D$, and as usual the eigenvectors $\{\mathbf{u}_i\}$ are chosen to be orthonormal. The corresponding value of the distortion measure is then given by

$$J = \sum_{i=M+1}^{D} \lambda_i \tag{12.18}$$

which is simply the sum of the eigenvalues of those eigenvectors that are orthogonal to the principal subspace. We therefore obtain the minimum value of J by selecting these eigenvectors to be those having the $D - M$ smallest eigenvalues, and hence the eigenvectors defining the principal subspace are those corresponding to the M largest eigenvalues.

Although we have considered $M < D$, the PCA analysis still holds if $M = D$, in which case there is no dimensionality reduction but simply a rotation of the coordinate axes to align with principal components.

Finally, it is worth noting that there exists a closely related linear dimensionality reduction technique called *canonical correlation analysis*, or *CCA* (Hotelling, 1936; Bach and Jordan, 2002). Whereas PCA works with a single random variable, CCA considers two (or more) variables and tries to find a corresponding pair of linear subspaces that have high cross-correlation, so that each component within one of the subspaces is correlated with a single component from the other subspace. Its solution can be expressed in terms of a generalized eigenvector problem.

12.1.3 Applications of PCA

We can illustrate the use of PCA for data compression by considering the off-line digits data set. Because each eigenvector of the covariance matrix is a vector

Appendix A

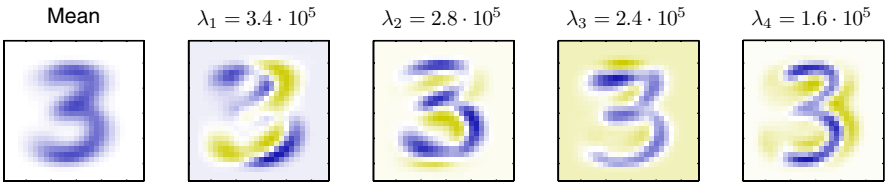

Figure 12.3 The mean vector $\overline{\mathbf{x}}$ along with the first four PCA eigenvectors $\mathbf{u}_1, \ldots, \mathbf{u}_4$ for the off-line digits data set, together with the corresponding eigenvalues.

in the original D-dimensional space, we can represent the eigenvectors as images of the same size as the data points. The first five eigenvectors, along with the corresponding eigenvalues, are shown in Figure 12.3. A plot of the complete spectrum of eigenvalues, sorted into decreasing order, is shown in Figure 12.4(a). The distortion measure J associated with choosing a particular value of M is given by the sum of the eigenvalues from $M+1$ up to D and is plotted for different values of M in Figure 12.4(b).

If we substitute (12.12) and (12.13) into (12.10), we can write the PCA approximation to a data vector $\mathbf{x}_n$ in the form

$$\widetilde{\mathbf{x}}_n = \sum_{i=1}^{M} (\mathbf{x}_n^{\mathrm{T}}\mathbf{u}_i)\mathbf{u}_i + \sum_{i=M+1}^{D} (\overline{\mathbf{x}}^{\mathrm{T}}\mathbf{u}_i)\mathbf{u}_i \tag{12.19}$$

$$= \overline{\mathbf{x}} + \sum_{i=1}^{M} \left(\mathbf{x}_n^{\mathrm{T}}\mathbf{u}_i - \overline{\mathbf{x}}^{\mathrm{T}}\mathbf{u}_i\right)\mathbf{u}_i \tag{12.20}$$

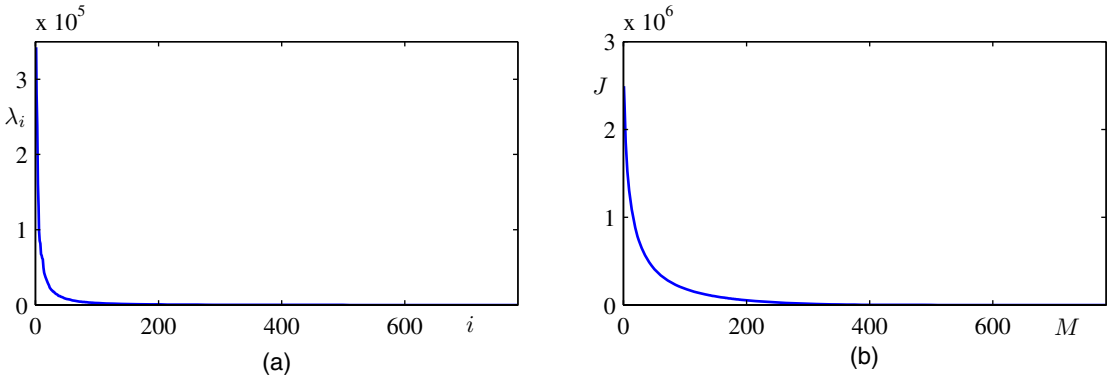

Figure 12.4 (a) Plot of the eigenvalue spectrum for the off-line digits data set. (b) Plot of the sum of the discarded eigenvalues, which represents the sum-of-squares distortion J introduced by projecting the data onto a principal component subspace of dimensionality M.

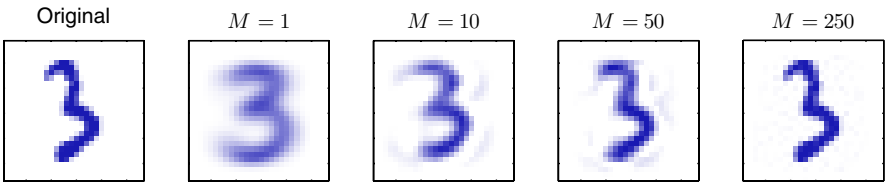

Figure 12.5 An original example from the off-line digits data set together with its PCA reconstructions obtained by retaining M principal components for various values of M. As M increases the reconstruction becomes more accurate and would become perfect when $M = D = 28 \times 28 = 784$.

where we have made use of the relation

$$\overline{\mathbf{x}} = \sum_{i=1}^{D} \left(\overline{\mathbf{x}}^{\mathrm{T}}\mathbf{u}_i\right)\mathbf{u}_i \tag{12.21}$$

which follows from the completeness of the $\{\mathbf{u}_i\}$. This represents a compression of the data set, because for each data point we have replaced the D-dimensional vector $\mathbf{x}_n$ with an M-dimensional vector having components $\left(\mathbf{x}_n^{\mathrm{T}}\mathbf{u}_i - \overline{\mathbf{x}}^{\mathrm{T}}\mathbf{u}_i\right)$. The smaller the value of M, the greater the degree of compression. Examples of PCA reconstructions of data points for the digits data set are shown in Figure 12.5.

Another application of principal component analysis is to data pre-processing. In this case, the goal is not dimensionality reduction but rather the transformation of a data set in order to standardize certain of its properties. This can be important in allowing subsequent pattern recognition algorithms to be applied successfully to the data set. Typically, it is done when the original variables are measured in various different units or have significantly different variability. For instance in the Old Faithful data set, the time between eruptions is typically an order of magnitude greater than the duration of an eruption. When we applied the K-means algorithm to this data set, we first made a separate linear re-scaling of the individual variables such that each variable had zero mean and unit variance. This is known as *standardizing* the data, and the covariance matrix for the standardized data has components

Appendix A

Section 9.1

$$\rho_{ij} = \frac{1}{N}\sum_{n=1}^{N}\frac{(x_{ni} - \overline{x}_i)}{\sigma_i}\frac{(x_{nj} - \overline{x}_j)}{\sigma_j} \tag{12.22}$$

where σ_i is the variance of x_i. This is known as the *correlation* matrix of the original data and has the property that if two components x_i and x_j of the data are perfectly correlated, then $\rho_{ij} = 1$, and if they are uncorrelated, then $\rho_{ij} = 0$.

However, using PCA we can make a more substantial normalization of the data to give it zero mean and unit covariance, so that different variables become decorrelated. To do this, we first write the eigenvector equation (12.17) in the form

$$\mathbf{SU} = \mathbf{UL} \tag{12.23}$$

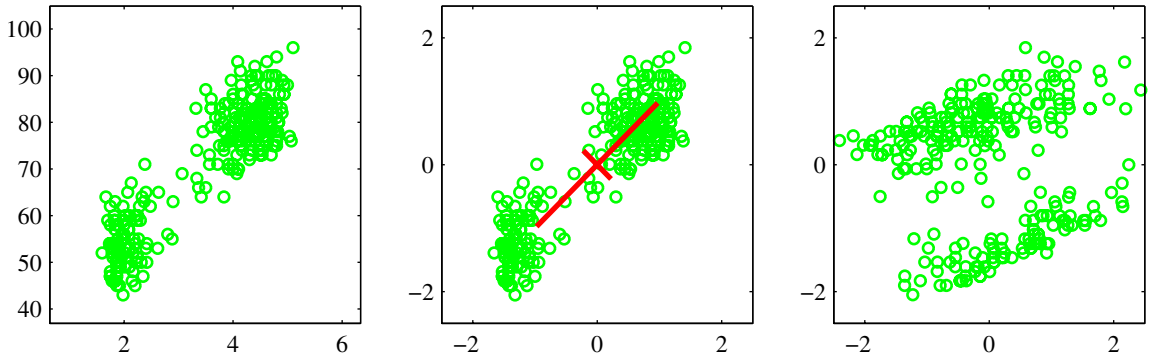

Figure 12.6 Illustration of the effects of linear pre-processing applied to the Old Faithful data set. The plot on the left shows the original data. The centre plot shows the result of standardizing the individual variables to zero mean and unit variance. Also shown are the principal axes of this normalized data set, plotted over the range $\pm\lambda_i^{1/2}$. The plot on the right shows the result of whitening of the data to give it zero mean and unit covariance.

where $\mathbf{L}$ is a $D \times D$ diagonal matrix with elements λ_i, and $\mathbf{U}$ is a $D \times D$ orthogonal matrix with columns given by $\mathbf{u}_i$. Then we define, for each data point $\mathbf{x}_n$, a transformed value given by

$$\mathbf{y}_n = \mathbf{L}^{-1/2}\mathbf{U}^{\mathrm{T}}(\mathbf{x}_n - \overline{\mathbf{x}}) \tag{12.24}$$

where $\overline{\mathbf{x}}$ is the sample mean defined by (12.1). Clearly, the set $\{\mathbf{y}_n\}$ has zero mean, and its covariance is given by the identity matrix because

$$\begin{aligned} \frac{1}{N}\sum_{n=1}^{N}\mathbf{y}_n\mathbf{y}_n^{\mathrm{T}} &= \frac{1}{N}\sum_{n=1}^{N}\mathbf{L}^{-1/2}\mathbf{U}^{\mathrm{T}}(\mathbf{x}_n - \overline{\mathbf{x}})(\mathbf{x}_n - \overline{\mathbf{x}})^{\mathrm{T}}\mathbf{U}\mathbf{L}^{-1/2} \\ &= \mathbf{L}^{-1/2}\mathbf{U}^{\mathrm{T}}\mathbf{S}\mathbf{U}\mathbf{L}^{-1/2} = \mathbf{L}^{-1/2}\mathbf{L}\mathbf{L}^{-1/2} = \mathbf{I}. \end{aligned} \tag{12.25}$$

This operation is known as *whitening* or *sphereing* the data and is illustrated for the Old Faithful data set in Figure 12.6.

Appendix A

It is interesting to compare PCA with the Fisher linear discriminant which was discussed in Section 4.1.4. Both methods can be viewed as techniques for linear dimensionality reduction. However, PCA is unsupervised and depends only on the values $\mathbf{x}_n$ whereas Fisher linear discriminant also uses class-label information. This difference is highlighted by the example in Figure 12.7.

Another common application of principal component analysis is to data visualization. Here each data point is projected onto a two-dimensional ($M = 2$) principal subspace, so that a data point $\mathbf{x}_n$ is plotted at Cartesian coordinates given by $\mathbf{x}_n^{\mathrm{T}}\mathbf{u}_1$ and $\mathbf{x}_n^{\mathrm{T}}\mathbf{u}_2$, where $\mathbf{u}_1$ and $\mathbf{u}_2$ are the eigenvectors corresponding to the largest and second largest eigenvalues. An example of such a plot, for the oil flow data set, is shown in Figure 12.8.

Appendix A

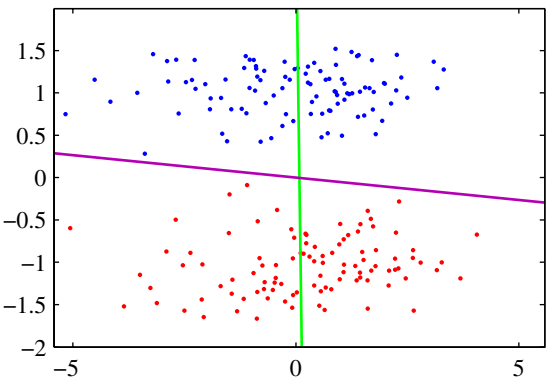

Figure 12.7 A comparison of principal component analysis with Fisher's linear discriminant for linear dimensionality reduction. Here the data in two dimensions, belonging to two classes shown in red and blue, is to be projected onto a single dimension. PCA chooses the direction of maximum variance, shown by the magenta curve, which leads to strong class overlap, whereas the Fisher linear discriminant takes account of the class labels and leads to a projection onto the green curve giving much better class separation.

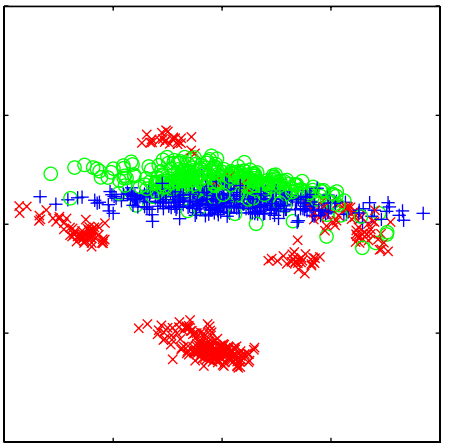

Figure 12.8 Visualization of the oil flow data set obtained by projecting the data onto the first two principal components. The red, blue, and green points correspond to the 'laminar', 'homogeneous', and 'annular' flow configurations respectively.

12.1.4 PCA for high-dimensional data

In some applications of principal component analysis, the number of data points is smaller than the dimensionality of the data space. For example, we might want to apply PCA to a data set of a few hundred images, each of which corresponds to a vector in a space of potentially several million dimensions (corresponding to three colour values for each of the pixels in the image). Note that in a D-dimensional space a set of N points, where $N < D$, defines a linear subspace whose dimensionality is at most $N - 1$, and so there is little point in applying PCA for values of M that are greater than $N - 1$. Indeed, if we perform PCA we will find that at least $D - N + 1$ of the eigenvalues are zero, corresponding to eigenvectors along whose directions the data set has zero variance. Furthermore, typical algorithms for finding the eigenvectors of a $D \times D$ matrix have a computational cost that scales like $O(D^3)$, and so for applications such as the image example, a direct application of PCA will be computationally infeasible.

We can resolve this problem as follows. First, let us define $\mathbf{X}$ to be the $(N \times D)$-

dimensional centred data matrix, whose n^{th} row is given by $(\mathbf{x}_n - \overline{\mathbf{x}})^{\mathrm{T}}$. The covariance matrix (12.3) can then be written as $\mathbf{S} = N^{-1}\mathbf{X}^{\mathrm{T}}\mathbf{X}$, and the corresponding eigenvector equation becomes

$$\frac{1}{N}\mathbf{X}^{\mathrm{T}}\mathbf{X}\mathbf{u}_i = \lambda_i \mathbf{u}_i. \tag{12.26}$$

Now pre-multiply both sides by $\mathbf{X}$ to give

$$\frac{1}{N}\mathbf{X}\mathbf{X}^{\mathrm{T}}(\mathbf{X}\mathbf{u}_i) = \lambda_i(\mathbf{X}\mathbf{u}_i). \tag{12.27}$$

If we now define $\mathbf{v}_i = \mathbf{X}\mathbf{u}_i$, we obtain

$$\frac{1}{N}\mathbf{X}\mathbf{X}^{\mathrm{T}}\mathbf{v}_i = \lambda_i \mathbf{v}_i \tag{12.28}$$

which is an eigenvector equation for the $N \times N$ matrix $N^{-1}\mathbf{X}\mathbf{X}^{\mathrm{T}}$. We see that this has the same $N-1$ eigenvalues as the original covariance matrix (which itself has an additional $D - N + 1$ eigenvalues of value zero). Thus we can solve the eigenvector problem in spaces of lower dimensionality with computational cost $O(N^3)$ instead of $O(D^3)$. In order to determine the eigenvectors, we multiply both sides of (12.28) by $\mathbf{X}^{\mathrm{T}}$ to give

$$\left(\frac{1}{N}\mathbf{X}^{\mathrm{T}}\mathbf{X}\right)(\mathbf{X}^{\mathrm{T}}\mathbf{v}_i) = \lambda_i(\mathbf{X}^{\mathrm{T}}\mathbf{v}_i) \tag{12.29}$$

from which we see that $(\mathbf{X}^{\mathrm{T}}\mathbf{v}_i)$ is an eigenvector of $\mathbf{S}$ with eigenvalue λ_i. Note, however, that these eigenvectors need not be normalized. To determine the appropriate normalization, we re-scale $\mathbf{u}_i \propto \mathbf{X}^{\mathrm{T}}\mathbf{v}_i$ by a constant such that $\|\mathbf{u}_i\| = 1$, which, assuming $\mathbf{v}_i$ has been normalized to unit length, gives

$$\mathbf{u}_i = \frac{1}{(N\lambda_i)^{1/2}}\mathbf{X}^{\mathrm{T}}\mathbf{v}_i. \tag{12.30}$$

In summary, to apply this approach we first evaluate $\mathbf{X}\mathbf{X}^{\mathrm{T}}$ and then find its eigenvectors and eigenvalues and then compute the eigenvectors in the original data space using (12.30).

12.2. Probabilistic PCA

The formulation of PCA discussed in the previous section was based on a linear projection of the data onto a subspace of lower dimensionality than the original data space. We now show that PCA can also be expressed as the maximum likelihood solution of a probabilistic latent variable model. This reformulation of PCA, known as *probabilistic PCA*, brings several advantages compared with conventional PCA:

- Probabilistic PCA represents a constrained form of the Gaussian distribution in which the number of free parameters can be restricted while still allowing the model to capture the dominant correlations in a data set.

- We can derive an EM algorithm for PCA that is computationally efficient in situations where only a few leading eigenvectors are required and that avoids having to evaluate the data covariance matrix as an intermediate step.

Section 12.2.2

- The combination of a probabilistic model and EM allows us to deal with missing values in the data set.
- Mixtures of probabilistic PCA models can be formulated in a principled way and trained using the EM algorithm.
- Probabilistic PCA forms the basis for a Bayesian treatment of PCA in which the dimensionality of the principal subspace can be found automatically from the data.

Section 12.2.3

- The existence of a likelihood function allows direct comparison with other probabilistic density models. By contrast, conventional PCA will assign a low reconstruction cost to data points that are close to the principal subspace even if they lie arbitrarily far from the training data.
- Probabilistic PCA can be used to model class-conditional densities and hence be applied to classification problems.
- The probabilistic PCA model can be run generatively to provide samples from the distribution.

This formulation of PCA as a probabilistic model was proposed independently by Tipping and Bishop (1997, 1999b) and by Roweis (1998). As we shall see later, it is closely related to *factor analysis* (Basilevsky, 1994).

Section 8.1.4

Probabilistic PCA is a simple example of the linear-Gaussian framework, in which all of the marginal and conditional distributions are Gaussian. We can formulate probabilistic PCA by first introducing an explicit latent variable $\mathbf{z}$ corresponding to the principal-component subspace. Next we define a Gaussian prior distribution $p(\mathbf{z})$ over the latent variable, together with a Gaussian conditional distribution $p(\mathbf{x}|\mathbf{z})$ for the observed variable $\mathbf{x}$ conditioned on the value of the latent variable. Specifically, the prior distribution over $\mathbf{z}$ is given by a zero-mean unit-covariance Gaussian

$$p(\mathbf{z}) = \mathcal{N}(\mathbf{z}|\mathbf{0}, \mathbf{I}). \tag{12.31}$$

Similarly, the conditional distribution of the observed variable $\mathbf{x}$, conditioned on the value of the latent variable $\mathbf{z}$, is again Gaussian, of the form

$$p(\mathbf{x}|\mathbf{z}) = \mathcal{N}(\mathbf{x}|\mathbf{W}\mathbf{z} + \boldsymbol{\mu}, \sigma^2\mathbf{I}) \tag{12.32}$$

in which the mean of $\mathbf{x}$ is a general linear function of $\mathbf{z}$ governed by the $D \times M$ matrix $\mathbf{W}$ and the D-dimensional vector $\boldsymbol{\mu}$. Note that this factorizes with respect to the elements of $\mathbf{x}$, in other words this is an example of the naive Bayes model. As we shall see shortly, the columns of $\mathbf{W}$ span a linear subspace within the data space that corresponds to the principal subspace. The other parameter in this model is the scalar σ^2 governing the variance of the conditional distribution. Note that there is no

Section 8.2.2

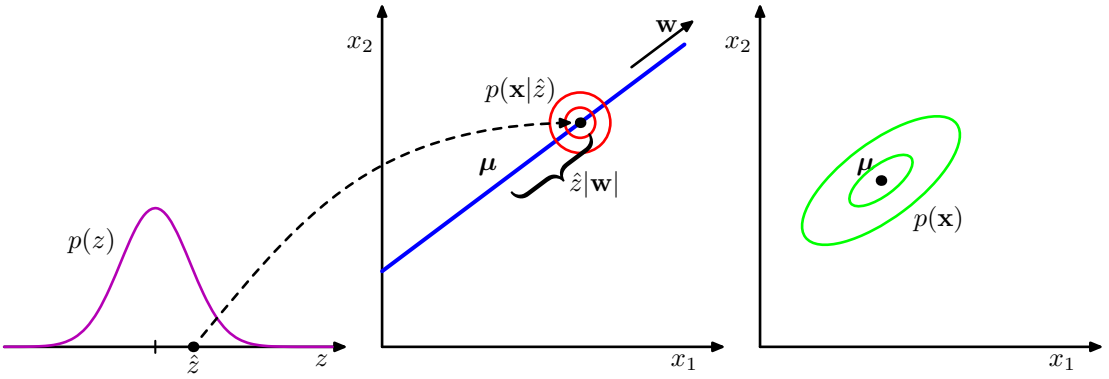

Figure 12.9 An illustration of the generative view of the probabilistic PCA model for a two-dimensional data space and a one-dimensional latent space. An observed data point $\mathbf{x}$ is generated by first drawing a value $\widehat{z}$ for the latent variable from its prior distribution $p(z)$ and then drawing a value for $\mathbf{x}$ from an isotropic Gaussian distribution (illustrated by the red circles) having mean $\mathbf{w}\widehat{z} + \boldsymbol{\mu}$ and covariance $\sigma^2\mathbf{I}$. The green ellipses show the density contours for the marginal distribution $p(\mathbf{x})$.

loss of generality in assuming a zero mean, unit covariance Gaussian for the latent distribution $p(\mathbf{z})$ because a more general Gaussian distribution would give rise to an equivalent probabilistic model.

Exercise 12.4

We can view the probabilistic PCA model from a generative viewpoint in which a sampled value of the observed variable is obtained by first choosing a value for the latent variable and then sampling the observed variable conditioned on this latent value. Specifically, the D-dimensional observed variable $\mathbf{x}$ is defined by a linear transformation of the M-dimensional latent variable $\mathbf{z}$ plus additive Gaussian 'noise', so that

$$\mathbf{x} = \mathbf{W}\mathbf{z} + \boldsymbol{\mu} + \boldsymbol{\epsilon} \tag{12.33}$$

where $\mathbf{z}$ is an M-dimensional Gaussian latent variable, and $\boldsymbol{\epsilon}$ is a D-dimensional zero-mean Gaussian-distributed noise variable with covariance $\sigma^2\mathbf{I}$. This generative process is illustrated in Figure 12.9. Note that this framework is based on a mapping from latent space to data space, in contrast to the more conventional view of PCA discussed above. The reverse mapping, from data space to the latent space, will be obtained shortly using Bayes' theorem.

Suppose we wish to determine the values of the parameters $\mathbf{W}$, $\boldsymbol{\mu}$ and σ^2 using maximum likelihood. To write down the likelihood function, we need an expression for the marginal distribution $p(\mathbf{x})$ of the observed variable. This is expressed, from the sum and product rules of probability, in the form

$$p(\mathbf{x}) = \int p(\mathbf{x}|\mathbf{z})p(\mathbf{z})\,\mathrm{d}\mathbf{z}. \tag{12.34}$$

Because this corresponds to a linear-Gaussian model, this marginal distribution is again Gaussian, and is given by

Exercise 12.7

$$p(\mathbf{x}) = \mathcal{N}(\mathbf{x}|\boldsymbol{\mu}, \mathbf{C}) \tag{12.35}$$

where the $D \times D$ covariance matrix $\mathbf{C}$ is defined by

$$\mathbf{C} = \mathbf{W}\mathbf{W}^{\mathrm{T}} + \sigma^2\mathbf{I}. \tag{12.36}$$

This result can also be derived more directly by noting that the predictive distribution will be Gaussian and then evaluating its mean and covariance using (12.33). This gives

$$\begin{aligned} \mathbb{E}[\mathbf{x}] &= \mathbb{E}[\mathbf{W}\mathbf{z} + \boldsymbol{\mu} + \boldsymbol{\epsilon}] = \boldsymbol{\mu} && (12.37) \\ \mathrm{cov}[\mathbf{x}] &= \mathbb{E}\left[(\mathbf{W}\mathbf{z} + \boldsymbol{\epsilon})(\mathbf{W}\mathbf{z} + \boldsymbol{\epsilon})^{\mathrm{T}}\right] \\ &= \mathbb{E}\left[\mathbf{W}\mathbf{z}\mathbf{z}^{\mathrm{T}}\mathbf{W}^{\mathrm{T}}\right] + \mathbb{E}[\boldsymbol{\epsilon}\boldsymbol{\epsilon}^{\mathrm{T}}] = \mathbf{W}\mathbf{W}^{\mathrm{T}} + \sigma^2\mathbf{I} && (12.38) \end{aligned}$$

where we have used the fact that $\mathbf{z}$ and $\boldsymbol{\epsilon}$ are independent random variables and hence are uncorrelated.

Intuitively, we can think of the distribution $p(\mathbf{x})$ as being defined by taking an isotropic Gaussian 'spray can' and moving it across the principal subspace spraying Gaussian ink with density determined by σ^2 and weighted by the prior distribution. The accumulated ink density gives rise to a 'pancake' shaped distribution representing the marginal density $p(\mathbf{x})$.

The predictive distribution $p(\mathbf{x})$ is governed by the parameters $\boldsymbol{\mu}$, $\mathbf{W}$, and σ^2. However, there is redundancy in this parameterization corresponding to rotations of the latent space coordinates. To see this, consider a matrix $\widetilde{\mathbf{W}} = \mathbf{W}\mathbf{R}$ where $\mathbf{R}$ is an orthogonal matrix. Using the orthogonality property $\mathbf{R}\mathbf{R}^{\mathrm{T}} = \mathbf{I}$, we see that the quantity $\widetilde{\mathbf{W}}\widetilde{\mathbf{W}}^{\mathrm{T}}$ that appears in the covariance matrix $\mathbf{C}$ takes the form

$$\widetilde{\mathbf{W}}\widetilde{\mathbf{W}}^{\mathrm{T}} = \mathbf{W}\mathbf{R}\mathbf{R}^{\mathrm{T}}\mathbf{W}^{\mathrm{T}} = \mathbf{W}\mathbf{W}^{\mathrm{T}} \tag{12.39}$$

and hence is independent of $\mathbf{R}$. Thus there is a whole family of matrices $\widetilde{\mathbf{W}}$ all of which give rise to the same predictive distribution. This invariance can be understood in terms of rotations within the latent space. We shall return to a discussion of the number of independent parameters in this model later.

When we evaluate the predictive distribution, we require $\mathbf{C}^{-1}$, which involves the inversion of a $D \times D$ matrix. The computation required to do this can be reduced by making use of the matrix inversion identity (C.7) to give

$$\mathbf{C}^{-1} = \sigma^{-1}\mathbf{I} - \sigma^{-2}\mathbf{W}\mathbf{M}^{-1}\mathbf{W}^{\mathrm{T}} \tag{12.40}$$

where the $M \times M$ matrix $\mathbf{M}$ is defined by

$$\mathbf{M} = \mathbf{W}^{\mathrm{T}}\mathbf{W} + \sigma^2\mathbf{I}. \tag{12.41}$$

Because we invert $\mathbf{M}$ rather than inverting $\mathbf{C}$ directly, the cost of evaluating $\mathbf{C}^{-1}$ is reduced from $O(D^3)$ to $O(M^3)$.

As well as the predictive distribution $p(\mathbf{x})$, we will also require the posterior distribution $p(\mathbf{z}|\mathbf{x})$, which can again be written down directly using the result (2.116) for linear-Gaussian models to give

Exercise 12.8

$$p(\mathbf{z}|\mathbf{x}) = \mathcal{N}\left(\mathbf{z}|\mathbf{M}^{-1}\mathbf{W}^{\mathrm{T}}(\mathbf{x} - \boldsymbol{\mu}), \sigma^{-2}\mathbf{M}\right). \tag{12.42}$$

Note that the posterior mean depends on $\mathbf{x}$, whereas the posterior covariance is independent of $\mathbf{x}$.

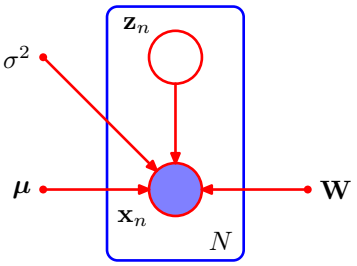

Figure 12.10 The probabilistic PCA model for a data set of N observations of $\mathbf{x}$ can be expressed as a directed graph in which each observation $\mathbf{x}_n$ is associated with a value $\mathbf{z}_n$ of the latent variable.

12.2.1 Maximum likelihood PCA

We next consider the determination of the model parameters using maximum likelihood. Given a data set $\mathbf{X} = \{\mathbf{x}_n\}$ of observed data points, the probabilistic PCA model can be expressed as a directed graph, as shown in Figure 12.10. The corresponding log likelihood function is given, from (12.35), by

$$\begin{aligned}\ln p(\mathbf{X}|\boldsymbol{\mu}, \mathbf{W}, \sigma^2) &= \sum_{n=1}^{N} \ln p(\mathbf{x}_n|\mathbf{W}, \boldsymbol{\mu}, \sigma^2) \\ &= -\frac{ND}{2}\ln(2\pi) - \frac{N}{2}\ln|\mathbf{C}| - \frac{1}{2}\sum_{n=1}^{N}(\mathbf{x}_n - \boldsymbol{\mu})^{\mathrm{T}}\mathbf{C}^{-1}(\mathbf{x}_n - \boldsymbol{\mu}). \quad (12.43)\end{aligned}$$

Setting the derivative of the log likelihood with respect to $\boldsymbol{\mu}$ equal to zero gives the expected result $\boldsymbol{\mu} = \overline{\mathbf{x}}$ where $\overline{\mathbf{x}}$ is the data mean defined by (12.1). Back-substituting we can then write the log likelihood function in the form

$$\ln p(\mathbf{X}|\mathbf{W}, \boldsymbol{\mu}, \sigma^2) = -\frac{N}{2}\left\{D\ln(2\pi) + \ln|\mathbf{C}| + \mathrm{Tr}\left(\mathbf{C}^{-1}\mathbf{S}\right)\right\} \quad (12.44)$$

where $\mathbf{S}$ is the data covariance matrix defined by (12.3). Because the log likelihood is a quadratic function of $\boldsymbol{\mu}$, this solution represents the unique maximum, as can be confirmed by computing second derivatives.

Maximization with respect to $\mathbf{W}$ and σ^2 is more complex but nonetheless has an exact closed-form solution. It was shown by Tipping and Bishop (1999b) that all of the stationary points of the log likelihood function can be written as

$$\mathbf{W}_{\mathrm{ML}} = \mathbf{U}_M(\mathbf{L}_M - \sigma^2\mathbf{I})^{1/2}\mathbf{R} \quad (12.45)$$

where $\mathbf{U}_M$ is a $D \times M$ matrix whose columns are given by any subset (of size M) of the eigenvectors of the data covariance matrix $\mathbf{S}$, the $M \times M$ diagonal matrix $\mathbf{L}_M$ has elements given by the corresponding eigenvalues λ_i, and $\mathbf{R}$ is an arbitrary $M \times M$ orthogonal matrix.

Furthermore, Tipping and Bishop (1999b) showed that the *maximum* of the likelihood function is obtained when the M eigenvectors are chosen to be those whose eigenvalues are the M largest (all other solutions being saddle points). A similar result was conjectured independently by Roweis (1998), although no proof was given.

Again, we shall assume that the eigenvectors have been arranged in order of decreasing values of the corresponding eigenvalues, so that the M principal eigenvectors are $\mathbf{u}_1, \ldots, \mathbf{u}_M$. In this case, the columns of $\mathbf{W}$ define the principal subspace of standard PCA. The corresponding maximum likelihood solution for σ^2 is then given by

$$\sigma^2_{\mathrm{ML}} = \frac{1}{D-M} \sum_{i=M+1}^{D} \lambda_i \tag{12.46}$$

so that σ^2_{ML} is the average variance associated with the discarded dimensions.

Because $\mathbf{R}$ is orthogonal, it can be interpreted as a rotation matrix in the $M \times M$ latent space. If we substitute the solution for $\mathbf{W}$ into the expression for $\mathbf{C}$, and make use of the orthogonality property $\mathbf{R}\mathbf{R}^{\mathrm{T}} = \mathbf{I}$, we see that $\mathbf{C}$ is independent of $\mathbf{R}$. This simply says that the predictive density is unchanged by rotations in the latent space as discussed earlier. For the particular case of $\mathbf{R} = \mathbf{I}$, we see that the columns of $\mathbf{W}$ are the principal component eigenvectors scaled by the variance parameters $\lambda_i - \sigma^2$. The interpretation of these scaling factors is clear once we recognize that for a convolution of independent Gaussian distributions (in this case the latent space distribution and the noise model) the variances are additive. Thus the variance λ_i in the direction of an eigenvector $\mathbf{u}_i$ is composed of the sum of a contribution $\lambda_i - \sigma^2$ from the projection of the unit-variance latent space distribution into data space through the corresponding column of $\mathbf{W}$, plus an isotropic contribution of variance σ^2 which is added in all directions by the noise model.

It is worth taking a moment to study the form of the covariance matrix given by (12.36). Consider the variance of the predictive distribution along some direction specified by the unit vector $\mathbf{v}$, where $\mathbf{v}^{\mathrm{T}}\mathbf{v} = 1$, which is given by $\mathbf{v}^{\mathrm{T}}\mathbf{C}\mathbf{v}$. First suppose that $\mathbf{v}$ is orthogonal to the principal subspace, in other words it is given by some linear combination of the discarded eigenvectors. Then $\mathbf{v}^{\mathrm{T}}\mathbf{U} = \mathbf{0}$ and hence $\mathbf{v}^{\mathrm{T}}\mathbf{C}\mathbf{v} = \sigma^2$. Thus the model predicts a noise variance orthogonal to the principal subspace, which, from (12.46), is just the average of the discarded eigenvalues. Now suppose that $\mathbf{v} = \mathbf{u}_i$ where $\mathbf{u}_i$ is one of the retained eigenvectors defining the principal subspace. Then $\mathbf{v}^{\mathrm{T}}\mathbf{C}\mathbf{v} = (\lambda_i - \sigma^2) + \sigma^2 = \lambda_i$. In other words, this model correctly captures the variance of the data along the principal axes, and approximates the variance in all remaining directions with a single average value σ^2.

One way to construct the maximum likelihood density model would simply be to find the eigenvectors and eigenvalues of the data covariance matrix and then to evaluate $\mathbf{W}$ and σ^2 using the results given above. In this case, we would choose $\mathbf{R} = \mathbf{I}$ for convenience. However, if the maximum likelihood solution is found by numerical optimization of the likelihood function, for instance using an algorithm such as conjugate gradients (Fletcher, 1987; Nocedal and Wright, 1999; Bishop and Nabney, 2008) or through the EM algorithm, then the resulting value of $\mathbf{R}$ is essentially arbitrary. This implies that the columns of $\mathbf{W}$ need not be orthogonal. If an orthogonal basis is required, the matrix $\mathbf{W}$ can be post-processed appropriately (Golub and Van Loan, 1996). Alternatively, the EM algorithm can be modified in such a way as to yield orthonormal principal directions, sorted in descending order of the corresponding eigenvalues, directly (Ahn and Oh, 2003).

Section 12.2.2

The rotational invariance in latent space represents a form of statistical nonidentifiability, analogous to that encountered for mixture models in the case of discrete latent variables. Here there is a continuum of parameters all of which lead to the same predictive density, in contrast to the discrete nonidentifiability associated with component re-labelling in the mixture setting.

If we consider the case of $M = D$, so that there is no reduction of dimensionality, then $\mathbf{U}_M = \mathbf{U}$ and $\mathbf{L}_M = \mathbf{L}$. Making use of the orthogonality properties $\mathbf{U}\mathbf{U}^{\mathrm{T}} = \mathbf{I}$ and $\mathbf{R}\mathbf{R}^{\mathrm{T}} = \mathbf{I}$, we see that the covariance $\mathbf{C}$ of the marginal distribution for $\mathbf{x}$ becomes

$$\mathbf{C} = \mathbf{U}(\mathbf{L} - \sigma^2\mathbf{I})^{1/2}\mathbf{R}\mathbf{R}^{\mathrm{T}}(\mathbf{L} - \sigma^2\mathbf{I})^{1/2}\mathbf{U}^{\mathrm{T}} + \sigma^2\mathbf{I} = \mathbf{U}\mathbf{L}\mathbf{U}^{\mathrm{T}} = \mathbf{S} \tag{12.47}$$

and so we obtain the standard maximum likelihood solution for an unconstrained Gaussian distribution in which the covariance matrix is given by the sample covariance.

Conventional PCA is generally formulated as a projection of points from the D-dimensional data space onto an M-dimensional linear subspace. Probabilistic PCA, however, is most naturally expressed as a mapping from the latent space into the data space via (12.33). For applications such as visualization and data compression, we can reverse this mapping using Bayes' theorem. Any point $\mathbf{x}$ in data space can then be summarized by its posterior mean and covariance in latent space. From (12.42) the mean is given by

$$\mathbb{E}[\mathbf{z}|\mathbf{x}] = \mathbf{M}^{-1}\mathbf{W}_{\mathrm{ML}}^{\mathrm{T}}(\mathbf{x} - \overline{\mathbf{x}}) \tag{12.48}$$

where $\mathbf{M}$ is given by (12.41). This projects to a point in data space given by

$$\mathbf{W}\mathbb{E}[\mathbf{z}|\mathbf{x}] + \boldsymbol{\mu}. \tag{12.49}$$

Section 3.3.1 Note that this takes the same form as the equations for regularized linear regression and is a consequence of maximizing the likelihood function for a linear Gaussian model. Similarly, the posterior covariance is given from (12.42) by $\sigma^2\mathbf{M}^{-1}$ and is independent of $\mathbf{x}$.

If we take the limit $\sigma^2 \to 0$, then the posterior mean reduces to

$$(\mathbf{W}_{\mathrm{ML}}^{\mathrm{T}}\mathbf{W}_{\mathrm{ML}})^{-1}\mathbf{W}_{\mathrm{ML}}^{\mathrm{T}}(\mathbf{x} - \overline{\mathbf{x}}) \tag{12.50}$$

which represents an orthogonal projection of the data point onto the latent space, *Exercise 12.11* and so we recover the standard PCA model. The posterior covariance in this limit is zero, however, and the density becomes singular. For $\sigma^2 > 0$, the latent projection *Exercise 12.12* is shifted towards the origin, relative to the orthogonal projection.

Finally, we note that an important role for the probabilistic PCA model is in defining a multivariate Gaussian distribution in which the number of degrees of freedom, in other words the number of independent parameters, can be controlled whilst still allowing the model to capture the dominant correlations in the data. Recall that a general Gaussian distribution has $D(D+1)/2$ independent parameters in its *Section 2.3* covariance matrix (plus another D parameters in its mean). Thus the number of parameters scales quadratically with D and can become excessive in spaces of high

dimensionality. If we restrict the covariance matrix to be diagonal, then it has only D independent parameters, and so the number of parameters now grows linearly with dimensionality. However, it now treats the variables as if they were independent and hence can no longer express any correlations between them. Probabilistic PCA provides an elegant compromise in which the M most significant correlations can be captured while still ensuring that the total number of parameters grows only linearly with D. We can see this by evaluating the number of degrees of freedom in the PPCA model as follows. The covariance matrix $\mathbf{C}$ depends on the parameters $\mathbf{W}$, which has size $D \times M$, and σ^2, giving a total parameter count of $DM + 1$. However, we have seen that there is some redundancy in this parameterization associated with rotations of the coordinate system in the latent space. The orthogonal matrix $\mathbf{R}$ that expresses these rotations has size $M \times M$. In the first column of this matrix there are $M - 1$ independent parameters, because the column vector must be normalized to unit length. In the second column there are $M - 2$ independent parameters, because the column must be normalized and also must be orthogonal to the previous column, and so on. Summing this arithmetic series, we see that $\mathbf{R}$ has a total of $M(M-1)/2$ independent parameters. Thus the number of degrees of freedom in the covariance matrix $\mathbf{C}$ is given by

$$DM + 1 - M(M-1)/2. \tag{12.51}$$

The number of independent parameters in this model therefore only grows linearly with D, for fixed M. If we take $M = D - 1$, then we recover the standard result for a full covariance Gaussian. In this case, the variance along $D - 1$ linearly independent directions is controlled by the columns of $\mathbf{W}$, and the variance along the remaining direction is given by σ^2. If $M = 0$, the model is equivalent to the isotropic covariance case.

Exercise 12.14

12.2.2 EM algorithm for PCA

As we have seen, the probabilistic PCA model can be expressed in terms of a marginalization over a continuous latent space $\mathbf{z}$ in which for each data point $\mathbf{x}_n$, there is a corresponding latent variable $\mathbf{z}_n$. We can therefore make use of the EM algorithm to find maximum likelihood estimates of the model parameters. This may seem rather pointless because we have already obtained an exact closed-form solution for the maximum likelihood parameter values. However, in spaces of high dimensionality, there may be computational advantages in using an iterative EM procedure rather than working directly with the sample covariance matrix. This EM procedure can also be extended to the factor analysis model, for which there is no closed-form solution. Finally, it allows missing data to be handled in a principled way.

Section 12.2.4

We can derive the EM algorithm for probabilistic PCA by following the general framework for EM. Thus we write down the complete-data log likelihood and take its expectation with respect to the posterior distribution of the latent distribution evaluated using 'old' parameter values. Maximization of this expected complete-data log likelihood then yields the 'new' parameter values. Because the data points

Section 9.4

are assumed independent, the complete-data log likelihood function takes the form

$$\ln p\left(\mathbf{X}, \mathbf{Z}|\boldsymbol{\mu}, \mathbf{W}, \sigma^2\right) = \sum_{n=1}^{N} \{\ln p(\mathbf{x}_n|\mathbf{z}_n) + \ln p(\mathbf{z}_n)\} \tag{12.52}$$

where the n^{th} row of the matrix $\mathbf{Z}$ is given by $\mathbf{z}_n$. We already know that the exact maximum likelihood solution for $\boldsymbol{\mu}$ is given by the sample mean $\overline{\mathbf{x}}$ defined by (12.1), and it is convenient to substitute for $\boldsymbol{\mu}$ at this stage. Making use of the expressions (12.31) and (12.32) for the latent and conditional distributions, respectively, and taking the expectation with respect to the posterior distribution over the latent variables, we obtain

$$\begin{aligned}\mathbb{E}[\ln p\left(\mathbf{X}, \mathbf{Z}|\boldsymbol{\mu}, \mathbf{W}, \sigma^2\right)] = -\sum_{n=1}^{N} \Bigg\{ & \frac{D}{2}\ln(2\pi\sigma^2) + \frac{1}{2}\mathrm{Tr}\left(\mathbb{E}[\mathbf{z}_n\mathbf{z}_n^{\mathrm{T}}]\right) \\ & + \frac{1}{2\sigma^2}\|\mathbf{x}_n - \boldsymbol{\mu}\|^2 - \frac{1}{\sigma^2}\mathbb{E}[\mathbf{z}_n]^{\mathrm{T}}\mathbf{W}^{\mathrm{T}}(\mathbf{x}_n - \boldsymbol{\mu}) \\ & + \frac{1}{2\sigma^2}\mathrm{Tr}\left(\mathbb{E}[\mathbf{z}_n\mathbf{z}_n^{\mathrm{T}}]\mathbf{W}^{\mathrm{T}}\mathbf{W}\right)\Bigg\}. \end{aligned} \tag{12.53}$$

Note that this depends on the posterior distribution only through the sufficient statistics of the Gaussian. Thus in the E step, we use the old parameter values to evaluate

$$\mathbb{E}[\mathbf{z}_n] = \mathbf{M}^{-1}\mathbf{W}^{\mathrm{T}}(\mathbf{x}_n - \overline{\mathbf{x}}) \tag{12.54}$$

$$\mathbb{E}[\mathbf{z}_n\mathbf{z}_n^{\mathrm{T}}] = \sigma^2\mathbf{M}^{-1} + \mathbb{E}[\mathbf{z}_n]\mathbb{E}[\mathbf{z}_n]^{\mathrm{T}} \tag{12.55}$$

which follow directly from the posterior distribution (12.42) together with the standard result $\mathbb{E}[\mathbf{z}_n\mathbf{z}_n^{\mathrm{T}}] = \mathrm{cov}[\mathbf{z}_n] + \mathbb{E}[\mathbf{z}_n]\mathbb{E}[\mathbf{z}_n]^{\mathrm{T}}$. Here $\mathbf{M}$ is defined by (12.41).

In the M step, we maximize with respect to $\mathbf{W}$ and σ^2, keeping the posterior statistics fixed. Maximization with respect to σ^2 is straightforward. For the maximization with respect to $\mathbf{W}$ we make use of (C.24), and obtain the M-step equations

Exercise 12.15

$$\mathbf{W}_{\text{new}} = \left[\sum_{n=1}^{N}(\mathbf{x}_n - \overline{\mathbf{x}})\mathbb{E}[\mathbf{z}_n]^{\mathrm{T}}\right]\left[\sum_{n=1}^{N}\mathbb{E}[\mathbf{z}_n\mathbf{z}_n^{\mathrm{T}}]\right]^{-1} \tag{12.56}$$

$$\begin{aligned}\sigma^2_{\text{new}} = & \frac{1}{ND}\sum_{n=1}^{N}\left\{\|\mathbf{x}_n - \overline{\mathbf{x}}\|^2 - 2\mathbb{E}[\mathbf{z}_n]^{\mathrm{T}}\mathbf{W}_{\text{new}}^{\mathrm{T}}(\mathbf{x}_n - \overline{\mathbf{x}})\right. \\ & \left. + \mathrm{Tr}\left(\mathbb{E}[\mathbf{z}_n\mathbf{z}_n^{\mathrm{T}}]\mathbf{W}_{\text{new}}^{\mathrm{T}}\mathbf{W}_{\text{new}}\right)\right\}. \end{aligned} \tag{12.57}$$

The EM algorithm for probabilistic PCA proceeds by initializing the parameters and then alternately computing the sufficient statistics of the latent space posterior distribution using (12.54) and (12.55) in the E step and revising the parameter values using (12.56) and (12.57) in the M step.

One of the benefits of the EM algorithm for PCA is computational efficiency for large-scale applications (Roweis, 1998). Unlike conventional PCA based on an

eigenvector decomposition of the sample covariance matrix, the EM approach is iterative and so might appear to be less attractive. However, each cycle of the EM algorithm can be computationally much more efficient than conventional PCA in spaces of high dimensionality. To see this, we note that the eigendecomposition of the covariance matrix requires $O(D^3)$ computation. Often we are interested only in the first M eigenvectors and their corresponding eigenvalues, in which case we can use algorithms that are $O(MD^2)$. However, the evaluation of the covariance matrix itself takes $O(ND^2)$ computations, where N is the number of data points. Algorithms such as the snapshot method (Sirovich, 1987), which assume that the eigenvectors are linear combinations of the data vectors, avoid direct evaluation of the covariance matrix but are $O(N^3)$ and hence unsuited to large data sets. The EM algorithm described here also does not construct the covariance matrix explicitly. Instead, the most computationally demanding steps are those involving sums over the data set that are $O(NDM)$. For large D, and $M \ll D$, this can be a significant saving compared to $O(ND^2)$ and can offset the iterative nature of the EM algorithm.

Note that this EM algorithm can be implemented in an on-line form in which each D-dimensional data point is read in and processed and then discarded before the next data point is considered. To see this, note that the quantities evaluated in the E step (an M-dimensional vector and an $M \times M$ matrix) can be computed for each data point separately, and in the M step we need to accumulate sums over data points, which we can do incrementally. This approach can be advantageous if both N and D are large.

Because we now have a fully probabilistic model for PCA, we can deal with missing data, provided that it is missing at random, by marginalizing over the distribution of the unobserved variables. Again these missing values can be treated using the EM algorithm. We give an example of the use of this approach for data visualization in Figure 12.11.

Another elegant feature of the EM approach is that we can take the limit $\sigma^2 \to 0$, corresponding to standard PCA, and still obtain a valid EM-like algorithm (Roweis, 1998). From (12.55), we see that the only quantity we need to compute in the E step is $\mathbb{E}[\mathbf{z}_n]$. Furthermore, the M step is simplified because $\mathbf{M} = \mathbf{W}^{\mathrm{T}}\mathbf{W}$. To emphasize the simplicity of the algorithm, let us define $\widetilde{\mathbf{X}}$ to be a matrix of size $N \times D$ whose n^{th} row is given by the vector $\mathbf{x}_n - \overline{\mathbf{x}}$ and similarly define $\boldsymbol{\Omega}$ to be a matrix of size $D \times M$ whose n^{th} row is given by the vector $\mathbb{E}[\mathbf{z}_n]$. The E step (12.54) of the EM algorithm for PCA then becomes

$$\boldsymbol{\Omega} = (\mathbf{W}_{\mathrm{old}}^{\mathrm{T}}\mathbf{W}_{\mathrm{old}})^{-1}\mathbf{W}_{\mathrm{old}}^{\mathrm{T}}\widetilde{\mathbf{X}} \tag{12.58}$$

and the M step (12.56) takes the form

$$\mathbf{W}_{\mathrm{new}} = \widetilde{\mathbf{X}}^{\mathrm{T}}\boldsymbol{\Omega}^{\mathrm{T}}(\boldsymbol{\Omega}\boldsymbol{\Omega}^{\mathrm{T}})^{-1}. \tag{12.59}$$

Again these can be implemented in an on-line form. These equations have a simple interpretation as follows. From our earlier discussion, we see that the E step involves an orthogonal projection of the data points onto the current estimate for the principal subspace. Correspondingly, the M step represents a re-estimation of the principal

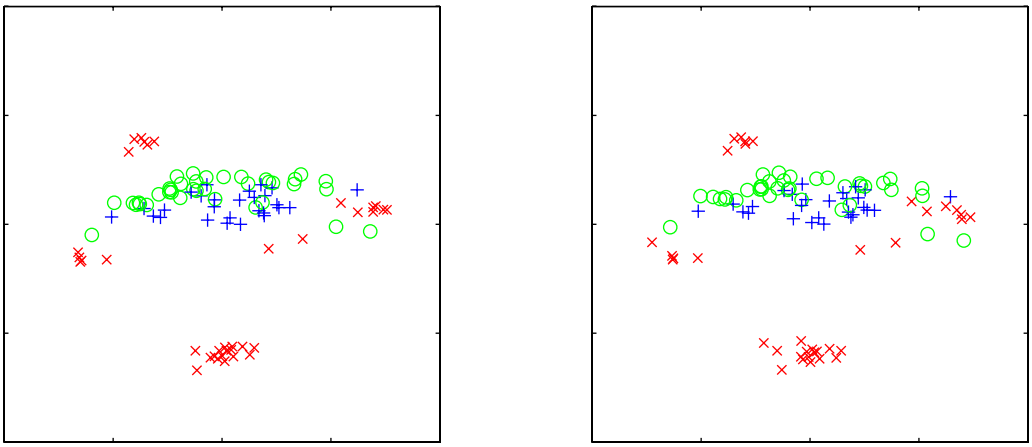

Figure 12.11 Probabilistic PCA visualization of a portion of the oil flow data set for the first 100 data points. The left-hand plot shows the posterior mean projections of the data points on the principal subspace. The right-hand plot is obtained by first randomly omitting 30% of the variable values and then using EM to handle the missing values. Note that each data point then has at least one missing measurement but that the plot is very similar to the one obtained without missing values.

Exercise 12.17

subspace to minimize the squared reconstruction error in which the projections are fixed.

We can give a simple physical analogy for this EM algorithm, which is easily visualized for $D = 2$ and $M = 1$. Consider a collection of data points in two dimensions, and let the one-dimensional principal subspace be represented by a solid rod. Now attach each data point to the rod via a spring obeying Hooke's law (stored energy is proportional to the square of the spring's length). In the E step, we keep the rod fixed and allow the attachment points to slide up and down the rod so as to minimize the energy. This causes each attachment point (independently) to position itself at the orthogonal projection of the corresponding data point onto the rod. In the M step, we keep the attachment points fixed and then release the rod and allow it to move to the minimum energy position. The E and M steps are then repeated until a suitable convergence criterion is satisfied, as is illustrated in Figure 12.12.

12.2.3 Bayesian PCA

So far in our discussion of PCA, we have assumed that the value M for the dimensionality of the principal subspace is given. In practice, we must choose a suitable value according to the application. For visualization, we generally choose $M = 2$, whereas for other applications the appropriate choice for M may be less clear. One approach is to plot the eigenvalue spectrum for the data set, analogous to the example in Figure 12.4 for the off-line digits data set, and look to see if the eigenvalues naturally form two groups comprising a set of small values separated by a significant gap from a set of relatively large values, indicating a natural choice for M. In practice, such a gap is often not seen.

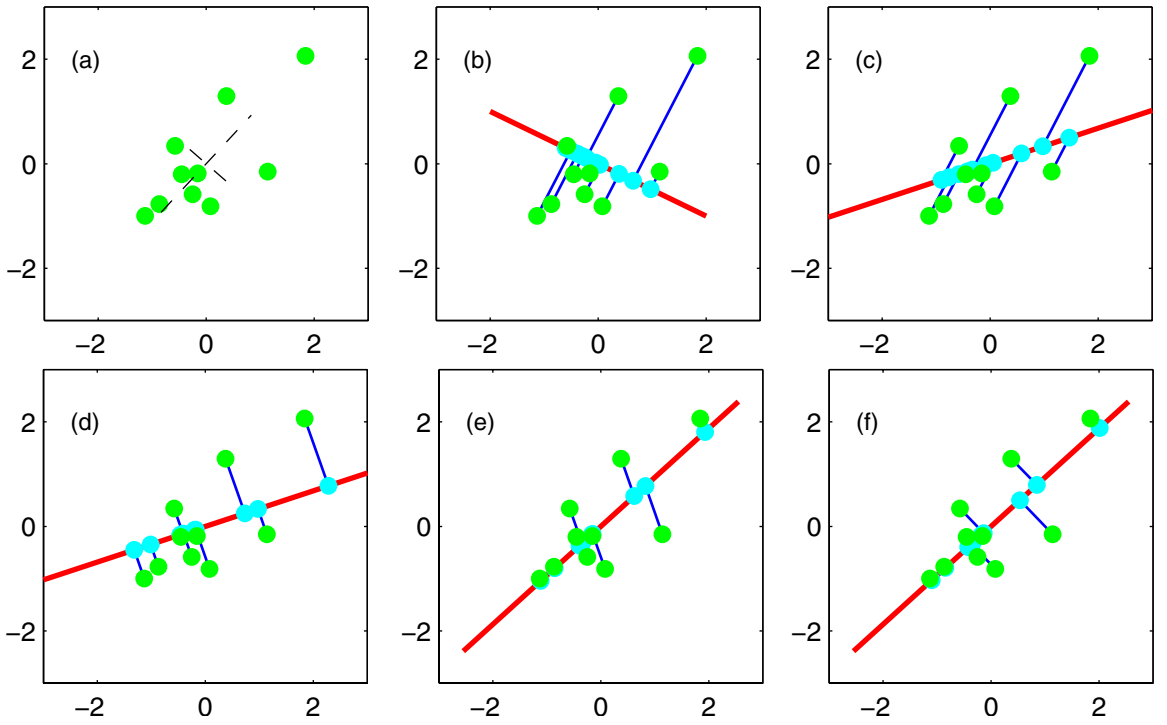

Figure 12.12 Synthetic data illustrating the EM algorithm for PCA defined by (12.58) and (12.59). (a) A data set $\mathbf{X}$ with the data points shown in green, together with the true principal components (shown as eigenvectors scaled by the square roots of the eigenvalues). (b) Initial configuration of the principal subspace defined by $\mathbf{W}$, shown in red, together with the projections of the latent points $\mathbf{Z}$ into the data space, given by $\mathbf{Z}\mathbf{W}^{\mathrm{T}}$, shown in cyan. (c) After one M step, the latent space has been updated with $\mathbf{Z}$ held fixed. (d) After the successive E step, the values of $\mathbf{Z}$ have been updated, giving orthogonal projections, with $\mathbf{W}$ held fixed. (e) After the second M step. (f) After the second E step.

Section 1.3

Because the probabilistic PCA model has a well-defined likelihood function, we could employ cross-validation to determine the value of dimensionality by selecting the largest log likelihood on a validation data set. Such an approach, however, can become computationally costly, particularly if we consider a probabilistic mixture of PCA models (Tipping and Bishop, 1999a) in which we seek to determine the appropriate dimensionality separately for each component in the mixture.

Given that we have a probabilistic formulation of PCA, it seems natural to seek a Bayesian approach to model selection. To do this, we need to marginalize out the model parameters $\boldsymbol{\mu}$, $\mathbf{W}$, and σ^2 with respect to appropriate prior distributions. This can be done by using a variational framework to approximate the analytically intractable marginalizations (Bishop, 1999b). The marginal likelihood values, given by the variational lower bound, can then be compared for a range of different values of M and the value giving the largest marginal likelihood selected.

Here we consider a simpler approach introduced by based on the *evidence ap-*

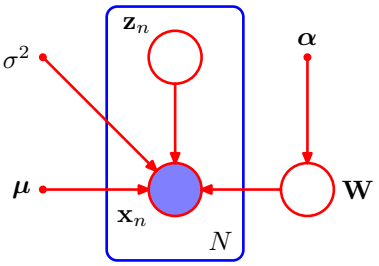

Figure 12.13 Probabilistic graphical model for Bayesian PCA in which the distribution over the parameter matrix $\mathbf{W}$ is governed by a vector $\boldsymbol{\alpha}$ of hyperparameters.

proximation, which is appropriate when the number of data points is relatively large and the corresponding posterior distribution is tightly peaked (Bishop, 1999a). It involves a specific choice of prior over $\mathbf{W}$ that allows surplus dimensions in the principal subspace to be pruned out of the model. This corresponds to an example of *automatic relevance determination*, or *ARD*, discussed in Section 7.2.2. Specifically, we define an independent Gaussian prior over each column of $\mathbf{W}$, which represent the vectors defining the principal subspace. Each such Gaussian has an independent variance governed by a precision hyperparameter α_i so that

$$p(\mathbf{W}|\boldsymbol{\alpha}) = \prod_{i=1}^{M} \left(\frac{\alpha_i}{2\pi}\right)^{D/2} \exp\left\{-\frac{1}{2}\alpha_i \mathbf{w}_i^{\mathrm{T}}\mathbf{w}_i\right\} \tag{12.60}$$

where $\mathbf{w}_i$ is the i^{th} column of $\mathbf{W}$. The resulting model can be represented using the directed graph shown in Figure 12.13.

The values for α_i will be found iteratively by maximizing the marginal likelihood function in which $\mathbf{W}$ has been integrated out. As a result of this optimization, some of the α_i may be driven to infinity, with the corresponding parameters vector $\mathbf{w}_i$ being driven to zero (the posterior distribution becomes a delta function at the origin) giving a sparse solution. The effective dimensionality of the principal subspace is then determined by the number of finite α_i values, and the corresponding vectors $\mathbf{w}_i$ can be thought of as 'relevant' for modelling the data distribution. In this way, the Bayesian approach is automatically making the trade-off between improving the fit to the data, by using a larger number of vectors $\mathbf{w}_i$ with their corresponding eigenvalues λ_i each tuned to the data, and reducing the complexity of the model by suppressing some of the $\mathbf{w}_i$ vectors. The origins of this sparsity were discussed earlier in the context of relevance vector machines.

Section 7.2

The values of α_i are re-estimated during training by maximizing the log marginal likelihood given by

$$p(\mathbf{X}|\boldsymbol{\alpha}, \boldsymbol{\mu}, \sigma^2) = \int p(\mathbf{X}|\mathbf{W}, \boldsymbol{\mu}, \sigma^2) p(\mathbf{W}|\boldsymbol{\alpha})\, \mathrm{d}\mathbf{W} \tag{12.61}$$

where the log of $p(\mathbf{X}|\mathbf{W}, \boldsymbol{\mu}, \sigma^2)$ is given by (12.43). Note that for simplicity we also treat $\boldsymbol{\mu}$ and σ^2 as parameters to be estimated, rather than defining priors over these parameters.

Section 4.4

Section 3.5.3

Because this integration is intractable, we make use of the Laplace approximation. If we assume that the posterior distribution is sharply peaked, as will occur for sufficiently large data sets, then the re-estimation equations obtained by maximizing the marginal likelihood with respect to α_i take the simple form

$$\alpha_i^{\text{new}} = \frac{D}{\mathbf{w}_i^{\mathrm{T}}\mathbf{w}_i} \tag{12.62}$$

which follows from (3.98), noting that the dimensionality of $\mathbf{w}_i$ is D. These re-estimations are interleaved with the EM algorithm updates for determining $\mathbf{W}$ and σ^2. The E-step equations are again given by (12.54) and (12.55). Similarly, the M-step equation for σ^2 is again given by (12.57). The only change is to the M-step equation for $\mathbf{W}$, which is modified to give

$$\mathbf{W}_{\text{new}} = \left[\sum_{n=1}^{N}(\mathbf{x}_n - \overline{\mathbf{x}})\mathbb{E}[\mathbf{z}_n]^{\mathrm{T}}\right]\left[\sum_{n=1}^{N}\mathbb{E}[\mathbf{z}_n\mathbf{z}_n^{\mathrm{T}}] + \sigma^2\mathbf{A}\right]^{-1} \tag{12.63}$$

where $\mathbf{A} = \text{diag}(\alpha_i)$. The value of $\boldsymbol{\mu}$ is given by the sample mean, as before.

If we choose $M = D - 1$ then, if all α_i values are finite, the model represents a full-covariance Gaussian, while if all the α_i go to infinity the model is equivalent to an isotropic Gaussian, and so the model can encompass all permissible values for the effective dimensionality of the principal subspace. It is also possible to consider smaller values of M, which will save on computational cost but which will limit the maximum dimensionality of the subspace. A comparison of the results of this algorithm with standard probabilistic PCA is shown in Figure 12.14.

Bayesian PCA provides an opportunity to illustrate the Gibbs sampling algorithm discussed in Section 11.3. Figure 12.15 shows an example of the samples from the hyperparameters $\ln \alpha_i$ for a data set in $D = 4$ dimensions in which the dimensionality of the latent space is $M = 3$ but in which the data set is generated from a probabilistic PCA model having one direction of high variance, with the remaining directions comprising low variance noise. This result shows clearly the presence of three distinct modes in the posterior distribution. At each step of the iteration, one of the hyperparameters has a small value and the remaining two have large values, so that two of the three latent variables are suppressed. During the course of the Gibbs sampling, the solution makes sharp transitions between the three modes.

The model described here involves a prior only over the matrix $\mathbf{W}$. A fully Bayesian treatment of PCA, including priors over $\boldsymbol{\mu}$, σ^2, and $\boldsymbol{\alpha}$, and solved using variational methods, is described in Bishop (1999b). For a discussion of various Bayesian approaches to determining the appropriate dimensionality for a PCA model, see Minka (2001c).

12.2.4 Factor analysis

Factor analysis is a linear-Gaussian latent variable model that is closely related to probabilistic PCA. Its definition differs from that of probabilistic PCA only in that the conditional distribution of the observed variable $\mathbf{x}$ given the latent variable $\mathbf{z}$ is

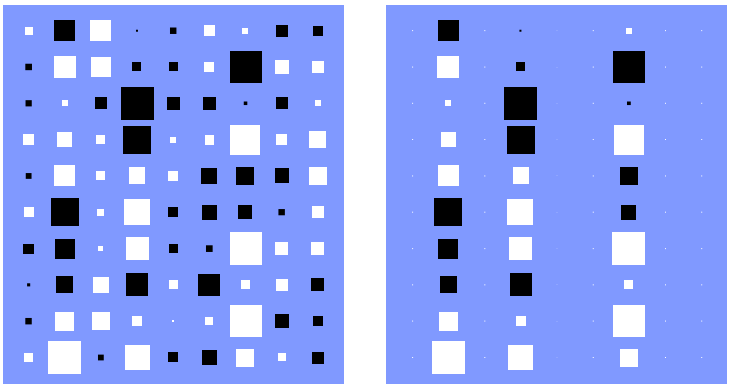

Figure 12.14 'Hinton' diagrams of the matrix $\mathbf{W}$ in which each element of the matrix is depicted as a square (white for positive and black for negative values) whose area is proportional to the magnitude of that element. The synthetic data set comprises 300 data points in $D = 10$ dimensions sampled from a Gaussian distribution having standard deviation 1.0 in 3 directions and standard deviation 0.5 in the remaining 7 directions for a data set in $D = 10$ dimensions having $M = 3$ directions with larger variance than the remaining 7 directions. The left-hand plot shows the result from maximum likelihood probabilistic PCA, and the left-hand plot shows the corresponding result from Bayesian PCA. We see how the Bayesian model is able to discover the appropriate dimensionality by suppressing the 6 surplus degrees of freedom.

taken to have a diagonal rather than an isotropic covariance so that

$$p(\mathbf{x}|\mathbf{z}) = \mathcal{N}(\mathbf{x}|\mathbf{W}\mathbf{z} + \boldsymbol{\mu}, \boldsymbol{\Psi}) \tag{12.64}$$

where $\boldsymbol{\Psi}$ is a $D \times D$ diagonal matrix. Note that the factor analysis model, in common with probabilistic PCA, assumes that the observed variables $x_1, \ldots, x_D$ are independent, given the latent variable $\mathbf{z}$. In essence, the factor analysis model is explaining the observed covariance structure of the data by representing the independent variance associated with each coordinate in the matrix $\boldsymbol{\Psi}$ and capturing the covariance between variables in the matrix $\mathbf{W}$. In the factor analysis literature, the columns of $\mathbf{W}$, which capture the correlations between observed variables, are called *factor loadings*, and the diagonal elements of $\boldsymbol{\Psi}$, which represent the independent noise variances for each of the variables, are called *uniquenesses*.

The origins of factor analysis are as old as those of PCA, and discussions of factor analysis can be found in the books by Everitt (1984), Bartholomew (1987), and Basilevsky (1994). Links between factor analysis and PCA were investigated by Lawley (1953) and Anderson (1963) who showed that at stationary points of the likelihood function, for a factor analysis model with $\boldsymbol{\Psi} = \sigma^2\mathbf{I}$, the columns of $\mathbf{W}$ are scaled eigenvectors of the sample covariance matrix, and σ^2 is the average of the discarded eigenvalues. Later, Tipping and Bishop (1999b) showed that the maximum of the log likelihood function occurs when the eigenvectors comprising $\mathbf{W}$ are chosen to be the principal eigenvectors.

Making use of (2.115), we see that the marginal distribution for the observed

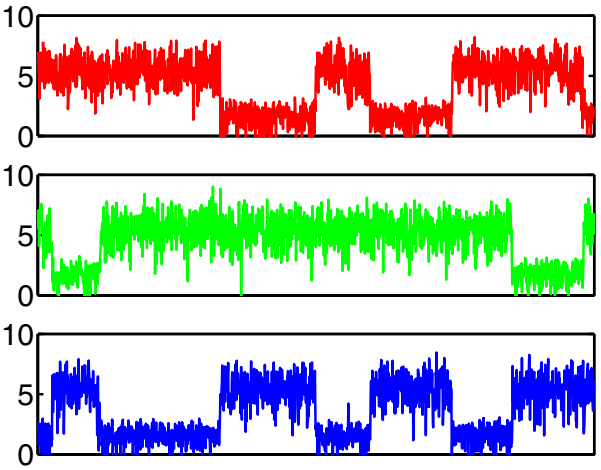

Figure 12.15 Gibbs sampling for Bayesian PCA showing plots of $\ln \alpha_i$ versus iteration number for three α values, showing transitions between the three modes of the posterior distribution.

variable is given by $p(\mathbf{x}) = \mathcal{N}(\mathbf{x}|\boldsymbol{\mu}, \mathbf{C})$ where now

$$\mathbf{C} = \mathbf{W}\mathbf{W}^{\mathrm{T}} + \boldsymbol{\Psi}. \tag{12.65}$$

Exercise 12.19

As with probabilistic PCA, this model is invariant to rotations in the latent space.

Historically, factor analysis has been the subject of controversy when attempts have been made to place an interpretation on the individual factors (the coordinates in $\mathbf{z}$-space), which has proven problematic due to the nonidentifiability of factor analysis associated with rotations in this space. From our perspective, however, we shall view factor analysis as a form of latent variable density model, in which the form of the latent space is of interest but not the particular choice of coordinates used to describe it. If we wish to remove the degeneracy associated with latent space rotations, we must consider non-Gaussian latent variable distributions, giving rise to

Section 12.4

independent component analysis (ICA) models.

We can determine the parameters $\boldsymbol{\mu}$, $\mathbf{W}$, and $\boldsymbol{\Psi}$ in the factor analysis model by maximum likelihood. The solution for $\boldsymbol{\mu}$ is again given by the sample mean. However, unlike probabilistic PCA, there is no longer a closed-form maximum likelihood solution for $\mathbf{W}$, which must therefore be found iteratively. Because factor analysis is

Exercise 12.21

a latent variable model, this can be done using an EM algorithm (Rubin and Thayer, 1982) that is analogous to the one used for probabilistic PCA. Specifically, the E-step equations are given by

$$\mathbb{E}[\mathbf{z}_n] = \mathbf{G}\mathbf{W}^{\mathrm{T}}\boldsymbol{\Psi}^{-1}(\mathbf{x}_n - \overline{\mathbf{x}}) \tag{12.66}$$

$$\mathbb{E}[\mathbf{z}_n\mathbf{z}_n^{\mathrm{T}}] = \mathbf{G} + \mathbb{E}[\mathbf{z}_n]\mathbb{E}[\mathbf{z}_n]^{\mathrm{T}} \tag{12.67}$$

where we have defined

$$\mathbf{G} = (\mathbf{I} + \mathbf{W}^{\mathrm{T}}\boldsymbol{\Psi}^{-1}\mathbf{W})^{-1}. \tag{12.68}$$

Note that this is expressed in a form that involves inversion of matrices of size $M \times M$ rather than $D \times D$ (except for the $D \times D$ diagonal matrix $\boldsymbol{\Psi}$ whose inverse is trivial

to compute in $O(D)$ steps), which is convenient because often $M \ll D$. Similarly, the M-step equations take the form

Exercise 12.22

$$\mathbf{W}^{\text{new}} = \left[\sum_{n=1}^{N}(\mathbf{x}_n - \overline{\mathbf{x}})\mathbb{E}[\mathbf{z}_n]^{\mathrm{T}}\right]\left[\sum_{n=1}^{N}\mathbb{E}[\mathbf{z}_n\mathbf{z}_n^{\mathrm{T}}]\right]^{-1} \tag{12.69}$$

$$\mathbf{\Psi}^{\text{new}} = \text{diag}\left\{\mathbf{S} - \mathbf{W}_{\text{new}}\frac{1}{N}\sum_{n=1}^{N}\mathbb{E}[\mathbf{z}_n](\mathbf{x}_n - \overline{\mathbf{x}})^{\mathrm{T}}\right\} \tag{12.70}$$

where the 'diag' operator sets all of the nondiagonal elements of a matrix to zero. A Bayesian treatment of the factor analysis model can be obtained by a straightforward application of the techniques discussed in this book.

Exercise 12.25

Another difference between probabilistic PCA and factor analysis concerns their different behaviour under transformations of the data set. For PCA and probabilistic PCA, if we rotate the coordinate system in data space, then we obtain exactly the same fit to the data but with the $\mathbf{W}$ matrix transformed by the corresponding rotation matrix. However, for factor analysis, the analogous property is that if we make a component-wise re-scaling of the data vectors, then this is absorbed into a corresponding re-scaling of the elements of $\mathbf{\Psi}$.

12.3. Kernel PCA

In Chapter 6, we saw how the technique of kernel substitution allows us to take an algorithm expressed in terms of scalar products of the form $\mathbf{x}^{\mathrm{T}}\mathbf{x}'$ and generalize that algorithm by replacing the scalar products with a nonlinear kernel. Here we apply this technique of kernel substitution to principal component analysis, thereby obtaining a nonlinear generalization called *kernel PCA* (Schölkopf *et al.*, 1998).

Consider a data set $\{\mathbf{x}_n\}$ of observations, where $n = 1, \ldots, N$, in a space of dimensionality D. In order to keep the notation uncluttered, we shall assume that we have already subtracted the sample mean from each of the vectors $\mathbf{x}_n$, so that $\sum_n \mathbf{x}_n = \mathbf{0}$. The first step is to express conventional PCA in such a form that the data vectors $\{\mathbf{x}_n\}$ appear only in the form of the scalar products $\mathbf{x}_n^{\mathrm{T}}\mathbf{x}_m$. Recall that the principal components are defined by the eigenvectors $\mathbf{u}_i$ of the covariance matrix

$$\mathbf{S}\mathbf{u}_i = \lambda_i\mathbf{u}_i \tag{12.71}$$

where $i = 1, \ldots, D$. Here the $D \times D$ sample covariance matrix $\mathbf{S}$ is defined by

$$\mathbf{S} = \frac{1}{N}\sum_{n=1}^{N}\mathbf{x}_n\mathbf{x}_n^{\mathrm{T}}, \tag{12.72}$$

and the eigenvectors are normalized such that $\mathbf{u}_i^{\mathrm{T}}\mathbf{u}_i = 1$.

Now consider a nonlinear transformation $\boldsymbol{\phi}(\mathbf{x})$ into an M-dimensional feature space, so that each data point $\mathbf{x}_n$ is thereby projected onto a point $\boldsymbol{\phi}(\mathbf{x}_n)$. We can

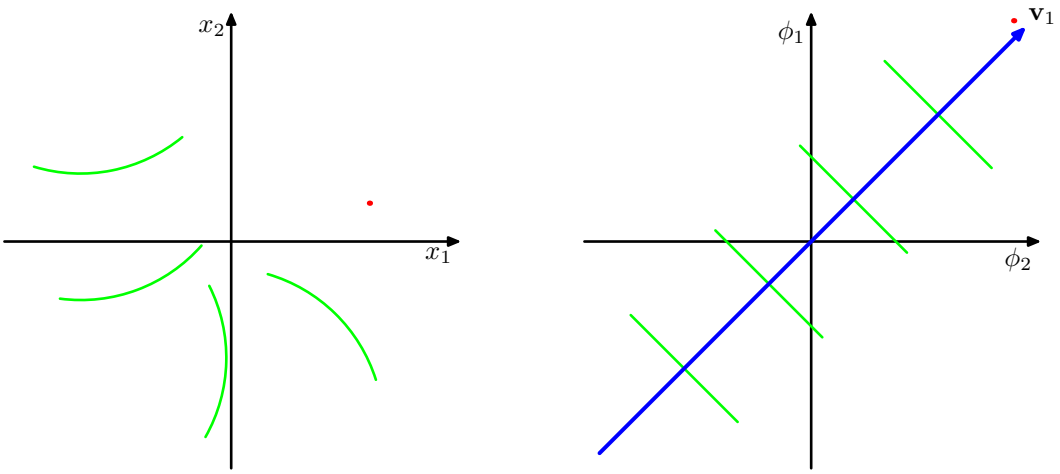

Figure 12.16 Schematic illustration of kernel PCA. A data set in the original data space (left-hand plot) is projected by a nonlinear transformation $\phi(\mathbf{x})$ into a feature space (right-hand plot). By performing PCA in the feature space, we obtain the principal components, of which the first is shown in blue and is denoted by the vector $\mathbf{v}_1$. The green lines in feature space indicate the linear projections onto the first principal component, which correspond to nonlinear projections in the original data space. Note that in general it is not possible to represent the nonlinear principal component by a vector in $\mathbf{x}$ space.

now perform standard PCA in the feature space, which implicitly defines a nonlinear principal component model in the original data space, as illustrated in Figure 12.16.

For the moment, let us assume that the projected data set also has zero mean, so that $\sum_n \boldsymbol{\phi}(\mathbf{x}_n) = \mathbf{0}$. We shall return to this point shortly. The $M \times M$ sample covariance matrix in feature space is given by

$$\mathbf{C} = \frac{1}{N}\sum_{n=1}^{N} \boldsymbol{\phi}(\mathbf{x}_n)\boldsymbol{\phi}(\mathbf{x}_n)^{\mathrm{T}} \tag{12.73}$$

and its eigenvector expansion is defined by

$$\mathbf{C}\mathbf{v}_i = \lambda_i \mathbf{v}_i \tag{12.74}$$

$i = 1, \ldots, M$. Our goal is to solve this eigenvalue problem without having to work explicitly in the feature space. From the definition of $\mathbf{C}$, the eigenvector equations tells us that $\mathbf{v}_i$ satisfies

$$\frac{1}{N}\sum_{n=1}^{N} \boldsymbol{\phi}(\mathbf{x}_n)\left\{\boldsymbol{\phi}(\mathbf{x}_n)^{\mathrm{T}}\mathbf{v}_i\right\} = \lambda_i \mathbf{v}_i \tag{12.75}$$

and so we see that (provided $\lambda_i > 0$) the vector $\mathbf{v}_i$ is given by a linear combination of the $\boldsymbol{\phi}(\mathbf{x}_n)$ and so can be written in the form

$$\mathbf{v}_i = \sum_{n=1}^{N} a_{in}\boldsymbol{\phi}(\mathbf{x}_n). \tag{12.76}$$

Substituting this expansion back into the eigenvector equation, we obtain

$$\frac{1}{N}\sum_{n=1}^{N}\boldsymbol{\phi}(\mathbf{x}_n)\boldsymbol{\phi}(\mathbf{x}_n)^{\mathrm{T}}\sum_{m=1}^{N}a_{im}\boldsymbol{\phi}(\mathbf{x}_m)=\lambda_i\sum_{n=1}^{N}a_{in}\boldsymbol{\phi}(\mathbf{x}_n). \tag{12.77}$$

The key step is now to express this in terms of the kernel function $k(\mathbf{x}_n,\mathbf{x}_m)=\boldsymbol{\phi}(\mathbf{x}_n)^{\mathrm{T}}\boldsymbol{\phi}(\mathbf{x}_m)$, which we do by multiplying both sides by $\boldsymbol{\phi}(\mathbf{x}_l)^{\mathrm{T}}$ to give

$$\frac{1}{N}\sum_{n=1}^{N}k(\mathbf{x}_l,\mathbf{x}_n)\sum_{m=1}^{m}a_{im}k(\mathbf{x}_n,\mathbf{x}_m)=\lambda_i\sum_{n=1}^{N}a_{in}k(\mathbf{x}_l,\mathbf{x}_n). \tag{12.78}$$

This can be written in matrix notation as

$$\mathbf{K}^2\mathbf{a}_i=\lambda_i N\mathbf{K}\mathbf{a}_i \tag{12.79}$$

where $\mathbf{a}_i$ is an N-dimensional column vector with elements a_{ni} for $n=1,\ldots,N$. We can find solutions for $\mathbf{a}_i$ by solving the following eigenvalue problem

$$\mathbf{K}\mathbf{a}_i=\lambda_i N\mathbf{a}_i \tag{12.80}$$

in which we have removed a factor of $\mathbf{K}$ from both sides of (12.79). Note that the solutions of (12.79) and (12.80) differ only by eigenvectors of $\mathbf{K}$ having zero eigenvalues that do not affect the principal components projection.

Exercise 12.26

The normalization condition for the coefficients $\mathbf{a}_i$ is obtained by requiring that the eigenvectors in feature space be normalized. Using (12.76) and (12.80), we have

$$1=\mathbf{v}_i^{\mathrm{T}}\mathbf{v}_i=\sum_{n=1}^{N}\sum_{m=1}^{N}a_{in}a_{im}\boldsymbol{\phi}(\mathbf{x}_n)^{\mathrm{T}}\boldsymbol{\phi}(\mathbf{x}_m)=\mathbf{a}_i^{\mathrm{T}}\mathbf{K}\mathbf{a}_i=\lambda_i N\mathbf{a}_i^{\mathrm{T}}\mathbf{a}_i. \tag{12.81}$$

Having solved the eigenvector problem, the resulting principal component projections can then also be cast in terms of the kernel function so that, using (12.76), the projection of a point $\mathbf{x}$ onto eigenvector i is given by

$$y_i(\mathbf{x})=\boldsymbol{\phi}(\mathbf{x})^{\mathrm{T}}\mathbf{v}_i=\sum_{n=1}^{N}a_{in}\boldsymbol{\phi}(\mathbf{x})^{\mathrm{T}}\boldsymbol{\phi}(\mathbf{x}_n)=\sum_{n=1}^{N}a_{in}k(\mathbf{x},\mathbf{x}_n) \tag{12.82}$$

and so again is expressed in terms of the kernel function.

In the original D-dimensional $\mathbf{x}$ space there are D orthogonal eigenvectors and hence we can find at most D linear principal components. The dimensionality M of the feature space, however, can be much larger than D (even infinite), and thus we can find a number of nonlinear principal components that can exceed D. Note, however, that the number of nonzero eigenvalues cannot exceed the number N of data points, because (even if $M>N$) the covariance matrix in feature space has rank at most equal to N. This is reflected in the fact that kernel PCA involves the eigenvector expansion of the $N\times N$ matrix $\mathbf{K}$.

So far we have assumed that the projected data set given by $\phi(\mathbf{x}_n)$ has zero mean, which in general will not be the case. We cannot simply compute and then subtract off the mean, since we wish to avoid working directly in feature space, and so again, we formulate the algorithm purely in terms of the kernel function. The projected data points after centralizing, denoted $\widetilde{\phi}(\mathbf{x}_n)$, are given by

$$\widetilde{\phi}(\mathbf{x}_n) = \phi(\mathbf{x}_n) - \frac{1}{N}\sum_{l=1}^{N}\phi(\mathbf{x}_l) \tag{12.83}$$

and the corresponding elements of the Gram matrix are given by

$$\begin{aligned}
\widetilde{K}_{nm} &= \widetilde{\phi}(\mathbf{x}_n)^{\mathrm{T}}\widetilde{\phi}(\mathbf{x}_m) \\
&= \phi(\mathbf{x}_n)^{\mathrm{T}}\phi(\mathbf{x}_m) - \frac{1}{N}\sum_{l=1}^{N}\phi(\mathbf{x}_n)^{\mathrm{T}}\phi(\mathbf{x}_l) \\
&\quad -\frac{1}{N}\sum_{l=1}^{N}\phi(\mathbf{x}_l)^{\mathrm{T}}\phi(\mathbf{x}_m) + \frac{1}{N^2}\sum_{j=1}^{N}\sum_{l=1}^{N}\phi(\mathbf{x}_j)^{\mathrm{T}}\phi(\mathbf{x}_l) \\
&= k(\mathbf{x}_n,\mathbf{x}_m) - \frac{1}{N}\sum_{l=1}^{N}k(\mathbf{x}_l,\mathbf{x}_m) \\
&\quad -\frac{1}{N}\sum_{l=1}^{N}k(\mathbf{x}_n,\mathbf{x}_l) + \frac{1}{N^2}\sum_{j=1}^{N}\sum_{l=1}^{N}k(\mathbf{x}_j,\mathbf{x}_l).
\end{aligned} \tag{12.84}$$

This can be expressed in matrix notation as

$$\widetilde{\mathbf{K}} = \mathbf{K} - \mathbf{1}_N\mathbf{K} - \mathbf{K}\mathbf{1}_N + \mathbf{1}_N\mathbf{K}\mathbf{1}_N \tag{12.85}$$

where $\mathbf{1}_N$ denotes the $N \times N$ matrix in which every element takes the value $1/N$. Thus we can evaluate $\widetilde{\mathbf{K}}$ using only the kernel function and then use $\widetilde{\mathbf{K}}$ to determine the eigenvalues and eigenvectors. Note that the standard PCA algorithm is recovered as a special case if we use a linear kernel $k(\mathbf{x},\mathbf{x}') = \mathbf{x}^{\mathrm{T}}\mathbf{x}'$. Figure 12.17 shows an example of kernel PCA applied to a synthetic data set (Schölkopf *et al.*, 1998). Here a 'Gaussian' kernel of the form

Exercise 12.27

$$k(\mathbf{x},\mathbf{x}') = \exp(-\|\mathbf{x}-\mathbf{x}'\|^2/0.1) \tag{12.86}$$

is applied to a synthetic data set. The lines correspond to contours along which the projection onto the corresponding principal component, defined by

$$\phi(\mathbf{x})^{\mathrm{T}}\mathbf{v}_i = \sum_{n=1}^{N}a_{in}k(\mathbf{x},\mathbf{x}_n) \tag{12.87}$$

is constant.

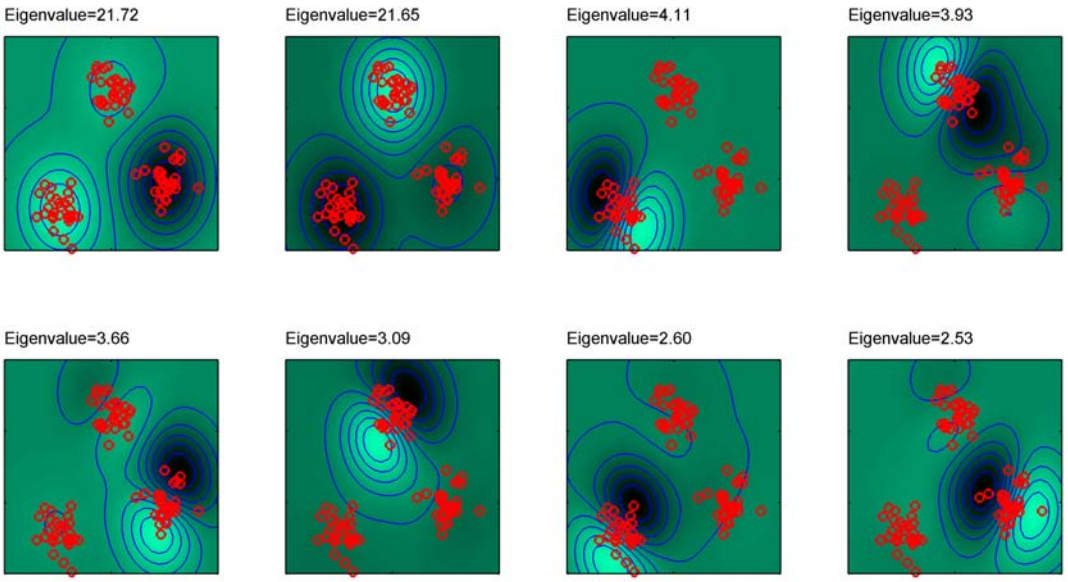

Figure 12.17 Example of kernel PCA, with a Gaussian kernel applied to a synthetic data set in two dimensions, showing the first eight eigenfunctions along with their eigenvalues. The contours are lines along which the projection onto the corresponding principal component is constant. Note how the first two eigenvectors separate the three clusters, the next three eigenvectors split each of the cluster into halves, and the following three eigenvectors again split the clusters into halves along directions orthogonal to the previous splits.

One obvious disadvantage of kernel PCA is that it involves finding the eigenvectors of the $N \times N$ matrix $\widetilde{\mathbf{K}}$ rather than the $D \times D$ matrix $\mathbf{S}$ of conventional linear PCA, and so in practice for large data sets approximations are often used.

Finally, we note that in standard linear PCA, we often retain some reduced number $L < D$ of eigenvectors and then approximate a data vector $\mathbf{x}_n$ by its projection $\widehat{\mathbf{x}}_n$ onto the L-dimensional principal subspace, defined by

$$\widehat{\mathbf{x}}_n = \sum_{i=1}^{L} \left(\mathbf{x}_n^{\mathrm{T}} \mathbf{u}_i\right) \mathbf{u}_i. \tag{12.88}$$

In kernel PCA, this will in general not be possible. To see this, note that the mapping $\boldsymbol{\phi}(\mathbf{x})$ maps the D-dimensional $\mathbf{x}$ space into a D-dimensional *manifold* in the M-dimensional feature space $\boldsymbol{\phi}$. The vector $\mathbf{x}$ is known as the *pre-image* of the corresponding point $\boldsymbol{\phi}(\mathbf{x})$. However, the projection of points in feature space onto the linear PCA subspace in that space will typically not lie on the nonlinear D-dimensional manifold and so will not have a corresponding pre-image in data space. Techniques have therefore been proposed for finding approximate pre-images (Bakir *et al.*, 2004).

12.4. Nonlinear Latent Variable Models

In this chapter, we have focussed on the simplest class of models having continuous latent variables, namely those based on linear-Gaussian distributions. As well as having great practical importance, these models are relatively easy to analyse and to fit to data and can also be used as components in more complex models. Here we consider briefly some generalizations of this framework to models that are either nonlinear or non-Gaussian, or both.

In fact, the issues of nonlinearity and non-Gaussianity are related because a general probability density can be obtained from a simple fixed reference density, such as a Gaussian, by making a nonlinear change of variables. This idea forms the basis of several practical latent variable models as we shall see shortly.

Exercise 12.28

12.4.1 Independent component analysis

We begin by considering models in which the observed variables are related linearly to the latent variables, but for which the latent distribution is non-Gaussian. An important class of such models, known as *independent component analysis*, or *ICA*, arises when we consider a distribution over the latent variables that factorizes, so that

$$p(\mathbf{z}) = \prod_{j=1}^{M} p(z_j). \tag{12.89}$$

To understand the role of such models, consider a situation in which two people are talking at the same time, and we record their voices using two microphones. If we ignore effects such as time delay and echoes, then the signals received by the microphones at any point in time will be given by linear combinations of the amplitudes of the two voices. The coefficients of this linear combination will be constant, and if we can infer their values from sample data, then we can invert the mixing process (assuming it is nonsingular) and thereby obtain two clean signals each of which contains the voice of just one person. This is an example of a problem called *blind source separation* in which 'blind' refers to the fact that we are given only the mixed data, and neither the original sources nor the mixing coefficients are observed (Cardoso, 1998).

This type of problem is sometimes addressed using the following approach (MacKay, 2003) in which we ignore the temporal nature of the signals and treat the successive samples as i.i.d. We consider a generative model in which there are two latent variables corresponding to the unobserved speech signal amplitudes, and there are two observed variables given by the signal values at the microphones. The latent variables have a joint distribution that factorizes as above, and the observed variables are given by a linear combination of the latent variables. There is no need to include a noise distribution because the number of latent variables equals the number of observed variables, and therefore the marginal distribution of the observed variables will not in general be singular, so the observed variables are simply deterministic linear combinations of the latent variables. Given a data set of observations, the

likelihood function for this model is a function of the coefficients in the linear combination. The log likelihood can be maximized using gradient-based optimization giving rise to a particular version of independent component analysis.

The success of this approach requires that the latent variables have non-Gaussian distributions. To see this, recall that in probabilistic PCA (and in factor analysis) the latent-space distribution is given by a zero-mean isotropic Gaussian. The model therefore cannot distinguish between two different choices for the latent variables where these differ simply by a rotation in latent space. This can be verified directly by noting that the marginal density (12.35), and hence the likelihood function, is unchanged if we make the transformation $\mathbf{W} \rightarrow \mathbf{WR}$ where $\mathbf{R}$ is an orthogonal matrix satisfying $\mathbf{RR}^{\mathrm{T}} = \mathbf{I}$, because the matrix $\mathbf{C}$ given by (12.36) is itself invariant. Extending the model to allow more general Gaussian latent distributions does not change this conclusion because, as we have seen, such a model is equivalent to the zero-mean isotropic Gaussian latent variable model.

Another way to see why a Gaussian latent variable distribution in a linear model is insufficient to find independent components is to note that the principal components represent a rotation of the coordinate system in data space such as to diagonalize the covariance matrix, so that the data distribution in the new coordinates is then uncorrelated. Although zero correlation is a necessary condition for independence it is not, however, sufficient. In practice, a common choice for the latent-variable distribution is given by

Exercise 12.29

$$p(z_j) = \frac{1}{\pi \cosh(z_j)} = \frac{1}{\pi(e^{z_j} + e^{-z_j})} \tag{12.90}$$

which has heavy tails compared to a Gaussian, reflecting the observation that many real-world distributions also exhibit this property.

The original ICA model (Bell and Sejnowski, 1995) was based on the optimization of an objective function defined by information maximization. One advantage of a probabilistic latent variable formulation is that it helps to motivate and formulate generalizations of basic ICA. For instance, *independent factor analysis* (Attias, 1999a) considers a model in which the number of latent and observed variables can differ, the observed variables are noisy, and the individual latent variables have flexible distributions modelled by mixtures of Gaussians. The log likelihood for this model is maximized using EM, and the reconstruction of the latent variables is approximated using a variational approach. Many other types of model have been considered, and there is now a huge literature on ICA and its applications (Jutten and Herault, 1991; Comon *et al.*, 1991; Amari *et al.*, 1996; Pearlmutter and Parra, 1997; Hyvärinen and Oja, 1997; Hinton *et al.*, 2001; Miskin and MacKay, 2001; Hojen-Sorensen *et al.*, 2002; Choudrey and Roberts, 2003; Chan *et al.*, 2003; Stone, 2004).

12.4.2 Autoassociative neural networks

In Chapter 5 we considered neural networks in the context of supervised learning, where the role of the network is to predict the output variables given values

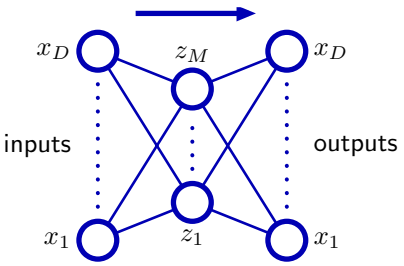

Figure 12.18 An autoassociative multilayer perceptron having two layers of weights. Such a network is trained to map input vectors onto themselves by minimization of a sum-of-squares error. Even with nonlinear units in the hidden layer, such a network is equivalent to linear principal component analysis. Links representing bias parameters have been omitted for clarity.

for the input variables. However, neural networks have also been applied to unsupervised learning where they have been used for dimensionality reduction. This is achieved by using a network having the same number of outputs as inputs, and optimizing the weights so as to minimize some measure of the reconstruction error between inputs and outputs with respect to a set of training data.

Consider first a multilayer perceptron of the form shown in Figure 12.18, having D inputs, D output units and M hidden units, with $M < D$. The targets used to train the network are simply the input vectors themselves, so that the network is attempting to map each input vector onto itself. Such a network is said to form an *autoassociative* mapping. Since the number of hidden units is smaller than the number of inputs, a perfect reconstruction of all input vectors is not in general possible. We therefore determine the network parameters $\mathbf{w}$ by minimizing an error function which captures the degree of mismatch between the input vectors and their reconstructions. In particular, we shall choose a sum-of-squares error of the form

$$E(\mathbf{w}) = \frac{1}{2}\sum_{n=1}^{N} \|\mathbf{y}(\mathbf{x}_n, \mathbf{w}) - \mathbf{x}_n\|^2. \tag{12.91}$$

If the hidden units have linear activations functions, then it can be shown that the error function has a unique global minimum, and that at this minimum the network performs a projection onto the M-dimensional subspace which is spanned by the first M principal components of the data (Bourlard and Kamp, 1988; Baldi and Hornik, 1989). Thus, the vectors of weights which lead into the hidden units in Figure 12.18 form a basis set which spans the principal subspace. Note, however, that these vectors need not be orthogonal or normalized. This result is unsurprising, since both principal component analysis and the neural network are using linear dimensionality reduction and are minimizing the same sum-of-squares error function.

It might be thought that the limitations of a linear dimensionality reduction could be overcome by using nonlinear (sigmoidal) activation functions for the hidden units in the network in Figure 12.18. However, even with nonlinear hidden units, the minimum error solution is again given by the projection onto the principal component subspace (Bourlard and Kamp, 1988). There is therefore no advantage in using two-layer neural networks to perform dimensionality reduction. Standard techniques for principal component analysis (based on singular value decomposition) are guaranteed to give the correct solution in finite time, and they also generate an ordered set of eigenvalues with corresponding orthonormal eigenvectors.

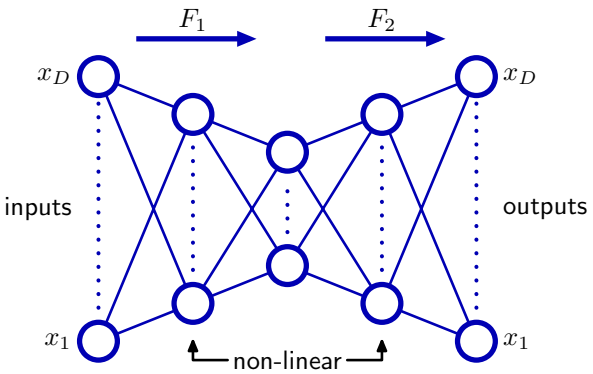

Figure 12.19 Addition of extra hidden layers of nonlinear units gives an autoassociative network which can perform a nonlinear dimensionality reduction.

The situation is different, however, if additional hidden layers are permitted in the network. Consider the four-layer autoassociative network shown in Figure 12.19. Again the output units are linear, and the M units in the second hidden layer can also be linear, however, the first and third hidden layers have sigmoidal nonlinear activation functions. The network is again trained by minimization of the error function (12.91). We can view this network as two successive functional mappings $\mathbf{F}_1$ and $\mathbf{F}_2$, as indicated in Figure 12.19. The first mapping $\mathbf{F}_1$ projects the original D-dimensional data onto an M-dimensional subspace $\mathcal{S}$ defined by the activations of the units in the second hidden layer. Because of the presence of the first hidden layer of nonlinear units, this mapping is very general, and in particular is not restricted to being linear. Similarly, the second half of the network defines an arbitrary functional mapping from the M-dimensional space back into the original D-dimensional input space. This has a simple geometrical interpretation, as indicated for the case $D = 3$ and $M = 2$ in Figure 12.20.

Such a network effectively performs a nonlinear principal component analysis.

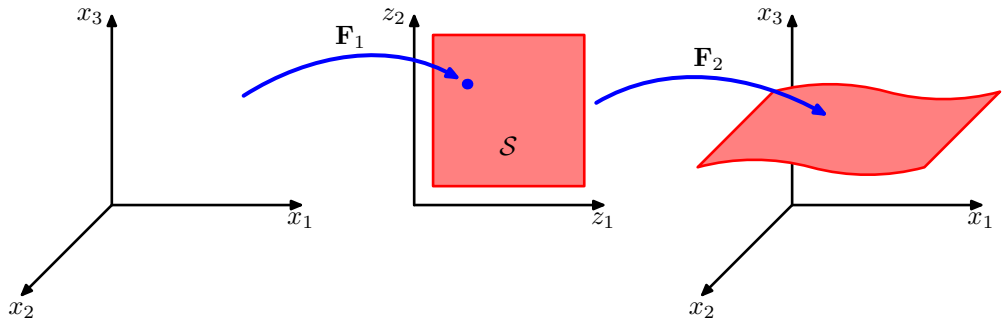

Figure 12.20 Geometrical interpretation of the mappings performed by the network in Figure 12.19 for the case of $D = 3$ inputs and $M = 2$ units in the middle hidden layer. The function $\mathbf{F}_2$ maps from an M-dimensional space $\mathcal{S}$ into a D-dimensional space and therefore defines the way in which the space $\mathcal{S}$ is embedded within the original $\mathbf{x}$-space. Since the mapping $\mathbf{F}_2$ can be nonlinear, the embedding of $\mathcal{S}$ can be nonplanar, as indicated in the figure. The mapping $\mathbf{F}_1$ then defines a projection of points in the original D-dimensional space into the M-dimensional subspace $\mathcal{S}$.

It has the advantage of not being limited to linear transformations, although it contains standard principal component analysis as a special case. However, training the network now involves a nonlinear optimization problem, since the error function (12.91) is no longer a quadratic function of the network parameters. Computationally intensive nonlinear optimization techniques must be used, and there is the risk of finding a suboptimal local minimum of the error function. Also, the dimensionality of the subspace must be specified before training the network.

12.4.3 Modelling nonlinear manifolds

As we have already noted, many natural sources of data correspond to low-dimensional, possibly noisy, nonlinear manifolds embedded within the higher dimensional observed data space. Capturing this property explicitly can lead to improved density modelling compared with more general methods. Here we consider briefly a range of techniques that attempt to do this.

One way to model the nonlinear structure is through a combination of linear models, so that we make a piece-wise linear approximation to the manifold. This can be obtained, for instance, by using a clustering technique such as K-means based on Euclidean distance to partition the data set into local groups with standard PCA applied to each group. A better approach is to use the reconstruction error for cluster assignment (Kambhatla and Leen, 1997; Hinton *et al.*, 1997) as then a common cost function is being optimized in each stage. However, these approaches still suffer from limitations due to the absence of an overall density model. By using probabilistic PCA it is straightforward to define a fully probabilistic model simply by considering a mixture distribution in which the components are probabilistic PCA models (Tipping and Bishop, 1999a). Such a model has both discrete latent variables, corresponding to the discrete mixture, as well as continuous latent variables, and the likelihood function can be maximized using the EM algorithm. A fully Bayesian treatment, based on variational inference (Bishop and Winn, 2000), allows the number of components in the mixture, as well as the effective dimensionalities of the individual models, to be inferred from the data. There are many variants of this model in which parameters such as the $\mathbf{W}$ matrix or the noise variances are tied across components in the mixture, or in which the isotropic noise distributions are replaced by diagonal ones, giving rise to a mixture of factor analysers (Ghahramani and Hinton, 1996a; Ghahramani and Beal, 2000). The mixture of probabilistic PCA models can also be extended hierarchically to produce an interactive data visualization algorithm (Bishop and Tipping, 1998).

An alternative to considering a mixture of linear models is to consider a single nonlinear model. Recall that conventional PCA finds a linear subspace that passes close to the data in a least-squares sense. This concept can be extended to one-dimensional nonlinear surfaces in the form of *principal curves* (Hastie and Stuetzle, 1989). We can describe a curve in a D-dimensional data space using a vector-valued function $\mathbf{f}(\lambda)$, which is a vector each of whose elements is a function of the scalar λ. There are many possible ways to parameterize the curve, of which a natural choice is the arc length along the curve. For any given point $\widehat{\mathbf{x}}$ in data space, we can find the point on the curve that is closest in Euclidean distance. We denote this point by

$\lambda = g_{\mathbf{f}}(\mathbf{x})$ because it depends on the particular curve $\mathbf{f}(\lambda)$. For a continuous data density $p(\mathbf{x})$, a principal curve is defined as one for which every point on the curve is the mean of all those points in data space that project to it, so that

$$\mathbb{E}\left[\mathbf{x}|g_{\mathbf{f}}(\mathbf{x}) = \lambda\right] = \mathbf{f}(\lambda). \tag{12.92}$$

For a given continuous density, there can be many principal curves. In practice, we are interested in finite data sets, and we also wish to restrict attention to smooth curves. Hastie and Stuetzle (1989) propose a two-stage iterative procedure for finding such principal curves, somewhat reminiscent of the EM algorithm for PCA. The curve is initialized using the first principal component, and then the algorithm alternates between a data projection step and curve re-estimation step. In the projection step, each data point is assigned to a value of λ corresponding to the closest point on the curve. Then in the re-estimation step, each point on the curve is given by a weighted average of those points that project to nearby points on the curve, with points closest on the curve given the greatest weight. In the case where the subspace is constrained to be linear, the procedure converges to the first principal component and is equivalent to the power method for finding the largest eigenvector of the covariance matrix. Principal curves can be generalized to multidimensional manifolds called *principal surfaces* although these have found limited use due to the difficulty of data smoothing in higher dimensions even for two-dimensional manifolds.

PCA is often used to project a data set onto a lower-dimensional space, for example two dimensional, for the purposes of visualization. Another linear technique with a similar aim is *multidimensional scaling*, or *MDS* (Cox and Cox, 2000). It finds a low-dimensional projection of the data such as to preserve, as closely as possible, the pairwise distances between data points, and involves finding the eigenvectors of the distance matrix. In the case where the distances are Euclidean, it gives equivalent results to PCA. The MDS concept can be extended to a wide variety of data types specified in terms of a similarity matrix, giving *nonmetric* MDS.

Two other nonprobabilistic methods for dimensionality reduction and data visualization are worthy of mention. *Locally linear embedding*, or *LLE* (Roweis and Saul, 2000) first computes the set of coefficients that best reconstructs each data point from its neighbours. These coefficients are arranged to be invariant to rotations, translations, and scalings of that data point and its neighbours, and hence they characterize the local geometrical properties of the neighbourhood. LLE then maps the high-dimensional data points down to a lower dimensional space while preserving these neighbourhood coefficients. If the local neighbourhood for a particular data point can be considered linear, then the transformation can be achieved using a combination of translation, rotation, and scaling, such as to preserve the angles formed between the data points and their neighbours. Because the weights are invariant to these transformations, we expect the same weight values to reconstruct the data points in the low-dimensional space as in the high-dimensional data space. In spite of the nonlinearity, the optimization for LLE does not exhibit local minima.

In *isometric feature mapping*, or *isomap* (Tenenbaum *et al.*, 2000), the goal is to project the data to a lower-dimensional space using MDS, but where the dissimilarities are defined in terms of the *geodesic distances* measured along the mani-

fold. For instance, if two points lie on a circle, then the geodesic is the arc-length distance measured around the circumference of the circle not the straight line distance measured along the chord connecting them. The algorithm first defines the neighbourhood for each data point, either by finding the K nearest neighbours or by finding all points within a sphere of radius ϵ. A graph is then constructed by linking all neighbouring points and labelling them with their Euclidean distance. The geodesic distance between any pair of points is then approximated by the sum of the arc lengths along the shortest path connecting them (which itself is found using standard algorithms). Finally, metric MDS is applied to the geodesic distance matrix to find the low-dimensional projection.

Our focus in this chapter has been on models for which the observed variables are continuous. We can also consider models having continuous latent variables together with discrete observed variables, giving rise to *latent trait* models (Bartholomew, 1987). In this case, the marginalization over the continuous latent variables, even for a linear relationship between latent and observed variables, cannot be performed analytically, and so more sophisticated techniques are required. Tipping (1999) uses variational inference in a model with a two-dimensional latent space, allowing a binary data set to be visualized analogously to the use of PCA to visualize continuous data. Note that this model is the dual of the Bayesian logistic regression problem discussed in Section 4.5. In the case of logistic regression we have N observations of the feature vector $\boldsymbol{\phi}_n$ which are parameterized by a single parameter vector $\mathbf{w}$, whereas in the latent space visualization model there is a single latent space variable $\mathbf{x}$ (analogous to $\boldsymbol{\phi}$) and N copies of the latent variable $\mathbf{w}_n$. A generalization of probabilistic latent variable models to general exponential family distributions is described in Collins *et al.* (2002).

We have already noted that an arbitrary distribution can be formed by taking a Gaussian random variable and transforming it through a suitable nonlinearity. This is exploited in a general latent variable model called a *density network* (MacKay, 1995; MacKay and Gibbs, 1999) in which the nonlinear function is governed by a multilayered neural network. If the network has enough hidden units, it can approximate a given nonlinear function to any desired accuracy. The downside of having such a flexible model is that the marginalization over the latent variables, required in order to obtain the likelihood function, is no longer analytically tractable. Instead, the likelihood is approximated using Monte Carlo techniques by drawing samples from the Gaussian prior. The marginalization over the latent variables then becomes a simple sum with one term for each sample. However, because a large number of sample points may be required in order to give an accurate representation of the marginal, this procedure can be computationally costly.

Chapter 5

Chapter 11

If we consider more restricted forms for the nonlinear function, and make an appropriate choice of the latent variable distribution, then we can construct a latent variable model that is both nonlinear and efficient to train. The *generative topographic mapping*, or *GTM* (Bishop *et al.*, 1996; Bishop *et al.*, 1997a; Bishop *et al.*, 1998b) uses a latent distribution that is defined by a finite regular grid of delta functions over the (typically two-dimensional) latent space. Marginalization over the latent space then simply involves summing over the contributions from each of the grid locations.

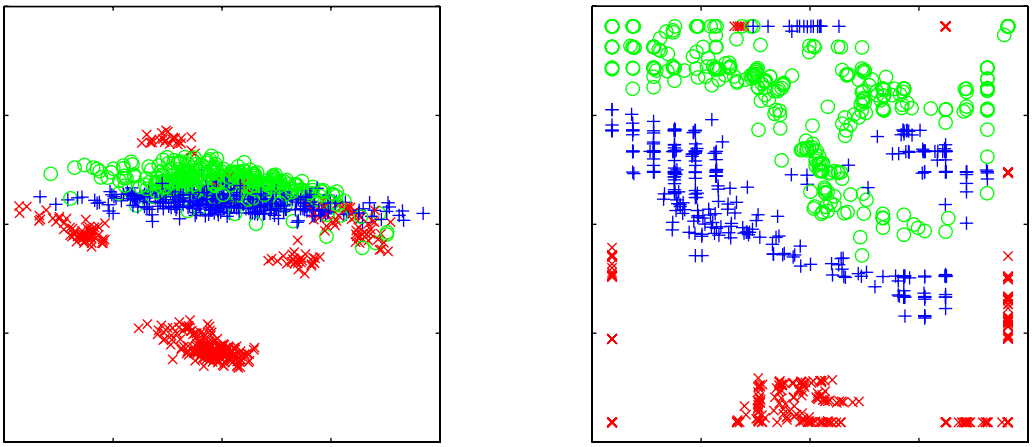

Figure 12.21 Plot of the oil flow data set visualized using PCA on the left and GTM on the right. For the GTM model, each data point is plotted at the mean of its posterior distribution in latent space. The nonlinearity of the GTM model allows the separation between the groups of data points to be seen more clearly.

Chapter 3

Section 1.4

The nonlinear mapping is given by a linear regression model that allows for general nonlinearity while being a linear function of the adaptive parameters. Note that the usual limitation of linear regression models arising from the curse of dimensionality does not arise in the context of the GTM since the manifold generally has two dimensions irrespective of the dimensionality of the data space. A consequence of these two choices is that the likelihood function can be expressed analytically in closed form and can be optimized efficiently using the EM algorithm. The resulting GTM model fits a two-dimensional nonlinear manifold to the data set, and by evaluating the posterior distribution over latent space for the data points, they can be projected back to the latent space for visualization purposes. Figure 12.21 shows a comparison of the oil data set visualized with linear PCA and with the nonlinear GTM.

The GTM can be seen as a probabilistic version of an earlier model called the *self organizing map*, or *SOM* (Kohonen, 1982; Kohonen, 1995), which also represents a two-dimensional nonlinear manifold as a regular array of discrete points. The SOM is somewhat reminiscent of the K-means algorithm in that data points are assigned to nearby prototype vectors that are then subsequently updated. Initially, the prototypes are distributed at random, and during the training process they 'self organize' so as to approximate a smooth manifold. Unlike K-means, however, the SOM is not optimizing any well-defined cost function (Erwin *et al.*, 1992) making it difficult to set the parameters of the model and to assess convergence. There is also no guarantee that the 'self-organization' will take place as this is dependent on the choice of appropriate parameter values for any particular data set.

By contrast, GTM optimizes the log likelihood function, and the resulting model defines a probability density in data space. In fact, it corresponds to a constrained mixture of Gaussians in which the components share a common variance, and the means are constrained to lie on a smooth two-dimensional manifold. This proba-

bilistic foundation also makes it very straightforward to define generalizations of GTM (Bishop *et al.*, 1998a) such as a Bayesian treatment, dealing with missing values, a principled extension to discrete variables, the use of Gaussian processes to define the manifold, or a hierarchical GTM model (Tino and Nabney, 2002).

Section 6.4

Because the manifold in GTM is defined as a continuous surface, not just at the prototype vectors as in the SOM, it is possible to compute the *magnification factors* corresponding to the local expansions and compressions of the manifold needed to fit the data set (Bishop *et al.*, 1997b) as well as the *directional curvatures* of the manifold (Tino *et al.*, 2001). These can be visualized along with the projected data and provide additional insight into the model.

Exercises

12.1 ($\star\star$) **www** In this exercise, we use proof by induction to show that the linear projection onto an M-dimensional subspace that maximizes the variance of the projected data is defined by the M eigenvectors of the data covariance matrix $\mathbf{S}$, given by (12.3), corresponding to the M largest eigenvalues. In Section 12.1, this result was proven for the case of $M = 1$. Now suppose the result holds for some general value of M and show that it consequently holds for dimensionality $M + 1$. To do this, first set the derivative of the variance of the projected data with respect to a vector $\mathbf{u}_{M+1}$ defining the new direction in data space equal to zero. This should be done subject to the constraints that $\mathbf{u}_{M+1}$ be orthogonal to the existing vectors $\mathbf{u}_1, \ldots, \mathbf{u}_M$, and also that it be normalized to unit length. Use Lagrange multipliers to enforce these constraints. Then make use of the orthonormality properties of the vectors $\mathbf{u}_1, \ldots, \mathbf{u}_M$ to show that the new vector $\mathbf{u}_{M+1}$ is an eigenvector of $\mathbf{S}$. Finally, show that the variance is maximized if the eigenvector is chosen to be the one corresponding to eigenvector λ_{M+1} where the eigenvalues have been ordered in decreasing value.

Appendix E

12.2 ($\star\star$) Show that the minimum value of the PCA distortion measure J given by (12.15) with respect to the $\mathbf{u}_i$, subject to the orthonormality constraints (12.7), is obtained when the $\mathbf{u}_i$ are eigenvectors of the data covariance matrix $\mathbf{S}$. To do this, introduce a matrix $\mathbf{H}$ of Lagrange multipliers, one for each constraint, so that the modified distortion measure, in matrix notation reads

$$\widetilde{J} = \mathrm{Tr}\left\{\widehat{\mathbf{U}}^{\mathrm{T}}\mathbf{S}\widehat{\mathbf{U}}\right\} + \mathrm{Tr}\left\{\mathbf{H}(\mathbf{I} - \widehat{\mathbf{U}}^{\mathrm{T}}\widehat{\mathbf{U}})\right\} \tag{12.93}$$

where $\widehat{\mathbf{U}}$ is a matrix of dimension $D \times (D - M)$ whose columns are given by $\mathbf{u}_i$. Now minimize $\widetilde{J}$ with respect to $\widehat{\mathbf{U}}$ and show that the solution satisfies $\mathbf{S}\widehat{\mathbf{U}} = \widehat{\mathbf{U}}\mathbf{H}$. Clearly, one possible solution is that the columns of $\widehat{\mathbf{U}}$ are eigenvectors of $\mathbf{S}$, in which case $\mathbf{H}$ is a diagonal matrix containing the corresponding eigenvalues. To obtain the general solution, show that $\mathbf{H}$ can be assumed to be a symmetric matrix, and by using its eigenvector expansion show that the general solution to $\mathbf{S}\widehat{\mathbf{U}} = \widehat{\mathbf{U}}\mathbf{H}$ gives the same value for $\widetilde{J}$ as the specific solution in which the columns of $\widehat{\mathbf{U}}$ are

the eigenvectors of $\mathbf{S}$. Because these solutions are all equivalent, it is convenient to choose the eigenvector solution.

12.3 ($\star$) Verify that the eigenvectors defined by (12.30) are normalized to unit length, assuming that the eigenvectors $\mathbf{v}_i$ have unit length.

12.4 ($\star$) **www** Suppose we replace the zero-mean, unit-covariance latent space distribution (12.31) in the probabilistic PCA model by a general Gaussian distribution of the form $\mathcal{N}(\mathbf{z}|\mathbf{m}, \mathbf{\Sigma})$. By redefining the parameters of the model, show that this leads to an identical model for the marginal distribution $p(\mathbf{x})$ over the observed variables for any valid choice of $\mathbf{m}$ and $\mathbf{\Sigma}$.

12.5 ($\star\star$) Let $\mathbf{x}$ be a D-dimensional random variable having a Gaussian distribution given by $\mathcal{N}(\mathbf{x}|\boldsymbol{\mu}, \mathbf{\Sigma})$, and consider the M-dimensional random variable given by $\mathbf{y} = \mathbf{A}\mathbf{x} + \mathbf{b}$ where $\mathbf{A}$ is an $M \times D$ matrix. Show that $\mathbf{y}$ also has a Gaussian distribution, and find expressions for its mean and covariance. Discuss the form of this Gaussian distribution for $M < D$, for $M = D$, and for $M > D$.

12.6 ($\star$) **www** Draw a directed probabilistic graph for the probabilistic PCA model described in Section 12.2 in which the components of the observed variable $\mathbf{x}$ are shown explicitly as separate nodes. Hence verify that the probabilistic PCA model has the same independence structure as the naive Bayes model discussed in Section 8.2.2.

12.7 ($\star\star$) By making use of the results (2.270) and (2.271) for the mean and covariance of a general distribution, derive the result (12.35) for the marginal distribution $p(\mathbf{x})$ in the probabilistic PCA model.

12.8 ($\star\star$) **www** By making use of the result (2.116), show that the posterior distribution $p(\mathbf{z}|\mathbf{x})$ for the probabilistic PCA model is given by (12.42).

12.9 ($\star$) Verify that maximizing the log likelihood (12.43) for the probabilistic PCA model with respect to the parameter $\boldsymbol{\mu}$ gives the result $\boldsymbol{\mu}_{\mathrm{ML}} = \overline{\mathbf{x}}$ where $\overline{\mathbf{x}}$ is the mean of the data vectors.

12.10 ($\star\star$) By evaluating the second derivatives of the log likelihood function (12.43) for the probabilistic PCA model with respect to the parameter $\boldsymbol{\mu}$, show that the stationary point $\boldsymbol{\mu}_{\mathrm{ML}} = \overline{\mathbf{x}}$ represents the unique maximum.

12.11 ($\star\star$) **www** Show that in the limit $\sigma^2 \to 0$, the posterior mean for the probabilistic PCA model becomes an orthogonal projection onto the principal subspace, as in conventional PCA.

12.12 ($\star\star$) For $\sigma^2 > 0$ show that the posterior mean in the probabilistic PCA model is shifted towards the origin relative to the orthogonal projection.

12.13 ($\star\star$) Show that the optimal reconstruction of a data point under probabilistic PCA, according to the least squares projection cost of conventional PCA, is given by

$$\widetilde{\mathbf{x}} = \mathbf{W}_{\mathrm{ML}}(\mathbf{W}_{\mathrm{ML}}^{\mathrm{T}}\mathbf{W}_{\mathrm{ML}})^{-1}\mathbf{M}\mathbb{E}[\mathbf{z}|\mathbf{x}]. \tag{12.94}$$

12.14 ($\star$) The number of independent parameters in the covariance matrix for the probabilistic PCA model with an M-dimensional latent space and a D-dimensional data space is given by (12.51). Verify that in the case of $M = D - 1$, the number of independent parameters is the same as in a general covariance Gaussian, whereas for $M = 0$ it is the same as for a Gaussian with an isotropic covariance.

12.15 ($\star\star$) **www** Derive the M-step equations (12.56) and (12.57) for the probabilistic PCA model by maximization of the expected complete-data log likelihood function given by (12.53).

12.16 ($\star\star\star$) In Figure 12.11, we showed an application of probabilistic PCA to a data set in which some of the data values were missing at random. Derive the EM algorithm for maximizing the likelihood function for the probabilistic PCA model in this situation. Note that the $\{\mathbf{z}_n\}$, as well as the missing data values that are components of the vectors $\{\mathbf{x}_n\}$, are now latent variables. Show that in the special case in which all of the data values are observed, this reduces to the EM algorithm for probabilistic PCA derived in Section 12.2.2.

12.17 ($\star\star$) **www** Let $\mathbf{W}$ be a $D \times M$ matrix whose columns define a linear subspace of dimensionality M embedded within a data space of dimensionality D, and let $\boldsymbol{\mu}$ be a D-dimensional vector. Given a data set $\{\mathbf{x}_n\}$ where $n = 1, \ldots, N$, we can approximate the data points using a linear mapping from a set of M-dimensional vectors $\{\mathbf{z}_n\}$, so that $\mathbf{x}_n$ is approximated by $\mathbf{W}\mathbf{z}_n + \boldsymbol{\mu}$. The associated sum-of-squares reconstruction cost is given by

$$J = \sum_{n=1}^{N} \|\mathbf{x}_n - \boldsymbol{\mu} - \mathbf{W}\mathbf{z}_n\|^2. \tag{12.95}$$

First show that minimizing J with respect to $\boldsymbol{\mu}$ leads to an analogous expression with $\mathbf{x}_n$ and $\mathbf{z}_n$ replaced by zero-mean variables $\mathbf{x}_n - \overline{\mathbf{x}}$ and $\mathbf{z}_n - \overline{\mathbf{z}}$, respectively, where $\overline{\mathbf{x}}$ and $\overline{\mathbf{z}}$ denote sample means. Then show that minimizing J with respect to $\mathbf{z}_n$, where $\mathbf{W}$ is kept fixed, gives rise to the PCA E step (12.58), and that minimizing J with respect to $\mathbf{W}$, where $\{\mathbf{z}_n\}$ is kept fixed, gives rise to the PCA M step (12.59).

12.18 ($\star$) Derive an expression for the number of independent parameters in the factor analysis model described in Section 12.2.4.

12.19 ($\star\star$) **www** Show that the factor analysis model described in Section 12.2.4 is invariant under rotations of the latent space coordinates.

12.20 ($\star\star$) By considering second derivatives, show that the only stationary point of the log likelihood function for the factor analysis model discussed in Section 12.2.4 with respect to the parameter $\boldsymbol{\mu}$ is given by the sample mean defined by (12.1). Furthermore, show that this stationary point is a maximum.

12.21 ($\star\star$) Derive the formulae (12.66) and (12.67) for the E step of the EM algorithm for factor analysis. Note that from the result of Exercise 12.20, the parameter $\boldsymbol{\mu}$ can be replaced by the sample mean $\overline{\mathbf{x}}$.

12.22 ($\star\star$) Write down an expression for the expected complete-data log likelihood function for the factor analysis model, and hence derive the corresponding M step equations (12.69) and (12.70).

12.23 ($\star$) **www** Draw a directed probabilistic graphical model representing a discrete mixture of probabilistic PCA models in which each PCA model has its own values of $\mathbf{W}$, $\boldsymbol{\mu}$, and σ^2. Now draw a modified graph in which these parameter values are shared between the components of the mixture.

12.24 ($\star\star\star$) We saw in Section 2.3.7 that Student's t-distribution can be viewed as an infinite mixture of Gaussians in which we marginalize with respect to a continuous latent variable. By exploiting this representation, formulate an EM algorithm for maximizing the log likelihood function for a multivariate Student's t-distribution given an observed set of data points, and derive the forms of the E and M step equations.

12.25 ($\star\star$) **www** Consider a linear-Gaussian latent-variable model having a latent space distribution $p(\mathbf{z}) = \mathcal{N}(\mathbf{x}|\mathbf{0}, \mathbf{I})$ and a conditional distribution for the observed variable $p(\mathbf{x}|\mathbf{z}) = \mathcal{N}(\mathbf{x}|\mathbf{W}\mathbf{z} + \boldsymbol{\mu}, \boldsymbol{\Phi})$ where $\boldsymbol{\Phi}$ is an arbitrary symmetric, positive-definite noise covariance matrix. Now suppose that we make a nonsingular linear transformation of the data variables $\mathbf{x} \rightarrow \mathbf{A}\mathbf{x}$, where $\mathbf{A}$ is a $D \times D$ matrix. If $\boldsymbol{\mu}_{\mathrm{ML}}$, $\mathbf{W}_{\mathrm{ML}}$ and $\boldsymbol{\Phi}_{\mathrm{ML}}$ represent the maximum likelihood solution corresponding to the original untransformed data, show that $\mathbf{A}\boldsymbol{\mu}_{\mathrm{ML}}$, $\mathbf{A}\mathbf{W}_{\mathrm{ML}}$, and $\mathbf{A}\boldsymbol{\Phi}_{\mathrm{ML}}\mathbf{A}^{\mathrm{T}}$ will represent the corresponding maximum likelihood solution for the transformed data set. Finally, show that the form of the model is preserved in two cases: (i) $\mathbf{A}$ is a diagonal matrix and $\boldsymbol{\Phi}$ is a diagonal matrix. This corresponds to the case of factor analysis. The transformed $\boldsymbol{\Phi}$ remains diagonal, and hence factor analysis is *covariant* under component-wise re-scaling of the data variables; (ii) $\mathbf{A}$ is orthogonal and $\boldsymbol{\Phi}$ is proportional to the unit matrix so that $\boldsymbol{\Phi} = \sigma^2\mathbf{I}$. This corresponds to probabilistic PCA. The transformed $\boldsymbol{\Phi}$ matrix remains proportional to the unit matrix, and hence probabilistic PCA is covariant under a rotation of the axes of data space, as is the case for conventional PCA.

12.26 ($\star\star$) Show that any vector $\mathbf{a}_i$ that satisfies (12.80) will also satisfy (12.79). Also, show that for any solution of (12.80) having eigenvalue λ, we can add any multiple of an eigenvector of $\mathbf{K}$ having zero eigenvalue, and obtain a solution to (12.79) that also has eigenvalue λ. Finally, show that such modifications do not affect the principal-component projection given by (12.82).

12.27 ($\star\star$) Show that the conventional linear PCA algorithm is recovered as a special case of kernel PCA if we choose the linear kernel function given by $k(\mathbf{x}, \mathbf{x}') = \mathbf{x}^{\mathrm{T}}\mathbf{x}'$.

12.28 ($\star\star$) **www** Use the transformation property (1.27) of a probability density under a change of variable to show that any density $p(y)$ can be obtained from a fixed density $q(x)$ that is everywhere nonzero by making a nonlinear change of variable $y = f(x)$ in which $f(x)$ is a monotonic function so that $0 \leqslant f'(x) < \infty$. Write down the differential equation satisfied by $f(x)$ and draw a diagram illustrating the transformation of the density.

12.29 (⋆⋆) **www** Suppose that two variables z_1 and z_2 are independent so that $p(z_1, z_2) = p(z_1)p(z_2)$. Show that the covariance matrix between these variables is diagonal. This shows that independence is a sufficient condition for two variables to be uncorrelated. Now consider two variables y_1 and y_2 in which $-1 \leqslant y_1 \leqslant 1$ and $y_2 = y_2^2$. Write down the conditional distribution $p(y_2|y_1)$ and observe that this is dependent on y_1, showing that the two variables are not independent. Now show that the covariance matrix between these two variables is again diagonal. To do this, use the relation $p(y_1, y_2) = p(y_1)p(y_2|y_1)$ to show that the off-diagonal terms are zero. This counter-example shows that zero correlation is not a sufficient condition for independence.

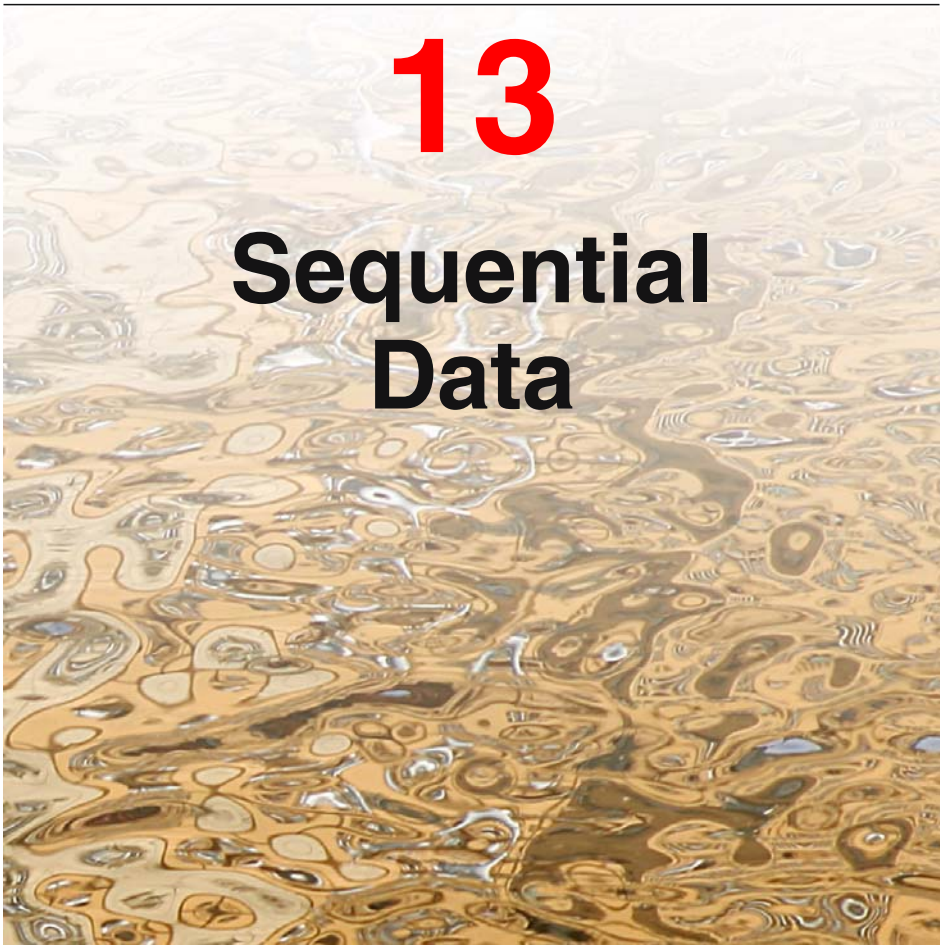

13 Sequential Data

So far in this book, we have focussed primarily on sets of data points that were assumed to be independent and identically distributed (i.i.d.). This assumption allowed us to express the likelihood function as the product over all data points of the probability distribution evaluated at each data point. For many applications, however, the i.i.d. assumption will be a poor one. Here we consider a particularly important class of such data sets, namely those that describe sequential data. These often arise through measurement of time series, for example the rainfall measurements on successive days at a particular location, or the daily values of a currency exchange rate, or the acoustic features at successive time frames used for speech recognition. An example involving speech data is shown in Figure 13.1. Sequential data can also arise in contexts other than time series, for example the sequence of nucleotide base pairs along a strand of DNA or the sequence of characters in an English sentence. For convenience, we shall sometimes refer to 'past' and 'future' observations in a sequence. However, the models explored in this chapter are equally applicable to all

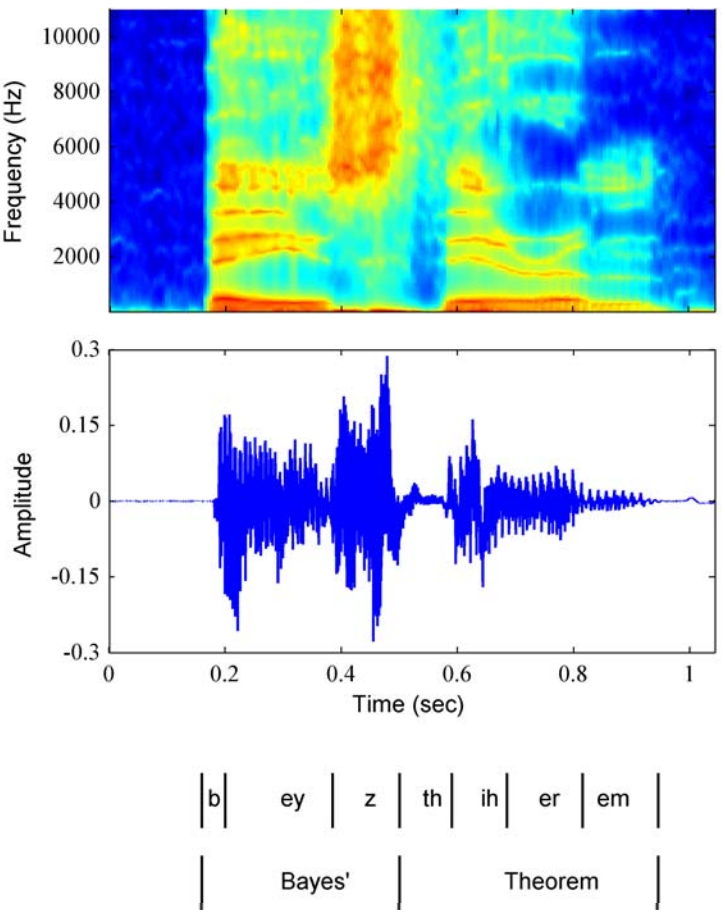

Figure 13.1 Example of a spectrogram of the spoken words "Bayes' theorem" showing a plot of the intensity of the spectral coefficients versus time index.

forms of sequential data, not just temporal sequences.

It is useful to distinguish between stationary and nonstationary sequential distributions. In the stationary case, the data evolves in time, but the distribution from which it is generated remains the same. For the more complex nonstationary situation, the generative distribution itself is evolving with time. Here we shall focus on the stationary case.

For many applications, such as financial forecasting, we wish to be able to predict the next value in a time series given observations of the previous values. Intuitively, we expect that recent observations are likely to be more informative than more historical observations in predicting future values. The example in Figure 13.1 shows that successive observations of the speech spectrum are indeed highly correlated. Furthermore, it would be impractical to consider a general dependence of future observations on all previous observations because the complexity of such a model would grow without limit as the number of observations increases. This leads us to consider *Markov models* in which we assume that future predictions are inde-

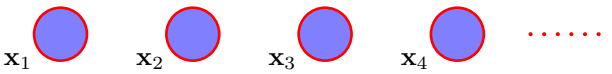

Figure 13.2 The simplest approach to modelling a sequence of observations is to treat them as independent, corresponding to a graph without links.

pendent of all but the most recent observations.

Although such models are tractable, they are also severely limited. We can obtain a more general framework, while still retaining tractability, by the introduction of latent variables, leading to *state space models*. As in Chapters 9 and 12, we shall see that complex models can thereby be constructed from simpler components (in particular, from distributions belonging to the exponential family) and can be readily characterized using the framework of probabilistic graphical models. Here we focus on the two most important examples of state space models, namely the *hidden Markov model*, in which the latent variables are discrete, and *linear dynamical systems*, in which the latent variables are Gaussian. Both models are described by directed graphs having a tree structure (no loops) for which inference can be performed efficiently using the sum-product algorithm.

13.1. Markov Models

The easiest way to treat sequential data would be simply to ignore the sequential aspects and treat the observations as i.i.d., corresponding to the graph in Figure 13.2. Such an approach, however, would fail to exploit the sequential patterns in the data, such as correlations between observations that are close in the sequence. Suppose, for instance, that we observe a binary variable denoting whether on a particular day it rained or not. Given a time series of recent observations of this variable, we wish to predict whether it will rain on the next day. If we treat the data as i.i.d., then the only information we can glean from the data is the relative frequency of rainy days. However, we know in practice that the weather often exhibits trends that may last for several days. Observing whether or not it rains today is therefore of significant help in predicting if it will rain tomorrow.

To express such effects in a probabilistic model, we need to relax the i.i.d. assumption, and one of the simplest ways to do this is to consider a *Markov model*. First of all we note that, without loss of generality, we can use the product rule to express the joint distribution for a sequence of observations in the form

$$p(\mathbf{x}_1, \ldots, \mathbf{x}_N) = \prod_{n=1}^{N} p(\mathbf{x}_n | \mathbf{x}_1, \ldots, \mathbf{x}_{n-1}). \tag{13.1}$$

If we now assume that each of the conditional distributions on the right-hand side is independent of all previous observations except the most recent, we obtain the *first-order Markov chain*, which is depicted as a graphical model in Figure 13.3. The

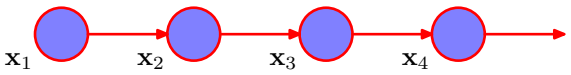

Figure 13.3 A first-order Markov chain of observations $\{\mathbf{x}_n\}$ in which the distribution $p(\mathbf{x}_n|\mathbf{x}_{n-1})$ of a particular observation $\mathbf{x}_n$ is conditioned on the value of the previous observation $\mathbf{x}_{n-1}$.

joint distribution for a sequence of N observations under this model is given by

$$p(\mathbf{x}_1, \ldots, \mathbf{x}_N) = p(\mathbf{x}_1) \prod_{n=2}^{N} p(\mathbf{x}_n|\mathbf{x}_{n-1}). \tag{13.2}$$

Section 8.2 From the d-separation property, we see that the conditional distribution for observation $\mathbf{x}_n$, given all of the observations up to time n, is given by

$$p(\mathbf{x}_n|\mathbf{x}_1, \ldots, \mathbf{x}_{n-1}) = p(\mathbf{x}_n|\mathbf{x}_{n-1}) \tag{13.3}$$

which is easily verified by direct evaluation starting from (13.2) and using the product rule of probability. Thus if we use such a model to predict the next observation in a sequence, the distribution of predictions will depend only on the value of the immediately preceding observation and will be independent of all earlier observations.

Exercise 13.1

In most applications of such models, the conditional distributions $p(\mathbf{x}_n|\mathbf{x}_{n-1})$ that define the model will be constrained to be equal, corresponding to the assumption of a stationary time series. The model is then known as a *homogeneous* Markov chain. For instance, if the conditional distributions depend on adjustable parameters (whose values might be inferred from a set of training data), then all of the conditional distributions in the chain will share the same values of those parameters.

Although this is more general than the independence model, it is still very restrictive. For many sequential observations, we anticipate that the trends in the data over several successive observations will provide important information in predicting the next value. One way to allow earlier observations to have an influence is to move to higher-order Markov chains. If we allow the predictions to depend also on the previous-but-one value, we obtain a second-order Markov chain, represented by the graph in Figure 13.4. The joint distribution is now given by

$$p(\mathbf{x}_1, \ldots, \mathbf{x}_N) = p(\mathbf{x}_1)p(\mathbf{x}_2|\mathbf{x}_1) \prod_{n=3}^{N} p(\mathbf{x}_n|\mathbf{x}_{n-1}, \mathbf{x}_{n-2}). \tag{13.4}$$

Again, using d-separation or by direct evaluation, we see that the conditional distribution of $\mathbf{x}_n$ given $\mathbf{x}_{n-1}$ and $\mathbf{x}_{n-2}$ is independent of all observations $\mathbf{x}_1, \ldots \mathbf{x}_{n-3}$.

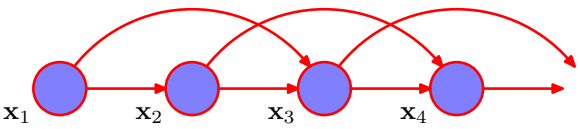

Figure 13.4 A second-order Markov chain, in which the conditional distribution of a particular observation $\mathbf{x}_n$ depends on the values of the two previous observations $\mathbf{x}_{n-1}$ and $\mathbf{x}_{n-2}$.

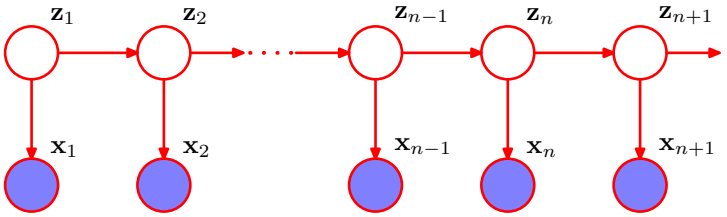

Figure 13.5 We can represent sequential data using a Markov chain of latent variables, with each observation conditioned on the state of the corresponding latent variable. This important graphical structure forms the foundation both for the hidden Markov model and for linear dynamical systems.

Each observation is now influenced by two previous observations. We can similarly consider extensions to an M^{th} order Markov chain in which the conditional distribution for a particular variable depends on the previous M variables. However, we have paid a price for this increased flexibility because the number of parameters in the model is now much larger. Suppose the observations are discrete variables having K states. Then the conditional distribution $p(\mathbf{x}_n|\mathbf{x}_{n-1})$ in a first-order Markov chain will be specified by a set of $K-1$ parameters for each of the K states of $\mathbf{x}_{n-1}$ giving a total of $K(K-1)$ parameters. Now suppose we extend the model to an M^{th} order Markov chain, so that the joint distribution is built up from conditionals $p(\mathbf{x}_n|\mathbf{x}_{n-M},\ldots,\mathbf{x}_{n-1})$. If the variables are discrete, and if the conditional distributions are represented by general conditional probability tables, then the number of parameters in such a model will have $K^{M-1}(K-1)$ parameters. Because this grows exponentially with M, it will often render this approach impractical for larger values of M.

For continuous variables, we can use linear-Gaussian conditional distributions in which each node has a Gaussian distribution whose mean is a linear function of its parents. This is known as an *autoregressive* or *AR* model (Box *et al.*, 1994; Thiesson *et al.*, 2004). An alternative approach is to use a parametric model for $p(\mathbf{x}_n|\mathbf{x}_{n-M},\ldots,\mathbf{x}_{n-1})$ such as a neural network. This technique is sometimes called a *tapped delay line* because it corresponds to storing (delaying) the previous M values of the observed variable in order to predict the next value. The number of parameters can then be much smaller than in a completely general model (for example it may grow linearly with M), although this is achieved at the expense of a restricted family of conditional distributions.

Suppose we wish to build a model for sequences that is not limited by the Markov assumption to any order and yet that can be specified using a limited number of free parameters. We can achieve this by introducing additional latent variables to permit a rich class of models to be constructed out of simple components, as we did with mixture distributions in Chapter 9 and with continuous latent variable models in Chapter 12. For each observation $\mathbf{x}_n$, we introduce a corresponding latent variable $\mathbf{z}_n$ (which may be of different type or dimensionality to the observed variable). We now assume that it is the latent variables that form a Markov chain, giving rise to the graphical structure known as a *state space model*, which is shown in Figure 13.5. It satisfies the key conditional independence property that $\mathbf{z}_{n-1}$ and $\mathbf{z}_{n+1}$ are independent given $\mathbf{z}_n$, so that

$$\mathbf{z}_{n+1} \perp\!\!\!\perp \mathbf{z}_{n-1} \,|\, \mathbf{z}_n. \tag{13.5}$$

The joint distribution for this model is given by

$$p(\mathbf{x}_1, \ldots, \mathbf{x}_N, \mathbf{z}_1, \ldots, \mathbf{z}_N) = p(\mathbf{z}_1) \left[\prod_{n=2}^{N} p(\mathbf{z}_n|\mathbf{z}_{n-1}) \right] \prod_{n=1}^{N} p(\mathbf{x}_n|\mathbf{z}_n). \tag{13.6}$$

Using the d-separation criterion, we see that there is always a path connecting any two observed variables $\mathbf{x}_n$ and $\mathbf{x}_m$ via the latent variables, and that this path is never blocked. Thus the predictive distribution $p(\mathbf{x}_{n+1}|\mathbf{x}_1, \ldots, \mathbf{x}_n)$ for observation $\mathbf{x}_{n+1}$ given all previous observations does not exhibit any conditional independence properties, and so our predictions for $\mathbf{x}_{n+1}$ depends on all previous observations. The observed variables, however, do not satisfy the Markov property at any order. We shall discuss how to evaluate the predictive distribution in later sections of this chapter.

There are two important models for sequential data that are described by this graph. If the latent variables are discrete, then we obtain the *hidden Markov model*, or *HMM* (Elliott *et al.*, 1995). Note that the observed variables in an HMM may be discrete or continuous, and a variety of different conditional distributions can be used to model them. If both the latent and the observed variables are Gaussian (with a linear-Gaussian dependence of the conditional distributions on their parents), then we obtain the *linear dynamical system*.

Section 13.2

Section 13.3

13.2. Hidden Markov Models

The hidden Markov model can be viewed as a specific instance of the state space model of Figure 13.5 in which the latent variables are discrete. However, if we examine a single time slice of the model, we see that it corresponds to a mixture distribution, with component densities given by $p(\mathbf{x}|\mathbf{z})$. It can therefore also be interpreted as an extension of a mixture model in which the choice of mixture component for each observation is not selected independently but depends on the choice of component for the previous observation. The HMM is widely used in speech recognition (Jelinek, 1997; Rabiner and Juang, 1993), natural language modelling (Manning and Schütze, 1999), on-line handwriting recognition (Nag *et al.*, 1986), and for the analysis of biological sequences such as proteins and DNA (Krogh *et al.*, 1994; Durbin *et al.*, 1998; Baldi and Brunak, 2001).

As in the case of a standard mixture model, the latent variables are the discrete multinomial variables $\mathbf{z}_n$ describing which component of the mixture is responsible for generating the corresponding observation $\mathbf{x}_n$. Again, it is convenient to use a 1-of-K coding scheme, as used for mixture models in Chapter 9. We now allow the probability distribution of $\mathbf{z}_n$ to depend on the state of the previous latent variable $\mathbf{z}_{n-1}$ through a conditional distribution $p(\mathbf{z}_n|\mathbf{z}_{n-1})$. Because the latent variables are K-dimensional binary variables, this conditional distribution corresponds to a table of numbers that we denote by $\mathbf{A}$, the elements of which are known as *transition probabilities*. They are given by $A_{jk} \equiv p(z_{nk} = 1|z_{n-1,j} = 1)$, and because they are probabilities, they satisfy $0 \leqslant A_{jk} \leqslant 1$ with $\sum_k A_{jk} = 1$, so that the matrix $\mathbf{A}$

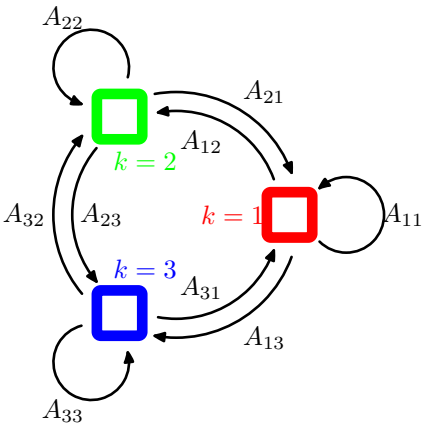

Figure 13.6 Transition diagram showing a model whose latent variables have three possible states corresponding to the three boxes. The black lines denote the elements of the transition matrix A_{jk}.

has $K(K-1)$ independent parameters. We can then write the conditional distribution explicitly in the form

$$p(\mathbf{z}_n|\mathbf{z}_{n-1,\mathbf{A}}) = \prod_{k=1}^{K}\prod_{j=1}^{K} A_{jk}^{z_{n-1,j}z_{nk}}. \tag{13.7}$$

The initial latent node $\mathbf{z}_1$ is special in that it does not have a parent node, and so it has a marginal distribution $p(\mathbf{z}_1)$ represented by a vector of probabilities $\boldsymbol{\pi}$ with elements $\pi_k \equiv p(z_{1k} = 1)$, so that

$$p(\mathbf{z}_1|\boldsymbol{\pi}) = \prod_{k=1}^{K} \pi_k^{z_{1k}} \tag{13.8}$$

where $\sum_k \pi_k = 1$.

The transition matrix is sometimes illustrated diagrammatically by drawing the states as nodes in a state transition diagram as shown in Figure 13.6 for the case of $K = 3$. Note that this does not represent a probabilistic graphical model, because the nodes are not separate variables but rather states of a single variable, and so we have shown the states as boxes rather than circles.

It is sometimes useful to take a state transition diagram, of the kind shown in Figure 13.6, and unfold it over time. This gives an alternative representation of the transitions between latent states, known as a *lattice* or *trellis* diagram, and which is shown for the case of the hidden Markov model in Figure 13.7.

Section 8.4.5

The specification of the probabilistic model is completed by defining the conditional distributions of the observed variables $p(\mathbf{x}_n|\mathbf{z}_n, \boldsymbol{\phi})$, where $\boldsymbol{\phi}$ is a set of parameters governing the distribution. These are known as *emission probabilities*, and might for example be given by Gaussians of the form (9.11) if the elements of $\mathbf{x}$ are continuous variables, or by conditional probability tables if $\mathbf{x}$ is discrete. Because $\mathbf{x}_n$ is observed, the distribution $p(\mathbf{x}_n|\mathbf{z}_n, \boldsymbol{\phi})$ consists, for a given value of $\boldsymbol{\phi}$, of a vector of K numbers corresponding to the K possible states of the binary vector $\mathbf{z}_n$.

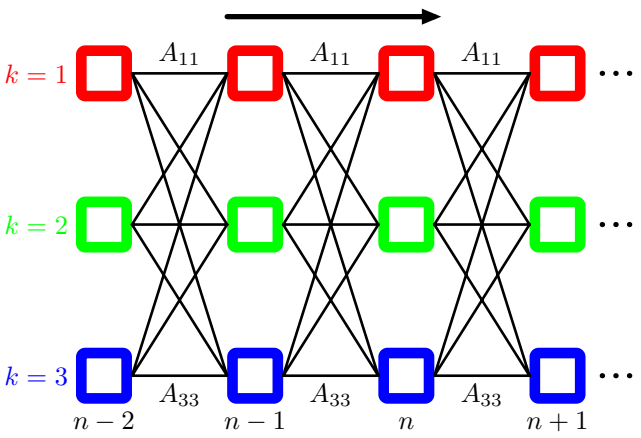

Figure 13.7 If we unfold the state transition diagram of Figure 13.6 over time, we obtain a lattice, or trellis, representation of the latent states. Each column of this diagram corresponds to one of the latent variables $\mathbf{z}_n$.

We can represent the emission probabilities in the form

$$p(\mathbf{x}_n|\mathbf{z}_n, \boldsymbol{\phi}) = \prod_{k=1}^{K} p(\mathbf{x}_n|\boldsymbol{\phi}_k)^{z_{nk}}. \tag{13.9}$$

We shall focuss attention on *homogeneous* models for which all of the conditional distributions governing the latent variables share the same parameters $\mathbf{A}$, and similarly all of the emission distributions share the same parameters $\boldsymbol{\phi}$ (the extension to more general cases is straightforward). Note that a mixture model for an i.i.d. data set corresponds to the special case in which the parameters A_{jk} are the same for all values of j, so that the conditional distribution $p(\mathbf{z}_n|\mathbf{z}_{n-1})$ is independent of $\mathbf{z}_{n-1}$. This corresponds to deleting the horizontal links in the graphical model shown in Figure 13.5.

The joint probability distribution over both latent and observed variables is then given by

$$p(\mathbf{X}, \mathbf{Z}|\boldsymbol{\theta}) = p(\mathbf{z}_1|\boldsymbol{\pi}) \left[\prod_{n=2}^{N} p(\mathbf{z}_n|\mathbf{z}_{n-1}, \mathbf{A}) \right] \prod_{m=1}^{N} p(\mathbf{x}_m|\mathbf{z}_m, \boldsymbol{\phi}) \tag{13.10}$$

where $\mathbf{X} = \{\mathbf{x}_1, \ldots, \mathbf{x}_N\}$, $\mathbf{Z} = \{\mathbf{z}_1, \ldots, \mathbf{z}_N\}$, and $\boldsymbol{\theta} = \{\boldsymbol{\pi}, \mathbf{A}, \boldsymbol{\phi}\}$ denotes the set of parameters governing the model. Most of our discussion of the hidden Markov model will be independent of the particular choice of the emission probabilities. Indeed, the model is tractable for a wide range of emission distributions including discrete tables, Gaussians, and mixtures of Gaussians. It is also possible to exploit discriminative models such as neural networks. These can be used to model the emission density $p(\mathbf{x}|\mathbf{z})$ directly, or to provide a representation for $p(\mathbf{z}|\mathbf{x})$ that can be converted into the required emission density $p(\mathbf{x}|\mathbf{z})$ using Bayes' theorem (Bishop *et al.*, 2004).

Exercise 13.4

We can gain a better understanding of the hidden Markov model by considering it from a generative point of view. Recall that to generate samples from a mixture of

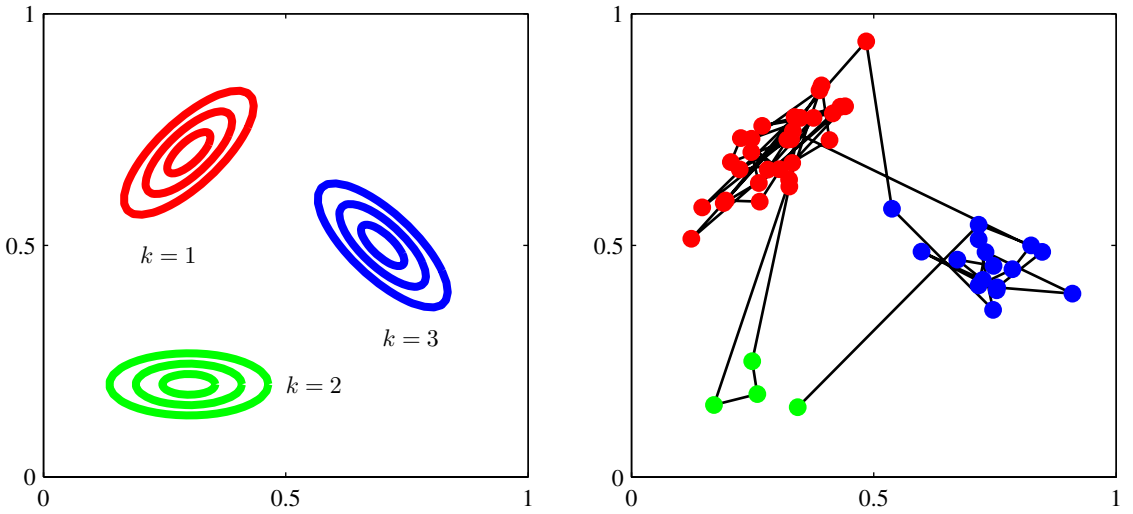

Figure 13.8 Illustration of sampling from a hidden Markov model having a 3-state latent variable $\mathbf{z}$ and a Gaussian emission model $p(\mathbf{x}|\mathbf{z})$ where $\mathbf{x}$ is 2-dimensional. (a) Contours of constant probability density for the emission distributions corresponding to each of the three states of the latent variable. (b) A sample of 50 points drawn from the hidden Markov model, colour coded according to the component that generated them and with lines connecting the successive observations. Here the transition matrix was fixed so that in any state there is a 5% probability of making a transition to each of the other states, and consequently a 90% probability of remaining in the same state.

Gaussians, we first chose one of the components at random with probability given by the mixing coefficients π_k and then generate a sample vector $\mathbf{x}$ from the corresponding Gaussian component. This process is repeated N times to generate a data set of N independent samples. In the case of the hidden Markov model, this procedure is modified as follows. We first choose the initial latent variable $\mathbf{z}_1$ with probabilities governed by the parameters π_k and then sample the corresponding observation $\mathbf{x}_1$. Now we choose the state of the variable $\mathbf{z}_2$ according to the transition probabilities $p(\mathbf{z}_2|\mathbf{z}_1)$ using the already instantiated value of $\mathbf{z}_1$. Thus suppose that the sample for $\mathbf{z}_1$ corresponds to state j. Then we choose the state k of $\mathbf{z}_2$ with probabilities A_{jk} for $k = 1, \ldots, K$. Once we know $\mathbf{z}_2$ we can draw a sample for $\mathbf{x}_2$ and also sample the next latent variable $\mathbf{z}_3$ and so on. This is an example of ancestral sampling for a directed graphical model. If, for instance, we have a model in which the diagonal transition elements A_{kk} are much larger than the off-diagonal elements, then a typical data sequence will have long runs of points generated from a single component, with infrequent transitions from one component to another. The generation of samples from a hidden Markov model is illustrated in Figure 13.8.

Section 8.1.2

There are many variants of the standard HMM model, obtained for instance by imposing constraints on the form of the transition matrix $\mathbf{A}$ (Rabiner, 1989). Here we mention one of particular practical importance called the *left-to-right* HMM, which is obtained by setting the elements A_{jk} of $\mathbf{A}$ to zero if $k < j$, as illustrated in the

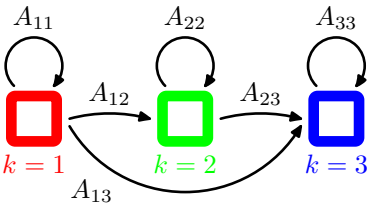

Figure 13.9 Example of the state transition diagram for a 3-state left-to-right hidden Markov model. Note that once a state has been vacated, it cannot later be re-entered.

state transition diagram for a 3-state HMM in Figure 13.9. Typically for such models the initial state probabilities for $p(\mathbf{z}_1)$ are modified so that $p(z_{11}) = 1$ and $p(z_{1j}) = 0$ for $j \neq 1$, in other words every sequence is constrained to start in state $j = 1$. The transition matrix may be further constrained to ensure that large changes in the state index do not occur, so that $A_{jk} = 0$ if $k > j + \Delta$. This type of model is illustrated using a lattice diagram in Figure 13.10.

Many applications of hidden Markov models, for example speech recognition, or on-line character recognition, make use of left-to-right architectures. As an illustration of the left-to-right hidden Markov model, we consider an example involving handwritten digits. This uses on-line data, meaning that each digit is represented by the trajectory of the pen as a function of time in the form of a sequence of pen coordinates, in contrast to the off-line digits data, discussed in Appendix A, which comprises static two-dimensional pixellated images of the ink. Examples of the on-line digits are shown in Figure 13.11. Here we train a hidden Markov model on a subset of data comprising 45 examples of the digit '2'. There are $K = 16$ states, each of which can generate a line segment of fixed length having one of 16 possible angles, and so the emission distribution is simply a 16×16 table of probabilities associated with the allowed angle values for each state index value. Transition probabilities are all set to zero except for those that keep the state index k the same or that increment it by 1, and the model parameters are optimized using 25 iterations of EM. We can gain some insight into the resulting model by running it generatively, as shown in Figure 13.11.

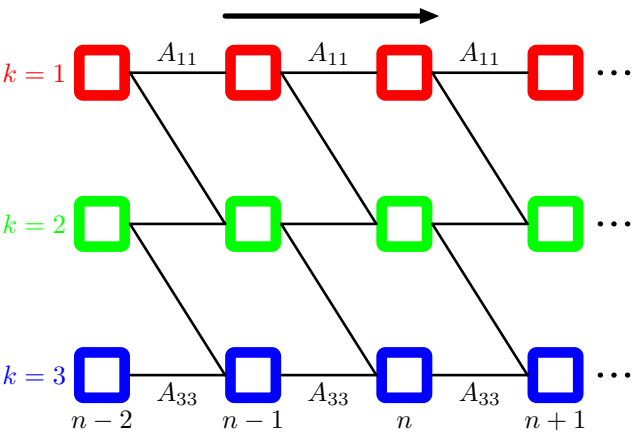

Figure 13.10 Lattice diagram for a 3-state left-to-right HMM in which the state index k is allowed to increase by at most 1 at each transition.

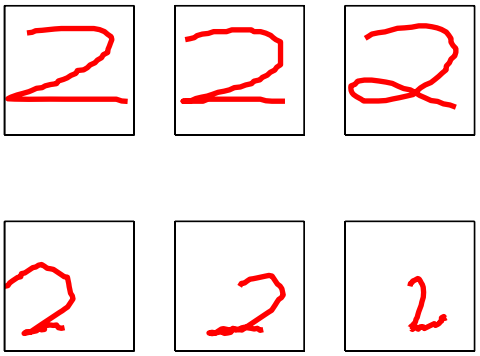

Figure 13.11 Top row: examples of on-line handwritten digits. Bottom row: synthetic digits sampled generatively from a left-to-right hidden Markov model that has been trained on a data set of 45 handwritten digits.

One of the most powerful properties of hidden Markov models is their ability to exhibit some degree of invariance to local warping (compression and stretching) of the time axis. To understand this, consider the way in which the digit '2' is written in the on-line handwritten digits example. A typical digit comprises two distinct sections joined at a cusp. The first part of the digit, which starts at the top left, has a sweeping arc down to the cusp or loop at the bottom left, followed by a second more-or-less straight sweep ending at the bottom right. Natural variations in writing style will cause the relative sizes of the two sections to vary, and hence the location of the cusp or loop within the temporal sequence will vary. From a generative perspective such variations can be accommodated by the hidden Markov model through changes in the number of transitions to the same state versus the number of transitions to the successive state. Note, however, that if a digit '2' is written in the reverse order, that is, starting at the bottom right and ending at the top left, then even though the pen tip coordinates may be identical to an example from the training set, the probability of the observations under the model will be extremely small. In the speech recognition context, warping of the time axis is associated with natural variations in the speed of speech, and again the hidden Markov model can accommodate such a distortion and not penalize it too heavily.

13.2.1 Maximum likelihood for the HMM

If we have observed a data set $\mathbf{X} = \{\mathbf{x}_1, \ldots, \mathbf{x}_N\}$, we can determine the parameters of an HMM using maximum likelihood. The likelihood function is obtained from the joint distribution (13.10) by marginalizing over the latent variables

$$p(\mathbf{X}|\boldsymbol{\theta}) = \sum_{\mathbf{Z}} p(\mathbf{X}, \mathbf{Z}|\boldsymbol{\theta}). \tag{13.11}$$

Because the joint distribution $p(\mathbf{X}, \mathbf{Z}|\boldsymbol{\theta})$ does not factorize over n (in contrast to the mixture distribution considered in Chapter 9), we cannot simply treat each of the summations over $\mathbf{z}_n$ independently. Nor can we perform the summations explicitly because there are N variables to be summed over, each of which has K states, resulting in a total of K^N terms. Thus the number of terms in the summation grows

exponentially with the length of the chain. In fact, the summation in (13.11) corresponds to summing over exponentially many paths through the lattice diagram in Figure 13.7.

We have already encountered a similar difficulty when we considered the inference problem for the simple chain of variables in Figure 8.32. There we were able to make use of the conditional independence properties of the graph to re-order the summations in order to obtain an algorithm whose cost scales linearly, instead of exponentially, with the length of the chain. We shall apply a similar technique to the hidden Markov model.

A further difficulty with the expression (13.11) for the likelihood function is that, because it corresponds to a generalization of a mixture distribution, it represents a summation over the emission models for different settings of the latent variables. Direct maximization of the likelihood function will therefore lead to complex expressions with no closed-form solutions, as was the case for simple mixture models (recall that a mixture model for i.i.d. data is a special case of the HMM).

Section 9.2

We therefore turn to the expectation maximization algorithm to find an efficient framework for maximizing the likelihood function in hidden Markov models. The EM algorithm starts with some initial selection for the model parameters, which we denote by $\boldsymbol{\theta}^{\text{old}}$. In the E step, we take these parameter values and find the posterior distribution of the latent variables $p(\mathbf{Z}|\mathbf{X}, \boldsymbol{\theta}^{\text{old}})$. We then use this posterior distribution to evaluate the expectation of the logarithm of the complete-data likelihood function, as a function of the parameters $\boldsymbol{\theta}$, to give the function $Q(\boldsymbol{\theta}, \boldsymbol{\theta}^{\text{old}})$ defined by

$$Q(\boldsymbol{\theta}, \boldsymbol{\theta}^{\text{old}}) = \sum_{\mathbf{Z}} p(\mathbf{Z}|\mathbf{X}, \boldsymbol{\theta}^{\text{old}}) \ln p(\mathbf{X}, \mathbf{Z}|\boldsymbol{\theta}). \tag{13.12}$$

At this point, it is convenient to introduce some notation. We shall use $\gamma(\mathbf{z}_n)$ to denote the marginal posterior distribution of a latent variable $\mathbf{z}_n$, and $\xi(\mathbf{z}_{n-1}, \mathbf{z}_n)$ to denote the joint posterior distribution of two successive latent variables, so that

$$\gamma(\mathbf{z}_n) = p(\mathbf{z}_n|\mathbf{X}, \boldsymbol{\theta}^{\text{old}}) \tag{13.13}$$

$$\xi(\mathbf{z}_{n-1}, \mathbf{z}_n) = p(\mathbf{z}_{n-1}, \mathbf{z}_n|\mathbf{X}, \boldsymbol{\theta}^{\text{old}}). \tag{13.14}$$

For each value of n, we can store $\gamma(\mathbf{z}_n)$ using a set of K nonnegative numbers that sum to unity, and similarly we can store $\xi(\mathbf{z}_{n-1}, \mathbf{z}_n)$ using a $K \times K$ matrix of nonnegative numbers that again sum to unity. We shall also use $\gamma(z_{nk})$ to denote the conditional probability of $z_{nk} = 1$, with a similar use of notation for $\xi(z_{n-1,j}, z_{nk})$ and for other probabilistic variables introduced later. Because the expectation of a binary random variable is just the probability that it takes the value 1, we have

$$\gamma(z_{nk}) = \mathbb{E}[z_{nk}] = \sum_{\mathbf{z}} \gamma(\mathbf{z}) z_{nk} \tag{13.15}$$

$$\xi(z_{n-1,j}, z_{nk}) = \mathbb{E}[z_{n-1,j} z_{nk}] = \sum_{\mathbf{z}} \gamma(\mathbf{z}) z_{n-1,j} z_{nk}. \tag{13.16}$$

If we substitute the joint distribution $p(\mathbf{X}, \mathbf{Z}|\boldsymbol{\theta})$ given by (13.10) into (13.12),

and make use of the definitions of γ and ξ , we obtain

$$\begin{aligned} Q(\boldsymbol{\theta}, \boldsymbol{\theta}^{\text{old}}) &= \sum_{k=1}^{K} \gamma(z_{1k}) \ln \pi_k + \sum_{n=2}^{N} \sum_{j=1}^{K} \sum_{k=1}^{K} \xi(z_{n-1,j}, z_{nk}) \ln A_{jk} \\ &\quad + \sum_{n=1}^{N} \sum_{k=1}^{K} \gamma(z_{nk}) \ln p(\mathbf{x}_n | \boldsymbol{\phi}_k). \end{aligned} \tag{13.17}$$

The goal of the E step will be to evaluate the quantities $\gamma(\mathbf{z}_n)$ and $\xi(\mathbf{z}_{n-1}, \mathbf{z}_n)$ efficiently, and we shall discuss this in detail shortly.

In the M step, we maximize $Q(\boldsymbol{\theta}, \boldsymbol{\theta}^{\text{old}})$ with respect to the parameters $\boldsymbol{\theta} = \{\boldsymbol{\pi}, \mathbf{A}, \boldsymbol{\phi}\}$ in which we treat $\gamma(\mathbf{z}_n)$ and $\xi(\mathbf{z}_{n-1}, \mathbf{z}_n)$ as constant. Maximization with respect to $\boldsymbol{\pi}$ and $\mathbf{A}$ is easily achieved using appropriate Lagrange multipliers with the results

Exercise 13.5

$$\pi_k = \frac{\gamma(z_{1k})}{\sum_{j=1}^{K} \gamma(z_{1j})} \tag{13.18}$$

$$A_{jk} = \frac{\sum_{n=2}^{N} \xi(z_{n-1,j}, z_{nk})}{\sum_{l=1}^{K} \sum_{n=2}^{N} \xi(z_{n-1,j}, z_{nl})}. \tag{13.19}$$

The EM algorithm must be initialized by choosing starting values for $\boldsymbol{\pi}$ and $\mathbf{A}$, which should of course respect the summation constraints associated with their probabilistic interpretation. Note that any elements of $\boldsymbol{\pi}$ or $\mathbf{A}$ that are set to zero initially will remain zero in subsequent EM updates. A typical initialization procedure would involve selecting random starting values for these parameters subject to the summation and non-negativity constraints. Note that no particular modification to the EM results are required for the case of left-to-right models beyond choosing initial values for the elements A_{jk} in which the appropriate elements are set to zero, because these will remain zero throughout.

Exercise 13.6

To maximize $Q(\boldsymbol{\theta}, \boldsymbol{\theta}^{\text{old}})$ with respect to $\boldsymbol{\phi}_k$, we notice that only the final term in (13.17) depends on $\boldsymbol{\phi}_k$, and furthermore this term has exactly the same form as the data-dependent term in the corresponding function for a standard mixture distribution for i.i.d. data, as can be seen by comparison with (9.40) for the case of a Gaussian mixture. Here the quantities $\gamma(z_{nk})$ are playing the role of the responsibilities. If the parameters $\boldsymbol{\phi}_k$ are independent for the different components, then this term decouples into a sum of terms one for each value of k, each of which can be maximized independently. We are then simply maximizing the weighted log likelihood function for the emission density $p(\mathbf{x}|\boldsymbol{\phi}_k)$ with weights $\gamma(z_{nk})$. Here we shall suppose that this maximization can be done efficiently. For instance, in the case of

Gaussian emission densities we have $p(\mathbf{x}|\boldsymbol{\phi}_k) = \mathcal{N}(\mathbf{x}|\boldsymbol{\mu}_k, \boldsymbol{\Sigma}_k)$, and maximization of the function $Q(\boldsymbol{\theta}, \boldsymbol{\theta}^{\text{old}})$ then gives

$$\boldsymbol{\mu}_k = \frac{\sum_{n=1}^{N} \gamma(z_{nk}) \mathbf{x}_n}{\sum_{n=1}^{N} \gamma(z_{nk})} \tag{13.20}$$

$$\boldsymbol{\Sigma}_k = \frac{\sum_{n=1}^{N} \gamma(z_{nk})(\mathbf{x}_n - \boldsymbol{\mu}_k)(\mathbf{x}_n - \boldsymbol{\mu}_k)^{\mathrm{T}}}{\sum_{n=1}^{N} \gamma(z_{nk})}. \tag{13.21}$$

For the case of discrete multinomial observed variables, the conditional distribution of the observations takes the form

$$p(\mathbf{x}|\mathbf{z}) = \prod_{i=1}^{D} \prod_{k=1}^{K} \mu_{ik}^{x_i z_k} \tag{13.22}$$

Exercise 13.8 and the corresponding M-step equations are given by

$$\mu_{ik} = \frac{\sum_{n=1}^{N} \gamma(z_{nk}) x_{ni}}{\sum_{n=1}^{N} \gamma(z_{nk})}. \tag{13.23}$$

An analogous result holds for Bernoulli observed variables.

The EM algorithm requires initial values for the parameters of the emission distribution. One way to set these is first to treat the data initially as i.i.d. and fit the emission density by maximum likelihood, and then use the resulting values to initialize the parameters for EM.

13.2.2 The forward-backward algorithm

Next we seek an efficient procedure for evaluating the quantities $\gamma(z_{nk})$ and $\xi(z_{n-1,j}, z_{nk})$, corresponding to the E step of the EM algorithm. The graph for the hidden Markov model, shown in Figure 13.5, is a tree, and so we know that the posterior distribution of the latent variables can be obtained efficiently using a two-stage message passing algorithm. In the particular context of the hidden Markov model, this is known as the *forward-backward* algorithm (Rabiner, 1989), or the *Baum-Welch* algorithm (Baum, 1972). There are in fact several variants of the basic algorithm, all of which lead to the exact marginals, according to the precise form of

Section 8.4

the messages that are propagated along the chain (Jordan, 2007). We shall focus on the most widely used of these, known as the alpha-beta algorithm.

As well as being of great practical importance in its own right, the forward-backward algorithm provides us with a nice illustration of many of the concepts introduced in earlier chapters. We shall therefore begin in this section with a 'conventional' derivation of the forward-backward equations, making use of the sum and product rules of probability, and exploiting conditional independence properties which we shall obtain from the corresponding graphical model using d-separation. Then in Section 13.2.3, we shall see how the forward-backward algorithm can be obtained very simply as a specific example of the sum-product algorithm introduced in Section 8.4.4.

It is worth emphasizing that evaluation of the posterior distributions of the latent variables is independent of the form of the emission density $p(\mathbf{x}|\mathbf{z})$ or indeed of whether the observed variables are continuous or discrete. All we require is the values of the quantities $p(\mathbf{x}_n|\mathbf{z}_n)$ for each value of $\mathbf{z}_n$ for every n. Also, in this section and the next we shall omit the explicit dependence on the model parameters $\boldsymbol{\theta}^{\text{old}}$ because these fixed throughout.

We therefore begin by writing down the following conditional independence properties (Jordan, 2007)

$$
\begin{aligned}
p(\mathbf{X}|\mathbf{z}_n) &= p(\mathbf{x}_1,\ldots,\mathbf{x}_n|\mathbf{z}_n) \\
&\quad\; p(\mathbf{x}_{n+1},\ldots,\mathbf{x}_N|\mathbf{z}_n) && (13.24)\\
p(\mathbf{x}_1,\ldots,\mathbf{x}_{n-1}|\mathbf{x}_n,\mathbf{z}_n) &= p(\mathbf{x}_1,\ldots,\mathbf{x}_{n-1}|\mathbf{z}_n) && (13.25)\\
p(\mathbf{x}_1,\ldots,\mathbf{x}_{n-1}|\mathbf{z}_{n-1},\mathbf{z}_n) &= p(\mathbf{x}_1,\ldots,\mathbf{x}_{n-1}|\mathbf{z}_{n-1}) && (13.26)\\
p(\mathbf{x}_{n+1},\ldots,\mathbf{x}_N|\mathbf{z}_n,\mathbf{z}_{n+1}) &= p(\mathbf{x}_{n+1},\ldots,\mathbf{x}_N|\mathbf{z}_{n+1}) && (13.27)\\
p(\mathbf{x}_{n+2},\ldots,\mathbf{x}_N|\mathbf{z}_{n+1},\mathbf{x}_{n+1}) &= p(\mathbf{x}_{n+2},\ldots,\mathbf{x}_N|\mathbf{z}_{n+1}) && (13.28)\\
p(\mathbf{X}|\mathbf{z}_{n-1},\mathbf{z}_n) &= p(\mathbf{x}_1,\ldots,\mathbf{x}_{n-1}|\mathbf{z}_{n-1}) \\
&\quad\; p(\mathbf{x}_n|\mathbf{z}_n)p(\mathbf{x}_{n+1},\ldots,\mathbf{x}_N|\mathbf{z}_n) && (13.29)\\
p(\mathbf{x}_{N+1}|\mathbf{X},\mathbf{z}_{N+1}) &= p(\mathbf{x}_{N+1}|\mathbf{z}_{N+1}) && (13.30)\\
p(\mathbf{z}_{N+1}|\mathbf{z}_N,\mathbf{X}) &= p(\mathbf{z}_{N+1}|\mathbf{z}_N) && (13.31)
\end{aligned}
$$

where $\mathbf{X} = \{\mathbf{x}_1,\ldots,\mathbf{x}_N\}$. These relations are most easily proved using d-separation. For instance in the first of these results, we note that every path from any one of the nodes $\mathbf{x}_1,\ldots,\mathbf{x}_{n-1}$ to the node $\mathbf{x}_n$ passes through the node $\mathbf{z}_n$, which is observed. Because all such paths are head-to-tail, it follows that the conditional independence property must hold. The reader should take a few moments to verify each of these properties in turn, as an exercise in the application of d-separation. These relations can also be proved directly, though with significantly greater effort, from the joint distribution for the hidden Markov model using the sum and product rules of probability.

Exercise 13.10

Let us begin by evaluating $\gamma(z_{nk})$. Recall that for a discrete multinomial random variable the expected value of one of its components is just the probability of that component having the value 1. Thus we are interested in finding the posterior distribution $p(\mathbf{z}_n|\mathbf{x}_1,\ldots,\mathbf{x}_N)$ of $\mathbf{z}_n$ given the observed data set $\mathbf{x}_1,\ldots,\mathbf{x}_N$. This

represents a vector of length K whose entries correspond to the expected values of z_{nk}. Using Bayes' theorem, we have

$$\gamma(\mathbf{z}_n) = p(\mathbf{z}_n|\mathbf{X}) = \frac{p(\mathbf{X}|\mathbf{z}_n)p(\mathbf{z}_n)}{p(\mathbf{X})}. \tag{13.32}$$

Note that the denominator $p(\mathbf{X})$ is implicitly conditioned on the parameters $\boldsymbol{\theta}^{\text{old}}$ of the HMM and hence represents the likelihood function. Using the conditional independence property (13.24), together with the product rule of probability, we obtain

$$\gamma(\mathbf{z}_n) = \frac{p(\mathbf{x}_1, \ldots, \mathbf{x}_n, \mathbf{z}_n)p(\mathbf{x}_{n+1}, \ldots, \mathbf{x}_N|\mathbf{z}_n)}{p(\mathbf{X})} = \frac{\alpha(\mathbf{z}_n)\beta(\mathbf{z}_n)}{p(\mathbf{X})} \tag{13.33}$$

where we have defined

$$\alpha(\mathbf{z}_n) \equiv p(\mathbf{x}_1, \ldots, \mathbf{x}_n, \mathbf{z}_n) \tag{13.34}$$

$$\beta(\mathbf{z}_n) \equiv p(\mathbf{x}_{n+1}, \ldots, \mathbf{x}_N|\mathbf{z}_n). \tag{13.35}$$

The quantity $\alpha(\mathbf{z}_n)$ represents the joint probability of observing all of the given data up to time n and the value of $\mathbf{z}_n$, whereas $\beta(\mathbf{z}_n)$ represents the conditional probability of all future data from time $n+1$ up to N given the value of $\mathbf{z}_n$. Again, $\alpha(\mathbf{z}_n)$ and $\beta(\mathbf{z}_n)$ each represent set of K numbers, one for each of the possible settings of the 1-of-K coded binary vector $\mathbf{z}_n$. We shall use the notation $\alpha(z_{nk})$ to denote the value of $\alpha(\mathbf{z}_n)$ when $z_{nk} = 1$, with an analogous interpretation of $\beta(z_{nk})$.

We now derive recursion relations that allow $\alpha(\mathbf{z}_n)$ and $\beta(\mathbf{z}_n)$ to be evaluated efficiently. Again, we shall make use of conditional independence properties, in particular (13.25) and (13.26), together with the sum and product rules, allowing us to express $\alpha(\mathbf{z}_n)$ in terms of $\alpha(\mathbf{z}_{n-1})$ as follows

$$\begin{aligned}
\alpha(\mathbf{z}_n) &= p(\mathbf{x}_1, \ldots, \mathbf{x}_n, \mathbf{z}_n) \\
&= p(\mathbf{x}_1, \ldots, \mathbf{x}_n|\mathbf{z}_n)p(\mathbf{z}_n) \\
&= p(\mathbf{x}_n|\mathbf{z}_n)p(\mathbf{x}_1, \ldots, \mathbf{x}_{n-1}|\mathbf{z}_n)p(\mathbf{z}_n) \\
&= p(\mathbf{x}_n|\mathbf{z}_n)p(\mathbf{x}_1, \ldots, \mathbf{x}_{n-1}, \mathbf{z}_n) \\
&= p(\mathbf{x}_n|\mathbf{z}_n) \sum_{\mathbf{z}_{n-1}} p(\mathbf{x}_1, \ldots, \mathbf{x}_{n-1}, \mathbf{z}_{n-1}, \mathbf{z}_n) \\
&= p(\mathbf{x}_n|\mathbf{z}_n) \sum_{\mathbf{z}_{n-1}} p(\mathbf{x}_1, \ldots, \mathbf{x}_{n-1}, \mathbf{z}_n|\mathbf{z}_{n-1})p(\mathbf{z}_{n-1}) \\
&= p(\mathbf{x}_n|\mathbf{z}_n) \sum_{\mathbf{z}_{n-1}} p(\mathbf{x}_1, \ldots, \mathbf{x}_{n-1}|\mathbf{z}_{n-1})p(\mathbf{z}_n|\mathbf{z}_{n-1})p(\mathbf{z}_{n-1}) \\
&= p(\mathbf{x}_n|\mathbf{z}_n) \sum_{\mathbf{z}_{n-1}} p(\mathbf{x}_1, \ldots, \mathbf{x}_{n-1}, \mathbf{z}_{n-1})p(\mathbf{z}_n|\mathbf{z}_{n-1})
\end{aligned}$$

Making use of the definition (13.34) for $\alpha(\mathbf{z}_n)$, we then obtain

$$\alpha(\mathbf{z}_n) = p(\mathbf{x}_n|\mathbf{z}_n) \sum_{\mathbf{z}_{n-1}} \alpha(\mathbf{z}_{n-1})p(\mathbf{z}_n|\mathbf{z}_{n-1}). \tag{13.36}$$

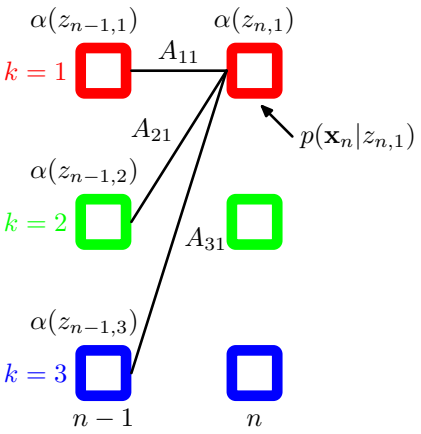

Figure 13.12 Illustration of the forward recursion (13.36) for evaluation of the α variables. In this fragment of the lattice, we see that the quantity $\alpha(z_{n1})$ is obtained by taking the elements $\alpha(z_{n-1,j})$ of $\alpha(\mathbf{z}_{n-1})$ at step $n-1$ and summing them up with weights given by A_{j1}, corresponding to the values of $p(\mathbf{z}_n|\mathbf{z}_{n-1})$, and then multiplying by the data contribution $p(\mathbf{x}_n|z_{n1})$.

It is worth taking a moment to study this recursion relation in some detail. Note that there are K terms in the summation, and the right-hand side has to be evaluated for each of the K values of $\mathbf{z}_n$ so each step of the α recursion has computational cost that scaled like $O(K^2)$. The forward recursion equation for $\alpha(\mathbf{z}_n)$ is illustrated using a lattice diagram in Figure 13.12.

In order to start this recursion, we need an initial condition that is given by

$$\alpha(\mathbf{z}_1) = p(\mathbf{x}_1, \mathbf{z}_1) = p(\mathbf{z}_1)p(\mathbf{x}_1|\mathbf{z}_1) = \prod_{k=1}^{K} \{\pi_k p(\mathbf{x}_1|\boldsymbol{\phi}_k)\}^{z_{1k}} \tag{13.37}$$

which tells us that $\alpha(z_{1k})$, for $k = 1, \ldots, K$, takes the value $\pi_k p(\mathbf{x}_1|\boldsymbol{\phi}_k)$. Starting at the first node of the chain, we can then work along the chain and evaluate $\alpha(\mathbf{z}_n)$ for every latent node. Because each step of the recursion involves multiplying by a $K \times K$ matrix, the overall cost of evaluating these quantities for the whole chain is of $O(K^2N)$.

We can similarly find a recursion relation for the quantities $\beta(\mathbf{z}_n)$ by making use of the conditional independence properties (13.27) and (13.28) giving

$$\begin{aligned}
\beta(\mathbf{z}_n) &= p(\mathbf{x}_{n+1}, \ldots, \mathbf{x}_N|\mathbf{z}_n) \\
&= \sum_{\mathbf{z}_{n+1}} p(\mathbf{x}_{n+1}, \ldots, \mathbf{x}_N, \mathbf{z}_{n+1}|\mathbf{z}_n) \\
&= \sum_{\mathbf{z}_{n+1}} p(\mathbf{x}_{n+1}, \ldots, \mathbf{x}_N|\mathbf{z}_n, \mathbf{z}_{n+1})p(\mathbf{z}_{n+1}|\mathbf{z}_n) \\
&= \sum_{\mathbf{z}_{n+1}} p(\mathbf{x}_{n+1}, \ldots, \mathbf{x}_N|\mathbf{z}_{n+1})p(\mathbf{z}_{n+1}|\mathbf{z}_n) \\
&= \sum_{\mathbf{z}_{n+1}} p(\mathbf{x}_{n+2}, \ldots, \mathbf{x}_N|\mathbf{z}_{n+1})p(\mathbf{x}_{n+1}|\mathbf{z}_{n+1})p(\mathbf{z}_{n+1}|\mathbf{z}_n).
\end{aligned}$$

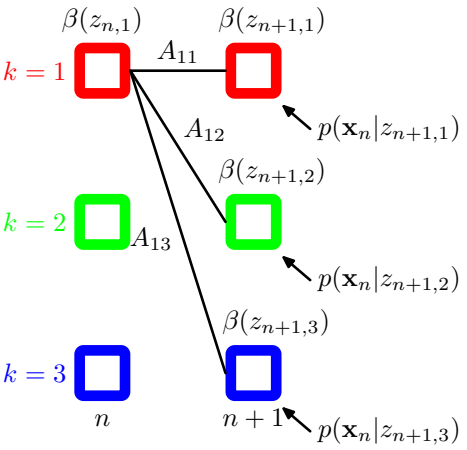

Figure 13.13 Illustration of the backward recursion (13.38) for evaluation of the β variables. In this fragment of the lattice, we see that the quantity $\beta(z_{n1})$ is obtained by taking the components $\beta(z_{n+1,k})$ of $\beta(\mathbf{z}_{n+1})$ at step $n+1$ and summing them up with weights given by the products of A_{1k}, corresponding to the values of $p(\mathbf{z}_{n+1}|\mathbf{z}_n)$ and the corresponding values of the emission density $p(\mathbf{x}_n|z_{n+1,k})$.

Making use of the definition (13.35) for $\beta(\mathbf{z}_n)$, we then obtain

$$\beta(\mathbf{z}_n) = \sum_{\mathbf{z}_{n+1}} \beta(\mathbf{z}_{n+1}) p(\mathbf{x}_{n+1}|\mathbf{z}_{n+1}) p(\mathbf{z}_{n+1}|\mathbf{z}_n). \tag{13.38}$$

Note that in this case we have a backward message passing algorithm that evaluates $\beta(\mathbf{z}_n)$ in terms of $\beta(\mathbf{z}_{n+1})$. At each step, we absorb the effect of observation $\mathbf{x}_{n+1}$ through the emission probability $p(\mathbf{x}_{n+1}|\mathbf{z}_{n+1})$, multiply by the transition matrix $p(\mathbf{z}_{n+1}|\mathbf{z}_n)$, and then marginalize out $\mathbf{z}_{n+1}$. This is illustrated in Figure 13.13.

Again we need a starting condition for the recursion, namely a value for $\beta(\mathbf{z}_N)$. This can be obtained by setting $n = N$ in (13.33) and replacing $\alpha(\mathbf{z}_N)$ with its definition (13.34) to give

$$p(\mathbf{z}_N|\mathbf{X}) = \frac{p(\mathbf{X}, \mathbf{z}_N)\beta(\mathbf{z}_N)}{p(\mathbf{X})} \tag{13.39}$$

which we see will be correct provided we take $\beta(\mathbf{z}_N) = 1$ for all settings of $\mathbf{z}_N$.

In the M step equations, the quantity $p(\mathbf{X})$ will cancel out, as can be seen, for instance, in the M-step equation for $\boldsymbol{\mu}_k$ given by (13.20), which takes the form

$$\boldsymbol{\mu}_k = \frac{\sum_{n=1}^{n} \gamma(z_{nk})\mathbf{x}_n}{\sum_{n=1}^{n} \gamma(z_{nk})} = \frac{\sum_{n=1}^{n} \alpha(z_{nk})\beta(z_{nk})\mathbf{x}_n}{\sum_{n=1}^{n} \alpha(z_{nk})\beta(z_{nk})}. \tag{13.40}$$

However, the quantity $p(\mathbf{X})$ represents the likelihood function whose value we typically wish to monitor during the EM optimization, and so it is useful to be able to evaluate it. If we sum both sides of (13.33) over $\mathbf{z}_n$, and use the fact that the left-hand side is a normalized distribution, we obtain

$$p(\mathbf{X}) = \sum_{\mathbf{z}_n} \alpha(\mathbf{z}_n)\beta(\mathbf{z}_n). \tag{13.41}$$

Thus we can evaluate the likelihood function by computing this sum, for any convenient choice of n. For instance, if we only want to evaluate the likelihood function, then we can do this by running the α recursion from the start to the end of the chain, and then use this result for $n = N$, making use of the fact that $\beta(\mathbf{z}_N)$ is a vector of 1s. In this case no β recursion is required, and we simply have

$$p(\mathbf{X}) = \sum_{\mathbf{z}_N} \alpha(\mathbf{z}_N). \tag{13.42}$$

Let us take a moment to interpret this result for $p(\mathbf{X})$. Recall that to compute the likelihood we should take the joint distribution $p(\mathbf{X}, \mathbf{Z})$ and sum over all possible values of $\mathbf{Z}$. Each such value represents a particular choice of hidden state for every time step, in other words every term in the summation is a path through the lattice diagram, and recall that there are exponentially many such paths. By expressing the likelihood function in the form (13.42), we have reduced the computational cost from being exponential in the length of the chain to being linear by swapping the order of the summation and multiplications, so that at each time step n we sum the contributions from all paths passing through each of the states z_{nk} to give the intermediate quantities $\alpha(\mathbf{z}_n)$.

Next we consider the evaluation of the quantities $\xi(\mathbf{z}_{n-1}, \mathbf{z}_n)$, which correspond to the values of the conditional probabilities $p(\mathbf{z}_{n-1}, \mathbf{z}_n|\mathbf{X})$ for each of the $K \times K$ settings for $(\mathbf{z}_{n-1}, \mathbf{z}_n)$. Using the definition of $\xi(\mathbf{z}_{n-1}, \mathbf{z}_n)$, and applying Bayes' theorem, we have

$$\begin{aligned}
\xi(\mathbf{z}_{n-1}, \mathbf{z}_n) &= p(\mathbf{z}_{n-1}, \mathbf{z}_n|\mathbf{X}) \\
&= \frac{p(\mathbf{X}|\mathbf{z}_{n-1}, \mathbf{z}_n)p(\mathbf{z}_{n-1}, \mathbf{z}_n)}{p(\mathbf{X})} \\
&= \frac{p(\mathbf{x}_1, \ldots, \mathbf{x}_{n-1}|\mathbf{z}_{n-1})p(\mathbf{x}_n|\mathbf{z}_n)p(\mathbf{x}_{n+1}, \ldots, \mathbf{x}_N|\mathbf{z}_n)p(\mathbf{z}_n|\mathbf{z}_{n-1})p(\mathbf{z}_{n-1})}{p(\mathbf{X})} \\
&= \frac{\alpha(\mathbf{z}_{n-1})p(\mathbf{x}_n|\mathbf{z}_n)p(\mathbf{z}_n|\mathbf{z}_{n-1})\beta(\mathbf{z}_n)}{p(\mathbf{X})}
\end{aligned} \tag{13.43}$$

where we have made use of the conditional independence property (13.29) together with the definitions of $\alpha(\mathbf{z}_n)$ and $\beta(\mathbf{z}_n)$ given by (13.34) and (13.35). Thus we can calculate the $\xi(\mathbf{z}_{n-1}, \mathbf{z}_n)$ directly by using the results of the α and β recursions.

Let us summarize the steps required to train a hidden Markov model using the EM algorithm. We first make an initial selection of the parameters $\boldsymbol{\theta}^{\text{old}}$ where $\boldsymbol{\theta} \equiv (\boldsymbol{\pi}, \mathbf{A}, \boldsymbol{\phi})$. The $\mathbf{A}$ and $\boldsymbol{\pi}$ parameters are often initialized either uniformly or randomly from a uniform distribution (respecting their non-negativity and summation constraints). Initialization of the parameters $\boldsymbol{\phi}$ will depend on the form of the distribution. For instance in the case of Gaussians, the parameters $\boldsymbol{\mu}_k$ might be initialized by applying the K-means algorithm to the data, and $\boldsymbol{\Sigma}_k$ might be initialized to the covariance matrix of the corresponding K means cluster. Then we run both the forward α recursion and the backward β recursion and use the results to evaluate $\gamma(\mathbf{z}_n)$ and $\xi(\mathbf{z}_{n-1}, \mathbf{z}_n)$. At this stage, we can also evaluate the likelihood function.

This completes the E step, and we use the results to find a revised set of parameters $\boldsymbol{\theta}^{\text{new}}$ using the M-step equations from Section 13.2.1. We then continue to alternate between E and M steps until some convergence criterion is satisfied, for instance when the change in the likelihood function is below some threshold.

Note that in these recursion relations the observations enter through conditional distributions of the form $p(\mathbf{x}_n|\mathbf{z}_n)$. The recursions are therefore independent of the type or dimensionality of the observed variables or the form of this conditional distribution, so long as its value can be computed for each of the K possible states of $\mathbf{z}_n$. Since the observed variables $\{\mathbf{x}_n\}$ are fixed, the quantities $p(\mathbf{x}_n|\mathbf{z}_n)$ can be pre-computed as functions of $\mathbf{z}_n$ at the start of the EM algorithm, and remain fixed throughout.

We have seen in earlier chapters that the maximum likelihood approach is most effective when the number of data points is large in relation to the number of parameters. Here we note that a hidden Markov model can be trained effectively, using maximum likelihood, provided the training sequence is sufficiently long. Alternatively, we can make use of multiple shorter sequences, which requires a straightforward modification of the hidden Markov model EM algorithm. In the case of left-to-right models, this is particularly important because, in a given observation sequence, a given state transition corresponding to a nondiagonal element of $\mathbf{A}$ will seen at most once.

Exercise 13.12

Another quantity of interest is the predictive distribution, in which the observed data is $\mathbf{X} = \{\mathbf{x}_1, \ldots, \mathbf{x}_N\}$ and we wish to predict $\mathbf{x}_{N+1}$, which would be important for real-time applications such as financial forecasting. Again we make use of the sum and product rules together with the conditional independence properties (13.29) and (13.31) giving

$$\begin{aligned}
p(\mathbf{x}_{N+1}|\mathbf{X}) &= \sum_{\mathbf{z}_{N+1}} p(\mathbf{x}_{N+1}, \mathbf{z}_{N+1}|\mathbf{X}) \\
&= \sum_{\mathbf{z}_{N+1}} p(\mathbf{x}_{N+1}|\mathbf{z}_{N+1}) p(\mathbf{z}_{N+1}|\mathbf{X}) \\
&= \sum_{\mathbf{z}_{N+1}} p(\mathbf{x}_{N+1}|\mathbf{z}_{N+1}) \sum_{\mathbf{z}_N} p(\mathbf{z}_{N+1}, \mathbf{z}_N|\mathbf{X}) \\
&= \sum_{\mathbf{z}_{N+1}} p(\mathbf{x}_{N+1}|\mathbf{z}_{N+1}) \sum_{\mathbf{z}_N} p(\mathbf{z}_{N+1}|\mathbf{z}_N) p(\mathbf{z}_N|\mathbf{X}) \\
&= \sum_{\mathbf{z}_{N+1}} p(\mathbf{x}_{N+1}|\mathbf{z}_{N+1}) \sum_{\mathbf{z}_N} p(\mathbf{z}_{N+1}|\mathbf{z}_N) \frac{p(\mathbf{z}_N, \mathbf{X})}{p(\mathbf{X})} \\
&= \frac{1}{p(\mathbf{X})} \sum_{\mathbf{z}_{N+1}} p(\mathbf{x}_{N+1}|\mathbf{z}_{N+1}) \sum_{\mathbf{z}_N} p(\mathbf{z}_{N+1}|\mathbf{z}_N) \alpha(\mathbf{z}_N) \qquad (13.44)
\end{aligned}$$

which can be evaluated by first running a forward α recursion and then computing the final summations over $\mathbf{z}_N$ and $\mathbf{z}_{N+1}$. The result of the first summation over $\mathbf{z}_N$ can be stored and used once the value of $\mathbf{x}_{N+1}$ is observed in order to run the α recursion forward to the next step in order to predict the subsequent value $\mathbf{x}_{N+2}$.

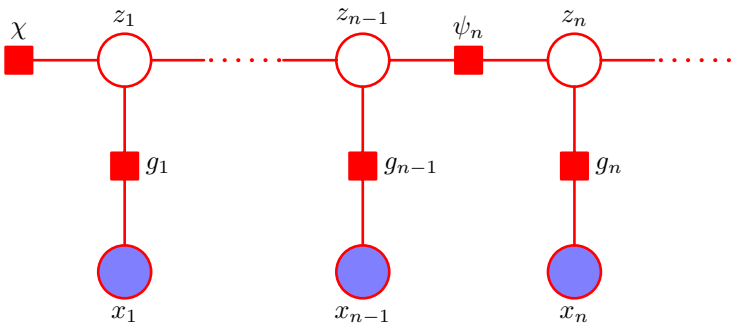

Figure 13.14 A fragment of the factor graph representation for the hidden Markov model.

Note that in (13.44), the influence of all data from $\mathbf{x}_1$ to $\mathbf{x}_N$ is summarized in the K values of $\alpha(\mathbf{z}_N)$. Thus the predictive distribution can be carried forward indefinitely using a fixed amount of storage, as may be required for real-time applications.

Here we have discussed the estimation of the parameters of an HMM using maximum likelihood. This framework is easily extended to regularized maximum likelihood by introducing priors over the model parameters $\boldsymbol{\pi}$, $\mathbf{A}$ and $\boldsymbol{\phi}$ whose values are then estimated by maximizing their posterior probability. This can again be done using the EM algorithm in which the E step is the same as discussed above, and the M step involves adding the log of the prior distribution $p(\boldsymbol{\theta})$ to the function $Q(\boldsymbol{\theta}, \boldsymbol{\theta}^{\text{old}})$ before maximization and represents a straightforward application of the techniques developed at various points in this book. Furthermore, we can use variational methods to give a fully Bayesian treatment of the HMM in which we marginalize over the parameter distributions (MacKay, 1997). As with maximum likelihood, this leads to a two-pass forward-backward recursion to compute posterior probabilities.

Section 10.1

13.2.3 The sum-product algorithm for the HMM

The directed graph that represents the hidden Markov model, shown in Figure 13.5, is a tree and so we can solve the problem of finding local marginals for the hidden variables using the sum-product algorithm. Not surprisingly, this turns out to be equivalent to the forward-backward algorithm considered in the previous section, and so the sum-product algorithm therefore provides us with a simple way to derive the alpha-beta recursion formulae.

Section 8.4.4

We begin by transforming the directed graph of Figure 13.5 into a factor graph, of which a representative fragment is shown in Figure 13.14. This form of the factor graph shows all variables, both latent and observed, explicitly. However, for the purpose of solving the inference problem, we shall always be conditioning on the variables $\mathbf{x}_1, \ldots, \mathbf{x}_N$, and so we can simplify the factor graph by absorbing the emission probabilities into the transition probability factors. This leads to the simplified factor graph representation in Figure 13.15, in which the factors are given by

$$h(\mathbf{z}_1) = p(\mathbf{z}_1)p(\mathbf{x}_1|\mathbf{z}_1) \tag{13.45}$$

$$f_n(\mathbf{z}_{n-1}, \mathbf{z}_n) = p(\mathbf{z}_n|\mathbf{z}_{n-1})p(\mathbf{x}_n|\mathbf{z}_n). \tag{13.46}$$

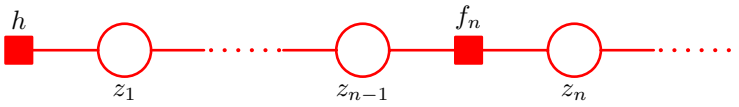

Figure 13.15 A simplified form of factor graph to describe the hidden Markov model.

To derive the alpha-beta algorithm, we denote the final hidden variable $\mathbf{z}_N$ as the root node, and first pass messages from the leaf node h to the root. From the general results (8.66) and (8.69) for message propagation, we see that the messages which are propagated in the hidden Markov model take the form

$$\mu_{\mathbf{z}_{n-1}\to f_n}(\mathbf{z}_{n-1}) = \mu_{f_{n-1}\to\mathbf{z}_{n-1}}(\mathbf{z}_{n-1}) \tag{13.47}$$

$$\mu_{f_n\to\mathbf{z}_n}(\mathbf{z}_n) = \sum_{\mathbf{z}_{n-1}} f_n(\mathbf{z}_{n-1},\mathbf{z}_n)\mu_{\mathbf{z}_{n-1}\to f_n}(\mathbf{z}_{n-1}) \tag{13.48}$$

These equations represent the propagation of messages forward along the chain and are equivalent to the alpha recursions derived in the previous section, as we shall now show. Note that because the variable nodes $\mathbf{z}_n$ have only two neighbours, they perform no computation.

We can eliminate $\mu_{\mathbf{z}_{n-1}\to f_n}(\mathbf{z}_{n-1})$ from (13.48) using (13.47) to give a recursion for the $f \to \mathbf{z}$ messages of the form

$$\mu_{f_n\to\mathbf{z}_n}(\mathbf{z}_n) = \sum_{\mathbf{z}_{n-1}} f_n(\mathbf{z}_{n-1},\mathbf{z}_n)\mu_{f_{n-1}\to\mathbf{z}_{n-1}}(\mathbf{z}_{n-1}). \tag{13.49}$$

If we now recall the definition (13.46), and if we define

$$\alpha(\mathbf{z}_n) = \mu_{f_n\to\mathbf{z}_n}(\mathbf{z}_n) \tag{13.50}$$

then we obtain the alpha recursion given by (13.36). We also need to verify that the quantities $\alpha(\mathbf{z}_n)$ are themselves equivalent to those defined previously. This is easily done by using the initial condition (8.71) and noting that $\alpha(\mathbf{z}_1)$ is given by $h(\mathbf{z}_1) = p(\mathbf{z}_1)p(\mathbf{x}_1|\mathbf{z}_1)$ which is identical to (13.37). Because the initial α is the same, and because they are iteratively computed using the same equation, all subsequent α quantities must be the same.

Next we consider the messages that are propagated from the root node back to the leaf node. These take the form

$$\mu_{f_{n+1}\to f_n}(\mathbf{z}_n) = \sum_{\mathbf{z}_{n+1}} f_{n+1}(\mathbf{z}_n,\mathbf{z}_{n+1})\mu_{f_{n+2}\to f_{n+1}}(\mathbf{z}_{n+1}) \tag{13.51}$$

where, as before, we have eliminated the messages of the type $\mathbf{z} \to f$ since the variable nodes perform no computation. Using the definition (13.46) to substitute for $f_{n+1}(\mathbf{z}_n,\mathbf{z}_{n+1})$, and defining

$$\beta(\mathbf{z}_n) = \mu_{f_{n+1}\to\mathbf{z}_n}(\mathbf{z}_n) \tag{13.52}$$

we obtain the beta recursion given by (13.38). Again, we can verify that the beta variables themselves are equivalent by noting that (8.70) implies that the initial message send by the root variable node is $\mu_{\mathbf{z}_N \to f_N}(\mathbf{z}_N) = 1$, which is identical to the initialization of $\beta(\mathbf{z}_N)$ given in Section 13.2.2.

The sum-product algorithm also specifies how to evaluate the marginals once all the messages have been evaluated. In particular, the result (8.63) shows that the local marginal at the node $\mathbf{z}_n$ is given by the product of the incoming messages. Because we have conditioned on the variables $\mathbf{X} = \{\mathbf{x}_1, \ldots, \mathbf{x}_N\}$, we are computing the joint distribution

$$p(\mathbf{z}_n, \mathbf{X}) = \mu_{f_n \to \mathbf{z}_n}(\mathbf{z}_n)\mu_{f_{n+1} \to \mathbf{z}_n}(\mathbf{z}_n) = \alpha(\mathbf{z}_n)\beta(\mathbf{z}_n). \tag{13.53}$$

Dividing both sides by $p(\mathbf{X})$, we then obtain

$$\gamma(\mathbf{z}_n) = \frac{p(\mathbf{z}_n, \mathbf{X})}{p(\mathbf{X})} = \frac{\alpha(\mathbf{z}_n)\beta(\mathbf{z}_n)}{p(\mathbf{X})} \tag{13.54}$$

Exercise 13.11 in agreement with (13.33). The result (13.43) can similarly be derived from (8.72).

13.2.4 Scaling factors

There is an important issue that must be addressed before we can make use of the forward backward algorithm in practice. From the recursion relation (13.36), we note that at each step the new value $\alpha(\mathbf{z}_n)$ is obtained from the previous value $\alpha(\mathbf{z}_{n-1})$ by multiplying by quantities $p(\mathbf{z}_n|\mathbf{z}_{n-1})$ and $p(\mathbf{x}_n|\mathbf{z}_n)$. Because these probabilities are often significantly less than unity, as we work our way forward along the chain, the values of $\alpha(\mathbf{z}_n)$ can go to zero exponentially quickly. For moderate lengths of chain (say 100 or so), the calculation of the $\alpha(\mathbf{z}_n)$ will soon exceed the dynamic range of the computer, even if double precision floating point is used.

In the case of i.i.d. data, we implicitly circumvented this problem with the evaluation of likelihood functions by taking logarithms. Unfortunately, this will not help here because we are forming sums of products of small numbers (we are in fact implicitly summing over all possible paths through the lattice diagram of Figure 13.7). We therefore work with re-scaled versions of $\alpha(\mathbf{z}_n)$ and $\beta(\mathbf{z}_n)$ whose values remain of order unity. As we shall see, the corresponding scaling factors cancel out when we use these re-scaled quantities in the EM algorithm.

In (13.34), we defined $\alpha(\mathbf{z}_n) = p(\mathbf{x}_1, \ldots, \mathbf{x}_n, \mathbf{z}_n)$ representing the joint distribution of all the observations up to $\mathbf{x}_n$ and the latent variable $\mathbf{z}_n$. Now we define a normalized version of α given by

$$\widehat{\alpha}(\mathbf{z}_n) = p(\mathbf{z}_n|\mathbf{x}_1, \ldots, \mathbf{x}_n) = \frac{\alpha(\mathbf{z}_n)}{p(\mathbf{x}_1, \ldots, \mathbf{x}_n)} \tag{13.55}$$

which we expect to be well behaved numerically because it is a probability distribution over K variables for any value of n. In order to relate the scaled and original alpha variables, we introduce scaling factors defined by conditional distributions over the observed variables

$$c_n = p(\mathbf{x}_n|\mathbf{x}_1, \ldots, \mathbf{x}_{n-1}). \tag{13.56}$$

From the product rule, we then have

$$p(\mathbf{x}_1, \ldots, \mathbf{x}_n) = \prod_{m=1}^{n} c_m \tag{13.57}$$

and so

$$\alpha(\mathbf{z}_n) = p(\mathbf{z}_n|\mathbf{x}_1, \ldots, \mathbf{x}_n)p(\mathbf{x}_1, \ldots, \mathbf{x}_n) = \left(\prod_{m=1}^{n} c_m\right)\widehat{\alpha}(\mathbf{z}_n). \tag{13.58}$$

We can then turn the recursion equation (13.36) for α into one for $\widehat{\alpha}$ given by

$$c_n\widehat{\alpha}(\mathbf{z}_n) = p(\mathbf{x}_n|\mathbf{z}_n)\sum_{\mathbf{z}_{n-1}}\widehat{\alpha}(\mathbf{z}_{n-1})p(\mathbf{z}_n|\mathbf{z}_{n-1}). \tag{13.59}$$

Note that at each stage of the forward message passing phase, used to evaluate $\widehat{\alpha}(\mathbf{z}_n)$, we have to evaluate and store c_n, which is easily done because it is the coefficient that normalizes the right-hand side of (13.59) to give $\widehat{\alpha}(\mathbf{z}_n)$.

We can similarly define re-scaled variables $\widehat{\beta}(\mathbf{z}_n)$ using

$$\beta(\mathbf{z}_n) = \left(\prod_{m=n+1}^{N} c_m\right)\widehat{\beta}(\mathbf{z}_n) \tag{13.60}$$

which will again remain within machine precision because, from (13.35), the quantities $\widehat{\beta}(\mathbf{z}_n)$ are simply the ratio of two conditional probabilities

$$\widehat{\beta}(\mathbf{z}_n) = \frac{p(\mathbf{x}_{n+1}, \ldots, \mathbf{x}_N|\mathbf{z}_n)}{p(\mathbf{x}_{n+1}, \ldots, \mathbf{x}_N|\mathbf{x}_1, \ldots, \mathbf{x}_n)}. \tag{13.61}$$

The recursion result (13.38) for β then gives the following recursion for the re-scaled variables

$$c_{n+1}\widehat{\beta}(\mathbf{z}_n) = \sum_{\mathbf{z}_{n+1}}\widehat{\beta}(\mathbf{z}_{n+1})p(\mathbf{x}_{n+1}|\mathbf{z}_{n+1})p(\mathbf{z}_{n+1}|\mathbf{z}_n). \tag{13.62}$$

In applying this recursion relation, we make use of the scaling factors c_n that were previously computed in the α phase.

From (13.57), we see that the likelihood function can be found using

$$p(\mathbf{X}) = \prod_{n=1}^{N} c_n. \tag{13.63}$$

Similarly, using (13.33) and (13.43), together with (13.63), we see that the required marginals are given by

Exercise 13.15

$$\gamma(\mathbf{z}_n) = \widehat{\alpha}(\mathbf{z}_n)\widehat{\beta}(\mathbf{z}_n) \tag{13.64}$$

$$\xi(\mathbf{z}_{n-1}, \mathbf{z}_n) = c_n\widehat{\alpha}(\mathbf{z}_{n-1})p(\mathbf{x}_n|\mathbf{z}_n)p(\mathbf{z}_n|\mathbf{z}_{-1})\widehat{\beta}(\mathbf{z}_n). \tag{13.65}$$

Finally, we note that there is an alternative formulation of the forward-backward algorithm (Jordan, 2007) in which the backward pass is defined by a recursion based the quantities $\gamma(\mathbf{z}_n) = \widehat{\alpha}(\mathbf{z}_n)\widehat{\beta}(\mathbf{z}_n)$ instead of using $\widehat{\beta}(\mathbf{z}_n)$. This α–γ recursion requires that the forward pass be completed first so that all the quantities $\widehat{\alpha}(\mathbf{z}_n)$ are available for the backward pass, whereas the forward and backward passes of the α–β algorithm can be done independently. Although these two algorithms have comparable computational cost, the α–β version is the most commonly encountered one in the case of hidden Markov models, whereas for linear dynamical systems a recursion analogous to the α–γ form is more usual.

Section 13.3

13.2.5 The Viterbi algorithm

In many applications of hidden Markov models, the latent variables have some meaningful interpretation, and so it is often of interest to find the most probable sequence of hidden states for a given observation sequence. For instance in speech recognition, we might wish to find the most probable phoneme sequence for a given series of acoustic observations. Because the graph for the hidden Markov model is a directed tree, this problem can be solved exactly using the max-sum algorithm. We recall from our discussion in Section 8.4.5 that the problem of finding the most probable sequence of latent states is not the same as that of finding the set of states that are individually the most probable. The latter problem can be solved by first running the forward-backward (sum-product) algorithm to find the latent variable marginals $\gamma(\mathbf{z}_n)$ and then maximizing each of these individually (Duda *et al.*, 2001). However, the set of such states will not, in general, correspond to the most probable sequence of states. In fact, this set of states might even represent a sequence having zero probability, if it so happens that two successive states, which in isolation are individually the most probable, are such that the transition matrix element connecting them is zero.

In practice, we are usually interested in finding the most probable *sequence* of states, and this can be solved efficiently using the max-sum algorithm, which in the context of hidden Markov models is known as the *Viterbi* algorithm (Viterbi, 1967). Note that the max-sum algorithm works with log probabilities and so there is no need to use re-scaled variables as was done with the forward-backward algorithm. Figure 13.16 shows a fragment of the hidden Markov model expanded as lattice diagram. As we have already noted, the number of possible paths through the lattice grows exponentially with the length of the chain. The Viterbi algorithm searches this space of paths efficiently to find the most probable path with a computational cost that grows only linearly with the length of the chain.

As with the sum-product algorithm, we first represent the hidden Markov model as a factor graph, as shown in Figure 13.15. Again, we treat the variable node $\mathbf{z}_N$ as the root, and pass messages to the root starting with the leaf nodes. Using the results (8.93) and (8.94), we see that the messages passed in the max-sum algorithm are given by

$$\mu_{\mathbf{z}_n \to f_{n+1}}(\mathbf{z}_n) = \mu_{f_n \to \mathbf{z}_n}(\mathbf{z}_n) \tag{13.66}$$

$$\mu_{f_{n+1} \to \mathbf{z}_{n+1}}(\mathbf{z}_{n+1}) = \max_{\mathbf{z}_n} \left\{ \ln f_{n+1}(\mathbf{z}_n, \mathbf{z}_{n+1}) + \mu_{\mathbf{z}_n \to f_{n+1}}(\mathbf{z}_n) \right\}. \tag{13.67}$$

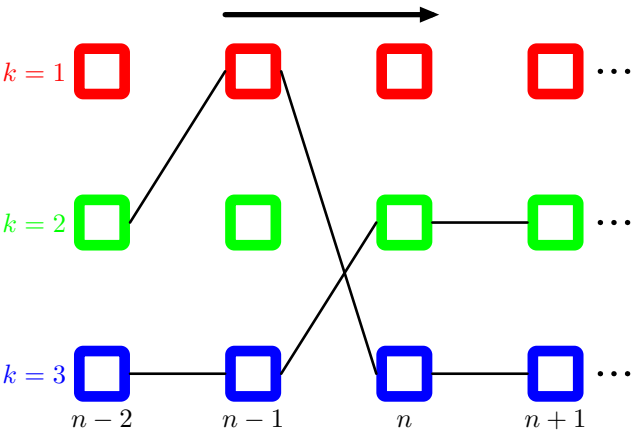

Figure 13.16 A fragment of the HMM lattice showing two possible paths. The Viterbi algorithm efficiently determines the most probable path from amongst the exponentially many possibilities. For any given path, the corresponding probability is given by the product of the elements of the transition matrix A_{jk}, corresponding to the probabilities $p(\mathbf{z}_{n+1}|\mathbf{z}_n)$ for each segment of the path, along with the emission densities $p(\mathbf{x}_n|k)$ associated with each node on the path.

If we eliminate $\mu_{\mathbf{z}_n \to f_{n+1}}(\mathbf{z}_n)$ between these two equations, and make use of (13.46), we obtain a recursion for the $f \to \mathbf{z}$ messages of the form

$$\omega(\mathbf{z}_{n+1}) = \ln p(\mathbf{x}_{n+1}|\mathbf{z}_{n+1}) + \max_{\mathbf{z}_n} \{\ln p(\mathbf{x}_{+1}|\mathbf{z}_n) + \omega(\mathbf{z}_n)\} \tag{13.68}$$

where we have introduced the notation $\omega(\mathbf{z}_n) \equiv \mu_{f_n \to \mathbf{z}_n}(\mathbf{z}_n)$.

From (8.95) and (8.96), these messages are initialized using

$$\omega(\mathbf{z}_1) = \ln p(\mathbf{z}_1) + \ln p(\mathbf{x}_1|\mathbf{z}_1). \tag{13.69}$$

where we have used (13.45). Note that to keep the notation uncluttered, we omit the dependence on the model parameters $\boldsymbol{\theta}$ that are held fixed when finding the most probable sequence.

The Viterbi algorithm can also be derived directly from the definition (13.6) of the joint distribution by taking the logarithm and then exchanging maximizations and summations. It is easily seen that the quantities $\omega(\mathbf{z}_n)$ have the probabilistic interpretation

Exercise 13.16

$$\omega(\mathbf{z}_n) = \max_{\mathbf{z}_1,\ldots,\mathbf{z}_{n-1}} p(\mathbf{x}_1,\ldots,\mathbf{x}_n,\mathbf{z}_1,\ldots,\mathbf{z}_n). \tag{13.70}$$

Once we have completed the final maximization over $\mathbf{z}_N$, we will obtain the value of the joint distribution $p(\mathbf{X},\mathbf{Z})$ corresponding to the most probable path. We also wish to find the sequence of latent variable values that corresponds to this path. To do this, we simply make use of the back-tracking procedure discussed in Section 8.4.5. Specifically, we note that the maximization over $\mathbf{z}_n$ must be performed for each of the K possible values of $\mathbf{z}_{n+1}$. Suppose we keep a record of the values of $\mathbf{z}_n$ that correspond to the maxima for each value of the K values of $\mathbf{z}_{n+1}$. Let us denote this function by $\psi(k_n)$ where $k \in \{1,\ldots,K\}$. Once we have passed messages to the end of the chain and found the most probable state of $\mathbf{z}_N$, we can then use this function to backtrack along the chain by applying it recursively

$$k_n^{\max} = \psi(k_{n+1}^{\max}). \tag{13.71}$$

Intuitively, we can understand the Viterbi algorithm as follows. Naively, we could consider explicitly all of the exponentially many paths through the lattice, evaluate the probability for each, and then select the path having the highest probability. However, we notice that we can make a dramatic saving in computational cost as follows. Suppose that for each path we evaluate its probability by summing up products of transition and emission probabilities as we work our way forward along each path through the lattice. Consider a particular time step n and a particular state k at that time step. There will be many possible paths converging on the corresponding node in the lattice diagram. However, we need only retain that particular path that so far has the highest probability. Because there are K states at time step n, we need to keep track of K such paths. At time step $n + 1$, there will be K^2 possible paths to consider, comprising K possible paths leading out of each of the K current states, but again we need only retain K of these corresponding to the best path for each state at time $n+1$. When we reach the final time step N we will discover which state corresponds to the overall most probable path. Because there is a unique path coming into that state we can trace the path back to step $N - 1$ to see what state it occupied at that time, and so on back through the lattice to the state $n = 1$.

13.2.6 Extensions of the hidden Markov model

The basic hidden Markov model, along with the standard training algorithm based on maximum likelihood, has been extended in numerous ways to meet the requirements of particular applications. Here we discuss a few of the more important examples.

We see from the digits example in Figure 13.11 that hidden Markov models can be quite poor generative models for the data, because many of the synthetic digits look quite unrepresentative of the training data. If the goal is sequence classification, there can be significant benefit in determining the parameters of hidden Markov models using discriminative rather than maximum likelihood techniques. Suppose we have a training set of R observation sequences $\mathbf{X}_r$, where $r = 1, \ldots, R$, each of which is labelled according to its class m, where $m = 1, \ldots, M$. For each class, we have a separate hidden Markov model with its own parameters $\boldsymbol{\theta}_m$, and we treat the problem of determining the parameter values as a standard classification problem in which we optimize the cross-entropy

$$\sum_{r=1}^{R} \ln p(m_r|\mathbf{X}_r). \tag{13.72}$$

Using Bayes' theorem this can be expressed in terms of the sequence probabilities associated with the hidden Markov models

$$\sum_{r=1}^{R} \ln \left\{ \frac{p(\mathbf{X}_r|\boldsymbol{\theta}_r)p(m_r)}{\sum_{l=1}^{M} p(\mathbf{X}_r|\boldsymbol{\theta}_l)p(l_r)} \right\} \tag{13.73}$$

where $p(m)$ is the prior probability of class m. Optimization of this cost function is more complex than for maximum likelihood (Kapadia, 1998), and in particular

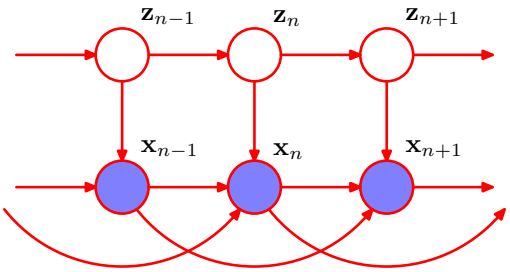

Figure 13.17 Section of an autoregressive hidden Markov model, in which the distribution of the observation $\mathbf{x}_n$ depends on a subset of the previous observations as well as on the hidden state $\mathbf{z}_n$. In this example, the distribution of $\mathbf{x}_n$ depends on the two previous observations $\mathbf{x}_{n-1}$ and $\mathbf{x}_{n-2}$.

requires that every training sequence be evaluated under each of the models in order to compute the denominator in (13.73). Hidden Markov models, coupled with discriminative training methods, are widely used in speech recognition (Kapadia, 1998).

A significant weakness of the hidden Markov model is the way in which it represents the distribution of times for which the system remains in a given state. To see the problem, note that the probability that a sequence sampled from a given hidden Markov model will spend precisely T steps in state k and then make a transition to a different state is given by

$$p(T) = (A_{kk})^T(1 - A_{kk}) \propto \exp\left(-T \ln A_{kk}\right) \tag{13.74}$$

and so is an exponentially decaying function of T. For many applications, this will be a very unrealistic model of state duration. The problem can be resolved by modelling state duration directly in which the diagonal coefficients A_{kk} are all set to zero, and each state k is explicitly associated with a probability distribution $p(T|k)$ of possible duration times. From a generative point of view, when a state k is entered, a value T representing the number of time steps that the system will remain in state k is then drawn from $p(T|k)$. The model then emits T values of the observed variable $\mathbf{x}_t$, which are generally assumed to be independent so that the corresponding emission density is simply $\prod_{t=1}^{T} p(\mathbf{x}_t|k)$. This approach requires some straightforward modifications to the EM optimization procedure (Rabiner, 1989).

Another limitation of the standard HMM is that it is poor at capturing long-range correlations between the observed variables (i.e., between variables that are separated by many time steps) because these must be mediated via the first-order Markov chain of hidden states. Longer-range effects could in principle be included by adding extra links to the graphical model of Figure 13.5. One way to address this is to generalize the HMM to give the *autoregressive hidden Markov model* (Ephraim *et al.*, 1989), an example of which is shown in Figure 13.17. For discrete observations, this corresponds to expanded tables of conditional probabilities for the emission distributions. In the case of a Gaussian emission density, we can use the linear-Gaussian framework in which the conditional distribution for $\mathbf{x}_n$ given the values of the previous observations, and the value of $\mathbf{z}_n$, is a Gaussian whose mean is a linear combination of the values of the conditioning variables. Clearly the number of additional links in the graph must be limited to avoid an excessive the number of free parameters. In the example shown in Figure 13.17, each observation depends on

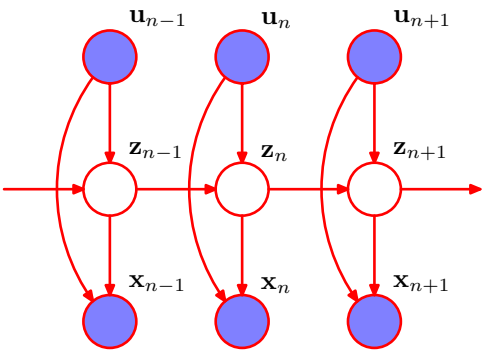

Figure 13.18 Example of an input-output hidden Markov model. In this case, both the emission probabilities and the transition probabilities depend on the values of a sequence of observations $\mathbf{u}_1, \ldots, \mathbf{u}_N$.

the two preceding observed variables as well as on the hidden state. Although this graph looks messy, we can again appeal to d-separation to see that in fact it still has a simple probabilistic structure. In particular, if we imagine conditioning on $\mathbf{z}_n$ we see that, as with the standard HMM, the values of $\mathbf{z}_{n-1}$ and $\mathbf{z}_{n+1}$ are independent, corresponding to the conditional independence property (13.5). This is easily verified by noting that every path from node $\mathbf{z}_{n-1}$ to node $\mathbf{z}_{n+1}$ passes through at least one observed node that is head-to-tail with respect to that path. As a consequence, we can again use a forward-backward recursion in the E step of the EM algorithm to determine the posterior distributions of the latent variables in a computational time that is linear in the length of the chain. Similarly, the M step involves only a minor modification of the standard M-step equations. In the case of Gaussian emission densities this involves estimating the parameters using the standard linear regression equations, discussed in Chapter 3.

We have seen that the autoregressive HMM appears as a natural extension of the standard HMM when viewed as a graphical model. In fact the probabilistic graphical modelling viewpoint motivates a plethora of different graphical structures based on the HMM. Another example is the *input-output* hidden Markov model (Bengio and Frasconi, 1995), in which we have a sequence of observed variables $\mathbf{u}_1, \ldots, \mathbf{u}_N$, in addition to the output variables $\mathbf{x}_1, \ldots, \mathbf{x}_N$, whose values influence either the distribution of latent variables or output variables, or both. An example is shown in Figure 13.18. This extends the HMM framework to the domain of supervised learning for sequential data. It is again easy to show, through the use of the d-separation criterion, that the Markov property (13.5) for the chain of latent variables still holds. To verify this, simply note that there is only one path from node $\mathbf{z}_{n-1}$ to node $\mathbf{z}_{n+1}$ and this is head-to-tail with respect to the observed node $\mathbf{z}_n$. This conditional independence property again allows the formulation of a computationally efficient learning algorithm. In particular, we can determine the parameters $\boldsymbol{\theta}$ of the model by maximizing the likelihood function $L(\boldsymbol{\theta}) = p(\mathbf{X}|\mathbf{U}, \boldsymbol{\theta})$ where $\mathbf{U}$ is a matrix whose rows are given by $\mathbf{u}_n^{\mathrm{T}}$. As a consequence of the conditional independence property (13.5) this likelihood function can be maximized efficiently using an EM algorithm in which the E step involves forward and backward recursions.

Exercise 13.18

Another variant of the HMM worthy of mention is the *factorial hidden Markov model* (Ghahramani and Jordan, 1997), in which there are multiple independent

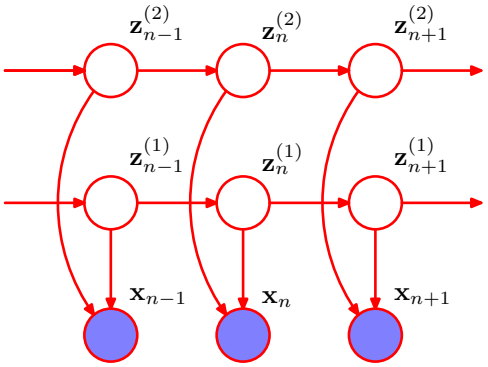

Figure 13.19 A factorial hidden Markov model comprising two Markov chains of latent variables. For continuous observed variables $\mathbf{x}$, one possible choice of emission model is a linear-Gaussian density in which the mean of the Gaussian is a linear combination of the states of the corresponding latent variables.

Markov chains of latent variables, and the distribution of the observed variable at a given time step is conditional on the states of all of the corresponding latent variables at that same time step. Figure 13.19 shows the corresponding graphical model. The motivation for considering factorial HMM can be seen by noting that in order to represent, say, 10 bits of information at a given time step, a standard HMM would need $K = 2^{10} = 1024$ latent states, whereas a factorial HMM could make use of 10 binary latent chains. The primary disadvantage of factorial HMMs, however, lies in the additional complexity of training them. The M step for the factorial HMM model is straightforward. However, observation of the $\mathbf{x}$ variables introduces dependencies between the latent chains, leading to difficulties with the E step. This can be seen by noting that in Figure 13.19, the variables $\mathbf{z}_n^{(1)}$ and $\mathbf{z}_n^{(2)}$ are connected by a path which is head-to-head at node $\mathbf{x}_n$ and hence they are not d-separated. The exact E step for this model does *not* correspond to running forward and backward recursions along the M Markov chains independently. This is confirmed by noting that the key conditional independence property (13.5) is not satisfied for the individual Markov chains in the factorial HMM model, as is shown using d-separation in Figure 13.20. Now suppose that there are M chains of hidden nodes and for simplicity suppose that all latent variables have the same number K of states. Then one approach would be to note that there are K^M combinations of latent variables at a given time step

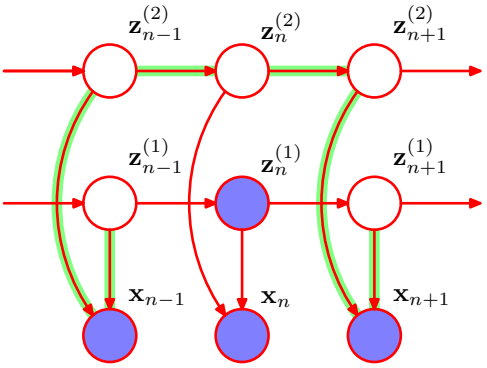

Figure 13.20 Example of a path, highlighted in green, which is head-to-head at the observed nodes $\mathbf{x}_{n-1}$ and $\mathbf{x}_{n+1}$, and head-to-tail at the unobserved nodes $\mathbf{z}_{n-1}^{(2)}$, $\mathbf{z}_n^{(2)}$ and $\mathbf{z}_{n+1}^{(2)}$. Thus the path is not blocked and so the conditional independence property (13.5) does not hold for the individual latent chains of the factorial HMM model. As a consequence, there is no efficient exact E step for this model.

and so we can transform the model into an equivalent standard HMM having a single chain of latent variables each of which has K^M latent states. We can then run the standard forward-backward recursions in the E step. This has computational complexity $O(NK^{2M})$ that is exponential in the number M of latent chains and so will be intractable for anything other than small values of M. One solution would be to use sampling methods (discussed in Chapter 11). As an elegant deterministic alternative, Ghahramani and Jordan (1997) exploited variational inference techniques to obtain a tractable algorithm for approximate inference. This can be done using a simple variational posterior distribution that is fully factorized with respect to the latent variables, or alternatively by using a more powerful approach in which the variational distribution is described by independent Markov chains corresponding to the chains of latent variables in the original model. In the latter case, the variational inference algorithms involves running independent forward and backward recursions along each chain, which is computationally efficient and yet is also able to capture correlations between variables within the same chain.

Section 10.1

Clearly, there are many possible probabilistic structures that can be constructed according to the needs of particular applications. Graphical models provide a general technique for motivating, describing, and analysing such structures, and variational methods provide a powerful framework for performing inference in those models for which exact solution is intractable.

13.3. Linear Dynamical Systems

In order to motivate the concept of linear dynamical systems, let us consider the following simple problem, which often arises in practical settings. Suppose we wish to measure the value of an unknown quantity $\mathbf{z}$ using a noisy sensor that returns a observation $\mathbf{x}$ representing the value of $\mathbf{z}$ plus zero-mean Gaussian noise. Given a single measurement, our best guess for $\mathbf{z}$ is to assume that $\mathbf{z} = \mathbf{x}$. However, we can improve our estimate for $\mathbf{z}$ by taking lots of measurements and averaging them, because the random noise terms will tend to cancel each other. Now let's make the situation more complicated by assuming that we wish to measure a quantity $\mathbf{z}$ that is changing over time. We can take regular measurements of $\mathbf{x}$ so that at some point in time we have obtained $\mathbf{x}_1, \ldots, \mathbf{x}_N$ and we wish to find the corresponding values $\mathbf{z}_1, \ldots, \mathbf{x}_N$. If we simply average the measurements, the error due to random noise will be reduced, but unfortunately we will just obtain a single averaged estimate, in which we have averaged over the changing value of $\mathbf{z}$, thereby introducing a new source of error.

Intuitively, we could imagine doing a bit better as follows. To estimate the value of $\mathbf{z}_N$, we take only the most recent few measurements, say $\mathbf{x}_{N-L}, \ldots, \mathbf{x}_N$ and just average these. If $\mathbf{z}$ is changing slowly, and the random noise level in the sensor is high, it would make sense to choose a relatively long window of observations to average. Conversely, if the signal is changing quickly, and the noise levels are small, we might be better just to use $\mathbf{x}_N$ directly as our estimate of $\mathbf{z}_N$. Perhaps we could do even better if we take a weighted average, in which more recent measurements

make a greater contribution than less recent ones.

Although this sort of intuitive argument seems plausible, it does not tell us how to form a weighted average, and any sort of hand-crafted weighing is hardly likely to be optimal. Fortunately, we can address problems such as this much more systematically by defining a probabilistic model that captures the time evolution and measurement processes and then applying the inference and learning methods developed in earlier chapters. Here we shall focus on a widely used model known as a *linear dynamical system*.

As we have seen, the HMM corresponds to the state space model shown in Figure 13.5 in which the latent variables are discrete but with arbitrary emission probability distributions. This graph of course describes a much broader class of probability distributions, all of which factorize according to (13.6). We now consider extensions to other distributions for the latent variables. In particular, we consider continuous latent variables in which the summations of the sum-product algorithm become integrals. The general form of the inference algorithms will, however, be the same as for the hidden Markov model. It is interesting to note that, historically, hidden Markov models and linear dynamical systems were developed independently. Once they are both expressed as graphical models, however, the deep relationship between them immediately becomes apparent.

One key requirement is that we retain an efficient algorithm for inference which is linear in the length of the chain. This requires that, for instance, when we take a quantity $\widehat{\alpha}(\mathbf{z}_{n-1})$, representing the posterior probability of $\mathbf{z}_n$ given observations $\mathbf{x}_1, \ldots, \mathbf{x}_n$, and multiply by the transition probability $p(\mathbf{z}_n|\mathbf{z}_{n-1})$ and the emission probability $p(\mathbf{x}_n|\mathbf{z}_n)$ and then marginalize over $\mathbf{z}_{n-1}$, we obtain a distribution over $\mathbf{z}_n$ that is of the same functional form as that over $\widehat{\alpha}(\mathbf{z}_{n-1})$. That is to say, the distribution must not become more complex at each stage, but must only change in its parameter values. Not surprisingly, the only distributions that have this property of being closed under multiplication are those belonging to the exponential family.

Here we consider the most important example from a practical perspective, which is the Gaussian. In particular, we consider a linear-Gaussian state space model so that the latent variables $\{\mathbf{z}_n\}$, as well as the observed variables $\{\mathbf{x}_n\}$, are multivariate Gaussian distributions whose means are linear functions of the states of their parents in the graph. We have seen that a directed graph of linear-Gaussian units is equivalent to a joint Gaussian distribution over all of the variables. Furthermore, marginals such as $\widehat{\alpha}(\mathbf{z}_n)$ are also Gaussian, so that the functional form of the messages is preserved and we will obtain an efficient inference algorithm. By contrast, suppose that the emission densities $p(\mathbf{x}_n|\mathbf{z}_n)$ comprise a mixture of K Gaussians each of which has a mean that is linear in $\mathbf{z}_n$. Then even if $\widehat{\alpha}(\mathbf{z}_1)$ is Gaussian, the quantity $\widehat{\alpha}(\mathbf{z}_2)$ will be a mixture of K Gaussians, $\widehat{\alpha}(\mathbf{z}_3)$ will be a mixture of K^2 Gaussians, and so on, and exact inference will not be of practical value.

We have seen that the hidden Markov model can be viewed as an extension of the mixture models of Chapter 9 to allow for sequential correlations in the data. In a similar way, we can view the linear dynamical system as a generalization of the continuous latent variable models of Chapter 12 such as probabilistic PCA and factor analysis. Each pair of nodes $\{\mathbf{z}_n, \mathbf{x}_n\}$ represents a linear-Gaussian latent variable

model for that particular observation. However, the latent variables $\{\mathbf{z}_n\}$ are no longer treated as independent but now form a Markov chain.

Because the model is represented by a tree-structured directed graph, inference problems can be solved efficiently using the sum-product algorithm. The forward recursions, analogous to the α messages of the hidden Markov model, are known as the *Kalman filter* equations (Kalman, 1960; Zarchan and Musoff, 2005), and the backward recursions, analogous to the β messages, are known as the *Kalman smoother* equations, or the *Rauch-Tung-Striebel* (RTS) equations (Rauch *et al.*, 1965). The Kalman filter is widely used in many real-time tracking applications.

Because the linear dynamical system is a linear-Gaussian model, the joint distribution over all variables, as well as all marginals and conditionals, will be Gaussian. It follows that the sequence of individually most probable latent variable values is the same as the most probable latent sequence. There is thus no need to consider the analogue of the Viterbi algorithm for the linear dynamical system.

Exercise 13.19

Because the model has linear-Gaussian conditional distributions, we can write the transition and emission distributions in the general form

$$p(\mathbf{z}_n|\mathbf{z}_{n-1}) = \mathcal{N}(\mathbf{z}_n|\mathbf{A}\mathbf{z}_{n-1}, \boldsymbol{\Gamma}) \tag{13.75}$$

$$p(\mathbf{x}_n|\mathbf{z}_n) = \mathcal{N}(\mathbf{x}_n|\mathbf{C}\mathbf{z}_n, \boldsymbol{\Sigma}). \tag{13.76}$$

The initial latent variable also has a Gaussian distribution which we write as

$$p(\mathbf{z}_1) = \mathcal{N}(\mathbf{z}_1|\boldsymbol{\mu}_0, \mathbf{V}_0). \tag{13.77}$$

Note that in order to simplify the notation, we have omitted additive constant terms from the means of the Gaussians. In fact, it is straightforward to include them if desired. Traditionally, these distributions are more commonly expressed in an equivalent form in terms of noisy linear equations given by

Exercise 13.24

$$\mathbf{z}_n = \mathbf{A}\mathbf{z}_{n-1} + \mathbf{w}_n \tag{13.78}$$

$$\mathbf{x}_n = \mathbf{C}\mathbf{z}_n + \mathbf{v}_n \tag{13.79}$$

$$\mathbf{z}_1 = \boldsymbol{\mu}_0 + \mathbf{u} \tag{13.80}$$

where the noise terms have the distributions

$$\mathbf{w} \sim \mathcal{N}(\mathbf{w}|\mathbf{0}, \boldsymbol{\Gamma}) \tag{13.81}$$

$$\mathbf{v} \sim \mathcal{N}(\mathbf{v}|\mathbf{0}, \boldsymbol{\Sigma}) \tag{13.82}$$

$$\mathbf{u} \sim \mathcal{N}(\mathbf{u}|\mathbf{0}, \mathbf{V}_0). \tag{13.83}$$

The parameters of the model, denoted by $\boldsymbol{\theta} = \{\mathbf{A}, \boldsymbol{\Gamma}, \mathbf{C}, \boldsymbol{\Sigma}, \boldsymbol{\mu}_0, \mathbf{V}_0\}$, can be determined using maximum likelihood through the EM algorithm. In the E step, we need to solve the inference problem of determining the local posterior marginals for the latent variables, which can be solved efficiently using the sum-product algorithm, as we discuss in the next section.

13.3.1 Inference in LDS

We now turn to the problem of finding the marginal distributions for the latent variables conditional on the observation sequence. For given parameter settings, we also wish to make predictions of the next latent state $\mathbf{z}_n$ and of the next observation $\mathbf{x}_n$ conditioned on the observed data $\mathbf{x}_1, \ldots, \mathbf{x}_{n-1}$ for use in real-time applications. These inference problems can be solved efficiently using the sum-product algorithm, which in the context of the linear dynamical system gives rise to the Kalman filter and Kalman smoother equations.

It is worth emphasizing that because the linear dynamical system is a linear-Gaussian model, the joint distribution over all latent and observed variables is simply a Gaussian, and so in principle we could solve inference problems by using the standard results derived in previous chapters for the marginals and conditionals of a multivariate Gaussian. The role of the sum-product algorithm is to provide a more efficient way to perform such computations.

Linear dynamical systems have the identical factorization, given by (13.6), to hidden Markov models, and are again described by the factor graphs in Figures 13.14 and 13.15. Inference algorithms therefore take precisely the same form except that summations over latent variables are replaced by integrations. We begin by considering the forward equations in which we treat $\mathbf{z}_N$ as the root node, and propagate messages from the leaf node $h(\mathbf{z}_1)$ to the root. From (13.77), the initial message will be Gaussian, and because each of the factors is Gaussian, all subsequent messages will also be Gaussian. By convention, we shall propagate messages that are normalized marginal distributions corresponding to $p(\mathbf{z}_n|\mathbf{x}_1, \ldots, \mathbf{x}_n)$, which we denote by

$$\widehat{\alpha}(\mathbf{z}_n) = \mathcal{N}(\mathbf{z}_n|\boldsymbol{\mu}_n, \mathbf{V}_n). \tag{13.84}$$

This is precisely analogous to the propagation of scaled variables $\widehat{\alpha}(\mathbf{z}_n)$ given by (13.59) in the discrete case of the hidden Markov model, and so the recursion equation now takes the form

$$c_n\widehat{\alpha}(\mathbf{z}_n) = p(\mathbf{x}_n|\mathbf{z}_n) \int \widehat{\alpha}(\mathbf{z}_{n-1})p(\mathbf{z}_n|\mathbf{z}_{n-1})\,\mathrm{d}\mathbf{z}_{n-1}. \tag{13.85}$$

Substituting for the conditionals $p(\mathbf{z}_n|\mathbf{z}_{n-1})$ and $p(\mathbf{x}_n|\mathbf{z}_n)$, using (13.75) and (13.76), respectively, and making use of (13.84), we see that (13.85) becomes

$$\begin{aligned} c_n\mathcal{N}(\mathbf{z}_n|\boldsymbol{\mu}_n, \mathbf{V}_n) &= \mathcal{N}(\mathbf{x}_n|\mathbf{C}\mathbf{z}_n, \boldsymbol{\Sigma}) \\ &\int \mathcal{N}(\mathbf{z}_n|\mathbf{A}\mathbf{z}_{n-1}, \boldsymbol{\Gamma})\mathcal{N}(\mathbf{z}_{n-1}|\boldsymbol{\mu}_{n-1}, \mathbf{V}_{n-1})\,\mathrm{d}\mathbf{z}_{n-1}. \end{aligned} \tag{13.86}$$

Here we are supposing that $\boldsymbol{\mu}_{n-1}$ and $\mathbf{V}_{n-1}$ are known, and by evaluating the integral in (13.86), we wish to determine values for $\boldsymbol{\mu}_n$ and $\mathbf{V}_n$. The integral is easily evaluated by making use of the result (2.115), from which it follows that

$$\begin{aligned} &\int \mathcal{N}(\mathbf{z}_n|\mathbf{A}\mathbf{z}_{n-1}, \boldsymbol{\Gamma})\mathcal{N}(\mathbf{z}_{n-1}|\boldsymbol{\mu}_{n-1}, \mathbf{V}_{n-1})\,\mathrm{d}\mathbf{z}_{n-1} \\ &\qquad = \mathcal{N}(\mathbf{z}_n|\mathbf{A}\boldsymbol{\mu}_{n-1}, \mathbf{P}_{n-1}) \end{aligned} \tag{13.87}$$

where we have defined

$$\mathbf{P}_{n-1} = \mathbf{A}\mathbf{V}_{n-1}\mathbf{A}^{\mathrm{T}} + \boldsymbol{\Gamma}. \tag{13.88}$$

We can now combine this result with the first factor on the right-hand side of (13.86) by making use of (2.115) and (2.116) to give

$$\begin{aligned}
\boldsymbol{\mu}_n &= \mathbf{A}\boldsymbol{\mu}_{n-1} + \mathbf{K}_n(\mathbf{x}_n - \mathbf{C}\mathbf{A}\boldsymbol{\mu}_{n-1}) && (13.89)\\
\mathbf{V}_n &= (\mathbf{I} - \mathbf{K}_n\mathbf{C})\mathbf{P}_{n-1} && (13.90)\\
c_n &= \mathcal{N}(\mathbf{x}_n|\mathbf{C}\mathbf{A}\boldsymbol{\mu}_{n-1}, \mathbf{C}\mathbf{P}_{n-1}\mathbf{C}^{\mathrm{T}} + \boldsymbol{\Sigma}). && (13.91)
\end{aligned}$$

Here we have made use of the matrix inverse identities (C.5) and (C.7) and also defined the *Kalman gain matrix*

$$\mathbf{K}_n = \mathbf{P}_{n-1}\mathbf{C}^{\mathrm{T}}\left(\mathbf{C}\mathbf{P}_{n-1}\mathbf{C}^{\mathrm{T}} + \boldsymbol{\Sigma}\right)^{-1}. \tag{13.92}$$

Thus, given the values of $\boldsymbol{\mu}_{n-1}$ and $\mathbf{V}_{n-1}$, together with the new observation $\mathbf{x}_n$, we can evaluate the Gaussian marginal for $\mathbf{z}_n$ having mean $\boldsymbol{\mu}_n$ and covariance $\mathbf{V}_n$, as well as the normalization coefficient c_n.

The initial conditions for these recursion equations are obtained from

$$c_1\widehat{\alpha}(\mathbf{z}_1) = p(\mathbf{z}_1)p(\mathbf{x}_1|\mathbf{z}_1). \tag{13.93}$$

Because $p(\mathbf{z}_1)$ is given by (13.77), and $p(\mathbf{x}_1|\mathbf{z}_1)$ is given by (13.76), we can again make use of (2.115) to calculate c_1 and (2.116) to calculate $\boldsymbol{\mu}_1$ and $\mathbf{V}_1$ giving

$$\begin{aligned}
\boldsymbol{\mu}_1 &= \boldsymbol{\mu}_0 + \mathbf{K}_1(\mathbf{x}_1 - \mathbf{C}\boldsymbol{\mu}_0) && (13.94)\\
\mathbf{V}_1 &= (\mathbf{I} - \mathbf{K}_1\mathbf{C})\mathbf{V}_0 && (13.95)\\
c_1 &= \mathcal{N}(\mathbf{x}_1|\mathbf{C}\boldsymbol{\mu}_0, \mathbf{C}\mathbf{V}_0\mathbf{C}^{\mathrm{T}} + \boldsymbol{\Sigma}) && (13.96)
\end{aligned}$$

where

$$\mathbf{K}_1 = \mathbf{V}_0\mathbf{C}^{\mathrm{T}}\left(\mathbf{C}\mathbf{V}_0\mathbf{C}^{\mathrm{T}} + \boldsymbol{\Sigma}\right)^{-1}. \tag{13.97}$$

Similarly, the likelihood function for the linear dynamical system is given by (13.63) in which the factors c_n are found using the Kalman filtering equations.

We can interpret the steps involved in going from the posterior marginal over $\mathbf{z}_{n-1}$ to the posterior marginal over $\mathbf{z}_n$ as follows. In (13.89), we can view the quantity $\mathbf{A}\boldsymbol{\mu}_{n-1}$ as the prediction of the mean over $\mathbf{z}_n$ obtained by simply taking the mean over $\mathbf{z}_{n-1}$ and projecting it forward one step using the transition probability matrix $\mathbf{A}$. This predicted mean would give a predicted observation for $\mathbf{x}_n$ given by $\mathbf{C}\mathbf{A}\mathbf{z}_{n-1}$ obtained by applying the emission probability matrix $\mathbf{C}$ to the predicted hidden state mean. We can view the update equation (13.89) for the mean of the hidden variable distribution as taking the predicted mean $\mathbf{A}\boldsymbol{\mu}_{n-1}$ and then adding a correction that is proportional to the error $\mathbf{x}_n - \mathbf{C}\mathbf{A}\mathbf{z}_{n-1}$ between the predicted observation and the actual observation. The coefficient of this correction is given by the Kalman gain matrix. Thus we can view the Kalman filter as a process of making successive predictions and then correcting these predictions in the light of the new observations. This is illustrated graphically in Figure 13.21.

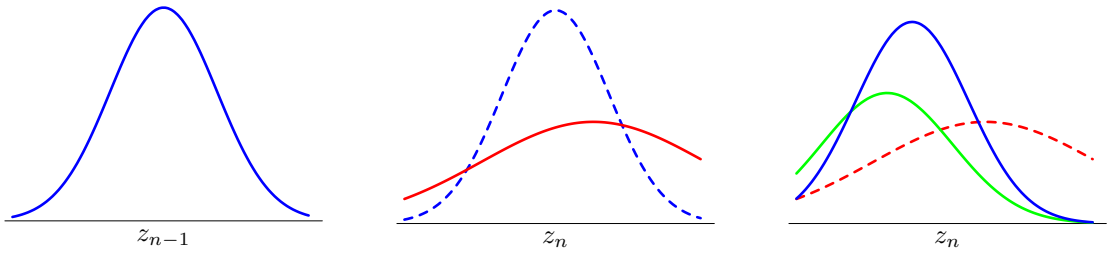

Figure 13.21 The linear dynamical system can be viewed as a sequence of steps in which increasing uncertainty in the state variable due to diffusion is compensated by the arrival of new data. In the left-hand plot, the blue curve shows the distribution $p(\mathbf{z}_{n-1}|\mathbf{x}_1, \ldots, \mathbf{x}_{n-1})$, which incorporates all the data up to step $n-1$. The diffusion arising from the nonzero variance of the transition probability $p(\mathbf{z}_n|\mathbf{z}_{n-1})$ gives the distribution $p(\mathbf{z}_n|\mathbf{x}_1, \ldots, \mathbf{x}_{n-1})$, shown in red in the centre plot. Note that this is broader and shifted relative to the blue curve (which is shown dashed in the centre plot for comparison). The next data observation $\mathbf{x}_n$ contributes through the emission density $p(\mathbf{x}_n|\mathbf{z}_n)$, which is shown as a function of $\mathbf{z}_n$ in green on the right-hand plot. Note that this is not a density with respect to $\mathbf{z}_n$ and so is not normalized to one. Inclusion of this new data point leads to a revised distribution $p(\mathbf{z}_n|\mathbf{x}_1, \ldots, \mathbf{x}_n)$ for the state density shown in blue. We see that observation of the data has shifted and narrowed the distribution compared to $p(\mathbf{z}_n|\mathbf{x}_1, \ldots, \mathbf{x}_{n-1})$ (which is shown in dashed in the right-hand plot for comparison).

Exercise 13.27 *Exercise 13.28*

If we consider a situation in which the measurement noise is small compared to the rate at which the latent variable is evolving, then we find that the posterior distribution for $\mathbf{z}_n$ depends only on the current measurement $\mathbf{x}_n$, in accordance with the intuition from our simple example at the start of the section. Similarly, if the latent variable is evolving slowly relative to the observation noise level, we find that the posterior mean for $\mathbf{z}_n$ is obtained by averaging all of the measurements obtained up to that time.

One of the most important applications of the Kalman filter is to tracking, and this is illustrated using a simple example of an object moving in two dimensions in Figure 13.22.

So far, we have solved the inference problem of finding the posterior marginal for a node $\mathbf{z}_n$ given observations from $\mathbf{x}_1$ up to $\mathbf{x}_n$. Next we turn to the problem of finding the marginal for a node $\mathbf{z}_n$ given all observations $\mathbf{x}_1$ to $\mathbf{x}_N$. For temporal data, this corresponds to the inclusion of future as well as past observations. Although this cannot be used for real-time prediction, it plays a key role in learning the parameters of the model. By analogy with the hidden Markov model, this problem can be solved by propagating messages from node $\mathbf{x}_N$ back to node $\mathbf{x}_1$ and combining this information with that obtained during the forward message passing stage used to compute the $\widehat{\alpha}(\mathbf{z}_n)$.

In the LDS literature, it is usual to formulate this backward recursion in terms of $\gamma(\mathbf{z}_n) = \widehat{\alpha}(\mathbf{z}_n)\widehat{\beta}(\mathbf{z}_n)$ rather than in terms of $\widehat{\beta}(\mathbf{z}_n)$. Because $\gamma(\mathbf{z}_n)$ must also be Gaussian, we write it in the form

$$\gamma(\mathbf{z}_n) = \widehat{\alpha}(\mathbf{z}_n)\widehat{\beta}(\mathbf{z}_n) = \mathcal{N}(\mathbf{z}_n|\widehat{\boldsymbol{\mu}}_n, \widehat{\mathbf{V}}_n). \tag{13.98}$$

To derive the required recursion, we start from the backward recursion (13.62) for

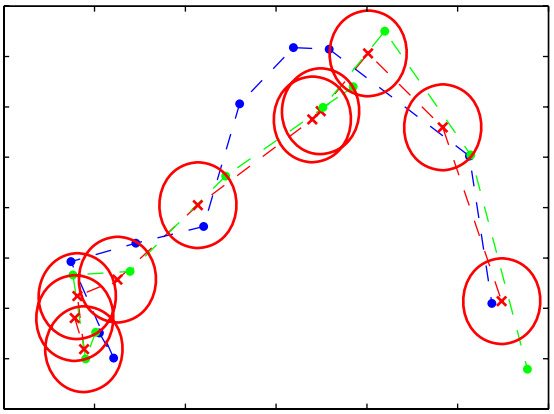

Figure 13.22 An illustration of a linear dynamical system being used to track a moving object. The blue points indicate the true positions of the object in a two-dimensional space at successive time steps, the green points denote noisy measurements of the positions, and the red crosses indicate the means of the inferred posterior distributions of the positions obtained by running the Kalman filtering equations. The covariances of the inferred positions are indicated by the red ellipses, which correspond to contours having one standard deviation.

$\widehat{\beta}(\mathbf{z}_n)$, which, for continuous latent variables, can be written in the form

$$c_{n+1}\widehat{\beta}(\mathbf{z}_n) = \int \widehat{\beta}(\mathbf{z}_{n+1})p(\mathbf{x}_{n+1}|\mathbf{z}_{n+1})p(\mathbf{z}_{n+1}|\mathbf{z}_n)\,\mathrm{d}\mathbf{z}_{n+1}. \tag{13.99}$$

We now multiply both sides of (13.99) by $\widehat{\alpha}(\mathbf{z}_n)$ and substitute for $p(\mathbf{x}_{n+1}|\mathbf{z}_{n+1})$ and $p(\mathbf{z}_{n+1}|\mathbf{z}_n)$ using (13.75) and (13.76). Then we make use of (13.89), (13.90) and (13.91), together with (13.98), and after some manipulation we obtain

Exercise 13.29

$$\widehat{\boldsymbol{\mu}}_n = \boldsymbol{\mu}_n + \mathbf{J}_n\left(\widehat{\boldsymbol{\mu}}_{n+1} - \mathbf{A}\boldsymbol{\mu}_N\right) \tag{13.100}$$

$$\widehat{\mathbf{V}}_n = \mathbf{V}_n + \mathbf{J}_n\left(\widehat{\mathbf{V}}_{n+1} - \mathbf{P}_n\right)\mathbf{J}_n^{\mathrm{T}} \tag{13.101}$$

where we have defined

$$\mathbf{J}_n = \mathbf{V}_n\mathbf{A}^{\mathrm{T}}\left(\mathbf{P}_n\right)^{-1} \tag{13.102}$$

and we have made use of $\mathbf{A}\mathbf{V}_n = \mathbf{P}_n\mathbf{J}_n^{\mathrm{T}}$. Note that these recursions require that the forward pass be completed first so that the quantities $\boldsymbol{\mu}_n$ and $\mathbf{V}_n$ will be available for the backward pass.

For the EM algorithm, we also require the pairwise posterior marginals, which can be obtained from (13.65) in the form

$$\begin{aligned}\xi(\mathbf{z}_{n-1},\mathbf{z}_n) &= (c_n)^{-1}\,\widehat{\alpha}(\mathbf{z}_{n-1})p(\mathbf{x}_n|\mathbf{z}_n)p(\mathbf{z}_n|\mathbf{z}_{-1})\widehat{\beta}(\mathbf{z}_n) \\ &= \frac{\mathcal{N}(\mathbf{z}_{n-1}|\boldsymbol{\mu}_{n-1},\mathbf{V}_{n-1})\mathcal{N}(\mathbf{z}_n|\mathbf{A}\mathbf{z}_{n-1},\boldsymbol{\Gamma})\mathcal{N}(\mathbf{x}_n|\mathbf{C}\mathbf{z}_n,\boldsymbol{\Sigma})\mathcal{N}(\mathbf{z}_n|\widehat{\boldsymbol{\mu}}_n,\widehat{\mathbf{V}}_n)}{c_n\widehat{\alpha}(\mathbf{z}_n)}.\end{aligned} \tag{13.103}$$

Substituting for $\widehat{\alpha}(\mathbf{z}_n)$ using (13.84) and rearranging, we see that $\xi(\mathbf{z}_{n-1},\mathbf{z}_n)$ is a Gaussian with mean given with components $\gamma(\mathbf{z}_{n-1})$ and $\gamma(\mathbf{z}_n)$, and a covariance between $\mathbf{z}_n$ and $\mathbf{z}_{n-1}$ given by

Exercise 13.31

$$\mathrm{cov}[\mathbf{z}_n,\mathbf{z}_{n-1}] = \mathbf{J}_{n-1}\widehat{\mathbf{V}}_n. \tag{13.104}$$

13.3.2 Learning in LDS

So far, we have considered the inference problem for linear dynamical systems, assuming that the model parameters $\boldsymbol{\theta} = \{\mathbf{A}, \boldsymbol{\Gamma}, \mathbf{C}, \boldsymbol{\Sigma}, \boldsymbol{\mu}_0, \mathbf{V}_0\}$ are known. Next, we consider the determination of these parameters using maximum likelihood (Ghahramani and Hinton, 1996b). Because the model has latent variables, this can be addressed using the EM algorithm, which was discussed in general terms in Chapter 9.

We can derive the EM algorithm for the linear dynamical system as follows. Let us denote the estimated parameter values at some particular cycle of the algorithm by $\boldsymbol{\theta}^{\text{old}}$. For these parameter values, we can run the inference algorithm to determine the posterior distribution of the latent variables $p(\mathbf{Z}|\mathbf{X}, \boldsymbol{\theta}^{\text{old}})$, or more precisely those local posterior marginals that are required in the M step. In particular, we shall require the following expectations

$$\mathbb{E}[\mathbf{z}_n] = \widehat{\boldsymbol{\mu}}_n \tag{13.105}$$

$$\mathbb{E}\left[\mathbf{z}_n \mathbf{z}_{n-1}^{\mathrm{T}}\right] = \mathbf{J}_{n-1}\widehat{\mathbf{V}}_n + \widehat{\boldsymbol{\mu}}_n \widehat{\boldsymbol{\mu}}_{n-1}^{\mathrm{T}} \tag{13.106}$$

$$\mathbb{E}\left[\mathbf{z}_n \mathbf{z}_n^{\mathrm{T}}\right] = \widehat{\mathbf{V}}_n + \widehat{\boldsymbol{\mu}}_n \widehat{\boldsymbol{\mu}}_n^{\mathrm{T}} \tag{13.107}$$

where we have used (13.104).

Now we consider the complete-data log likelihood function, which is obtained by taking the logarithm of (13.6) and is therefore given by

$$\begin{aligned} \ln p(\mathbf{X}, \mathbf{Z}|\boldsymbol{\theta}) = {} & \ln p(\mathbf{z}_1|\boldsymbol{\mu}_0, \mathbf{V}_0) + \sum_{n=2}^{N} \ln p(\mathbf{z}_n|\mathbf{z}_{n-1}, \mathbf{A}, \boldsymbol{\Gamma}) \\ & + \sum_{n=1}^{N} \ln p(\mathbf{x}_n|\mathbf{z}_n, \mathbf{C}, \boldsymbol{\Sigma}) \end{aligned} \tag{13.108}$$

in which we have made the dependence on the parameters explicit. We now take the expectation of the complete-data log likelihood with respect to the posterior distribution $p(\mathbf{Z}|\mathbf{X}, \boldsymbol{\theta}^{\text{old}})$ which defines the function

$$Q(\boldsymbol{\theta}, \boldsymbol{\theta}^{\text{old}}) = \mathbb{E}_{\mathbf{Z}|\boldsymbol{\theta}^{\text{old}}}\left[\ln p(\mathbf{X}, \mathbf{Z}|\boldsymbol{\theta})\right]. \tag{13.109}$$

In the M step, this function is maximized with respect to the components of $\boldsymbol{\theta}$.

Consider first the parameters $\boldsymbol{\mu}_0$ and $\mathbf{V}_0$. If we substitute for $p(\mathbf{z}_1|\boldsymbol{\mu}_0, \mathbf{V}_0)$ in (13.108) using (13.77), and then take the expectation with respect to $\mathbf{Z}$, we obtain

$$Q(\boldsymbol{\theta}, \boldsymbol{\theta}^{\text{old}}) = -\frac{1}{2}\ln|\mathbf{V}_0| - \mathbb{E}_{\mathbf{Z}|\boldsymbol{\theta}^{\text{old}}}\left[\frac{1}{2}(\mathbf{z}_1 - \boldsymbol{\mu}_0)^{\mathrm{T}}\mathbf{V}_0^{-1}(\mathbf{z}_1 - \boldsymbol{\mu}_0)\right] + \text{const}$$

where all terms not dependent on $\boldsymbol{\mu}_0$ or $\mathbf{V}_0$ have been absorbed into the additive constant. Maximization with respect to $\boldsymbol{\mu}_0$ and $\mathbf{V}_0$ is easily performed by making use of the maximum likelihood solution for a Gaussian distribution discussed in Section 2.3.4, giving

Exercise 13.32

$$\boldsymbol{\mu}_0^{\text{new}} = \mathbb{E}[\mathbf{z}_1] \tag{13.110}$$
$$\mathbf{V}_0^{\text{new}} = \mathbb{E}[\mathbf{z}_1\mathbf{z}_1^{\mathrm{T}}] - \mathbb{E}[\mathbf{z}_1]\mathbb{E}[\mathbf{z}_1^{\mathrm{T}}]. \tag{13.111}$$

Similarly, to optimize $\mathbf{A}$ and $\boldsymbol{\Gamma}$, we substitute for $p(\mathbf{z}_n|\mathbf{z}_{n-1}, \mathbf{A}, \boldsymbol{\Gamma})$ in (13.108) using (13.75) giving

$$Q(\boldsymbol{\theta}, \boldsymbol{\theta}^{\text{old}}) = -\frac{N-1}{2}\ln|\boldsymbol{\Gamma}| - \mathbb{E}_{\mathbf{Z}|\boldsymbol{\theta}^{\text{old}}}\left[\frac{1}{2}\sum_{n=2}^{N}(\mathbf{z}_n - \mathbf{A}\mathbf{z}_{n-1})^{\mathrm{T}}\boldsymbol{\Gamma}^{-1}(\mathbf{z}_n - \mathbf{A}\mathbf{z}_{n-1})\right] + \text{const} \tag{13.112}$$

in which the constant comprises terms that are independent of $\mathbf{A}$ and $\boldsymbol{\Gamma}$. Maximizing with respect to these parameters then gives

Exercise 13.33

$$\mathbf{A}^{\text{new}} = \left(\sum_{n=2}^{N}\mathbb{E}\left[\mathbf{z}_n\mathbf{z}_{n-1}^{\mathrm{T}}\right]\right)\left(\sum_{n=2}^{N}\mathbb{E}\left[\mathbf{z}_{n-1}\mathbf{z}_{n-1}^{\mathrm{T}}\right]\right)^{-1} \tag{13.113}$$

$$\boldsymbol{\Gamma}^{\text{new}} = \frac{1}{N-1}\sum_{n=2}^{N}\left\{\mathbb{E}\left[\mathbf{z}_n\mathbf{z}_n^{\mathrm{T}}\right] - \mathbf{A}^{\text{new}}\mathbb{E}\left[\mathbf{z}_{n-1}\mathbf{z}_n^{\mathrm{T}}\right] - \mathbb{E}\left[\mathbf{z}_n\mathbf{z}_{n-1}^{\mathrm{T}}\right]\mathbf{A}^{\text{new}} + \mathbf{A}^{\text{new}}\mathbb{E}\left[\mathbf{z}_{n-1}\mathbf{z}_{n-1}^{\mathrm{T}}\right](\mathbf{A}^{\text{new}})^{\mathrm{T}}\right\}. \tag{13.114}$$

Note that $\mathbf{A}^{\text{new}}$ must be evaluated first, and the result can then be used to determine $\boldsymbol{\Gamma}^{\text{new}}$.

Finally, in order to determine the new values of $\mathbf{C}$ and $\boldsymbol{\Sigma}$, we substitute for $p(\mathbf{x}_n|\mathbf{z}_n, \mathbf{C}, \boldsymbol{\Sigma})$ in (13.108) using (13.76) giving

$$Q(\boldsymbol{\theta}, \boldsymbol{\theta}^{\text{old}}) = -\frac{N}{2}\ln|\boldsymbol{\Sigma}| - \mathbb{E}_{\mathbf{Z}|\boldsymbol{\theta}^{\text{old}}}\left[\frac{1}{2}\sum_{n=1}^{N}(\mathbf{x}_n - \mathbf{C}\mathbf{z}_n)^{\mathrm{T}}\boldsymbol{\Sigma}^{-1}(\mathbf{x}_n - \mathbf{C}\mathbf{z}_n)\right] + \text{const}.$$

Exercise 13.34

Maximizing with respect to $\mathbf{C}$ and $\boldsymbol{\Sigma}$ then gives

$$\mathbf{C}^{\text{new}} = \left(\sum_{n=1}^{N}\mathbf{x}_n\mathbb{E}\left[\mathbf{z}_n^{\mathrm{T}}\right]\right)\left(\sum_{n=1}^{N}\mathbb{E}\left[\mathbf{z}_n\mathbf{z}_n^{\mathrm{T}}\right]\right)^{-1} \tag{13.115}$$

$$\boldsymbol{\Sigma}^{\text{new}} = \frac{1}{N}\sum_{n=1}^{N}\left\{\mathbf{x}_n\mathbf{x}_n^{\mathrm{T}} - \mathbf{C}^{\text{new}}\mathbb{E}\left[\mathbf{z}_n\right]\mathbf{x}_n^{\mathrm{T}} - \mathbf{x}_n\mathbb{E}\left[\mathbf{z}_n^{\mathrm{T}}\right]\mathbf{C}^{\text{new}} + \mathbf{C}^{\text{new}}\mathbb{E}\left[\mathbf{z}_n\mathbf{z}_n^{\mathrm{T}}\right]\mathbf{C}^{\text{new}}\right\}. \tag{13.116}$$

We have approached parameter learning in the linear dynamical system using maximum likelihood. Inclusion of priors to give a MAP estimate is straightforward, and a fully Bayesian treatment can be found by applying the analytical approximation techniques discussed in Chapter 10, though a detailed treatment is precluded here due to lack of space.

13.3.3 Extensions of LDS

As with the hidden Markov model, there is considerable interest in extending the basic linear dynamical system in order to increase its capabilities. Although the assumption of a linear-Gaussian model leads to efficient algorithms for inference and learning, it also implies that the marginal distribution of the observed variables is simply a Gaussian, which represents a significant limitation. One simple extension of the linear dynamical system is to use a Gaussian mixture as the initial distribution for $\mathbf{z}_1$. If this mixture has K components, then the forward recursion equations (13.85) will lead to a mixture of K Gaussians over each hidden variable $\mathbf{z}_n$, and so the model is again tractable.

For many applications, the Gaussian emission density is a poor approximation. If instead we try to use a mixture of K Gaussians as the emission density, then the posterior $\widehat{\alpha}(\mathbf{z}_1)$ will also be a mixture of K Gaussians. However, from (13.85) the posterior $\widehat{\alpha}(\mathbf{z}_2)$ will comprise a mixture of K^2 Gaussians, and so on, with $\widehat{\alpha}(\mathbf{z}_n)$ being given by a mixture of K^n Gaussians. Thus the number of components grows exponentially with the length of the chain, and so this model is impractical.

More generally, introducing transition or emission models that depart from the linear-Gaussian (or other exponential family) model leads to an intractable inference problem. We can make deterministic approximations such as assumed density filtering or expectation propagation, or we can make use of sampling methods, as discussed in Section 13.3.4. One widely used approach is to make a Gaussian approximation by linearizing around the mean of the predicted distribution, which gives rise to the *extended Kalman filter* (Zarchan and Musoff, 2005).

Chapter 10

As with hidden Markov models, we can develop interesting extensions of the basic linear dynamical system by expanding its graphical representation. For example, the *switching state space model* (Ghahramani and Hinton, 1998) can be viewed as a combination of the hidden Markov model with a set of linear dynamical systems. The model has multiple Markov chains of continuous linear-Gaussian latent variables, each of which is analogous to the latent chain of the linear dynamical system discussed earlier, together with a Markov chain of discrete variables of the form used in a hidden Markov model. The output at each time step is determined by stochastically choosing one of the continuous latent chains, using the state of the discrete latent variable as a switch, and then emitting an observation from the corresponding conditional output distribution. Exact inference in this model is intractable, but variational methods lead to an efficient inference scheme involving forward-backward recursions along each of the continuous and discrete Markov chains independently. Note that, if we consider multiple chains of discrete latent variables, and use one as the switch to select from the remainder, we obtain an analogous model having only discrete latent variables known as the *switching hidden Markov model*.

13.3.4 Particle filters

Chapter 11

For dynamical systems which do not have a linear-Gaussian, for example, if they use a non-Gaussian emission density, we can turn to sampling methods in order to find a tractable inference algorithm. In particular, we can apply the sampling-importance-resampling formalism of Section 11.1.5 to obtain a sequential Monte Carlo algorithm known as the particle filter.

Consider the class of distributions represented by the graphical model in Figure 13.5, and suppose we are given the observed values $\mathbf{X}_n = (\mathbf{x}_1, \ldots, \mathbf{x}_n)$ and we wish to draw L samples from the posterior distribution $p(\mathbf{z}_n|\mathbf{X}_n)$. Using Bayes' theorem, we have

$$\begin{aligned}
\mathbb{E}[f(\mathbf{z}_n)] &= \int f(\mathbf{z}_n) p(\mathbf{z}_n|\mathbf{X}_n)\, \mathrm{d}\mathbf{z}_n \\
&= \int f(\mathbf{z}_n) p(\mathbf{z}_n|\mathbf{x}_n, \mathbf{X}_{n-1})\, \mathrm{d}\mathbf{z}_n \\
&= \frac{\displaystyle\int f(\mathbf{z}_n) p(\mathbf{x}_n|\mathbf{z}_n) p(\mathbf{z}_n|\mathbf{X}_{n-1})\, \mathrm{d}\mathbf{z}_n}{\displaystyle\int p(\mathbf{x}_n|\mathbf{z}_n) p(\mathbf{z}_n|\mathbf{X}_{n-1})\, \mathrm{d}\mathbf{z}_n} \\
&\simeq \sum_{l=1}^{L} w_n^{(l)} f(\mathbf{z}_n^{(l)})
\end{aligned} \tag{13.117}$$

where $\{\mathbf{z}_n^{(l)}\}$ is a set of samples drawn from $p(\mathbf{z}_n|\mathbf{X}_{n-1})$ and we have made use of the conditional independence property $p(\mathbf{x}_n|\mathbf{z}_n, \mathbf{X}_{n-1}) = p(\mathbf{x}_n|\mathbf{z}_n)$, which follows from the graph in Figure 13.5. The sampling weights $\{w_n^{(l)}\}$ are defined by

$$w_n^{(l)} = \frac{p(\mathbf{x}_n|\mathbf{z}_n^{(l)})}{\sum_{m=1}^{L} p(\mathbf{x}_n|\mathbf{z}_n^{(m)})} \tag{13.118}$$

where the same samples are used in the numerator as in the denominator. Thus the posterior distribution $p(\mathbf{z}_n|\mathbf{x}_n)$ is represented by the set of samples $\{\mathbf{z}_n^{(l)}\}$ together with the corresponding weights $\{w_n^{(l)}\}$. Note that these weights satisfy $0 \leqslant w_n^{(l)} 1$ and $\sum_l w_n^{(l)} = 1$.

Because we wish to find a sequential sampling scheme, we shall suppose that a set of samples and weights have been obtained at time step n, and that we have subsequently observed the value of $\mathbf{x}_{n+1}$, and we wish to find the weights and samples at time step $n + 1$. We first sample from the distribution $p(\mathbf{z}_{n+1}|\mathbf{X}_n)$. This is

straightforward since, again using Bayes' theorem

$$\begin{aligned} p(\mathbf{z}_{n+1}|\mathbf{X}_n) &= \int p(\mathbf{z}_{n+1}|\mathbf{z}_n, \mathbf{X}_n) p(\mathbf{z}_n|\mathbf{X}_n)\, \mathrm{d}\mathbf{z}_n \\ &= \int p(\mathbf{z}_{n+1}|\mathbf{z}_n) p(\mathbf{z}_n|\mathbf{X}_n)\, \mathrm{d}\mathbf{z}_n \\ &= \int p(\mathbf{z}_{n+1}|\mathbf{z}_n) p(\mathbf{z}_n|\mathbf{x}_n, \mathbf{X}_{n-1})\, \mathrm{d}\mathbf{z}_n \\ &= \frac{\displaystyle\int p(\mathbf{z}_{n+1}|\mathbf{z}_n) p(\mathbf{x}_n|\mathbf{z}_n) p(\mathbf{z}_n|\mathbf{X}_{n-1})\, \mathrm{d}\mathbf{z}_n}{\displaystyle\int p(\mathbf{x}_n|\mathbf{z}_n) p(\mathbf{z}_n|\mathbf{X}_{n-1})\, \mathrm{d}\mathbf{z}_n} \\ &= \sum_l w_n^{(l)} p(\mathbf{z}_{n+1}|\mathbf{z}_n^{(l)}) \end{aligned} \tag{13.119}$$

where we have made use of the conditional independence properties

$$p(\mathbf{z}_{n+1}|\mathbf{z}_n, \mathbf{X}_n) = p(\mathbf{z}_{n+1}|\mathbf{z}_n) \tag{13.120}$$

$$p(\mathbf{x}_n|\mathbf{z}_n, \mathbf{X}_{n-1}) = p(\mathbf{x}_n|\mathbf{z}_n) \tag{13.121}$$

which follow from the application of the d-separation criterion to the graph in Figure 13.5. The distribution given by (13.119) is a mixture distribution, and samples can be drawn by choosing a component l with probability given by the mixing coefficients $w^{(l)}$ and then drawing a sample from the corresponding component.

In summary, we can view each step of the particle filter algorithm as comprising two stages. At time step n, we have a sample representation of the posterior distribution $p(\mathbf{z}_n|\mathbf{X}_n)$ expressed as samples $\{\mathbf{z}_n^{(l)}\}$ with corresponding weights $\{w_n^{(l)}\}$. This can be viewed as a mixture representation of the form (13.119). To obtain the corresponding representation for the next time step, we first draw L samples from the mixture distribution (13.119), and then for each sample we use the new observation $\mathbf{x}_{n+1}$ to evaluate the corresponding weights $w_{n+1}^{(l)} \propto p(\mathbf{x}_{n+1}|\mathbf{z}_{n+1}^{(l)})$. This is illustrated, for the case of a single variable z, in Figure 13.23.

The particle filtering, or sequential Monte Carlo, approach has appeared in the literature under various names including the *bootstrap filter* (Gordon *et al.*, 1993), *survival of the fittest* (Kanazawa *et al.*, 1995), and the *condensation* algorithm (Isard and Blake, 1998).

Exercises

13.1 (⋆) **WWW** Use the technique of d-separation, discussed in Section 8.2, to verify that the Markov model shown in Figure 13.3 having N nodes in total satisfies the conditional independence properties (13.3) for $n = 2, \ldots, N$. Similarly, show that a model described by the graph in Figure 13.4 in which there are N nodes in total

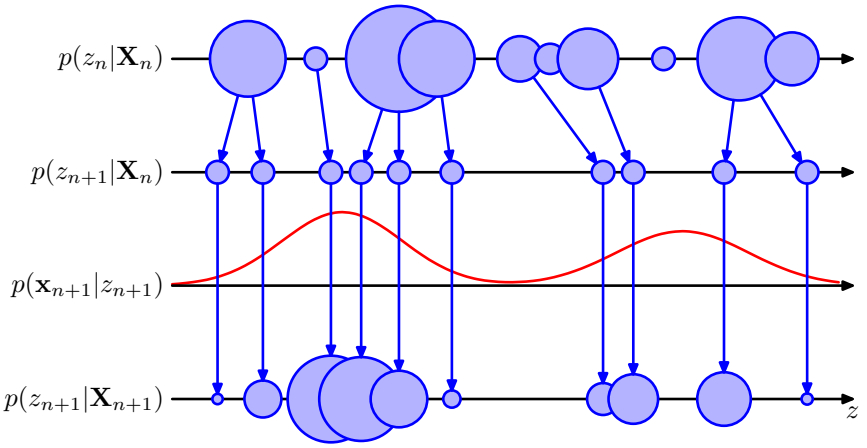

Figure 13.23 Schematic illustration of the operation of the particle filter for a one-dimensional latent space. At time step n, the posterior $p(z_n|\mathbf{x}_n)$ is represented as a mixture distribution, shown schematically as circles whose sizes are proportional to the weights $w_n^{(l)}$. A set of L samples is then drawn from this distribution and the new weights $w_{n+1}^{(l)}$ evaluated using $p(\mathbf{x}_{n+1}|\mathbf{z}_{n+1}^{(l)})$.

satisfies the conditional independence properties

$$p(\mathbf{x}_n|\mathbf{x}_1,\ldots,\mathbf{x}_{n-1}) = p(\mathbf{x}_n|\mathbf{x}_{n-1},\mathbf{x}_{n-2}) \tag{13.122}$$

for $n = 3,\ldots,N$.

13.2 ($\star\star$) Consider the joint probability distribution (13.2) corresponding to the directed graph of Figure 13.3. Using the sum and product rules of probability, verify that this joint distribution satisfies the conditional independence property (13.3) for $n = 2,\ldots,N$. Similarly, show that the second-order Markov model described by the joint distribution (13.4) satisfies the conditional independence property

$$p(\mathbf{x}_n|\mathbf{x}_1,\ldots,\mathbf{x}_{n-1}) = p(\mathbf{x}_n|\mathbf{x}_{n-1},\mathbf{x}_{n-2}) \tag{13.123}$$

for $n = 3,\ldots,N$.

13.3 ($\star$) By using d-separation, show that the distribution $p(\mathbf{x}_1,\ldots,\mathbf{x}_N)$ of the observed data for the state space model represented by the directed graph in Figure 13.5 does not satisfy any conditional independence properties and hence does not exhibit the Markov property at any finite order.

13.4 ($\star\star$) **WWW** Consider a hidden Markov model in which the emission densities are represented by a parametric model $p(\mathbf{x}|\mathbf{z},\mathbf{w})$, such as a linear regression model or a neural network, in which $\mathbf{w}$ is a vector of adaptive parameters. Describe how the parameters $\mathbf{w}$ can be learned from data using maximum likelihood.

13.5 ($\star\star$) Verify the M-step equations (13.18) and (13.19) for the initial state probabilities and transition probability parameters of the hidden Markov model by maximization of the expected complete-data log likelihood function (13.17), using appropriate Lagrange multipliers to enforce the summation constraints on the components of $\boldsymbol{\pi}$ and $\mathbf{A}$.

13.6 ($\star$) Show that if any elements of the parameters $\boldsymbol{\pi}$ or $\mathbf{A}$ for a hidden Markov model are initially set to zero, then those elements will remain zero in all subsequent updates of the EM algorithm.

13.7 ($\star$) Consider a hidden Markov model with Gaussian emission densities. Show that maximization of the function $Q(\boldsymbol{\theta}, \boldsymbol{\theta}^{\text{old}})$ with respect to the mean and covariance parameters of the Gaussians gives rise to the M-step equations (13.20) and (13.21).

13.8 ($\star\star$) **www** For a hidden Markov model having discrete observations governed by a multinomial distribution, show that the conditional distribution of the observations given the hidden variables is given by (13.22) and the corresponding M step equations are given by (13.23). Write down the analogous equations for the conditional distribution and the M step equations for the case of a hidden Markov with multiple binary output variables each of which is governed by a Bernoulli conditional distribution. Hint: refer to Sections 2.1 and 2.2 for a discussion of the corresponding maximum likelihood solutions for i.i.d. data if required.

13.9 ($\star\star$) **www** Use the d-separation criterion to verify that the conditional independence properties (13.24)–(13.31) are satisfied by the joint distribution for the hidden Markov model defined by (13.6).

13.10 ($\star\star\star$) By applying the sum and product rules of probability, verify that the conditional independence properties (13.24)–(13.31) are satisfied by the joint distribution for the hidden Markov model defined by (13.6).

13.11 ($\star\star$) Starting from the expression (8.72) for the marginal distribution over the variables of a factor in a factor graph, together with the results for the messages in the sum-product algorithm obtained in Section 13.2.3, derive the result (13.43) for the joint posterior distribution over two successive latent variables in a hidden Markov model.

13.12 ($\star\star$) Suppose we wish to train a hidden Markov model by maximum likelihood using data that comprises R independent sequences of observations, which we denote by $\mathbf{X}^{(r)}$ where $r = 1, \ldots, R$. Show that in the E step of the EM algorithm, we simply evaluate posterior probabilities for the latent variables by running the α and β recursions independently for each of the sequences. Also show that in the M step, the initial probability and transition probability parameters are re-estimated

using modified forms of (13.18) and (13.19) given by

$$\pi_k = \frac{\sum_{r=1}^{R} \gamma(z_{1k}^{(r)})}{\sum_{r=1}^{R}\sum_{j=1}^{K} \gamma(z_{1j}^{(r)})} \tag{13.124}$$

$$A_{jk} = \frac{\sum_{r=1}^{R}\sum_{n=2}^{N} \xi(z_{n-1,j}^{(r)}, z_{n,k}^{(r)})}{\sum_{r=1}^{R}\sum_{l=1}^{K}\sum_{n=2}^{N} \xi(z_{n-1,j}^{(r)}, z_{n,l}^{(r)})} \tag{13.125}$$

where, for notational convenience, we have assumed that the sequences are of the same length (the generalization to sequences of different lengths is straightforward). Similarly, show that the M-step equation for re-estimation of the means of Gaussian emission models is given by

$$\boldsymbol{\mu}_k = \frac{\sum_{r=1}^{R}\sum_{n=1}^{N} \gamma(z_{nk}^{(r)})\mathbf{x}_n^{(r)}}{\sum_{r=1}^{R}\sum_{n=1}^{N} \gamma(z_{nk}^{(r)})}. \tag{13.126}$$

Note that the M-step equations for other emission model parameters and distributions take an analogous form.

13.13 (⋆⋆) **www** Use the definition (8.64) of the messages passed from a factor node to a variable node in a factor graph, together with the expression (13.6) for the joint distribution in a hidden Markov model, to show that the definition (13.50) of the alpha message is the same as the definition (13.34).

13.14 (⋆⋆) Use the definition (8.67) of the messages passed from a factor node to a variable node in a factor graph, together with the expression (13.6) for the joint distribution in a hidden Markov model, to show that the definition (13.52) of the beta message is the same as the definition (13.35).

13.15 (⋆⋆) Use the expressions (13.33) and (13.43) for the marginals in a hidden Markov model to derive the corresponding results (13.64) and (13.65) expressed in terms of re-scaled variables.

13.16 (⋆⋆⋆) In this exercise, we derive the forward message passing equation for the Viterbi algorithm directly from the expression (13.6) for the joint distribution. This involves maximizing over all of the hidden variables $\mathbf{z}_1, \ldots, \mathbf{z}_N$. By taking the logarithm and then exchanging maximizations and summations, derive the recursion

(13.68) where the quantities $\omega(\mathbf{z}_n)$ are defined by (13.70). Show that the initial condition for this recursion is given by (13.69).

13.17 ($\star$) **www** Show that the directed graph for the input-output hidden Markov model, given in Figure 13.18, can be expressed as a tree-structured factor graph of the form shown in Figure 13.15 and write down expressions for the initial factor $h(\mathbf{z}_1)$ and for the general factor $f_n(\mathbf{z}_{n-1}, \mathbf{z}_n)$ where $2 \leqslant n \leqslant N$.

13.18 ($\star\star\star$) Using the result of Exercise 13.17, derive the recursion equations, including the initial conditions, for the forward-backward algorithm for the input-output hidden Markov model shown in Figure 13.18.

13.19 ($\star$) **www** The Kalman filter and smoother equations allow the posterior distributions over individual latent variables, conditioned on all of the observed variables, to be found efficiently for linear dynamical systems. Show that the sequence of latent variable values obtained by maximizing each of these posterior distributions individually is the same as the most probable sequence of latent values. To do this, simply note that the joint distribution of all latent and observed variables in a linear dynamical system is Gaussian, and hence all conditionals and marginals will also be Gaussian, and then make use of the result (2.98).

13.20 ($\star\star$) **www** Use the result (2.115) to prove (13.87).

13.21 ($\star\star$) Use the results (2.115) and (2.116), together with the matrix identities (C.5) and (C.7), to derive the results (13.89), (13.90), and (13.91), where the Kalman gain matrix $\mathbf{K}_n$ is defined by (13.92).

13.22 ($\star\star$) **www** Using (13.93), together with the definitions (13.76) and (13.77) and the result (2.115), derive (13.96).

13.23 ($\star\star$) Using (13.93), together with the definitions (13.76) and (13.77) and the result (2.116), derive (13.94), (13.95) and (13.97).

13.24 ($\star\star$) **www** Consider a generalization of (13.75) and (13.76) in which we include constant terms $\mathbf{a}$ and $\mathbf{c}$ in the Gaussian means, so that

$$p(\mathbf{z}_n|\mathbf{z}_{n-1}) = \mathcal{N}(\mathbf{z}_n|\mathbf{A}\mathbf{z}_{n-1} + \mathbf{a}, \boldsymbol{\Gamma}) \tag{13.127}$$

$$p(\mathbf{x}_n|\mathbf{z}_n) = \mathcal{N}(\mathbf{x}_n|\mathbf{C}\mathbf{z}_n + \mathbf{c}, \boldsymbol{\Sigma}). \tag{13.128}$$

Show that this extension can be re-case in the framework discussed in this chapter by defining a state vector $\mathbf{z}$ with an additional component fixed at unity, and then augmenting the matrices $\mathbf{A}$ and $\mathbf{C}$ using extra columns corresponding to the parameters $\mathbf{a}$ and $\mathbf{c}$.

13.25 ($\star\star$) In this exercise, we show that when the Kalman filter equations are applied to independent observations, they reduce to the results given in Section 2.3 for the maximum likelihood solution for a single Gaussian distribution. Consider the problem of finding the mean μ of a single Gaussian random variable x, in which we are given a set of independent observations $\{x_1, \ldots, x_N\}$. To model this we can use

a linear dynamical system governed by (13.75) and (13.76), with latent variables $\{z_1, \ldots, z_N\}$ in which $\mathbf{C}$ becomes the identity matrix and where the transition probability $\mathbf{A} = \mathbf{0}$ because the observations are independent. Let the parameters $\mathbf{m}_0$ and $\mathbf{V}_0$ of the initial state be denoted by μ_0 and σ_0^2, respectively, and suppose that $\boldsymbol{\Sigma}$ becomes σ^2. Write down the corresponding Kalman filter equations starting from the general results (13.89) and (13.90), together with (13.94) and (13.95). Show that these are equivalent to the results (2.141) and (2.142) obtained directly by considering independent data.

13.26 ($\star\star\star$) Consider a special case of the linear dynamical system of Section 13.3 that is equivalent to probabilistic PCA, so that the transition matrix $\mathbf{A} = \mathbf{0}$, the covariance $\boldsymbol{\Gamma} = \mathbf{I}$, and the noise covariance $\boldsymbol{\Sigma} = \sigma^2\mathbf{I}$. By making use of the matrix inversion identity (C.7) show that, if the emission density matrix $\mathbf{C}$ is denoted $\mathbf{W}$, then the posterior distribution over the hidden states defined by (13.89) and (13.90) reduces to the result (12.42) for probabilistic PCA.

13.27 ($\star$) **www** Consider a linear dynamical system of the form discussed in Section 13.3 in which the amplitude of the observation noise goes to zero, so that $\boldsymbol{\Sigma} = \mathbf{0}$. Show that the posterior distribution for $\mathbf{z}_n$ has mean $\mathbf{x}_n$ and zero variance. This accords with our intuition that if there is no noise, we should just use the current observation $\mathbf{x}_n$ to estimate the state variable $\mathbf{z}_n$ and ignore all previous observations.

13.28 ($\star\star\star$) Consider a special case of the linear dynamical system of Section 13.3 in which the state variable $\mathbf{z}_n$ is constrained to be equal to the previous state variable, which corresponds to $\mathbf{A} = \mathbf{I}$ and $\boldsymbol{\Gamma} = \mathbf{0}$. For simplicity, assume also that $\mathbf{V}_0 \to \infty$ so that the initial conditions for $\mathbf{z}$ are unimportant, and the predictions are determined purely by the data. Use proof by induction to show that the posterior mean for state $\mathbf{z}_n$ is determined by the average of $\mathbf{x}_1, \ldots, \mathbf{x}_n$. This corresponds to the intuitive result that if the state variable is constant, our best estimate is obtained by averaging the observations.

13.29 ($\star\star\star$) Starting from the backwards recursion equation (13.99), derive the RTS smoothing equations (13.100) and (13.101) for the Gaussian linear dynamical system.

13.30 ($\star\star$) Starting from the result (13.65) for the pairwise posterior marginal in a state space model, derive the specific form (13.103) for the case of the Gaussian linear dynamical system.

13.31 ($\star\star$) Starting from the result (13.103) and by substituting for $\widehat{\alpha}(\mathbf{z}_n)$ using (13.84), verify the result (13.104) for the covariance between $\mathbf{z}_n$ and $\mathbf{z}_{n-1}$.

13.32 ($\star\star$) **www** Verify the results (13.110) and (13.111) for the M-step equations for $\boldsymbol{\mu}_0$ and $\mathbf{V}_0$ in the linear dynamical system.

13.33 ($\star\star$) Verify the results (13.113) and (13.114) for the M-step equations for $\mathbf{A}$ and $\boldsymbol{\Gamma}$ in the linear dynamical system.

13.34 ($\star\star$) Verify the results (13.115) and (13.116) for the M-step equations for $\mathbf{C}$ and $\boldsymbol{\Sigma}$ in the linear dynamical system.

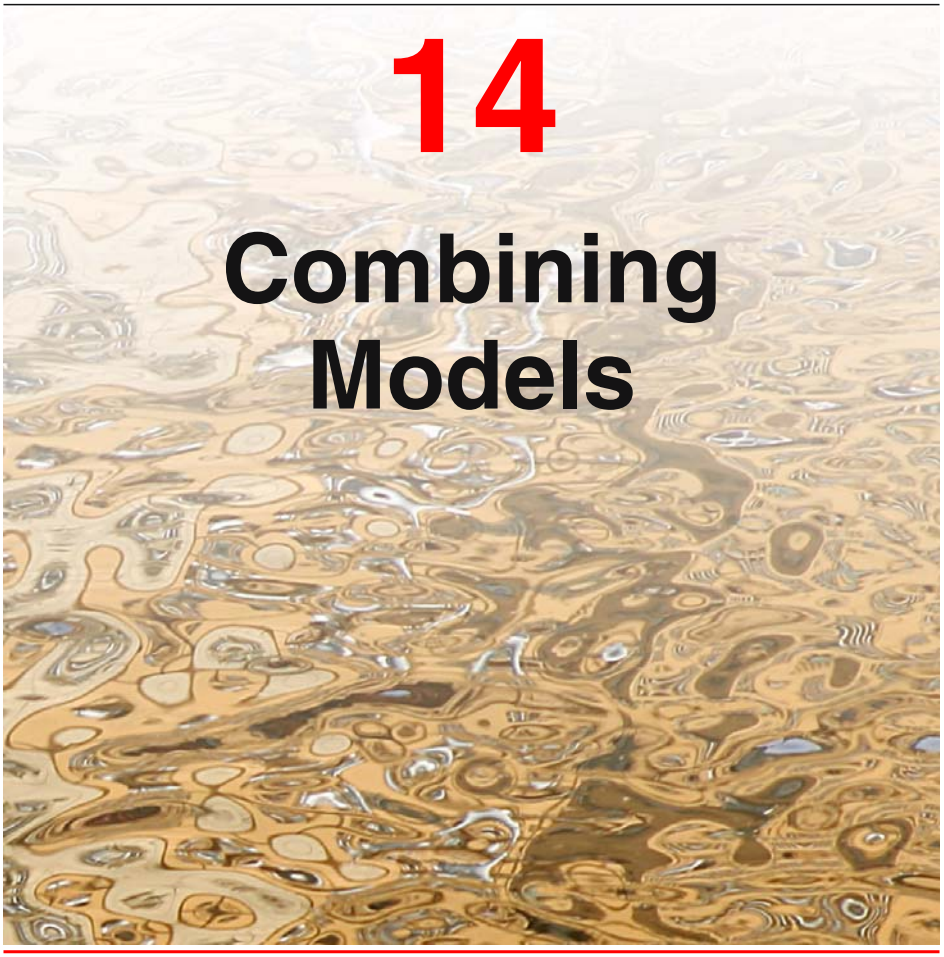

14 Combining Models

In earlier chapters, we have explored a range of different models for solving classification and regression problems. It is often found that improved performance can be obtained by combining multiple models together in some way, instead of just using a single model in isolation. For instance, we might train L different models and then make predictions using the average of the predictions made by each model. Such combinations of models are sometimes called *committees*. In Section 14.2, we discuss ways to apply the committee concept in practice, and we also give some insight into why it can sometimes be an effective procedure.

One important variant of the committee method, known as *boosting*, involves training multiple models in sequence in which the error function used to train a particular model depends on the performance of the previous models. This can produce substantial improvements in performance compared to the use of a single model and is discussed in Section 14.3.

Instead of averaging the predictions of a set of models, an alternative form of

model combination is to select one of the models to make the prediction, in which the choice of model is a function of the input variables. Thus different models become responsible for making predictions in different regions of input space. One widely used framework of this kind is known as a *decision tree* in which the selection process can be described as a sequence of binary selections corresponding to the traversal of a tree structure and is discussed in Section 14.4. In this case, the individual models are generally chosen to be very simple, and the overall flexibility of the model arises from the input-dependent selection process. Decision trees can be applied to both classification and regression problems.

One limitation of decision trees is that the division of input space is based on hard splits in which only one model is responsible for making predictions for any given value of the input variables. The decision process can be softened by moving to a probabilistic framework for combining models, as discussed in Section 14.5. For example, if we have a set of K models for a conditional distribution $p(t|\mathbf{x}, k)$ where $\mathbf{x}$ is the input variable, t is the target variable, and $k = 1, \ldots, K$ indexes the model, then we can form a probabilistic mixture of the form

$$p(t|\mathbf{x}) = \sum_{k=1}^{K} \pi_k(\mathbf{x}) p(t|\mathbf{x}, k) \tag{14.1}$$

in which $\pi_k(\mathbf{x}) = p(k|\mathbf{x})$ represent the input-dependent mixing coefficients. Such models can be viewed as mixture distributions in which the component densities, as well as the mixing coefficients, are conditioned on the input variables and are known as *mixtures of experts*. They are closely related to the mixture density network model discussed in Section 5.6.

14.1. Bayesian Model Averaging

Section 9.2

It is important to distinguish between model combination methods and Bayesian model averaging, as the two are often confused. To understand the difference, consider the example of density estimation using a mixture of Gaussians in which several Gaussian components are combined probabilistically. The model contains a binary latent variable $\mathbf{z}$ that indicates which component of the mixture is responsible for generating the corresponding data point. Thus the model is specified in terms of a joint distribution

$$p(\mathbf{x}, \mathbf{z}) \tag{14.2}$$

and the corresponding density over the observed variable $\mathbf{x}$ is obtained by marginalizing over the latent variable

$$p(\mathbf{x}) = \sum_{\mathbf{z}} p(\mathbf{x}, \mathbf{z}). \tag{14.3}$$

In the case of our Gaussian mixture example, this leads to a distribution of the form

$$p(\mathbf{x}) = \sum_{k=1}^{K} \pi_k \mathcal{N}(\mathbf{x}|\boldsymbol{\mu}_k, \boldsymbol{\Sigma}_k) \tag{14.4}$$

with the usual interpretation of the symbols. This is an example of model combination. For independent, identically distributed data, we can use (14.3) to write the marginal probability of a data set $\mathbf{X} = \{\mathbf{x}_1, \ldots, \mathbf{x}_N\}$ in the form

$$p(\mathbf{X}) = \prod_{n=1}^{N} p(\mathbf{x}_n) = \prod_{n=1}^{N} \left[\sum_{\mathbf{z}_n} p(\mathbf{x}_n, \mathbf{z}_n) \right]. \tag{14.5}$$

Thus we see that each observed data point $\mathbf{x}_n$ has a corresponding latent variable $\mathbf{z}_n$.

Now suppose we have several different models indexed by $h = 1, \ldots, H$ with prior probabilities $p(h)$. For instance one model might be a mixture of Gaussians and another model might be a mixture of Cauchy distributions. The marginal distribution over the data set is given by

$$p(\mathbf{X}) = \sum_{h=1}^{H} p(\mathbf{X}|h)p(h). \tag{14.6}$$

This is an example of Bayesian model averaging. The interpretation of this summation over h is that just one model is responsible for generating the whole data set, and the probability distribution over h simply reflects our uncertainty as to which model that is. As the size of the data set increases, this uncertainty reduces, and the posterior probabilities $p(h|\mathbf{X})$ become increasingly focussed on just one of the models.

This highlights the key difference between Bayesian model averaging and model combination, because in Bayesian model averaging the whole data set is generated by a single model. By contrast, when we combine multiple models, as in (14.5), we see that different data points within the data set can potentially be generated from different values of the latent variable $\mathbf{z}$ and hence by different components.

Although we have considered the marginal probability $p(\mathbf{X})$, the same considerations apply for the predictive density $p(\mathbf{x}|\mathbf{X})$ or for conditional distributions such as $p(\mathbf{t}|\mathbf{x}, \mathbf{X}, \mathbf{T})$.

Exercise 14.1

14.2. Committees

The simplest way to construct a committee is to average the predictions of a set of individual models. Such a procedure can be motivated from a frequentist perspective by considering the trade-off between bias and variance, which decomposes the error due to a model into the bias component that arises from differences between the model and the true function to be predicted, and the variance component that represents the sensitivity of the model to the individual data points. Recall from Figure 3.5

Section 3.2

that when we trained multiple polynomials using the sinusoidal data, and then averaged the resulting functions, the contribution arising from the variance term tended to cancel, leading to improved predictions. When we averaged a set of low-bias models (corresponding to higher order polynomials), we obtained accurate predictions for the underlying sinusoidal function from which the data were generated.

In practice, of course, we have only a single data set, and so we have to find a way to introduce variability between the different models within the committee. One approach is to use *bootstrap* data sets, discussed in Section 1.2.3. Consider a regression problem in which we are trying to predict the value of a single continuous variable, and suppose we generate M bootstrap data sets and then use each to train a separate copy $y_m(\mathbf{x})$ of a predictive model where $m = 1, \ldots, M$. The committee prediction is given by

$$y_{\mathrm{COM}}(\mathbf{x}) = \frac{1}{M}\sum_{m=1}^{M} y_m(\mathbf{x}). \tag{14.7}$$

This procedure is known as bootstrap aggregation or *bagging* (Breiman, 1996).

Suppose the true regression function that we are trying to predict is given by $h(\mathbf{x})$, so that the output of each of the models can be written as the true value plus an error in the form

$$y_m(\mathbf{x}) = h(\mathbf{x}) + \epsilon_m(\mathbf{x}). \tag{14.8}$$

The average sum-of-squares error then takes the form

$$\mathbb{E}_{\mathbf{x}}\left[\{y_m(\mathbf{x}) - h(\mathbf{x})\}^2\right] = \mathbb{E}_{\mathbf{x}}\left[\epsilon_m(\mathbf{x})^2\right] \tag{14.9}$$

where $\mathbb{E}_{\mathbf{x}}[\cdot]$ denotes a frequentist expectation with respect to the distribution of the input vector $\mathbf{x}$. The average error made by the models acting individually is therefore

$$E_{\mathrm{AV}} = \frac{1}{M}\sum_{m=1}^{M} \mathbb{E}_{\mathbf{x}}\left[\epsilon_m(\mathbf{x})^2\right]. \tag{14.10}$$

Similarly, the expected error from the committee (14.7) is given by

$$\begin{aligned} E_{\mathrm{COM}} &= \mathbb{E}_{\mathbf{x}}\left[\left\{\frac{1}{M}\sum_{m=1}^{M} y_m(\mathbf{x}) - h(\mathbf{x})\right\}^2\right] \\ &= \mathbb{E}_{\mathbf{x}}\left[\left\{\frac{1}{M}\sum_{m=1}^{M} \epsilon_m(\mathbf{x})\right\}^2\right] \end{aligned} \tag{14.11}$$

If we assume that the errors have zero mean and are uncorrelated, so that

$$\mathbb{E}_{\mathbf{x}}\left[\epsilon_m(\mathbf{x})\right] = 0 \tag{14.12}$$

$$\mathbb{E}_{\mathbf{x}}\left[\epsilon_m(\mathbf{x})\epsilon_l(\mathbf{x})\right] = 0, \qquad m \neq l \tag{14.13}$$

Exercise 14.2

then we obtain

$$E_{\mathrm{COM}} = \frac{1}{M} E_{\mathrm{AV}}. \tag{14.14}$$

This apparently dramatic result suggests that the average error of a model can be reduced by a factor of M simply by averaging M versions of the model. Unfortunately, it depends on the key assumption that the errors due to the individual models are uncorrelated. In practice, the errors are typically highly correlated, and the reduction in overall error is generally small. It can, however, be shown that the expected committee error will not exceed the expected error of the constituent models, so that $E_{\mathrm{COM}} \leqslant E_{\mathrm{AV}}$. In order to achieve more significant improvements, we turn to a more sophisticated technique for building committees, known as boosting.

Exercise 14.3

14.3. Boosting

Boosting is a powerful technique for combining multiple 'base' classifiers to produce a form of committee whose performance can be significantly better than that of any of the base classifiers. Here we describe the most widely used form of boosting algorithm called *AdaBoost*, short for 'adaptive boosting', developed by Freund and Schapire (1996). Boosting can give good results even if the base classifiers have a performance that is only slightly better than random, and hence sometimes the base classifiers are known as *weak learners*. Originally designed for solving classification problems, boosting can also be extended to regression (Friedman, 2001).

The principal difference between boosting and the committee methods such as bagging discussed above, is that the base classifiers are trained in sequence, and each base classifier is trained using a weighted form of the data set in which the weighting coefficient associated with each data point depends on the performance of the previous classifiers. In particular, points that are misclassified by one of the base classifiers are given greater weight when used to train the next classifier in the sequence. Once all the classifiers have been trained, their predictions are then combined through a weighted majority voting scheme, as illustrated schematically in Figure 14.1.

Consider a two-class classification problem, in which the training data comprises input vectors $\mathbf{x}_1, \ldots, \mathbf{x}_N$ along with corresponding binary target variables $t_1, \ldots, t_N$ where $t_n \in \{-1, 1\}$. Each data point is given an associated weighting parameter w_n, which is initially set $1/N$ for all data points. We shall suppose that we have a procedure available for training a base classifier using weighted data to give a function $y(\mathbf{x}) \in \{-1, 1\}$. At each stage of the algorithm, AdaBoost trains a new classifier using a data set in which the weighting coefficients are adjusted according to the performance of the previously trained classifier so as to give greater weight to the misclassified data points. Finally, when the desired number of base classifiers have been trained, they are combined to form a committee using coefficients that give different weight to different base classifiers. The precise form of the AdaBoost algorithm is given below.

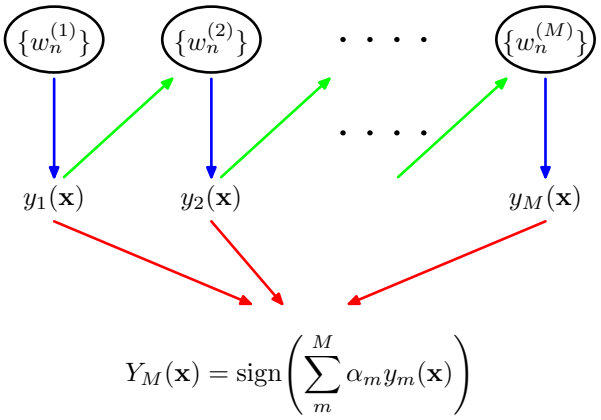

Figure 14.1 Schematic illustration of the boosting framework. Each base classifier $y_m(\mathbf{x})$ is trained on a weighted form of the training set (blue arrows) in which the weights $w_n^{(m)}$ depend on the performance of the previous base classifier $y_{m-1}(\mathbf{x})$ (green arrows). Once all base classifiers have been trained, they are combined to give the final classifier $Y_M(\mathbf{x})$ (red arrows).

AdaBoost

1. Initialize the data weighting coefficients $\{w_n\}$ by setting $w_n^{(1)} = 1/N$ for $n = 1, \ldots, N$.
2. For $m = 1, \ldots, M$:
   (a) Fit a classifier $y_m(\mathbf{x})$ to the training data by minimizing the weighted error function

$$J_m = \sum_{n=1}^{N} w_n^{(m)} I(y_m(\mathbf{x}_n) \neq t_n) \tag{14.15}$$

   where $I(y_m(\mathbf{x}_n) \neq t_n)$ is the indicator function and equals 1 when $y_m(\mathbf{x}_n) \neq t_n$ and 0 otherwise.

   (b) Evaluate the quantities

$$\epsilon_m = \frac{\sum_{n=1}^{N} w_n^{(m)} I(y_m(\mathbf{x}_n) \neq t_n)}{\sum_{n=1}^{N} w_n^{(m)}} \tag{14.16}$$

   and then use these to evaluate

$$\alpha_m = \ln\left\{\frac{1-\epsilon_m}{\epsilon_m}\right\}. \tag{14.17}$$

   (c) Update the data weighting coefficients

$$w_n^{(m+1)} = w_n^{(m)} \exp\left\{\alpha_m I(y_m(\mathbf{x}_n) \neq t_n)\right\} \tag{14.18}$$

3. Make predictions using the final model, which is given by

$$Y_M(\mathbf{x}) = \text{sign}\left(\sum_{m=1}^{M} \alpha_m y_m(\mathbf{x})\right). \tag{14.19}$$

We see that the first base classifier $y_1(\mathbf{x})$ is trained using weighting coefficients $w_n^{(1)}$ that are all equal, which therefore corresponds to the usual procedure for training a single classifier. From (14.18), we see that in subsequent iterations the weighting coefficients $w_n^{(m)}$ are increased for data points that are misclassified and decreased for data points that are correctly classified. Successive classifiers are therefore forced to place greater emphasis on points that have been misclassified by previous classifiers, and data points that continue to be misclassified by successive classifiers receive ever greater weight. The quantities ϵ_m represent weighted measures of the error rates of each of the base classifiers on the data set. We therefore see that the weighting coefficients α_m defined by (14.17) give greater weight to the more accurate classifiers when computing the overall output given by (14.19).

The AdaBoost algorithm is illustrated in Figure 14.2, using a subset of 30 data points taken from the toy classification data set shown in Figure A.7. Here each base learners consists of a threshold on one of the input variables. This simple classifier corresponds to a form of decision tree known as a 'decision stumps', i.e., a decision tree with a single node. Thus each base learner classifies an input according to whether one of the input features exceeds some threshold and therefore simply partitions the space into two regions separated by a linear decision surface that is parallel to one of the axes.

Section 14.4

14.3.1 Minimizing exponential error

Boosting was originally motivated using statistical learning theory, leading to upper bounds on the generalization error. However, these bounds turn out to be too loose to have practical value, and the actual performance of boosting is much better than the bounds alone would suggest. Friedman *et al.* (2000) gave a different and very simple interpretation of boosting in terms of the sequential minimization of an exponential error function.

Consider the exponential error function defined by

$$E = \sum_{n=1}^{N} \exp\{-t_n f_m(\mathbf{x}_n)\} \tag{14.20}$$

where $f_m(\mathbf{x})$ is a classifier defined in terms of a linear combination of base classifiers $y_l(\mathbf{x})$ of the form

$$f_m(\mathbf{x}) = \frac{1}{2}\sum_{l=1}^{m} \alpha_l y_l(\mathbf{x}) \tag{14.21}$$

and $t_n \in \{-1, 1\}$ are the training set target values. Our goal is to minimize E with respect to both the weighting coefficients α_l and the parameters of the base classifiers $y_l(\mathbf{x})$.

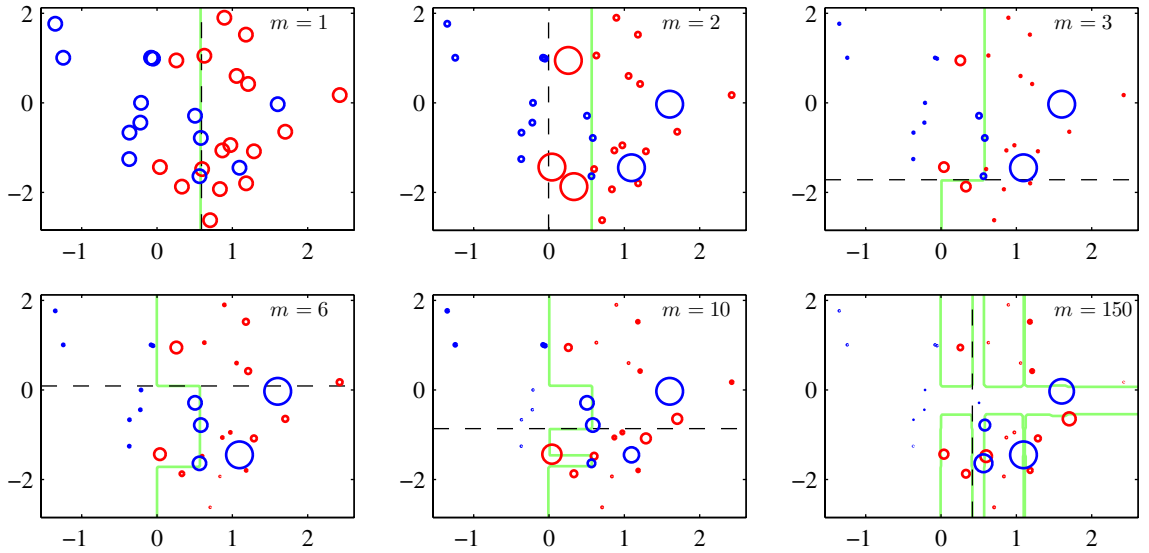

Figure 14.2 Illustration of boosting in which the base learners consist of simple thresholds applied to one or other of the axes. Each figure shows the number m of base learners trained so far, along with the decision boundary of the most recent base learner (dashed black line) and the combined decision boundary of the ensemble (solid green line). Each data point is depicted by a circle whose radius indicates the weight assigned to that data point when training the most recently added base learner. Thus, for instance, we see that points that are misclassified by the $m = 1$ base learner are given greater weight when training the $m = 2$ base learner.

Instead of doing a global error function minimization, however, we shall suppose that the base classifiers $y_1(\mathbf{x}), \ldots, y_{m-1}(\mathbf{x})$ are fixed, as are their coefficients $\alpha_1, \ldots, \alpha_{m-1}$, and so we are minimizing only with respect to α_m and $y_m(\mathbf{x})$. Separating off the contribution from base classifier $y_m(\mathbf{x})$, we can then write the error function in the form

$$\begin{aligned} E &= \sum_{n=1}^{N} \exp\left\{-t_n f_{m-1}(\mathbf{x}_n) - \frac{1}{2} t_n \alpha_m y_m(\mathbf{x}_n)\right\} \\ &= \sum_{n=1}^{N} w_n^{(m)} \exp\left\{-\frac{1}{2} t_n \alpha_m y_m(\mathbf{x}_n)\right\} \end{aligned} \tag{14.22}$$

where the coefficients $w_n^{(m)} = \exp\{-t_n f_{m-1}(\mathbf{x}_n)\}$ can be viewed as constants because we are optimizing only α_m and $y_m(\mathbf{x})$. If we denote by $\mathcal{T}_m$ the set of data points that are correctly classified by $y_m(\mathbf{x})$, and if we denote the remaining misclassified points by $\mathcal{M}_m$, then we can in turn rewrite the error function in the

form

$$\begin{aligned} E &= e^{-\alpha_m/2} \sum_{n\in\mathcal{T}_m} w_n^{(m)} + e^{\alpha_m/2} \sum_{n\in\mathcal{M}_m} w_n^{(m)} \\ &= (e^{\alpha_m/2} - e^{-\alpha_m/2}) \sum_{n=1}^{N} w_n^{(m)} I(y_m(\mathbf{x}_n) \neq t_n) + e^{-\alpha_m/2} \sum_{n=1}^{N} w_n^{(m)}. \end{aligned} \tag{14.23}$$

When we minimize this with respect to $y_m(\mathbf{x})$, we see that the second term is constant, and so this is equivalent to minimizing (14.15) because the overall multiplicative factor in front of the summation does not affect the location of the minimum. Similarly, minimizing with respect to α_m, we obtain (14.17) in which ϵ_m is defined by (14.16).

Exercise 14.6

From (14.22) we see that, having found α_m and $y_m(\mathbf{x})$, the weights on the data points are updated using

$$w_n^{(m+1)} = w_n^{(m)} \exp\left\{-\frac{1}{2} t_n \alpha_m y_m(\mathbf{x}_n)\right\}. \tag{14.24}$$

Making use of the fact that

$$t_n y_m(\mathbf{x}_n) = 1 - 2I(y_m(\mathbf{x}_n) \neq t_n) \tag{14.25}$$

we see that the weights $w_n^{(m)}$ are updated at the next iteration using

$$w_n^{(m+1)} = w_n^{(m)} \exp(-\alpha_m/2) \exp\left\{\alpha_m I(y_m(\mathbf{x}_n) \neq t_n)\right\}. \tag{14.26}$$

Because the term $\exp(-\alpha_m/2)$ is independent of n, we see that it weights all data points by the same factor and so can be discarded. Thus we obtain (14.18).

Finally, once all the base classifiers are trained, new data points are classified by evaluating the sign of the combined function defined according to (14.21). Because the factor of $1/2$ does not affect the sign it can be omitted, giving (14.19).

14.3.2 Error functions for boosting

The exponential error function that is minimized by the AdaBoost algorithm differs from those considered in previous chapters. To gain some insight into the nature of the exponential error function, we first consider the expected error given by

$$\mathbb{E}_{\mathbf{x},t}\left[\exp\{-ty(\mathbf{x})\}\right] = \sum_t \int \exp\{-ty(\mathbf{x})\} p(t|\mathbf{x}) p(\mathbf{x})\, \mathrm{d}\mathbf{x}. \tag{14.27}$$

If we perform a variational minimization with respect to all possible functions $y(\mathbf{x})$, we obtain

Exercise 14.7

$$y(\mathbf{x}) = \frac{1}{2} \ln\left\{\frac{p(t=1|\mathbf{x})}{p(t=-1|\mathbf{x})}\right\} \tag{14.28}$$

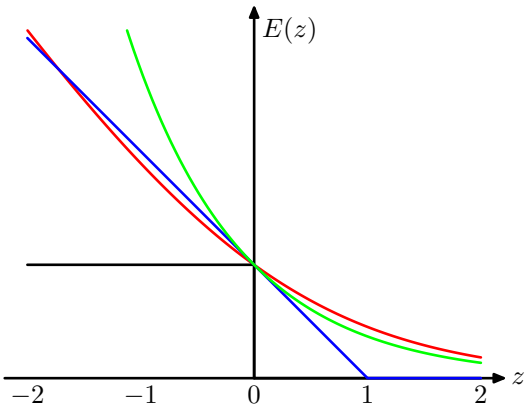

Figure 14.3 Plot of the exponential (green) and rescaled cross-entropy (red) error functions along with the hinge error (blue) used in support vector machines, and the misclassification error (black). Note that for large negative values of $z = ty(\mathbf{x})$, the cross-entropy gives a linearly increasing penalty, whereas the exponential loss gives an exponentially increasing penalty.

which is half the log-odds. Thus the AdaBoost algorithm is seeking the best approximation to the log odds ratio, within the space of functions represented by the linear combination of base classifiers, subject to the constrained minimization resulting from the sequential optimization strategy. This result motivates the use of the sign function in (14.19) to arrive at the final classification decision.

Section 7.1.2

We have already seen that the minimizer $y(\mathbf{x})$ of the cross-entropy error (4.90) for two-class classification is given by the posterior class probability. In the case of a target variable $t \in \{-1, 1\}$, we have seen that the error function is given by $\ln(1 + \exp(-yt))$. This is compared with the exponential error function in Figure 14.3, where we have divided the cross-entropy error by a constant factor $\ln(2)$ so that it passes through the point $(0, 1)$ for ease of comparison. We see that both can be seen as continuous approximations to the ideal misclassification error function. An advantage of the exponential error is that its sequential minimization leads to the simple AdaBoost scheme. One drawback, however, is that it penalizes large negative values of $ty(\mathbf{x})$ much more strongly than cross-entropy. In particular, we see that for large negative values of ty, the cross-entropy grows linearly with $|ty|$, whereas the exponential error function grows exponentially with $|ty|$. Thus the exponential error function will be much less robust to outliers or misclassified data points. Another important difference between cross-entropy and the exponential error function is that the latter cannot be interpreted as the log likelihood function of any well-defined probabilistic model. Furthermore, the exponential error does not generalize to classification problems having $K > 2$ classes, again in contrast to the cross-entropy for a probabilistic model, which is easily generalized to give (4.108).

Exercise 14.8

Section 4.3.4

The interpretation of boosting as the sequential optimization of an additive model under an exponential error (Friedman *et al.*, 2000) opens the door to a wide range of boosting-like algorithms, including multiclass extensions, by altering the choice of error function. It also motivates the extension to regression problems (Friedman, 2001). If we consider a sum-of-squares error function for regression, then sequential minimization of an additive model of the form (14.21) simply involves fitting each new base classifier to the residual errors $t_n - f_{m-1}(\mathbf{x}_n)$ from the previous model. As we have noted, however, the sum-of-squares error is not robust to outliers, and this

Exercise 14.9

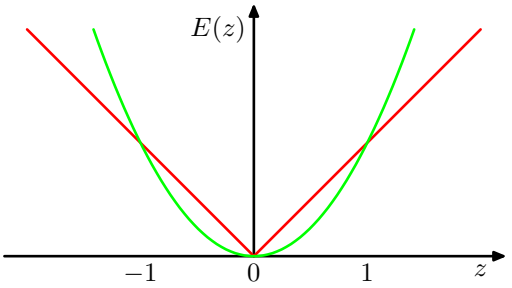

Figure 14.4 Comparison of the squared error (green) with the absolute error (red) showing how the latter places much less emphasis on large errors and hence is more robust to outliers and mislabelled data points.

can be addressed by basing the boosting algorithm on the absolute deviation $|y - t|$ instead. These two error functions are compared in Figure 14.4.

14.4. Tree-based Models

There are various simple, but widely used, models that work by partitioning the input space into cuboid regions, whose edges are aligned with the axes, and then assigning a simple model (for example, a constant) to each region. They can be viewed as a model combination method in which only one model is responsible for making predictions at any given point in input space. The process of selecting a specific model, given a new input $\mathbf{x}$, can be described by a sequential decision making process corresponding to the traversal of a binary tree (one that splits into two branches at each node). Here we focus on a particular tree-based framework called *classification and regression trees*, or *CART* (Breiman *et al.*, 1984), although there are many other variants going by such names as ID3 and C4.5 (Quinlan, 1986; Quinlan, 1993).

Figure 14.5 shows an illustration of a recursive binary partitioning of the input space, along with the corresponding tree structure. In this example, the first step

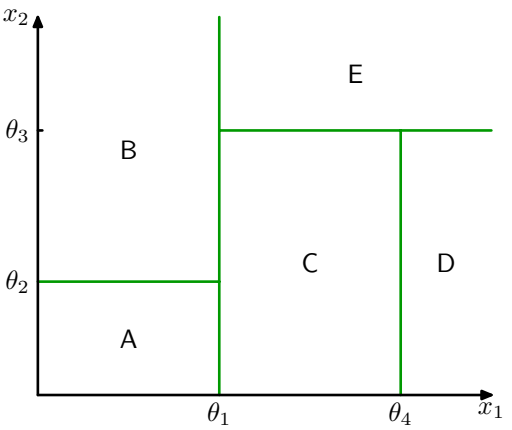

Figure 14.5 Illustration of a two-dimensional input space that has been partitioned into five regions using axis-aligned boundaries.

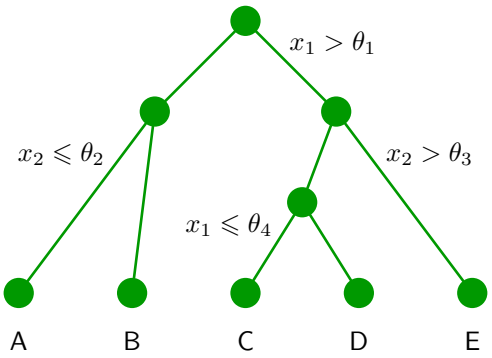

Figure 14.6 Binary tree corresponding to the partitioning of input space shown in Figure 14.5.

divides the whole of the input space into two regions according to whether $x_1 \leqslant \theta_1$ or $x_1 > \theta_1$ where θ_1 is a parameter of the model. This creates two subregions, each of which can then be subdivided independently. For instance, the region $x_1 \leqslant \theta_1$ is further subdivided according to whether $x_2 \leqslant \theta_2$ or $x_2 > \theta_2$, giving rise to the regions denoted A and B. The recursive subdivision can be described by the traversal of the binary tree shown in Figure 14.6. For any new input $\mathbf{x}$, we determine which region it falls into by starting at the top of the tree at the root node and following a path down to a specific leaf node according to the decision criteria at each node. Note that such decision trees are not probabilistic graphical models.

Within each region, there is a separate model to predict the target variable. For instance, in regression we might simply predict a constant over each region, or in classification we might assign each region to a specific class. A key property of tree-based models, which makes them popular in fields such as medical diagnosis, for example, is that they are readily interpretable by humans because they correspond to a sequence of binary decisions applied to the individual input variables. For instance, to predict a patient's disease, we might first ask "is their temperature greater than some threshold?". If the answer is yes, then we might next ask "is their blood pressure less than some threshold?". Each leaf of the tree is then associated with a specific diagnosis.

In order to learn such a model from a training set, we have to determine the structure of the tree, including which input variable is chosen at each node to form the split criterion as well as the value of the threshold parameter θ_i for the split. We also have to determine the values of the predictive variable within each region.

Consider first a regression problem in which the goal is to predict a single target variable t from a D-dimensional vector $\mathbf{x} = (x_1, \ldots, x_D)^{\mathrm{T}}$ of input variables. The training data consists of input vectors $\{\mathbf{x}_1, \ldots, \mathbf{x}_N\}$ along with the corresponding continuous labels $\{t_1, \ldots, t_N\}$. If the partitioning of the input space is given, and we minimize the sum-of-squares error function, then the optimal value of the predictive variable within any given region is just given by the average of the values of t_n for those data points that fall in that region.

Exercise 14.10

Now consider how to determine the structure of the decision tree. Even for a fixed number of nodes in the tree, the problem of determining the optimal structure (including choice of input variable for each split as well as the corresponding thresh-

olds) to minimize the sum-of-squares error is usually computationally infeasible due to the combinatorially large number of possible solutions. Instead, a greedy optimization is generally done by starting with a single root node, corresponding to the whole input space, and then growing the tree by adding nodes one at a time. At each step there will be some number of candidate regions in input space that can be split, corresponding to the addition of a pair of leaf nodes to the existing tree. For each of these, there is a choice of which of the D input variables to split, as well as the value of the threshold. The joint optimization of the choice of region to split, and the choice of input variable and threshold, can be done efficiently by exhaustive search noting that, for a given choice of split variable and threshold, the optimal choice of predictive variable is given by the local average of the data, as noted earlier. This is repeated for all possible choices of variable to be split, and the one that gives the smallest residual sum-of-squares error is retained.

Given a greedy strategy for growing the tree, there remains the issue of when to stop adding nodes. A simple approach would be to stop when the reduction in residual error falls below some threshold. However, it is found empirically that often none of the available splits produces a significant reduction in error, and yet after several more splits a substantial error reduction is found. For this reason, it is common practice to grow a large tree, using a stopping criterion based on the number of data points associated with the leaf nodes, and then prune back the resulting tree. The pruning is based on a criterion that balances residual error against a measure of model complexity. If we denote the starting tree for pruning by T_0, then we define $T \subset T_0$ to be a subtree of T_0 if it can be obtained by pruning nodes from T_0 (in other words, by collapsing internal nodes by combining the corresponding regions). Suppose the leaf nodes are indexed by $\tau = 1, \ldots, |T|$, with leaf node τ representing a region $\mathcal{R}_\tau$ of input space having N_τ data points, and $|T|$ denoting the total number of leaf nodes. The optimal prediction for region $\mathcal{R}_\tau$ is then given by

$$y_\tau = \frac{1}{N_\tau} \sum_{\mathbf{x}_n \in \mathcal{R}_\tau} t_n \tag{14.29}$$

and the corresponding contribution to the residual sum-of-squares is then

$$Q_\tau(T) = \sum_{\mathbf{x}_n \in \mathcal{R}_\tau} \{t_n - y_\tau\}^2 . \tag{14.30}$$

The pruning criterion is then given by

$$C(T) = \sum_{\tau=1}^{|T|} Q_\tau(T) + \lambda |T| \tag{14.31}$$

The regularization parameter λ determines the trade-off between the overall residual sum-of-squares error and the complexity of the model as measured by the number $|T|$ of leaf nodes, and its value is chosen by cross-validation.

For classification problems, the process of growing and pruning the tree is similar, except that the sum-of-squares error is replaced by a more appropriate measure

of performance. If we define $p_{\tau k}$ to be the proportion of data points in region $\mathcal{R}_\tau$ assigned to class k, where $k = 1, \ldots, K$, then two commonly used choices are the cross-entropy

$$Q_\tau(T) = \sum_{k=1}^{K} p_{\tau k} \ln p_{\tau k} \tag{14.32}$$

and the *Gini index*

$$Q_\tau(T) = \sum_{k=1}^{K} p_{\tau k} \left(1 - p_{\tau k}\right). \tag{14.33}$$

These both vanish for $p_{\tau k} = 0$ and $p_{\tau k} = 1$ and have a maximum at $p_{\tau k} = 0.5$. They encourage the formation of regions in which a high proportion of the data points are assigned to one class. The cross entropy and the Gini index are better measures than the misclassification rate for growing the tree because they are more sensitive to the node probabilities. Also, unlike misclassification rate, they are differentiable and hence better suited to gradient based optimization methods. For subsequent pruning of the tree, the misclassification rate is generally used.

Exercise 14.11

The human interpretability of a tree model such as CART is often seen as its major strength. However, in practice it is found that the particular tree structure that is learned is very sensitive to the details of the data set, so that a small change to the training data can result in a very different set of splits (Hastie *et al.*, 2001).

There are other problems with tree-based methods of the kind considered in this section. One is that the splits are aligned with the axes of the feature space, which may be very suboptimal. For instance, to separate two classes whose optimal decision boundary runs at 45 degrees to the axes would need a large number of axis-parallel splits of the input space as compared to a single non-axis-aligned split. Furthermore, the splits in a decision tree are hard, so that each region of input space is associated with one, and only one, leaf node model. The last issue is particularly problematic in regression where we are typically aiming to model smooth functions, and yet the tree model produces piecewise-constant predictions with discontinuities at the split boundaries.

14.5. Conditional Mixture Models

We have seen that standard decision trees are restricted by hard, axis-aligned splits of the input space. These constraints can be relaxed, at the expense of interpretability, by allowing soft, probabilistic splits that can be functions of all of the input variables, not just one of them at a time. If we also give the leaf models a probabilistic interpretation, we arrive at a fully probabilistic tree-based model called the *hierarchical mixture of experts*, which we consider in Section 14.5.3.

An alternative way to motivate the hierarchical mixture of experts model is to start with a standard probabilistic mixtures of unconditional density models such as Gaussians and replace the component densities with conditional distributions. Here we consider mixtures of linear regression models (Section 14.5.1) and mixtures of

Chapter 9

logistic regression models (Section 14.5.2). In the simplest case, the mixing coefficients are independent of the input variables. If we make a further generalization to allow the mixing coefficients also to depend on the inputs then we obtain a *mixture of experts* model. Finally, if we allow each component in the mixture model to be itself a mixture of experts model, then we obtain a hierarchical mixture of experts.

14.5.1 Mixtures of linear regression models

One of the many advantages of giving a probabilistic interpretation to the linear regression model is that it can then be used as a component in more complex probabilistic models. This can be done, for instance, by viewing the conditional distribution representing the linear regression model as a node in a directed probabilistic graph. Here we consider a simple example corresponding to a mixture of linear regression models, which represents a straightforward extension of the Gaussian mixture model discussed in Section 9.2 to the case of conditional Gaussian distributions.

We therefore consider K linear regression models, each governed by its own weight parameter $\mathbf{w}_k$. In many applications, it will be appropriate to use a common noise variance, governed by a precision parameter β, for all K components, and this is the case we consider here. We will once again restrict attention to a single target variable t, though the extension to multiple outputs is straightforward. If we denote the mixing coefficients by π_k, then the mixture distribution can be written

Exercise 14.12

$$p(t|\boldsymbol{\theta}) = \sum_{k=1}^{K} \pi_k \mathcal{N}(t|\mathbf{w}_k^{\mathrm{T}}\boldsymbol{\phi}, \beta^{-1}) \tag{14.34}$$

where $\boldsymbol{\theta}$ denotes the set of all adaptive parameters in the model, namely $\mathbf{W} = \{\mathbf{w}_k\}$, $\boldsymbol{\pi} = \{\pi_k\}$, and β. The log likelihood function for this model, given a data set of observations $\{\boldsymbol{\phi}_n, t_n\}$, then takes the form

$$\ln p(\mathbf{t}|\boldsymbol{\theta}) = \sum_{n=1}^{N} \ln \left(\sum_{k=1}^{K} \pi_k \mathcal{N}(t_n|\mathbf{w}_k^{\mathrm{T}}\boldsymbol{\phi}_n, \beta^{-1}) \right) \tag{14.35}$$

where $\mathbf{t} = (t_1, \ldots, t_N)^{\mathrm{T}}$ denotes the vector of target variables.

In order to maximize this likelihood function, we can once again appeal to the EM algorithm, which will turn out to be a simple extension of the EM algorithm for unconditional Gaussian mixtures of Section 9.2. We can therefore build on our experience with the unconditional mixture and introduce a set $\mathbf{Z} = \{\mathbf{z}_n\}$ of binary latent variables where $z_{nk} \in \{0, 1\}$ in which, for each data point n, all of the elements $k = 1, \ldots, K$ are zero except for a single value of 1 indicating which component of the mixture was responsible for generating that data point. The joint distribution over latent and observed variables can be represented by the graphical model shown in Figure 14.7.

The complete-data log likelihood function then takes the form

Exercise 14.13

$$\ln p(\mathbf{t}, \mathbf{Z}|\boldsymbol{\theta}) = \sum_{n=1}^{N} \sum_{k=1}^{K} z_{nk} \ln \left\{ \pi_k \mathcal{N}(t_n|\mathbf{w}_k^{\mathrm{T}}\boldsymbol{\phi}_n, \beta^{-1}) \right\}. \tag{14.36}$$

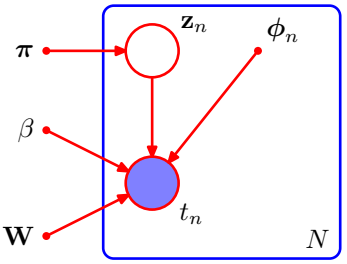

Figure 14.7 Probabilistic directed graph representing a mixture of linear regression models, defined by (14.35).

The EM algorithm begins by first choosing an initial value $\boldsymbol{\theta}^{\text{old}}$ for the model parameters. In the E step, these parameter values are then used to evaluate the posterior probabilities, or responsibilities, of each component k for every data point n given by

$$\gamma_{nk} = \mathbb{E}[z_{nk}] = p(k|\boldsymbol{\phi}_n, \boldsymbol{\theta}^{\text{old}}) = \frac{\pi_k \mathcal{N}(t_n|\mathbf{w}_k^{\text{T}}\boldsymbol{\phi}_n, \beta^{-1})}{\sum_j \pi_j \mathcal{N}(t_n|\mathbf{w}_j^{\text{T}}\boldsymbol{\phi}_n, \beta^{-1})}. \tag{14.37}$$

The responsibilities are then used to determine the expectation, with respect to the posterior distribution $p(\mathbf{Z}|\mathbf{t}, \boldsymbol{\theta}^{\text{old}})$, of the complete-data log likelihood, which takes the form

$$Q(\boldsymbol{\theta}, \boldsymbol{\theta}^{\text{old}}) = \mathbb{E}_{\mathbf{Z}}\left[\ln p(\mathbf{t}, \mathbf{Z}|\boldsymbol{\theta})\right] = \sum_{n=1}^{N}\sum_{k=1}^{K} \gamma_{nk}\left\{\ln \pi_k + \ln \mathcal{N}(t_n|\mathbf{w}_k^{\text{T}}\boldsymbol{\phi}_n, \beta^{-1})\right\}.$$

In the M step, we maximize the function $Q(\boldsymbol{\theta}, \boldsymbol{\theta}^{\text{old}})$ with respect to $\boldsymbol{\theta}$, keeping the γ_{nk} fixed. For the optimization with respect to the mixing coefficients π_k we need to take account of the constraint $\sum_k \pi_k = 1$, which can be done with the aid of a Lagrange multiplier, leading to an M-step re-estimation equation for π_k in the form

Exercise 14.14

$$\pi_k = \frac{1}{N}\sum_{n=1}^{N} \gamma_{nk}. \tag{14.38}$$

Note that this has exactly the same form as the corresponding result for a simple mixture of unconditional Gaussians given by (9.22).

Next consider the maximization with respect to the parameter vector $\mathbf{w}_k$ of the k^{th} linear regression model. Substituting for the Gaussian distribution, we see that the function $Q(\boldsymbol{\theta}, \boldsymbol{\theta}^{\text{old}})$, as a function of the parameter vector $\mathbf{w}_k$, takes the form

$$Q(\boldsymbol{\theta}, \boldsymbol{\theta}^{\text{old}}) = \sum_{n=1}^{N} \gamma_{nk}\left\{-\frac{\beta}{2}\left(t_n - \mathbf{w}_k^{\text{T}}\boldsymbol{\phi}_n\right)^2\right\} + \text{const} \tag{14.39}$$

where the constant term includes the contributions from other weight vectors $\mathbf{w}_j$ for $j \neq k$. Note that the quantity we are maximizing is similar to the (negative of the) standard sum-of-squares error (3.12) for a single linear regression model, but with the inclusion of the responsibilities γ_{nk}. This represents a *weighted least squares*

problem, in which the term corresponding to the n^{th} data point carries a weighting coefficient given by $\beta\gamma_{nk}$, which could be interpreted as an effective precision for each data point. We see that each component linear regression model in the mixture, governed by its own parameter vector $\mathbf{w}_k$, is fitted separately to the whole data set in the M step, but with each data point n weighted by the responsibility γ_{nk} that model k takes for that data point. Setting the derivative of (14.39) with respect to $\mathbf{w}_k$ equal to zero gives

$$0 = \sum_{n=1}^{N} \gamma_{nk} \left(t_n - \mathbf{w}_k^{\mathrm{T}} \boldsymbol{\phi}_n\right) \boldsymbol{\phi}_n \tag{14.40}$$

which we can write in matrix notation as

$$0 = \boldsymbol{\Phi}^{\mathrm{T}} \mathbf{R}_k (\mathbf{t} - \boldsymbol{\Phi} \mathbf{w}_k) \tag{14.41}$$

where $\mathbf{R}_k = \mathrm{diag}(\gamma_{nk})$ is a diagonal matrix of size $N \times N$. Solving for $\mathbf{w}_k$, we obtain

$$\mathbf{w}_k = \left(\boldsymbol{\Phi}^{\mathrm{T}} \mathbf{R}_k \boldsymbol{\Phi}\right)^{-1} \boldsymbol{\Phi}^{\mathrm{T}} \mathbf{R}_k \mathbf{t}. \tag{14.42}$$

This represents a set of modified normal equations corresponding to the weighted least squares problem, of the same form as (4.99) found in the context of logistic regression. Note that after each E step, the matrix $\mathbf{R}_k$ will change and so we will have to solve the normal equations afresh in the subsequent M step.

Finally, we maximize $Q(\boldsymbol{\theta}, \boldsymbol{\theta}^{\mathrm{old}})$ with respect to β. Keeping only terms that depend on β, the function $Q(\boldsymbol{\theta}, \boldsymbol{\theta}^{\mathrm{old}})$ can be written

$$Q(\boldsymbol{\theta}, \boldsymbol{\theta}^{\mathrm{old}}) = \sum_{n=1}^{N} \sum_{k=1}^{K} \gamma_{nk} \left\{ \frac{1}{2} \ln \beta - \frac{\beta}{2} \left(t_n - \mathbf{w}_k^{\mathrm{T}} \boldsymbol{\phi}_n\right)^2 \right\}. \tag{14.43}$$

Setting the derivative with respect to β equal to zero, and rearranging, we obtain the M-step equation for β in the form

$$\frac{1}{\beta} = \frac{1}{N} \sum_{n=1}^{N} \sum_{k=1}^{K} \gamma_{nk} \left(t_n - \mathbf{w}_k^{\mathrm{T}} \boldsymbol{\phi}_n\right)^2. \tag{14.44}$$

In Figure 14.8, we illustrate this EM algorithm using the simple example of fitting a mixture of two straight lines to a data set having one input variable x and one target variable t. The predictive density (14.34) is plotted in Figure 14.9 using the converged parameter values obtained from the EM algorithm, corresponding to the right-hand plot in Figure 14.8. Also shown in this figure is the result of fitting a single linear regression model, which gives a unimodal predictive density. We see that the mixture model gives a much better representation of the data distribution, and this is reflected in the higher likelihood value. However, the mixture model also assigns significant probability mass to regions where there is no data because its predictive distribution is bimodal for all values of x. This problem can be resolved by extending the model to allow the mixture coefficients themselves to be functions of x, leading to models such as the mixture density networks discussed in Section 5.6, and hierarchical mixture of experts discussed in Section 14.5.3.

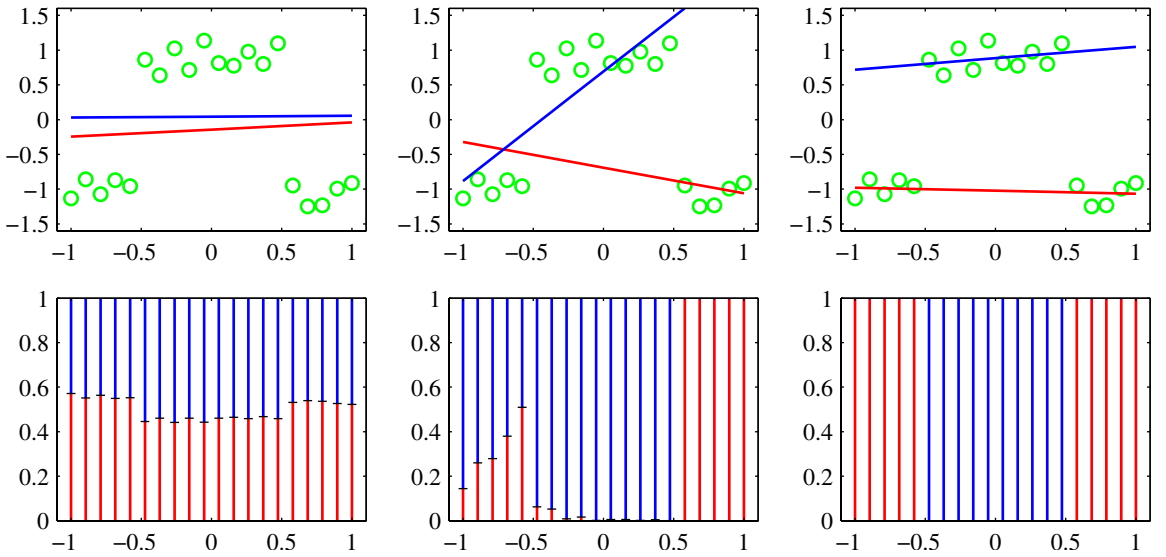

Figure 14.8 Example of a synthetic data set, shown by the green points, having one input variable x and one target variable t, together with a mixture of two linear regression models whose mean functions $y(x, \mathbf{w}_k)$, where $k \in \{1, 2\}$, are shown by the blue and red lines. The upper three plots show the initial configuration (left), the result of running 30 iterations of EM (centre), and the result after 50 iterations of EM (right). Here β was initialized to the reciprocal of the true variance of the set of target values. The lower three plots show the corresponding responsibilities plotted as a vertical line for each data point in which the length of the blue segment gives the posterior probability of the blue line for that data point (and similarly for the red segment).

14.5.2 Mixtures of logistic models

Because the logistic regression model defines a conditional distribution for the target variable, given the input vector, it is straightforward to use it as the component distribution in a mixture model, thereby giving rise to a richer family of conditional distributions compared to a single logistic regression model. This example involves a straightforward combination of ideas encountered in earlier sections of the book and will help consolidate these for the reader.

The conditional distribution of the target variable, for a probabilistic mixture of K logistic regression models, is given by

$$p(t|\boldsymbol{\phi}, \boldsymbol{\theta}) = \sum_{k=1}^{K} \pi_k y_k^t \left[1 - y_k\right]^{1-t} \tag{14.45}$$

where $\boldsymbol{\phi}$ is the feature vector, $y_k = \sigma\left(\mathbf{w}_k^{\mathrm{T}} \boldsymbol{\phi}\right)$ is the output of component k, and $\boldsymbol{\theta}$ denotes the adjustable parameters namely $\{\pi_k\}$ and $\{\mathbf{w}_k\}$.

Now suppose we are given a data set $\{\boldsymbol{\phi}_n, t_n\}$. The corresponding likelihood

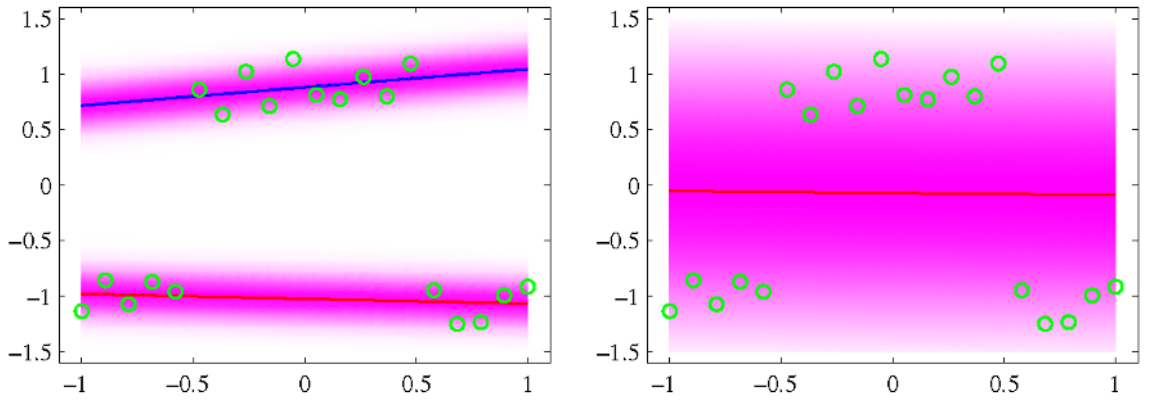

Figure 14.9 The left plot shows the predictive conditional density corresponding to the converged solution in Figure 14.8. This gives a log likelihood value of -3.0. A vertical slice through one of these plots at a particular value of x represents the corresponding conditional distribution $p(t|x)$, which we see is bimodal. The plot on the right shows the predictive density for a single linear regression model fitted to the same data set using maximum likelihood. This model has a smaller log likelihood of -27.6.

function is then given by

$$p(\mathbf{t}|\boldsymbol{\theta}) = \prod_{n=1}^{N} \left(\sum_{k=1}^{K} \pi_k y_{nk}^{t_n} \left[1 - y_{nk}\right]^{1-t_n} \right) \tag{14.46}$$

where $y_{nk} = \sigma(\mathbf{w}_k^{\mathrm{T}} \boldsymbol{\phi}_n)$ and $\mathbf{t} = (t_1, \ldots, t_N)^{\mathrm{T}}$. We can maximize this likelihood function iteratively by making use of the EM algorithm. This involves introducing latent variables z_{nk} that correspond to a 1-of-K coded binary indicator variable for each data point n. The complete-data likelihood function is then given by

$$p(\mathbf{t}, \mathbf{Z}|\boldsymbol{\theta}) = \prod_{n=1}^{N} \prod_{k=1}^{K} \left\{ \pi_k y_{nk}^{t_n} \left[1 - y_{nk}\right]^{1-t_n} \right\}^{z_{nk}} \tag{14.47}$$

where $\mathbf{Z}$ is the matrix of latent variables with elements z_{nk}. We initialize the EM algorithm by choosing an initial value $\boldsymbol{\theta}^{\mathrm{old}}$ for the model parameters. In the E step, we then use these parameter values to evaluate the posterior probabilities of the components k for each data point n, which are given by

$$\gamma_{nk} = \mathbb{E}[z_{nk}] = p(k|\boldsymbol{\phi}_n, \boldsymbol{\theta}^{\mathrm{old}}) = \frac{\pi_k y_{nk}^{t_n} \left[1 - y_{nk}\right]^{1-t_n}}{\sum_j \pi_j y_{nj}^{t_n} \left[1 - y_{nj}\right]^{1-t_n}}. \tag{14.48}$$

These responsibilities are then used to find the expected complete-data log likelihood as a function of $\boldsymbol{\theta}$, given by

$$\begin{aligned} Q(\boldsymbol{\theta}, \boldsymbol{\theta}^{\mathrm{old}}) &= \mathbb{E}_{\mathbf{Z}} \left[\ln p(\mathbf{t}, \mathbf{Z}|\boldsymbol{\theta})\right] \\ &= \sum_{n=1}^{N} \sum_{k=1}^{K} \gamma_{nk} \left\{ \ln \pi_k + t_n \ln y_{nk} + (1 - t_n) \ln \left(1 - y_{nk}\right) \right\}. \end{aligned} \tag{14.49}$$

The M step involves maximization of this function with respect to $\boldsymbol{\theta}$, keeping $\boldsymbol{\theta}^{\text{old}}$, and hence γ_{nk}, fixed. Maximization with respect to π_k can be done in the usual way, with a Lagrange multiplier to enforce the summation constraint $\sum_k \pi_k = 1$, giving the familiar result

$$\pi_k = \frac{1}{N} \sum_{n=1}^{N} \gamma_{nk}. \tag{14.50}$$

To determine the $\{\mathbf{w}_k\}$, we note that the $Q(\boldsymbol{\theta}, \boldsymbol{\theta}^{\text{old}})$ function comprises a sum over terms indexed by k each of which depends only on one of the vectors $\mathbf{w}_k$, so that the different vectors are decoupled in the M step of the EM algorithm. In other words, the different components interact only via the responsibilities, which are fixed during the M step. Note that the M step does not have a closed-form solution and must be solved iteratively using, for instance, the iterative reweighted least squares (IRLS) algorithm. The gradient and the Hessian for the vector $\mathbf{w}_k$ are given by

Section 4.3.3

$$\nabla_k Q = \sum_{n=1}^{N} \gamma_{nk}(t_n - y_{nk})\boldsymbol{\phi}_n \tag{14.51}$$

$$\mathbf{H}_k = -\nabla_k \nabla_k Q = \sum_{n=1}^{N} \gamma_{nk} y_{nk}(1 - y_{nk})\boldsymbol{\phi}_n \boldsymbol{\phi}_n^{\mathrm{T}} \tag{14.52}$$

where ∇_k denotes the gradient with respect to $\mathbf{w}_k$. For fixed γ_{nk}, these are independent of $\{\mathbf{w}_j\}$ for $j \neq k$ and so we can solve for each $\mathbf{w}_k$ separately using the IRLS algorithm. Thus the M-step equations for component k correspond simply to fitting a single logistic regression model to a weighted data set in which data point n carries a weight γ_{nk}. Figure 14.10 shows an example of the mixture of logistic regression models applied to a simple classification problem. The extension of this model to a mixture of softmax models for more than two classes is straightforward.

Section 4.3.3

Exercise 14.16

14.5.3 Mixtures of experts

In Section 14.5.1, we considered a mixture of linear regression models, and in Section 14.5.2 we discussed the analogous mixture of linear classifiers. Although these simple mixtures extend the flexibility of linear models to include more complex (e.g., multimodal) predictive distributions, they are still very limited. We can further increase the capability of such models by allowing the mixing coefficients themselves to be functions of the input variable, so that

$$p(\mathbf{t}|\mathbf{x}) = \sum_{k=1}^{K} \pi_k(\mathbf{x}) p_k(\mathbf{t}|\mathbf{x}). \tag{14.53}$$

This is known as a *mixture of experts* model (Jacobs *et al.*, 1991) in which the mixing coefficients $\pi_k(\mathbf{x})$ are known as *gating* functions and the individual component densities $p_k(\mathbf{t}|\mathbf{x})$ are called *experts*. The notion behind the terminology is that different components can model the distribution in different regions of input space (they

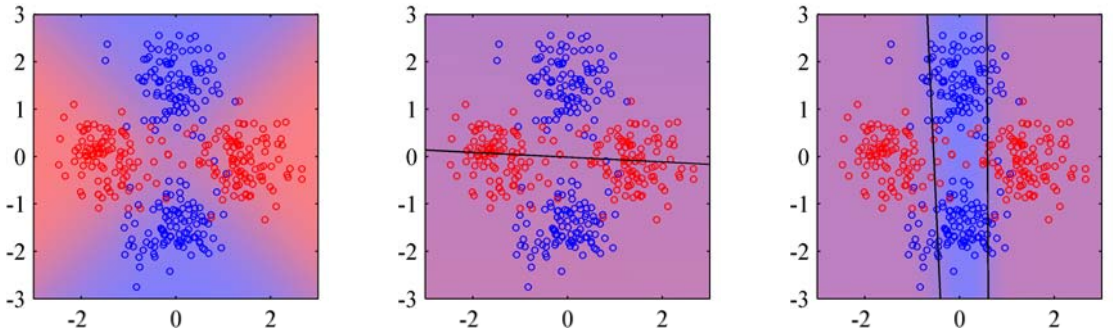

Figure 14.10 Illustration of a mixture of logistic regression models. The left plot shows data points drawn from two classes denoted red and blue, in which the background colour (which varies from pure red to pure blue) denotes the true probability of the class label. The centre plot shows the result of fitting a single logistic regression model using maximum likelihood, in which the background colour denotes the corresponding probability of the class label. Because the colour is a near-uniform purple, we see that the model assigns a probability of around 0.5 to each of the classes over most of input space. The right plot shows the result of fitting a mixture of two logistic regression models, which now gives much higher probability to the correct labels for many of the points in the blue class.

are 'experts' at making predictions in their own regions), and the gating functions determine which components are dominant in which region.

The gating functions $\pi_k(\mathbf{x})$ must satisfy the usual constraints for mixing coefficients, namely $0 \leqslant \pi_k(\mathbf{x}) \leqslant 1$ and $\sum_k \pi_k(\mathbf{x}) = 1$. They can therefore be represented, for example, by linear softmax models of the form (4.104) and (4.105). If the experts are also linear (regression or classification) models, then the whole model can be fitted efficiently using the EM algorithm, with iterative reweighted least squares being employed in the M step (Jordan and Jacobs, 1994).

Such a model still has significant limitations due to the use of linear models for the gating and expert functions. A much more flexible model is obtained by using a multilevel gating function to give the *hierarchical mixture of experts*, or *HME* model (Jordan and Jacobs, 1994). To understand the structure of this model, imagine a mixture distribution in which each component in the mixture is itself a mixture distribution. For simple unconditional mixtures, this hierarchical mixture is trivially equivalent to a single flat mixture distribution. However, when the mixing coefficients are input dependent, this hierarchical model becomes nontrivial. The HME model can also be viewed as a probabilistic version of *decision trees* discussed in Section 14.4 and can again be trained efficiently by maximum likelihood using an EM algorithm with IRLS in the M step. A Bayesian treatment of the HME has been given by Bishop and Svensén (2003) based on variational inference.

Exercise 14.17

Section 4.3.3

We shall not discuss the HME in detail here. However, it is worth pointing out the close connection with the *mixture density network* discussed in Section 5.6. The principal advantage of the mixtures of experts model is that it can be optimized by EM in which the M step for each mixture component and gating model involves a convex optimization (although the overall optimization is nonconvex). By contrast, the advantage of the mixture density network approach is that the component

densities and the mixing coefficients share the hidden units of the neural network. Furthermore, in the mixture density network, the splits of the input space are further relaxed compared to the hierarchical mixture of experts in that they are not only soft, and not constrained to be axis aligned, but they can also be nonlinear.

Exercises

14.1 (⋆⋆) **www** Consider a set models of the form $p(\mathbf{t}|\mathbf{x}, \mathbf{z}_h, \boldsymbol{\theta}_h, h)$ in which $\mathbf{x}$ is the input vector, $\mathbf{t}$ is the target vector, h indexes the different models, $\mathbf{z}_h$ is a latent variable for model h, and $\boldsymbol{\theta}_h$ is the set of parameters for model h. Suppose the models have prior probabilities $p(h)$ and that we are given a training set $\mathbf{X} = \{\mathbf{x}_1, \ldots, \mathbf{x}_N\}$ and $\mathbf{T} = \{\mathbf{t}_1, \ldots, \mathbf{t}_N\}$. Write down the formulae needed to evaluate the predictive distribution $p(\mathbf{t}|\mathbf{x}, \mathbf{X}, \mathbf{T})$ in which the latent variables and the model index are marginalized out. Use these formulae to highlight the difference between Bayesian averaging of different models and the use of latent variables within a single model.

14.2 (⋆) The expected sum-of-squares error E_{AV} for a simple committee model can be defined by (14.10), and the expected error of the committee itself is given by (14.11). Assuming that the individual errors satisfy (14.12) and (14.13), derive the result (14.14).

14.3 (⋆) **www** By making use of Jensen's inequality (1.115), for the special case of the convex function $f(x) = x^2$, show that the average expected sum-of-squares error E_{AV} of the members of a simple committee model, given by (14.10), and the expected error E_{COM} of the committee itself, given by (14.11), satisfy

$$E_{\mathrm{COM}} \leqslant E_{\mathrm{AV}}. \tag{14.54}$$

14.4 (⋆⋆) By making use of Jensen's in equality (1.115), show that the result (14.54) derived in the previous exercise hods for any error function $E(y)$, not just sum-of-squares, provided it is a convex function of y.

14.5 (⋆⋆) **www** Consider a committee in which we allow unequal weighting of the constituent models, so that

$$y_{\mathrm{COM}}(\mathbf{x}) = \sum_{m=1}^{M} \alpha_m y_m(\mathbf{x}). \tag{14.55}$$

In order to ensure that the predictions $y_{\mathrm{COM}}(\mathbf{x})$ remain within sensible limits, suppose that we require that they be bounded at each value of $\mathbf{x}$ by the minimum and maximum values given by any of the members of the committee, so that

$$y_{\min}(\mathbf{x}) \leqslant y_{\mathrm{COM}}(\mathbf{x}) \leqslant y_{\max}(\mathbf{x}). \tag{14.56}$$

Show that a necessary and sufficient condition for this constraint is that the coefficients α_m satisfy

$$\alpha_m \geqslant 0, \qquad \sum_{m=1}^{M} \alpha_m = 1. \tag{14.57}$$

14.6 (⋆) **www** By differentiating the error function (14.23) with respect to α_m, show that the parameters α_m in the AdaBoost algorithm are updated using (14.17) in which ϵ_m is defined by (14.16).

14.7 (⋆) By making a variational minimization of the expected exponential error function given by (14.27) with respect to all possible functions $y(\mathbf{x})$, show that the minimizing function is given by (14.28).

14.8 (⋆) Show that the exponential error function (14.20), which is minimized by the AdaBoost algorithm, does not correspond to the log likelihood of any well-behaved probabilistic model. This can be done by showing that the corresponding conditional distribution $p(t|\mathbf{x})$ cannot be correctly normalized.

14.9 (⋆) **www** Show that the sequential minimization of the sum-of-squares error function for an additive model of the form (14.21) in the style of boosting simply involves fitting each new base classifier to the residual errors $t_n - f_{m-1}(\mathbf{x}_n)$ from the previous model.

14.10 (⋆) Verify that if we minimize the sum-of-squares error between a set of training values $\{t_n\}$ and a single predictive value t, then the optimal solution for t is given by the mean of the $\{t_n\}$.

14.11 (⋆⋆) Consider a data set comprising 400 data points from class $\mathcal{C}_1$ and 400 data points from class $\mathcal{C}_2$. Suppose that a tree model A splits these into $(300, 100)$ at the first leaf node and $(100, 300)$ at the second leaf node, where (n, m) denotes that n points are assigned to $\mathcal{C}_1$ and m points are assigned to $\mathcal{C}_2$. Similarly, suppose that a second tree model B splits them into $(200, 400)$ and $(200, 0)$. Evaluate the misclassification rates for the two trees and hence show that they are equal. Similarly, evaluate the cross-entropy (14.32) and Gini index (14.33) for the two trees and show that they are both lower for tree B than for tree A.

14.12 (⋆⋆) Extend the results of Section 14.5.1 for a mixture of linear regression models to the case of multiple target values described by a vector $\mathbf{t}$. To do this, make use of the results of Section 3.1.5.

14.13 (⋆) **www** Verify that the complete-data log likelihood function for the mixture of linear regression models is given by (14.36).

14.14 (⋆) Use the technique of Lagrange multipliers (Appendix E) to show that the M-step re-estimation equation for the mixing coefficients in the mixture of linear regression models trained by maximum likelihood EM is given by (14.38).

14.15 (⋆) **www** We have already noted that if we use a squared loss function in a regression problem, the corresponding optimal prediction of the target variable for a new input vector is given by the conditional mean of the predictive distribution. Show that the conditional mean for the mixture of linear regression models discussed in Section 14.5.1 is given by a linear combination of the means of each component distribution. Note that if the conditional distribution of the target data is multimodal, the conditional mean can give poor predictions.

14.16 ($\star\star\star$) Extend the logistic regression mixture model of Section 14.5.2 to a mixture of softmax classifiers representing $C \geqslant 2$ classes. Write down the EM algorithm for determining the parameters of this model through maximum likelihood.

14.17 ($\star\star$) **WWW** Consider a mixture model for a conditional distribution $p(t|\mathbf{x})$ of the form

$$p(t|\mathbf{x}) = \sum_{k=1}^{K} \pi_k \psi_k(t|\mathbf{x}) \tag{14.58}$$

in which each mixture component $\psi_k(t|\mathbf{x})$ is itself a mixture model. Show that this two-level hierarchical mixture is equivalent to a conventional single-level mixture model. Now suppose that the mixing coefficients in both levels of such a hierarchical model are arbitrary functions of $\mathbf{x}$. Again, show that this hierarchical model is again equivalent to a single-level model with $\mathbf{x}$-dependent mixing coefficients. Finally, consider the case in which the mixing coefficients at both levels of the hierarchical mixture are constrained to be linear classification (logistic or softmax) models. Show that the hierarchical mixture cannot in general be represented by a single-level mixture having linear classification models for the mixing coefficients. Hint: to do this it is sufficient to construct a single counter-example, so consider a mixture of two components in which one of those components is itself a mixture of two components, with mixing coefficients given by linear-logistic models. Show that this cannot be represented by a single-level mixture of 3 components having mixing coefficients determined by a linear-softmax model.

Appendix A. Data Sets

In this appendix, we give a brief introduction to the data sets used to illustrate some of the algorithms described in this book. Detailed information on file formats for these data sets, as well as the data files themselves, can be obtained from the book web site:

http://research.microsoft.com/∼cmbishop/PRML

Handwritten Digits

The digits data used in this book is taken from the MNIST data set (LeCun *et al.*, 1998), which itself was constructed by modifying a subset of the much larger data set produced by NIST (the National Institute of Standards and Technology). It comprises a training set of $60,000$ examples and a test set of $10,000$ examples. Some of the data was collected from Census Bureau employees and the rest was collected from high-school children, and care was taken to ensure that the test examples were written by different individuals to the training examples.

The original NIST data had binary (black or white) pixels. To create MNIST, these images were size normalized to fit in a 20×20 pixel box while preserving their aspect ratio. As a consequence of the anti-aliasing used to change the resolution of the images, the resulting MNIST digits are grey scale. These images were then centred in a 28×28 box. Examples of the MNIST digits are shown in Figure A.1.

Error rates for classifying the digits range from 12% for a simple linear classifier, through 0.56% for a carefully designed support vector machine, to 0.4% for a convolutional neural network (LeCun *et al.*, 1998).

Figure A.1 One hundred examples of the MNIST digits chosen at random from the training set.

Oil Flow

This is a synthetic data set that arose out of a project aimed at measuring noninvasively the proportions of oil, water, and gas in North Sea oil transfer pipelines (Bishop and James, 1993). It is based on the principle of *dual-energy gamma densitometry*. The ideas is that if a narrow beam of gamma rays is passed through the pipe, the attenuation in the intensity of the beam provides information about the density of material along its path. Thus, for instance, the beam will be attenuated more strongly by oil than by gas.

A single attenuation measurement alone is not sufficient because there are two degrees of freedom corresponding to the fraction of oil and the fraction of water (the fraction of gas is redundant because the three fractions must add to one). To address this, two gamma beams of different energies (in other words different frequencies or wavelengths) are passed through the pipe along the same path, and the attenuation of each is measured. Because the absorbtion properties of different materials vary differently as a function of energy, measurement of the attenuations at the two energies provides two independent pieces of information. Given the known absorbtion properties of oil, water, and gas at the two energies, it is then a simple matter to calculate the average fractions of oil and water (and hence of gas) measured *along the path* of the gamma beams.

There is a further complication, however, associated with the motion of the materials along the pipe. If the flow velocity is small, then the oil floats on top of the water with the gas sitting above the oil. This is known as a *laminar* or *stratified*

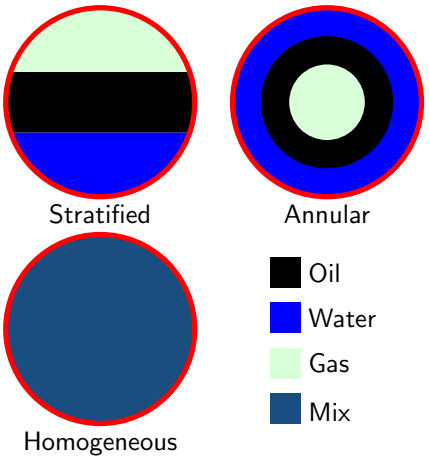

Figure A.2 The three geometrical configurations of the oil, water, and gas phases used to generate the oil-flow data set. For each configuration, the proportions of the three phases can vary.

flow configuration and is illustrated in Figure A.2. As the flow velocity is increased, more complex geometrical configurations of the oil, water, and gas can arise. For the purposes of this data set, two specific idealizations are considered. In the *annular* configuration the oil, water, and gas form concentric cylinders with the water around the outside and the gas in the centre, whereas in the *homogeneous* configuration the oil, water and gas are assumed to be intimately mixed as might occur at high flow velocities under turbulent conditions. These configurations are also illustrated in Figure A.2.

We have seen that a single dual-energy beam gives the oil and water fractions measured along the path length, whereas we are interested in the volume fractions of oil and water. This can be addressed by using multiple dual-energy gamma densitometers whose beams pass through different regions of the pipe. For this particular data set, there are six such beams, and their spatial arrangement is shown in Figure A.3. A single observation is therefore represented by a 12-dimensional vector comprising the fractions of oil and water measured along the paths of each of the beams. We are, however, interested in obtaining the overall volume fractions of the three phases in the pipe. This is much like the classical problem of tomographic reconstruction, used in medical imaging for example, in which a two-dimensional dis-

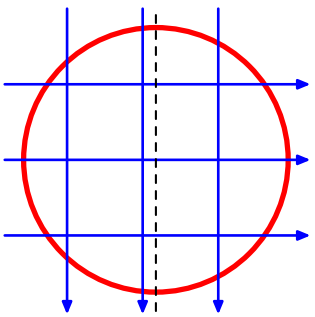

Figure A.3 Cross section of the pipe showing the arrangement of the six beam lines, each of which comprises a single dual-energy gamma densitometer. Note that the vertical beams are asymmetrically arranged relative to the central axis (shown by the dotted line).

tribution is to be reconstructed from an number of one-dimensional averages. Here there are far fewer line measurements than in a typical tomography application. On the other hand the range of geometrical configurations is much more limited, and so the configuration, as well as the phase fractions, can be predicted with reasonable accuracy from the densitometer data.

For safety reasons, the intensity of the gamma beams is kept relatively weak and so to obtain an accurate measurement of the attenuation, the measured beam intensity is integrated over a specific time interval. For a finite integration time, there are random fluctuations in the measured intensity due to the fact that the gamma beams comprise discrete packets of energy called photons. In practice, the integration time is chosen as a compromise between reducing the noise level (which requires a long integration time) and detecting temporal variations in the flow (which requires a short integration time). The oil flow data set is generated using realistic known values for the absorption properties of oil, water, and gas at the two gamma energies used, and with a specific choice of integration time (10 seconds) chosen as characteristic of a typical practical setup.

Each point in the data set is generated independently using the following steps:

1. Choose one of the three phase configurations at random with equal probability.

2. Choose three random numbers f_1, f_2 and f_3 from the uniform distribution over $(0, 1)$ and define

$$f_{\text{oil}} = \frac{f_1}{f_1 + f_2 + f_3}, \qquad f_{\text{water}} = \frac{f_2}{f_1 + f_2 + f_3}. \tag{A.1}$$

   This treats the three phases on an equal footing and ensures that the volume fractions add to one.

3. For each of the six beam lines, calculate the effective path lengths through oil and water for the given phase configuration.

4. Perturb the path lengths using the Poisson distribution based on the known beam intensities and integration time to allow for the effect of photon statistics.

Each point in the data set comprises the 12 path length measurements, together with the fractions of oil and water and a binary label describing the phase configuration. The data set is divided into training, validation, and test sets, each of which comprises $1,000$ independent data points. Details of the data format are available from the book web site.

In Bishop and James (1993), statistical machine learning techniques were used to predict the volume fractions and also the geometrical configuration of the phases shown in Figure A.2, from the 12-dimensional vector of measurements. The 12-dimensional observation vectors can also be used to test data visualization algorithms.

This data set has a rich and interesting structure, as follows. For any given configuration there are two degrees of freedom corresponding to the fractions of

oil and water, and so for infinite integration time the data will locally live on a two-dimensional manifold. For a finite integration time, the individual data points will be perturbed away from the manifold by the photon noise. In the homogeneous phase configuration, the path lengths in oil and water are linearly related to the fractions of oil and water, and so the data points lie close to a linear manifold. For the annular configuration, the relationship between phase fraction and path length is nonlinear and so the manifold will be nonlinear. In the case of the laminar configuration the situation is even more complex because small variations in the phase fractions can cause one of the horizontal phase boundaries to move across one of the horizontal beam lines leading to a discontinuous jump in the 12-dimensional observation space. In this way, the two-dimensional nonlinear manifold for the laminar configuration is broken into six distinct segments. Note also that some of the manifolds for different phase configurations meet at specific points, for example if the pipe is filled entirely with oil, it corresponds to specific instances of the laminar, annular, and homogeneous configurations.

Old Faithful

Old Faithful, shown in Figure A.4, is a hydrothermal geyser in Yellowstone National Park in the state of Wyoming, U.S.A., and is a popular tourist attraction. Its name stems from the supposed regularity of its eruptions.

The data set comprises 272 observations, each of which represents a single eruption and contains two variables corresponding to the duration in minutes of the eruption, and the time until the next eruption, also in minutes. Figure A.5 shows a plot of the time to the next eruption versus the duration of the eruptions. It can be seen that the time to the next eruption varies considerably, although knowledge of the duration of the current eruption allows it to be predicted more accurately. Note that there exist several other data sets relating to the eruptions of Old Faithful.

Figure A.4 The Old Faithful geyser in Yellowstone National Park. ©Bruce T. Gourley www.brucegourley.com.

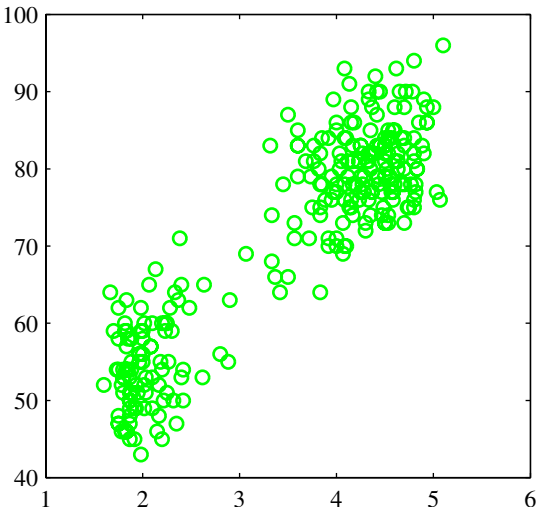

Figure A.5 Plot of the time to the next eruption in minutes (vertical axis) versus the duration of the eruption in minutes (horizontal axis) for the Old Faithful data set.

Synthetic Data

Throughout the book, we use two simple synthetic data sets to illustrate many of the algorithms. The first of these is a regression problem, based on the sinusoidal function, shown in Figure A.6. The input values $\{x_n\}$ are generated uniformly in range $(0, 1)$, and the corresponding target values $\{t_n\}$ are obtained by first computing the corresponding values of the function $\sin(2\pi x)$, and then adding random noise with a Gaussian distribution having standard deviation 0.3. Various forms of this data set, having different numbers of data points, are used in the book.

The second data set is a classification problem having two classes, with equal prior probabilities, and is shown in Figure A.7. The blue class is generated from a single Gaussian while the red class comes from a mixture of two Gaussians. Because we know the class priors and the class-conditional densities, it is straightforward to evaluate and plot the true posterior probabilities as well as the minimum misclassification-rate decision boundary, as shown in Figure A.7.

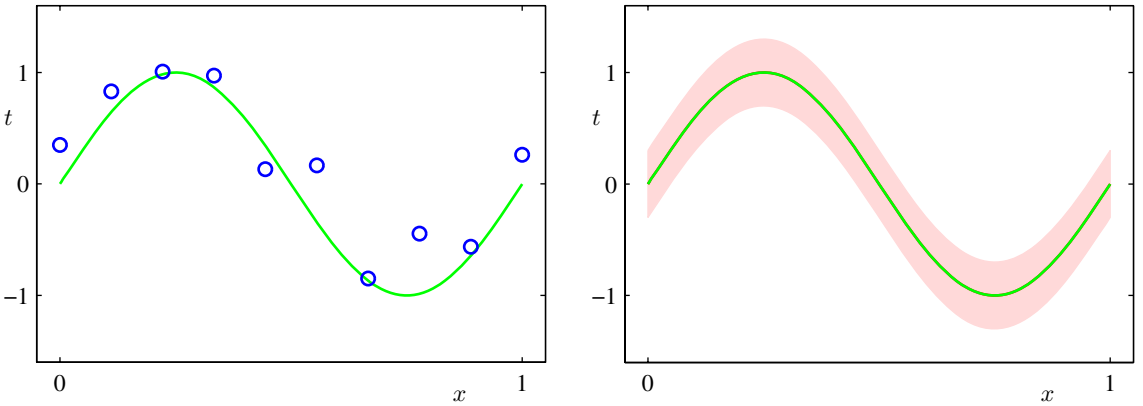

Figure A.6 The left-hand plot shows the synthetic regression data set along with the underlying sinusoidal function from which the data points were generated. The right-hand plot shows the true conditional distribution $p(t|x)$ from which the labels are generated, in which the green curve denotes the mean, and the shaded region spans one standard deviation on each side of the mean.

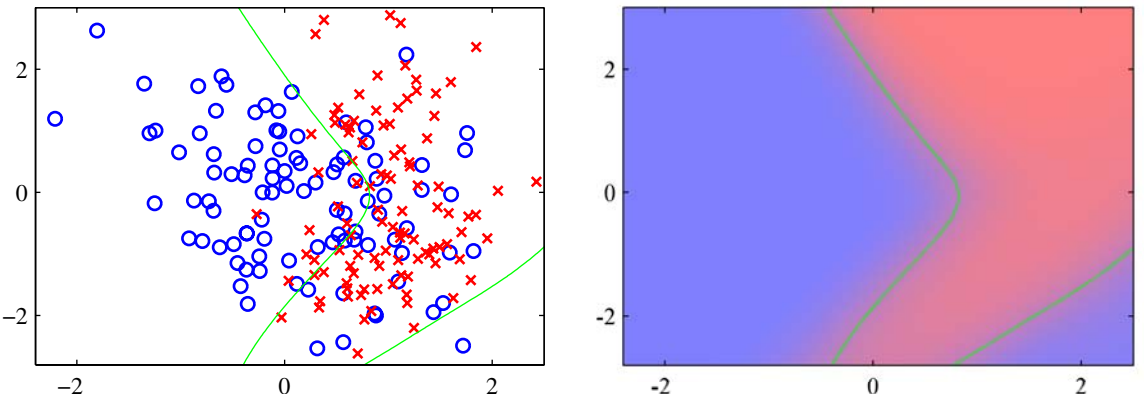

Figure A.7 The left plot shows the synthetic classification data set with data from the two classes shown in red and blue. On the right is a plot of the true posterior probabilities, shown on a colour scale going from pure red denoting probability of the red class is 1 to pure blue denoting probability of the red class is 0. Because these probabilities are known, the optimal decision boundary for minimizing the misclassification rate (which corresponds to the contour along which the posterior probabilities for each class equal 0.5) can be evaluated and is shown by the green curve. This decision boundary is also plotted on the left-hand figure.

Appendix B. Probability Distributions

In this appendix, we summarize the main properties of some of the most widely used probability distributions, and for each distribution we list some key statistics such as the expectation $\mathbb{E}[\mathbf{x}]$, the variance (or covariance), the mode, and the entropy $\mathrm{H}[\mathbf{x}]$. All of these distributions are members of the exponential family and are widely used as building blocks for more sophisticated probabilistic models.

Bernoulli

This is the distribution for a single binary variable $x \in \{0, 1\}$ representing, for example, the result of flipping a coin. It is governed by a single continuous parameter $\mu \in [0, 1]$ that represents the probability of $x = 1$.

$$\mathrm{Bern}(x|\mu) = \mu^x(1-\mu)^{1-x} \tag{B.1}$$

$$\mathbb{E}[x] = \mu \tag{B.2}$$

$$\mathrm{var}[x] = \mu(1-\mu) \tag{B.3}$$

$$\mathrm{mode}[x] = \begin{cases} 1 & \text{if } \mu \geqslant 0.5, \\ 0 & \text{otherwise} \end{cases} \tag{B.4}$$

$$\mathrm{H}[x] = -\mu \ln \mu - (1-\mu)\ln(1-\mu). \tag{B.5}$$

The Bernoulli is a special case of the binomial distribution for the case of a single observation. Its conjugate prior for μ is the beta distribution.

Beta

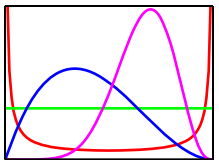

This is a distribution over a continuous variable $\mu \in [0, 1]$, which is often used to represent the probability for some binary event. It is governed by two parameters a and b that are constrained by $a > 0$ and $b > 0$ to ensure that the distribution can be normalized.

$$\text{Beta}(\mu|a, b) = \frac{\Gamma(a+b)}{\Gamma(a)\Gamma(b)}\mu^{a-1}(1-\mu)^{b-1} \tag{B.6}$$

$$\mathbb{E}[\mu] = \frac{a}{a+b} \tag{B.7}$$

$$\text{var}[\mu] = \frac{ab}{(a+b)^2(a+b+1)} \tag{B.8}$$

$$\text{mode}[\mu] = \frac{a-1}{a+b-2}. \tag{B.9}$$

The beta is the conjugate prior for the Bernoulli distribution, for which a and b can be interpreted as the effective prior number of observations of $x = 1$ and $x = 0$, respectively. Its density is finite if $a \geqslant 1$ and $b \geqslant 1$, otherwise there is a singularity at $\mu = 0$ and/or $\mu = 1$. For $a = b = 1$, it reduces to a uniform distribution. The beta distribution is a special case of the K-state Dirichlet distribution for $K = 2$.

Binomial

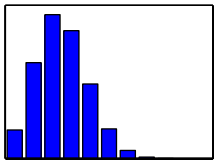

The binomial distribution gives the probability of observing m occurrences of $x = 1$ in a set of N samples from a Bernoulli distribution, where the probability of observing $x = 1$ is $\mu \in [0, 1]$.

$$\text{Bin}(m|N, \mu) = \binom{N}{m}\mu^m(1-\mu)^{N-m} \tag{B.10}$$

$$\mathbb{E}[m] = N\mu \tag{B.11}$$

$$\text{var}[m] = N\mu(1-\mu) \tag{B.12}$$

$$\text{mode}[m] = \lfloor (N+1)\mu \rfloor \tag{B.13}$$

where $\lfloor (N+1)\mu \rfloor$ denotes the largest integer that is less than or equal to $(N+1)\mu$, and the quantity

$$\binom{N}{m} = \frac{N!}{m!(N-m)!} \tag{B.14}$$

denotes the number of ways of choosing m objects out of a total of N identical objects. Here $m!$, pronounced 'factorial m', denotes the product $m \times (m-1) \times \ldots, \times 2 \times 1$. The particular case of the binomial distribution for $N = 1$ is known as the Bernoulli distribution, and for large N the binomial distribution is approximately Gaussian. The conjugate prior for μ is the beta distribution.

Dirichlet

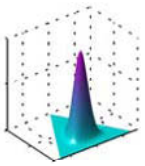

The Dirichlet is a multivariate distribution over K random variables $0 \leqslant \mu_k \leqslant 1$, where $k = 1, \ldots, K$, subject to the constraints

$$0 \leqslant \mu_k \leqslant 1, \qquad \sum_{k=1}^{K} \mu_k = 1. \tag{B.15}$$

Denoting $\boldsymbol{\mu} = (\mu_1, \ldots, \mu_K)^{\mathrm{T}}$ and $\boldsymbol{\alpha} = (\alpha_1, \ldots, \alpha_K)^{\mathrm{T}}$, we have

$$\begin{aligned}
\mathrm{Dir}(\boldsymbol{\mu}|\boldsymbol{\alpha}) &= C(\boldsymbol{\alpha}) \prod_{k=1}^{K} \mu_k^{\alpha_k - 1} && \text{(B.16)}\\
\mathbb{E}[\mu_k] &= \frac{\alpha_k}{\widehat{\alpha}} && \text{(B.17)}\\
\mathrm{var}[\mu_k] &= \frac{\alpha_k(\widehat{\alpha} - \alpha_k)}{\widehat{\alpha}^2(\widehat{\alpha} + 1)} && \text{(B.18)}\\
\mathrm{cov}[\mu_j \mu_k] &= -\frac{\alpha_j \alpha_k}{\widehat{\alpha}^2(\widehat{\alpha} + 1)} && \text{(B.19)}\\
\mathrm{mode}[\mu_k] &= \frac{\alpha_k - 1}{\widehat{\alpha} - K} && \text{(B.20)}\\
\mathbb{E}[\ln \mu_k] &= \psi(\alpha_k) - \psi(\widehat{\alpha}) && \text{(B.21)}\\
\mathrm{H}[\boldsymbol{\mu}] &= -\sum_{k=1}^{K} (\alpha_k - 1)\{\psi(\alpha_k) - \psi(\widehat{\alpha})\} - \ln C(\boldsymbol{\alpha}) && \text{(B.22)}
\end{aligned}$$

where

$$C(\boldsymbol{\alpha}) = \frac{\Gamma(\widehat{\alpha})}{\Gamma(\alpha_1) \cdots \Gamma(\alpha_K)} \tag{B.23}$$

and

$$\widehat{\alpha} = \sum_{k=1}^{K} \alpha_k. \tag{B.24}$$

Here

$$\psi(a) \equiv \frac{d}{da} \ln \Gamma(a) \tag{B.25}$$

is known as the *digamma* function (Abramowitz and Stegun, 1965). The parameters α_k are subject to the constraint $\alpha_k > 0$ in order to ensure that the distribution can be normalized.

The Dirichlet forms the conjugate prior for the multinomial distribution and represents a generalization of the beta distribution. In this case, the parameters α_k can be interpreted as effective numbers of observations of the corresponding values of the K-dimensional binary observation vector $\mathbf{x}$. As with the beta distribution, the Dirichlet has finite density everywhere provided $\alpha_k \geqslant 1$ for all k.

Gamma

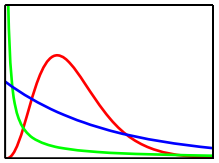

The Gamma is a probability distribution over a positive random variable $\tau > 0$ governed by parameters a and b that are subject to the constraints $a > 0$ and $b > 0$ to ensure that the distribution can be normalized.

$$\mathrm{Gam}(\tau|a,b) = \frac{1}{\Gamma(a)} b^a \tau^{a-1} e^{-b\tau} \tag{B.26}$$

$$\mathbb{E}[\tau] = \frac{a}{b} \tag{B.27}$$

$$\mathrm{var}[\tau] = \frac{a}{b^2} \tag{B.28}$$

$$\mathrm{mode}[\tau] = \frac{a-1}{b} \quad \text{for } \alpha \geqslant 1 \tag{B.29}$$

$$\mathbb{E}[\ln \tau] = \psi(a) - \ln b \tag{B.30}$$

$$\mathrm{H}[\tau] = \ln \Gamma(a) - (a-1)\psi(a) - \ln b + a \tag{B.31}$$

where $\psi(\cdot)$ is the digamma function defined by (B.25). The gamma distribution is the conjugate prior for the precision (inverse variance) of a univariate Gaussian. For $a \geqslant 1$ the density is everywhere finite, and the special case of $a = 1$ is known as the *exponential* distribution.

Gaussian

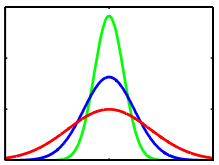

The Gaussian is the most widely used distribution for continuous variables. It is also known as the *normal* distribution. In the case of a single variable $x \in (-\infty, \infty)$ it is governed by two parameters, the mean $\mu \in (-\infty, \infty)$ and the variance $\sigma^2 > 0$.

$$\mathcal{N}(x|\mu,\sigma^2) = \frac{1}{(2\pi\sigma^2)^{1/2}} \exp\left\{-\frac{1}{2\sigma^2}(x-\mu)^2\right\} \tag{B.32}$$

$$\mathbb{E}[x] = \mu \tag{B.33}$$

$$\mathrm{var}[x] = \sigma^2 \tag{B.34}$$

$$\mathrm{mode}[x] = \mu \tag{B.35}$$

$$\mathrm{H}[x] = \frac{1}{2}\ln\sigma^2 + \frac{1}{2}\left(1 + \ln(2\pi)\right). \tag{B.36}$$

The inverse of the variance $\tau = 1/\sigma^2$ is called the precision, and the square root of the variance σ is called the standard deviation. The conjugate prior for μ is the Gaussian, and the conjugate prior for τ is the gamma distribution. If both μ and τ are unknown, their joint conjugate prior is the Gaussian-gamma distribution.

For a D-dimensional vector $\mathbf{x}$, the Gaussian is governed by a D-dimensional mean vector $\boldsymbol{\mu}$ and a $D \times D$ covariance matrix $\boldsymbol{\Sigma}$ that must be symmetric and

positive-definite.

$$\mathcal{N}(\mathbf{x}|\boldsymbol{\mu},\boldsymbol{\Sigma}) = \frac{1}{(2\pi)^{D/2}}\frac{1}{|\boldsymbol{\Sigma}|^{1/2}}\exp\left\{-\frac{1}{2}(\mathbf{x}-\boldsymbol{\mu})^{\mathrm{T}}\boldsymbol{\Sigma}^{-1}(\mathbf{x}-\boldsymbol{\mu})\right\} \quad \text{(B.37)}$$

$$\mathbb{E}[\mathbf{x}] = \boldsymbol{\mu} \quad \text{(B.38)}$$

$$\mathrm{cov}[\mathbf{x}] = \boldsymbol{\Sigma} \quad \text{(B.39)}$$

$$\mathrm{mode}[\mathbf{x}] = \boldsymbol{\mu} \quad \text{(B.40)}$$

$$\mathrm{H}[\mathbf{x}] = \frac{1}{2}\ln|\boldsymbol{\Sigma}| + \frac{D}{2}\left(1+\ln(2\pi)\right). \quad \text{(B.41)}$$

The inverse of the covariance matrix $\boldsymbol{\Lambda} = \boldsymbol{\Sigma}^{-1}$ is the precision matrix, which is also symmetric and positive definite. Averages of random variables tend to a Gaussian, by the central limit theorem, and the sum of two Gaussian variables is again Gaussian. The Gaussian is the distribution that maximizes the entropy for a given variance (or covariance). Any linear transformation of a Gaussian random variable is again Gaussian. The marginal distribution of a multivariate Gaussian with respect to a subset of the variables is itself Gaussian, and similarly the conditional distribution is also Gaussian. The conjugate prior for $\boldsymbol{\mu}$ is the Gaussian, the conjugate prior for $\boldsymbol{\Lambda}$ is the Wishart, and the conjugate prior for $(\boldsymbol{\mu},\boldsymbol{\Lambda})$ is the Gaussian-Wishart.

If we have a marginal Gaussian distribution for $\mathbf{x}$ and a conditional Gaussian distribution for $\mathbf{y}$ given $\mathbf{x}$ in the form

$$p(\mathbf{x}) = \mathcal{N}(\mathbf{x}|\boldsymbol{\mu},\boldsymbol{\Lambda}^{-1}) \quad \text{(B.42)}$$

$$p(\mathbf{y}|\mathbf{x}) = \mathcal{N}(\mathbf{y}|\mathbf{A}\mathbf{x}+\mathbf{b},\mathbf{L}^{-1}) \quad \text{(B.43)}$$

then the marginal distribution of $\mathbf{y}$, and the conditional distribution of $\mathbf{x}$ given $\mathbf{y}$, are given by

$$p(\mathbf{y}) = \mathcal{N}(\mathbf{y}|\mathbf{A}\boldsymbol{\mu}+\mathbf{b},\mathbf{L}^{-1}+\mathbf{A}\boldsymbol{\Lambda}^{-1}\mathbf{A}^{\mathrm{T}}) \quad \text{(B.44)}$$

$$p(\mathbf{x}|\mathbf{y}) = \mathcal{N}(\mathbf{x}|\boldsymbol{\Sigma}\{\mathbf{A}^{\mathrm{T}}\mathbf{L}(\mathbf{y}-\mathbf{b})+\boldsymbol{\Lambda}\boldsymbol{\mu}\},\boldsymbol{\Sigma}) \quad \text{(B.45)}$$

where

$$\boldsymbol{\Sigma} = (\boldsymbol{\Lambda}+\mathbf{A}^{\mathrm{T}}\mathbf{L}\mathbf{A})^{-1}. \quad \text{(B.46)}$$

If we have a joint Gaussian distribution $\mathcal{N}(\mathbf{x}|\boldsymbol{\mu},\boldsymbol{\Sigma})$ with $\boldsymbol{\Lambda} \equiv \boldsymbol{\Sigma}^{-1}$ and we define the following partitions

$$\mathbf{x} = \begin{pmatrix}\mathbf{x}_a\\ \mathbf{x}_b\end{pmatrix}, \qquad \boldsymbol{\mu} = \begin{pmatrix}\boldsymbol{\mu}_a\\ \boldsymbol{\mu}_b\end{pmatrix} \quad \text{(B.47)}$$

$$\boldsymbol{\Sigma} = \begin{pmatrix}\boldsymbol{\Sigma}_{aa} & \boldsymbol{\Sigma}_{ab}\\ \boldsymbol{\Sigma}_{ba} & \boldsymbol{\Sigma}_{bb}\end{pmatrix}, \qquad \boldsymbol{\Lambda} = \begin{pmatrix}\boldsymbol{\Lambda}_{aa} & \boldsymbol{\Lambda}_{ab}\\ \boldsymbol{\Lambda}_{ba} & \boldsymbol{\Lambda}_{bb}\end{pmatrix} \quad \text{(B.48)}$$

then the conditional distribution $p(\mathbf{x}_a|\mathbf{x}_b)$ is given by

$$p(\mathbf{x}_a|\mathbf{x}_b) = \mathcal{N}(\mathbf{x}|\boldsymbol{\mu}_{a|b},\boldsymbol{\Lambda}_{aa}^{-1}) \quad \text{(B.49)}$$

$$\boldsymbol{\mu}_{a|b} = \boldsymbol{\mu}_a - \boldsymbol{\Lambda}_{aa}^{-1}\boldsymbol{\Lambda}_{ab}(\mathbf{x}_b-\boldsymbol{\mu}_b) \quad \text{(B.50)}$$

and the marginal distribution $p(\mathbf{x}_a)$ is given by

$$p(\mathbf{x}_a) = \mathcal{N}(\mathbf{x}_a|\boldsymbol{\mu}_a, \boldsymbol{\Sigma}_{aa}). \tag{B.51}$$

Gaussian-Gamma

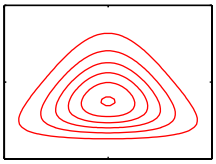

This is the conjugate prior distribution for a univariate Gaussian $\mathcal{N}(x|\mu, \lambda^{-1})$ in which the mean μ and the precision λ are both unknown and is also called the *normal-gamma* distribution. It comprises the product of a Gaussian distribution for μ, whose precision is proportional to λ, and a gamma distribution over λ.

$$p(\mu, \lambda|\mu_0, \beta, a, b) = \mathcal{N}\left(\mu|\mu_o, (\beta\lambda)^{-1}\right) \mathrm{Gam}(\lambda|a, b). \tag{B.52}$$

Gaussian-Wishart

This is the conjugate prior distribution for a multivariate Gaussian $\mathcal{N}(\mathbf{x}|\boldsymbol{\mu}, \boldsymbol{\Lambda})$ in which both the mean $\boldsymbol{\mu}$ and the precision $\boldsymbol{\Lambda}$ are unknown, and is also called the normal-Wishart distribution. It comprises the product of a Gaussian distribution for $\boldsymbol{\mu}$, whose precision is proportional to $\boldsymbol{\Lambda}$, and a Wishart distribution over $\boldsymbol{\Lambda}$.

$$p(\boldsymbol{\mu}, \boldsymbol{\Lambda}|\boldsymbol{\mu}_0, \beta, \mathbf{W}, \nu) = \mathcal{N}\left(\boldsymbol{\mu}|\boldsymbol{\mu}_0, (\beta\boldsymbol{\Lambda})^{-1}\right) \mathcal{W}(\boldsymbol{\Lambda}|\mathbf{W}, \nu). \tag{B.53}$$

For the particular case of a scalar x, this is equivalent to the Gaussian-gamma distribution.

Multinomial

If we generalize the Bernoulli distribution to an K-dimensional binary variable $\mathbf{x}$ with components $x_k \in \{0, 1\}$ such that $\sum_k x_k = 1$, then we obtain the following discrete distribution

$$p(\mathbf{x}) = \prod_{k=1}^{K} \mu_k^{x_k} \tag{B.54}$$

$$\mathbb{E}[x_k] = \mu_k \tag{B.55}$$

$$\mathrm{var}[x_k] = \mu_k(1 - \mu_k) \tag{B.56}$$

$$\mathrm{cov}[x_j x_k] = I_{jk}\mu_k \tag{B.57}$$

$$\mathrm{H}[\mathbf{x}] = -\sum_{k=1}^{M} \mu_k \ln \mu_k \tag{B.58}$$

where I_{jk} is the j, k element of the identity matrix. Because $p(x_k = 1) = \mu_k$, the parameters must satisfy $0 \leqslant \mu_k \leqslant 1$ and $\sum_k \mu_k = 1$.

The multinomial distribution is a multivariate generalization of the binomial and gives the distribution over counts m_k for a K-state discrete variable to be in state k given a total number of observations N.

$$\text{Mult}(m_1, m_2, \ldots, m_K|\boldsymbol{\mu}, N) = \binom{N}{m_1 m_2 \ldots m_M} \prod_{k=1}^{M} \mu_k^{m_k} \tag{B.59}$$

$$\mathbb{E}[m_k] = N\mu_k \tag{B.60}$$

$$\text{var}[m_k] = N\mu_k(1 - \mu_k) \tag{B.61}$$

$$\text{cov}[m_j m_k] = -N\mu_j\mu_k \tag{B.62}$$

where $\boldsymbol{\mu} = (\mu_1, \ldots, \mu_K)^{\text{T}}$, and the quantity

$$\binom{N}{m_1 m_2 \ldots m_K} = \frac{N!}{m_1! \ldots m_K!} \tag{B.63}$$

gives the number of ways of taking N identical objects and assigning m_k of them to bin k for $k = 1, \ldots, K$. The value of μ_k gives the probability of the random variable taking state k, and so these parameters are subject to the constraints $0 \leqslant \mu_k \leqslant 1$ and $\sum_k \mu_k = 1$. The conjugate prior distribution for the parameters $\{\mu_k\}$ is the Dirichlet.

Normal

The normal distribution is simply another name for the Gaussian. In this book, we use the term Gaussian throughout, although we retain the conventional use of the symbol $\mathcal{N}$ to denote this distribution. For consistency, we shall refer to the normal-gamma distribution as the Gaussian-gamma distribution, and similarly the normal-Wishart is called the Gaussian-Wishart.

Student's t

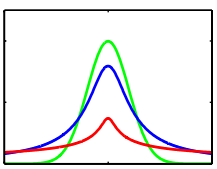

This distribution was published by William Gosset in 1908, but his employer, Guiness Breweries, required him to publish under a pseudonym, so he chose 'Student'. In the univariate form, Student's t-distribution is obtained by placing a conjugate gamma prior over the precision of a univariate Gaussian distribution and then integrating out the precision variable. It can therefore be viewed as an infinite mixture

of Gaussians having the same mean but different variances.

$$\mathrm{St}(x|\mu,\lambda,\nu) = \frac{\Gamma(\nu/2+1/2)}{\Gamma(\nu/2)}\left(\frac{\lambda}{\pi\nu}\right)^{1/2}\left[1+\frac{\lambda(x-\mu)^2}{\nu}\right]^{-\nu/2-1/2} \tag{B.64}$$

$$\mathbb{E}[x] = \mu \quad \text{for } \nu > 1 \tag{B.65}$$

$$\mathrm{var}[x] = \frac{1}{\lambda}\frac{\nu}{\nu-2} \quad \text{for } \nu > 2 \tag{B.66}$$

$$\mathrm{mode}[x] = \mu. \tag{B.67}$$

Here $\nu > 0$ is called the number of degrees of freedom of the distribution. The particular case of $\nu = 1$ is called the *Cauchy* distribution.

For a D-dimensional variable $\mathbf{x}$, Student's t-distribution corresponds to marginalizing the precision matrix of a multivariate Gaussian with respect to a conjugate Wishart prior and takes the form

$$\mathrm{St}(\mathbf{x}|\boldsymbol{\mu},\boldsymbol{\Lambda},\nu) = \frac{\Gamma(\nu/2+D/2)}{\Gamma(\nu/2)}\frac{|\boldsymbol{\Lambda}|^{1/2}}{(\nu\pi)^{D/2}}\left[1+\frac{\Delta^2}{\nu}\right]^{-\nu/2-D/2} \tag{B.68}$$

$$\mathbb{E}[\mathbf{x}] = \boldsymbol{\mu} \quad \text{for } \nu > 1 \tag{B.69}$$

$$\mathrm{cov}[\mathbf{x}] = \frac{\nu}{\nu-2}\boldsymbol{\Lambda}^{-1} \quad \text{for } \nu > 2 \tag{B.70}$$

$$\mathrm{mode}[\mathbf{x}] = \boldsymbol{\mu} \tag{B.71}$$

where Δ^2 is the squared Mahalanobis distance defined by

$$\Delta^2 = (\mathbf{x}-\boldsymbol{\mu})^{\mathrm{T}}\boldsymbol{\Lambda}(\mathbf{x}-\boldsymbol{\mu}). \tag{B.72}$$

In the limit $\nu \to \infty$, the t-distribution reduces to a Gaussian with mean μ and precision $\boldsymbol{\Lambda}$. Student's t-distribution provides a generalization of the Gaussian whose maximum likelihood parameter values are robust to outliers.

Uniform

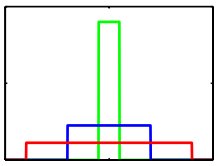

This is a simple distribution for a continuous variable x defined over a finite interval $x \in [a,b]$ where $b > a$.

$$\mathrm{U}(x|a,b) = \frac{1}{b-a} \tag{B.73}$$

$$\mathbb{E}[x] = \frac{(b+a)}{2} \tag{B.74}$$

$$\mathrm{var}[x] = \frac{(b-a)^2}{12} \tag{B.75}$$

$$\mathrm{H}[x] = \ln(b-a). \tag{B.76}$$

If x has distribution $\mathrm{U}(x|0,1)$, then $a+(b-a)x$ will have distribution $\mathrm{U}(x|a,b)$.

Von Mises

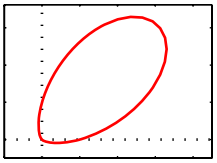

The von Mises distribution, also known as the circular normal or the circular Gaussian, is a univariate Gaussian-like periodic distribution for a variable $\theta \in [0, 2\pi)$.

$$p(\theta|\theta_0, m) = \frac{1}{2\pi I_0(m)} \exp\{m\cos(\theta - \theta_0)\} \tag{B.77}$$

where $I_0(m)$ is the zeroth-order Bessel function of the first kind. The distribution has period 2π so that $p(\theta + 2\pi) = p(\theta)$ for all θ. Care must be taken in interpreting this distribution because simple expectations will be dependent on the (arbitrary) choice of origin for the variable θ. The parameter θ_0 is analogous to the mean of a univariate Gaussian, and the parameter $m > 0$, known as the *concentration* parameter, is analogous to the precision (inverse variance). For large m, the von Mises distribution is approximately a Gaussian centred on θ_0.

Wishart

The Wishart distribution is the conjugate prior for the precision matrix of a multivariate Gaussian.

$$\mathcal{W}(\mathbf{\Lambda}|\mathbf{W}, \nu) = B(\mathbf{W}, \nu)|\mathbf{\Lambda}|^{(\nu-D-1)/2} \exp\left(-\frac{1}{2}\mathrm{Tr}(\mathbf{W}^{-1}\mathbf{\Lambda})\right) \tag{B.78}$$

where

$$B(\mathbf{W}, \nu) \equiv |\mathbf{W}|^{-\nu/2} \left(2^{\nu D/2}\, \pi^{D(D-1)/4} \prod_{i=1}^{D} \Gamma\left(\frac{\nu + 1 - i}{2}\right)\right)^{-1} \tag{B.79}$$

$$\mathbb{E}[\mathbf{\Lambda}] = \nu\mathbf{W} \tag{B.80}$$

$$\mathbb{E}\left[\ln|\mathbf{\Lambda}|\right] = \sum_{i=1}^{D} \psi\left(\frac{\nu + 1 - i}{2}\right) + D\ln 2 + \ln|\mathbf{W}| \tag{B.81}$$

$$\mathrm{H}[\mathbf{\Lambda}] = -\ln B(\mathbf{W}, \nu) - \frac{(\nu - D - 1)}{2}\mathbb{E}\left[\ln|\mathbf{\Lambda}|\right] + \frac{\nu D}{2} \tag{B.82}$$

where $\mathbf{W}$ is a $D \times D$ symmetric, positive definite matrix, and $\psi(\cdot)$ is the digamma function defined by (B.25). The parameter ν is called the *number of degrees of freedom* of the distribution and is restricted to $\nu > D - 1$ to ensure that the Gamma function in the normalization factor is well-defined. In one dimension, the Wishart reduces to the gamma distribution $\mathrm{Gam}(\lambda|a, b)$ given by (B.26) with parameters $a = \nu/2$ and $b = 1/2W$.

Appendix C. Properties of Matrices

In this appendix, we gather together some useful properties and identities involving matrices and determinants. This is not intended to be an introductory tutorial, and it is assumed that the reader is already familiar with basic linear algebra. For some results, we indicate how to prove them, whereas in more complex cases we leave the interested reader to refer to standard textbooks on the subject. In all cases, we assume that inverses exist and that matrix dimensions are such that the formulae are correctly defined. A comprehensive discussion of linear algebra can be found in Golub and Van Loan (1996), and an extensive collection of matrix properties is given by Lütkepohl (1996). Matrix derivatives are discussed in Magnus and Neudecker (1999).

Basic Matrix Identities

A matrix $\mathbf{A}$ has elements A_{ij} where i indexes the rows, and j indexes the columns. We use $\mathbf{I}_N$ to denote the $N \times N$ identity matrix (also called the unit matrix), and where there is no ambiguity over dimensionality we simply use $\mathbf{I}$. The transpose matrix $\mathbf{A}^{\mathrm{T}}$ has elements $(\mathbf{A}^{\mathrm{T}})_{ij} = A_{ji}$. From the definition of transpose, we have

$$(\mathbf{AB})^{\mathrm{T}} = \mathbf{B}^{\mathrm{T}}\mathbf{A}^{\mathrm{T}} \tag{C.1}$$

which can be verified by writing out the indices. The inverse of $\mathbf{A}$, denoted $\mathbf{A}^{-1}$, satisfies

$$\mathbf{A}\mathbf{A}^{-1} = \mathbf{A}^{-1}\mathbf{A} = \mathbf{I}. \tag{C.2}$$

Because $\mathbf{ABB}^{-1}\mathbf{A}^{-1} = \mathbf{I}$, we have

$$(\mathbf{AB})^{-1} = \mathbf{B}^{-1}\mathbf{A}^{-1}. \tag{C.3}$$

Also we have

$$\left(\mathbf{A}^{\mathrm{T}}\right)^{-1} = \left(\mathbf{A}^{-1}\right)^{\mathrm{T}} \tag{C.4}$$

which is easily proven by taking the transpose of (C.2) and applying (C.1).

A useful identity involving matrix inverses is the following

$$(\mathbf{P}^{-1} + \mathbf{B}^{\mathrm{T}}\mathbf{R}^{-1}\mathbf{B})^{-1}\mathbf{B}^{\mathrm{T}}\mathbf{R}^{-1} = \mathbf{P}\mathbf{B}^{\mathrm{T}}(\mathbf{B}\mathbf{P}\mathbf{B}^{\mathrm{T}} + \mathbf{R})^{-1}. \tag{C.5}$$

which is easily verified by right multiplying both sides by $(\mathbf{B}\mathbf{P}\mathbf{B}^{\mathrm{T}} + \mathbf{R})$. Suppose that $\mathbf{P}$ has dimensionality $N \times N$ while $\mathbf{R}$ has dimensionality $M \times M$, so that $\mathbf{B}$ is $M \times N$. Then if $M \ll N$, it will be much cheaper to evaluate the right-hand side of (C.5) than the left-hand side. A special case that sometimes arises is

$$(\mathbf{I} + \mathbf{A}\mathbf{B})^{-1}\mathbf{A} = \mathbf{A}(\mathbf{I} + \mathbf{B}\mathbf{A})^{-1}. \tag{C.6}$$

Another useful identity involving inverses is the following:

$$(\mathbf{A} + \mathbf{B}\mathbf{D}^{-1}\mathbf{C})^{-1} = \mathbf{A}^{-1} - \mathbf{A}^{-1}\mathbf{B}(\mathbf{D} + \mathbf{C}\mathbf{A}^{-1}\mathbf{B})^{-1}\mathbf{C}\mathbf{A}^{-1} \tag{C.7}$$

which is known as the *Woodbury identity* and which can be verified by multiplying both sides by $(\mathbf{A} + \mathbf{B}\mathbf{D}^{-1}\mathbf{C})$. This is useful, for instance, when $\mathbf{A}$ is large and diagonal, and hence easy to invert, while $\mathbf{B}$ has many rows but few columns (and conversely for $\mathbf{C}$) so that the right-hand side is much cheaper to evaluate than the left-hand side.

A set of vectors $\{\mathbf{a}_1, \ldots, \mathbf{a}_N\}$ is said to be *linearly independent* if the relation $\sum_n \alpha_n \mathbf{a}_n = 0$ holds only if all $\alpha_n = 0$. This implies that none of the vectors can be expressed as a linear combination of the remainder. The rank of a matrix is the maximum number of linearly independent rows (or equivalently the maximum number of linearly independent columns).

Traces and Determinants

Trace and determinant apply to square matrices. The trace $\mathrm{Tr}(\mathbf{A})$ of a matrix $\mathbf{A}$ is defined as the sum of the elements on the leading diagonal. By writing out the indices, we see that

$$\mathrm{Tr}(\mathbf{A}\mathbf{B}) = \mathrm{Tr}(\mathbf{B}\mathbf{A}). \tag{C.8}$$

By applying this formula multiple times to the product of three matrices, we see that

$$\mathrm{Tr}(\mathbf{A}\mathbf{B}\mathbf{C}) = \mathrm{Tr}(\mathbf{C}\mathbf{A}\mathbf{B}) = \mathrm{Tr}(\mathbf{B}\mathbf{C}\mathbf{A}) \tag{C.9}$$

which is known as the *cyclic* property of the trace operator and which clearly extends to the product of any number of matrices. The determinant $|\mathbf{A}|$ of an $N \times N$ matrix $\mathbf{A}$ is defined by

$$|\mathbf{A}| = \sum (\pm 1) A_{1i_1} A_{2i_2} \cdots A_{Ni_N} \tag{C.10}$$

in which the sum is taken over all products consisting of precisely one element from each row and one element from each column, with a coefficient $+1$ or -1 according

to whether the permutation $i_1 i_2 \ldots i_N$ is even or odd, respectively. Note that $|\mathbf{I}| = 1$. Thus, for a 2×2 matrix, the determinant takes the form

$$|\mathbf{A}| = \begin{vmatrix} a_{11} & a_{12} \\ a_{21} & a_{22} \end{vmatrix} = a_{11}a_{22} - a_{12}a_{21}. \tag{C.11}$$

The determinant of a product of two matrices is given by

$$|\mathbf{AB}| = |\mathbf{A}||\mathbf{B}| \tag{C.12}$$

as can be shown from (C.10). Also, the determinant of an inverse matrix is given by

$$\left|\mathbf{A}^{-1}\right| = \frac{1}{|\mathbf{A}|} \tag{C.13}$$

which can be shown by taking the determinant of (C.2) and applying (C.12).

If $\mathbf{A}$ and $\mathbf{B}$ are matrices of size $N \times M$, then

$$\left|\mathbf{I}_N + \mathbf{AB}^{\mathrm{T}}\right| = \left|\mathbf{I}_M + \mathbf{A}^{\mathrm{T}}\mathbf{B}\right|. \tag{C.14}$$

A useful special case is

$$\left|\mathbf{I}_N + \mathbf{ab}^{\mathrm{T}}\right| = 1 + \mathbf{a}^{\mathrm{T}}\mathbf{b} \tag{C.15}$$

where $\mathbf{a}$ and $\mathbf{b}$ are N-dimensional column vectors.

Matrix Derivatives

Sometimes we need to consider derivatives of vectors and matrices with respect to scalars. The derivative of a vector $\mathbf{a}$ with respect to a scalar x is itself a vector whose components are given by

$$\left(\frac{\partial \mathbf{a}}{\partial x}\right)_i = \frac{\partial a_i}{\partial x} \tag{C.16}$$

with an analogous definition for the derivative of a matrix. Derivatives with respect to vectors and matrices can also be defined, for instance

$$\left(\frac{\partial x}{\partial \mathbf{a}}\right)_i = \frac{\partial x}{\partial a_i} \tag{C.17}$$

and similarly

$$\left(\frac{\partial \mathbf{a}}{\partial \mathbf{b}}\right)_{ij} = \frac{\partial a_i}{\partial b_j}. \tag{C.18}$$

The following is easily proven by writing out the components

$$\frac{\partial}{\partial \mathbf{x}}\left(\mathbf{x}^{\mathrm{T}}\mathbf{a}\right) = \frac{\partial}{\partial \mathbf{x}}\left(\mathbf{a}^{\mathrm{T}}\mathbf{x}\right) = \mathbf{a}. \tag{C.19}$$

Similarly

$$\frac{\partial}{\partial \mathbf{x}}(\mathbf{AB}) = \frac{\partial \mathbf{A}}{\partial \mathbf{x}}\mathbf{B} + \mathbf{A}\frac{\partial \mathbf{B}}{\partial \mathbf{x}}. \tag{C.20}$$

The derivative of the inverse of a matrix can be expressed as

$$\frac{\partial}{\partial x}\left(\mathbf{A}^{-1}\right) = -\mathbf{A}^{-1}\frac{\partial \mathbf{A}}{\partial x}\mathbf{A}^{-1} \tag{C.21}$$

as can be shown by differentiating the equation $\mathbf{A}^{-1}\mathbf{A} = \mathbf{I}$ using (C.20) and then right multiplying by $\mathbf{A}^{-1}$. Also

$$\frac{\partial}{\partial x}\ln|\mathbf{A}| = \mathrm{Tr}\left(\mathbf{A}^{-1}\frac{\partial \mathbf{A}}{\partial x}\right) \tag{C.22}$$

which we shall prove later. If we choose x to be one of the elements of $\mathbf{A}$, we have

$$\frac{\partial}{\partial A_{ij}}\mathrm{Tr}\,(\mathbf{AB}) = B_{ji} \tag{C.23}$$

as can be seen by writing out the matrices using index notation. We can write this result more compactly in the form

$$\frac{\partial}{\partial \mathbf{A}}\mathrm{Tr}\,(\mathbf{AB}) = \mathbf{B}^{\mathrm{T}}. \tag{C.24}$$

With this notation, we have the following properties

$$\frac{\partial}{\partial \mathbf{A}}\mathrm{Tr}\left(\mathbf{A}^{\mathrm{T}}\mathbf{B}\right) = \mathbf{B} \tag{C.25}$$

$$\frac{\partial}{\partial \mathbf{A}}\mathrm{Tr}(\mathbf{A}) = \mathbf{I} \tag{C.26}$$

$$\frac{\partial}{\partial \mathbf{A}}\mathrm{Tr}(\mathbf{ABA}^{\mathrm{T}}) = \mathbf{A}(\mathbf{B} + \mathbf{B}^{\mathrm{T}}) \tag{C.27}$$

which can again be proven by writing out the matrix indices. We also have

$$\frac{\partial}{\partial \mathbf{A}}\ln|\mathbf{A}| = \left(\mathbf{A}^{-1}\right)^{\mathrm{T}} \tag{C.28}$$

which follows from (C.22) and (C.26).

Eigenvector Equation

For a square matrix $\mathbf{A}$ of size $M \times M$, the eigenvector equation is defined by

$$\mathbf{A}\mathbf{u}_i = \lambda_i \mathbf{u}_i \tag{C.29}$$

for $i = 1, \ldots, M$, where $\mathbf{u}_i$ is an *eigenvector* and λ_i is the corresponding *eigenvalue*. This can be viewed as a set of M simultaneous homogeneous linear equations, and the condition for a solution is that

$$|\mathbf{A} - \lambda_i \mathbf{I}| = 0 \tag{C.30}$$

which is known as the *characteristic equation*. Because this is a polynomial of order M in λ_i, it must have M solutions (though these need not all be distinct). The rank of $\mathbf{A}$ is equal to the number of nonzero eigenvalues.

Of particular interest are symmetric matrices, which arise as covariance matrices, kernel matrices, and Hessians. Symmetric matrices have the property that $A_{ij} = A_{ji}$, or equivalently $\mathbf{A}^{\mathrm{T}} = \mathbf{A}$. The inverse of a symmetric matrix is also symmetric, as can be seen by taking the transpose of $\mathbf{A}^{-1}\mathbf{A} = \mathbf{I}$ and using $\mathbf{A}\mathbf{A}^{-1} = \mathbf{I}$ together with the symmetry of $\mathbf{I}$.

In general, the eigenvalues of a matrix are complex numbers, but for symmetric matrices the eigenvalues λ_i are real. This can be seen by first left multiplying (C.29) by $(\mathbf{u}_i^\star)^{\mathrm{T}}$, where $\star$ denotes the complex conjugate, to give

$$(\mathbf{u}_i^\star)^{\mathrm{T}} \mathbf{A}\mathbf{u}_i = \lambda_i (\mathbf{u}_i^\star)^{\mathrm{T}} \mathbf{u}_i. \tag{C.31}$$

Next we take the complex conjugate of (C.29) and left multiply by $\mathbf{u}_i^{\mathrm{T}}$ to give

$$\mathbf{u}_i^{\mathrm{T}} \mathbf{A}\mathbf{u}_i^\star = \lambda_i^\star \mathbf{u}_i^{\mathrm{T}} \mathbf{u}_i^\star. \tag{C.32}$$

where we have used $\mathbf{A}^\star = \mathbf{A}$ because we consider only real matrices $\mathbf{A}$. Taking the transpose of the second of these equations, and using $\mathbf{A}^{\mathrm{T}} = \mathbf{A}$, we see that the left-hand sides of the two equations are equal, and hence that $\lambda_i^\star = \lambda_i$ and so λ_i must be real.

The eigenvectors $\mathbf{u}_i$ of a real symmetric matrix can be chosen to be orthonormal (i.e., orthogonal and of unit length) so that

$$\mathbf{u}_i^{\mathrm{T}} \mathbf{u}_j = I_{ij} \tag{C.33}$$

where I_{ij} are the elements of the identity matrix $\mathbf{I}$. To show this, we first left multiply (C.29) by $\mathbf{u}_j^{\mathrm{T}}$ to give

$$\mathbf{u}_j^{\mathrm{T}} \mathbf{A}\mathbf{u}_i = \lambda_i \mathbf{u}_j^{\mathrm{T}} \mathbf{u}_i \tag{C.34}$$

and hence, by exchange of indices, we have

$$\mathbf{u}_i^{\mathrm{T}} \mathbf{A}\mathbf{u}_j = \lambda_j \mathbf{u}_i^{\mathrm{T}} \mathbf{u}_j. \tag{C.35}$$

We now take the transpose of the second equation and make use of the symmetry property $\mathbf{A}^{\mathrm{T}} = \mathbf{A}$, and then subtract the two equations to give

$$(\lambda_i - \lambda_j)\, \mathbf{u}_i^{\mathrm{T}} \mathbf{u}_j = 0. \tag{C.36}$$

Hence, for $\lambda_i \neq \lambda_j$, we have $\mathbf{u}_i^{\mathrm{T}} \mathbf{u}_j = 0$, and hence $\mathbf{u}_i$ and $\mathbf{u}_j$ are orthogonal. If the two eigenvalues are equal, then any linear combination $\alpha\mathbf{u}_i + \beta\mathbf{u}_j$ is also an eigenvector with the same eigenvalue, so we can select one linear combination arbitrarily,

and then choose the second to be orthogonal to the first (it can be shown that the degenerate eigenvectors are never linearly dependent). Hence the eigenvectors can be chosen to be orthogonal, and by normalizing can be set to unit length. Because there are M eigenvalues, the corresponding M orthogonal eigenvectors form a complete set and so any M-dimensional vector can be expressed as a linear combination of the eigenvectors.

We can take the eigenvectors $\mathbf{u}_i$ to be the columns of an $M \times M$ matrix $\mathbf{U}$, which from orthonormality satisfies

$$\mathbf{U}^{\mathrm{T}}\mathbf{U} = \mathbf{I}. \tag{C.37}$$

Such a matrix is said to be *orthogonal*. Interestingly, the rows of this matrix are also orthogonal, so that $\mathbf{U}\mathbf{U}^{\mathrm{T}} = \mathbf{I}$. To show this, note that (C.37) implies $\mathbf{U}^{\mathrm{T}}\mathbf{U}\mathbf{U}^{-1} = \mathbf{U}^{-1} = \mathbf{U}^{\mathrm{T}}$ and so $\mathbf{U}\mathbf{U}^{-1} = \mathbf{U}\mathbf{U}^{\mathrm{T}} = \mathbf{I}$. Using (C.12), it also follows that $|\mathbf{U}| = 1$.

The eigenvector equation (C.29) can be expressed in terms of $\mathbf{U}$ in the form

$$\mathbf{A}\mathbf{U} = \mathbf{U}\boldsymbol{\Lambda} \tag{C.38}$$

where $\boldsymbol{\Lambda}$ is an $M \times M$ diagonal matrix whose diagonal elements are given by the eigenvalues λ_i.

If we consider a column vector $\mathbf{x}$ that is transformed by an orthogonal matrix $\mathbf{U}$ to give a new vector

$$\widetilde{\mathbf{x}} = \mathbf{U}\mathbf{x} \tag{C.39}$$

then the length of the vector is preserved because

$$\widetilde{\mathbf{x}}^{\mathrm{T}}\widetilde{\mathbf{x}} = \mathbf{x}^{\mathrm{T}}\mathbf{U}^{\mathrm{T}}\mathbf{U}\mathbf{x} = \mathbf{x}^{\mathrm{T}}\mathbf{x} \tag{C.40}$$

and similarly the angle between any two such vectors is preserved because

$$\widetilde{\mathbf{x}}^{\mathrm{T}}\widetilde{\mathbf{y}} = \mathbf{x}^{\mathrm{T}}\mathbf{U}^{\mathrm{T}}\mathbf{U}\mathbf{y} = \mathbf{x}^{\mathrm{T}}\mathbf{y}. \tag{C.41}$$

Thus, multiplication by $\mathbf{U}$ can be interpreted as a rigid rotation of the coordinate system.

From (C.38), it follows that

$$\mathbf{U}^{\mathrm{T}}\mathbf{A}\mathbf{U} = \boldsymbol{\Lambda} \tag{C.42}$$

and because $\boldsymbol{\Lambda}$ is a diagonal matrix, we say that the matrix $\mathbf{A}$ is *diagonalized* by the matrix $\mathbf{U}$. If we left multiply by $\mathbf{U}$ and right multiply by $\mathbf{U}^{\mathrm{T}}$, we obtain

$$\mathbf{A} = \mathbf{U}\boldsymbol{\Lambda}\mathbf{U}^{\mathrm{T}} \tag{C.43}$$

Taking the inverse of this equation, and using (C.3) together with $\mathbf{U}^{-1} = \mathbf{U}^{\mathrm{T}}$, we have

$$\mathbf{A}^{-1} = \mathbf{U}\boldsymbol{\Lambda}^{-1}\mathbf{U}^{\mathrm{T}}. \tag{C.44}$$

These last two equations can also be written in the form

$$\mathbf{A} = \sum_{i=1}^{M} \lambda_i \mathbf{u}_i \mathbf{u}_i^{\mathrm{T}} \tag{C.45}$$

$$\mathbf{A}^{-1} = \sum_{i=1}^{M} \frac{1}{\lambda_i} \mathbf{u}_i \mathbf{u}_i^{\mathrm{T}}. \tag{C.46}$$

If we take the determinant of (C.43), and use (C.12), we obtain

$$|\mathbf{A}| = \prod_{i=1}^{M} \lambda_i. \tag{C.47}$$

Similarly, taking the trace of (C.43), and using the cyclic property (C.8) of the trace operator together with $\mathbf{U}^{\mathrm{T}}\mathbf{U} = \mathbf{I}$, we have

$$\mathrm{Tr}(\mathbf{A}) = \sum_{i=1}^{M} \lambda_i. \tag{C.48}$$

We leave it as an exercise for the reader to verify (C.22) by making use of the results (C.33), (C.45), (C.46), and (C.47).

A matrix $\mathbf{A}$ is said to be *positive definite*, denoted by $\mathbf{A} \succ 0$, if $\mathbf{w}^{\mathrm{T}}\mathbf{A}\mathbf{w} > 0$ for all values of the vector $\mathbf{w}$. Equivalently, a positive definite matrix has $\lambda_i > 0$ for all of its eigenvalues (as can be seen by setting $\mathbf{w}$ to each of the eigenvectors in turn, and by noting that an arbitrary vector can be expanded as a linear combination of the eigenvectors). Note that positive definite is not the same as all the elements being positive. For example, the matrix

$$\begin{pmatrix} 1 & 2 \\ 3 & 4 \end{pmatrix} \tag{C.49}$$

has eigenvalues $\lambda_1 \simeq 5.37$ and $\lambda_2 \simeq -0.37$. A matrix is said to be *positive semidefinite* if $\mathbf{w}^{\mathrm{T}}\mathbf{A}\mathbf{w} \geqslant 0$ holds for all values of $\mathbf{w}$, which is denoted $\mathbf{A} \succeq 0$, and is equivalent to $\lambda_i \geqslant 0$.

Appendix D. Calculus of Variations

We can think of a function $y(x)$ as being an operator that, for any input value x, returns an output value y. In the same way, we can define a *functional* $F[y]$ to be an operator that takes a function $y(x)$ and returns an output value F. An example of a functional is the length of a curve drawn in a two-dimensional plane in which the path of the curve is defined in terms of a function. In the context of machine learning, a widely used functional is the entropy $\mathrm{H}[x]$ for a continuous variable x because, for any choice of probability density function $p(x)$, it returns a scalar value representing the entropy of x under that density. Thus the entropy of $p(x)$ could equally well have been written as $\mathrm{H}[p]$.

A common problem in conventional calculus is to find a value of x that maximizes (or minimizes) a function $y(x)$. Similarly, in the calculus of variations we seek a function $y(x)$ that maximizes (or minimizes) a functional $F[y]$. That is, of all possible functions $y(x)$, we wish to find the particular function for which the functional $F[y]$ is a maximum (or minimum). The calculus of variations can be used, for instance, to show that the shortest path between two points is a straight line or that the maximum entropy distribution is a Gaussian.

If we weren't familiar with the rules of ordinary calculus, we could evaluate a conventional derivative $\mathrm{d}y/\mathrm{d}x$ by making a small change ϵ to the variable x and then expanding in powers of ϵ, so that

$$y(x+\epsilon) = y(x) + \frac{\mathrm{d}y}{\mathrm{d}x}\epsilon + O(\epsilon^2) \tag{D.1}$$

and finally taking the limit $\epsilon \to 0$. Similarly, for a function of several variables $y(x_1, \ldots, x_D)$, the corresponding partial derivatives are defined by

$$y(x_1+\epsilon_1, \ldots, x_D+\epsilon_D) = y(x_1, \ldots, x_D) + \sum_{i=1}^{D} \frac{\partial y}{\partial x_i}\epsilon_i + O(\epsilon^2). \tag{D.2}$$

The analogous definition of a functional derivative arises when we consider how much a functional $F[y]$ changes when we make a small change $\epsilon\eta(x)$ to the function

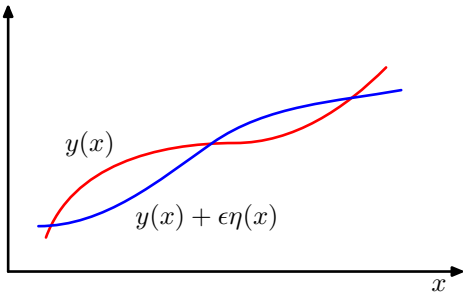

Figure D.1 A functional derivative can be defined by considering how the value of a functional $F[y]$ changes when the function $y(x)$ is changed to $y(x) + \epsilon\eta(x)$ where $\eta(x)$ is an arbitrary function of x.

$y(x)$, where $\eta(x)$ is an arbitrary function of x, as illustrated in Figure D.1. We denote the functional derivative of $E[f]$ with respect to $f(x)$ by $\delta F/\delta f(x)$, and define it by the following relation:

$$F[y(x) + \epsilon\eta(x)] = F[y(x)] + \epsilon \int \frac{\delta F}{\delta y(x)} \eta(x)\, \mathrm{d}x + O(\epsilon^2). \tag{D.3}$$

This can be seen as a natural extension of (D.2) in which $F[y]$ now depends on a continuous set of variables, namely the values of y at all points x. Requiring that the functional be stationary with respect to small variations in the function $y(x)$ gives

$$\int \frac{\delta E}{\delta y(x)} \eta(x)\, \mathrm{d}x = 0. \tag{D.4}$$

Because this must hold for an arbitrary choice of $\eta(x)$, it follows that the functional derivative must vanish. To see this, imagine choosing a perturbation $\eta(x)$ that is zero everywhere except in the neighbourhood of a point $\widehat{x}$, in which case the functional derivative must be zero at $x = \widehat{x}$. However, because this must be true for every choice of $\widehat{x}$, the functional derivative must vanish for all values of x.

Consider a functional that is defined by an integral over a function $G(y, y', x)$ that depends on both $y(x)$ and its derivative $y'(x)$ as well as having a direct dependence on x

$$F[y] = \int G\left(y(x), y'(x), x\right)\, \mathrm{d}x \tag{D.5}$$

where the value of $y(x)$ is assumed to be fixed at the boundary of the region of integration (which might be at infinity). If we now consider variations in the function $y(x)$, we obtain

$$F[y(x) + \epsilon\eta(x)] = F[y(x)] + \epsilon \int \left\{ \frac{\partial G}{\partial y}\eta(x) + \frac{\partial G}{\partial y'}\eta'(x) \right\} \mathrm{d}x + O(\epsilon^2). \tag{D.6}$$

We now have to cast this in the form (D.3). To do so, we integrate the second term by parts and make use of the fact that $\eta(x)$ must vanish at the boundary of the integral (because $y(x)$ is fixed at the boundary). This gives

$$F[y(x) + \epsilon\eta(x)] = F[y(x)] + \epsilon \int \left\{ \frac{\partial G}{\partial y} - \frac{\mathrm{d}}{\mathrm{d}x}\left(\frac{\partial G}{\partial y'}\right) \right\} \eta(x)\, \mathrm{d}x + O(\epsilon^2) \tag{D.7}$$

from which we can read off the functional derivative by comparison with (D.3). Requiring that the functional derivative vanishes then gives

$$\frac{\partial G}{\partial y} - \frac{\mathrm{d}}{\mathrm{d}x}\left(\frac{\partial G}{\partial y'}\right) = 0 \tag{D.8}$$

which are known as the *Euler-Lagrange* equations. For example, if

$$G = y(x)^2 + (y'(x))^2 \tag{D.9}$$

then the Euler-Lagrange equations take the form

$$y(x) - \frac{\mathrm{d}^2 y}{\mathrm{d}x^2} = 0. \tag{D.10}$$

This second order differential equation can be solved for $y(x)$ by making use of the boundary conditions on $y(x)$.

Often, we consider functionals defined by integrals whose integrands take the form $G(y, x)$ and that do not depend on the derivatives of $y(x)$. In this case, stationarity simply requires that $\partial G/\partial y(x) = 0$ for all values of x.

If we are optimizing a functional with respect to a probability distribution, then we need to maintain the normalization constraint on the probabilities. This is often most conveniently done using a Lagrange multiplier, which then allows an unconstrained optimization to be performed.

Appendix E

The extension of the above results to a multidimensional variable $\mathbf{x}$ is straightforward. For a more comprehensive discussion of the calculus of variations, see Sagan (1969).

Appendix E. Lagrange Multipliers

Lagrange multipliers, also sometimes called *undetermined multipliers*, are used to find the stationary points of a function of several variables subject to one or more constraints.

Consider the problem of finding the maximum of a function $f(x_1, x_2)$ subject to a constraint relating x_1 and x_2, which we write in the form

$$g(x_1, x_2) = 0. \tag{E.1}$$

One approach would be to solve the constraint equation (E.1) and thus express x_2 as a function of x_1 in the form $x_2 = h(x_1)$. This can then be substituted into $f(x_1, x_2)$ to give a function of x_1 alone of the form $f(x_1, h(x_1))$. The maximum with respect to x_1 could then be found by differentiation in the usual way, to give the stationary value $x_1^\star$, with the corresponding value of x_2 given by $x_2^\star = h(x_1^\star)$.

One problem with this approach is that it may be difficult to find an analytic solution of the constraint equation that allows x_2 to be expressed as an explicit function of x_1. Also, this approach treats x_1 and x_2 differently and so spoils the natural symmetry between these variables.

A more elegant, and often simpler, approach is based on the introduction of a parameter λ called a Lagrange multiplier. We shall motivate this technique from a geometrical perspective. Consider a D-dimensional variable $\mathbf{x}$ with components $x_1, \ldots, x_D$. The constraint equation $g(\mathbf{x}) = 0$ then represents a $(D-1)$-dimensional surface in $\mathbf{x}$-space as indicated in Figure E.1.

We first note that at any point on the constraint surface the gradient $\nabla g(\mathbf{x})$ of the constraint function will be orthogonal to the surface. To see this, consider a point $\mathbf{x}$ that lies on the constraint surface, and consider a nearby point $\mathbf{x} + \boldsymbol{\epsilon}$ that also lies on the surface. If we make a Taylor expansion around $\mathbf{x}$, we have

$$g(\mathbf{x} + \boldsymbol{\epsilon}) \simeq g(\mathbf{x}) + \boldsymbol{\epsilon}^{\mathrm{T}} \nabla g(\mathbf{x}). \tag{E.2}$$

Because both $\mathbf{x}$ and $\mathbf{x} + \boldsymbol{\epsilon}$ lie on the constraint surface, we have $g(\mathbf{x}) = g(\mathbf{x} + \boldsymbol{\epsilon})$ and hence $\boldsymbol{\epsilon}^{\mathrm{T}} \nabla g(\mathbf{x}) \simeq 0$. In the limit $\|\boldsymbol{\epsilon}\| \to 0$ we have $\boldsymbol{\epsilon}^{\mathrm{T}} \nabla g(\mathbf{x}) = 0$, and because $\boldsymbol{\epsilon}$ is

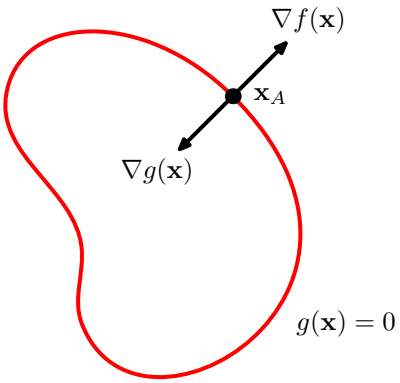

Figure E.1 A geometrical picture of the technique of Lagrange multipliers in which we seek to maximize a function $f(\mathbf{x})$, subject to the constraint $g(\mathbf{x}) = 0$. If $\mathbf{x}$ is D dimensional, the constraint $g(\mathbf{x}) = 0$ corresponds to a subspace of dimensionality $D - 1$, indicated by the red curve. The problem can be solved by optimizing the Lagrangian function $L(\mathbf{x}, \lambda) = f(\mathbf{x}) + \lambda g(\mathbf{x})$.

then parallel to the constraint surface $g(\mathbf{x}) = 0$, we see that the vector ∇g is normal to the surface.

Next we seek a point $\mathbf{x}^\star$ on the constraint surface such that $f(\mathbf{x})$ is maximized. Such a point must have the property that the vector $\nabla f(\mathbf{x})$ is also orthogonal to the constraint surface, as illustrated in Figure E.1, because otherwise we could increase the value of $f(\mathbf{x})$ by moving a short distance along the constraint surface. Thus ∇f and ∇g are parallel (or anti-parallel) vectors, and so there must exist a parameter λ such that

$$\nabla f + \lambda \nabla g = 0 \tag{E.3}$$

where $\lambda \neq 0$ is known as a *Lagrange multiplier*. Note that λ can have either sign.

At this point, it is convenient to introduce the *Lagrangian* function defined by

$$L(\mathbf{x}, \lambda) \equiv f(\mathbf{x}) + \lambda g(\mathbf{x}). \tag{E.4}$$

The constrained stationarity condition (E.3) is obtained by setting $\nabla_{\mathbf{x}} L = 0$. Furthermore, the condition $\partial L/\partial \lambda = 0$ leads to the constraint equation $g(\mathbf{x}) = 0$.

Thus to find the maximum of a function $f(\mathbf{x})$ subject to the constraint $g(\mathbf{x}) = 0$, we define the Lagrangian function given by (E.4) and we then find the stationary point of $L(\mathbf{x}, \lambda)$ with respect to both $\mathbf{x}$ and λ. For a D-dimensional vector $\mathbf{x}$, this gives $D + 1$ equations that determine both the stationary point $\mathbf{x}^\star$ and the value of λ. If we are only interested in $\mathbf{x}^\star$, then we can eliminate λ from the stationarity equations without needing to find its value (hence the term 'undetermined multiplier').

As a simple example, suppose we wish to find the stationary point of the function $f(x_1, x_2) = 1 - x_1^2 - x_2^2$ subject to the constraint $g(x_1, x_2) = x_1 + x_2 - 1 = 0$, as illustrated in Figure E.2. The corresponding Lagrangian function is given by

$$L(\mathbf{x}, \lambda) = 1 - x_1^2 - x_2^2 + \lambda(x_1 + x_2 - 1). \tag{E.5}$$

The conditions for this Lagrangian to be stationary with respect to x_1, x_2, and λ give the following coupled equations:

$$-2x_1 + \lambda = 0 \tag{E.6}$$

$$-2x_2 + \lambda = 0 \tag{E.7}$$

$$x_1 + x_2 - 1 = 0. \tag{E.8}$$

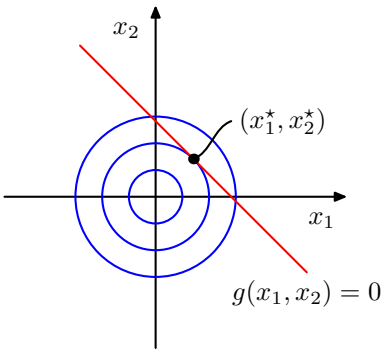

Figure E.2 A simple example of the use of Lagrange multipliers in which the aim is to maximize $f(x_1, x_2) = 1 - x_1^2 - x_2^2$ subject to the constraint $g(x_1, x_2) = 0$ where $g(x_1, x_2) = x_1 + x_2 - 1$. The circles show contours of the function $f(x_1, x_2)$, and the diagonal line shows the constraint surface $g(x_1, x_2) = 0$.

Solution of these equations then gives the stationary point as $(x_1^\star, x_2^\star) = (\frac{1}{2}, \frac{1}{2})$, and the corresponding value for the Lagrange multiplier is $\lambda = 1$.

So far, we have considered the problem of maximizing a function subject to an *equality constraint* of the form $g(\mathbf{x}) = 0$. We now consider the problem of maximizing $f(\mathbf{x})$ subject to an *inequality constraint* of the form $g(\mathbf{x}) \geqslant 0$, as illustrated in Figure E.3.

There are now two kinds of solution possible, according to whether the constrained stationary point lies in the region where $g(\mathbf{x}) > 0$, in which case the constraint is *inactive*, or whether it lies on the boundary $g(\mathbf{x}) = 0$, in which case the constraint is said to be *active*. In the former case, the function $g(\mathbf{x})$ plays no role and so the stationary condition is simply $\nabla f(\mathbf{x}) = 0$. This again corresponds to a stationary point of the Lagrange function (E.4) but this time with $\lambda = 0$. The latter case, where the solution lies on the boundary, is analogous to the equality constraint discussed previously and corresponds to a stationary point of the Lagrange function (E.4) with $\lambda \neq 0$. Now, however, the sign of the Lagrange multiplier is crucial, because the function $f(\mathbf{x})$ will only be at a maximum if its gradient is oriented away from the region $g(\mathbf{x}) > 0$, as illustrated in Figure E.3. We therefore have $\nabla f(\mathbf{x}) = -\lambda \nabla g(\mathbf{x})$ for some value of $\lambda > 0$.

For either of these two cases, the product $\lambda g(\mathbf{x}) = 0$. Thus the solution to the

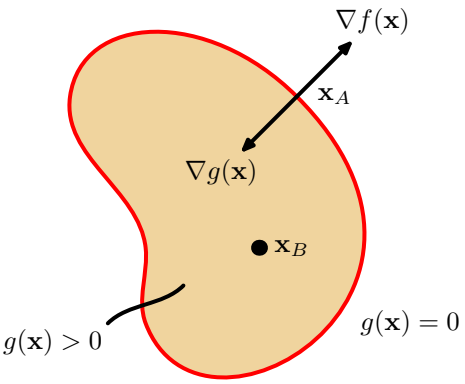

Figure E.3 Illustration of the problem of maximizing $f(\mathbf{x})$ subject to the inequality constraint $g(\mathbf{x}) \geqslant 0$.

problem of maximizing $f(\mathbf{x})$ subject to $g(\mathbf{x}) \geqslant 0$ is obtained by optimizing the Lagrange function (E.4) with respect to $\mathbf{x}$ and λ subject to the conditions

$$g(\mathbf{x}) \geqslant 0 \tag{E.9}$$

$$\lambda \geqslant 0 \tag{E.10}$$

$$\lambda g(\mathbf{x}) = 0 \tag{E.11}$$

These are known as the *Karush-Kuhn-Tucker* (KKT) conditions (Karush, 1939; Kuhn and Tucker, 1951).

Note that if we wish to minimize (rather than maximize) the function $f(\mathbf{x})$ subject to an inequality constraint $g(\mathbf{x}) \geqslant 0$, then we minimize the Lagrangian function $L(\mathbf{x}, \lambda) = f(\mathbf{x}) - \lambda g(\mathbf{x})$ with respect to $\mathbf{x}$, again subject to $\lambda \geqslant 0$.

Finally, it is straightforward to extend the technique of Lagrange multipliers to the case of multiple equality and inequality constraints. Suppose we wish to maximize $f(\mathbf{x})$ subject to $g_j(\mathbf{x}) = 0$ for $j = 1, \ldots, J$, and $h_k(\mathbf{x}) \geqslant 0$ for $k = 1, \ldots, K$. We then introduce Lagrange multipliers $\{\lambda_j\}$ and $\{\mu_k\}$, and then optimize the Lagrangian function given by

$$L(\mathbf{x}, \{\lambda_j\}, \{\mu_k\}) = f(\mathbf{x}) + \sum_{j=1}^{J} \lambda_j g_j(\mathbf{x}) + \sum_{k=1}^{K} \mu_k h_k(\mathbf{x}) \tag{E.12}$$

subject to $\mu_k \geqslant 0$ and $\mu_k h_k(\mathbf{x}) = 0$ for $k = 1, \ldots, K$. Extensions to constrained functional derivatives are similarly straightforward. For a more detailed discussion of the technique of Lagrange multipliers, see Nocedal and Wright (1999).

Appendix D

References

Abramowitz, M. and I. A. Stegun (1965). *Handbook of Mathematical Functions*. Dover.

Adler, S. L. (1981). Over-relaxation method for the Monte Carlo evaluation of the partition function for multiquadratic actions. *Physical Review D* **23**, 2901–2904.

Ahn, J. H. and J. H. Oh (2003). A constrained EM algorithm for principal component analysis. *Neural Computation* **15**(1), 57–65.

Aizerman, M. A., E. M. Braverman, and L. I. Rozonoer (1964). The probability problem of pattern recognition learning and the method of potential functions. *Automation and Remote Control* **25**, 1175–1190.

Akaike, H. (1974). A new look at statistical model identification. *IEEE Transactions on Automatic Control* **19**, 716–723.

Ali, S. M. and S. D. Silvey (1966). A general class of coefficients of divergence of one distribution from another. *Journal of the Royal Statistical Society, B* **28**(1), 131–142.

Allwein, E. L., R. E. Schapire, and Y. Singer (2000). Reducing multiclass to binary: a unifying approach for margin classifiers. *Journal of Machine Learning Research* **1**, 113–141.

Amari, S. (1985). *Differential-Geometrical Methods in Statistics*. Springer.

Amari, S., A. Cichocki, and H. H. Yang (1996). A new learning algorithm for blind signal separation. In D. S. Touretzky, M. C. Mozer, and M. E. Hasselmo (Eds.), *Advances in Neural Information Processing Systems*, Volume 8, pp. 757–763. MIT Press.

Amari, S. I. (1998). Natural gradient works efficiently in learning. *Neural Computation* **10**, 251–276.

Anderson, J. A. and E. Rosenfeld (Eds.) (1988). *Neurocomputing: Foundations of Research*. MIT Press.

Anderson, T. W. (1963). Asymptotic theory for principal component analysis. *Annals of Mathematical Statistics* **34**, 122–148.

Andrieu, C., N. de Freitas, A. Doucet, and M. I. Jordan (2003). An introduction to MCMC for machine learning. *Machine Learning* **50**, 5–43.

Anthony, M. and N. Biggs (1992). *An Introduction to Computational Learning Theory*. Cambridge University Press.

Attias, H. (1999a). Independent factor analysis. *Neural Computation* **11**(4), 803–851.

Attias, H. (1999b). Inferring parameters and structure of latent variable models by variational Bayes. In K. B. Laskey and H. Prade (Eds.),

Uncertainty in Artificial Intelligence: Proceedings of the Fifth Conference, pp. 21–30. Morgan Kaufmann.

Bach, F. R. and M. I. Jordan (2002). Kernel independent component analysis. *Journal of Machine Learning Research* **3**, 1–48.

Bakir, G. H., J. Weston, and B. Schölkopf (2004). Learning to find pre-images. In S. Thrun, L. K. Saul, and B. Schölkopf (Eds.), *Advances in Neural Information Processing Systems*, Volume 16, pp. 449–456. MIT Press.

Baldi, P. and S. Brunak (2001). *Bioinformatics: The Machine Learning Approach* (Second ed.). MIT Press.

Baldi, P. and K. Hornik (1989). Neural networks and principal component analysis: learning from examples without local minima. *Neural Networks* **2**(1), 53–58.

Barber, D. and C. M. Bishop (1997). Bayesian model comparison by Monte Carlo chaining. In M. Mozer, M. Jordan, and T. Petsche (Eds.), *Advances in Neural Information Processing Systems*, Volume 9, pp. 333–339. MIT Press.

Barber, D. and C. M. Bishop (1998a). Ensemble learning for multi-layer networks. In M. I. Jordan, K. J. Kearns, and S. A. Solla (Eds.), *Advances in Neural Information Processing Systems*, Volume 10, pp. 395–401.

Barber, D. and C. M. Bishop (1998b). Ensemble learning in Bayesian neural networks. In C. M. Bishop (Ed.), *Generalization in Neural Networks and Machine Learning*, pp. 215–237. Springer.

Bartholomew, D. J. (1987). *Latent Variable Models and Factor Analysis*. Charles Griffin.

Basilevsky, A. (1994). *Statistical Factor Analysis and Related Methods: Theory and Applications*. Wiley.

Bather, J. (2000). *Decision Theory: An Introduction to Dynamic Programming and Sequential Decisions*. Wiley.

Baudat, G. and F. Anouar (2000). Generalized discriminant analysis using a kernel approach. *Neural Computation* **12**(10), 2385–2404.

Baum, L. E. (1972). An inequality and associated maximization technique in statistical estimation of probabilistic functions of Markov processes. *Inequalities* **3**, 1–8.

Becker, S. and Y. Le Cun (1989). Improving the convergence of back-propagation learning with second order methods. In D. Touretzky, G. E. Hinton, and T. J. Sejnowski (Eds.), *Proceedings of the 1988 Connectionist Models Summer School*, pp. 29–37. Morgan Kaufmann.

Bell, A. J. and T. J. Sejnowski (1995). An information maximization approach to blind separation and blind deconvolution. *Neural Computation* **7**(6), 1129–1159.

Bellman, R. (1961). *Adaptive Control Processes: A Guided Tour*. Princeton University Press.

Bengio, Y. and P. Frasconi (1995). An input output HMM architecture. In G. Tesauro, D. S. Touretzky, and T. K. Leen (Eds.), *Advances in Neural Information Processing Systems*, Volume 7, pp. 427–434. MIT Press.

Bennett, K. P. (1992). Robust linear programming discrimination of two linearly separable sets. *Optimization Methods and Software* **1**, 23–34.

Berger, J. O. (1985). *Statistical Decision Theory and Bayesian Analysis* (Second ed.). Springer.

Bernardo, J. M. and A. F. M. Smith (1994). *Bayesian Theory*. Wiley.

Berrou, C., A. Glavieux, and P. Thitimajshima (1993). Near Shannon limit error-correcting coding and decoding: Turbo-codes (1). In *Proceedings ICC'93*, pp. 1064–1070.

Besag, J. (1974). On spatio-temporal models and Markov fields. In *Transactions of the 7th Prague Conference on Information Theory, Statistical Decision Functions and Random Processes*, pp. 47–75. Academia.

Besag, J. (1986). On the statistical analysis of dirty pictures. *Journal of the Royal Statistical Society* **B-48**, 259–302.

Besag, J., P. J. Green, D. Hidgon, and K. Megersen (1995). Bayesian computation and stochastic systems. *Statistical Science* **10**(1), 3–66.

Bishop, C. M. (1991). A fast procedure for retraining the multilayer perceptron. *International Journal of Neural Systems* **2**(3), 229–236.

Bishop, C. M. (1992). Exact calculation of the Hessian matrix for the multilayer perceptron. *Neural Computation* **4**(4), 494–501.

Bishop, C. M. (1993). Curvature-driven smoothing: a learning algorithm for feedforward networks. *IEEE Transactions on Neural Networks* **4**(5), 882–884.

Bishop, C. M. (1994). Novelty detection and neural network validation. *IEE Proceedings: Vision, Image and Signal Processing* **141**(4), 217–222. Special issue on applications of neural networks.

Bishop, C. M. (1995a). *Neural Networks for Pattern Recognition*. Oxford University Press.

Bishop, C. M. (1995b). Training with noise is equivalent to Tikhonov regularization. *Neural Computation* **7**(1), 108–116.

Bishop, C. M. (1999a). Bayesian PCA. In M. S. Kearns, S. A. Solla, and D. A. Cohn (Eds.), *Advances in Neural Information Processing Systems*, Volume 11, pp. 382–388. MIT Press.

Bishop, C. M. (1999b). Variational principal components. In *Proceedings Ninth International Conference on Artificial Neural Networks, ICANN'99*, Volume 1, pp. 509–514. IEE.

Bishop, C. M. and G. D. James (1993). Analysis of multiphase flows using dual-energy gamma densitometry and neural networks. *Nuclear Instruments and Methods in Physics Research* **A327**, 580–593.

Bishop, C. M. and I. T. Nabney (1996). Modelling conditional probability distributions for periodic variables. *Neural Computation* **8**(5), 1123–1133.

Bishop, C. M. and I. T. Nabney (2008). *Pattern Recognition and Machine Learning: A Matlab Companion*. Springer. In preparation.

Bishop, C. M., D. Spiegelhalter, and J. Winn (2003). VIBES: A variational inference engine for Bayesian networks. In S. Becker, S. Thrun, and K. Obermeyer (Eds.), *Advances in Neural Information Processing Systems*, Volume 15, pp. 793–800. MIT Press.

Bishop, C. M. and M. Svensén (2003). Bayesian hierarchical mixtures of experts. In U. Kjaerulff and C. Meek (Eds.), *Proceedings Nineteenth Conference on Uncertainty in Artificial Intelligence*, pp. 57–64. Morgan Kaufmann.

Bishop, C. M., M. Svensén, and G. E. Hinton (2004). Distinguishing text from graphics in online handwritten ink. In F. Kimura and H. Fujisawa (Eds.), *Proceedings Ninth International Workshop on Frontiers in Handwriting Recognition, IWFHR-9*, Tokyo, Japan, pp. 142–147.

Bishop, C. M., M. Svensén, and C. K. I. Williams (1996). EM optimization of latent variable density models. In D. S. Touretzky, M. C. Mozer, and M. E. Hasselmo (Eds.), *Advances in Neural Information Processing Systems*, Volume 8, pp. 465–471. MIT Press.

Bishop, C. M., M. Svensén, and C. K. I. Williams (1997a). GTM: a principled alternative to the Self-Organizing Map. In M. C. Mozer, M. I. Jordan, and T. Petche (Eds.), *Advances in Neural Information Processing Systems*, Volume 9, pp. 354–360. MIT Press.

Bishop, C. M., M. Svensén, and C. K. I. Williams (1997b). Magnification factors for the GTM algorithm. In *Proceedings IEE Fifth International Conference on Artificial Neural Networks, Cambridge, U.K.*, pp. 64–69. Institute of Electrical Engineers.

Bishop, C. M., M. Svensén, and C. K. I. Williams (1998a). Developments of the Generative Topographic Mapping. *Neurocomputing* **21**, 203–224.

Bishop, C. M., M. Svensén, and C. K. I. Williams (1998b). GTM: the Generative Topographic Mapping. *Neural Computation* **10**(1), 215–234.

Bishop, C. M. and M. E. Tipping (1998). A hierarchical latent variable model for data visualization. *IEEE Transactions on Pattern Analysis and Machine Intelligence* **20**(3), 281–293.

Bishop, C. M. and J. Winn (2000). Non-linear Bayesian image modelling. In *Proceedings Sixth European Conference on Computer Vision, Dublin*, Volume 1, pp. 3–17. Springer.

Blei, D. M., M. I. Jordan, and A. Y. Ng (2003). Hierarchical Bayesian models for applications in information retrieval. In J. M. B. *et al.* (Ed.), *Bayesian Statistics, 7*, pp. 25–43. Oxford University Press.

Block, H. D. (1962). The perceptron: a model for brain functioning. *Reviews of Modern Physics* **34**(1), 123–135. Reprinted in Anderson and Rosenfeld (1988).

Blum, J. A. (1965). Multidimensional stochastic approximation methods. *Annals of Mathematical Statistics* **25**, 737–744.

Bodlaender, H. (1993). A tourist guide through treewidth. *Acta Cybernetica* **11**, 1–21.

Boser, B. E., I. M. Guyon, and V. N. Vapnik (1992). A training algorithm for optimal margin classifiers. In D. Haussler (Ed.), *Proceedings Fifth Annual Workshop on Computational Learning Theory (COLT)*, pp. 144–152. ACM.

Bourlard, H. and Y. Kamp (1988). Auto-association by multilayer perceptrons and singular value decomposition. *Biological Cybernetics* **59**, 291–294.

Box, G. E. P., G. M. Jenkins, and G. C. Reinsel (1994). *Time Series Analysis*. Prentice Hall.

Box, G. E. P. and G. C. Tao (1973). *Bayesian Inference in Statistical Analysis*. Wiley.

Boyd, S. and L. Vandenberghe (2004). *Convex Optimization*. Cambridge University Press.

Boyen, X. and D. Koller (1998). Tractable inference for complex stochastic processes. In G. F. Cooper and S. Moral (Eds.), *Proceedings 14th Annual Conference on Uncertainty in Artificial Intelligence (UAI)*, pp. 33–42. Morgan Kaufmann.

Boykov, Y., O. Veksler, and R. Zabih (2001). Fast approximate energy minimization via graph cuts. *IEEE Transactions on Pattern Analysis and Machine Intelligence* **23**(11), 1222–1239.

Breiman, L. (1996). Bagging predictors. *Machine Learning* **26**, 123–140.

Breiman, L., J. H. Friedman, R. A. Olshen, and P. J. Stone (1984). *Classification and Regression Trees*. Wadsworth.

Brooks, S. P. (1998). Markov chain Monte Carlo method and its application. *The Statistician* **47**(1), 69–100.

Broomhead, D. S. and D. Lowe (1988). Multivariable functional interpolation and adaptive networks. *Complex Systems* **2**, 321–355.

Buntine, W. and A. Weigend (1991). Bayesian backpropagation. *Complex Systems* **5**, 603–643.

Buntine, W. L. and A. S. Weigend (1993). Computing second derivatives in feed-forward networks: a review. *IEEE Transactions on Neural Networks* **5**(3), 480–488.

Burges, C. J. C. (1998). A tutorial on support vector machines for pattern recognition. *Knowledge Discovery and Data Mining* **2**(2), 121–167.

Cardoso, J.-F. (1998). Blind signal separation: statistical principles. *Proceedings of the IEEE* **9**(10), 2009–2025.

Casella, G. and R. L. Berger (2002). *Statistical Inference* (Second ed.). Duxbury.

Castillo, E., J. M. Gutiérrez, and A. S. Hadi (1997). *Expert Systems and Probabilistic Network Models*. Springer.

Chan, K., T. Lee, and T. J. Sejnowski (2003). Variational Bayesian learning of ICA with missing data. *Neural Computation* **15**(8), 1991–2011.

Chen, A. M., H. Lu, and R. Hecht-Nielsen (1993). On the geometry of feedforward neural network error surfaces. *Neural Computation* **5**(6), 910–927.

Chen, M. H., Q. M. Shao, and J. G. Ibrahim (Eds.) (2001). *Monte Carlo Methods for Bayesian Computation*. Springer.

Chen, S., C. F. N. Cowan, and P. M. Grant (1991). Orthogonal least squares learning algorithm for radial basis function networks. *IEEE Transactions on Neural Networks* **2**(2), 302–309.

Choudrey, R. A. and S. J. Roberts (2003). Variational mixture of Bayesian independent component analyzers. *Neural Computation* **15**(1), 213–252.

Clifford, P. (1990). Markov random fields in statistics. In G. R. Grimmett and D. J. A. Welsh (Eds.), *Disorder in Physical Systems. A Volume in Honour of John M. Hammersley*, pp. 19–32. Oxford University Press.

Collins, M., S. Dasgupta, and R. E. Schapire (2002). A generalization of principal component analysis to the exponential family. In T. G. Dietterich, S. Becker, and Z. Ghahramani (Eds.), *Advances in Neural Information Processing Systems*, Volume 14, pp. 617–624. MIT Press.

Comon, P., C. Jutten, and J. Herault (1991). Blind source separation, 2: problems statement. *Signal Processing* **24**(1), 11–20.

Corduneanu, A. and C. M. Bishop (2001). Variational Bayesian model selection for mixture distributions. In T. Richardson and T. Jaakkola (Eds.), *Proceedings Eighth International Conference on Artificial Intelligence and Statistics*, pp. 27–34. Morgan Kaufmann.

Cormen, T. H., C. E. Leiserson, R. L. Rivest, and C. Stein (2001). *Introduction to Algorithms* (Second ed.). MIT Press.

Cortes, C. and V. N. Vapnik (1995). Support vector networks. *Machine Learning* **20**, 273–297.

Cotter, N. E. (1990). The Stone-Weierstrass theorem and its application to neural networks. *IEEE Transactions on Neural Networks* **1**(4), 290–295.

Cover, T. and P. Hart (1967). Nearest neighbor pattern classification. *IEEE Transactions on Information Theory* **IT-11**, 21–27.

Cover, T. M. and J. A. Thomas (1991). *Elements of Information Theory*. Wiley.

Cowell, R. G., A. P. Dawid, S. L. Lauritzen, and D. J. Spiegelhalter (1999). *Probabilistic Networks and Expert Systems*. Springer.

Cox, R. T. (1946). Probability, frequency and reasonable expectation. *American Journal of Physics* **14**(1), 1–13.

Cox, T. F. and M. A. A. Cox (2000). *Multidimensional Scaling* (Second ed.). Chapman and Hall.

Cressie, N. (1993). *Statistics for Spatial Data*. Wiley.

Cristianini, N. and J. Shawe-Taylor (2000). *Support vector machines and other kernel-based learning methods*. Cambridge University Press.

Csató, L. and M. Opper (2002). Sparse on-line Gaussian processes. *Neural Computation* **14**(3), 641–668.

Csiszàr, I. and G. Tusnàdy (1984). Information geometry and alternating minimization procedures. *Statistics and Decisions* **1**(1), 205–237.

Cybenko, G. (1989). Approximation by superpositions of a sigmoidal function. *Mathematics of Control, Signals and Systems* **2**, 304–314.

Dawid, A. P. (1979). Conditional independence in statistical theory (with discussion). *Journal of the Royal Statistical Society, Series B* **4**, 1–31.

Dawid, A. P. (1980). Conditional independence for statistical operations. *Annals of Statistics* **8**, 598–617.

deFinetti, B. (1970). *Theory of Probability*. Wiley and Sons.

Dempster, A. P., N. M. Laird, and D. B. Rubin (1977). Maximum likelihood from incomplete data via the EM algorithm. *Journal of the Royal Statistical Society, B* **39**(1), 1–38.

Denison, D. G. T., C. C. Holmes, B. K. Mallick, and A. F. M. Smith (2002). *Bayesian Methods for Nonlinear Classification and Regression*. Wiley.

Diaconis, P. and L. Saloff-Coste (1998). What do we know about the Metropolis algorithm? *Journal of Computer and System Sciences* **57**, 20–36.

Dietterich, T. G. and G. Bakiri (1995). Solving multiclass learning problems via error-correcting output codes. *Journal of Artificial Intelligence Research* **2**, 263–286.

Duane, S., A. D. Kennedy, B. J. Pendleton, and D. Roweth (1987). Hybrid Monte Carlo. *Physics Letters B* **195**(2), 216–222.

Duda, R. O. and P. E. Hart (1973). *Pattern Classification and Scene Analysis*. Wiley.

Duda, R. O., P. E. Hart, and D. G. Stork (2001). *Pattern Classification* (Second ed.). Wiley.

Durbin, R., S. Eddy, A. Krogh, and G. Mitchison (1998). *Biological Sequence Analysis*. Cambridge University Press.

Dybowski, R. and S. Roberts (2005). An anthology of probabilistic models for medical informatics. In D. Husmeier, R. Dybowski, and S. Roberts (Eds.), *Probabilistic Modeling in Bioinformatics and Medical Informatics*, pp. 297–349. Springer.

Efron, B. (1979). Bootstrap methods: another look at the jackknife. *Annals of Statistics* **7**, 1–26.

Elkan, C. (2003). Using the triangle inequality to accelerate k-means. In *Proceedings of the Twelfth International Conference on Machine Learning*, pp. 147–153. AAAI.

Elliott, R. J., L. Aggoun, and J. B. Moore (1995). *Hidden Markov Models: Estimation and Control*. Springer.

Ephraim, Y., D. Malah, and B. H. Juang (1989). On the application of hidden Markov models for enhancing noisy speech. *IEEE Transactions on Acoustics, Speech and Signal Processing* **37**(12), 1846–1856.

Erwin, E., K. Obermayer, and K. Schulten (1992). Self-organizing maps: ordering, convergence properties and energy functions. *Biological Cybernetics* **67**, 47–55.

Everitt, B. S. (1984). *An Introduction to Latent Variable Models*. Chapman and Hall.

Faul, A. C. and M. E. Tipping (2002). Analysis of sparse Bayesian learning. In T. G. Dietterich, S. Becker, and Z. Ghahramani (Eds.), *Advances in Neural Information Processing Systems*, Volume 14, pp. 383–389. MIT Press.

Feller, W. (1966). *An Introduction to Probability Theory and its Applications* (Second ed.), Volume 2. Wiley.

Feynman, R. P., R. B. Leighton, and M. Sands (1964). *The Feynman Lectures of Physics*, Volume Two. Addison-Wesley. Chapter 19.

Fletcher, R. (1987). *Practical Methods of Optimization* (Second ed.). Wiley.

Forsyth, D. A. and J. Ponce (2003). *Computer Vision: A Modern Approach*. Prentice Hall.

Freund, Y. and R. E. Schapire (1996). Experiments with a new boosting algorithm. In L. Saitta (Ed.), *Thirteenth International Conference on Machine Learning*, pp. 148–156. Morgan Kaufmann.

Frey, B. J. (1998). *Graphical Models for Machine Learning and Digital Communication*. MIT Press.

Frey, B. J. and D. J. C. MacKay (1998). A revolution: Belief propagation in graphs with cycles. In M. I. Jordan, M. J. Kearns, and S. A. Solla (Eds.), *Advances in Neural Information Processing Systems*, Volume 10. MIT Press.

Friedman, J. H. (2001). Greedy function approximation: a gradient boosting machine. *Annals of Statistics* **29**(5), 1189–1232.

Friedman, J. H., T. Hastie, and R. Tibshirani (2000). Additive logistic regression: a statistical view of boosting. *Annals of Statistics* **28**, 337–407.

Friedman, N. and D. Koller (2003). Being Bayesian about network structure: A Bayesian approach to structure discovery in Bayesian networks. *Machine Learning* **50**, 95–126.

Frydenberg, M. (1990). The chain graph Markov property. *Scandinavian Journal of Statistics* **17**, 333–353.

Fukunaga, K. (1990). *Introduction to Statistical Pattern Recognition* (Second ed.). Academic Press.

Funahashi, K. (1989). On the approximate realization of continuous mappings by neural networks. *Neural Networks* **2**(3), 183–192.

Fung, R. and K. C. Chang (1990). Weighting and integrating evidence for stochastic simulation in Bayesian networks. In P. P. Bonissone, M. Henrion, L. N. Kanal, and J. F. Lemmer (Eds.), *Uncertainty in Artificial Intelligence*, Volume 5, pp. 208–219. Elsevier.

Gallager, R. G. (1963). *Low-Density Parity-Check Codes*. MIT Press.

Gamerman, D. (1997). *Markov Chain Monte Carlo: Stochastic Simulation for Bayesian Inference*. Chapman and Hall.

Gelman, A., J. B. Carlin, H. S. Stern, and D. B. Rubin (2004). *Bayesian Data Analysis* (Second ed.). Chapman and Hall.

Geman, S. and D. Geman (1984). Stochastic relaxation, Gibbs distributions, and the Bayesian restoration of images. *IEEE Transactions on Pattern Analysis and Machine Intelligence* **6**(1), 721–741.

Ghahramani, Z. and M. J. Beal (2000). Variational inference for Bayesian mixtures of factor analyzers. In S. A. Solla, T. K. Leen, and K. R. Müller (Eds.), *Advances in Neural Information Processing Systems*, Volume 12, pp. 449–455. MIT Press.

Ghahramani, Z. and G. E. Hinton (1996a). The EM algorithm for mixtures of factor analyzers. Technical Report CRG-TR-96-1, University of Toronto.

Ghahramani, Z. and G. E. Hinton (1996b). Parameter estimation for linear dynamical systems. Technical Report CRG-TR-96-2, University of Toronto.

Ghahramani, Z. and G. E. Hinton (1998). Variational learning for switching state-space models. *Neural Computation* **12**(4), 963–996.

Ghahramani, Z. and M. I. Jordan (1994). Supervised learning from incomplete data via an EM appproach. In J. D. Cowan, G. T. Tesauro, and J. Alspector (Eds.), *Advances in Neural Information Processing Systems*, Volume 6, pp. 120–127. Morgan Kaufmann.

Ghahramani, Z. and M. I. Jordan (1997). Factorial hidden Markov models. *Machine Learning* **29**, 245–275.

Gibbs, M. N. (1997). *Bayesian Gaussian processes for regression and classification*. Phd thesis, University of Cambridge.

Gibbs, M. N. and D. J. C. MacKay (2000). Variational Gaussian process classifiers. *IEEE Transactions on Neural Networks* **11**, 1458–1464.

Gilks, W. R. (1992). Derivative-free adaptive rejection sampling for Gibbs sampling. In J. Bernardo, J. Berger, A. P. Dawid, and A. F. M. Smith (Eds.), *Bayesian Statistics*, Volume 4. Oxford University Press.

Gilks, W. R., N. G. Best, and K. K. C. Tan (1995). Adaptive rejection Metropolis sampling. *Applied Statistics* **44**, 455–472.

Gilks, W. R., S. Richardson, and D. J. Spiegelhalter (Eds.) (1996). *Markov Chain Monte Carlo in Practice*. Chapman and Hall.

Gilks, W. R. and P. Wild (1992). Adaptive rejection sampling for Gibbs sampling. *Applied Statistics* **41**, 337–348.

Gill, P. E., W. Murray, and M. H. Wright (1981). *Practical Optimization*. Academic Press.

Goldberg, P. W., C. K. I. Williams, and C. M. Bishop (1998). Regression with input-dependent noise: A Gaussian process treatment. In *Advances in Neural Information Processing Systems*, Volume 10, pp. 493–499. MIT Press.

Golub, G. H. and C. F. Van Loan (1996). *Matrix Computations* (Third ed.). John Hopkins University Press.

Good, I. (1950). *Probability and the Weighing of Evidence*. Hafners.

Gordon, N. J., D. J. Salmond, and A. F. M. Smith (1993). Novel approach to nonlinear/non-Gaussian Bayesian state estimation. *IEE Proceedings-F* **140**(2), 107–113.

Graepel, T. (2003). Solving noisy linear operator equations by Gaussian processes: Application to ordinary and partial differential equations. In *Proceedings of the Twentieth International Conference on Machine Learning*, pp. 234–241.

Greig, D., B. Porteous, and A. Seheult (1989). Exact maximum a-posteriori estimation for binary images. *Journal of the Royal Statistical Society, Series B* **51**(2), 271–279.

Gull, S. F. (1989). Developments in maximum entropy data analysis. In J. Skilling (Ed.), *Maximum Entropy and Bayesian Methods*, pp. 53–71. Kluwer.

Hassibi, B. and D. G. Stork (1993). Second order derivatives for network pruning: optimal brain surgeon. In S. J. Hanson, J. D. Cowan, and C. L. Giles (Eds.), *Advances in Neural Information Processing Systems*, Volume 5, pp. 164–171. Morgan Kaufmann.

Hastie, T. and W. Stuetzle (1989). Principal curves. *Journal of the American Statistical Association* **84**(106), 502–516.

Hastie, T., R. Tibshirani, and J. Friedman (2001). *The Elements of Statistical Learning*. Springer.

Hastings, W. K. (1970). Monte Carlo sampling methods using Markov chains and their applications. *Biometrika* **57**, 97–109.

Hathaway, R. J. (1986). Another interpretation of the EM algorithm for mixture distributions. *Statistics and Probability Letters* **4**, 53–56.

Haussler, D. (1999). Convolution kernels on discrete structures. Technical Report UCSC-CRL-99-10, University of California, Santa Cruz, Computer Science Department.

Henrion, M. (1988). Propagation of uncertainty by logic sampling in Bayes' networks. In J. F. Lemmer and L. N. Kanal (Eds.), *Uncertainty in Artificial Intelligence*, Volume 2, pp. 149–164. North Holland.

Herbrich, R. (2002). *Learning Kernel Classifiers*. MIT Press.

Hertz, J., A. Krogh, and R. G. Palmer (1991). *Introduction to the Theory of Neural Computation*. Addison Wesley.

Hinton, G. E., P. Dayan, and M. Revow (1997). Modelling the manifolds of images of handwritten digits. *IEEE Transactions on Neural Networks* **8**(1), 65–74.

Hinton, G. E. and D. van Camp (1993). Keeping neural networks simple by minimizing the description length of the weights. In *Proceedings of the Sixth Annual Conference on Computational Learning Theory*, pp. 5–13. ACM.

Hinton, G. E., M. Welling, Y. W. Teh, and S. Osindero (2001). A new view of ICA. In *Proceedings of the International Conference on Independent Component Analysis and Blind Signal Separation*, Volume 3.

Hodgson, M. E. (1998). Reducing computational requirements of the minimum-distance classifier. *Remote Sensing of Environments* **25**, 117–128.

Hoerl, A. E. and R. Kennard (1970). Ridge regression: biased estimation for nonorthogonal problems. *Technometrics* **12**, 55–67.

Hofmann, T. (2000). Learning the similarity of documents: an information-geometric approach to document retrieval and classification. In S. A. Solla, T. K. Leen, and K. R. Müller (Eds.), *Advances in Neural Information Processing Systems*, Volume 12, pp. 914–920. MIT Press.

Hojen-Sorensen, P. A., O. Winther, and L. K. Hansen (2002). Mean field approaches to independent component analysis. *Neural Computation* **14**(4), 889–918.

Hornik, K. (1991). Approximation capabilities of multilayer feedforward networks. *Neural Networks* **4**(2), 251–257.

Hornik, K., M. Stinchcombe, and H. White (1989). Multilayer feedforward networks are universal approximators. *Neural Networks* **2**(5), 359–366.

Hotelling, H. (1933). Analysis of a complex of statistical variables into principal components. *Journal of Educational Psychology* **24**, 417–441.

Hotelling, H. (1936). Relations between two sets of variables. *Biometrika* **28**, 321–377.

Hyvärinen, A. and E. Oja (1997). A fast fixed-point algorithm for independent component analysis. *Neural Computation* **9**(7), 1483–1492.

Isard, M. and A. Blake (1998). CONDENSATION – conditional density propagation for visual tracking. *International Journal of Computer Vision* **29**(1), 5–18.

Ito, Y. (1991). Representation of functions by superpositions of a step or sigmoid function and their applications to neural network theory. *Neural Networks* **4**(3), 385–394.

Jaakkola, T. and M. I. Jordan (2000). Bayesian parameter estimation via variational methods. *Statistics and Computing* **10**, 25–37.

Jaakkola, T. S. (2001). Tutorial on variational approximation methods. In M. Opper and D. Saad (Eds.), *Advances in Mean Field Methods*, pp. 129–159. MIT Press.

Jaakkola, T. S. and D. Haussler (1999). Exploiting generative models in discriminative classifiers. In M. S. Kearns, S. A. Solla, and D. A. Cohn (Eds.), *Advances in Neural Information Processing Systems*, Volume 11. MIT Press.

Jacobs, R. A., M. I. Jordan, S. J. Nowlan, and G. E. Hinton (1991). Adaptive mixtures of local experts. *Neural Computation* **3**(1), 79–87.

Jaynes, E. T. (2003). *Probability Theory: The Logic of Science*. Cambridge University Press.

Jebara, T. (2004). *Machine Learning: Discriminative and Generative*. Kluwer.

Jeffries, H. (1946). An invariant form for the prior probability in estimation problems. *Pro. Roy. Soc. AA* **186**, 453–461.

Jelinek, F. (1997). *Statistical Methods for Speech Recognition*. MIT Press.

Jensen, C., A. Kong, and U. Kjaerulff (1995). Blocking gibbs sampling in very large probabilistic expert systems. *International Journal of Human Computer Studies. Special Issue on Real-World Applications of Uncertain Reasoning.* **42**, 647–666.

Jensen, F. V. (1996). *An Introduction to Bayesian Networks*. UCL Press.

Jerrum, M. and A. Sinclair (1996). The Markov chain Monte Carlo method: an approach to approximate counting and integration. In D. S. Hochbaum (Ed.), *Approximation Algorithms for NP-Hard Problems*. PWS Publishing.

Jolliffe, I. T. (2002). *Principal Component Analysis* (Second ed.). Springer.

Jordan, M. I. (1999). *Learning in Graphical Models*. MIT Press.

Jordan, M. I. (2007). *An Introduction to Probabilistic Graphical Models*. In preparation.

Jordan, M. I., Z. Ghahramani, T. S. Jaakkola, and L. K. Saul (1999). An introduction to variational methods for graphical models. In M. I. Jordan (Ed.), *Learning in Graphical Models*, pp. 105–162. MIT Press.

Jordan, M. I. and R. A. Jacobs (1994). Hierarchical mixtures of experts and the EM algorithm. *Neural Computation* **6**(2), 181–214.

Jutten, C. and J. Herault (1991). Blind separation of sources, 1: An adaptive algorithm based on neuromimetic architecture. *Signal Processing* **24**(1), 1–10.

Kalman, R. E. (1960). A new approach to linear filtering and prediction problems. *Transactions of the American Society for Mechanical Engineering, Series D, Journal of Basic Engineering* **82**, 35–45.

Kambhatla, N. and T. K. Leen (1997). Dimension reduction by local principal component analysis. *Neural Computation* **9**(7), 1493–1516.

Kanazawa, K., D. Koller, and S. Russel (1995). Stochastic simulation algorithms for dynamic probabilistic networks. In *Uncertainty in Artificial Intelligence*, Volume 11. Morgan Kaufmann.

Kapadia, S. (1998). *Discriminative Training of Hidden Markov Models*. Phd thesis, University of Cambridge, U.K.

Kapur, J. (1989). *Maximum entropy methods in science and engineering*. Wiley.

Karush, W. (1939). Minima of functions of several variables with inequalities as side constraints. Master's thesis, Department of Mathematics, University of Chicago.

Kass, R. E. and A. E. Raftery (1995). Bayes factors. *Journal of the American Statistical Association* **90**, 377–395.

Kearns, M. J. and U. V. Vazirani (1994). *An Introduction to Computational Learning Theory*. MIT Press.

Kindermann, R. and J. L. Snell (1980). *Markov Random Fields and Their Applications*. American Mathematical Society.

Kittler, J. and J. Föglein (1984). Contextual classification of multispectral pixel data. *Image and Vision Computing* **2**, 13–29.

Kohonen, T. (1982). Self-organized formation of topologically correct feature maps. *Biological Cybernetics* **43**, 59–69.

Kohonen, T. (1995). *Self-Organizing Maps*. Springer.

Kolmogorov, V. and R. Zabih (2004). What energy functions can be minimized via graph cuts? *IEEE Transactions on Pattern Analysis and Machine Intelligence* **26**(2), 147–159.

Kreinovich, V. Y. (1991). Arbitrary nonlinearity is sufficient to represent all functions by neural networks: a theorem. *Neural Networks* **4**(3), 381–383.

Krogh, A., M. Brown, I. S. Mian, K. Sjölander, and D. Haussler (1994). Hidden Markov models in computational biology: Applications to protein modelling. *Journal of Molecular Biology* **235**, 1501–1531.

Kschischnang, F. R., B. J. Frey, and H. A. Loeliger (2001). Factor graphs and the sum-product algorithm. *IEEE Transactions on Information Theory* **47**(2), 498–519.

Kuhn, H. W. and A. W. Tucker (1951). Nonlinear programming. In *Proceedings of the 2nd Berkeley Symposium on Mathematical Statistics and Probabilities*, pp. 481–492. University of California Press.

Kullback, S. and R. A. Leibler (1951). On information and sufficiency. *Annals of Mathematical Statistics* **22**(1), 79–86.

Kùrková, V. and P. C. Kainen (1994). Functionally equivalent feed-forward neural networks. *Neural Computation* **6**(3), 543–558.

Kuss, M. and C. Rasmussen (2006). Assessing approximations for Gaussian process classification. In *Advances in Neural Information Processing Systems*, Number 18. MIT Press. in press.

Lasserre, J., C. M. Bishop, and T. Minka (2006). Principled hybrids of generative and discriminative models. In *Proceedings 2006 IEEE Conference on Computer Vision and Pattern Recognition, New York*.

Lauritzen, S. and N. Wermuth (1989). Graphical models for association between variables, some of which are qualitative some quantitative. *Annals of Statistics* **17**, 31–57.

Lauritzen, S. L. (1992). Propagation of probabilities, means and variances in mixed graphical association models. *Journal of the American Statistical Association* **87**, 1098–1108.

Lauritzen, S. L. (1996). *Graphical Models*. Oxford University Press.

Lauritzen, S. L. and D. J. Spiegelhalter (1988). Local computations with probabailities on graphical structures and their application to expert systems. *Journal of the Royal Statistical Society* **50**, 157–224.

Lawley, D. N. (1953). A modified method of estimation in factor analysis and some large sample results. In *Uppsala Symposium on Psychological Factor Analysis*, Number 3 in Nordisk Psykologi Monograph Series, pp. 35–42. Uppsala: Almqvist and Wiksell.

Lawrence, N. D., A. I. T. Rowstron, C. M. Bishop, and M. J. Taylor (2002). Optimising synchronisation times for mobile devices. In T. G. Dietterich, S. Becker, and Z. Ghahramani (Eds.), *Advances in Neural Information Processing Systems*, Volume 14, pp. 1401–1408. MIT Press.

Lazarsfeld, P. F. and N. W. Henry (1968). *Latent Structure Analysis*. Houghton Mifflin.

Le Cun, Y., B. Boser, J. S. Denker, D. Henderson, R. E. Howard, W. Hubbard, and L. D. Jackel (1989). Backpropagation applied to handwritten zip code recognition. *Neural Computation* **1**(4), 541–551.

Le Cun, Y., J. S. Denker, and S. A. Solla (1990). Optimal brain damage. In D. S. Touretzky (Ed.),

Advances in Neural Information Processing Systems, Volume 2, pp. 598–605. Morgan Kaufmann.

LeCun, Y., L. Bottou, Y. Bengio, and P. Haffner (1998). Gradient-based learning applied to document recognition. *Proceedings of the IEEE* **86**, 2278–2324.

Lee, Y., Y. Lin, and G. Wahba (2001). Multicategory support vector machines. Technical Report 1040, Department of Statistics, University of Madison, Wisconsin.

Leen, T. K. (1995). From data distributions to regularization in invariant learning. *Neural Computation* **7**, 974–981.

Lindley, D. V. (1982). Scoring rules and the inevitability of probability. *International Statistical Review* **50**, 1–26.

Liu, J. S. (Ed.) (2001). *Monte Carlo Strategies in Scientific Computing*. Springer.

Lloyd, S. P. (1982). Least squares quantization in PCM. *IEEE Transactions on Information Theory* **28**(2), 129–137.

Lütkepohl, H. (1996). *Handbook of Matrices*. Wiley.

MacKay, D. J. C. (1992a). Bayesian interpolation. *Neural Computation* **4**(3), 415–447.

MacKay, D. J. C. (1992b). The evidence framework applied to classification networks. *Neural Computation* **4**(5), 720–736.

MacKay, D. J. C. (1992c). A practical Bayesian framework for back-propagation networks. *Neural Computation* **4**(3), 448–472.

MacKay, D. J. C. (1994). Bayesian methods for backprop networks. In E. Domany, J. L. van Hemmen, and K. Schulten (Eds.), *Models of Neural Networks, III*, Chapter 6, pp. 211–254. Springer.

MacKay, D. J. C. (1995). Bayesian neural networks and density networks. *Nuclear Instruments and Methods in Physics Research, A* **354**(1), 73–80.

MacKay, D. J. C. (1997). Ensemble learning for hidden Markov models. Unpublished manuscript, Department of Physics, University of Cambridge.

MacKay, D. J. C. (1998). Introduction to Gaussian processes. In C. M. Bishop (Ed.), *Neural Networks and Machine Learning*, pp. 133–166. Springer.

MacKay, D. J. C. (1999). Comparison of approximate methods for handling hyperparameters. *Neural Computation* **11**(5), 1035–1068.

MacKay, D. J. C. (2003). *Information Theory, Inference and Learning Algorithms*. Cambridge University Press.

MacKay, D. J. C. and M. N. Gibbs (1999). Density networks. In J. W. Kay and D. M. Titterington (Eds.), *Statistics and Neural Networks: Advances at the Interface*, Chapter 5, pp. 129–145. Oxford University Press.

MacKay, D. J. C. and R. M. Neal (1999). Good error-correcting codes based on very sparse matrices. *IEEE Transactions on Information Theory* **45**, 399–431.

MacQueen, J. (1967). Some methods for classification and analysis of multivariate observations. In L. M. LeCam and J. Neyman (Eds.), *Proceedings of the Fifth Berkeley Symposium on Mathematical Statistics and Probability*, Volume I, pp. 281–297. University of California Press.

Magnus, J. R. and H. Neudecker (1999). *Matrix Differential Calculus with Applications in Statistics and Econometrics*. Wiley.

Mallat, S. (1999). *A Wavelet Tour of Signal Processing* (Second ed.). Academic Press.

Manning, C. D. and H. Schütze (1999). *Foundations of Statistical Natural Language Processing*. MIT Press.

Mardia, K. V. and P. E. Jupp (2000). *Directional Statistics*. Wiley.

Maybeck, P. S. (1982). *Stochastic models, estimation and control*. Academic Press.

McAllester, D. A. (2003). PAC-Bayesian stochastic model selection. *Machine Learning* **51**(1), 5–21.

McCullagh, P. and J. A. Nelder (1989). *Generalized Linear Models* (Second ed.). Chapman and Hall.

McCulloch, W. S. and W. Pitts (1943). A logical calculus of the ideas immanent in nervous activity. *Bulletin of Mathematical Biophysics* **5**, 115–133. Reprinted in Anderson and Rosenfeld (1988).

McEliece, R. J., D. J. C. MacKay, and J. F. Cheng (1998). Turbo decoding as an instance of Pearl's 'Belief Ppropagation' algorithm. *IEEE Journal on Selected Areas in Communications* **16**, 140–152.

McLachlan, G. J. and K. E. Basford (1988). *Mixture Models: Inference and Applications to Clustering*. Marcel Dekker.

McLachlan, G. J. and T. Krishnan (1997). *The EM Algorithm and its Extensions*. Wiley.

McLachlan, G. J. and D. Peel (2000). *Finite Mixture Models*. Wiley.

Meng, X. L. and D. B. Rubin (1993). Maximum likelihood estimation via the ECM algorithm: a general framework. *Biometrika* **80**, 267–278.

Metropolis, N., A. W. Rosenbluth, M. N. Rosenbluth, A. H. Teller, and E. Teller (1953). Equation of state calculations by fast computing machines. *Journal of Chemical Physics* **21**(6), 1087–1092.

Metropolis, N. and S. Ulam (1949). The Monte Carlo method. *Journal of the American Statistical Association* **44**(247), 335–341.

Mika, S., G. Rätsch, J. Weston, and B. Schölkopf (1999). Fisher discriminant analysis with kernels. In Y. H. Hu, J. Larsen, E. Wilson, and S. Douglas (Eds.), *Neural Networks for Signal Processing IX*, pp. 41–48. IEEE.

Minka, T. (2001a). Expectation propagation for approximate Bayesian inference. In J. Breese and D. Koller (Eds.), *Proceedings of the Seventeenth Conference on Uncertainty in Artificial Intelligence*, pp. 362–369. Morgan Kaufmann.

Minka, T. (2001b). *A family of approximate algorithms for Bayesian inference*. Ph. D. thesis, MIT.

Minka, T. (2004). Power EP. Technical Report MSR-TR-2004-149, Microsoft Research Cambridge.

Minka, T. (2005). Divergence measures and message passing. Technical Report MSR-TR-2005-173, Microsoft Research Cambridge.

Minka, T. P. (2001c). Automatic choice of dimensionality for PCA. In T. K. Leen, T. G. Dietterich, and V. Tresp (Eds.), *Advances in Neural Information Processing Systems*, Volume 13, pp. 598–604. MIT Press.

Minsky, M. L. and S. A. Papert (1969). *Perceptrons*. MIT Press. Expanded edition 1990.

Miskin, J. W. and D. J. C. MacKay (2001). Ensemble learning for blind source separation. In S. J. Roberts and R. M. Everson (Eds.), *Independent Component Analysis: Principles and Practice*. Cambridge University Press.

Møller, M. (1993). Efficient Training of Feed-Forward Neural Networks. Ph. D. thesis, Aarhus University, Denmark.

Moody, J. and C. J. Darken (1989). Fast learning in networks of locally-tuned processing units. *Neural Computation* **1**(2), 281–294.

Moore, A. W. (2000). The anchors hierarch: using the triangle inequality to survive high dimensional data. In *Proceedings of the Twelfth Conference on Uncertainty in Artificial Intelligence*, pp. 397–405.

Müller, K. R., S. Mika, G. Rätsch, K. Tsuda, and B. Schölkopf (2001). An introduction to kernel-based learning algorithms. *IEEE Transactions on Neural Networks* **12**(2), 181–202.

Müller, P. and F. A. Quintana (2004). Nonparametric Bayesian data analysis. *Statistical Science* **19**(1), 95–110.

Nabney, I. T. (2002). *Netlab: Algorithms for Pattern Recognition*. Springer.

Nadaraya, É. A. (1964). On estimating regression. *Theory of Probability and its Applications* **9**(1), 141–142.

Nag, R., K. Wong, and F. Fallside (1986). Script recognition using hidden markov models. In *ICASSP86*, pp. 2071–2074. IEEE.

Neal, R. M. (1993). Probabilistic inference using Markov chain Monte Carlo methods. Technical Report CRG-TR-93-1, Department of Computer Science, University of Toronto, Canada.

Neal, R. M. (1996). *Bayesian Learning for Neural Networks*. Springer. Lecture Notes in Statistics 118.

Neal, R. M. (1997). Monte Carlo implementation of Gaussian process models for Bayesian regression and classification. Technical Report 9702, Department of Computer Statistics, University of Toronto.

Neal, R. M. (1999). Suppressing random walks in Markov chain Monte Carlo using ordered overrelaxation. In M. I. Jordan (Ed.), *Learning in Graphical Models*, pp. 205–228. MIT Press.

Neal, R. M. (2000). Markov chain sampling for Dirichlet process mixture models. *Journal of Computational and Graphical Statistics* **9**, 249–265.

Neal, R. M. (2003). Slice sampling. *Annals of Statistics* **31**, 705–767.

Neal, R. M. and G. E. Hinton (1999). A new view of the EM algorithm that justifies incremental and other variants. In M. I. Jordan (Ed.), *Learning in Graphical Models*, pp. 355–368. MIT Press.

Nelder, J. A. and R. W. M. Wedderburn (1972). Generalized linear models. *Journal of the Royal Statistical Society, A* **135**, 370–384.

Nilsson, N. J. (1965). *Learning Machines*. McGraw-Hill. Reprinted as *The Mathematical Foundations of Learning Machines*, Morgan Kaufmann, (1990).

Nocedal, J. and S. J. Wright (1999). *Numerical Optimization*. Springer.

Nowlan, S. J. and G. E. Hinton (1992). Simplifying neural networks by soft weight sharing. *Neural Computation* **4**(4), 473–493.

Ogden, R. T. (1997). *Essential Wavelets for Statistical Applications and Data Analysis*. Birkhäuser.

Opper, M. and O. Winther (1999). A Bayesian approach to on-line learning. In D. Saad (Ed.), *On-Line Learning in Neural Networks*, pp. 363–378. Cambridge University Press.

Opper, M. and O. Winther (2000a). Gaussian processes and SVM: mean field theory and leave-one-out. In A. J. Smola, P. L. Bartlett, B. Schölkopf, and D. Shuurmans (Eds.), *Advances in Large Margin Classifiers*, pp. 311–326. MIT Press.

Opper, M. and O. Winther (2000b). Gaussian processes for classification. *Neural Computation* **12**(11), 2655–2684.

Osuna, E., R. Freund, and F. Girosi (1996). Support vector machines: training and applications. A.I. Memo AIM-1602, MIT.

Papoulis, A. (1984). *Probability, Random Variables, and Stochastic Processes* (Second ed.). McGraw-Hill.

Parisi, G. (1988). *Statistical Field Theory*. Addison-Wesley.

Pearl, J. (1988). *Probabilistic Reasoning in Intelligent Systems*. Morgan Kaufmann.

Pearlmutter, B. A. (1994). Fast exact multiplication by the Hessian. *Neural Computation* **6**(1), 147–160.

Pearlmutter, B. A. and L. C. Parra (1997). Maximum likelihood source separation: a context-sensitive generalization of ICA. In M. C. Mozer, M. I. Jordan, and T. Petsche (Eds.), *Advances in Neural Information Processing Systems*, Volume 9, pp. 613–619. MIT Press.

Pearson, K. (1901). On lines and planes of closest fit to systems of points in space. *The London, Edinburgh and Dublin Philosophical Magazine and Journal of Science, Sixth Series* **2**, 559–572.

Platt, J. C. (1999). Fast training of support vector machines using sequential minimal optimization. In B. Schölkopf, C. J. C. Burges, and A. J. Smola (Eds.), *Advances in Kernel Methods – Support Vector Learning*, pp. 185–208. MIT Press.

Platt, J. C. (2000). Probabilities for SV machines. In A. J. Smola, P. L. Bartlett, B. Schölkopf, and D. Shuurmans (Eds.), *Advances in Large Margin Classifiers*, pp. 61–73. MIT Press.

Platt, J. C., N. Cristianini, and J. Shawe-Taylor (2000). Large margin DAGs for multiclass classification. In S. A. Solla, T. K. Leen, and K. R. Müller (Eds.), *Advances in Neural Information Processing Systems*, Volume 12, pp. 547–553. MIT Press.

Poggio, T. and F. Girosi (1990). Networks for approximation and learning. *Proceedings of the IEEE* **78**(9), 1481–1497.

Powell, M. J. D. (1987). Radial basis functions for multivariable interpolation: a review. In J. C. Mason and M. G. Cox (Eds.), *Algorithms for Approximation*, pp. 143–167. Oxford University Press.

Press, W. H., S. A. Teukolsky, W. T. Vetterling, and B. P. Flannery (1992). *Numerical Recipes in C: The Art of Scientific Computing* (Second ed.). Cambridge University Press.

Qazaz, C. S., C. K. I. Williams, and C. M. Bishop (1997). An upper bound on the Bayesian error bars for generalized linear regression. In S. W. Ellacott, J. C. Mason, and I. J. Anderson (Eds.), *Mathematics of Neural Networks: Models, Algorithms and Applications*, pp. 295–299. Kluwer.

Quinlan, J. R. (1986). Induction of decision trees. *Machine Learning* **1**(1), 81–106.

Quinlan, J. R. (1993). *C4.5: Programs for Machine Learning*. Morgan Kaufmann.

Rabiner, L. and B. H. Juang (1993). *Fundamentals of Speech Recognition*. Prentice Hall.

Rabiner, L. R. (1989). A tutorial on hidden Markov models and selected applications in speech recognition. *Proceedings of the IEEE* **77**(2), 257–285.

Ramasubramanian, V. and K. K. Paliwal (1990). A generalized optimization of the k-d tree for fast nearest-neighbour search. In *Proceedings Fourth IEEE Region 10 International Conference (TENCON'89)*, pp. 565–568.

Ramsey, F. (1931). Truth and probability. In R. Braithwaite (Ed.), *The Foundations of Mathematics and other Logical Essays*. Humanities Press.

Rao, C. R. and S. K. Mitra (1971). *Generalized Inverse of Matrices and Its Applications*. Wiley.

Rasmussen, C. E. (1996). *Evaluation of Gaussian Processes and Other Methods for Non-Linear Regression*. Ph. D. thesis, University of Toronto.

Rasmussen, C. E. and J. Quiñonero-Candela (2005). Healing the relevance vector machine by augmentation. In L. D. Raedt and S. Wrobel (Eds.), *Proceedings of the 22nd International Conference on Machine Learning*, pp. 689–696.

Rasmussen, C. E. and C. K. I. Williams (2006). *Gaussian Processes for Machine Learning*. MIT Press.

Rauch, H. E., F. Tung, and C. T. Striebel (1965). Maximum likelihood estimates of linear dynamical systems. *AIAA Journal* **3**, 1445–1450.

Ricotti, L. P., S. Ragazzini, and G. Martinelli (1988). Learning of word stress in a sub-optimal second order backpropagation neural network. In *Proceedings of the IEEE International Conference on Neural Networks*, Volume 1, pp. 355–361. IEEE.

Ripley, B. D. (1996). *Pattern Recognition and Neural Networks*. Cambridge University Press.

Robbins, H. and S. Monro (1951). A stochastic approximation method. *Annals of Mathematical Statistics* **22**, 400–407.

Robert, C. P. and G. Casella (1999). *Monte Carlo Statistical Methods*. Springer.

Rockafellar, R. (1972). *Convex Analysis*. Princeton University Press.

Rosenblatt, F. (1962). *Principles of Neurodynamics: Perceptrons and the Theory of Brain Mechanisms*. Spartan.

Roth, V. and V. Steinhage (2000). Nonlinear discriminant analysis using kernel functions. In S. A.

Solla, T. K. Leen, and K. R. Müller (Eds.), *Advances in Neural Information Processing Systems*, Volume 12. MIT Press.

Roweis, S. (1998). EM algorithms for PCA and SPCA. In M. I. Jordan, M. J. Kearns, and S. A. Solla (Eds.), *Advances in Neural Information Processing Systems*, Volume 10, pp. 626–632. MIT Press.

Roweis, S. and Z. Ghahramani (1999). A unifying review of linear Gaussian models. *Neural Computation* **11**(2), 305–345.

Roweis, S. and L. Saul (2000, December). Nonlinear dimensionality reduction by locally linear embedding. *Science* **290**, 2323–2326.

Rubin, D. B. (1983). Iteratively reweighted least squares. In *Encyclopedia of Statistical Sciences*, Volume 4, pp. 272–275. Wiley.

Rubin, D. B. and D. T. Thayer (1982). EM algorithms for ML factor analysis. *Psychometrika* **47**(1), 69–76.

Rumelhart, D. E., G. E. Hinton, and R. J. Williams (1986). Learning internal representations by error propagation. In D. E. Rumelhart, J. L. McClelland, and the PDP Research Group (Eds.), *Parallel Distributed Processing: Explorations in the Microstructure of Cognition*, Volume 1: Foundations, pp. 318–362. MIT Press. Reprinted in Anderson and Rosenfeld (1988).

Rumelhart, D. E., J. L. McClelland, and the PDP Research Group (Eds.) (1986). *Parallel Distributed Processing: Explorations in the Microstructure of Cognition*, Volume 1: Foundations. MIT Press.

Sagan, H. (1969). *Introduction to the Calculus of Variations*. Dover.

Savage, L. J. (1961). The subjective basis of statistical practice. Technical report, Department of Statistics, University of Michigan, Ann Arbor.

Schölkopf, B., J. Platt, J. Shawe-Taylor, A. Smola, and R. C. Williamson (2001). Estimating the support of a high-dimensional distribution. *Neural Computation* **13**(7), 1433–1471.

Schölkopf, B., A. Smola, and K.-R. Müller (1998). Nonlinear component analysis as a kernel eigenvalue problem. *Neural Computation* **10**(5), 1299–1319.

Schölkopf, B., A. Smola, R. C. Williamson, and P. L. Bartlett (2000). New support vector algorithms. *Neural Computation* **12**(5), 1207–1245.

Schölkopf, B. and A. J. Smola (2002). *Learning with Kernels*. MIT Press.

Schwarz, G. (1978). Estimating the dimension of a model. *Annals of Statistics* **6**, 461–464.

Schwarz, H. R. (1988). *Finite element methods*. Academic Press.

Seeger, M. (2003). *Bayesian Gaussian Process Models: PAC-Bayesian Generalization Error Bounds and Sparse Approximations*. Ph. D. thesis, University of Edinburg.

Seeger, M., C. K. I. Williams, and N. Lawrence (2003). Fast forward selection to speed up sparse Gaussian processes. In C. M. Bishop and B. Frey (Eds.), *Proceedings Ninth International Workshop on Artificial Intelligence and Statistics, Key West, Florida*.

Shachter, R. D. and M. Peot (1990). Simulation approaches to general probabilistic inference on belief networks. In P. P. Bonissone, M. Henrion, L. N. Kanal, and J. F. Lemmer (Eds.), *Uncertainty in Artificial Intelligence*, Volume 5. Elsevier.

Shannon, C. E. (1948). A mathematical theory of communication. *The Bell System Technical Journal* **27**(3), 379–423 and 623–656.

Shawe-Taylor, J. and N. Cristianini (2004). *Kernel Methods for Pattern Analysis*. Cambridge University Press.

Sietsma, J. and R. J. F. Dow (1991). Creating artificial neural networks that generalize. *Neural Networks* **4**(1), 67–79.

Simard, P., Y. Le Cun, and J. Denker (1993). Efficient pattern recognition using a new transformation distance. In S. J. Hanson, J. D. Cowan, and

C. L. Giles (Eds.), *Advances in Neural Information Processing Systems*, Volume 5, pp. 50–58. Morgan Kaufmann.

Simard, P., B. Victorri, Y. Le Cun, and J. Denker (1992). Tangent prop – a formalism for specifying selected invariances in an adaptive network. In J. E. Moody, S. J. Hanson, and R. P. Lippmann (Eds.), *Advances in Neural Information Processing Systems*, Volume 4, pp. 895–903. Morgan Kaufmann.

Simard, P. Y., D. Steinkraus, and J. Platt (2003). Best practice for convolutional neural networks applied to visual document analysis. In *Proceedings International Conference on Document Analysis and Recognition (ICDAR)*, pp. 958–962. IEEE Computer Society.

Sirovich, L. (1987). Turbulence and the dynamics of coherent structures. *Quarterly Applied Mathematics* **45**(3), 561–590.

Smola, A. J. and P. Bartlett (2001). Sparse greedy Gaussian process regression. In T. K. Leen, T. G. Dietterich, and V. Tresp (Eds.), *Advances in Neural Information Processing Systems*, Volume 13, pp. 619–625. MIT Press.

Spiegelhalter, D. and S. Lauritzen (1990). Sequential updating of conditional probabilities on directed graphical structures. *Networks* **20**, 579–605.

Stinchecombe, M. and H. White (1989). Universal approximation using feed-forward networks with non-sigmoid hidden layer activation functions. In *International Joint Conference on Neural Networks*, Volume 1, pp. 613–618. IEEE.

Stone, J. V. (2004). *Independent Component Analysis: A Tutorial Introduction*. MIT Press.

Sung, K. K. and T. Poggio (1994). Example-based learning for view-based human face detection. A.I. Memo 1521, MIT.

Sutton, R. S. and A. G. Barto (1998). *Reinforcement Learning: An Introduction*. MIT Press.

Svensén, M. and C. M. Bishop (2004). Robust Bayesian mixture modelling. *Neurocomputing* **64**, 235–252.

Tarassenko, L. (1995). Novelty detection for the identification of masses in mamograms. In *Proceedings Fourth IEE International Conference on Artificial Neural Networks*, Volume 4, pp. 442–447. IEE.

Tax, D. and R. Duin (1999). Data domain description by support vectors. In M. Verleysen (Ed.), *Proceedings European Symposium on Artificial Neural Networks, ESANN*, pp. 251–256. D. Facto Press.

Teh, Y. W., M. I. Jordan, M. J. Beal, and D. M. Blei (2006). Hierarchical Dirichlet processes. *Journal of the Americal Statistical Association*. to appear.

Tenenbaum, J. B., V. de Silva, and J. C. Langford (2000, December). A global framework for nonlinear dimensionality reduction. *Science* **290**, 2319–2323.

Tesauro, G. (1994). TD-Gammon, a self-teaching backgammon program, achieves master-level play. *Neural Computation* **6**(2), 215–219.

Thiesson, B., D. M. Chickering, D. Heckerman, and C. Meek (2004). ARMA time-series modelling with graphical models. In M. Chickering and J. Halpern (Eds.), *Proceedings of the Twentieth Conference on Uncertainty in Artificial Intelligence, Banff, Canada*, pp. 552–560. AUAI Press.

Tibshirani, R. (1996). Regression shrinkage and selection via the lasso. *Journal of the Royal Statistical Society, B* **58**, 267–288.

Tierney, L. (1994). Markov chains for exploring posterior distributions. *Annals of Statistics* **22**(4), 1701–1762.

Tikhonov, A. N. and V. Y. Arsenin (1977). *Solutions of Ill-Posed Problems*. V. H. Winston.

Tino, P. and I. T. Nabney (2002). Hierarchical GTM: constructing localized non-linear projection manifolds in a principled way. *IEEE Transactions on Pattern Analysis and Machine Intelligence* **24**(5), 639–656.

Tino, P., I. T. Nabney, and Y. Sun (2001). Using directional curvatures to visualize folding patterns of the GTM projection manifolds. In

G. Dorffner, H. Bischof, and K. Hornik (Eds.), *Artificial Neural Networks – ICANN 2001*, pp. 421–428. Springer.

Tipping, M. E. (1999). Probabilistic visualisation of high-dimensional binary data. In M. S. Kearns, S. A. Solla, and D. A. Cohn (Eds.), *Advances in Neural Information Processing Systems*, Volume 11, pp. 592–598. MIT Press.

Tipping, M. E. (2001). Sparse Bayesian learning and the relevance vector machine. *Journal of Machine Learning Research* **1**, 211–244.

Tipping, M. E. and C. M. Bishop (1997). Probabilistic principal component analysis. Technical Report NCRG/97/010, Neural Computing Research Group, Aston University.

Tipping, M. E. and C. M. Bishop (1999a). Mixtures of probabilistic principal component analyzers. *Neural Computation* **11**(2), 443–482.

Tipping, M. E. and C. M. Bishop (1999b). Probabilistic principal component analysis. *Journal of the Royal Statistical Society, Series B* **21**(3), 611–622.

Tipping, M. E. and A. Faul (2003). Fast marginal likelihood maximization for sparse Bayesian models. In C. M. Bishop and B. Frey (Eds.), *Proceedings Ninth International Workshop on Artificial Intelligence and Statistics, Key West, Florida*.

Tong, S. and D. Koller (2000). Restricted Bayes optimal classifiers. In *Proceedings 17th National Conference on Artificial Intelligence*, pp. 658–664. AAAI.

Tresp, V. (2001). Scaling kernel-based systems to large data sets. *Data Mining and Knowledge Discovery* **5**(3), 197–211.

Uhlenbeck, G. E. and L. S. Ornstein (1930). On the theory of Brownian motion. *Phys. Rev.* **36**, 823–841.

Valiant, L. G. (1984). A theory of the learnable. *Communications of the Association for Computing Machinery* **27**, 1134–1142.

Vapnik, V. N. (1982). *Estimation of dependences based on empirical data*. Springer.

Vapnik, V. N. (1995). *The nature of statistical learning theory*. Springer.

Vapnik, V. N. (1998). *Statistical learning theory*. Wiley.

Veropoulos, K., C. Campbell, and N. Cristianini (1999). Controlling the sensitivity of support vector machines. In *Proceedings of the International Joint Conference on Artificial Intelligence (IJCAI99), Workshop ML3*, pp. 55–60.

Vidakovic, B. (1999). *Statistical Modelling by Wavelets*. Wiley.

Viola, P. and M. Jones (2004). Robust real-time face detection. *International Journal of Computer Vision* **57**(2), 137–154.

Viterbi, A. J. (1967). Error bounds for convolutional codes and an asymptotically optimum decoding algorithm. *IEEE Transactions on Information Theory* **IT-13**, 260–267.

Viterbi, A. J. and J. K. Omura (1979). *Principles of Digital Communication and Coding*. McGraw-Hill.

Wahba, G. (1975). A comparison of GCV and GML for choosing the smoothing parameter in the generalized spline smoothing problem. *Numerical Mathematics* **24**, 383–393.

Wainwright, M. J., T. S. Jaakkola, and A. S. Willsky (2005). A new class of upper bounds on the log partition function. *IEEE Transactions on Information Theory* **51**, 2313–2335.

Walker, A. M. (1969). On the asymptotic behaviour of posterior distributions. *Journal of the Royal Statistical Society, B* **31**(1), 80–88.

Walker, S. G., P. Damien, P. W. Laud, and A. F. M. Smith (1999). Bayesian nonparametric inference for random distributions and related functions (with discussion). *Journal of the Royal Statistical Society, B* **61**(3), 485–527.

Watson, G. S. (1964). Smooth regression analysis. *Sankhyā: The Indian Journal of Statistics. Series A* **26**, 359–372.

Webb, A. R. (1994). Functional approximation by feed-forward networks: a least-squares approach to generalisation. *IEEE Transactions on Neural Networks* **5**(3), 363–371.

Weisstein, E. W. (1999). *CRC Concise Encyclopedia of Mathematics*. Chapman and Hall, and CRC.

Weston, J. and C. Watkins (1999). Multi-class support vector machines. In M. Verlysen (Ed.), *Proceedings ESANN'99, Brussels*. D-Facto Publications.

Whittaker, J. (1990). *Graphical Models in Applied Multivariate Statistics*. Wiley.

Widrow, B. and M. E. Hoff (1960). Adaptive switching circuits. In *IRE WESCON Convention Record*, Volume 4, pp. 96–104. Reprinted in Anderson and Rosenfeld (1988).

Widrow, B. and M. A. Lehr (1990). 30 years of adaptive neural networks: perceptron, madeline, and backpropagation. *Proceedings of the IEEE* **78**(9), 1415–1442.

Wiegerinck, W. and T. Heskes (2003). Fractional belief propagation. In S. Becker, S. Thrun, and K. Obermayer (Eds.), *Advances in Neural Information Processing Systems*, Volume 15, pp. 455–462. MIT Press.

Williams, C. K. I. (1998). Computation with infinite neural networks. *Neural Computation* **10**(5), 1203–1216.

Williams, C. K. I. (1999). Prediction with Gaussian processes: from linear regression to linear prediction and beyond. In M. I. Jordan (Ed.), *Learning in Graphical Models*, pp. 599–621. MIT Press.

Williams, C. K. I. and D. Barber (1998). Bayesian classification with Gaussian processes. *IEEE Transactions on Pattern Analysis and Machine Intelligence* **20**, 1342–1351.

Williams, C. K. I. and M. Seeger (2001). Using the Nystrom method to speed up kernel machines. In T. K. Leen, T. G. Dietterich, and V. Tresp (Eds.), *Advances in Neural Information Processing Systems*, Volume 13, pp. 682–688. MIT Press.

Williams, O., A. Blake, and R. Cipolla (2005). Sparse Bayesian learning for efficient visual tracking. *IEEE Transactions on Pattern Analysis and Machine Intelligence* **27**(8), 1292–1304.

Williams, P. M. (1996). Using neural networks to model conditional multivariate densities. *Neural Computation* **8**(4), 843–854.

Winn, J. and C. M. Bishop (2005). Variational message passing. *Journal of Machine Learning Research* **6**, 661–694.

Zarchan, P. and H. Musoff (2005). *Fundamentals of Kalman Filtering: A Practical Approach* (Second ed.). AIAA.

Index

Page numbers in **bold** indicate the primary source of information for the corresponding topic.